TRANSITION METAL CATALYZED CARBON-HYDROGEN BOND FUNCTIONALIZATIONS FOR AROMATIC CARBON-NITROGEN BOND FORMATION. DEVELOPMENT OF PALLADIUM-CATALYZED INTERMOLECULAR AMIDATION OF ANILIDES AND BENZOIC ACIDS AND RHODIUM-CATALYZED DIRECT ARYL C-H AMINATION USING *N*-CHLOROAMINES.

NG KA HO

Ph.D

The Hong Kong Polytechnic University

2015

The Hong Kong Polytechnic University

Department of Applied Biology and Chemical Technology

Transition Metal Catalyzed Carbon-Hydrogen Bond Functionalizations for Aromatic Carbon-Nitrogen Bond Formation. Development of Palladium-Catalyzed Intermolecular Amidation of Anilides and Benzoic Acids and Rhodium-Catalyzed Direct Aryl C-H Amination Using *N*-Chloroamines.

NG KA HO

A thesis submitted in partial fulfillment

of the requirements for the degree of

Doctor of Philosophy

January 2014

CERTIFICATION OF ORIGINALITY

I hereby declare that this thesis is my own work and that, to the best of my knowledge and belief, it reproduces no material previously published or written, nor material that has been accepted for the award of any other degree or diploma, except where due acknowledgement has been made in the text.

NG Ka Ho

ABSTRACT

Abstract of the thesis entitled

Transition Metal Catalyzed Carbon-Hydrogen Bond Functionalizations for Aromatic Carbon-Nitrogen Bond Formation. Development of Palladium-Catalyzed Intermolecular Amidation of Anilides and Benzoic Acids and Rhodium-Catalyzed Direct Aryl C-H Amination Using *N*-Chloroamines.

Submitted by NG Ka Ho

for the degree of Doctor of Philosophy

at The Hong Kong Polytechnic University in June 2014

Site-selective aromatic C-N bond formation is an attractive approach of fundamental importance in organic synthesis, since arylamines are common motifs in pharmaceutical products and advanced functional materials. Currently, palladium-catalyzed cross coupling of aryl halides with amines (Buchwald-Hartwig amination) remains a widely employed method for arylamines synthesis. However, the reliance of prefunctionalized arenes and the need for strongly basic medium constitute the major drawback of this method. It is envisioned that direct amination of

aryl C-H bonds should improve atom-economy and synthetic efficiency for arylamine synthesis.

Transition metal-mediated nitrenoid insertion to aliphatic C-H bonds has been extensively investigated over the past decades. Reactive metal-nitrene/imido complexes are known to react with sp^3 C-H bonds with a reactivity order of tertiary C-H > secondary C-H >> primary C-H bonds. This reactivity order is reminiscent of the hydrogen atom abstraction mechanism for the C-H bond cleavage. Due to the higher bond dissociation energy of aromatic C-H bonds, nitrenoid insertion to arene C-H bonds is largely unsuccessful.

In this work, palladium(II)-catalyzed aromatic amidation of pivalanilides with ethyl *N*-nosyloxycarbamate (1.2 equiv) and $[Pd(OTs)_2(MeCN)_2]$ (OTs = *p*-toluenesulfonate) (10 mol%) in 1,4-dioxane at 80 °C to afford *ortho*-amidated pivalanilides in up to 87% yields. Excellent functional group tolerance was achieved, for instance, substrates bearing halogens and -OMe as substituents were smoothly transformed to the desired amides under mild conditions. Notably, benzyl and vinyl moiety, which are known to react with nitrenes, were well tolerated.

This Pd-catalyzed approach has been extended successfully to the direct *ortho*-C-H amidation of benzoic acids to give anthranilic acids. Reaction of lithium benzoates with $Pd(OAc)_2$ (10 mol%) and ethyl

N-(2,4,6-trimethylbenzenesulfonyloxy)carbamates gave anthranilic acids in up to 73% yields. Strong dependence on the counter ion of the benzoates was observed; when Li^+ is the counter ion (versus Na^+, K^+ and $N\textit{n}Bu_4^+$), the reaction gave the best results.

A kinetic study on the $[Pd(OTs)_2(MeCN)_2]$-catalyzed amidation of 2,4-dimethylpivalanilide (**1a**) with ethyl *N*-nosyloxycarbamate (**2aNs**) was performed; an experimental rate law: rate = k[**1a**][**2aNs**][**Pd**]^2 was observed. Also, a significant primary kinetic isotope effect (k_H / k_D = 2.8) was observed, implying that the turnover-limiting step involves substantial C-H bond cleavage. The palladacyclic complex $[Pd(C\sim O)(\mu\text{-}OTs)]_2$ (C~O = 2,4-dimethylpivalanilide) (**1aPd**) was prepared and structurally characterized, and a stoichiometric reaction of **1aPd** with **2aNs** (1.2 equiv) in 1,4-dioxane afforded amide **3aa** in 45% yield. A plot of log k_{rel} versus the Hammett substituent σ_{para} constants for the amidation of pivalanilides revealed a linear free energy relationship with a ρ value of -0.53. The small negative ρ value implies that the Pd(II)-mediated C-H bond cleavage should not proceed through an cationic arene intermediate (arenium intermediate).

Apart from C-H amidation reactions, we also achieved the aromatic C-H amination with *N*-chloroamines under Rh(III) catalysis. With $[Cp^*RhCl_2]_2$ (Cp* = 1,2,3,4,5-pentamethylcyclopentadienyl) (2.5 mol%) as catalyst, treating acetophenone *O*-methyloximes with secondary *N*-chloroamines, $AgSbF_6$ (1.5 equiv) and CsOAc

(0.3 equiv) in THF at 40 °C afforded the *N*-arylamines in up to 85% yield. Both electron-donating and electron-withdrawing substituents were well tolerated. A one-pot C-H amination protocol was also developed; this involves *in situ* generation of the *N*-chloroamines by reacting N-H amines with *N*-chlorosuccinimide.

The Rh-catalyzed C-N bond coupling reaction was also extended to primary *N*-chloroamines (ClNHR) as coupling partners. In the literature, primary *N*-chloroamines are poor substrates for electrophilic amination. In this work, when acetophenone *O*-methyloximes reacted with primary *N*-chloroamines in the presence of $[Cp^*RhCl_2]_2$ (5 mol%), $AgSbF_6$ (1.5 equiv) and CsOAc (1.3 equiv) in THF at 40 °C, the C-N coupled products were obtained in up to 92% yield. Regarding the reaction mechanism, an apparent primary kinetic isotope effect (k_H / k_D = 2.1) indicates C-H rhodation being turnover-limiting in the catalysis. Furthermore, the cyclorhodated complex [Cp*Rh(C~N)Cl] (C~N = 2-phenylpyridine) (**11aRh**) was prepared and spectroscopically characterized. The stoichiometric reaction of **11aRh** with *N*-chloroamines afforded the amination products in 52 — 93% yields.

PUBLICATIONS AND CONFERENCE

PUBLICATIONS

Ng, K.-H.; Zhou, Z.; Yu, W.-Y. "$[Cp^*RhCl_2]_2$-catalyzed *ortho*-C-H bond amination of acetophenone *O*-methyloximes with primary *N*-chloroalkylamines: convenient synthesis of *N*-alkyl-2-acylanilines", *Chemical Communications*, **2013**, *49*, 7031.

Ng, K.-H.; Ng, F.-N.; Yu, W.-Y. "A convenient synthesis of anthranilic acids by Pd-catalyzed direct intermolecular *ortho*-C-H amidation of benzoic acids", *Chemical Communications*, **2012**, *48*, 11680.

Ng, K.-H.; Zhou, Z.; Yu, W.-Y. "Rhodium(III)-Catalyzed Intermolecular Direct Amination of Aromatic C-H Bonds with *N*-Chloroamines", *Organic Letters*, **2012**, *14*, 272.

Ng, K.-H.; Chan, A. S. C.; Yu, W.-Y. "Pd-Catalyzed Intermolecular *ortho*-C-H Amidation of Anilides by *N*-Nosyloxycarbamate", *Journal of American Chemical Society*, **2010,** *132*, 12862.

CONFERENCE

Ng, K.-H.; Chan, A. S. C.; Yu, W.-Y. "Pd-Catalyzed Intermolecular *ortho*-C-H Amidation of Anilides by *N*-Nosyloxycarbamate", 17th European Symposium on Organic Chemistry, Crete, Greece, 10th-15th July 2011.

SYMPOSIUMS

Ng, K.-H.; Zhou, Z.; Yu, W.-Y. "Rhodium(III)-Catalyzed Intermolecular Direct Aromatic C-H Bonds Amination Using *N*-Chloroamines", The 19th Symposium on Chemistry Postgraduate Research in Hong Kong, 14th April 2012.

Ng, K.-H.; Chan, A. S. C.; Yu, W.-Y. "Pd-Catalyzed Intermolecular *ortho*-C-H Amidation of Anilides by *N*-Nosyloxycarbamate", The 18th Symposium on Chemistry Postgraduate Research in Hong Kong, 30th April 2011.

ACKNOWLEDGEMENTS

I would like to take this opportunity to thank all those people for their contributions and support on the projects.

First, I would like to express my deepest gratitude to my chief supervisor Dr. Michael Wing-Yiu Yu for his professional and insightful advice and guidance on both practical and theoretical aspects of organometallic chemistry during the course of my study. I also appreciate his patience for taking in-depth discussions with me in the investigation. I am grateful to have an opportunity to carry out my postgraduate study under Yu's supervision and it was truly an unforgettable experience working in Yu's research group.

I would also like to thank my co-supervisor, Prof. Albert Sun-Chi Chan for his advice and support. He has been a role model of being successful to me.

Special thank should be granted to Dr. Yuk-Tai Tsoi for his constant guidance and support in my research.

Sincere thanks must be given to Dr. Hong-Yee Chueng, Dr. Wing-Nga Sit, Dr Jun Wang, Dr. Wai-Wing Chan, Mr. Hon-Wah Lam, Mr. Chun-Wo Chan, Mr. Fo-Ling Ng and others in PolyU Y 1307 for their countless support.

Furthermore, the technical support from the staff and technicians in the

Department of Applied Biology and Chemical Technology is highly appreciated. I would like to tank Prof. Zhonyuan Zhou for his assistance in X-ray crystallography studies. Also, I would like to thank Dr. Pui-Kin So for his support on the operation of ESI-HRMS and Mr. Wing-Kong Kwan for his technical advice on NMR issues.

More importantly, I would like to express my love and apology to my family: My father Mr. Sai-Kit Ng, my mother Mrs. Pui-Ling Lau and my sister Miss Ka-Ying Ng. Thank you for their encouragement and support in housework, so that I can focus on my research more. Sorry for my occasionally bad attitude when I felt stuck in my works.

I would like to acknowledge the financial support from the State Key Laboratory for Chirosciences, the Hong Kong Research Grants Council and the Hong Kong Polytechnic University for my postgraduate studentship and the travel grants to conference participation in the 17th European Symposium on Organic Chemistry, which was held in Crete, Greece in 10th-15th July 2011.

TABLE OF CONTENTS

ABBREVIATIONS AND SYMBOLS

Ac	Acetyl
Ad	1-Adamantyl
AcOH	Acetic acid
Ar	Aryl
Å	Anstom
BDE	Bond dissociation energy
Bn	Benzoyl
Boc	*tert*-Butoxy carbonyl
BQ	Benzoquinolone
Bz	Benzyl
CO	Carbon monoxide
cod	1,5-Cyclooctadiene
coe	Cyclooctene
Cp	Cyclopentadienyl
Cp*	Pentamethylcyclopentadienyl
CMD	Concerted metalation deprotonation
dba	Dibenzylideneacetone

DCE	1,2-Dichloroethane
DCM	Dichloromethane
DMA	*N*,*N*-Dimethylacetamide
DMF	*N*,*N*-Dimethylformamide
DMSO	Dimethyl sulfoxide
EtOAc	Ethyl acetate
ESI	Electrospray-ionization
GC	Gas chromatography
GC-MS	Gas chromatography—mass spectrometry
IR	Infrared spectrometry
KIE	Kinetic isotope effect
MeCN	Acetonitrile
MO	Molecular orbital
NEt_3	Triethylamine
NMR	Nuclear magnetic resonance
phen	1,10-Phenanthroline
Piv	2,2,2-Trimethylacetyl
PPh_3	Triphenylphosphine
OAc	Acetate

OPiv	2,2,2-Trimethylacetate
OTf	Trifluoromethanesulfonate
OTs	*p*-Toluenesulfonate
ONs	*p*-Nitrobenzenesulfonate
rt	Room temperature
THF	Tetrahydrofuran
TLC	Thin layer chromatography
TPP	Tetraphenylporphyrin
TPFPP	Tetrakis(pentafluorophenyl)porphyrin
TFA	Trifuoroacetic acid
s	Singlet
d	Doublet
t	Triplet
q	Quartet
m	Multiplet
δ	Chemical shift in NMR
ρ	rho value in Hammett plot

LIST OF FIGURES

Appendices

LIST OF TABLES

Appendices

LIST OF SCHEMES

Chapter 1

Introduction

1.1 General Background

Construction of aromatic C-N bond is a subject that has been extensively investigated.[1a,b] Indeed, arylamines (anilines) are versatile scaffolds that are frequently found in polymers, pharmaceutical agents and natural products. For example, in materials science, polyaniline (PANI) is a class electrically conductive polymers that are widely used in bio-sensors and light-emitting diodes.[2] Arylamines are also found in many pharmaceutical products such as paracetamol and Zyvox, which are painkiller and anti-bacterial agent, respectively (Figure 1.1).[3]

Figure 1.1 Examples of Drug and Material Containing Arylamine as Scaffold

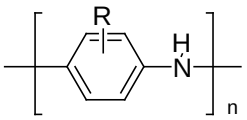

Polyaniline (PANI)

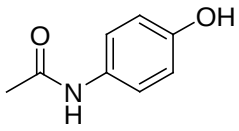

Paracetamol

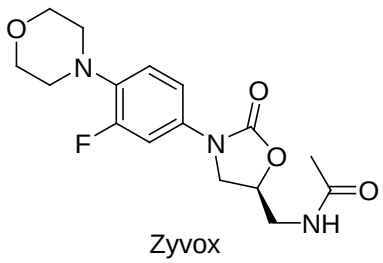

Zyvox

Conventional methods such as electrophilic nitration—nitro-group reduction, S_NAr type nucleophilic substitution and benzyne generation of aryl haildes have long been employed to prepare anilines (Scheme 1.1).[1a] However, these methods suffer from poor regio- and chemo-selectivity and they require harsh reaction conditions (e.g. high temperature, excess of reagents). In the past two decades, Buchwald-Hartwig type amination / amidation of aryl (pseudo)halides has emerged as a powerful approach to synthesize a large variety of arylamines.[4] This method utilizes Pd(0)-phosphine as catalyst to mediate the coupling reaction of aryl halides or aryl triflates with amines or amides, and a generally accepted mechanism is depicted in Scheme 1.2. Despite significant advances in the Pd-catalysis for arylamine synthesis, the Buchwald-Hartwig amination requires pre-functionalized substrates, and the functional group tolerance for substrates bearing multiple halogens is usually poor.

To improve the atom economy for the synthesis of arylamines, direct amination / amidation of unactivated aromatic carbon-hydrogen (C-H) bonds with good regio- and chemo-selectivity should be highly desirable.

Scheme 1.1 Three Conventional Methods for Arylamine Synthesis

(1) electrophilic nitration–nitro group reduction

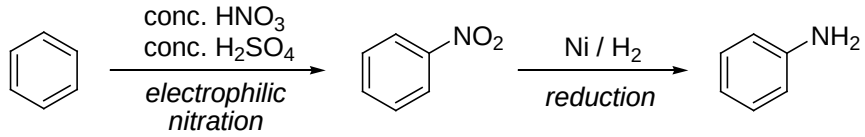

(2) S_NAr type nucleophilic substitution

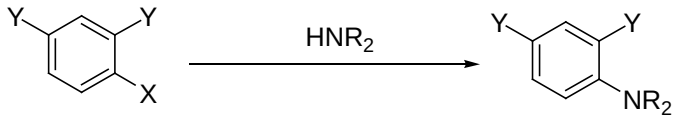

X= F, Cl, Br, I
Y = NO_2, CO_2R, SO_3R

(3) benzyne generation

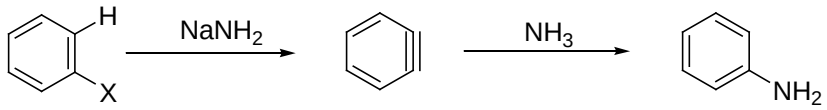

X= F, Cl, Br

benzyne

Scheme 1.2 The Generally Accepted Mechanism for Buchwald-Hartwig Amination

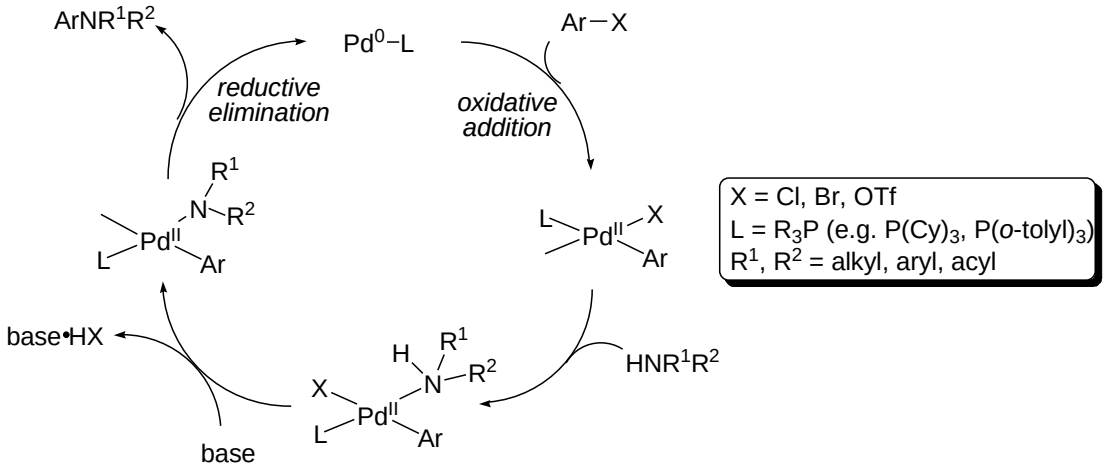

X = Cl, Br, OTf
L = R_3P (e.g. $P(Cy)_3$, $P(o\text{-tolyl})_3$)
R^1, R^2 = alkyl, aryl, acyl

1.2 Challenges and Approaches for Transition-Metal Mediated C-H Bond Activation

1.2.1 Challenges for C-H Activation

Direct C-H bond functionalization is the most straightforward approach to cross coupling reactions. However, the apparent conceptual simplicity comes with various challenging issues. First of all, C-H bonds are chemically inert because of high bond dissociation energy (BDE) and low acidity of the "proton". For instance, BDE values of the C-H bonds in benzene and methane are 112.9 and 104.9 kcal mol^{-1} respectively. Compared to that of C-X bonds (e.g. BDE for C-Cl in chlorobenzene = 97.1 kcal mol^{-1}; for C-Br in bromobenzene = 84.0 kcal mol^{-1}) the strong C-H bond constitutes a major kinetic barrier of direct C-H bond cross-coupling reactions (Table 1.1).[5b] It should be noted that an aromatic C-H bond in benzene is highest among other C-H bonds listed in Table 1.1; activation of aromatic C-H activation is therefore more difficult. Having a range of pK_a values of from 45 to 60, typical C-H bonds are non-acidic and heterolytic cleavage of C-H bonds (deprotonation) by strong bases is not viable.[5a]

Table 1.1 Bond Dissociation Enthalpies Calculated Based on Radical Heats of Formation

Bond type	BDE (kcal mol^{-1})	Bond type	BDE (kcal mol^{-1})
C_6H_5—I	67.0	$(CH_3)_3C$—H	96.5
C_6H_5—Br	84.0	CH_3CH_2—H	101.1
C_6H_5—Cl	97.1	H_3C—H	104.9
C_6H_5—OMe	101.0	C_6H_5—H	112.9

The control of selectivities in C-H bond activation is highly challenging. For example, activation of a strong C-H bond in the presence of other weaker bonds with lower BDE (i.e. carbon-halogen bonds) would be difficult. When different types of C-H bond are present, non-selective functionalization (e.g. radical reactions) would give a mixture of products, and this would render the coupling reactions inefficient for synthesizing the target molecules. Similarly, the regioselectivity of aromatic C-H bond functionalization is also a concern.

1.2.2 Approaches for Transition-Metal Mediated C-H Functionalization

To date, there are two major approaches for C-H bond activation / functionalization: (1) the outer-sphere and (2) the inner-sphere approaches (Scheme 1.3).[6b]

Scheme 1.3 Two General Approaches for C-H Activation / Functionalization

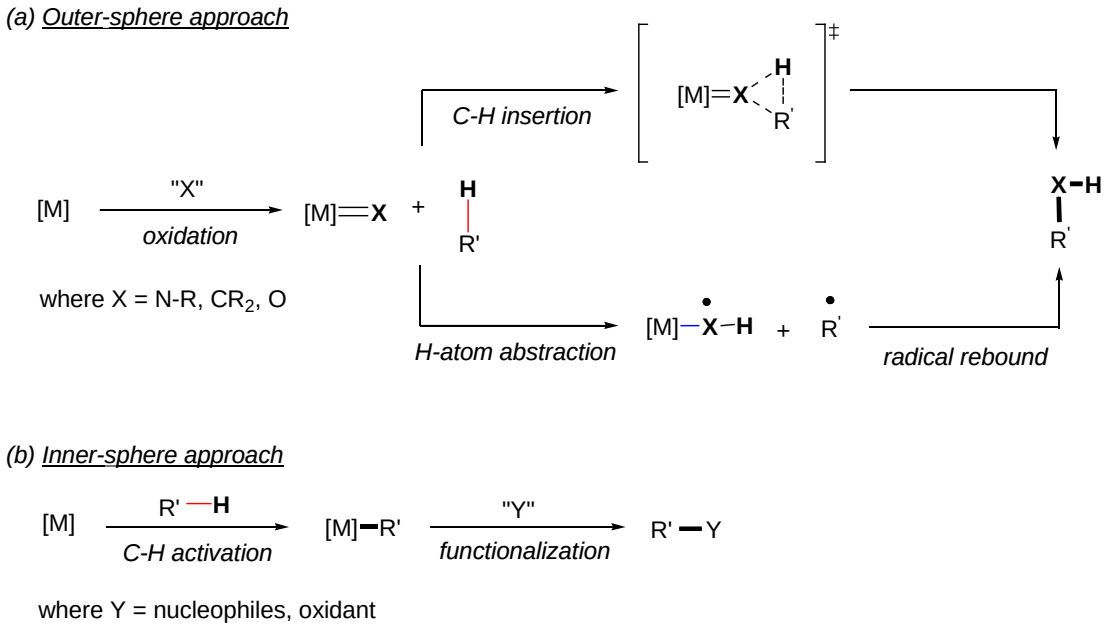

For the outer-sphere approach, the transition metal would first be oxidized to form the reactive "[M]=X" intermediate where X can be O (oxo), CR_2 (carbenoid) or NR (nitrenoid). The carbon-hydrogen bond can react with the reactive "[M]=X" intermediate *via* either concerted C-H insertion or a stepwise hydrogen atom abstraction—radical rebound sequence to afford the formal C-H functionalized products.

Unlike the outer-sphere approach, the inner-sphere involves the initial C-H bond cleavage by the metal catalyst to form an organometallic complex "[M]-R" (Scheme 1.3b). Several mechanisms for the C-H bond metalation have been discussed in the literature,[7, 8, 9b, 10c,d] and they are: (1) electrophilic metalation; (2) oxidative addition;

(3) agostic C-H complex formation followed by facile deprotonation and (4) concerted metalation deprotonation (CMD). The metalated complex could react with either nucleophiles or electrophiles to yield the functionalized products.

1.3 Transition Metal-Mediated C-H Amidation *via* Outer-sphere Nitrenoid Insertion Mechanism

As mentioned in Scheme 1.3, the C-H bond activation *via* the outer-sphere pathway would involve the initial formation of a reactive "[M]=X" complex. For C-H bond amidation reactions, the metal-nitrenoid intermediate (i.e., "[M]=NR") has been proposed to be generated by the reaction of a metal catalysts with nitrene precursors (e.g. PhINTs, chloramine-T).[11]

1.3.1 Structure of Nitrenes

Nitrene is a monovalent nitrogen having six valence electrons. Analogous to carbenes, nitrenes can exist in either singlet state or triplet state. For singlet nitrenes, the non-bonding electrons would pair up forming two lone pairs of electrons, and each pair occupies an sp^2-hybrid orbital. For the triplet state, two non-bonding electrons

with opposite spin pair up occupying an sp^2-hybrid orbital, and the other two electrons having the same spin fill up an sp^2-hybrid orbital and a p orbital (Figure 1.2).[1c, 11f]

Figure 1.2 Singlet and Triplet States of Nitrene

Singlet state Triplet state

1.3.2 Methods for Nitrene Generation

Scheme 1.4 depicts several reported method for nitrene generation. Similar to carbene generation from diazo compounds, organic azides can decompose *via* thermolysis or photolysis along with extrusion of nitrogen gas to form free nitrenes.[1c] Amines or amides bearing an N-X bond (X = Br, Cl, OMe, OCOR, OSO_2Ar) were known to generate nitrene *via* a deprotonation — α-elimination sequence. It is noteworthy that free alkyl-, aryl- and acyl-nitrenes are very reactive species which would rapidly undergo intramolecular rearrangement (Scheme 1.5).

In recent years, transition metal-mediated nitrene generation using nitrene precursors such as hypervalent iodine reagents (i.e. $PhINSO_2Ar$) and chloramine-T

has been thoroughly studied,[11a, c] and the associated C-H bond amidation reactions will be discussed in the following sections.

Scheme 1.4 Methods for Nitrene Generation

(1) decomposition of organic azide

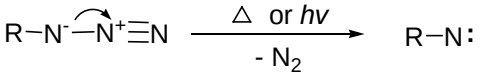

R = alkyl, aryl, acyl, CO_2R, SO_2Ar

(2) deprotonation–α-elimination of N-X amide / amine

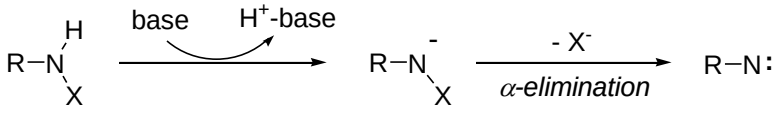

R = alkyl, aryl, acyl, CO_2R, SO_2Ar
X = Br, Cl, OMe, OCOR, OSO_2Ar

(3) transition metal-mediated nitrene formation

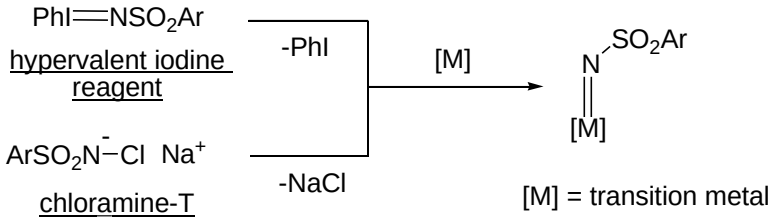

[M] = transition metal

Scheme 1.5 Rearrangement Reactions of Alkyl-, Aryl- and Acyl-nitrenes

Alkyl-nitrene rearrangement

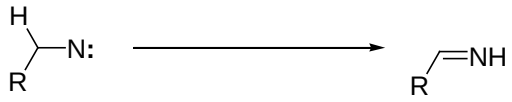

R = alkyl, H

Aryl-nitrene rearrangement

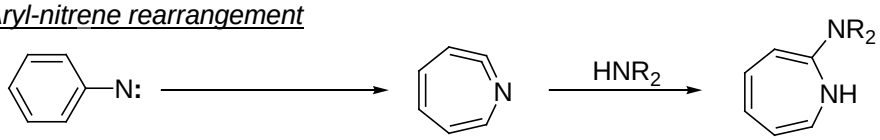

Acyl-nitrene rearrangement

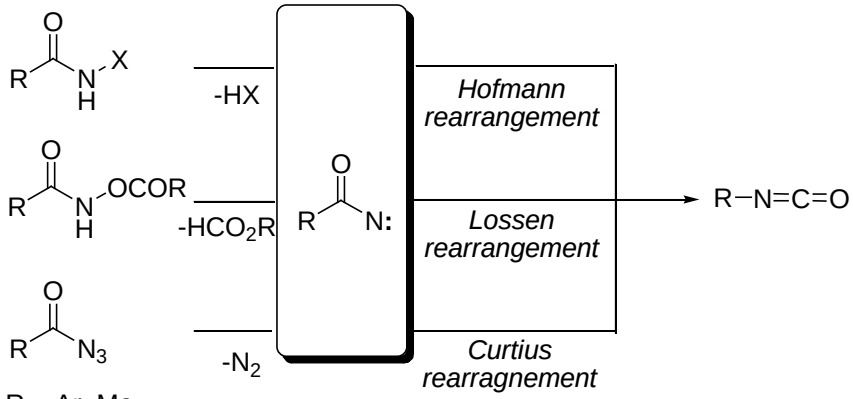

R = Ar, Me

1.3.3 Manganese-Catalyzed Nitrenoid C-H Insertions

Metalloporphyrin-catalyzed nitrene transfer reaction to C-H bonds was first discovered by Breslow and co-workers in 1982. Inspired by the cytochrome-P450 enzymatic activity on oxygen atom (oxene) transfer, it was anticipated that the analogous nitrene transfer reaction to C-H bonds should be possible. With Mn(III)-porphyrin or Fe(III)-porphyrin complexes as catalysts, it was found that the reaction of cyclohexane with PhINTs (125 mM) and [Mn^{III}(TPP)Cl] (TPP = dianionic tetraphenylporphyrin; 2.5 mM) in dichloromethane at room temperature for 4.5 h afforded the corresponding *N*-cyclohexyltosylamide in approximately 6% yield (turnover number = ~3; Scheme 1.6). [12b]

Scheme 1.6 [Mn^{III}(TPP)Cl]-Mediated Tosylamidation of Cyclohexane

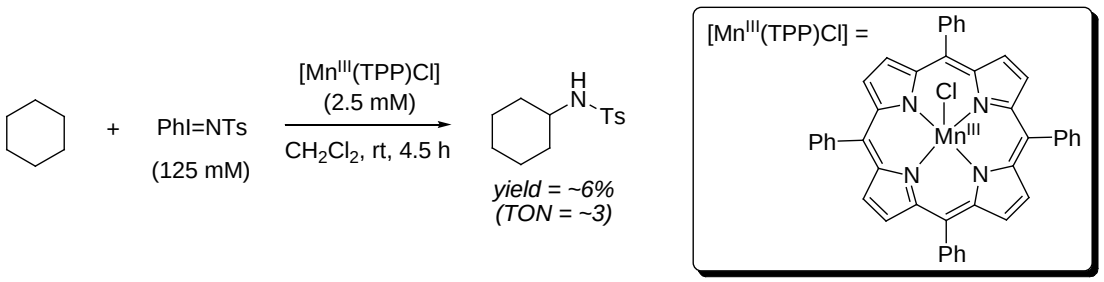

The more efficient Mn(III)-porphyrin-catalyzed C-H nitrenoid insertion reaction was later reported by the research group of Mansuy. In their study, allyllic C-H bond

from cyclohexene was successfully amided with PhINTs (50 mM) as nitrene precursor under [Mn^{III}(TPP)(ClO_4)] (2.5 mM) catalysis to give 3-tosylamidocyclohexene in 40% yield based on the PhINTs (Scheme 1.7**)**.[13d] Notably, the amidation of *trans*-hex-2-ene in their study gave a mixture of allylic tosylamides (Scheme 1.8). To account for this interesting result, the authors explained that the nitrenoid insertion reaction should proceed through a sequential hydrogen atom abstraction—radical delocalization—radical rebound pathway.

Scheme 1.7 **[**Mn^{III}(TPP)(ClO_4)]-Catalyzed Allylic C-H Tosylamination of Cyclohexene

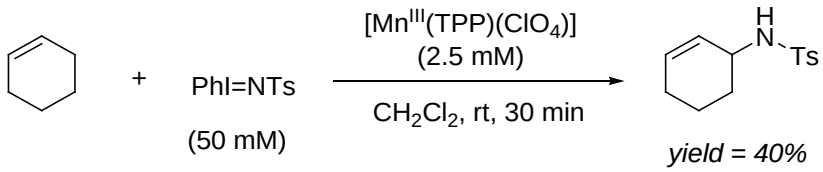

Scheme 1.8 $Mn^{III}(TPP)(ClO_4)$-Catalyzed Allylic C-H Tosylamination of *tran*-Hex-2-ene and the Proposed Mechansim

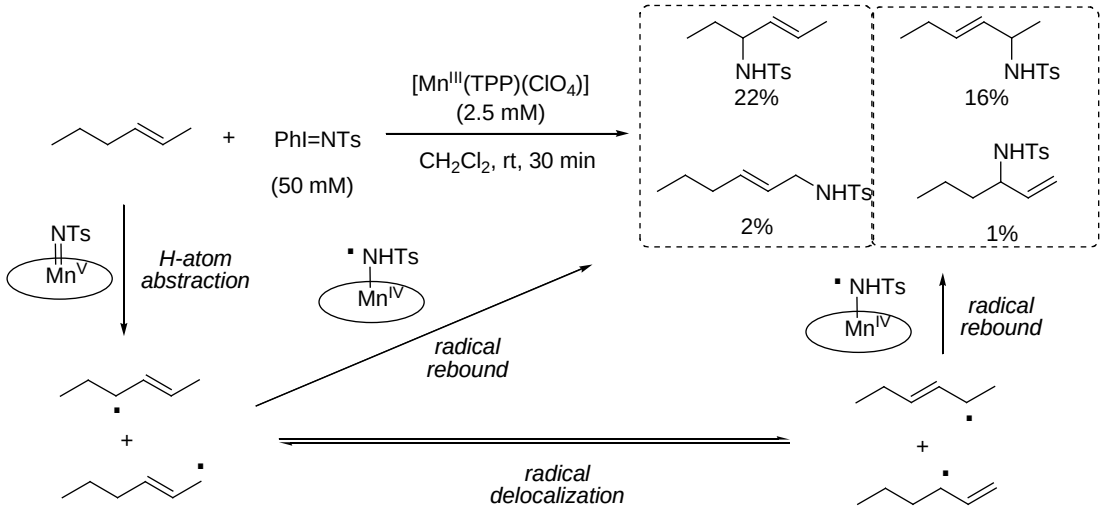

Despite the apparent success in Mn(III)-porphyrin catalyzed allylic C-H amidation, the catalyst efficiency (i.e., catalyst turnover number) and the scope of substrate remained quite limited. To tackle these issues, Che and co-workers found that by modifying the electronic property of the porphyrin ligand, the Mn(III)-porphyrin catalyst efficiency can be significantly improved. For example, $[Mn^{III}(TPFPP)Cl]$ (TPFPP = dianionic *meso*-tetrakis(pentafluorophenyl)porphyrin) was found to be a highly effective catalyst for the nitrenoid insertion of allylic, benzylic and tertiary C-H bonds to give amidation products in up to 92% yield (Scheme 1.9).[13c] Notably, apart from using PhINTs as nitrene precursor, the combination of $PhI(OAc)_2$ and amides such as tosylamine, nosylamide and methylsulfonylamide (1:1) was also successfully employed for the nitrenoid insetion

reactions in their study.

Scheme 1.9 [Mn^{III}(TPFPP)Cl]-Catalyzed Allyic, Benzylic and Tertiary C-H Bond Amidation

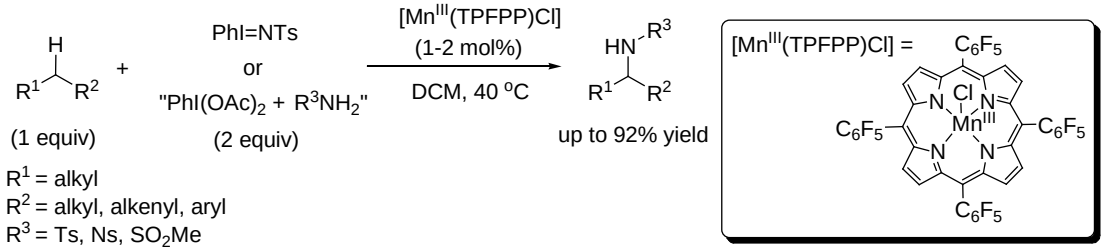

Apart from metalloporphyrins, manganese complexes of salens were also reported to mediate catalytic nitrenoid C-H insertion. Katsuki and co-workers have examined a series of substituted salen ligands for the [Mn^{III}(salen)(PF_6)]-catalyzed nitrenoid insertion reaction of benzylic and allylic C-H bonds, and it was found that the bromo-substituted salen gave the best results (Scheme 1.10).[13b]

Scheme 1.10 [Mn^{III}(salen)(PF_6)]-Catalyzed Allyic and Benzylic C-H Bond Amidation

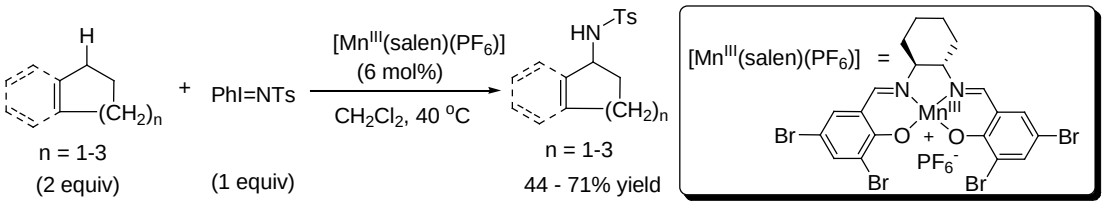

1.3.4 Charaterization of Reactive Imidoruthenium(VI) Complexes as Model System for Catalytic C-H Amidation

Although metal-imido intermediate had been proposed to be the active intermediate for both nitrenoid C-H insertion and aziridination, the metal-imido complex was never isolated or spectroscopically characterized. Ruthenium(II)-porpyrins, similar to manganese(III)-porphyrins, were also known to mediate nitrenoid C-H insertion reactions.[13a,c,14b,c] More importantly, Ru(II)-porphyrin was the only complex that can form stable (at -20 °C for several days) metal-imido species for structural characterization. Yet, the metal-imido complexes are capable of mediating nitrenoid transfer reactions.[15] As reported by Che and co-workers, treating $[Ru^{II}(por)(CO)(MeOH)]$ (por = dianoinic porphyrin; 0.2 mmol) with PhINTs (0.6 mmol) in dichloromethane at room temperature for 5 min, the $[Ru^{VI}(por)(NTs)_2]$ was isolated in about 60% yield (Scheme 1.11).[14d]

Scheme 1.11 Synthesis of Isolable $[Ru^{VI}(por)(NTs)_2]$ Complexes

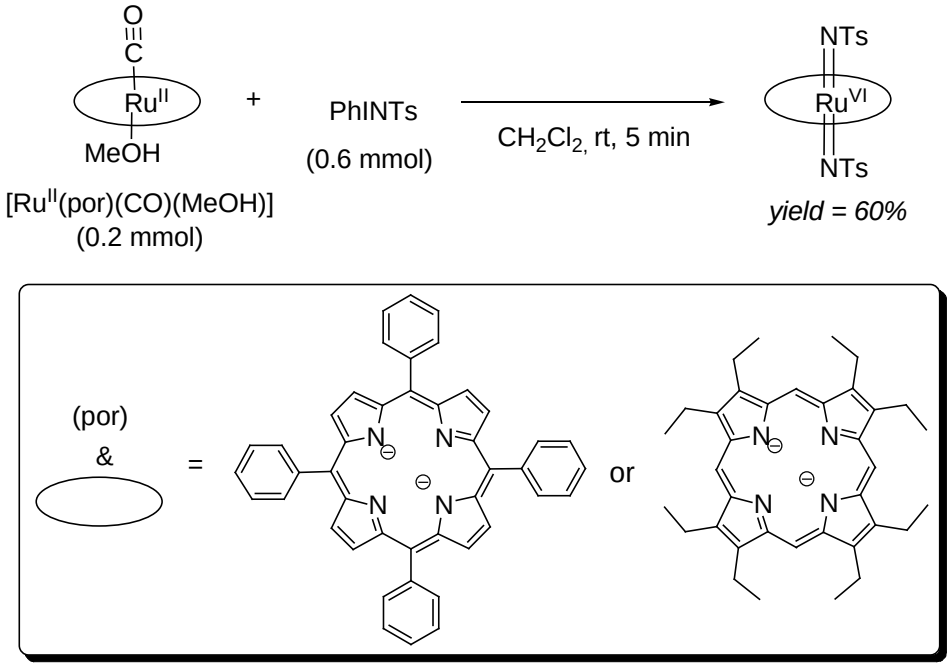

The follow-up studies by Che and co-workers revealed that the $[Ru^{VI}(por)(NTs)_2]$ complexes were capable of mediating nitrenoid insertion to benzylic, allylic and aliphatic C-H bonds (Table 1.2).[14b] Notably, the amidations of methyl C-H bonds on toluene and aliphatic C-H bonds on cyclohexane were rather unfavorable, and only ~10% yields of the corresponding tosylamides were produced. The tertiary C-H bond on adamentane, the allylic C-H bond on cyclohexene and the α-C-H bonds on ethylbenzene and cumene were amidated in good yields. These results collaboratively implied that the $[Ru^{II}(por)(NTs)_2]$-mediated preferentially reacted with weaker C-H bonds (i.e., benzylic C-H BDE = 89.7 kcal mol^{-1}, allylic C-H BDE = 88.8 kcal mol^{-1}). In addition, the tosylamidations of ethylbenzene and d_{10}-ethylbenzene revealed a

large primary kinetic isotope effect (k_H / k_D = 11). This suggests a head-on hydrogen abstraction mechanism in the C-H bond cleavage step followed by a carboradical rebound to give the amidation product (Scheme 1.12**)**.

Table 1.2 [Ru^{VI}(por)$(NTs)_2$]-Mediated Nitrenoid C-H Insertion[a]

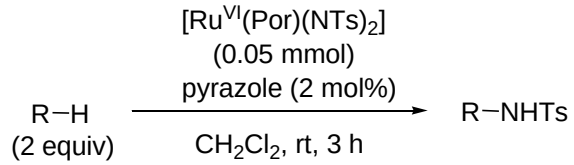

R−H	R−NHTs	yield%
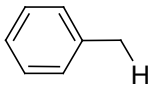	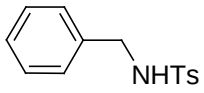	11
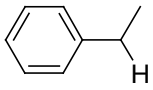	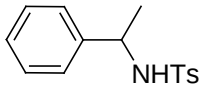	80
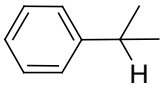	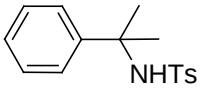	77
	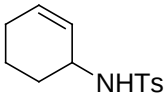	88
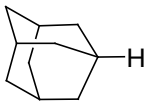	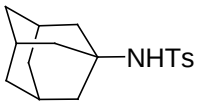	60
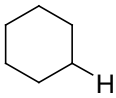	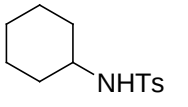	10

[a]por = dianionic octethylporphyrin

Scheme 1.12 Reaction Mechanism for $[Ru^{VI}(por)(NTs)_2]$-Mediated C-H Nitrenoid Insertion

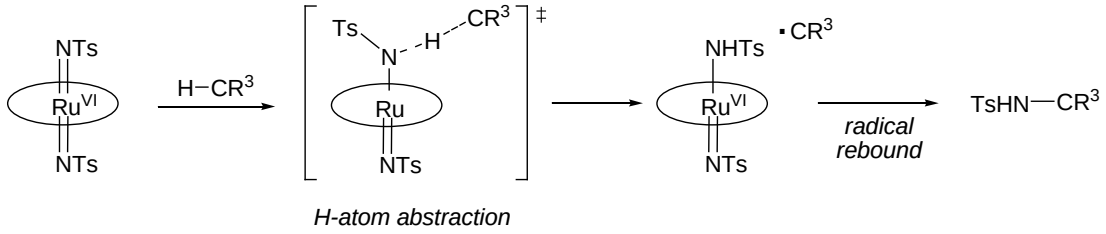

The Ru-catalyzed nitrenoid C-H insertion reaction typically requires a rigid and square-planar ligand set (i.e., porphyrin, salen) to support the formation of a high oxidation state metal-imido intermediate, and example of using a non-porphyrin ligated ruthenium complex was rare. Interestingly, ruthenium complexes such as $[Ru^{III}(Me_3tacn)(CF_3CO_2)_3]$ and *cis*-$[Ru^{II}(6,6'\text{-}Cl_2bpy)_2Cl_2]$ have been developed for catalytic benzylic C-H amidation with PhINTs as reagent **(**Scheme 1.13).[14a,c] In their studies, the "amides + $PhI(OAc)_2$" protocol can also be employed for the amidation reaction. Surprisingly, benzamides which are susceptible to Hoffmann-Lossen rearrangement under oxidizing conditions, were also successfully coupled to the benzylic C-H bonds when the "amide + $PhI(OAc)_2$" protocol was employed.

Scheme 1.13 $Ru^{III}(Me_3tacn)(CF_3CO_2)_3$ and *cis*-$[Ru^{II}(6,6'\text{-}Cl_2bpy)_2Cl_2]$ Catalyzed Benzylic C-H Amidation

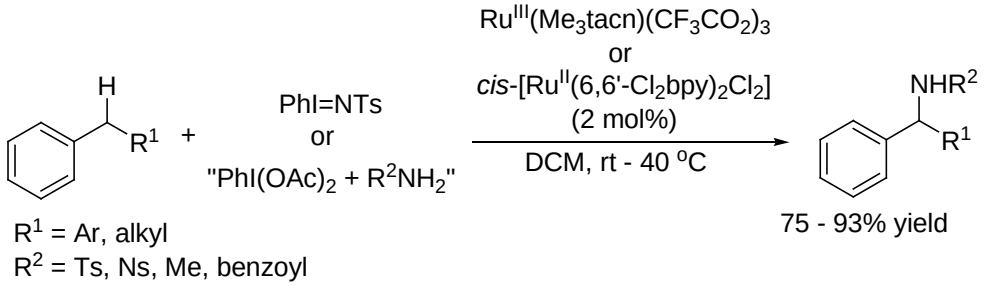

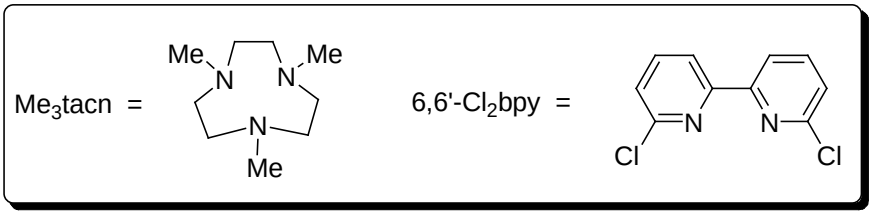

1.3.5 Copper-Catalyzed Nitrenoid C-H Insertions

In 1998, Taylor and co-workers reported the first example of Cu-catalyzed nitrenoid insertion into benzylic C-H bonds with chloramine-T as nitrene precursor. With the use of catalytic amounts of CuOTf (5 mol%) and *N*-(2-pyridinylmethylene)-1-pentanamine (6 mol%) as ligand, the benzylic C-H bonds of cyclohexene and tetralin were successfully amidated, despite moderate yields (Scheme 1.14).[16b] Interestingly, they later found that CuCl (10 mol%) alone in acetonitrile is also an effective catalyst for the amidations of the α-C-H bonds of cyclic ethers and benzylic C-H bonds with chloramine-T as reagent (Scheme 1.15**)**.[16a] It is noteworthy that although the method only produced moderate yields of products, both CuCl and chloramine-T are inexpensive reagents and no special precautions (e.g. dehydration of reagents, N_2 atmosphere) were needed for the amidation.

Scheme 1.14 First Example of Cu(I)-Catalyzed Allylic and Benzylic C-H Bond Amidation with Chloramine-T as Nitrene Precursor

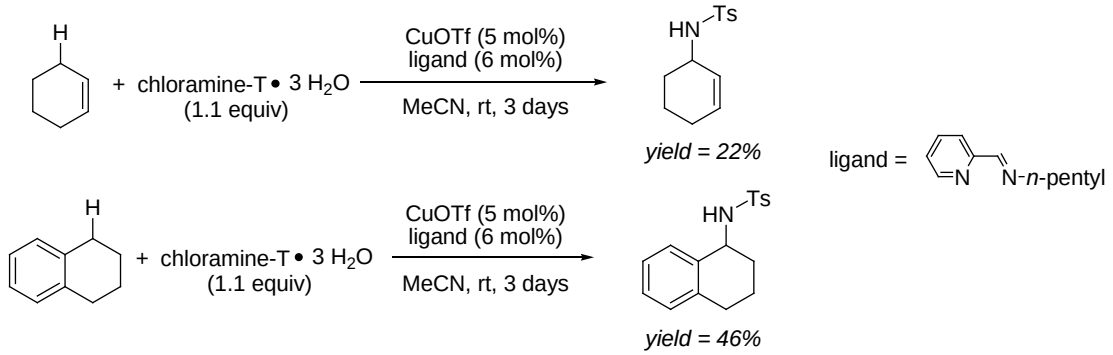

Scheme 1.15 CuCl-Catalyzed Amidation of Benzylic C-H Bonds and α-C-H Bonds of Cyclic Ethers with Chloramine-T in Acetonitrile

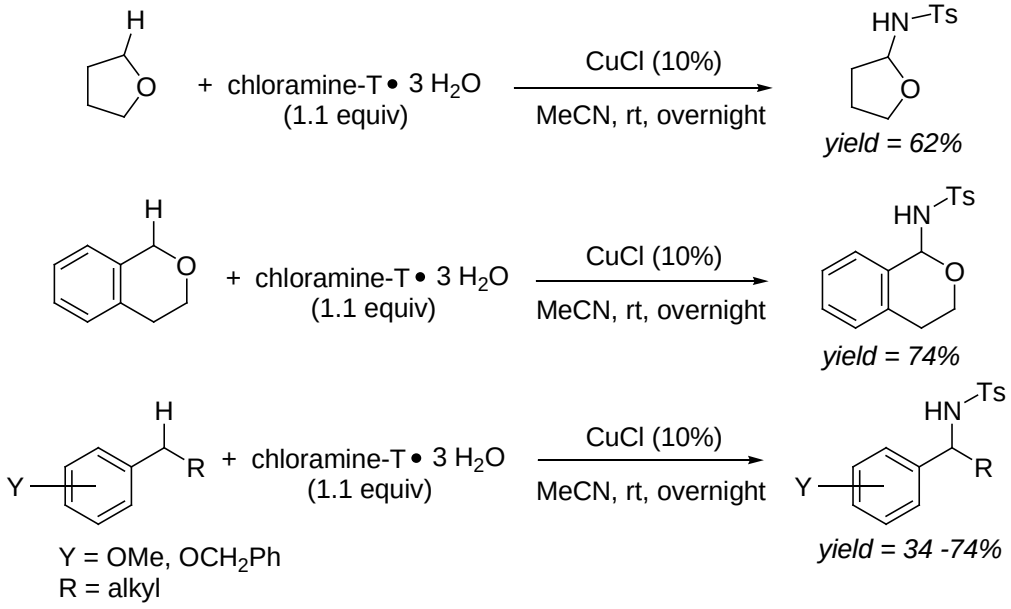

More recently, [Tp^{Br3}Cu(MeCN)] (Tp^{Br3} = trsi(3,4,5-tribromopyrazolyl)borate) was found to be a highly effective catalyst in nitrenoid C-H insertion reactions by the research group of Pérez (Scheme 1.16).[17] With [Tp^{Br3}Cu(MeCN)] (5 mol%) as

catalyst and *N*-(*p*-tolylsulfonyl)iminophenyliodinane (PhINTs) as nitrene precursor, the aliphatic C-H bond on cyclohexane (neat) was inserted at room temperature to give *N*-cyclohexyltosylamide in 65% yield. Apart from aliphatic C-H amidation, the strong aromatic C-H bonds in benzene can also be amidated to afford *N*-phenyltosylamide in good yield. However, when toluene was used as solvent, the amidation exclusively occurred on the methyl group (yield = 95%) without aromatic C-H bond nitrenoid insertion. Interestingly, the reaction with 4-methylethylbenzene gave a variety of products, in which the benzylic C-H bond was predominantly amidated (yield = 58%) and the amidations of the benzylic methyl group (yield = 19%) and *para*-methyl group (yield = 9%) were minor. Apparently, the nitrenoid insertion follows the order of benzylic C-H > methyl C-H > aromatic C-H, and this parallels the order of the increasing C-H bond dissociation energy (BDE). Although the selectivity of [Tp^{Br3}Cu(MeCN)]-catalyzed C-H amidation was seemingly only controlled by the C-H BDE, this study is still a valuable example that demonstrated the possibility of the aromatic C-H amidation *via* the outer-sphere mechanism, which is rare in the literature.[11a,b,c]

Scheme 1.16 [Tp^{Br3}Cu(MeCN)]-Catalyzed Aliphatic and Aromatic C-H Amidation with PhINTs as Reagent

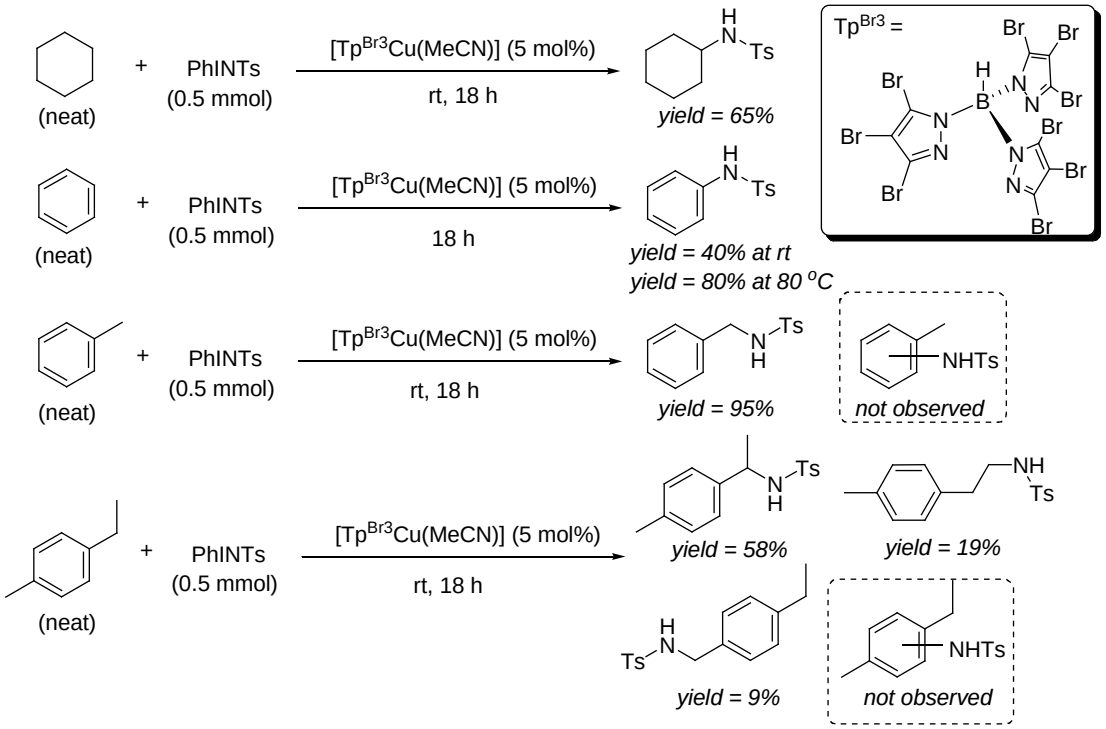

1.3.6 Rhodium-Catalyzed C-H Nitrenoid C-H Insertions

Dirhodium(II, II) carboxylate-catalyzed nitrenoid C-H insertion reaction has been extensively investigated in recent years.[11a,b, 18a] Structurally different from other catalysts, dirhodium(II, II) carboxylate ($[Rh_2(CO_2R)_4]$) is a paddlewheel-like complex, in which the two rhodium(II) metal centres were connected by four bridging μ-carboxylates and a Rh-Rh metal bond (Figure 1.3).

Figure 1.3 Paddlewheel-like Structure of $[Rh_2(CO_2R)_4]$

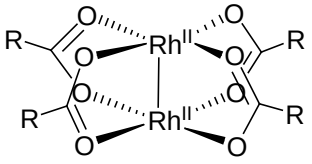

This unique paddlewheel structure of $[Rh_2(CO_2R)_4]$ is key to catalyst robustness for carbene and nitrene transfer reactions. In a mechanistic study on $[Rh_2(CO_2R)_4]$-mediated carbenoid transfer reaction, Nakamura and co-workers suggested that only one of the rhodium centre functions as a carbene binding site, and the other rhodium centre serves as an "auxiliary ligand" that provides an electron sink to enhance the electrophilicity of the carbene function and facilitate the Rh-C bond cleavage on the completion of functionalization.[19]

The pioneering study on [$Rh_2(CO_2R)$]-catalyzed C-H nitrenoid insertion reaction was reported by Breslow and co-workers in 1983. In their study, it was found that [$Rh_2(OAc)_4$] (5 mol%) was found to efficiently catalyze the intramolecular nitrenoid C-H insertion of the hypervalent iodine(III) reagent derivative, which was synthesized from 2,5-diisopropylbenzenesulfonamide. The corresponding amide was produced in 86% yield (Scheme 1.17).[12a]

Scheme 1.17 An Early Example of [$Rh_2(OAc)_4$]-Catalyzed Intramolecular C-H Amidation

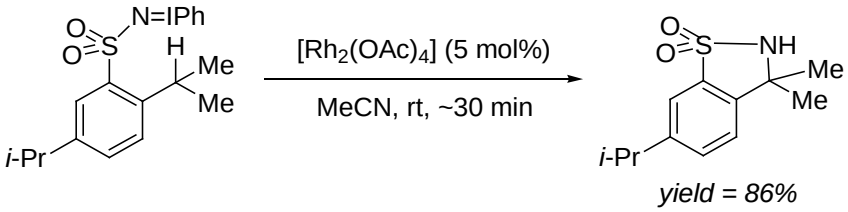

Due to limitation in the preparation of hypervalent iminoiodinane reagents, the scope of metal-mediated nitrenoid C-H insertion reaction was usually very limited.[20] Du Bois and co-workers later found that the iminoiodinane reagents can be generated *in situ* by mixing the desired amides with $PhI(OAc)_2$,. Thus, the research group of Du Bois achieved an initial success in [$Rh_2(OAc)_4$]-catalyzed intramolecular cyclization of carbamate[18f] and sulfamate[18e] esters (Scheme 1.18).

Scheme 1.18 $[Rh_2(OAc)_4]$-Catalyzed Intramolecular Cyclization of Carbamate and Sulfamate Esters Using *in situ* Iminoiodinane Generation Method

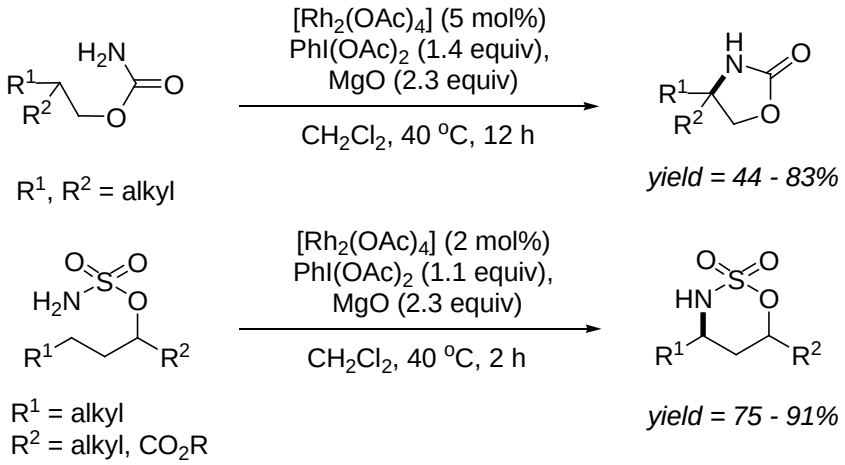

More importantly, Du Bois and co-workers have discovered that $[Rh_2(esp)_2]$ was an exceptionally efficient catalyst for the intramolecular amidation.[18a-d] For example, the intramolecular insertion reaction of sulfamate ester at very low catalyst loading ($[Rh_2(CO_2tBu)_4]$; 0.15 mol%) typically gave poor yield of the cyclization product, but when $[Rh_2(esp)_4]$ (0.15 mol%) was employed, significant improvement in product yield was observed (Scheme 1.19).[18d] Apart from higher catalyst efficiency, the use of $[Rh_2(esp)_2]$ has also further extended the intramolecular amidation substrate scope to ureas, [18c] guanidines[18c] and sulfamides[18b] (Scheme 1.20).

Scheme 1.19 Catalyst Performance Comparison on Sulfamate Ester Cyclization ([$Rh_2(CO_2tBu)_4$] versus [$Rh_2(esp)_2$])

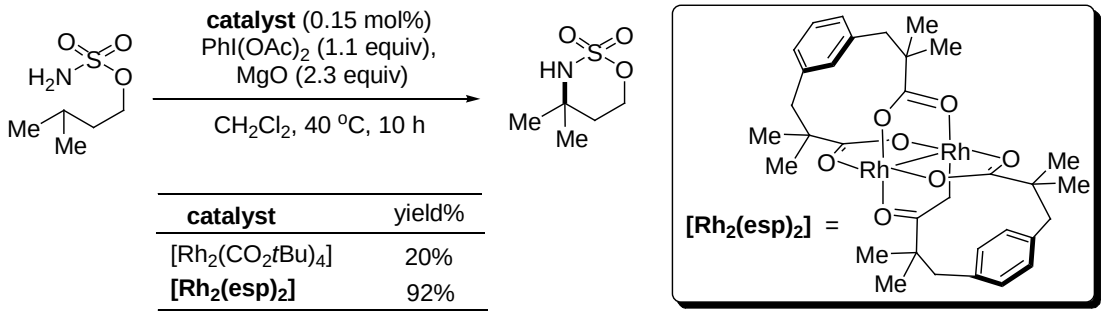

catalyst	yield%
[$Rh_2(CO_2tBu)_4$]	20%
[$Rh_2(esp)_2$]	92%

Scheme 1.20 [$Rh_2(esp)_2$]-Catalyzed Intramolecular C-H Amidation with Urea, Guanidine and Sulfamide as Substrates

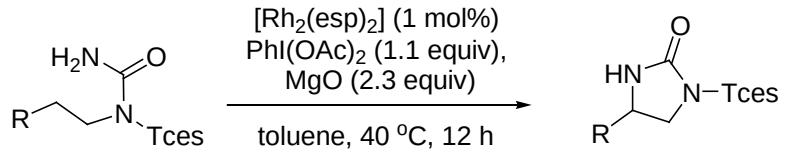

R = alkyl, aryl
Tces = 2,2,2-trichloroethoxysulfonyl

yield =31 - 93%

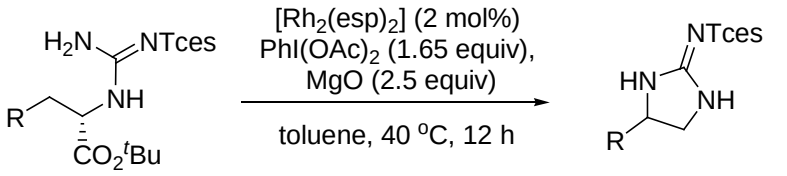

R = alkyl, aryl
Tces = 2,2,2-trichloroethoxysulfonyl

yield =30 - 91%

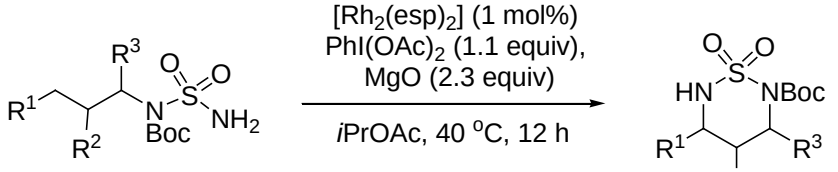

R^1, R^3 = alkyl, aryl, CO_2R
R^2 = H, phthalimide

yield = 73 - 99%

Apart from the use of hypervalent iodine(III) reagents, the research group of Lebel has reported the Rh(II)-catalyzed intramolecular[21b] and intermolecular[21a] aliphatic C-H amidation reactions with the use of *N*-tosyloxycarbamates as reagents (Scheme 1.21).

Scheme 1.21 Rh(II)-Catalyzed Intra- and Intermolecular Aliphatic C-H Amidation using *N*-Tosyloxycarbamates as Nitrene Precursors

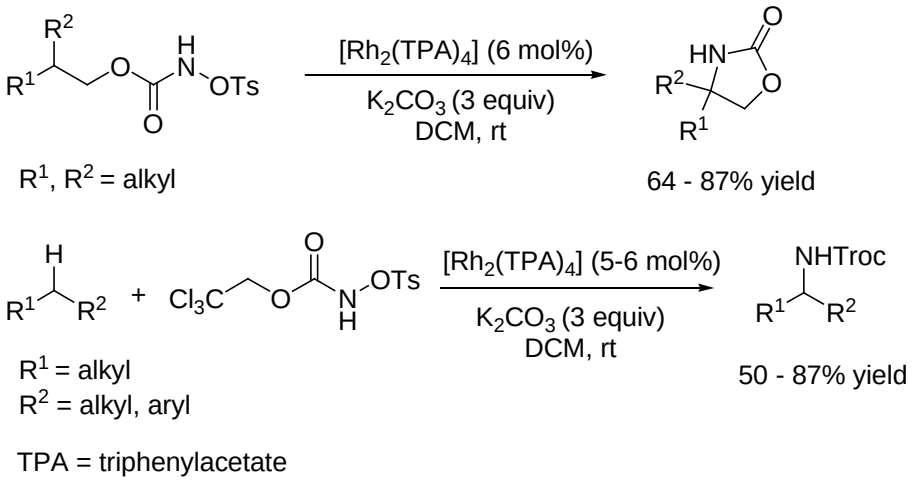

Notably, examples of Rh(II)-catalyzed intramolecular C-H amidation using vinylazides[22b] and phenylazides[22a] to prepare indole derivatives were also reported (Scheme 1.22). Since the nitrene generation from azides would only produce nitrogen as the side product, the use of azides as reagents significantly improved the atom economy of the nitrenoid C-H insertion reactions..

Scheme 1.22 Rh(II)-Catalyzed Intrarmolecular Aliphatic C-H Amidation using Azides as Nitrene Precursors

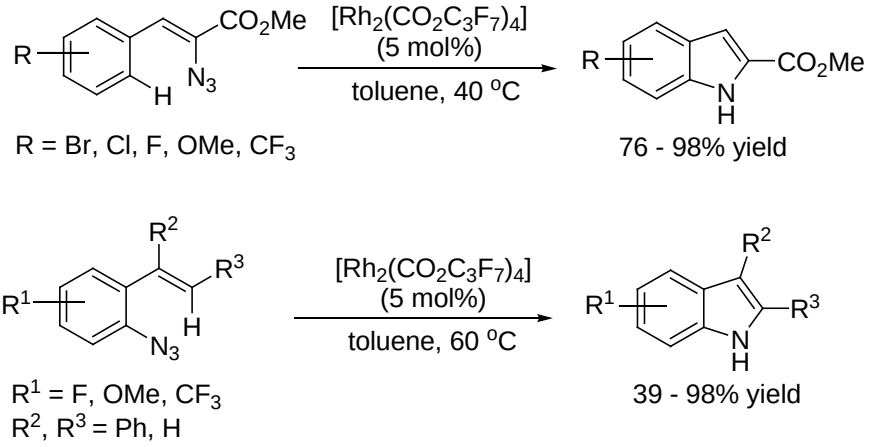

1.4 General Background for Transition Metal-Mediated Aromatic C-H Bond Activation / Functionalizations

Apart from the outer-sphere pathway for aliphatic C-H insertions, the transition metal-mediated direct arene C-H activation / functionalization (i.e., inner-sphere pathway) has been extensively investigated in recent years.[6,7, 23]

In 1967, a pioneering study by Fujiwara and co-workers described the Pd-mediated alkenylation of benzene. It was found that refluxing styrene palladium(II) chloride dimer in a mixture of benzene and acetic acid (approx. 4:1) for 8 h afforded *trans*-stilbene in 56% yield (Scheme 1.23).[24c] In their later studies, $Pd(OAc)_2$ was found to be efficient for the alkenylation of mono-substituted arenes (C_6H_5-**Y**) with styrene. Refluxing styrene (5 mmol) and $Pd(OAc)_2$ (1 equiv) in C_6H_5-**Y** / acetic acid (approx. 4:1) gave the corresponding *trans*-stilbenes in up to 90% yields (Scheme 1.24**)**. Attempts on turning the reaction into a catalysis by employing a smaller amount of Pd(OAc) (10 mol%) and a reoxidant (i.e., $Cu(OAc)_2$, AgOAc) were proven successful, despite low catalytic turnover (TON = ~5).[24b] Although the actual Ar-Pd(II) complex was not isolated in their reports, they proposed that their result on the Hammett correlation (ρ = -1.4)[24a] of the $Pd(OAc)_2$-mediated alkenylation of C_6H_5-**Y** was indicative of a rate-limiting electrophilic aromatic palladation of the arenes (c.f.

Ryabov's Hammett correlation study (ρ = -1.6)[7b] on $Pd(OAc)_2$-mediated *ortho*-C-H metalation of *N*,*N*-dimethylbenzylamine; see later sections).

Scheme 1.23 Reaction of Styrene-Palladium(II) Chloride Dimer with Benzene

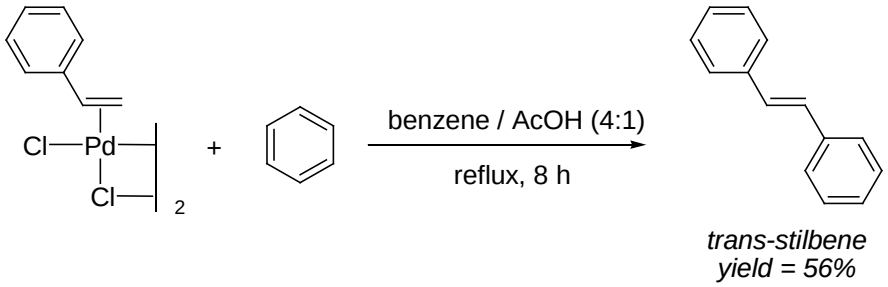

Scheme 1.24 $Pd(OAc)_2$-Mediated Alkenylation of C_6H_5-**Y** with Styrene

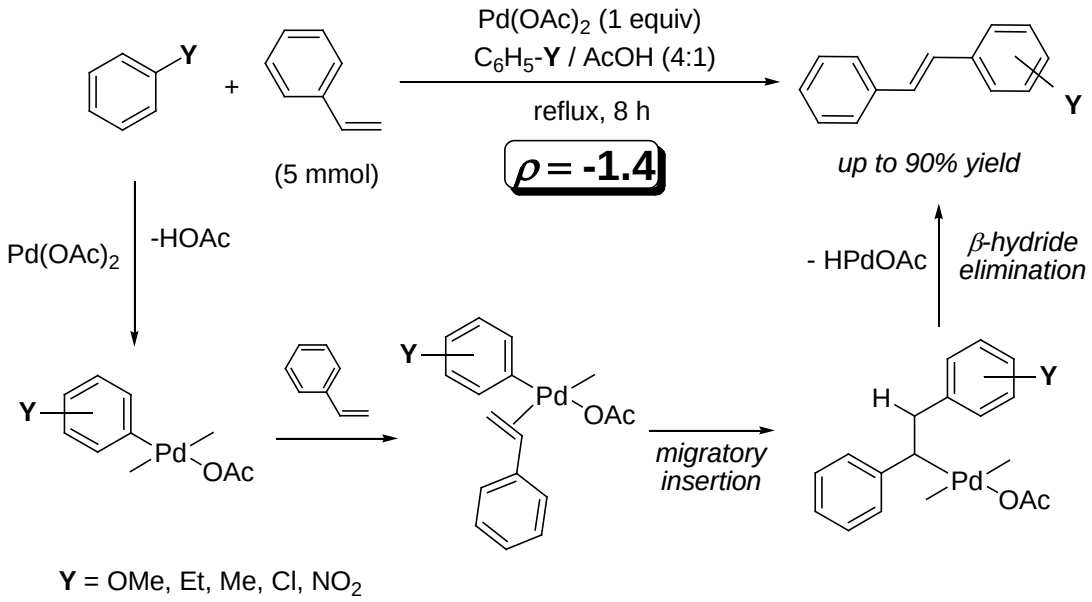

1.4.1 Directing Group-Assisted *ortho*-Selective Aromatic C-H Activation

The regioselectivity is one of the major challenges for arene C-H bond functionalization, and as in Fujiwara's studies, the Pd(II)-mediated mono-substituted benzene alkenylation generally gave a mixture of regioisomers, and the yields of the isomers were highly dependent on the electronic properties of the arenes (Table 1.3**)**.[24a]

Table 1.3 Regioisomer Distribution for $Pd(OAc)_2$-Mediated C_6H_5-**Y** Alkenylation with Styrene in Fujiwara's Study

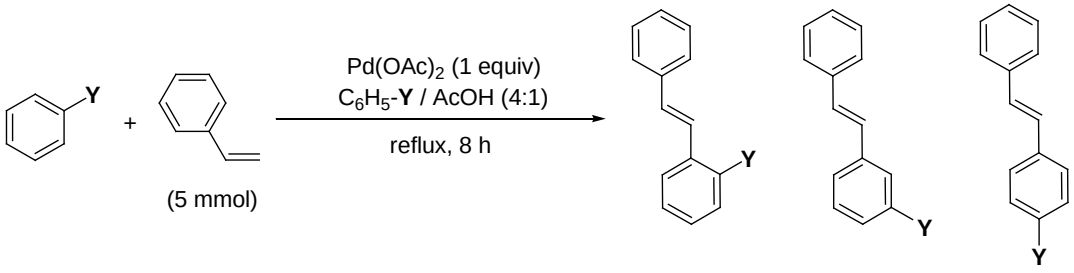

Y	yield% for *ortho*-product	yield% for *meta*-product	yield% for *para*-product
Me	11.6	15.3	21.6
OMe	26.0	3.8	41.5
Cl	4.1	10.5	15.0

To gain control of the regioselectivity in arene C-H bond functionalization,

directing group (DG)-assisted *ortho*-selective arene C-H activation approach has been extensively investigated in recent years.[6.7a]

According to the literature, the first example for DG-assisted arene *ortho*-C-H activation was demonstrated by Kleiman and Dubeck.[25] By heating the mixture of dicyclopentyldienyl nickel(II) and azobenzene at 135 ˚C for 4 h, a cyclonickelated complex of azobenzene was obtained (Scheme 1.25). The pioneering work on palladacyclic complex synthesis was later reported by the research group of Cope. In their study, potassium tetrachloropalladium(II) was treated with azobenzene (1 equiv) in methanol at room temperature to afford the corresponding chloro-bridged dimeric cyclopalladated complex of azobenzene in 95% yield within 2 hours (Scheme 1.26).[26b] In both examples, azobenzene acts as a bidentate ligand that it coordinates to the metal center through the azo nitrogen and the *ortho*-sp^2-carbon atom.

Scheme 1.25 Early Example of Preparation of the Cyclonickelated Complex of Azobenzene

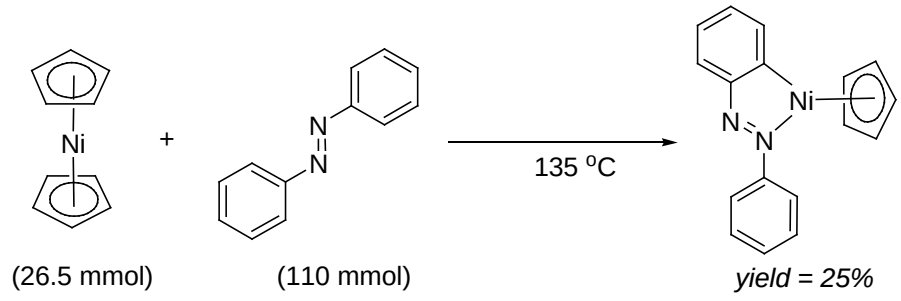

Scheme 1.26 Preparation of the Cyclopalladated Complex of Azobenzene

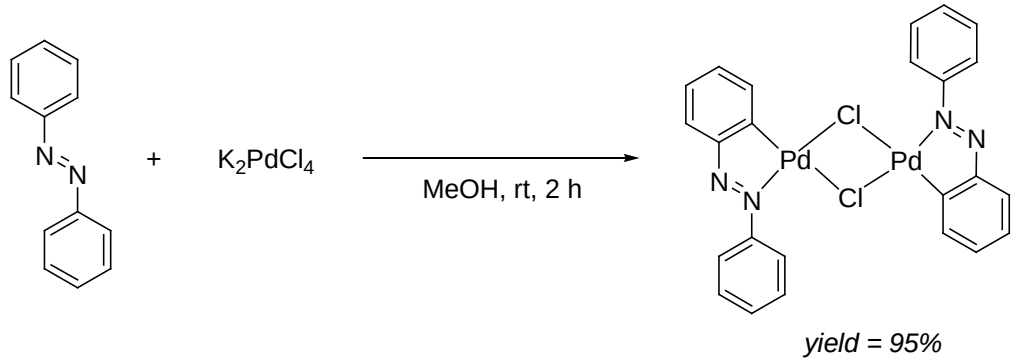

yield = 95%

Since Cope's report on the cyclopalladated complex synthesis, enormous number of examples for palladacyclic complex synthesis emerged in the literature, and some examples were illustrated in Figure 1.4. Analogous to nitrogen donors, the oxygen atom of a carbonyl group was found to bind to palladium centre.[41a,j] Apart from the palladium examples, other transition metals such as rhodium, iridium and ruthenium were also reported to form cyclometalated complexes with arenes bearing a directing group (Figure 1.5).[28]

Figure 1.4 Selected Examples of Cyclopalladated Complexes

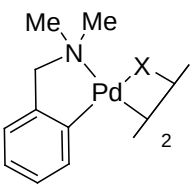

X = Cl; Cope (1965)[26a]
X = OAc; Ryabov (1985)[7b]

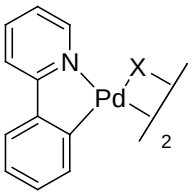

X = Cl; Kasahara (1968)[27b]
X = OAc; Constable (1987)[27a]

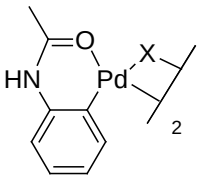

X = OAc; Horino (1981)[41j]
X = OTs; Yu (2010)[41a]

Figure 1.5 Selected Examples of Cyclometalated Complexes

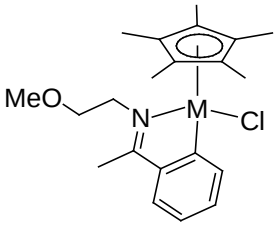

M = Rh, Ir

Davies (2003)[28c]

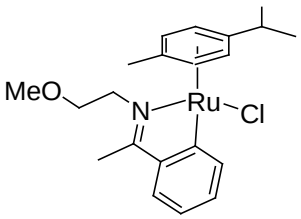

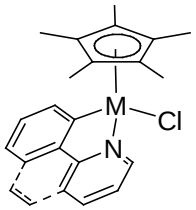

M = Rh, Ir

Jones (2008)[28a,b]

The pioneering work on transition metal-catalyzed *ortho*-selective aromatic C-H functionalizations was first reported Fahey and co-workers.[29] In their study, when a mixture of azobenzene (5.5 mmol) and $PdCl_2$ (20 mol%) in dioxane / H_2O (2:1) was slowly bubbled with chlorine gas at 85 °C for 16 h, *ortho*-chlorinated azobenzenes were exclusively formed (Scheme 1.27). More importantly, the stoichiometric chlorination reaction using the cyclopalladated azobenzene complex also successfully produced 2,6,2',6'-tetrachloroazobenzene in 39% yield. It was proposed that the C-H chlorination reaction should proceed *via* the initial cyclopalladation of azobenzene, followed by oxidative addition of chlorine to give a putative Pd(IV) intermediate. Subsequent reductive elimination of the Pd(IV) complex would yield the C-Cl bond formation products. In the absence of $PdCl_2$, the chlorination of azobenzene predominantly occurred at the *para*-positions (yield for the total *para*-chlorinated azobenzene = ~80%). This result was consistent with aromatic chlorination *via* electrophilic aromatic substitution mechanism.

Scheme 1.27 Pd(II)-Catalyzed *ortho*-Chlorination of Azobenzene and the Stoichiometric Reaction with the Cyclopalladated Azobenzene Complex

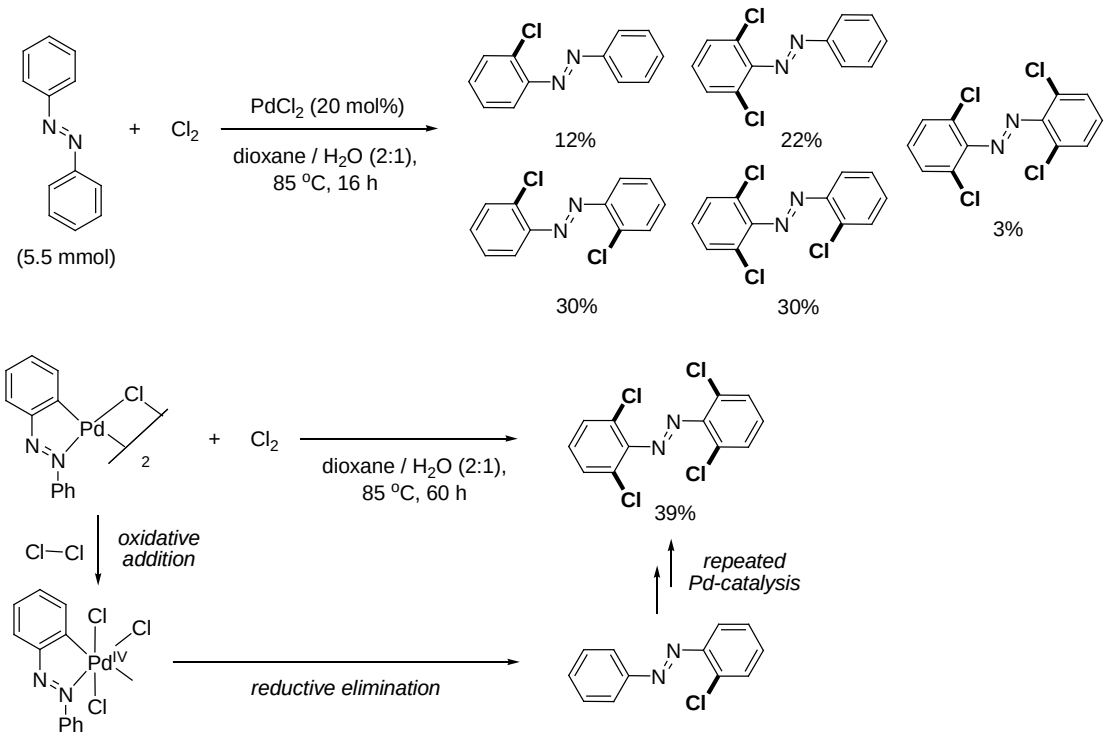

1.5 Transition Metal-Catalyzed Chelation-Assisted Arene C-H Functionalizations *via* Inner-sphere Mechanism

1.5.1 Ruthenium-Catalyzed Chelation-Assisted Aromatic C-H Functionalizations[30]

In 1993, Murai, Kakiuchi and Chatani disclosed a seminal work on Ru(0)-catalysis for *ortho*-selective alkylation of aromatic ketones. With the use of $[RuH_2(CO)(PPh_3)_3]$ (2 mol%) as catalyst, aromatic ketones reacted effectively with a variety of alkenes in toluene at 135 ℃ to give the *ortho*-alkylated products in 66 — >99% yields (Scheme 1.28).[31a] The reaction was proposed that *ortho*-C-H bond of the aromatic ketones would be cleaved by Ru(0) *via* oxidative addition to generate the aryl-hydrido ruthenium(II) complex. Alkenes would then coordinate to the Ru(II) complex followed by hydride migration, and the resulting alkyl-aryl-Ru(II) complex would undergo reductive elimination to yield the alkylation products.[31d]

The research group of Kakiuchi later further extended the Ru(0)-catalysis to *ortho*-arylation of aromatic ketones (Scheme 1.29).[31b,c] The reaction was also believed to proceed by the *ortho*-C-H bond activation *via* Ru(0)-mediated oxidative addition. Interestingly, an extra equivalent of aromatic ketones was needed for good product

yields. For example, with 1 equiv of aromatic ketones, only a maximum of 47% yield of product was obtained. It was suggested that the extra ketones would react with the aryl-hydrido-Ru(II) complex to give the aryl-alkoxy-Ru(II) complex, which then underwent transmetalation with the arylboronates to generate di(aryl)-Ru(II) complex. Reductive elimination would give the biaryl products.

Scheme 1.28 $[RuH_2(CO)(PPh_3)_3]$-Catalyzed *ortho*-Selective Alkylation of Aromatic Ketones with Alkenes

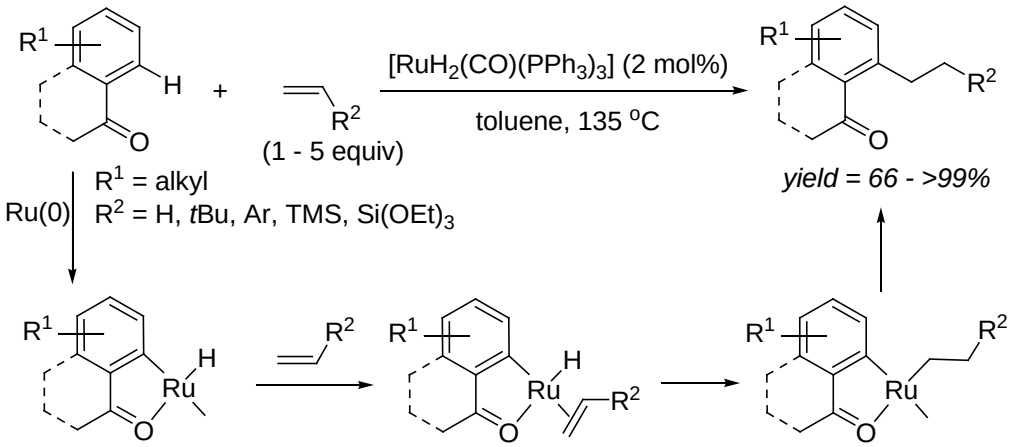

Apart from the Ru(0)-catalysis, Oi and Inoue reported the $[\eta^6\text{-}(C_6H_6)RuCl_2]_2$-catalyzed *ortho*-selective arylation of 2-arylpyridine with aryl bromides (Scheme 1.30) Treatment of 2-arylpyridines with aryl bromides (1 equiv), $[\eta^6\text{-}(C_6H_6)RuCl_2]_2$ (2.5 mol%), triphenylphosphine (10 mol%) and K_2CO_3 (2 equiv) in *N*-methylpyrrolidinone at 120 °C for 20 h produced the arylation products in 40 —

95% yields.[32c] Apart from 2-arylpyridines, aromatic imines,[32b] 2-aryloxazolines and 2-arylimidazolines[32a] were found to be effective substrates for the Ru(II)-catalyzed arylation reactions.

Scheme 1.29 $[RuH_2(CO)(PPh_3)_3]$-Catalyzed *ortho*-Selective Arylation of Aromatic Ketones with Arylboronates

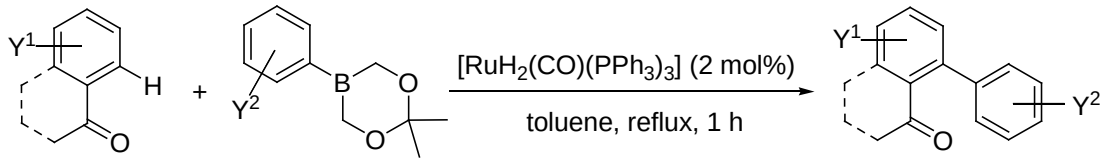

(2 equiv)

up to 95% yield

Y^1 = OMe, F, CF_3, alkyl
Y^2 = NMe_2, OMe, F, CF_3, alkyl

Scheme 1.30 $[\eta^6\text{-}(C_6H_6)RuCl_2]_2$-Catalyzed *ortho*-Selective Arylation of 2-Arylpyridine with Aryl Bromides

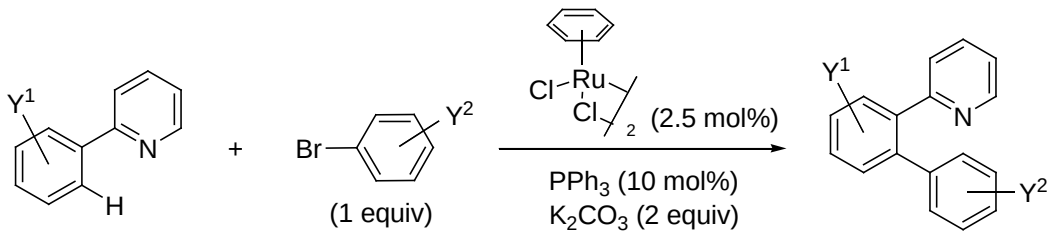

(1 equiv)

yield = 40 - 95%

Y^1 = aryl, alkyl, CF_3
Y^2 = F, alkyl
NMP = *N*-methylpyrrolidinone

1.5.2 Rhodium-Catalyzed Chelation-Assisted Aromatic C-H Functionalizations

Rh(I)-catalyzed *ortho*-selective arene C-H bond functionalization, especially C-C bond coupling, has been extensively studied in recent years.[33] Early examples were reported by Kim and co-workers[34] that Wilkinson's catalyst ($[RhCl(PPh_3)_3]$ was found to effectively mediate the *ortho*-C-H alkylation of 2-phenylpyridines (Scheme 1.31). Analogous to the Ru(0)-catalysis, the Rh(I) catalyst was believed to undergo the oxidative addition of the *ortho*-C-H bonds of 2-phenylpyridines to give a hydrido-cyclometalated rhodium(III) complex, which would further react with alkenes to give an alkyl-cyclorhodated complex. Subsequent reductive elimination would yield the alkylation products. Jun and co-workers have further extended the scope of the $[RhCl(PPh_3)_3]$-catalyzed *ortho*-alkylation reactions to aromatic aldimines and ketimines,[35] and a large variety of functionalizaed alkenes such as acrylates, *N*,*N*-dimethylacrylamide, phenyl vinyl sulfone and acrylonitrile were also found to be effective coupling partners.[35a]

Scheme 1.31 [RhCl(PPh$_3$)]-Catalyzed *ortho*-C-H Alkylation of 2-Phenylpyridines

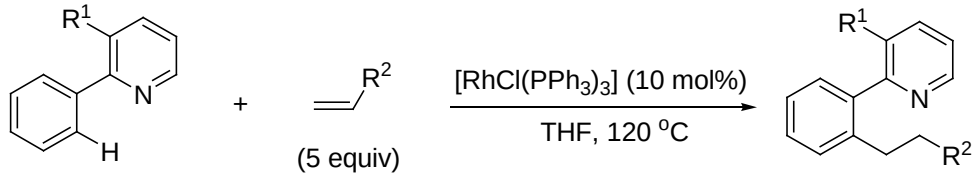

R^1 = H, Me
R^2 = alkyl, TMS, Si(OEt)$_3$

up to 99% yield

More recently, Cp*Rh(III) complexes was also found to be effective catalysts for arene C-H bond activation / C-C bond coupling reactions. For example, Miura and co-workers demonstrated that the cyclization of benzoic acids with alkynes and alkenes to give coumerins and 7-vinylphthalides respectively under [Cp*RhCl$_2$]$_2$ catalysis (Scheme 1.32).[36] Unlike to Rh(I)-catalysis, the reaction was proposed to be initiated by cyclorhodation of the benzoic acids with concomitant elimination HX (X = Cl or OAc), followed by alkynes / alkenes insertion. Reductive elimination would result in the C-C coupled cyclization products. It is noteworthy that Cu(OAc)$_2$ was crucial for the catalysis; possibly, Cu(OAc)$_2$ would act as re-oxidant for regenerating the active Rh(III) catalyst (Scheme 1.33).

Scheme 1.32 $[Cp^*RhCl_2]_2$-Catalyzed Cyclization Reactions of Benzoic Acids

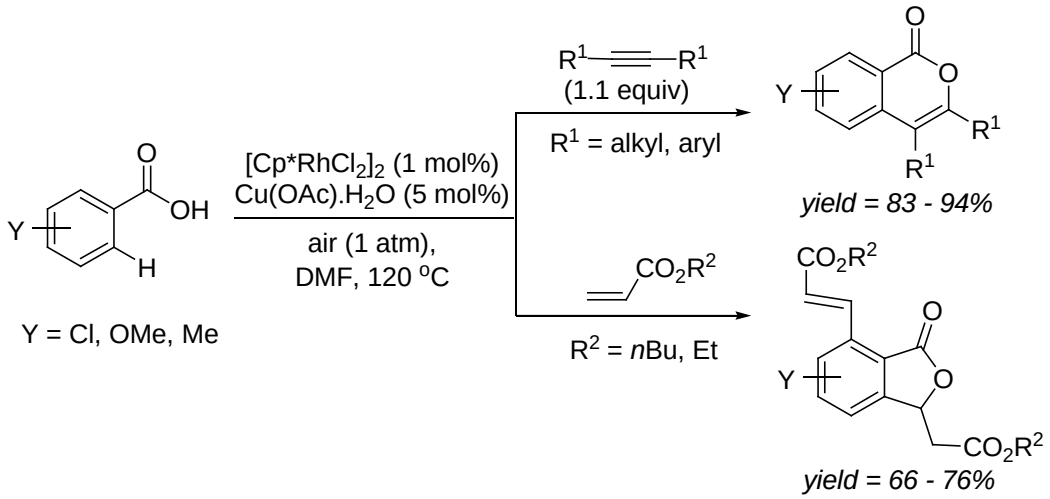

Scheme 1.33 The Proposed Mechanism for the Rh(III)-Catalyzed Cyclization of Benzoic Acids with Alkynes

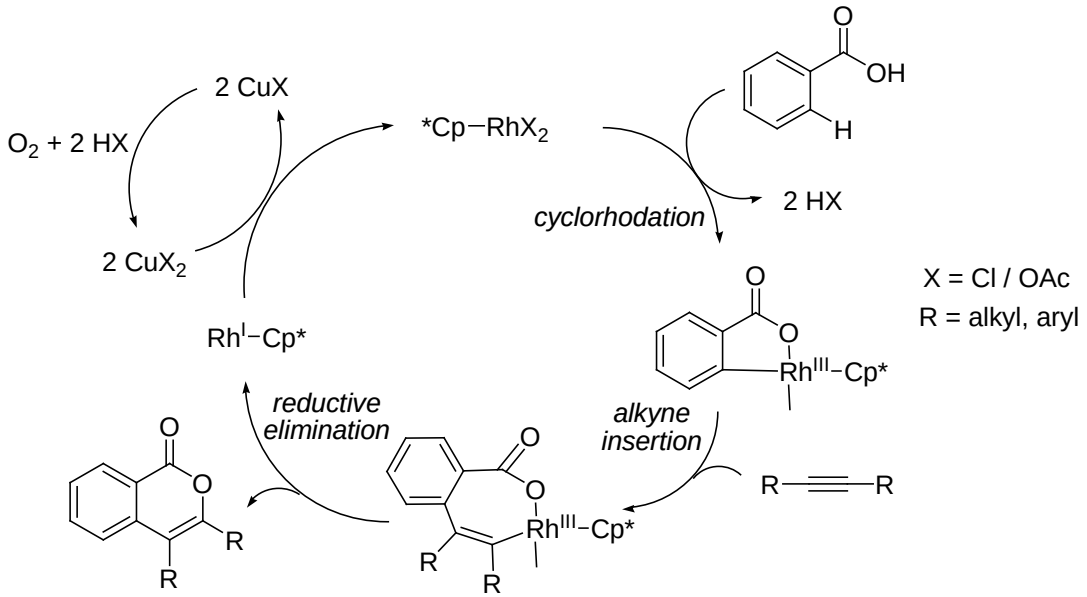

Bergmen and Ellmen recently reported an interesting Rh(III)-catalyzed arene C-H alkylation with *N*-protected aldimines as reagents.[37] It was found that when

2-arylpyridines / benzo[*h*]quinolines were treated with aldimines (1 equiv), $[Cp^*RhCl_2]_2$ (10 mol%) and $AgSbF_6$ (40 mol%) in dichloromethane at 75 °C for 20 h, the C-C bond coupled products were furnished in up to 95% yield (Scheme 1.34). Recently, Rh(III)-catalyzed *ortho*-C-H acylation of *N*,*N*-diethylbenzamide was also achieved by employing benzaldehydes as coupling partners (Scheme 1.35).[38]

Scheme 1.34 $[Cp^*RhCl_2]_2$-Catalyzed *ortho*-C-H Alkylation of 2-Arylpyridines / Benzo[*h*]quinolines with *N*-Protected Aldimines

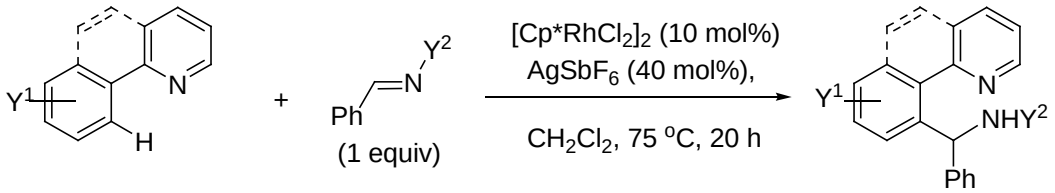

Y^1 = OMe, Ac, Cl, NHAc, alkyl
Y^2 = Boc, Ts, Ns, $P(O)Ph_2$

up to 95% yield

Scheme 1.35 $[Cp^*RhCl_2]_2$-Catalyzed *ortho*-C-H Acylation of *N*,*N*-Dimethylbenzamides with Benzaldehydes

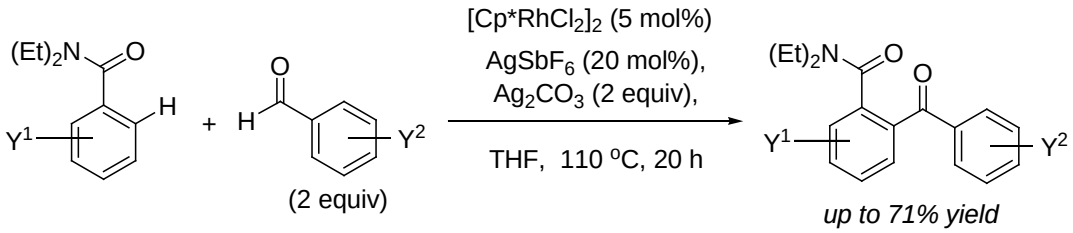

Y^1 = halogens, OMe, OAc, alkyl
Y^2 = halogens, OMe, NO_2

up to 71% yield

1.5.3 Palladium-Catalyzed Chelation-Assisted Aromatic C-H Activation / Functionalizations

1.5.3.1 Pd-Mediated Arene *ortho*-C-H Activation

The mechanism for $Pd(OAc)_2$-mediated directing group-assisted arene *ortho*-C-H activation, which leads to palldacyclic complexes, has been extensively investigated in the literature.[7,8,9,10] As depicted in Scheme 1.36, there are generally three proposed pathways: (1) electrophilic aromatic substitution *via* a Wheland intermediate;[7] (2) proton-transfer *via* a four-membered transition state[39] and (3) agostic C-H complex formation followed by facile intramolecular deprotonation.[9b]

In Ryabov's study on the cyclopalladation of *N*,*N*-dimethylbenzylamine (DMBA), it was found that the reaction exhibited a primary kinetic isotope effect (k_H / k_D = 2.2) indicating a rate-limiting C-H bond cleavage step. In addition, the Hammett correlation study on cyclopalladation of *para*-substituted DMBA revealed a ρ value of -1.6; thus, the C-H bond cleavage step should be electrophilic in nature. Based on these results, Ryabov and co-workers have proposed that the cyclopalladation of DMBA by $Pd(OAc)_2$ should proceed through electrophilic aromatic substitution *via* the Wheland intermediate (arenium intermediate).[7b] In the

mechanistic study of cyclopalladation reported by Martinez and co-workers, it was proposed that the C-H activation would go through an proton abstraction mechanism involving a four-membered transition state.[39] In Davies and Macgregor DFT calculation study on the cyclopalladation of *N*,*N*-dimethylbenzylamine, it was found that the pathway involving the rate-limting agostic C-H complex formation followed by a facile acetate deprotonation (*via* a six-membered transition state) was thermodynamically favorable.[9b]

It is noteworthy that Fagnou and co-workers have recently proposed the concerted metalation deprotonation (CMD) mechanism for $Pd(OAc)_2$-mediated C-H activation of simple arenes. Interestingly, in their study of the $Pd(OAc)_2$-catalyzed coupling of pyridine *N*-oxides and aryl bromides, the reaction exhibited a linear Hammett correlation with a positive slope (ρ = +1.53) for the arylation of C-4 substituted pyridine *N*-oxide. The positive ρ value indicated a negative charge buildup in the transition state for C-H bond cleavage (Scheme 1.37).[10c,d]

Scheme 1.36 Various Proposed Mechanisms for $Pd(OAc)_2$-Mediated DG-Assisted *ortho*-C-H Bond Activation

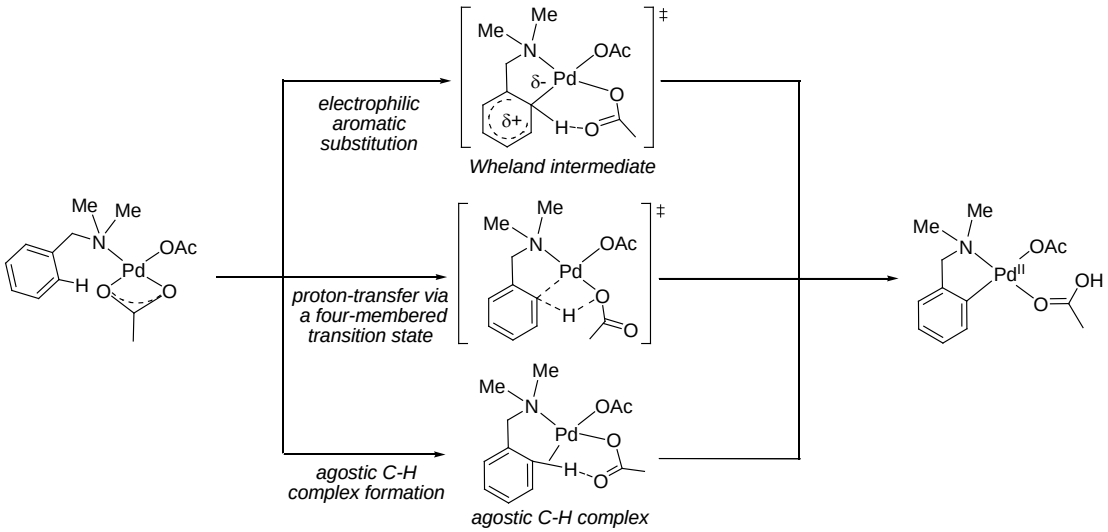

Scheme 1.37 Concerted Metalation Deprotonation Mechanism Proposed By Fagnou and Co-workers

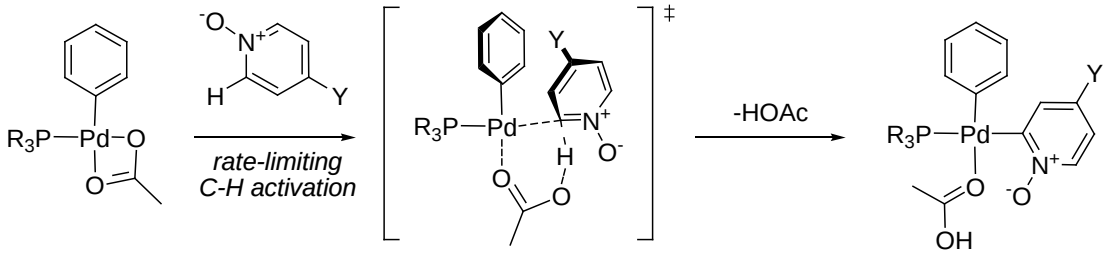

Y = OMe, Me, H, CO_2Me, NO_2 **ρ = +1.53**

1.5.3.2 Pd-Catalyzed Aromatic *ortho*-C-H Activation for C-C Bond Formations

Pd-catalyzed arene C-H activation / C-C bond formation has been attracting widespread interest. In particular, C-C bond formation reactions such as alkenylation, alkylation, arylation and carbonylation have been extensively investigated.[40]

1.5.3.2.1 Pd-Catalyzed Aromatic *ortho*-C-H Alkenylation

A pioneering work by de Vries, van Leeuwen and co-workers reported that acetanilides would couple with *n*-butyl acrylate (1.1 equiv) in AcOH at room temperature in the presence of $Pd(OAc)_2$ (5 mol%) **(**Scheme 1.38).[41h] The analogous reaction employing *N*,*N*-dimethyl-*N*'-aryl urea as substrates was later reported by Brown and co-workers in 2009.[41b] With *N*,*N*-dimethylbenzylamines as substrates, Shi and co-workers further extended that the scope of alkenes in the Pd-catalyzed arene C-H alkenylation to benzyl acrylate, acrylamide and *N*,*N*-disubstituted acrylamide (Scheme 1.39).[42]

Scheme 1.38 $Pd(OAc)_2$-Catalyzed Acetanilides *ortho*-C-H Alkenylation

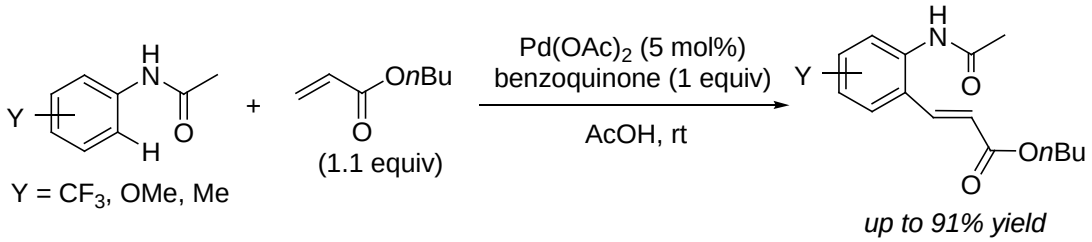

Y = CF_3, OMe, Me

up to 91% yield

Scheme 1.39 Pd-Catalyzed *N*,*N*-Dimethylbenzylamine *ortho*-C-H Alkenylation

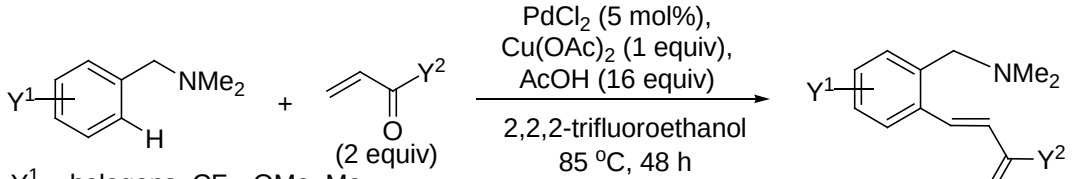

Y^1 = halogens, CF_3, OMe, Me

Y^2 = O*n*Bu, OMe, OEt, NH_2, pyrrolidinyl

yield = 53 - 86%

In general, re-oxidants such as benzoquinone (BQ) and $Cu(OAc)_2$ are required for regenerating the Pd(II) catalyst from Pd(0), which would probably be generated from *β*-hydride elimination and the subsequent reductive elimination. Daugulis and co-workers demonstrated that with 3-bromoacrylates as the coupling partners the Pd-catalyzed anilides *ortho*-C-H alkenylation can be achieved without reoxidants (Scheme 1.40).[41g]

Scheme 1.40 Pd-Catalyzed Anilides *ortho*-C-H Alkenylation with 3-Bromo Acrylates

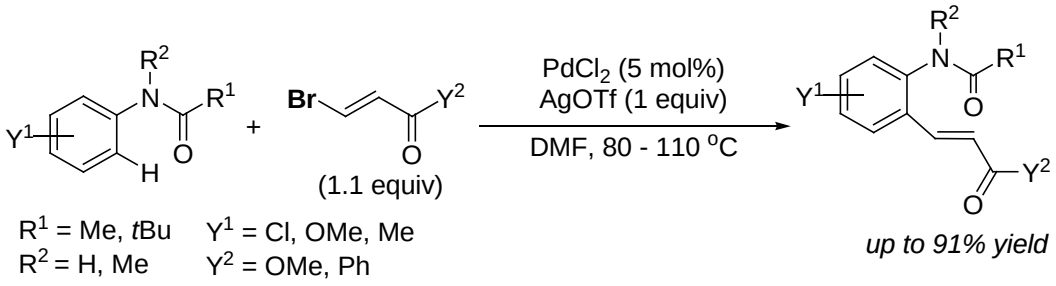

1.5.3.2.2 Pd-Catalyzed Aromatic *ortho*-C-H Alkylation

The first example of Pd(II)-catalyzed alkylation of aromatic C-H bonds with primary-alkyl tin reagents was reported by Yu (J.-Q.) and co-workers. Their study revealed that with a 4,4-dimethyloxazoline group as directing group the arene *ortho*-C-H bonds can be alkylated with tetraalkyl tin (0.075 equiv × 10) in the presence of BQ (1 equiv), $Cu(OAc)_2$ (1 equiv) and $Pd(OAc)_2$ (10 mol%) in acetonitrile at 100 °C (Scheme 1.41).[43b] The same research group also reported the analogous Pd-catalyzed *ortho*-C-H alkylation of 2-arylpyridines with methylboroxine and alkyl boronic acids as reagents (Scheme 1.42).[43a] It is noteworthy that the use alkyl boronic acids significantly broadened the scope of the C-H alkylation reaction.

Scheme 1.41 $Pd(OAc)_2$-Catalyzed Alkylation of Arenes Bearing an Oxazoline Directing Group with Tetraalkyl Tin

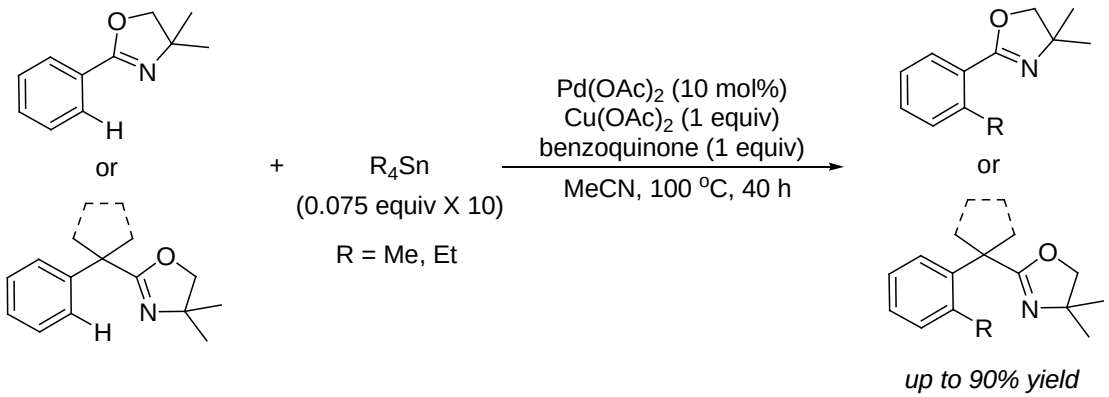

Scheme 1.42 $Pd(OAc)_2$-Catalyzed Alkylation of 2-Arylpyridines with Methylboroxane or Alkyl Boronic Acids

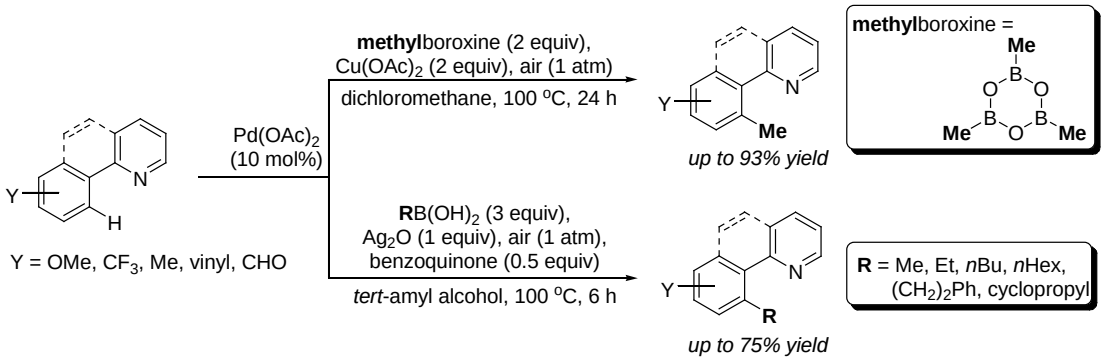

1.5.3.2.3 Pd-Catalyzed Aromatic *ortho*-C-H Arylation

Daugulis and co-workers have investigated the Pd(II)-catalyzed directing group-assisted arylation reaction using aryl iodides as reagents. In their initial study, treatment of anilides with $Pd(OAc)_2$ (10 mol%), aryl iodides (2 — 9 equiv) and

silver acetate (1 equiv) in trifluoroacetic acid at 90 — 130 °C afforded the 2,6-diarylated anilides in 55 — 95% yields (Scheme 1.43).[41f] The "aryl iodide + AgOAc" protocol was also applicable to the *ortho*-selective arylation 2-arylpyridine derivatives[44b] and benzoic acids[44a] as substrates. It is noteworthy that aryl chlorides were also found to be compatible arylation reagents for *ortho*-arylation of benzoic acids (Scheme 1.44).[44a]

Scheme 1.43 $Pd(OAc)_2$-Catalyzed Arylation of Anilides with Aryl iodides

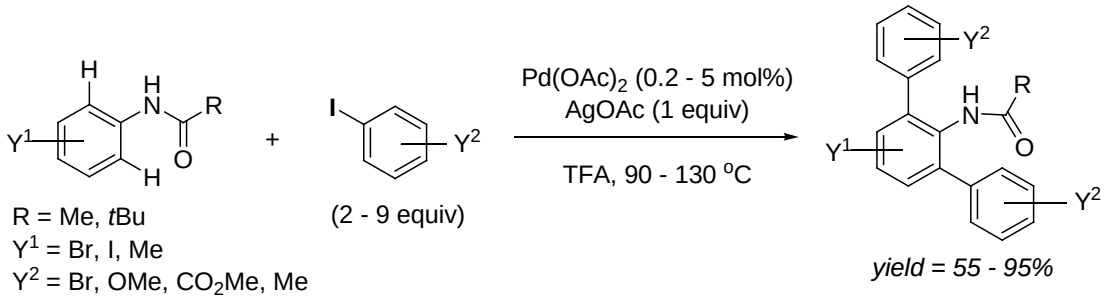

Scheme 1.44 $Pd(OAc)_2$-Catalyzed Arylation of Benzoic Acids with Aryl Chlorides

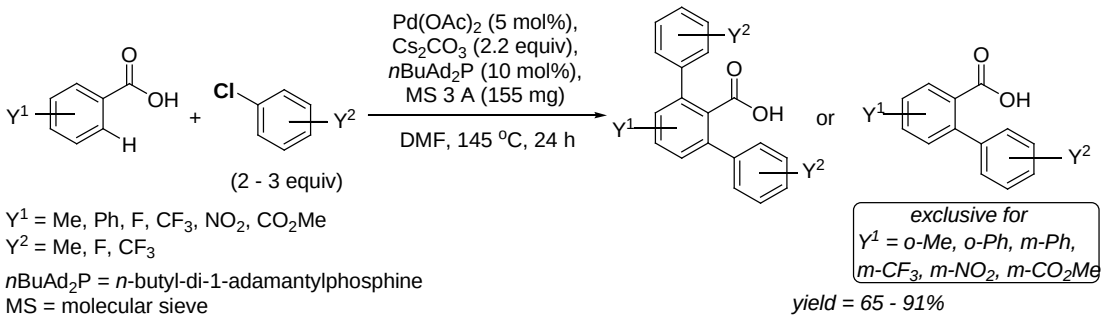

In 2007, Sanford and co-workers reported the Pd-catalyzed arene C-H arylation

using unsymmetrical mesityl/aryl-substituted iodinium(III) reagents ([Ar-I-Mes]BF_4). It was found that various directing groups such as 2-pyridyl, pyrrolidinyl and acetamide were effective directing groups for the *ortho*-selective arylation of arenes (Scheme 1.45).[45] According to the mechanistic study, the arylation was proposed to go through turnover-limiting oxidation of palladium(II) by the [Ar-I-Mes]BF_4,[45a] rather than turnover-limiting C-H bond cleavage.[40]

Scheme 1.45 $Pd(OAc)_2$-Catalyzed *ortho*-Selective Arylation of Arenes using [Ar-I-Mes]BF_4

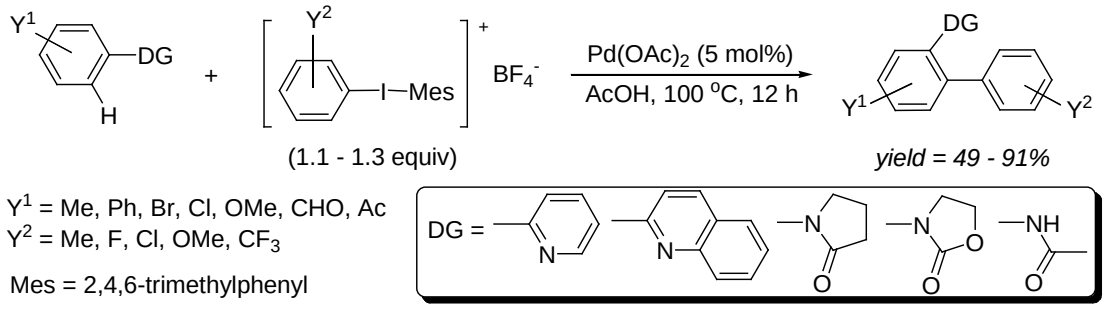

Apart from the arylation reactions employing pre-functionalized arylation reagents, Pd-catalyzed directing group-assisted arene C-H coupling with unactivated arene C-H bonds has also been extensively investigated in recent years. For example, Sanford and co-workers found that with $Pd(OAc)_2$ (10 mol%) as catalyst, BQ (0.5 equiv) and Ag_2CO_3 (2 equiv) as oxidants and DMSO (4 equiv) as additive, benzo[*h*]quinoline can effectively couple with various substituted benzenes to give the

ortho-arylation products in up to 93% yield.[46a,d] *ortho*-C-H arylation of anilides was also investigated by the research groups of Buchwald[46b] and Shi[46c] (Scheme 1.46).

Scheme 1.46 Pd-Catalyzed *ortho*-Selective Arenes C-H Coupling with Unactivated Arene C-H Bonds

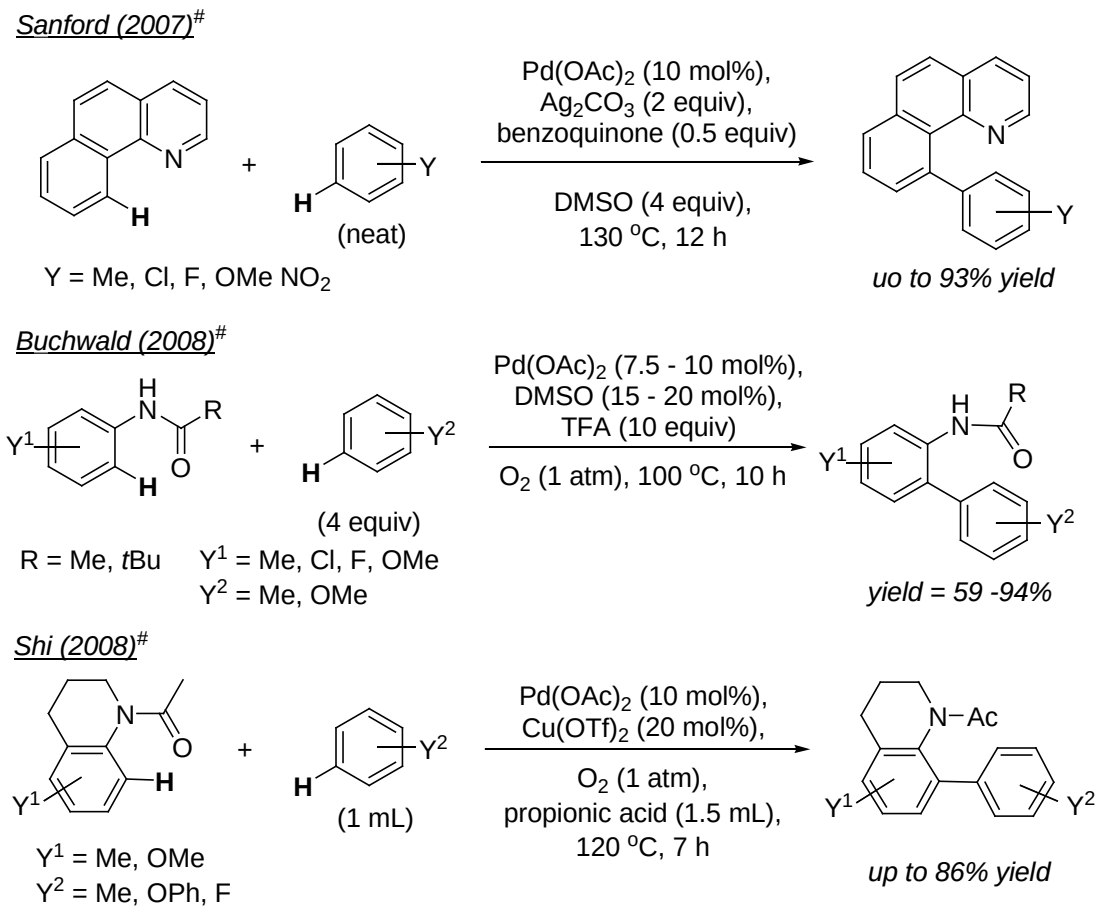

1.5.3.2.4 Pd-Catalyzed Aromatic *ortho*-C-H Carbonylation

Pd(II)-catalyzed aromatic *ortho*-C-H carbonylation using carbon monoxide (CO) as coupling partner has been demonstrated in the literature. Yu (J.-Q.) and co-workers achieved the Pd-catalyzed *ortho*-carboxylation of benzoic acids[47b] and acetanilides[41a] in 2008 and 2009, respectively. Lloyd-Jones, Booker-Milburn and co-workers also found that *N*-alkyl-*N'*-aryl ureas or *N*,*N*-dialkyl-*N'*-aryl ureas were effective substrates for Pd-mediated *ortho*-carboxyation (Scheme 1.47).[47a]

Scheme 1.47 Pd-Catalyzed Aromatic *ortho*-C-H Carboxylation with CO

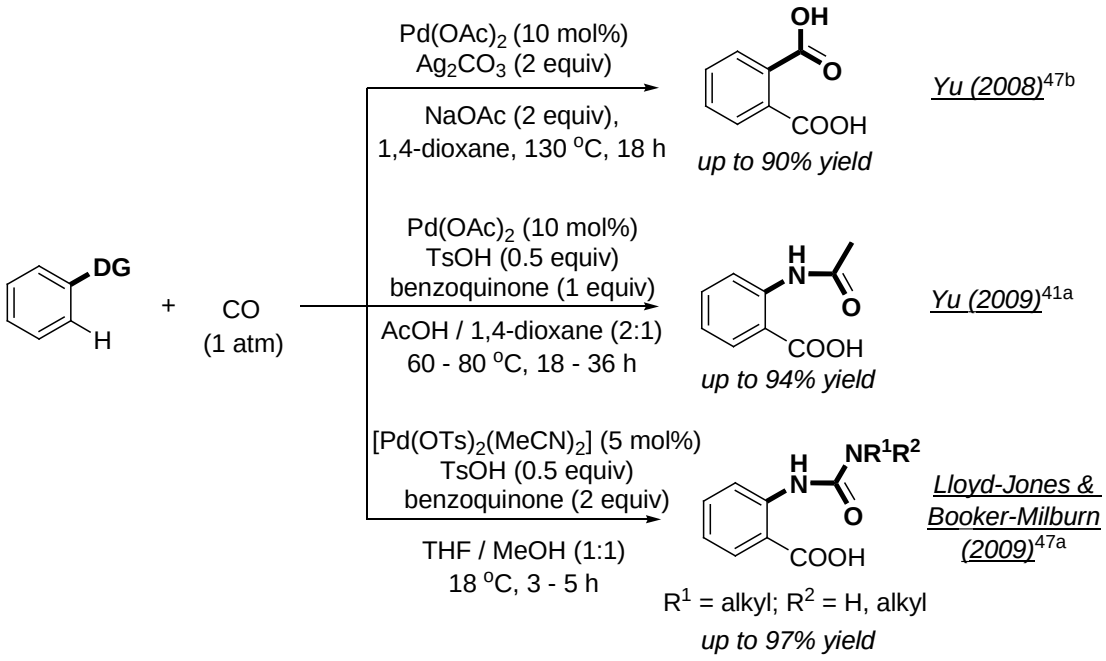

The research group of Yu (W.-Y) employed an alternative strategy for Pd-catalyzed arene C-H carbonylation. Instead of carbon monoxide, diethyl azodicarboxylate (DEAD) was found to be an effective reagent for directing group-assisted arene C-H ethoxycarbonylation. With $Pd(OAc)_2$ (5 mol%) as catalyst and DEAD (0.5 equiv × 4) as reagent, the arenes bearing a variety of directing groups (e.g. 2-pyridyl, pyrrolidinonyl, *O*-methyloxime) can be effectively *ortho*-carbonylated (Scheme 1.48).[48c]

Scheme 1.48 Pd-Catalyzed Directing Group-Assisted Arene C-H Ethoxycarbonylation with DEAD

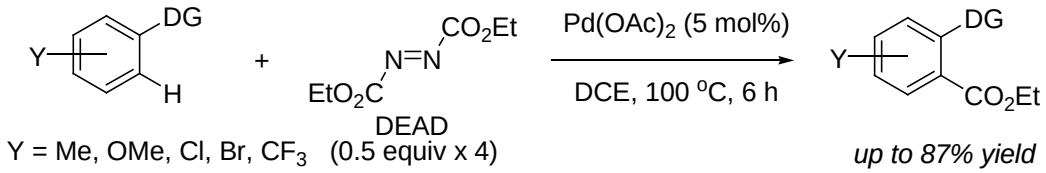

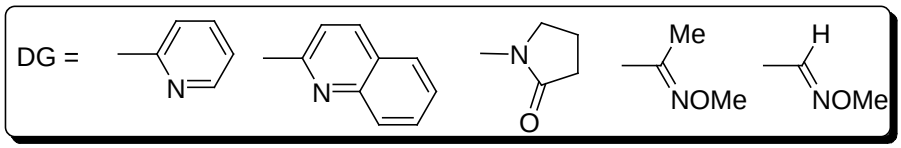

Apart from using DEAD as reagent, Yu (W.-Y.) also devised a C-H / C-H coupling reaction for Pd-catalyzed aromatic *ortho*-C-H acylation using aldehydes as coupling partners. It was found that treatment of *O*-methyloximes with aldehydes (6 equiv), $Pd(OAc)_2$ (5 mol%), *tert*-butyl hydroperoxide (TBHP; 2 equiv) and AcOH

(0.5 equiv) in toluene at 100 °C for 2 h afforded the *ortho*-C-H acylation products in 40 — 95% yields (Scheme 1.49).[48b] The acylation reaction of anilides with aldehyde and TBHP was also investigated in their recent works.[48a]

Notably, in the studies of ethoxycarbonylation and the coupling reactions with aldehydes, Yu (W.-Y) and co-workers proposed that the Pd-catalyzed acylations may involve acyl radicals, which would react with the cyclopalladated complexes to generate the putative Pd(III) or Pd(IV) intermediates.

Scheme 1.49 Pd-Catalyzed *ortho*-Acylation of *O*-Methyloximes with Aldehydes and TBHP

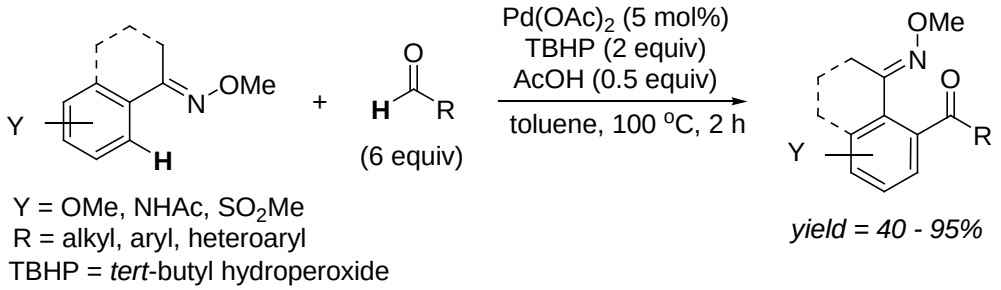

Y = OMe, NHAc, SO_2Me
R = alkyl, aryl, heteroaryl
TBHP = *tert*-butyl hydroperoxide

1.5.3.3 Pd-Catalyzed Intramolecular Arene *ortho*-C-H Amidations / Aminations

For the Pd-catalyzed intramolecular C-N bond formation reactions, the nitrogen donor groups on the arenes serve as the directing groups for the arene *ortho*-C-H activation and the coupling partner.

Buchwald and co-workers reported the first example of Pd-catalyzed intramolecular aromatic C-H amidation.[49f] When 2-phenylacetanilides were treated with $Pd(OAc)_2$ (5 mol%), $Cu(OAc)_2$ (1 equiv) and O_2 (1 atm) in toluene at 120 °C, *N*-acetylcarbazoles were produced in 88 — 94% yields (Scheme 1.50). The reaction was proposed to go through a nitrogen-directed *ortho*-C-H activation of the adjacent arene group to form a cyclopalladated complex, which would furnish the carbazole by reductive elimination. The combination of $Cu(OAc)_2$ and oxygen would re-oxidize the Pd(0) back to the Pd(II) catalyst (Scheme 1.51).

Scheme 1.50 $Pd(OAc)_2$-Catalyzed Cyclization of 2-Phenylacetanilides

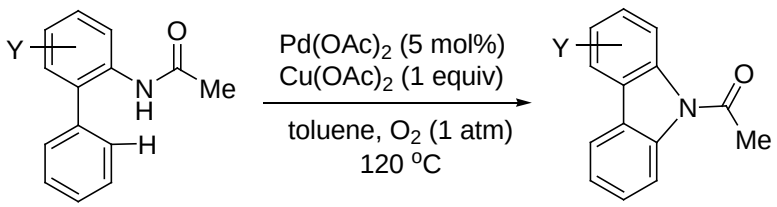

Y = F, CF_3, Me

yield = 88 - 94%

Scheme 1.51 Proposed Catalytic Cycle for the Pd-Catalyzed Cyclization of 2-Phenylacetanilides

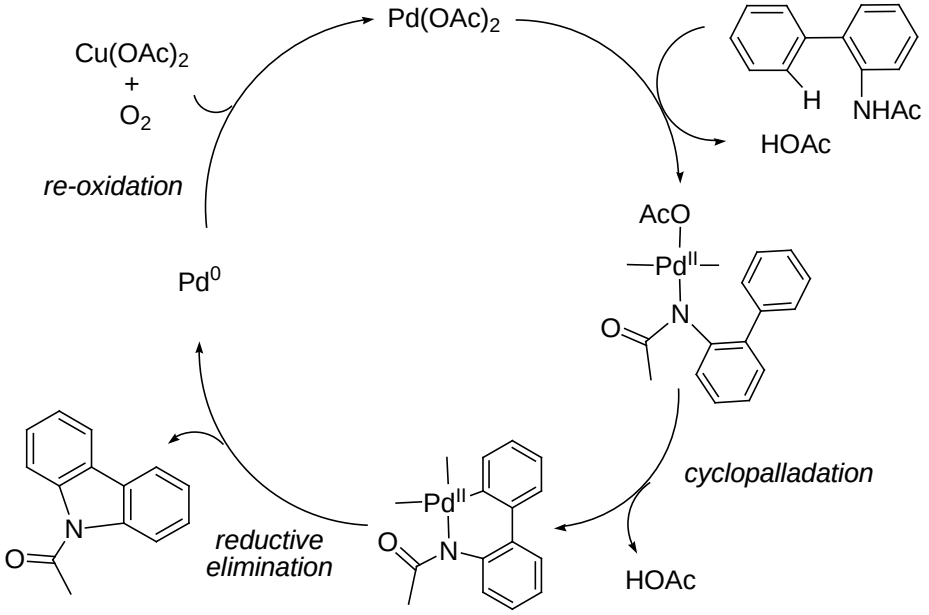

A remarkable Pd-catalyzed intramolecular C-N coupling reaction using *O*-acetyloxime as substrate was developed by Hartwig and coworkers.[49a] In their study, treatment of *O*-acetyl 2-phenylpropanone oximes $Pd(dba)_2$ (1 mol%) and Cs_2CO_3 (1 equiv) in toluene at 150 °C for 24 h afforded indole derivatives in 40 — 71% yield (Scheme 1.52**)**. Notably, the Pd(II) complex generated from oxidative addition of N-O bond was also prepared by the reaction of *O*-pentafluorobenzoyl 2,2-diphenylpropanone oxime with $Pd(PCy_3)_2$ (1 equiv) in toluene. When the complex was heated in the presence of Cs_2CO_3 (1 equiv) in toluene at 150 °C for 2 h, 2-methyl-3-phenylindole was obtained in 31% yield. Based on these results, it was proposed that the reaction would go through four steps: (1) oxidative N-O bond

addition of *O*-acyloxime to give a Pd(II) complex; (2) tautomerization of the imido ligand; (3) intramolecular *ortho*-directed C-H activation to give a cyclopalladated complex and (4) reductive elimination to produce the substituted indole with the concomitant Pd(0) regeneration (Scheme 1.53).

Scheme 1.52 Pd(0)-Catalyzed Cyclization of *O*-Acyloximes and the Pd(II) Complex Generated from the Oxidative Addition of N-O Bond

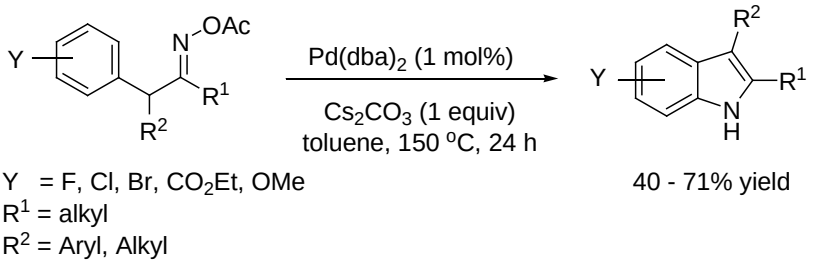

Y = F, Cl, Br, CO_2Et, OMe
R^1 = alkyl
R^2 = Aryl, Alkyl

40 - 71% yield

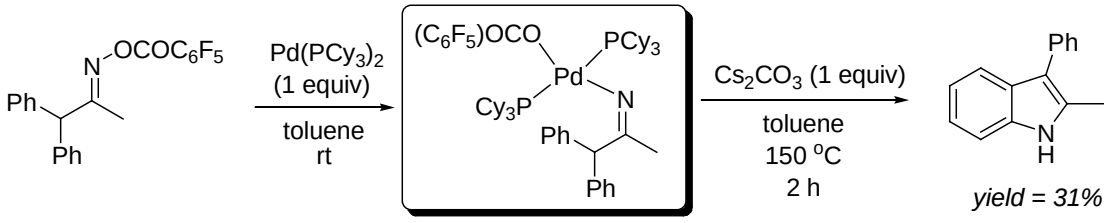

X-ray characterized
yield = 56%

yield = 31%

Scheme 1.53 Proposed Mechanism for Pd(0)-Catalyzed Cyclization of *O*-Acyloximes

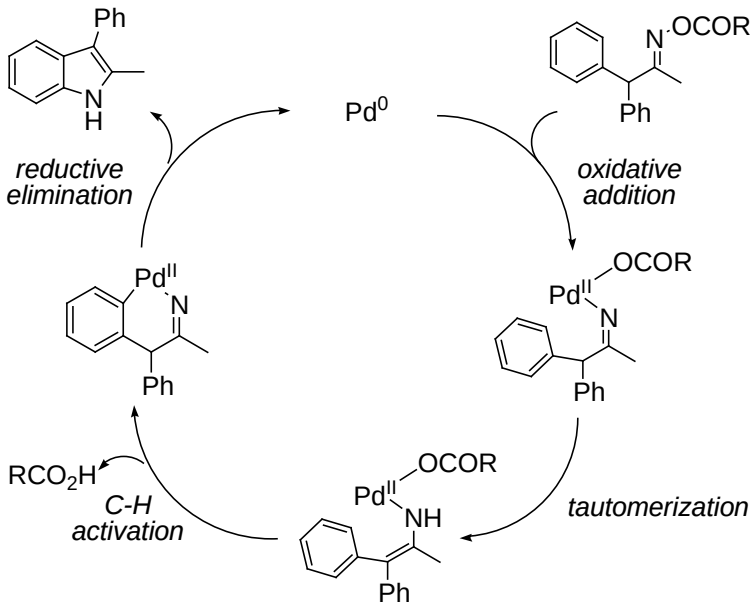

Scheme 1.54 General Mechanism for Intramolecular Arene C-H Amidation / Amination *via* the Pd(II)/(IV) Manifold

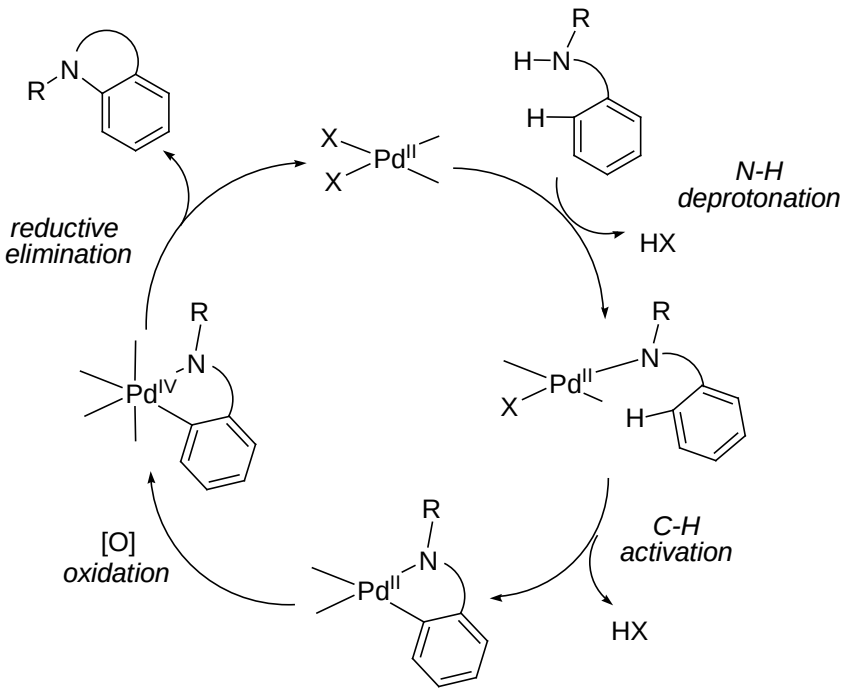

While the early examples of Pd-catalyzed intramolecular C-H activation / C-N bond formation were proposed to go through a Pd(0)/(II) catalytic cycle, Gaunt[49e] and Yu (J.-Q.)[49b,c] later demonstrated the plausible operation of Pd(II)/(IV) reaction manifold for the intramolecular C-N bond coupling, and the general mechanism was shown in Scheme 1.54.

In 2008, Gaunt and co-workers reported the Pd(II)-catalyzed cyclization of *N*-alkyl(2-aryl)anilines for the synthesis of *N*-alkylcarbazoles under mild reaction conditions.[49e] For Buchwald's Pd(II)-catalyzed cyclization of 2-phenylacetanilides, the reaction employed $Cu(OAc)_2$ and O_2 as oxidants and high temperature for success. In Gaunt's work on the Pd(II)-catalyzed intramolecular amination of *N*-alkyl(2-aryl)anilines employed $PhI(OAc)_2$ as oxidant, and the reaction proceeded smoothly even at room temperature furnishing *N*-alkylcarbazoles in good to excellent yields (Scheme 1.55). It was proposed that reaction would involve the formation of a Pd(IV) intermediate, which would undergo reductive elimination to effect the C-N bond formation.

Scheme 1.55 $Pd(OAc)_2$-Catalyzed Cyclization of *N*-alkyl(2-aryl)anilines at Room Temperature

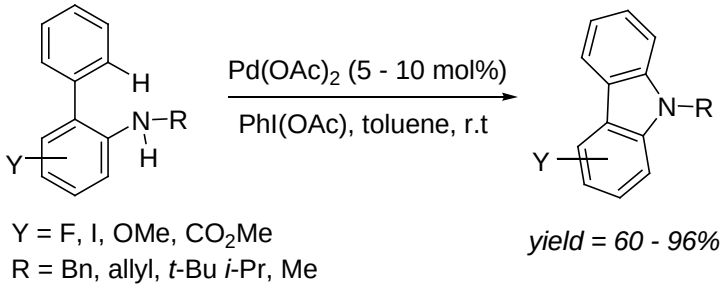

Y = F, I, OMe, CO_2Me
R = Bn, allyl, *t*-Bu *i*-Pr, Me

yield = 60 - 96%

Yu (J.-Q.) and co-workers recognized that the use of oxidants such as *N*-chlorosuccinimide and $PhI(OAc)_2$ in the intramolecular C-H amidation reaction could result in undesirable products (i.e., *ortho*-chlorination or *ortho*-acetoxylation products), and that it would adversely affect the yield for C-N bond coupled product. In this regard, it was proposed that the use of weakly / non-coordinating oxidants for the Pd-catalyzed intramolecular amidation should render C-N bond coupling predominant. In their study on the Pd(II)-catalyzed 2-phenylalkylamine cyclization, it was demonstrated that 1-fluoro-2,4,6-trimethylpyridinium triflate was a potent oxidant for effecting C-N bond coupling without any observable carbon-heteroatom bond formation (Scheme 1.56).[49b]

Scheme 1.56 Pd(II)-Catalyzed Intramolecular C-N Coupling with 1-Fluoro-2,4,6-trimethylpyridinium Triflate as Oxidant

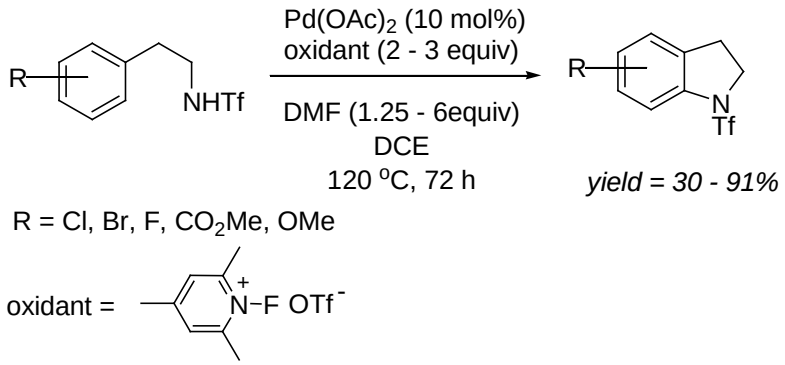

1.5.3.4 Pd-Catalyzed Intermolecular Arene *ortho*-C-H Amidations

While Pd-catalyzed intramolecular aromatic C-H activation / C-N fomration reactions have been extensively studied, the analogous intermolecular amidations are rare.

The Pd(II)-catalyzed intermolecular direct amidation of *O*-methyloximes was the first example reported by Yu (W.-Y.) and Che.[50d] Employing potassium persulfate ($K_2S_2O_8$) as oxidant, *O*-methyloximes and amides such as carbamates, arylsulfonylamides and acylamides can be effectively coupled under $Pd(OAc)_2$ catalysis (Scheme 1.57**)**. It is noteworthy that the amidation reaction with benzamide as reagent using the "$Pd(OAc)_2$ + $K_2S_2O_8$" protocol in the presence of methanol (3 equiv) gave methyl *N*-(2-methoxyphenyl)carbamate exclusively in quantitative yield

(Scheme 1.58). This result led to the hypothesis that a nitrene intermediate could have been involved, since the *N*-benzoylnitrene generated *in situ* should quickly undergo Hoffmann-Lossen rearrangement to give *N*-phenylisocyanate, which should further react with methanol to yield methyl *N*-phenylcarbamate. The proposed mechanism was depicted in Scheme 1.59.

Scheme 1.57 Pd(II)-Catalyzed Intermolecular Coupling of *O*-Methyloximes with Amides using Potassium Persulfate as Oxidant

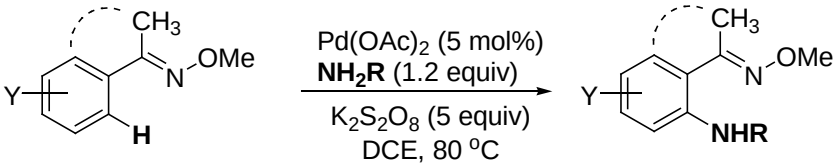

Y = Br, I, OMe
R = CO_2CH_3, $COCF_3$, CO_2tBu, SO_2CH_3
$SO_2(p\text{-}ClC_6H_4)$, $COCHC{=}CHC_6H_4$

yield = 68 - 95%

Scheme 1.58 Conversion of Benzamide to Methyl *N*-(2-Methoxyphenyl)carbamate

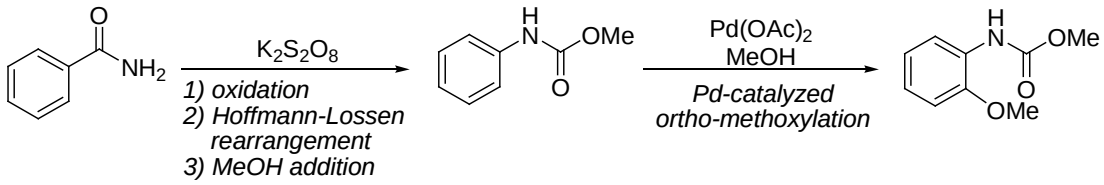

Scheme 1.59 Postulated Mechanism for Pd(II)-Catalyzed Intermolecular Amidation of *O*-Methyloximes

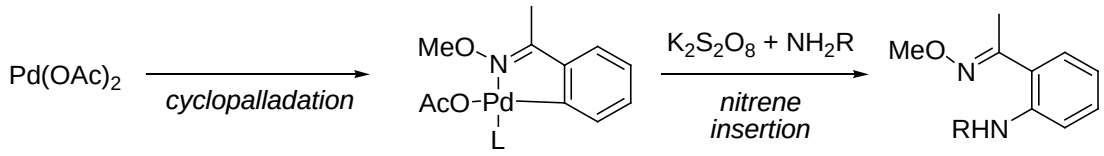

Sanford and co-workers examined the stoichiometric amidation reactions of cyclopalladated complexes with PhINTs. When the cyclopalladated complexes of benzo[*h*]quinoline was treated with PhINTs (1.3 equiv) in the presence of pyridine (8 equiv) in THF at room temperature the [(N~NTs)(Py)ClPd] was obtained in 78% yield (Scheme 1.60; N~NTs = tosylamidated benzo[*h*]quinoline, py = pyridine).[50c] Two possible mechanisms for the formation of "NTs-inserted" products were proposed — (A) a stepwise mechanism (formal Pd(IV)-imido formation) and (B) a concerted mechanism (Scheme 1.61). Although the two mechanisms were indistinguishable, Sanford suggested the nitrenoid mechanism is more likely due to the following reasons: (1) similar reactions of palladacycle with ArI=O and inorganic / organic peroxide were previously proposed to go through a similar Pd(IV)-oxo intermediate;[51] (2) the observation on the formation of chlorination and acetoxylation products of benzo[*h*]quinoline was consistent with a stepwise mechanism involving a Pd(IV) intermediate, since the concerted mechanism should exclusively lead to

amidation.

Scheme 1.60 Stoichiometric Amidation of Cyclopalladated Complexes of Benzo[*h*]quinoline with PhINTs

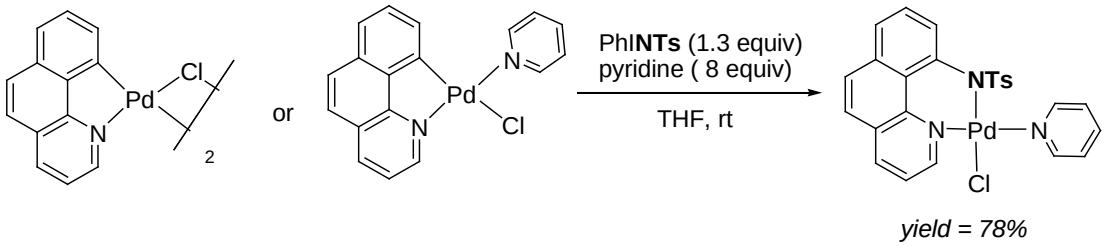

Scheme 1.61 Two Possible Mechanisms for "NTs-Insertion" into the Pd-C Bond

(A) Stepwise Mechanism

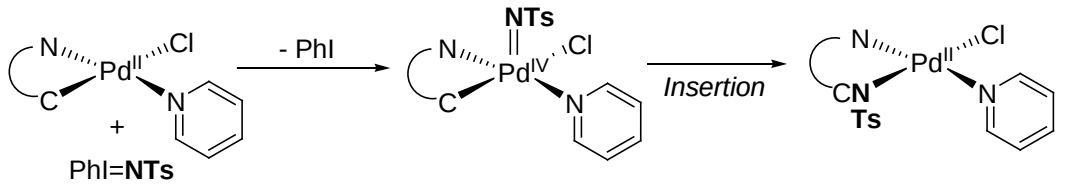

(B) Concerted Mechanism

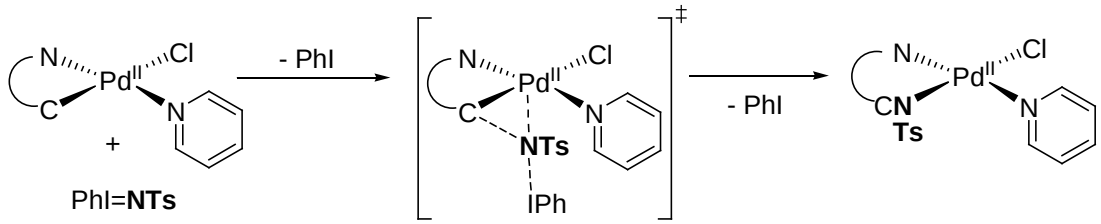

More recently, aromatic ketones were found to be effective substrates for the intermolecular amidation. According to Liu's study, treatment of alkyl aryl ketone with $Pd(OTf)_2$ (10 mol%), arylsulfonylamide (2 equiv) and

N-fluoro-2,4,6-trimethylpyridinium triflate (2 equiv) in 1,2-dichloroethane at 80 °C for 8 h afforded the *ortho*-amidation products in up to 82% yield (Scheme 1.62). The reaction was proposed to proceed *via* a Pd(II)/(IV) reaction manifold involving ketone-directed cyclopalladation. The oxidation of the amido-aryl-Pd(II) complex by *N*-fluoro-2,4,6-trimethylpyridinium triflate would generate the putative Pd(IV) intermediate; reductive elimination of which would afford the *ortho*-amidated aryl ketones.[50a]

Scheme 1.62 Pd-Catalyzed *ortho*-Amidation of Aryl Ketones

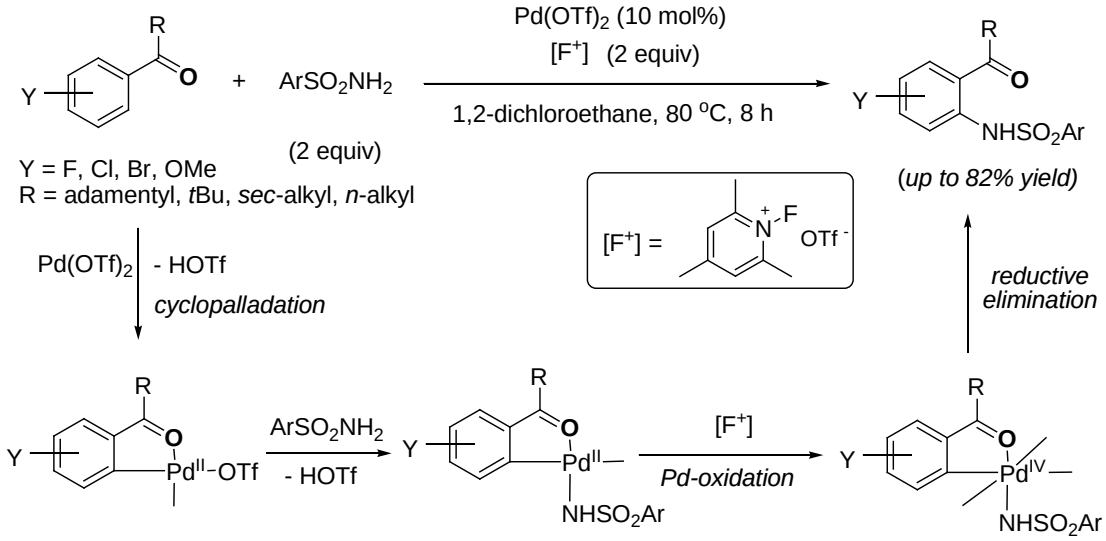

1.5.4 Copper-Catalyzed (Hetero)Arene C-H Amination

In 2009, Mori[52e] and Schreiber[52d] independently reported the pioneering works on Cu-catalyzed intermolecular direct heterocyclic C-H amination with dialkylamines. With $Cu(OAc)_2$ as catalyst, heterocycles such as azoles, benzothiazoles and *N*-methylbenzimidazoles effectively couple with *N*,*N*-dialkylamines in the presence of a base (e.g. NaOAc, Na_2CO_3) and O_2 as oxidant in toluene to afford C-2 amination products (Scheme 1.63). The reaction was proposed to be initiated by a base-assisted aryl C-H bond metalation followed by deprotonation and coordination of *N*,*N*-dialkylamine to give the (hetero)arylcopper-amido complex. The following reductive elimination of the complex would furnish the product arylamine, and the copper catalyst would be re-generated by re-oxidation with oxygen (Scheme 1.64). However, a radical mechanism involving single-electron transfer can also be possible.

Scheme 1.63 Copper-Catalyzed Direct Heterocyclic C-H Amination

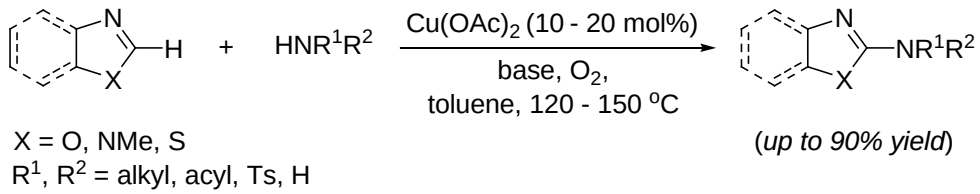

X = O, NMe, S
R^1, R^2 = alkyl, acyl, Ts, H

(*up to 90% yield*)

Scheme 1.64 Proposed Mechanism for the Copper-Catalyzed Heterocyclic C-H Amination

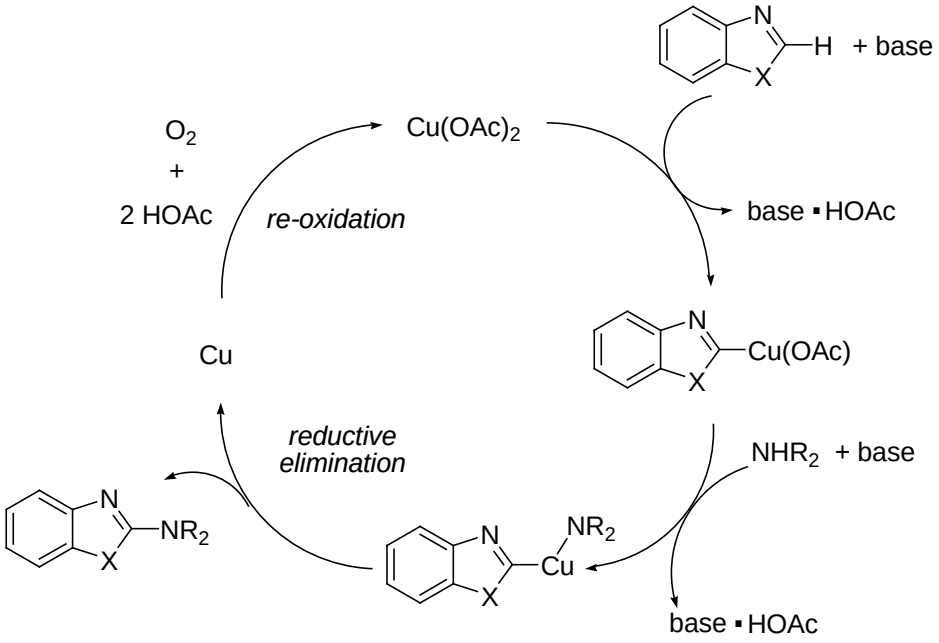

The substrate scopes of both arenes and amines for the Cu-catalyzed direct aromatic C-H amination reaction was further extended by Su and coworkers.[52b] In their study, with $Cu(OAc)_2$ as catalyst, potassium *tert*-butoxide as base and oxygen and TEMPO ((2,2,6,6-tetramethylpiperidin-1-yl)oxy) as oxidants, polyfluoroarenes effectively coupled with electron-deficient anilines in DMF at 40 ˚C to give highly functionalized diarylamines in up to 83% yields (Scheme 1.65).

Scheme 1.65 Copper-Catalyzed Aromatic C-H Amination of Polyfluoroarenes with Electron-deficient Anilines

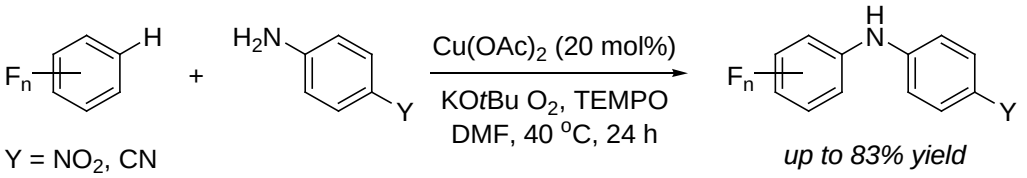

Interestingly, instead of using the "Cu(II) + O_2" couple for the Cu-catalyzed arene C-H amination, Miura and co-workers reported successful examples of Cu-catalyzed (hetero)aryl C-H amination using *N*-chloroamines[52c] and *O*-benzoylhydroxylamines[52a] as effective reagents. In their studies, treating the arene (e.g. benzoxazoles, polyfluorinated benzenes) with *N*-chloro / *N*-benzoyloxyamines (1.2 equiv), $Cu(OAc)_2$ (10 mol%), 1,10-phenanthroline (10 mol%) and lithium *tert*-butoxide (2 equiv) in 1,4-dioxane at room temperature afforded the corresponding arylamines in up to 84% yields (Scheme 1.66). It should be noted that the reaction temperature was significantly lower than that applied in the previously mentioned Cu-catalyzed cross coupling reactions of arenes and *N*-H *N*,*N*-dialkylamine. Regarding the reaction mechanism, Miura proposed that the reaction would proceed *via* initial base-assisted cupration of the arene, followed by oxidative addition of the N-X bond across the Cu(I) metal centre to give a aryl-amido-copper(III) complex, and reductive elimination would effect the C-N bond formation.

Scheme 1.66 Copper-Catalyzed Direct Aminations of (Benz)oxazoles and Polyfluorinated Arenes with *N*-Chloroamines and *O*-Benzoylhydroxylamines

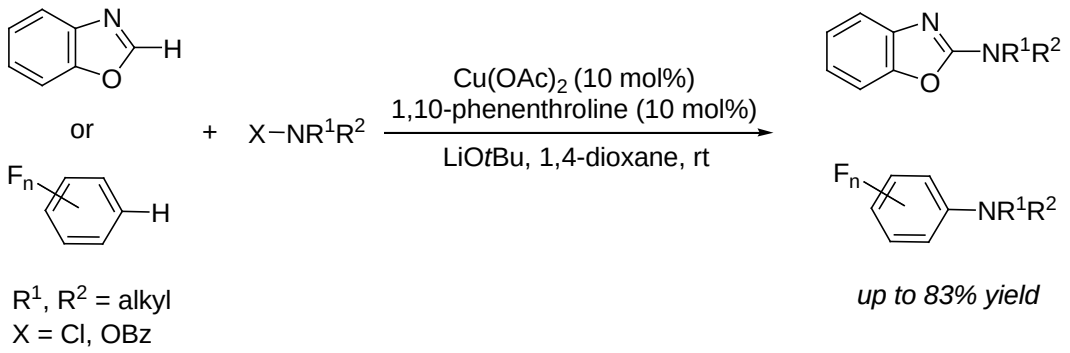

R^1, R^2 = alkyl
X = Cl, OBz

up to 83% yield

1.6 Aims and Objectives

In this research, we aim to develop efficient transition metal-catalyzed direct regioselective arene C-H amidation and amination methods.

Major advancements on catalytic C-H amidation based on the nitrenoid sp^3-C-H bond insertion reactions have been made, the arene C-H amidation has been challenging. Although various Pd(II)-catalyzed intramolecular aromatic C-H amidation reactions were reported, the related intermolecular reaction remained scarce. Our focus of the first part in this research is to develop a Pd(II)-catalyzed intermolecular C-H amidation reaction of pivalanilides with *N*-arylsulfonyloxycarbamates for synthesis of 2-aminoanilines and anthranilic acids, which are key intermediates for the synthesis of some pharmaceutically important

hetercycles.

In the second part of this thesis, we would pursue mechanistic investigation for the Pd-catalyzed arene C-H amidation reaction. We hope to determine the reaction rate orders for the reactants, and propose a mechanism based on our kinetic study.

Direct amination of unactivated arene C-H bonds has been a very challenging reaction. Since both arenes and amines are electron-rich molecules, and the π-electrons on the arenes would tend to repel nucleophilic amines. Little advances have been achieved by the Pd(II)-catalyzed intramolecular arene C-H activation / amination approach, the intermolecular counterpart has never been accomplished. In final part of this thesis, we employ an “umpolung strategy” to achieve the Rh(III)-catalyzed intermolecular arene C-H amination with electrophilic reagents such as *N*-chloroamines.

Chapter 2

Palladium-Catalyzed Intermolecular Aromatic C-H Bond Amidation

2.1 Introduction

2-Aminoaniline is a privileged structure found in many pharmaceutically important heterocycles such as benzimidazoles, 1,5-benzodiazepines, quinoxalines and benzotriazoles.[53] Notable examples include omaprazoles (Nexium), olanzapine (Zyprexa) and bromonidine (Alphagan P) (Figure 2.1).

Figure 2.1 Examples of Pharmaceuticals with a 2-Aminoaniline Scaffold

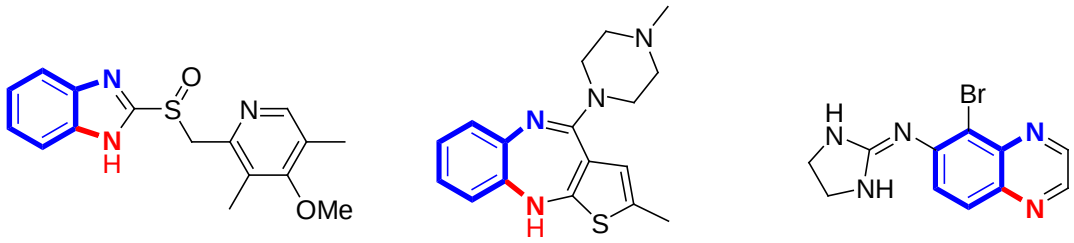

Nexium
for dyspepsia

Zyprexa
for pyschotic disorder

Alphagan P
for glaucoma

Conventionally, the synthesis of 2-aminoanilines involves a nucleophilic

substitution-nitro group reduction sequence with 2-fluoronitrobenzene as starting material. Alternatively, an electrophilic nitration of anilines followed by nitro group reduction is also known (Scheme 2.1).[1a,c] However, apart from the requirement of a functionalized substrates, these routes suffer from poor synthetic efficiency and a limited substrate scope.

Scheme 2.1 Conventional Methods for Synthesis of 2-Aminoanilines

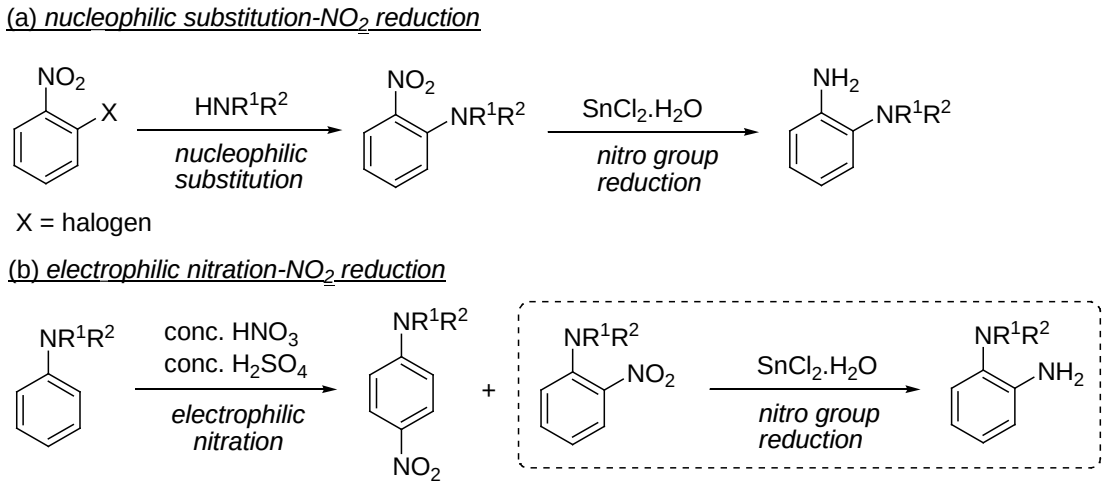

Chelation-assisted Pd-catalyzed *ortho*-C-H activation for C-C bond formation have received considerable attention over the past decade.[40] With an amide function as a directing group, anilide has been frequently employed as substrate for the C-H functionalization reactions. Notable examples include alkenylation,[41b,g,h,j] arylation,[41d,f] alkylation[41i] and carboxylation.[41a] It is conceivable that the direct

ortho-C-H amidation of anilides would afford 2-aminoaniline derivatives in one step (Scheme 2.2). In this work, we investigated the *ortho*-C-H amidation of anilides by *N*-arylsulfonyloxycarbamates.

Scheme 2.2 Catalytic Direct *ortho*-C-H Amidation

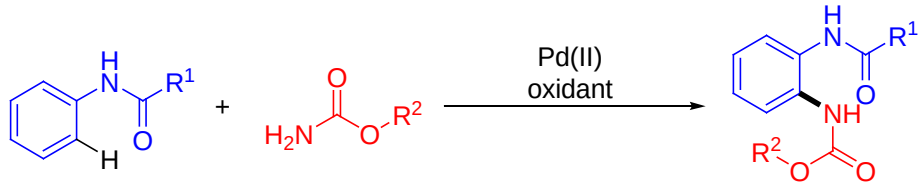

2.2 Pd-Catalyzed Direct Aromatic C-H Bond Amidation of Anilides

At the beginning, we tested the amidation reaction of 2,4-dimethylpivalanilide (**1a**) with ethyl carbamate (1 equiv), $Pd(OAc)_2$ (10 mol%), $K_2S_2O_8$ (5 equiv), AcOH (20 equiv) in 1,2-dichloroethane at 100 °C for 14 h. However, the expected amide **3aa** was not obtained, and **1a** was almost completely recovered (Table 2.1, entry 1). While there are many successful examples of Pd(II)-catalyzed *ortho*-C-H functionalizations of anilides,[41] the "$K_2S_2O_8$ + carbamate" protocol is apparently not applicable to the C-H amidation of anilides. This prompted us to search for a more general protocol for the C-H amidation.

We hypothesized that cyclometalated palladium(II) complexes could readily

react with nitrene to produce arylamide products *via* palladium-imido intermediates.[50b-d] According to the literature, *N*-arylsulfonyloxycarbamates were known to be nitrene precusors for Rh(II)-catalyzed amidation of sp^3 C-H bonds.[21] We surmised that *N*-arylsulfonyloxycarbamates or *N*-carbonyloxycarbamates would be effective reagents for the Pd(II)-catalyzed amidation of anilides. To test the effectiveness of these reagents, we prepared a series of carbamates— *N*-pivaloyloxy (OPiv); *N*-pentafluorobenzoyloxy (OPFB); *N*-tosyloxy (OTs) and *N*-nosyloxy (ONs) for the catalytic amidation.

Table 2.1 Study on the *N*-Leaving Group (Y) on Ethyl Carbamate[a]

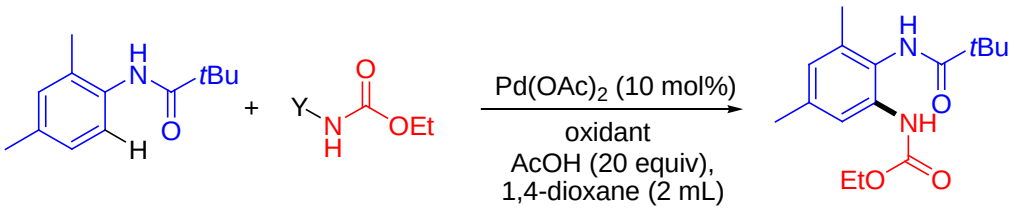

1a (1 equiv) **3aa**

entry	Y	oxidant (equiv)	temp (°C)	time (h)	conversion of **1a**[b] (%)	yield[b] (%)
1[c]	H	$K_2S_2O_8$ (5)	100	14	<5	0
2	OPiv	--	100	2	<5	0
3	OPFB	--	100	2	<5	<5
4	OPiv	--	120	18	<5	<5
5	OPFB	--	120	18	40	10
6	OTs	--	100	2	73	57
7	ONs	--	100	2	99	75, 70[d]
8[e]	ONs	--	100	2	<5	0

[a]Reaction conditions: 2,4-dimethylpivalanilide (0.2 mmol), *N*-Y carbamate (1 equiv),

$Pd(OAc)_2$ (10 mol%), additives, 1,4-dioxane (2 mL). TsO = *p*-toluenesulfonyloxy; OPiv = 2,2-dimethylpropionyloxy (pivaloyloxy); OPFB = pentafluorobenzoyloxy; NsO = *p*-nitrobenzenesulfonyloxy. [b]Conversions and yields were determined by ^1H NMR with dibromomethane as internal standard. [c]Reaction was performed in 1,2-dichloroethane (2 mL). [d] Isolated yields. [e]No $Pd(OAc)_2$.

When **1a** was treated with ethyl *N*-pivaloyloxycarbamate (1 equiv), $Pd(OAc)_2$ (10 mol%) and AcOH (20 equiv) in 1,4-dioxane at 100 °C for 2 h, no **3aa** formation was observed (entry 2). With ethyl *N*-pentafluorobenzoyloxycarbamate as reagent, <5% of **3aa** was obtained (entry 3). Increasing the reaction temperature to 120 °C and extending the reaction time to 18 h afforded **3aa** in less than 5% yield for the reaction with ethyl *N*-pivaloyloxycarbamate (entry 4). Likewise, 10% yield of **3aa** was obtained for the reaction with ethyl *N*-pentafluorobenzoyloxycarbamate (entry 5). Gratifyingly, when ethyl *N*-tosyloxycarbamate was employed, **3aa** was produced in 57% yield (entry 6). When ethyl *N*-nosyloxycarbamate (**2aNs**) was used for the amidation, **3aa** was isolated in 70% yield (entry 7). Notably, without $Pd(OAc)_2$, no **3aa** formation was detected with **1a** being completely recovered (entry 8).

2.2.1 Reaction Optimization

Table 2.2 depicts the temperature effect on the amidation reaction with *N*-nosyloxycarbamate as reagent. Performing the reaction at 120 °C, we obtained **3aa** in 70% yield (entry 2), which is comparable to the result of 100 °C (entry 1). A similar result was obtained when performing the reaction at 90 °C for 6 h (entry 3). When the reaction temperature was adjusted to 80 °C, 84% of **3aa** was obtained (entry 4). However, performing the reaction at lower temperatures (i.e. 70 °C and 60 °C) with prolonged reaction time did not give better results (entries 5 and 6).

Table 2.2 Temperature Effect[a]

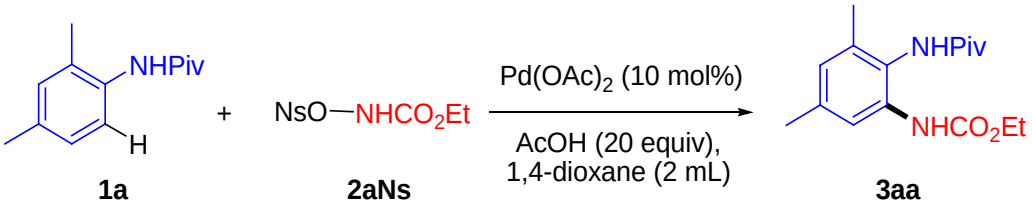

1a **2aNs** **3aa**

entry	temp (˚C)	time (h)	yield (%)[b]
1	100	2	75, 70[c]
2	120	2	70
3	90	6	75
4	80	6	84, 75[c]
5	70	12	79
6	60	16	64

[a]Reaction conditions: **1a** (0.2 mmol), **2aNs** (1 equiv), $Pd(OAc)_2$ (10 mol%), AcOH (20 equiv), 1,4-dioxane (2 mL). [b]Yields were determined by ^1H NMR with dibromomethane as internal standard. [c]Isolated yields.

Table 2.3 depicts the results with various solvents. While 1,4-dioxane provided **3aa** in 84% yield (entry 1), less polar solvents such as 1,2-dichloroethane and toluene were found to afford moderate yields of 58 — 67% (entries 2 and 3). With THF as solvent, **3aa** was obtained in 34% yield (entry 4). Poor yield of **3aa** was obtained when using DMA (12%) and DMF (28%) as solvents (entries 5 — 6). Acetonitrile was an ineffective solvent for the amidation (entry 7). Notably the reaction was equally effective without AcOH as co-solvent, and **3aa** was produced in 76% yield (entry 8).

Table 2.3 Solvent Effect[a]

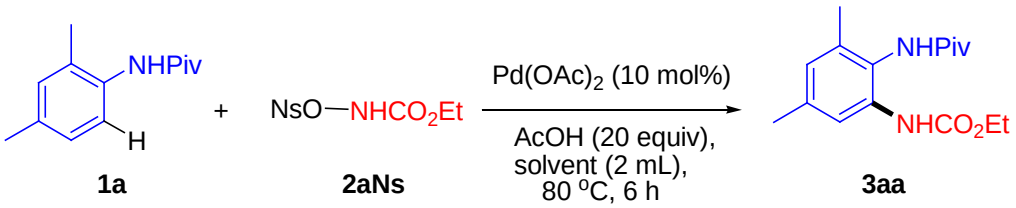

1a **2aNs** **3aa**

entry	solvent	yield (%)[b]
1	1,4-dioxane	84, 75[c]
2	toluene	58
3	1,2-dichloroethane	67
4	THF	34
5	DMA	12
6	DMF	28
7	MeCN	0
8[d]	1,4-dioxane	76

[a]Reaction conditions: **1a** (0.2 mmol), **2aNs** (1 equiv), $Pd(OAc)_2$ (10 mol%), AcOH (20 equiv), solvent (2 mL). [b]Yields were determined by ^1H NMR with dibromomethane as internal standard. [c]Isolated yields. [d]No AcOH was added.

Furthermore, we evaluated some Pd(II) complexes for the catalytic C-H amidation (Table 2.4). With $Pd(TFA)_2$ as catalyst, **3aa** was obtained in 78% yield. This result is comparable to the reaction with $Pd(OAc)_2$ as catalyst (entry 2). When $Pd(OPiv)_2$ was used, the yield of **3aa** was improved to 86% (entry 3). However, when a palladium(II) catalyst with non-carboxylate ligands such as $[PdCl_2(MeCN)_2]$ was employed, the product yield was diminished to 56% (entry 4). In this work, we found that when $[Pd(OTs)_2(MeCN)_2]$ was chosen as catalyst, **3aa** was produced in 86% yield (entry 5). This is in agreement with the earlier findings by Yu's and Jone's research groups on Pd-catalyzed *ortho*-C-H bond carboxylation of anilides and urea. After considering the ease of catalyst preparation, $[Pd(OTs)_2(MeCN)_2]$ was chosen for further optimization.

Table 2.4 Catalyst Screening[a]

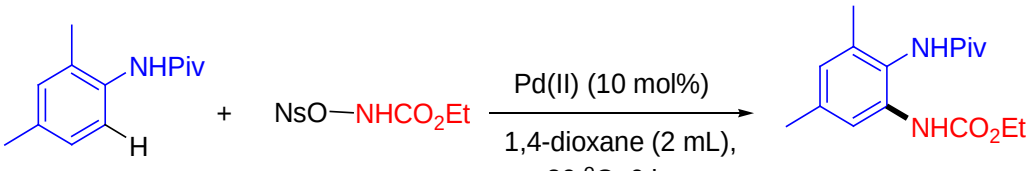

1a **2aNs** **3aa**

entry	Pd(II) (10 mol%)	yield (%)[b]
1	$Pd(OAc)_2$	76%
2	$Pd(TFA)_2$	78%
3	$Pd(OPiv)_2$	86%
4	$[PdCl_2(MeCN)_2]$	56%
5	$[Pd(OTs)_2(MeCN)_2]$	86%

[a]Reaction conditions: **1a** (0.2 mmol), **2aNs** (1 equiv), Pd(II) (10 mol%), 1,4-dioxane (2 mL). [b]Yields were determined by ^{1}H NMR with dibromomethane as internal standard.

Effect of the amounts of **2aNs** and [$Pd(OTs)_2(MeCN)_2$] was also examined, and the results were shown in Table 2.5. When the amount of **2aNs** was increased to 0.24 mmol, **3aa** was formed in 90% yield (entry 2). However, employing 0.30 mmol of **2aNs** resulted in a lower yield of 67% (entry 3). When 5 mol% of [$Pd(OTs)_2(MeCN)_2$] was used, **3aa** was obtained in 83% yield (entry 4). Extended reaction time of 15 h gave a similar yield of 85% (entry 5). Lowering the catalyst loading to 1 mol%, **3aa** was formed in 45% yield (entry 6). Running the reaction for 15 h with 1 mol% of catalyst did not improve the yield (entry 7).

Thus, the optimal reaction conditions for the anilide amidation were found to be: **1a** (0.2 mmol), **2aNs** (1.2 equiv) and [$Pd(OTs)_2(MeCN)_2$] (10 mol%) in 1,4-dioxane (2 mL) at 80 °C for 6 h, and **3aa** was obtained in 84% isolated yield.

Table 2.5 Effect of **2aNs** Amount and Catalyst Loading[a]

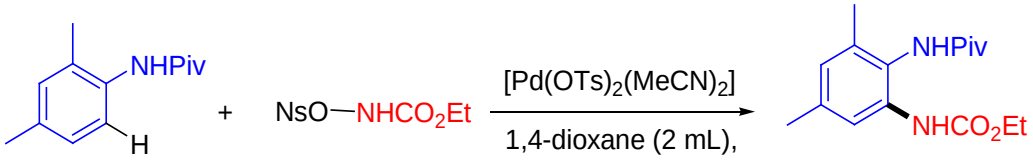

1a **2aNs** **3aa**

entry	**2aNs** (mmol)	$[Pd(OTs)_2(MeCN)_2]$ (mol%)	time (h)	yield (%)[b]
1	0.20	10	6	86
2	0.24	10	6	90, 84[c]
3	0.30	10	6	67
4	0.24	5	6	83
5	0.24	5	15	85
6	0.24	1	6	46
7	0.24	1	15	45

[a]Reaction conditions: **1a** (0.2 mmol), **2aNs**, $[Pd(OTs)_2(MeCN)_2]$, 1,4-dioxane (2 mL). [b]Yields were determined by ^1H NMR with dibromomethane as internal standard. [c]Isolated yields.

2.2.2 Scopes and Limitations

With the optimized conditions in hand, we turned to examine the scope of the Pd-catalyzed amidation reaction (Table 2.6). Acetanilides and benzamides were converted to their respective amides **3ba** (52%) and **3ca** (57%). However, pivalanilides produced better product yields (**3aa**: 84% yield), presumably due to the favorable conformational properties of the *tert*-butyl group. Analogous to this finding, substrates with a tertiary amide group were found to undergo facile *ortho*-C-H

amidation in 68—85% yields for **3da**—**3fa**. We considered that the synthetic applications of this C-H amidation reaction would be enhanced if amide groups of orthogonal reactivity can be introduced to the anilides. Thus, further transformations of the anilide scaffolds can be pursued by selective manipulation of the nitrogen protecting groups. In this work, the C-H amidation reactions with 2,2,2-trichloroethyl (Troc) *N*-nosyloxycarbamate **2b** and benzyl *N*-nosyloxycarbamate **2c** as reagents afforded the corresponding amides **3ab** and **3ac** in 87% and 75% yields, respectively.

Electron-donating (Me, benzyl, OMe) and -withdrawing (F, Cl, Br) groups were well tolerated under the amidation conditions, and **3ga—3oa** was furnished in 45—82% yields. 3,4-Dimethylpivalanilide (**1p**) and 1-pivalamidonaphthanlene (**1q**) were also amidated to **3pa** (73%) and **3qa** (72%). Interestingly, anilides bearing a vinyl substituent can be transformed to the expected amide **3ra** in 50% yield. Noted that 40% of the starting anilide was recovered after the reaction; this reaction exhibits a mass balance of about 85%. Liu and Xu reported earlier that *O*-pivaloyl esters would undergo Pd-catalyzed *ortho*-C-H arylations.[54] In this work, treating the pivalanilide containing a pivaloyl ester moiety with **2a** afforded **3sa** exclusively in 67% yield. This result indicates that the amide group is a stronger directing group than the ester group.

Table 2.6 Reaction Scope [a,b]

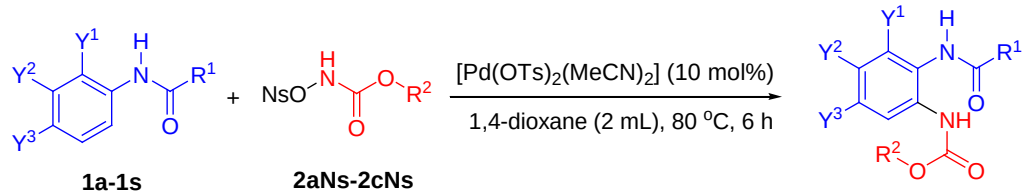

1a-1s + **2aNs-2cNs** → **3aa-3sa, 3ab, 3ac**

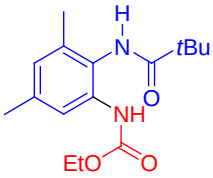

3aa, 84%

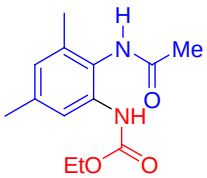

3ba, 52%

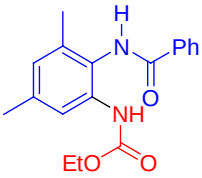

3ca, 57%

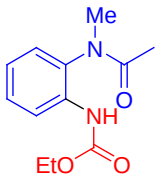

3da, 72%

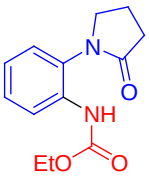

3ea, 85%

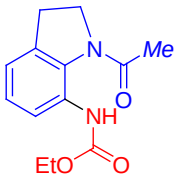

3fa, 68%

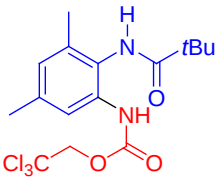

3ab, 87%

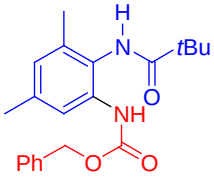

3ac, 75%

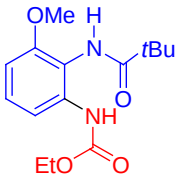

3ga, 62%

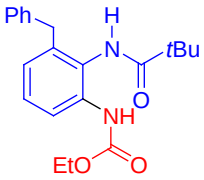

3ha, 70%

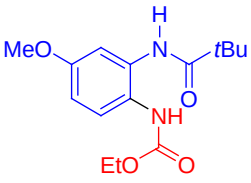

3ia, 45%

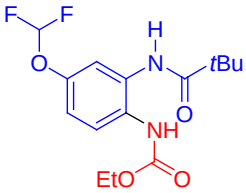

3ja, 60%

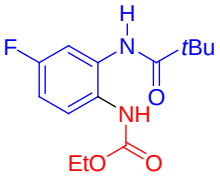

3ka, 66%

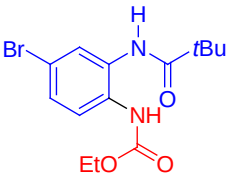

3la, 68%

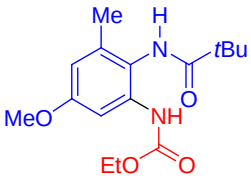

3ma, 59%

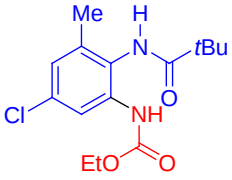

3na, 65%

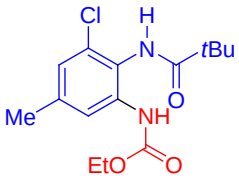

3oa, 82%

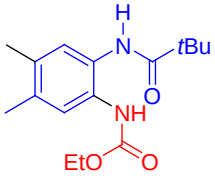

3pa, 73%

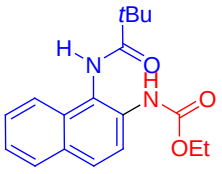

3qa, 72%

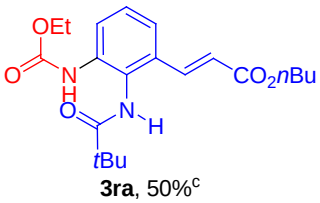

3ra, 50%[c]

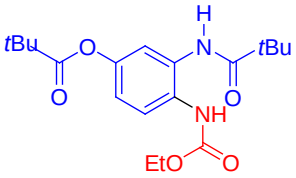

3sa, 67%[d]

[a]Reaction conditons: anilide (0.2 mmol), *N*-nosyloxycarbamate (1.2 equiv), $[Pd(OTs)_2(MeCN)_2]$ (10 mol%), 1,4-dioxane (2 mL), 80 °C, 6 h. [b]Isolated yields. [c]Batchwise addition of **2a** (2 × 1.2 equiv / 6 h), 12 h; 40% starting anilide was recovered. [d]Reaction run for 12 h.

2.3 Anthranilic Acid Synthesis *via* Pd-Catalyzed Direct Aromatic C-H Bond Amidation of Benzoic Acids

Encouraged by the success in catalytic *ortho*-C-H amidation of anilides, we hoped to extend the current method to synthesize other synthetically important molecules.

Anthranilic acids are key building blocks to a large variety of pharmaceutically important heterocycles such as acridinones, indoles, quinazolinones, and benzoxazinones.[55] The current industial method for the production of anthranilic acid involves the ring opening of phthalic anhydride by ammonia, followed by Hofmann rearrangement with hypochlorite (Scheme 2.3, route A). For the synthesis of substituted anthranilic acids, Sandmeyer methodology[56] (Scheme 2.3, route B), Ullmann reactions[57] and Buchwald-Hartwig type amination[4] of *ortho*-haloabenzoic acids (Scheme 2.3, route C) were also known to be effective routes. We envisioned that the direct *ortho*-amidation of benzoic acids would furnish anthranilic acid derivatives in one step.

Scheme 2.3 Synthesis of Anthranilic Acids

(A) Industrial Method for Simple Anthranilic Acid

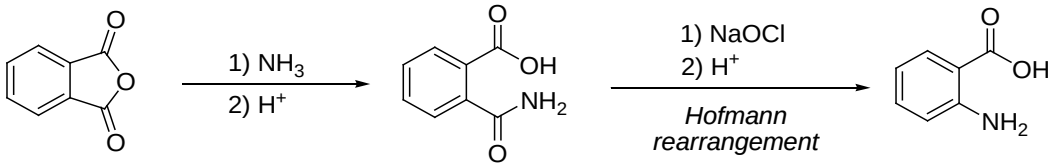

(B) Sandmeyer Method

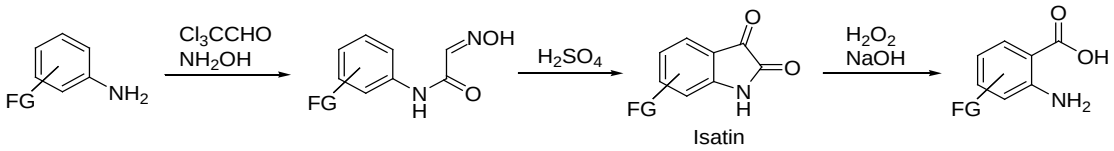

(C) Ullmann coupling / Buchwald-Hartwig Type Amination

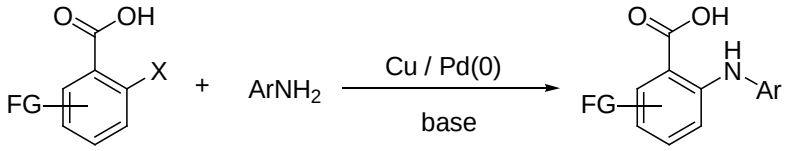

However, when compared to those substrates with nitrogen donor groups, benzoic acids bearing a carboxylate as directing group are less common substrates for catalytic *ortho*-C-H functionalizations. Pioneering works reported by Yu[58] and Daugulis[44a] revealed the direct *ortho*-C-H functionalization of benzoic acids, presumably *via* the cyclometalated palladium(II) complexes.[47b] Examples of direct regioselective amidation of benzoic acids are rare.

To test the feasibility of direct benzoic acid amidation, we treated 3,4-dimethylbenozic acid (**4a**, 0.2 mmol) with ethyl *N*-nosyloxycarbamate (**2aNs**, 1.2 equiv; batchwise addition: 4 × 0.3 equiv / 3 h), K_2CO_3 (1 equiv) and a stoichiometric amount of $Pd(OAc)_2$ (1 equiv) in 1,4-dioxane (2 mL) at 80 °C for 12 h (Table 2.7,

entry 1), and the desired anthranilic acid **5aa** was obtained in 30% yield. The reaction did not occur in the absence of either K_2CO_3 or $Pd(OAc)_2$ (entries 2 and 3). The requirement of K_2CO_3 for benzoic acid functionalization is consistent with the earlier report by Yu and co-workers.[58e] Motivated by these findings, we turned to develop a catalytic transformation.

Table 2.7 Stoichiometric Pd-mediated *ortho*-Amidation of 3,4-Dimethylbenzoic Acid[a]

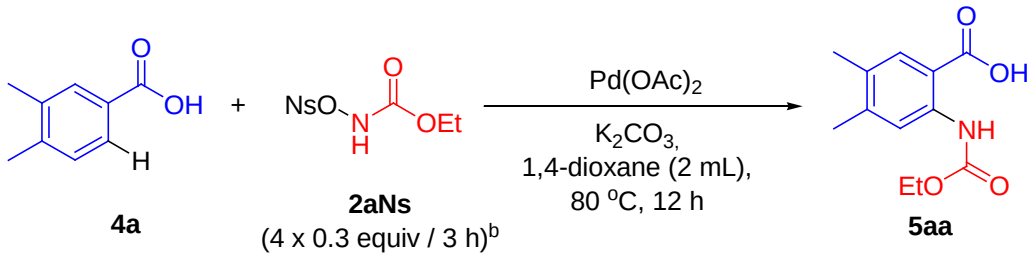

4a **2aNs** (4 x 0.3 equiv / 3 h)[b] **5aa**

entry	$Pd(OAc)_2$ (equiv)	K_2CO_3 (equiv)	conversion of **4a** (%)[c]	yield (%)[d]
1	1	1	92	30
2	1	--	<5	0
3	--	1	<5	0

[a]Reaction conditons: **4a** (0.2 mmol), **2aNs** (1.2 equiv), K_2CO_3, $Pd(OAc)_2$, 1,4-dioxane (2 mL), 80 °C, 12 h. [b]Batchwise addition of **2aNs** (4 × 0.3 equiv / 3 h). [c]Conversions were determined by ^1H NMR with dibromomethane as internal standard. [d]Isolated yields.

2.3.1 Reaction Optimization

We first evaluated the effect of carbamate reagents bearing different *N*-leaving groups (Table 2.8). To begin, we performed the reaction with ethyl *N*-nosyloxycarbamate as reagent, sodium benzoate (**4aNa**) as substrate and a catalytic amount of $Pd(OAc)_2$ (10 mol%) in 1,4-dioxane (2 mL) at 90 °C for 4 h, and only a trace amount of **5aa** was produced (entry 1, <5%). Interestingly, when *N*-tosylate (OTs) was employed as the leaving group, **5aa** was obtained in 27% yield (entry 2). With *N*-mesitylsulfonate (OMes) as the leaving group, a comparable yield of 30% was obtained (entry 3). Unlike the analogous amidations of anilides, ethyl *N*-pentafluorobenzoate (PFB) and *N*-pivalate (OPiv) carbamates were effective reagents for the benzoic acid amidation with **5aa** being obtained in 25% and 32%, respectively. Notably, when ethyl *N*-mesitylsulfonyloxycarbamate (**2aMes**) was employed as reagent, the reaction exhibited better mass balance than the reaction with ethyl *N*-pivaloyloxycarbamate as reagent (entry 3 vs. entry 5). Therefore, **2aMes** was chosen for further reaction optimization.

Table 2.8 Effect of the *N*-Leaving Groups on Ethyl Carbamate[a]

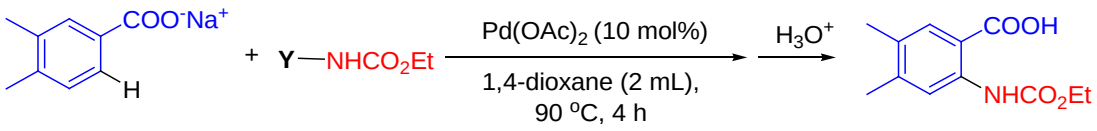

4aNa (4 x 0.3 equiv / h)[b] **5aa**

entry	Y	conversion of **4aNa** (%)[c]	yield (%)[c]
1	NsO	50	<5
2	TsO	50	27
3	MesO	67	30
4	PFB	64	25
5	PivO	76	32

[a]Reaction conditons: **4aNa** (0.2 mmol), ethyl *N*-Y carbamate (1.2 equiv), $Pd(OAc)_2$ (10 mol%), 1,4-dioxane (2 mL), 90 °C, 4 h. [b]Batchwise addition of ethyl *N*-Y carbamate (4 × 0.3 equiv / 1 h). [c]Conversions and yields were determined by ^1H NMR with dibromomethane as internal standard.

Next, we investigated the effect of counter ions (Table 2.9). Without counter ions, 3,4-dimethylbenzoic acid (**4a**) is an ineffective substrate for the amidation (entry 1). When lithium benzoate (**4aLi**) was treated with **2aMes** (1.2 equiv; batchwise addition: 4 × 0.3 equiv / h) and $Pd(OAc)_2$ (10 mol%) in 1,4-dioxane (2 mL) at 90 °C for 4 h, **5aa** was obtained in 40% yield (entry 2). However, with the same reaction conditions, potassium benzoate and tetrabutylammonium benzoate were less effective substrates, and **5aa** were obtained in 16% and 14% yields, respectively (entries 4—5). Based on the above findings, the effectiveness of the reaction was apparently affected by the size of the counter ions in a descending order: $Li^+ > Na^+ > K^+ \sim= (n\text{-}Bu)_4N^+$; the

harder the counter ion, the more effective the reaction. Probably, the harder counter ions would induce a stronger polarization effect on the benzoate resulting in a stronger covalent metal-carboxylate linkage, with which the formation of the κ^1-benzoate-palladium(II) complex should be more favorable than that of the κ^2-benzoate-palladium(II) complex. Therefore, the proximal *ortho*-C-H bond of lithium benzoate could be more readily activated to generate the cyclopalladated complex (Scheme 2.4).

Table 2.9 Effect of Counter Ion[a]

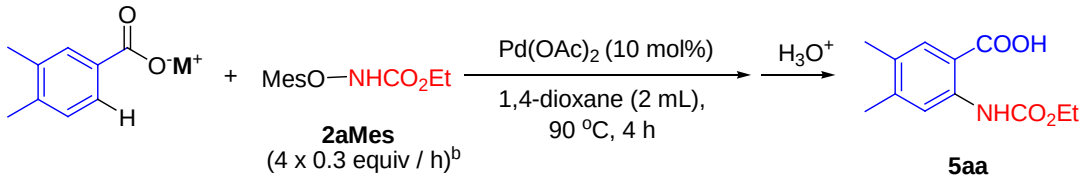

Entry	M^+	yield (%)[c]
1	H^+	0
2	Li^+	40
3	Na^+	30
4	K^+	16
5	$(n\text{-Bu})_4N^+$	14

[a]Reaction conditons: 3,4-dimethylbenzoate (0.2 mmol), **2aMes** (1.2 equiv), $Pd(OAc)_2$ (10 mol%), 1,4-dioxane (2 mL), 90 °C, 4 h. [b]Batchwise addition of **2aMes** (4 × 0.3 equiv / 1 h). [c]Yields were determined by ^1H NMR with dibromomethane as internal standard.

Scheme 2.4 Cyclopalladation of Benzoates

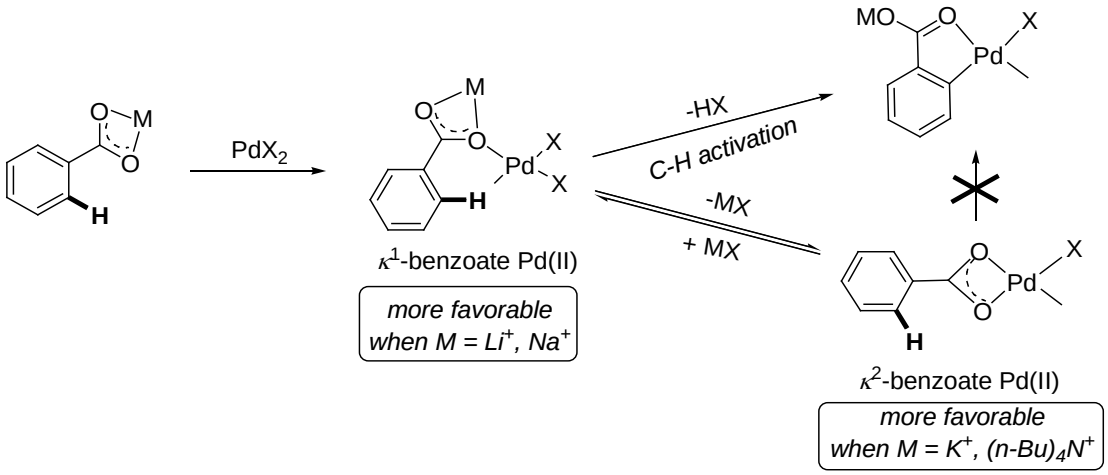

We also examined the effect of the addition method of **2aMes** to the amidation (Table 2.10). Batchwise addition and syringe pump addition of **2aMes** gave similar yields (~40%) of **5aa** (entries 1 — 2). Increasing the amount of **2aMes** to 1.5 equiv with syringe pump addition at the same rate (0.3 equiv / h) afforded **5aa** in 45% yield (entry 3). When the reaction was carried out under a nitrogen atmosphere with 1.5 equivalent of **2aMes** being added by a syringe pump at a rate of 0.3 equiv / h, the yield of **5aa** was improved to 52% (entry 4). Therefore, syringe pump addition of **2aMes** under a nitrogen atmosphere was employed for further optimization study.

Table 2.10 Effect of the Amount and Addition Method of **2aMes**[a]

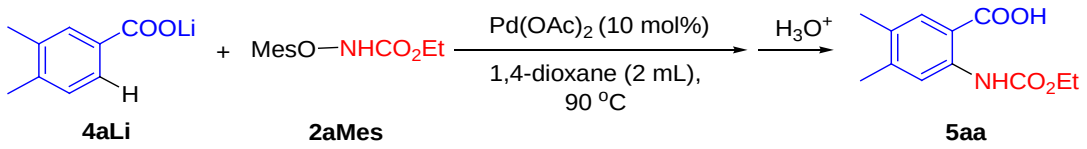

4aLi **2aMes** **5aa**

entry	**2aMes** (equiv)	addition method[b]	rate	time (h)	yield (%)[c]
1	1.2	A	4 × 0.3 equiv / h	4	40
2	1.2	B	0.3 equiv / h	4	41
3	1.5	B	0.3 equiv / h	6	45
4[d]	1.5	B	0.3 equiv / h	6	52

[a]Reaction conditons: **4aLi** (0.2 mmol), **2aMes**, $Pd(OAc)_2$ (10 mol%), 1,4-dioxane (2 mL), 90 °C, 4 h. [b]A = batchwise addition of **2aMes**; B = dropwise addition of **2aMes** by a syringe pump. [c]Yields were determined by ^1H NMR with dibromomethane as internal standard. [d]Reaction was performed under N_2.

In the catalytic cycle, AcOH and MesOH would be generated as side products. The accumulation of the acids may eventually turn the benzoate salt back to benzoic acid, which was shown to be an ineffective substrate for the amidation. As anticipated, when KOAc (1 equiv) was added to the reaction mixture, 65% of **5aa** was obtained (Table 2.11, entry 2). However, the use of KOPiv (1 equiv) led to lower **5aa** yield of 41% (entry 3). With K_2HPO_4 (1 equiv) or $KHCO_3$ (1 equiv) as base, **5aa** was produced in 54% and 59%, respectively (entries 4 — 5). When 0.5 equivalent of K_2CO_3 was used, 60% yield of **5aa** was obtained (entry 6). Increasing the amount of K_2CO_3 to 0.75 did not improve the yield (56%) of **5aa** (entry 7). Similarly, with 1 equivalent of K_2CO_3, **5aa** was obtained in 48% yield (entry 8). Probably, a larger

amount of K_2CO_3 would lead to faster decomposition of **2aMes** and lower the product yields.

Table 2.11 Effect of Base[a]

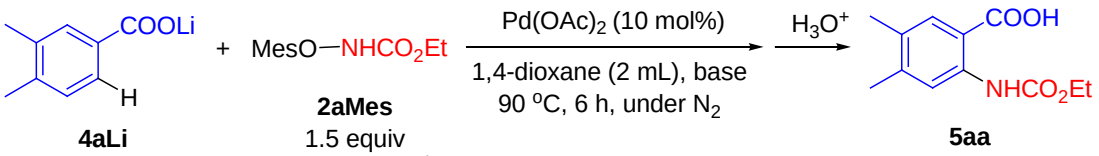

entry	base (equiv)	yield (%)[c]
1	--	52
2	KOAc (1.0)	65, 63[d]
3	KOPiv (1.0)	41
4	K_2HPO_4 (1.0)	54
5	$KHCO_3$ (1.0)	59
6	K_2CO_3 (0.5)	60
7	K_2CO_3 (0.75)	56
8	K_2CO_3 (1.0)	48

[a]Reaction conditons: **4aLi** (0.2 mmol), **2aMes** (1.5 equiv in 0.5 mL 1,4-dioxane), base, $Pd(OAc)_2$ (10 mol%), 1,4-dioxane (1.5 mL), 90 °C, 6 h, under N_2. [b]Syringe pump addition of **2aMes** at a rate of 0.3 equiv / h. [c]Yields were determined by ^1H NMR with dibromomethane as internal standard. [d]Isolated yield.

Solvent effect was also examined (Table 2.12). DMF, DMA and DMSO were undesirable solvents for the amidation, and **5aa** was formed in 5—20% yields (entries 1 — 3). Diglyme and 1,2-dichloroethane were effective solvents for the reaction, albeit with lower **5aa** yields of 45% (entries 4 — 5). Employing *tert*-butanol as solvent produced **5aa** in 57% yield (entry 6). Eventually, 1,4-dioxane remained the

best solvent on the basis of the product yield (entry 7, 65%).

Table 2.12 Effect of Solvent[a]

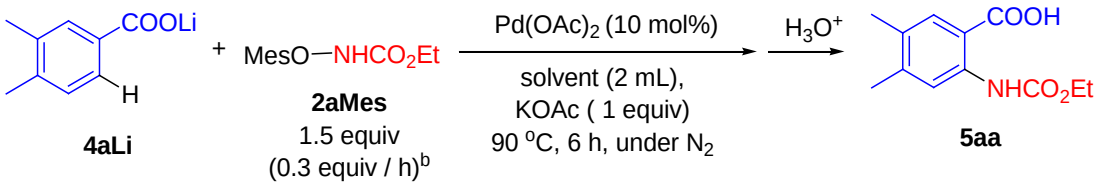

entry	solvent	yield (%)[c]
1	DMF	20
2	DMSO	5
3	DMA	13
4	diglyme	45
5	1,2-dichloroethane	45
6	*t*-butanol	57
7	1,4-dioxane	65, 63[d]

[a]Reaction conditons: **4aLi** (0.2 mmol), **2aMes** (1.5 equiv in 0.5 mL 1,4-dioxane), KOAc (1 equiv), $Pd(OAc)_2$ (10 mol%), solvent (1.5 mL), 90 °C, 6 h, under N_2. [b]Syringe pump addition of **2aMes** at a rate of 0.3 equiv / h. [c]Yields were determined by ^1H NMR with dibromomethane as internal standard. [d]Isolated yield.

Finally, we examined the temperature effect of the amidation (Table 2.13). When the reaction was performed at 130 °C, a diminished yield (20%) of **5aa** was obtained (entry 1). At 70 °C, the reaction produced **5aa** in 33% yield (entry 3). At 40 °C, less than 5% of **5aa** was obtained (entry 4). Thus, the optimal reaction conditions were found to be: **4aLi** (0.2 mmol), **2aMes** (1.5 equiv in 0.5 mL 1,4-dioxane; syringe pump addition: 0.3 equiv / h), KOAc (1 equiv) and $Pd(OAc)_2$ (10 mol%) in 1,4-dioxane at 90 °C under a nitrogen atmosphere for 6 h, and **5aa** was obtained in 63% isolated

yield.

Table 2.13 Effect of Temperature[a]

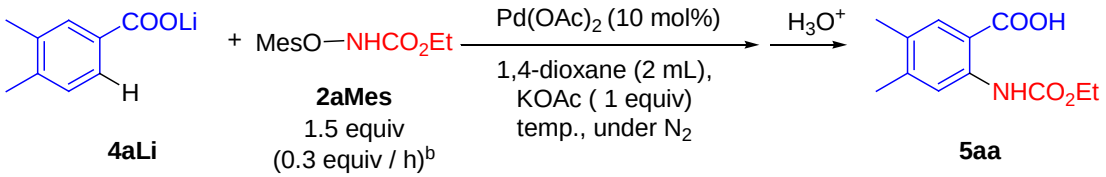

entry	temperature (°C)	time (h)	yield (%)[c]
1	130	4	20
2	90	6	65, 63[d]
3	70	6	33
4	40	18	<5

[a]Reaction conditons: **4aLi** (0.2 mmol), **2aMes** (1.5 equiv in 0.5 mL 1,4-dioxane), KOAc (1 equiv), $Pd(OAc)_2$ (10 mol%), 1,4-dioxane (1.5 mL), under N_2. [b]Syringe pump addition of **2aMes** at a rate of 0.3 equiv / h. [c]Yields were determined by ^1H NMR with dibromomethane as internal standard. [d]Isolated yield.

2.3.2 Scopes and Limitations

With the optimized conditions in hand, we examined the reaction scope (Table 2.14). In general, *meta*-substituted benzoic acids having electron-donating (-OMe, -Ph) and electron-withdrawing (-Cl, -Br, $-CF_3$) groups were transformed to the analogous anthranilic acids **5ba—5fa** in 47% — 70% yields. Since nitrene may be involved for the amidation, we tested the chemoselectivity of the reaction by employing lithium 2-benzylbenzoate (**4gLi**) as substrate. The amidation of **4gLi** with **2aMes** afforded

anthranilic acid **5ga** exclusively in 71% yield without benzylic C-H inserted product formation. The reactions with 2,4-disubstituted lithium benzoates were also examined. With lithium 2,4-dimethylbenzoate (**4hLi**) as substrate, the corresponding **5ha** was produced in 73% yield. When compared to **4hLi**, the reaction with 4-fluoro-2-methylbenzoate (**4iLi**) only afforded **5ia** in 46% yield. Probably, the C-H activation of electron-deficient arenes is slower than the electron-rich counterpart. Similarly, the methoxy group should be electron-withdrawing to the *meta*-C-H bond, the amidation of 2-methoxy-4-methylbenzoate (**4jLi**) resulted in 50% yield of **5ja**. Lithium benzoates with fused ring scaffolds were also effective substrates. For example, lithium 1,4-benzodioxane-6-carboxylate (**4kLi**) and lithium 2-naphthoate (**4lLi**) were transformed to the corresponding anthranilic acids **5ka** and **5la** in 40% and 55% yields, respectively. However, lithium 1-naphthoate (**4mLi**) is a less effective substrate, and **5ma** was produced in only 21% yield.

Table 2.14 Reaction Scope[a,b]

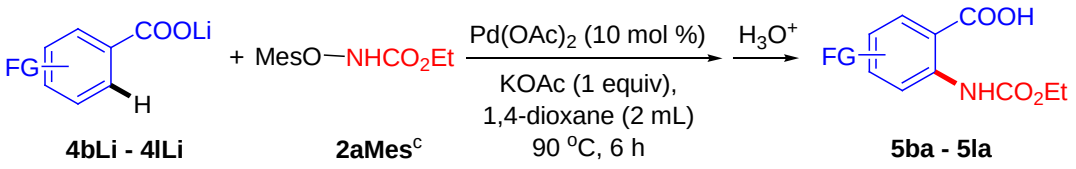

4bLi - 4lLi **2aMes**[c] **5ba - 5la**

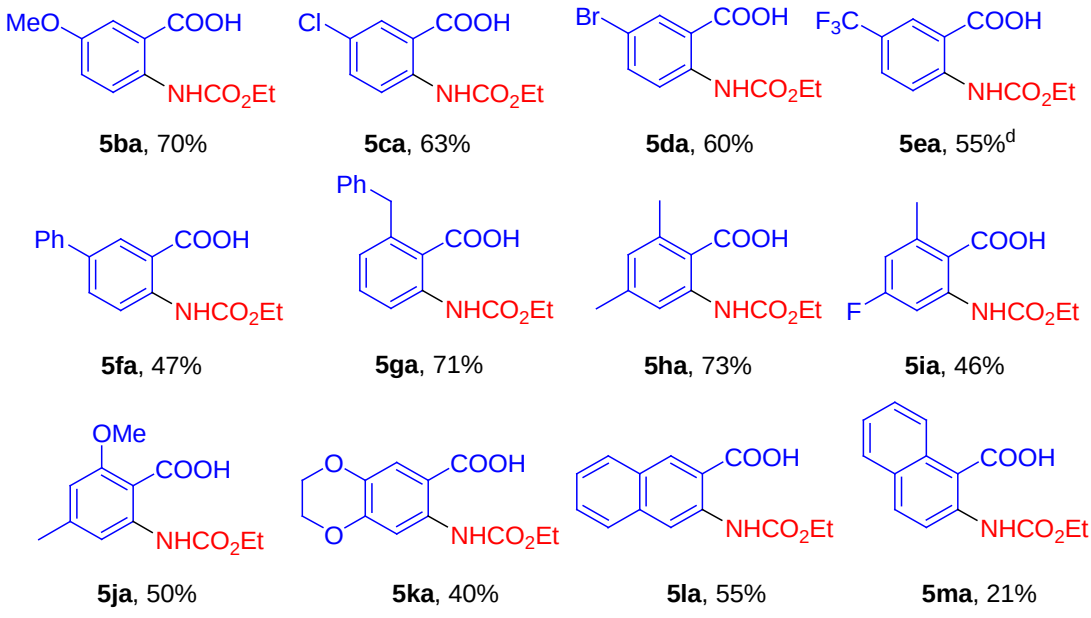

5ba, 70% **5ca**, 63% **5da**, 60% **5ea**, 55%[d]

5fa, 47% **5ga**, 71% **5ha**, 73% **5ia**, 46%

5ja, 50% **5ka**, 40% **5la**, 55% **5ma**, 21%

[a]Reaction conditons: Lithium benzoate (0.2 mmol), **2aMes** (1.5 equiv in 0.5 mL 1,4-dioxane), KOAc (1 equiv), $Pd(OAc)_2$ (10 mol%), 1,4-dioxane (1.5 mL) at 90 °C for 6 h under N_2. [b]Isolated yields. [c]Syringe pump addition of **2aMes** at a rate of 0.3 equiv / h. [d]KOAc (2 equiv) was employed, reaction was performed at 130 °C.

2.4 Proposed Mechanism

A plausible mechanism is shown in Scheme 2.5. The amidation may be initiated by Pd(II)-catalyzed *ortho*-C-H activation of arenes to generate palladacyclic complexes **A**. *N*-arylsulfonyloxycarbamate would react with complex **A** (or assisted by a base, if present) to form the putative palladium(IV)-imido intermediate **B**.

Migratory insertion of the aryl would afford the palladacyclic complex **C**. Upon protonation, the arylamine would be released and the Pd(II) catalyst was regenerated.

Scheme 2.5 Proposed Mechanism

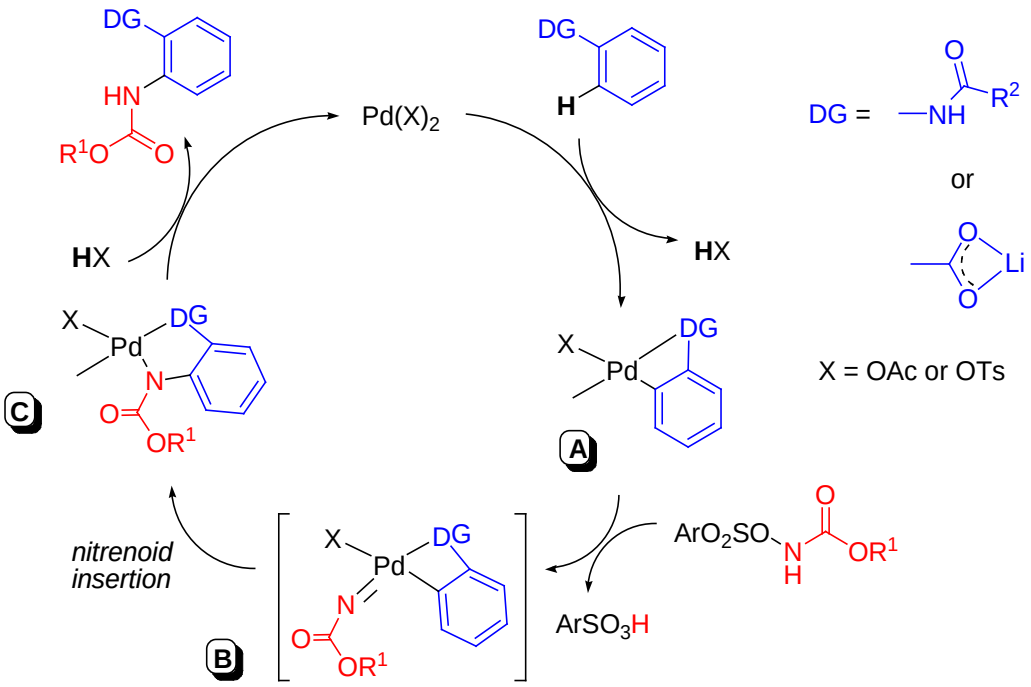

A more detailed mechanistic investigation of the Pd(II)-catalyzed arene amidation will be presented in the next chapter.

2.5 Concluding Summary

In conclusion, we developed the Pd(II)-catalyzed intermolecular arene C-H amidation of anilides and benzoic acids using *N*-arylsulfonyloxycarbamates as reagent for the synthesis of 2-aminoanilines and anthranilic acids. For the amidation of anilides, *N*-nosyloxycarbamate was found to be the most effective amidation reagent when compared to the carbamates with different *N*-leaving groups (i.e. OTs, OPiv and OPFB). Anilides with different protecting groups such as pivaloyl, acetyl and benzoyl can also be functionalized to produce 2-aminoanilines derivatives in good yields and regioselectivity. Functional groups such as halogens, methoxy, benzyl and alkenyl groups were also well tolerated. For amidation of benzoic acids, *N*-mesitylsulfonylcarbamates were more effective reagents providing a better mass balance for the amidation. The effectiveness of the amidation was dependent on the size of the counter ions in a descending order: $Li^+ > Na^+ > K^+ \sim=> (n\text{-}Bu_4)N^+$. Without counter ion, benzoic acid is ineffective substrate for the amidation. Lithium benzoates bearing different functional groups such as halogen, $-CF_3$, methoxy and benzyl groups were effectively transformed to corresponding anthranilic acids derivatives in good yields. The reactions were proposed to be initiated by Pd(II)-mediated *ortho*-C-H bond cleavage to generate a cyclopalladated complex. The

N-arylsulfonyloxycarbamates would generate nitrene and react with the cyclopalladated complex forming the putative palladium(IV)-imido intermediate. The following migratory insertion and protonation would furnish the amidation products.

2.6 Experimental Section

All reagents were obtained from commercial source, and they used as received without purification. 1,4-dioxane was dried with metallic sodium and distilled before use. All the pivalanilides (except for **1r** and **1s)** were synthesized from anilines and pivaloyl chloride with triethylamine as base in EtOAc.[41] All lithium benzoates were prepared by reacting benzoic acids with lithium hydroxide in methanol, and were then dried at 100 ˚C under high vacuum (~0.05 mmHg) for 12 h. $[Pd(OTs)_2(MeCN)_2]$,[59c] $Pd(OPiv)_2$,[59d] ethyl *N*-carboxylate carbamates,[59a] ethyl *N*-arylsulfonyloxycarbamates[21] and 3-phenylbenzoic acid[59b] were prepared according to the literature procedures. All the amidation reactions with pivalanilides were performed in 8 mL-vials equipped with Teflon® liner caps without special precautions unless otherwise specified. The amidation reactions with lithium benzoates were performed in a 10-mL Schlenk tube under an atmosphere of nitrogen.

Flash column chromatography was performed on 230-400 mesh silica gel (NA Chemical) (or aluminum oxide (NA Chemical) where specified). Preparative TLC was performed on a silica gel coated glass. GC-MS analyses were performed on a 6890N-GC (Agilent Technology) with 5973Network-MS (Agilent Technology). ^1H, ^{13}C, DEPT 135^o NMR analyses were performed on either a Bruker (400 MHz) or a Varian (500 MHz) spectrometer. Chemical shifts (δ) were given in ppm, and the signals were referenced with the solvent residual peak(s). NMR yields or conversions were determined by ^1H NMR with dibromomethane (0.1 mmol) as the internal standard which has a singlet signal (2H) at δ_H 4.9 ppm in $CDCl_3$ or δ_H 5.3 ppm in d_6-acetone. IR spectra were obtained by a Nicolet-380 FT-IR spectrometer. Melting points were recorded on a BÜCHI-B-545 instrument and were uncorrected. High resolution mass spectra were obtained using VG MICROMASS Fison VG

platform, with electrospray ionization mode.

2.6.1 General Experimental Procedures and Characterizations

2.6.1.1 Preparation of *N*-Nosyloxycarbamates

Step 1: Hydoxylamine hydrochloride (13.9 g, 0.200 mol) was added to 1.5 M aqueous solution of sodium hydroxide (160 mL, 0.240 mol). The solution was cooled to 0 ˚C and the suitable chloroformate (38 mmol) was added dropwise. Upon complete addition of the chloroformate, the reaction mixture was warmed to room temperature and stirred for 2 h. The reaction mixture was acidified with 6 M HCl to pH 4—5. The mixture was extracted with diethyl ether (10 × 200 mL), and the combined organic fractions were washed with brine, then dried over Na_2SO_4. After the removal of solvent *in vacuo*, the desired crude *N*-hydroxycarbamate was weighed and used directly for **step 2** without further purification.

Step 2: The crude *N*-hydroxycarbamate was dissolved in diethyl ether (1 mmol / 10 mL), and the solution was cooled to 0 ˚C. *p*-nitrobenzenesulfonyl chloride (1.1 equiv) was added, and triethylamine (1.1 equiv) was added dropwise to the reaction mixture. Upon complete addition of triethylamine, the dropping funnel was rinsed with a small amount of diethyl ether, and the resulting white suspension was warmed to room temperature and stirred for 3 h. Water was added to the solution until a clear solution was obtained. The two layers were separated, and the aqueous layer was extracted with DCM (2 × 20 mL). The combined organic layers were washed with brine and dried over Na_2SO_4. After removal of solvent, the crude product was recrystallized by a chloroform-hexanes mixture to afford the pure *N*-nosyloxycarbamate as a pale yellow solid.

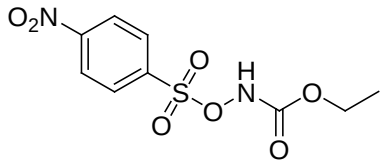

2aNs

Ethyl *N*-Nosyloxycarbamate (2aNs) was prepared from ethyl chloroformate according to the general procedure. The yield of the corresponding *N*-hydroxycarbamate produced in **step 1** was 85%. In **step 2**, after recrystallisation from chloroform and hexane, **2a** was obtained as a pale yellow solid (8.4 g, 90%); R_f = 0.2 (8 : 2 hexane : EtOAc); mp = 115-116.5 ^oC; ^1H NMR ($CDCl_3$, 400 MHz): δ_H 8.41 (d, J = 8.8Hz, 2H), 8.22 (d, J = 8.8Hz, 2H), 7.94 (s, 1H), 4.09 (q, J = 7.2Hz, 2H), 1.16 (t, J = 7.2Hz, 3H); ^{13}C NMR ($CDCl_3$, 100 MHz) δ_C 155.20 (C), 151.37 (C), 139.18 (C), 131.03 (2CH), 124.14 (2CH), 63.73 (CH_2) 14.06 (CH_3); IR (KBr, cm^{-1}): 3196, 3117, 1735, 1540, 1414, 1350, 1337, 1190, 747; HRMS m/z (ESI): calculated for $C_9H_{10}N_2O_7SNa^+$: 313.0106, found: 313.0108.

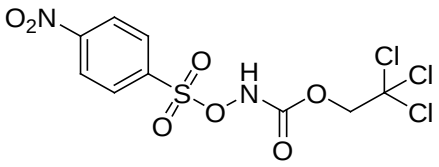

2bNs

2,2,2-Trichloroethyl *N*-Nosyloxycarbamate (2bNs) was prepared from 2,2,2-trichloroethyl chloroformate according to the general procedure. The yield of the corresponding *N*-hydroxycarbamate produced in **step 1** was 75%. In **step 2**, after recrystallisation from chloroform and hexane, **2b** was obtained as a pale yellow solid (9.2 g, 82%); R_f = 0.2 (8 : 2 hexane : EtOAc); mp = 125.5-127.5 ^oC; ^1H NMR ($CDCl_3$, 400 MHz): δ_H 8.42-8.40 (m, 2H), 8.32 (br.s, 1H), 8.25-8.23 (m, 2H), 4.65 (s, 2H); ^{13}C NMR ($CDCl_3$, 100 MHz) δ_C 153.48 (C), 151.53 (C), 138.74 (C), 131.15

(2CH), 124.30 (2CH), 93.87 (C) 75.31 (CH_2); IR (KBr, cm^{-1}): 3274, 1783, 1531, 1395, 1240, 1193, 752; HRMS m/z (ESI): calculated for $C_9H_7N_2O_7SCl_3Na^+$: 414.8937, found: 414.8918.

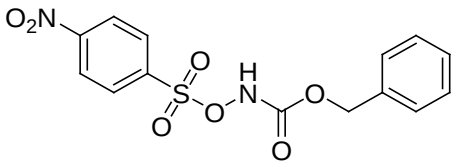

2cNs

Benzyl *N*-Nosyloxycarbamate (2cNs) was prepared from benzyl chloroformate according to the general procedure. The yield of the corresponding *N*-hydroxycarbamate produced in **step 1** was 83%. In **step 2**, after recrystallisation from chloroform and hexane, **2c** was obtained as a pale yellow solid (7.2 g, 65%); R_f = 0.2 (8 : 2 hexane : EtOAc); mp = 104-106.5 ^oC; ^1H NMR ($CDCl_3$, 400 MHz): δ_H 8.19 (d, *J* = 8.8Hz, 2H), 8.09 (d, *J* = 8.8Hz, 2H), 8.05 (s, 1H), 7.35-7.29 (m, 3H), 7.16-7.13 (m, 2H), 5.00 (s, 2H); ^{13}C NMR ($CDCl_3$, 100 MHz) δ_C 154.89 (C), 151.18 (C), 138.80 (C), 133.97 (C), 130.89 (CH), 129.18 (CH), 128.66 (2CH), 123.99 (CH), 69.11 (CH_2); IR (KBr, cm^{-1}): 3294, 1729, 1532, 1407, 1390, 1348, 1316, 1189, 754; HRMS m/z (ESI): calculated for $C_{14}H_{12}N_2O_7SNa^+$: 375.0263, found: 375.0246. (Note: **2cNs** should be stored at below -20 ^oC to prevent decomposition; it is stable within one month at -20 ^oC)

2.6.2 Preparation of Substrates 1r[41h] and 1s

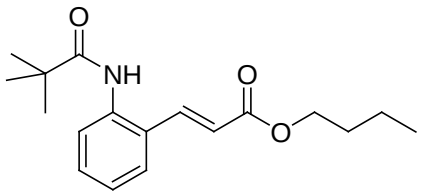

1r

1r was prepared according to the literature procedures[41h] with pivalanilide (0.5 mmol) as substrate, and it was obtained as a white solid (121.2 mg, 80%); R_f = 0.4 (6 : 4 hexane : Et_2O); mp = 73.5-75 ^oC; ^1H NMR ($CDCl_3$, 400 MHz): δ_H 7.78-7.74 (m, 2H), 7.55 (dd, *J* = 7.6Hz, 1.6Hz, 1H), 7.41-7.36 (m, 2H), 7.21 (t, *J* = 7.6Hz, 1H), 7.40 (d, *J* = 16Hz, 1H), 4.21 (t, *J* = 7.2Hz, 2H), 1.72-1.65 (m, 2H), 1.48-1.41 (m, 2H), 1.36 (s, 9H), 0.979 (t, *J* = 7.2Hz, 3H); ^{13}C NMR ($CDCl_3$, 100 MHz) δ_C 176.90 (C), 166.59 (C), 139.06 (CH), 135.93 (C), 130.70 (CH), 127.98 (C), 127.21 (CH), 125.79 (CH), 125.06 (CH), 120.99 (CH), 64.57 (CH_2), 39.71 (C), 30.73 (CH_2), 27.64 (CH_3), 19.22 (CH_2), 13.72 (CH_3); IR (KBr, cm^{-1}): 3274, 2955, 1710, 1646, 1638, 1481, 1319, 1176, 762; HRMS m/z (ESI): calculated for $C_{18}H_{25}NO_3H^+$: 304.1913, found: 304.1925.

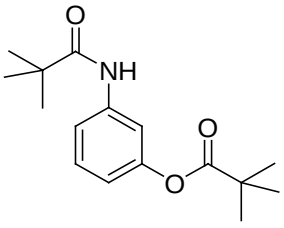

1s

To a mixture of 3-aminophenol (10 mmol) and K_2CO_3 (2 equiv) in acetonitrile (20 mL), pivaloyl chloride (2.2 equiv) was added in one portion. The reaction mixture was stirred at 120 ˚C for about 3 h. After cooling down to room temperature, the reaction mixture was diluted with Et_2O, and de-ionized water was also added. Two

layers were separated and the aqueous layer was washed with Et_2O (2 × 20 mL). The combined organic fractions were washed with brine and dried over Na_2SO_4. Solvent was removed by rotary evaporation, and **1s** was isolated by flash column chromatography on silica gel and obtained as a white solid (0.83 mg, 30% yield). R_f = 0.6 (8 : 2 hexane : EtOAc); mp = 118-120 °C; ^{1}H NMR ($CDCl_3$, 400 MHz): δ_H 7.48 (t, *J* = 2Hz, 1H), 7.35 (br.s, 1H), 7.31-7.23 (m, 2H), 6.81-6.79 (m, 1H), 1.34 (s, 9H), 1.30 (s, 9H); ^{13}C NMR ($CDCl_3$, 100 MHz) δ_C 176.99 (C), 176.55 (C), 151.54 (C), 139.09 (C), 129.44 (CH), 117.16 (CH), 116.76 (CH), 113.42 (CH), 39.66 (C), 39.07 (C), 27.57 (CH_3), 27.13 (CH_3); IR (KBr, cm^{-1}): 3313, 2978, 1742, 1653, 1604, 1541, 1481, 1425, 1265, 1183, 1136, 1117; HRMS m/z (ESI): calculated for $C_{16}H_{23}NO_3Na^+$: 300.1576, found: 300.1577.

2.6.3 General Procedures for the Pd(II)-Catalyzed C-H Amidation of Anilides and Its Analogs with *N*-Nosyloxycarbamates

To a mixture of anilide (0.2 mmol) and $[Pd(OTs)_2(MeCN)_2]$ (10 mol%) in 1,4-dioxane (2 mL) in an 8 mL-vial, *N*-nosyloxycarbamate (1.2 equiv) was added in one portion, and the vial was sealed with a Teflon® liner cap. The mixture was stirred at 80 °C for 6 hours. After cooling to room temperature, the reaction mixture was diluted with about 4 mL of EtOAc. The diluted mixture was washed with 5 mL of a saturated $NaHCO_3$ solution, and the aqueous layer was extracted with EtOAc (5 mL × 3). The combined organic extracts were dried over anhydrous Na_2SO_4 and then filtered through a short plug of silica gel. The silica gel was washed with EtOAc (40 mL) and the filtrate was evaporated to dryness by rotary evaporation. The residue was redissolved with small amount of dichloromethane (DCM), and it was loaded on a

silica gel / aluminum oxide packed column with hexanes-EtOAc mixture as mobile phase for purification.

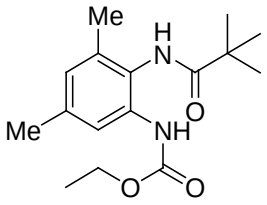

3aa

3aa was isolated by flash column chromatography on silica gel as a white solid (49.1 mg, 84% yield). R_f = 0.2 (8 : 2 hexane : EtOAc); mp = 152-153°C; ^{1}H NMR ($CDCl_3$, 400 MHz): δ_H 7.56 (br.s, 1H), 7.10 (br.s, 1H), 7.03 (s, 1H), 6.80 (s, 1H), 4.15 (q, *J* = 7.2Hz, 2H), 2.23 (s, 3H), 2.13 (s, 3H), 1.30 (s, 9H), 1.26 (t, *J* = 7.2Hz, 3H); ^{13}C NMR ($CDCl_3$, 100 MHz) δ_C 177.71 (C), 154.84 (C), 136.77 (C), 134.98 (C), 132.87 (C), 127.80 (CH), 125.77 (C), 122.25 (CH), 61.17 (CH_2), 39.26 (C), 27.51 (CH_3), 20.91 (CH_3), 18.08 (CH_3), 14.45 (CH_3); IR (KBr, cm^{-1}): 3322, 1730, 1632, 1546, 1502, 1243, 1212; HRMS m/z (ESI): calculated for $C_{16}H_{24}N_2O_3H^+$: 293.1865, found: 293.1862.

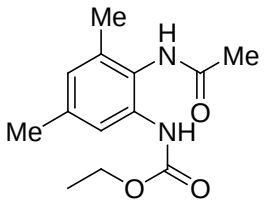

3ba

3ba was isolated by flash column chromatography on silica gel as a white solid (26.0 mg, 52% yield). R_f = 0.4 (20% EtOAc in DCM); mp = 131-133.5°C; ^{1}H NMR (CD_2Cl_2, 400 MHz): δ_H 7.53 (br.s, 1H), 7.30 (s, 1H), 7.14 (br.s, 1H), 6.78 (s, 1H),

4.18 (q, *J* = 7.2Hz, 2H), 2.28 (s, 3H), 2.13 (s, 3H), 1.30 (t, *J* = 7.2Hz, 3H); ^{13}C NMR (CD_2Cl_2, 100 MHz) δ_C 169.69 (C), 154.31 (C), 137.12 (C), 134.79 (C), 133.43 (C), 126.95 (CH), 124.59 (C), 121.01 (CH), 61.17 (CH_2), 22.83 (CH_3), 20.76 (CH_3), 17.90 (CH_3), 14.26 (CH_3); IR (KBr, cm^{-1}): 3274, 1700, 1655, 1559, 1278, 1256; HRMS m/z (ESI): calculated for $C_{13}H_{18}N_2O_3Na^+$: 273.1215, found: 273.1202.

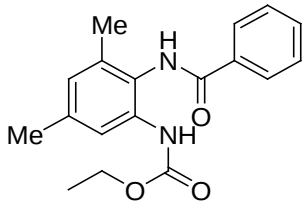

3ca

3ca was isolated by flash column chromatography on silica gel as a white solid (35.6 mg, 57% yield). R_f = 0.2 (8 : 2 hexane : EtOAc); mp = 61-63.5 ^{o}C; ^{1}H NMR ($CDCl_3$, 400MHz): δ_H 8.20 (br.s, 1H), 7.95-7.93 (m, 2H), 7.58-7.54 (m, 1H), 7.50-7.47 (m, 2H), 7.18 (s, 1H), 7.11 (br.s, 1H), 6.87 (s, 1H), 4.14 (q, *J* = 7.2Hz, 2H), 2.28 (s, 3H), 2.25 (s, 3H), 1.22 (t, *J* = 7.2Hz, 3H); ^{13}C NMR ($CDCl_3$, 100 MHz) δ_C 165.96 (C), 154.81 (C), 137.28 (C), 135.26 (C), 133.75 (C), 132.98 (CH), 131.92 (C), 128.65 (CH), 127.99 (CH), 127.36 (CH), 125.38 (C), 122.03 (CH), 61.38 (CH_2), 20.98 (CH_3), 18.42 (CH_3), 14.40 (CH_3); IR (KBr, cm^{-1}): 3291, 1734, 1647, 1533, 1237, 1104, 1029, 709; HRMS m/z (ESI): calculated for $C_{18}H_{20}N_2O_3H^+$: 313.1552, found: 313.1551.

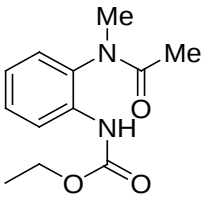

3da

3da was isolated by flash column chromatography on silica gel as a pink solid (34.0 mg, 72% yield). R_f = 0.3 (1 : 1 hexane : EtOAc); mp = 105.106.5 ^oC; ^1H NMR ($CDCl_3$, 400 MHz): δ_H 8.19 (d, *J* = 8.4, 1H), 7.37-7.32 (m, 1H), 7.12-7.05 (m, 2H), 6.89 (br.s, 1H) 4.21 (q, *J* = 7.2Hz, 2H), 3.17 (s, 3H), 1.81 (s, 3H), 1.31 (t, *J* = 7.2Hz, 3H); ^{13}C NMR ($CDCl_3$, 100 MHz) δ_C 171.74 (C), 153.25 (C), 134.68 (C), 132.18 (C), 129.38 (CH), 127.71 (CH), 123.74 (CH), 119.89 (CH), 61.55 (CH_2), 35.81 (CH_3), 21.91 (CH_3), 14.35 (CH_3); IR (KBr, cm^{-1}): 3229, 2981, 1735, 1654, 1593, 1534, 1224, 1059; HRMS m/z (ESI): calculated for $C_{12}H_{16}N_2O_3H^+$: 237.1239, found: 237.1236.

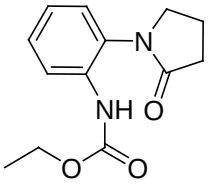

3ea

3ea was isolated by flash column chromatography on silica gel as a pale yellow semi-solid (42.2 mg, 85 % yield). R_f = 0.4 (10% EtOAc in DCM); ^1H NMR ($CDCl_3$, 400 MHz): δ_H 7.8 (d, *J* = 8Hz, 1H), 7.52 (br.s, 1H), 7.29-7.25 (m, 1H), 7.16-7.09 (m, 2H), 4.18 (q, *J* = 7.2Hz, 2H), 3.85 (t, *J* = 7.2Hz, 2H), 2.62 (t, *J* = 8Hz, 2H), 2.26-2.18 (m, 2H), 1.29 (t, *J* = 7.2Hz, 3H); ^{13}C NMR ($CDCl_3$, 100 MHz) δ_C 175.16 (C), 154.32 (C), 133.23 (C), 130.24 (C), 127.56 (CH), 124.63 (CH), 124.54 (CH), 123.73 (CH), 61.10 (CH_2), 50.99 (CH_2), 31.68 (CH_2), 19.17 (CH_2), 14.49 (CH_3); IR (Thin film,

DCM, cm^{-1}): 3053, 2985, 1724, 1679, 1521,1269, 1261; HRMS m/z (ESI): calculated for $C_{13}H_{16}N_2O_3Na^+$: 271.1059, found: 271.1057.

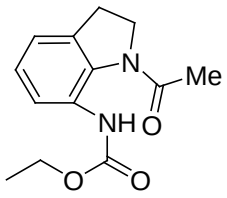

3fa

3fa was isolated by preparative TLC plate (silica gel) as a white solid (33.7 mg, 68% yield). R_f = 0.6 (5% EtOAc in DCM); mp = 118.5-120 ^oC; ^1H NMR ($CDCl_3$, 400 MHz): δ_H 9.54 (br.s, 1H), 7.80 (d, *J* = 8Hz, 2H), 7.15 (t, *J* = 7.6Hz, 1H), 6.92 (d. *J* = 7.2Hz. 1H), 4.18 (q, *J* = 7.2Hz, 2H), 4.06 (t, *J* = 8Hz, 2H), 3.06 (t, *J* = 8Hz, 2H), 2.33 (s, 3H), 1.29 (t, *J* = 7.2Hz, 3H); ^{13}C NMR ($CDCl_3$, 100 MHz) δ_C 169.23 (C), 154.18 (C), 134.65 (C), 132.06 (C), 128.53 (C), 126.30 (CH), 121.18 (CH), 119.40 (CH), 60.73 (CH_2), 51.47 (CH_2), 29.04 (CH_2), 24.43 (CH_3), 14.58 (CH_3); IR (KBr, cm^{-1}): 1728, 1639, 1602, 1517, 1433, 1407, 1231, 1079; HRMS m/z (ESI): calculated for $C_{13}H_{16}N_2O_3Na^+$: 271.1059, found: 271.1047.

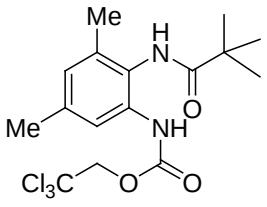

3ab

3ab was isolated by flash column chromatography on silica gel as a white solid (68.8 mg, 87% yield). R_f = 0.15 (9 : 1 hexane : EtOAc); mp = 171-173 ^oC; ^1H NMR ($CDCl_3$, 400 MHz): δ_H 7.50 (br.s, 1H), 7.30 (br.s, 1H), 7.21 (s, 1H), 6.87 (s, 1H),

4.77 (s, 2H), 2.29 (s, 3H), 2.19 (s, 3H), 1.34 (s, 9H); ^{13}C NMR ($CDCl_3$, 100 MHz) δ_C 177.99 (C), 152.77 (C), 137.17 (C), 133.87 (C), 132.25 (C), 128.48 (CH), 125.74 (C), 123.17 (CH), 95.35 (C), 74.50 (CH_2), 39.43 (C), 27.58 (CH_3), 20.94 (CH_3), 18.06 (CH_3); IR (KBr, cm^{-1}): 3355, 3293, 2967, 1726, 1646, 1543, 1499, 1252, 1119, 724; HRMS m/z (ESI): calculated for $C_{16}H_{21}N_2O_3Cl_3H^+$: 395.0696, found: 395.0704.

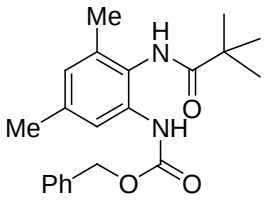

3ac

3ac was isolated by flash column chromatography on aluminum oxide as a white solid (53.1 mg, 75% yield). R_f = 0.15 (9 : 1 hexane : EtOAc on aluminum oxide TLC plate); mp = 142-144 ^{o}C; ^{1}H NMR (CD_2Cl_2, 400 MHz): δ_H 7.43 (br.s, 1H), 7.40-7.33 (m, 5H), 7.18 (s, 2H), 6.89 (s, 1H), 5.16 (s, 2H), 2.30 (s, 3H), 2.18 (s, 3H), 1.27 (s, 9H); ^{13}C NMR (CD_2Cl_2, 100 MHz) δ_C 177.56 (C), 154.28 (C), 136.96 (C), 136.46 (C), 135.00 (C), 133.03 (C), 128.38 (CH), 128.01 (CH), 127.90 (CH), 127.73 (CH), 125.83 (C), 122.11 (CH), 66.77 (CH_2), 39.14 (C), 27.26 (CH_3), 20.68 (CH_3), 17.88 (CH_3); IR (KBr, cm^{-1}): 3296, 1729, 1630, 1552, 1499, 1242, 1209, 1096; HRMS m/z (ESI): calculated for $C_{21}H_{26}N_2O_3H^+$: 355.2022, found: 355.2007.

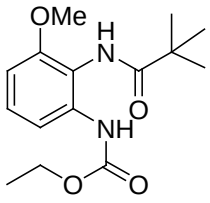

3ga

3ga was isolated by flash column chromatography on aluminum oxide as a pale yellow solid (36.5 mg, 62% yield). R_f = 0.4 (8 :2 hexane : EtOAc on aluminum oxide TLC plate); mp = 100-101 ^oC; ^1H NMR (CD_2Cl_2, 400 MHz): δ_H 8.01 (br.s, 1H), 7.67 (br.s, 1H), 7.39 (d, *J* = 8.4Hz, 1H), 7.21 (t, *J* = 8.4Hz, 1H), 6.72 (d, *J* = 8.8Hz, 1H), 4.17 (q, *J* = 7.2Hz, 2H), 3.87 (s, 3H), 1.35 (s, 9H), 1.29 (t, *J* = 7.2Hz, 3H); ^{13}C NMR (CD_2Cl_2, 100 MHz) δ_C 178.62 (C), 154.08 (C), 152.44 (C), 133.29 (C), 126.18 (CH), 118.21 (C), 115.97 (CH), 105.90 (CH), 60.83 (CH_2), 55.93 (CH_3), 39.61 (C), 27.31 (CH_3), 14.29 (CH_3); IR (KBr, cm^{-1}): 3296, 1732, 1635, 1604, 1474, 1240, 1217, 1053; HRMS m/z (ESI): calculated for $C_{15}H_{22}N_2O_4H^+$: 295.1658, found: 295.1644.

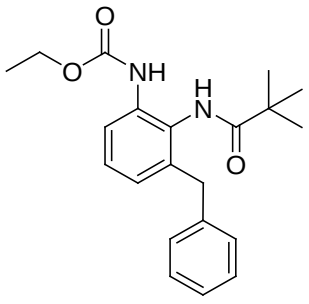

3ha

3ha was isolated by flash column chromatography on silica gel as a light yellow solid (60.0 mg, 70% yield). R_f = 0.2 (8 : 2 hexane : EtOAc); mp = 115-118 ^oC; ^1H NMR (CD_2Cl_2, 400 MHz): δ_H 7.55 (d, *J* = 8Hz, 1H), 7.34-7.24 (m, 5H), 7.20 (br.s, 1H),

7.13 (d, *J* = 6.8Hz, 2H), 7.06 (d, *J* = 7.2Hz, 1H), 4.17 (q, *J* = 7.2Hz, 2H), 4.00 (s, 2H), 1.28 (t, *J* = 7.2Hz, 3H), 1.17 (s, 9H); ^{13}C NMR (CD_2Cl_2, 100 MHz) δ_C 177.77 (C), 154.39 (C), 139.25 (C), 136.87 (C), 134.23 (C), 128.71 (CH), 128.26 (CH), 128.10 (C), 127.11 (CH), 127.02 (CH), 126.47 (CH), 122.72 (CH), 61.12 (CH_2), 39.14 (C), 38.30 (CH_2), 27.07 (CH_3), 14.29 (CH_3); IR (KBr, cm^{-1}): 3316, 2985, 1726, 1628, 1542, 1498, 1232, 1087, 775; HRMS m/z (ESI): calculated for $C_{21}H_{26}N_2O_3H^+$: 355.2022, found: 355.2017.

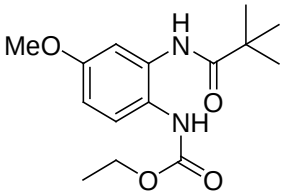

3ia

The crude product of **3ia** was isolated by flash column chromatography on aluminum oxide. The crude product was then re-dissolved in EtOAc and washed with 1M HCl (20 ml), then sat. $NaHCO_3$ and brine, and dried over anhydrous Na_2SO_4. Solvent was removed *in vacuo.* NMR pure product of **3ia** was obtained as a yellow solid (26.5 mg, 45% yield). R_f = 0.3 (8 : 2 hexane : EtOAc, on aluminum oxide TLC plate); mp = 110-111.5 ^{o}C; ^{1}H NMR (CD_2Cl_2, 400 MHz): δ_H 8.11 (br.s, 1H), 7.22 (s, 1H), 7.71 (d, *J* = 8.8Hz, 1H), 6.79 (br.s, 1H), 6.71 (dd, *J* = 8.8Hz, 2.4Hz, 1H), 4.19 (q, *J* = 7.2Hz, 2H), 3.79 (s, 3H), 1.31-1.28 (m, 12H); ^{13}C NMR (CD_2Cl_2, 100 MHz) δ_C 177.21 (C), 157.76 (C), 155.36 (C), 133.04 (C), 126.29 (CH), 122.53 (C), 111.19 (CH), 109.62 (CH), 61.51 (CH_2), 55.42 (CH_3), 39.38(C), 27.25 (CH_3), 14.30 (CH_3); IR (KBr, cm^{-1}): 3312, 3283, 1729, 1635, 1522, 1220, 1031; HRMS m/z (ESI): calculated for $C_{15}H_{22}N_2O_4H^+$: 295.1658, found: 295.1655.

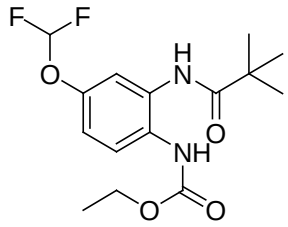

3ja

3ja was isolated by flash column chromatography on aluminum oxide as a light yellow solid (39.6 mg, 60% yield). R_f = 0.2 (9 : 1 hexane : EtOAc, on aluminum oxide TLC plate); mp = 90-92.5 ^oC; ^1H NMR (CD_2Cl_2, 400 MHz): δ_H 8.26 (br.s, 1H), 7.43 (d, *J* = 2.4Hz, 1H), 7.28 (d, *J* = 8.8Hz, 1H), 7.05 (br.s, 1H), 6.92 (dd, *J* = 8.8Hz, 2.8Hz, 1H), 6.55 (t, *J* = 74.4Hz, 1H), 4.21 (q, *J* = 7.2Hz, 2H), 1.32-1.29 (m, 12H); ^{13}C NMR (CD_2Cl_2, 100 MHz) δ_C 177.54 (C), 155.03 (C), 148.49 (C), 132.58 (C), 127.25 (C), 125.93 (CH), 116.44 (CH), 115.94 (CH), 118.62, 116.04, 113.47 (t, *J* = 257Hz, CH), 61.81 (CH_2), 39.41 (C), 27.10 (CH_3), 14.23 (CH_3); IR (KBr, cm^{-1}):3338, 1720, 1560, 1522, 1244, 1133, 1035; HRMS m/z (ESI): calculated for $C_{15}H_{20}N_2O_4F_2H^+$: 331.1469, found: 331.1458.

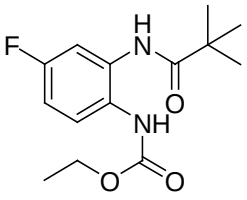

3ka

3ka was isolated by flash column chromatography on silica gel as a pale yellow solid (37.2 mg, 66% yield). R_f = 0.25 (8 : 2 hexane : EtOAc); mp = 81-83 ^oC; ^1H NMR (CD_2Cl_2, 400MHz): δ_H 8.30 (br.s, 1H), 7.45 (d, *J* = 8.4Hz, 1H), 7.22-7.19 (m, 1H), 6.99 (br.s, 1H), 6.87-6.82 (m, 1H), 4.20 (q, *J* = 7.2Hz, 2H), 1.32-1.27 (m, 12H); ^{13}C NMR (CD_2Cl_2, 100 MHz) δ_C 177.38 (C), 161.41, 158.99 (d, *J* = 242Hz, C), 155.21

(C), 133.22 (C), 126.35 (CH), 125.49 (C), 112.01, 111.78 (d, *J* = 23Hz, CH), 111.39 (CH), 61.80 (CH_2), 39.44 (C), 27.09 (CH_3), 14.26 (CH_3); IR (KBr, cm^{-1}): 3305, 1709, 1532, 1490, 1261, 1252; HRMS m/z (ESI): calculated for $C_{14}H_{19}N_2O_3FH^+$: 283.1458, found: 283.1455.

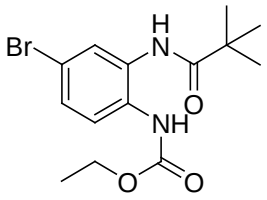

3la

3la was isolated by flash column chromatography on silica gel as a light brown solid (46.5 mg, 68% yield). R_f = 0.3 (8 : 2 hexane : EtOAc); mp = 140.5-142°C; ^{1}H NMR ($CDCl_3$, 400 MHz): δ_H 8.31 (br.s, 1H), 7.58 (d, *J* = 1.6Hz, 1H), 7.21 (dd, *J* = 8.8Hz, 2Hz, 1H), 7.10 (d, *J* =8.8Hz, 2H), 4.19 (q, *J* = 7.2Hz, 2H), 1.31-1.28 (m, 12H); ^{13}C NMR ($CDCl_3$, 100 MHz) δ_C 178.09 (C), 155.01 (C), 131.88 (C), 129.51 (C), 128.88 (CH), 128.45 (CH), 125.92 (CH), 118.23 (C), 61.81 (CH_2), 39.45 (C), 27.36 (CH_3), 14.49 (CH_3); IR (KBr, cm^{-1}): 3300, 2968, 1698, 1658, 1529, 1499, 1478, 1255, 1061; HRMS m/z (ESI): calculated for $C_{14}H_{19}N_2O_3BrH^+$: 343.0657, found: 343.0670.

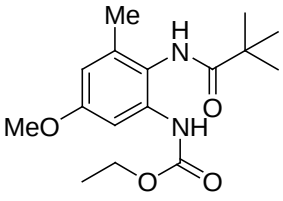

3ma

3ma was isolated by flash column chromatography on silica gel as a light brown solid (36.3 mg, 59% yield). R_f = 0.25 (5% EtOAc in DCM); mp = 155.5-157.5 °C; ^{1}H

NMR ($CDCl_3$, 400 MHz): δ_H 7.44 (br.s, 1H), 7.19 (br.s, 1H), 6.81 (d, *J* = 2.4Hz, 1H), 6.53 (d, *J* = 2.4Hz, 1H), 4.16 (q, *J* = 7.2Hz, 2H), 3.72 (s, 3H), 1.31 (s, 9H), 1.27 (t, *J* = 7.2Hz, 3H); ^{13}C NMR ($CDCl_3$, 100 MHz) δ_C 177.97 (C), 158.12 (C), 154.60 (C), 136.33 (C), 134.28 (C), 120.81 (C), 112.94 (CH), 106.03 (CH), 61.22 (CH_2), 55.21 (CH_3), 39.24 (C), 27.54 (CH_3), 18.43 (CH_3), 14.51 (CH_3); IR (KBr, cm^{-1}): 3320, 1734, 1635, 1541, 1506, 1245; HRMS m/z (ESI): calculated for $C_{16}H_{24}N_2O_4H^+$: 309.1814, found: 309.1802.

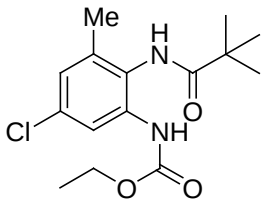

3na

3na was isolated by flash column chromatography on silica gel as a white solid (40.6 mg, 65% yield). R_f = 0.3 (8 : 2 hexane : EtOAc); mp = 166.5-168°C; ^1H NMR ($CDCl_3$, 400 MHz): δ_H 7.63 (br.s, 1H), 7.24-7.23 (m, 2H), 6.97 (d, *J* = 2Hz, 1H), 4.16 (q, *J* = 7.2Hz, 2H), 2.14 (s, 3H), 1.31 (s, 9H), 1.27 (t, *J* = 7.2Hz, 3H); ^{13}C NMR ($CDCl_3$, 100 MHz) δ_C 178.01 (C), 154.55 (C), 137.02 (C), 134.22 (C), 132.17 (C), 126.67 (CH), 126.58 (C), 121.24 (CH), 61.51 (CH_2), 39.36 (C), 27.45 (CH_3), 18.14 (CH_3), 14.45 (CH_3); IR (KBr, cm^{-1}): 3324, 3268, 2986, 1732, 1706, 1635, 1601, 1541, 1490, 1240, 1208, 1103, 1031; HRMS m/z (ESI): calculated for $C_{15}H_{21}N_2O_3ClH^+$: 313.1319, found: 313.1313.

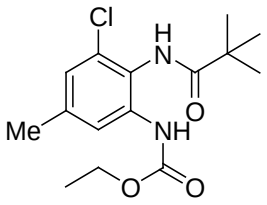

3oa

3oa was isolated by flash column chromatography on silica gel as a white solid (51.25 mg, 82% yield). R_f = 0.3 (8 : 2 hexane : EtOAc); mp = 106-107 ^oC; ^1H NMR ($CDCl_3$, 400 MHz): δ_H 8.19 (br.s, 1H), 7.35 (s, 1H), 7.14 (s, 1H), 7.08 (br.s, 1H), 4.19 (q, J = 7.2Hz, 2H), 2.27 (s, 3H), 1.30-1.26 (m, 12H); ^{13}C NMR ($CDCl_3$, 100 MHz) δ_C 178.14 (C), 155.07 (C), 133.82 (C), 130.64 (C), 129.13 (2C), 126.45 (CH), 125.90 (CH), 61.66 (CH_2), 39.34 (C), 27.34 (CH_3), 19.50 (CH_3), 14.49 (CH_3); IR (KBr, cm^{-1}): 3348, 3270, 2982, 1735, 1637, 1592, 1527, 1224, 1070; HRMS m/z (ESI): calculated for $C_{15}H_{21}N_2O_3ClH^+$: 313.1319, found: 313.1321.

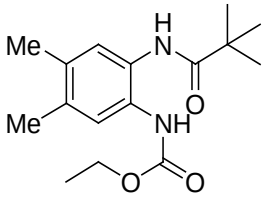

3pa

3pa was isolated by flash column chromatography on silica gel as a pale yellow solid (42 mg, 73% yield). R_f = 0.25 (8 : 2 hexane : EtOAc); mp = 122-123 ^oC; ^1H NMR ($CDCl_3$, 400 MHz): δ_H 8.04 (br.s, 1H), 7.16 (s, 1H), 7.06 (s, 1H), 6.94 (br.s, 1H), 4.18 (q, J = 7.2Hz, 2H), 2.17 (s, 6H), 1.30-1.26 (m, 12H); ^{13}C NMR ($CDCl_3$, 100 MHz) δ_C 177.68 (C), 155.19 (C), 134.54 (C), 134.21 (C), 128.15 (C), 127.98 (C), 126.48 (CH), 125.72 (CH), 61.38 (CH_2), 39.27 (C), 27.46 (CH_3), 19.20 (CH_3), 19.13

(CH_3), 14.54 (CH_3); IR (KBr, cm^{-1}): 3313, 3271, 1739, 1728, 1636, 1527, 1227; HRMS m/z (ESI): calculated for $C_{16}H_{24}N_2O_3H^+$: 293.1865, found: 293.1853.

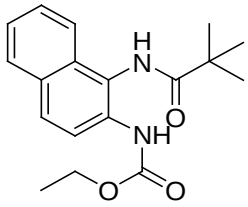

3qa

3qa was isolated by flash column chromatography on silica gel as a yellow solid (44.6 mg, 72% yield). R_f = 0.25 (8 : 2 hexane : EtOAc); mp = 138-140 ^oC; ^1H NMR (CD_2Cl_2, 400 MHz): δ_H 7.98 (br.s, 1H), 7.83 (d, *J* = 7.6Hz, 1H), 7.74 (d, *J* = 8.4Hz, 1H), 7.69 (d, *J* = 9.2Hz, 1H), 7.61 (d, *J* = 8.8Hz, 1H) 7.54-7.45 (m, 2H), 4.20 (q, *J* = 7.2Hz, 2H), 1.38 (s, 9H), 1.31 (t, *J* = 7.2Hz, 3H); ^{13}C NMR (CD_2Cl_2, 100 MHz) δ_C 178.20 (C), 154.37 (C), 131.27 (C), 131.02 (C), 130.01 (C), 128.04 (CH), 127.51 (CH), 126.64 (CH), 125.23 (CH), 123.12 (C), 122.43 (CH), 122.02 (CH), 61.40 (CH_2), 39.40 (C), 27.35 (CH_3), 14.31 (CH_3); IR (KBr, cm^{-1}): 3292, 3269, 1729, 1629, 1502, 1228; HRMS m/z (ESI): calculated for $C_{18}H_{22}N_2O_3H^+$: 315.1709, found: 315.1696.

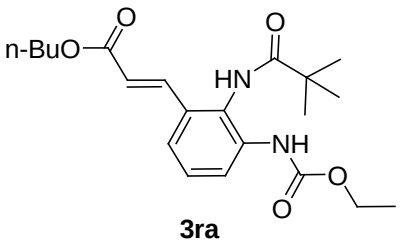

3ra

3ra was synthesized according to the general procedure, but after stirring at 80^{o}C for 6 hours, a second batch of **2a** (1.2 equiv) was added to the reaction mixture, and it was stirred at 80^{o}C for additional 6 hours. Crude product of **3ra** was isolated by flash

column chromatography on aluminum oxide. The crude product was re-dissolved in EtOAc and washed with 1M HCl (20 ml), then sat. $NaHCO_3$ and brine, and dried over anhydrous Na_2SO_4. Solvent was removed *in vacuo*. ^{1}H NMR pure product of **3ra** was obtained as a pale yellow solid (39.0 mg, 50% yield). R_f = 0.4 (7 : 3 hexane : EtOAc on aluminum oxide TLC plate); mp = 106.5-108 ^{o}C; ^{1}H NMR ($CDCl_3$, 400 MHz): δ_H 7.80 (br.s, 1H), 7.68 (d, *J* = 16Hz, 1H), 7.45 (d, *J* = 8Hz, 1H), 7.41 (d, *J* = 8Hz, 1H), 7.22 (t, *J* = 8Hz, 1H), 7.09 (br.s, 1H), 6.37 (d, *J* = 16Hz, 1H), 4.21-4.15 (m, 4H), 1.69-1.62 (m, 2H), 1.44-1.39 (m, 2H), 1.35 (s, 9H), 1.28 (t, *J* = 7.2Hz, 3H), 0.95 (t, *J* = 7.2Hz, 3H); ^{13}C NMR ($CDCl_3$, 100 MHz) δ_C 178.23 (C), 166.56 (C), 154.66 (C), 139.54 (CH), 133.99 (C), 132.43 (C), 128.69 (C), 127.54 (CH), 125.57 (CH), 123.31 (CH), 120.60 (CH), 64.43 (CH_2), 61.54 (CH_2), 39.47 (C), 30.65 (CH_2), 27.46 (CH_3), 19.13 (CH_2), 14.47 (CH_3), 13.62 (CH_3); IR (KBr, cm^{-1}): 3294, 2962, 1739, 1713, 1635, 1541, 1247, 1223; HRMS m/z (ESI): calculated for $C_{21}H_{30}N_2O_5H^+$: 391.2233, found: 391.2227.

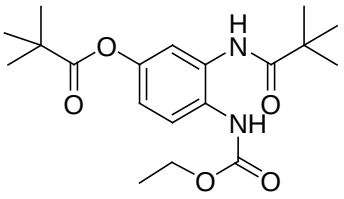

3sa

3sa was synthesized according to the general procedure but run for 12 h and was isolated by flash column chromatography on aluminum oxide as a light yellow solid (48.8 mg, 67% yield). R_f = 0.45 (8 : 2 hexane : EtOAc, on aluminum oxide TLC plate); mp = 126.5-128.5 ^{o}C; ^{1}H NMR (CD_2Cl_2, 400 MHz): δ_H 8.26 (br.s, 1H), 7.31 (d, *J* = 2Hz, 1H), 7.25 (d, *J* = 8.4Hz, 1H), 7.16 (br.s, 1H), 6.82 (dd, *J* = 8.8Hz, 2.4Hz, 1H), 4.21 (q, *J* =7.2 Hz, 2H), 1.36 (s, 9H), 1.33-1.28 (m, 12H); ^{13}C NMR (CD_2Cl_2,

100 MHz) δ_C 177.44 (C), 177.02 (C), 155.05 (C), 148.36 (C), 132.01 (C), 127.51 (C), 125.23 (CH), 118.58 (CH), 118.18 (CH), 61.66 (CH_2), 39.35 (C), 38.88 (C), 27.13 (CH_3), 26.77 (CH_3), 14.29 (CH_3); IR (KBr, cm^{-1}):3319, 2972, 1755, 1701, 1534, 1480, 1262, 1247, 1122, 1064; HRMS m/z (ESI): calculated for $C_{19}H_{28}N_2O_5H^+$: 365.2076, found: 365.2082.

2.6.4 General Procedures for Pd(II)-Catalyzed Amidation of Lithium Benzoates

A mixture of lithium benzoate (0.2 mmol), $Pd(OAc)_2$ (10 mol%) and KOAc (1 equiv) was dissolved in 1,4-dioxane (0.5 mL) in a 10-mL Schlenk tube, and ethyl *N*-mesitylsulfonyloxycarbamate (1.5 equiv) in 1,4-dioxane (1 mL) was added dropwise by a syringe pump at the rate of 0.3 equiv / h. The reaction was stirred at 90 ^oC for 6 h under an atmosphere of nitrogen. After cooling to room temperature, the reaction mixture was diluted with EtOAc (ca. 4 mL), and the mixture was acidified with 2 M HCl (2 mL) solution. The aqueous layer was extracted with EtOAc (5 mL × 3). The combined organic extracts were dried over anhydrous Na_2SO_4 and then filtered through a short plug of Celite®, and the filtrate was evaporated to dryness by rotary evaporation. The residue was redissolved with dichloromethane (DCM). A minimum amount of MeOH may be added (when the reaction crude mixture was barely-soluble in DCM). It was then purified by flash column chromatography on silica gel by gradient elution with 10-50% EtOAc in hexanes (5% increment of EtOAc).

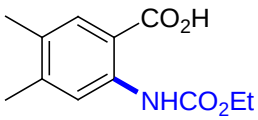

5aa was isolated as a brown solid (30.0 mg, 63% yield). mp = 140-142 °C; ^{1}H NMR ($CDCl_3$, 400 MHz): δ_H 10.1 (s, 1H), 8.26 (s, 1H), 7.84 (s, 1H), 4.23 (q, *J* = 7.2 Hz, 2H), 2.32 (s, 3H), 2.23 (s, 3H), 1.34 (t, *J* = 7.2 Hz, 3H); ^{13}C NMR ($CDCl_3$, 100 MHz): δ_C 172.6 (C), 153.7 (C), 145.8 (C), 140.4 (C), 132.3 (CH), 130.2 (C), 119.9 (CH), 111.1 (C), 61.2 (CH_2), 20.6 (CH_3), 18.9 (CH_3), 14.5 (CH_3); IR (KBr, cm^{-1}): 3324, 2980, 1735, 1670, 1584, 1521, 1263, 1226, 1093, 1034; HRMS *m/z* (ESI): calculated for $C_{12}H_{15}NO_4Na^+$: 260.0899, found: 260.0907.

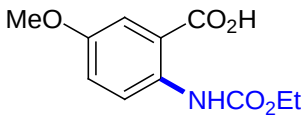

5ba was isolated as a pale yellow solid (33.5 mg, 70% yield). mp = 146-148 °C; ^{1}H NMR (*d*$_6$-acetone, 400 MHz): δ_H 10.4 (s, 1H), 8.36 (d, *J* = 9.2 Hz, 1H), 7.57 (d, *J* = 3.2 Hz, 1H), 7.20 (dd, *J* = 9.2 Hz, 2.8 Hz, 1H), 4.16 (q, *J* = 7.2 Hz, 2H), 3.81 (s, 3H), 1.26 (t, *J* = 7.2 Hz, 3H); ^{13}C NMR (*d*$_6$-acetone, 100 MHz): δ_C 170.1 (C), 154.9 (C), 154.2 (C), 136.8 (C), 121.9 (CH), 120.8 (CH), 116.4 (C), 115.9 (CH), 61.5 (CH_2), 56.0 (CH_3), 14.9 (CH_3); IR (KBr, cm^{-1}): 3348, 1738, 1536, 1280, 1250, 1210, 1091, 1063, 1042; HRMS *m/z* (ESI): calculated for $C_{11}H_{13}NO_5Na^+$: 262.0685, found: 262.0685.

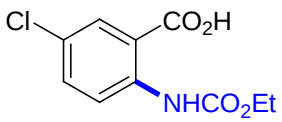

5ca was isolated as a pale yellow solid (30.6 mg, 63% yield). mp = 146-148 °C; ^{1}H

NMR (d_6-DMSO, 400 MHz): δ_H 12.9 (s, 1H), 8.19 (d, J = 8.8 Hz, 1H), 7.97 (d, J = 2.8 Hz, 1H), 7.38 dd, J = 8.8 Hz, 2.8 Hz, 1H), 4.10 (q, J = 7.2 Hz, 2H), 1.22 (t, J = 7.2 Hz, 3H); ^{13}C NMR (d_6-DMSO, 100 MHz): δ_C 169.5 (C), 153.6 (C), 140.1 (C), 131.2 (CH), 131.0 (CH), 124.91 (C), 124.8 (C), 119.2 (CH), 60.7 (CH_2), 15.0 (CH_3); IR (KBr, cm^{-1}): 3217, 3201, 1706, 1664, 1428, 1282, 1224; HRMS *m/z* (ESI): calculated for $C_{10}H_{10}NO_4ClNa^+$: 265.0118, found: 265.0119.

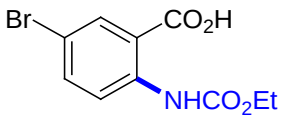

5da was isolated as a pale yellow solid (34.3 mg, 60% yield). mp = 146-148 ^{o}C; ^{1}H NMR ($CDCl_3$, 400 MHz): δ_H 10.2 (s, 1H), 8.42 (d, J = 9.2 Hz, 1H), 8.22 (d, J = 2 Hz, 1H), 7.67 (dd, J = 9.2 Hz, 2 Hz, 1H), 4.25 (q, J = 7.2 Hz, 2H), 1.34 (t, J = 7.2 Hz, 3H); ^{13}C NMR ($CDCl_3$, 100 MHz): δ_C 171.3 (C), 154.4 (C), 142.6 (C), 139.3 (CH), 135.1 (CH), 121.7 (CH), 115.7 (C), 114.8 (C), 62.6 (CH_2), 15.4 (CH_3); IR (KBr, cm^{-1}): 3233, 1742, 1686, 1606, 1532, 1508, 1246, 1198, 1154, 1037; HRMS *m/z* (ESI): calculated for $C_{10}H_{10}NO_4BrNa^+$: 309.9691, found: 309.9687.

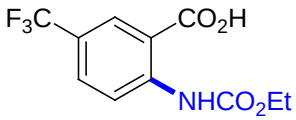

5ea was synthesized according to the general procedures but with 2 equivalents of KOAc, and run at 130 ˚C. It was isolated as a pale yellow solid (30.5 mg, 55% yield). mp = 187-188 ^{o}C; ^{1}H NMR (d_6-acetone, 400 MHz): δ_H 10.9 (s, 1H), 8.64 (d, J = 8.8 Hz, 1H), 8.33 (s, 1H), 7.90 (d, J = 7.6 Hz, 1H), 4.23 (q, J = 7.2 Hz, 2H), 1.29 (t, J = 7.2 Hz, 3H); ^{13}C NMR (d_6-acetone, 100 MHz): δ_C 169.7 (C), 154.0 (C), 146.3 (C), 131.6 (CH), 129.4 (CH), 129.1, 126.4, 123.8, 121.1 (q, J_{CF} = 269 Hz, CF_3), 124.0,

123.6, 123.3, 121.1 (q, J_{CF} = 33 Hz, C), 119.6 (CH), 116.2 (C), 62.2 (CH_2), 14.7 (CH_3); IR (KBr, cm^{-1}): 3332, 1732, 1689, 1592, 1542, 1409, 1249, 1121, 1087; HRMS *m/z* (ESI): calculated for $C_{11}H_{10}NO_4F_3Na^+$: 322.0279, found: 322.265.

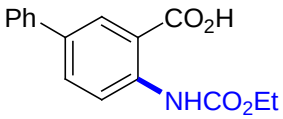

5fa was isolated as a pale yellow solid (26.8 mg, 47% yield). mp = 187-188 ^oC; ^1H NMR (*d*$_4$-methanol, 400 MHz): δ_H 8.43 (d, *J* = 8.8, 1H), 8.29 (s, 1H), 7.79 (d, *J* = 8.8, 1H), 7.59 (d, *J* = 7.2 Hz, 2H), 7.43 (t, *J* = 7.6 Hz, 2H), 7.32 (t, *J* = 7.2 Hz, 1H), 4.22 (q, *J* = 7.2 Hz, 2H), 1.32 (t, *J* = 7.2 Hz, 3H); ^{13}C NMR (*d*$_4$-methanol, 100 MHz): δ_C 153.7 (C), 140.7 (C), 139.5 (C), 134.3 (C), 132.4 (C), 132.0 (CH), 129.2 (CH), 128.5 (CH), 126.9 (CH), 126.5 (C), 126.1 (CH), 118.6 (CH), 60.8 (CH_2), 13.3 (CH_3); IR (KBr, cm^{-1}): 3339, 3028, 2485, 1742, 1670, 1247; HRMS *m/z* (ESI): calculated for $C_{16}H_{15}NNaO_4^+$: 308.0899, found: 308.0890.

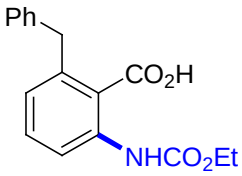

5ga was isolated as a pale yellow solid (42.5 mg, 71% yield). mp = 117-118^oC; ^1H NMR ($CDCl_3$, 400 MHz): δ_H 8.78 (s, 1H), 8.06 (d, *J* = 6.8 Hz, 1H), 7.39 (t, *J* = 8.0 Hz, 1H), 7.26-7.10 (m, 5H), 6.92 (d, *J* = 7.6 Hz, 1H), 4.26-4.20 (m, 4H), 1.30 (t, *J* = 7.2 Hz, 3H); ^{13}C NMR ($CDCl_3$, 100 MHz): δ_C 154.0 (C), 142.1 (C), 140.4 (C), 139.2 (C), 138.7 (C), 132.2 (CH), 128.9 (CH), 128.3 (CH), 126.2 (CH), 126.1 (CH), 119.2 (CH), 61.5 (CH_2), 40.5 (CH_2), 14.4 (CH_3); IR (KBr, cm^{-1}): 3360, 3027, 1739, 1653, 1528, 1266, 1216, 1089; HRMS *m/z* (ESI): calculated for $C_{17}H_{17}NO_4Na^+$: 322.1055, found: 322.1059.

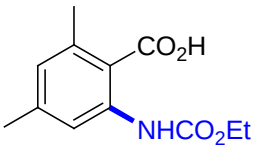

5ha was isolated as a yellow solid (34.6 mg, 73% yield). mp = 145-146 °C; ^{1}H NMR (d_4-methanol, 400 MHz): δ_H 7.69 (s, 1H), 6.80 (s, 1H), 4.17 (q, J = 7.2 Hz, 2H), 2.44 (s, 3H), 2.30 (s, 3H), 1.29 (t, J = 7.2 Hz, 3H); ^{13}C NMR (d_4-methanol, 100 MHz): δ_C 171.4 (C), 155.3 (C), 142.6 (C), 139.8 (C), 139.4 (C), 127.6 (CH), 119.6 (CH), 61.8 (CH_2), 22.1 (CH_3), 21.1 (CH_3), 14.4 (CH_3); IR (KBr, cm^{-1}): 3217, 2372, 1706, 1664, 1428, 1224; HRMS *m/z* (ESI): calculated for $C_{12}H_{15}NO_4Na^+$: 260.0899, found: 260.0898.

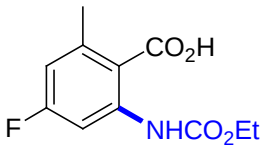

5ia was isolated as a brown solid (22.2 mg, 46% yield). mp = 133-134 °C; ^{1}H NMR ($CDCl_3$, 400 MHz): δ_H 9.71 (s, 1H), 8.03 (dd, J = 11.2 Hz, 2 Hz, 1H), 6.66 (dd, J = 8.8 Hz, 2 Hz, 1H), 4.24 (q, J = 7.2 Hz, 2H), 1.33 (t, J = 7.2 Hz, 3H); ^{13}C NMR ($CDCl_3$, 100 MHz): δ_C 172.4 (C), 166.2, 163.7 (d, J = 250 Hz, CF), 153.4 (C), 144.5, 144.4 (d, J = 11 Hz, C), 143.5, 143.4 (d, J = 13 Hz, C), 113.1, 112.9 (d, J = 22 Hz, CH), 104.9, 104.7 (d, J = 28 Hz, CH), 61.5 (CH_2), 23.8 (CH_3), 14.4 (CH_3); IR (KBr, cm^{-1}): 3256, 1725, 1606, 1523, 1446, 1245, 1197; HRMS *m/z* (ESI): calculated for $C_{11}H_{12}NO_4FNa^+$: 264.0648, found: 264.0659.

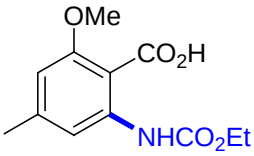

5ja was isolated as a yellow solid (25.3 mg, 50% yield). mp = 102-103 °C; ^{1}H NMR (d_4-methanol, 400 MHz): δ_H 7.64 (s, 1H), 6.64 (s, 1H), 4.17 (q, J = 7.2 Hz, 2H), 3.90 (s, 3H), 2.34 (s, 3H), 1.29 (t, J = 7.2 Hz, 3H); ^{13}C NMR (d_4-methanol, 100 MHz): δ_C 169.9 (C), 159.9 (C), 154.9 (C), 145.6 (C), 141.5 (C), 114.0 (CH), 107.7 (CH), 106.6 (C), 61.9 (CH_2), 56.6 (CH_3), 21.9 (CH_3), 14.4 (CH_3); IR (KBr, cm^{-1}): 3199, 2990, 1735, 1707, 1583, 1442, 1366, 1254, 1223, 1049; HRMS *m/z* (ESI): calculated for $C_{12}H_{15}NO_5Na^+$: 276.0848, found: 276.0843.

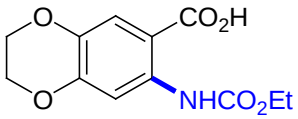

5ka was isolated as a white solid (21.4 mg, 40% yield). mp = 210-211 °C; ^{1}H NMR (d_4-methanol, 400 MHz): δ_H 7.83 (s, 1H), 7.50 (s, 1H), 4.31-4.29 (m, 2H), 4.23-4.21 (m, 2H), 4.18 (q, J = 7.2 Hz, 2H), 1.29 (t, J = 7.2 Hz, 3H); ^{13}C NMR (d_6-DMSO, 100 MHz): δ_C 170.5 (C), 154.2 (C), 149.7 (C), 139.1 (C), 137.4 (C), 120.4 (CH), 109.8 (C), 107.9 (CH), 66.3 (CH_2), 65.2 (CH_2), 62.1 (CH_2), 15.8 (CH_3); IR (KBr, cm^{-1}): 1736, 1646, 1565, 1308, 1266, 1064; HRMS *m/z* (ESI): calculated for $C_{12}H_{13}NO_6Na^+$: 290.0641, found: 296.0650.

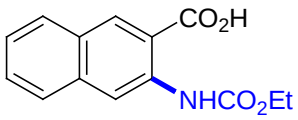

5la was isolated as a yellow solid (28.5 mg, 55% yield). mp = 197-198 °C; ^{1}H NMR (d_6-acetone, 400 MHz): δ_H 10.7 (bs, 1H), 8.82 (s, 1H), 8.76 (s, 1H), 7.98 (d, J = 8.0 Hz, 1H), 7.86 (d, J = 8.4 Hz, 1H), 7.61 (t, J = 8.0 Hz, 1H), 7.45 (t, J = 8.0 Hz, 1H),

4.23 (q, J = 7.2, 2H), 1.31 (t, J = 7.2 Hz, 3H); ^{13}C NMR (d_6-acetone, 100 MHz): δ_C 169.4 (C), 153.2 (C), 137.1 (C), 136.5 (C), 133.6 (CH), 129.2 (CH), 129.0 (CH), 128.0 (C), 127.0 (CH), 125.0 (CH), 115.6 (C), 114.6 (CH), 60.6 (CH_2), 13.9 (CH_3); IR (KBr, cm^{-1}): 3330, 2987, 1723, 1678, 1541, 1284, 1247, 1220, 1041; HRMS *m/z* (ESI): calculated for $C_{14}H_{13}NO_4Na^+$: 282.0742, found: 282.0748.

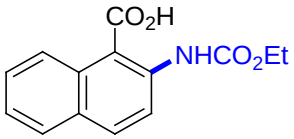

5ma was isolated as a brown solid (10.9 mg, 21% yield). mp = 140-142 ^{o}C; ^{1}H NMR ($CDCl_3$, 400 MHz): δ_H 9.58 (s, 1H), 8.55 (d, J = 8.4 Hz, 1H), 8.46 (d, J = 9.2 Hz, 1H), 7.98 (d, J = 9.2 Hz, 1H), 7.81 (d, J = 8.0 Hz, 1H), 7.56 (t, J = 8.0 Hz, 1H), 7.44 (t, J = 7.6 Hz, 1H), 4.27 (q, J = 7.2 Hz, 2H), 1.35 (t, J = 7.2 Hz, 3H); ^{13}C NMR ($CDCl_3$, 100 MHz): δ_C 172.9 (C), 153.8 (C), 140.0 (C), 134.3 (CH), 131.4 (C), 129.9 (C), 128.4 (CH), 128.0 (CH), 125.7 (CH), 124.9 (CH), 119.3 (CH), 61.6 (CH_2), 14.4 (CH_3); IR (KBr, cm^{-1}): 1729, 1654, 1577, 1508, 1251, 1214, 1085, 825; HRMS *m/z* (ESI): calculated for $C_{14}H_{13}NO_4Na^+$: 282.0742, found: 282.0747.

Chapter 3

Kinetic Investigation on the Palladium-Catalyzed Intermolecular Arene C-H Bond Amidation of Anilides by *N*-Nosyloxycarbamates

3.1 Introduction

In Chapter 2, we described the Pd(II)-catalyzed arene C-H amidation of anilides with *N*-sulfonyloxycarbamates as reagent. It was hypothesized that the catalytic reaction should involve three major steps: (1) directing group-assisted *ortho*-C-H bond cleavage by Pd(II) complex to form cyclopalladated complexes; (2) coupling of the cyclopalladated complexes with *N*-sulfonyloxycarbamate to give a putative arylamido-palladium complex, and (3) protonation of the amido complex to release the product amide with concomitant regeneration of the Pd(II) catalyst (Scheme 3.1).

Pertaining to the mechanism of the catalytic C-H amidation, several questions remain outstanding: (1) Which reaction manifold, Pd(0)/(II) or Pd(II)/(IV), would the reaction proceed? (2) What is the catalyst resting state? (3) What is the nature of the reaction of the *N*-nosyloxycarbamate with the arylpalladium(II) resulting in the C-N

bond formation?

Scheme 3.1 Previously Proposed Catalytic Cycle

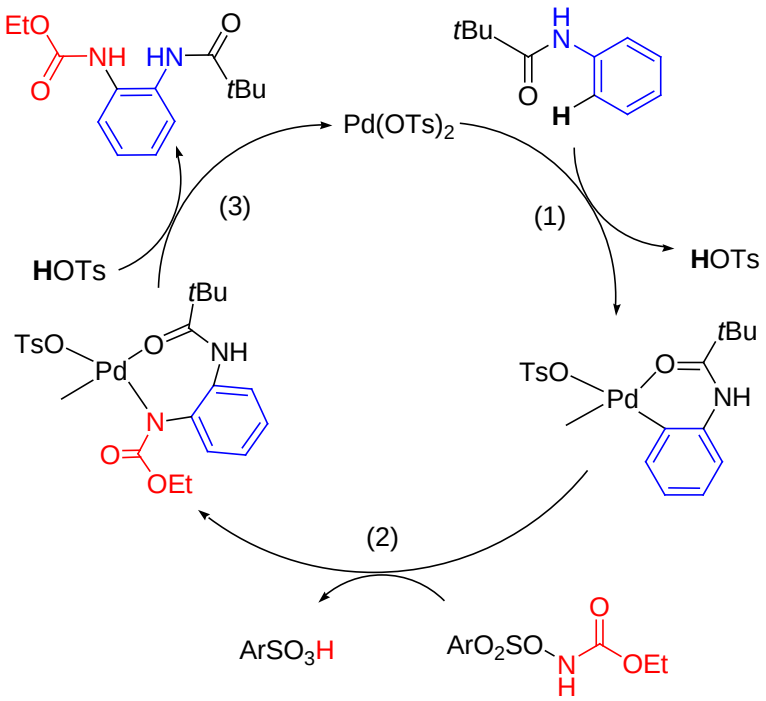

To address these issues, we herein present a kinetic study on the Pd(II)-catalyzed *ortho*-C-H amidation of pivalanilides with *N*-sulfonyloxycarbamates. On the basis of our findings, a plausible mechanism will be discussed.

3.2 Results

3.2.1 Testing the Feasibility of the Pd(0)/(II) Reaction Manifold

It is generally accepted that the mechanism of the Buchwald-Hartwig amination reaction should operate by a Pd(0)/(II) cycle. Reaction of arylpalladium(II) complexes with amines / amides would afford the arylpalladium(II)-amido complexes. Reductive elimination of the arylpalladium(II) amido complex should furnish the arylamine products and a Pd(0) complex. Similar to other amides, carbamates are known to be effective coupling partners for the Pd(II)-catalyzed amidation of aryl halides.[4c,d]

To test the viability of the Pd(0)/(II) cycle for the direct C-H amidation reaction, we reacted 2,4-dimethylpivalanilide (**1a**) and ethyl carbamate (1 equiv) with K_2CO_3 (1.2 equiv) and [$Pd(OTs)_2(MeCN)_2$] (10 mol%) in 1,4-dioxane (2 mL) at 80 °C for 6 h; no **3aa** formation was observed with full recovery of **1a** and the ethyl carbamate. Notably, the stoichiometric reaction between the cyclopalladated complex of **1a** (i.e., **1aPd**, 0.05 mmol) and ethyl carbamate (2 equiv) in the presence of K_2CO_3 (2 equiv) in 1,4-dioxane (2 mL) at 80 °C for 2 h failed to produce any **3aa** with complete recovery of the starting materials (Scheme 3.2). Based on these results, reductive elimination of the arylpalladium(II)-amido complex for the C-N bond formation

should not be a plausible pathway for the direct amidation of **1a**.

Scheme 3.2 Ethyl Carbamates are Ineffective Coupling Partners for the Direct C-H Amidation of Anilides

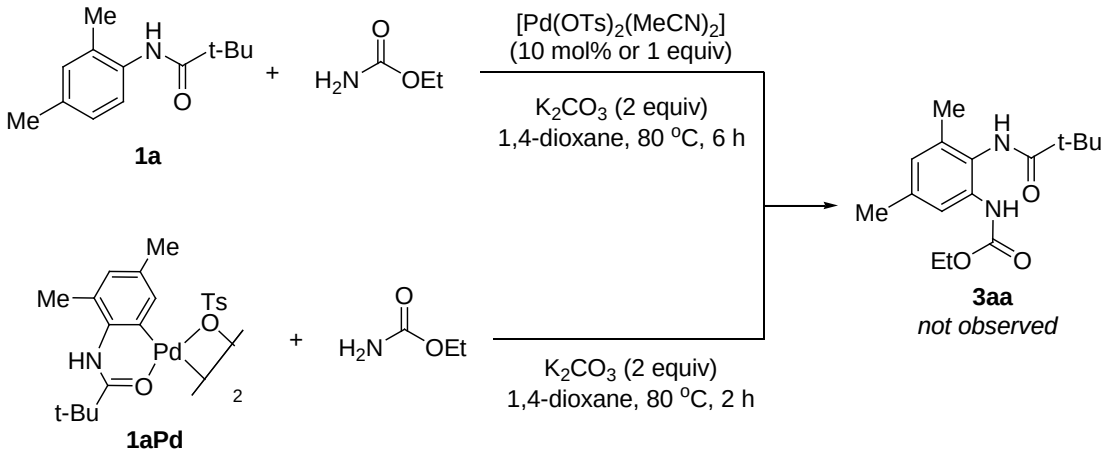

3.2.2 Reaction Rate Order

To gain more mechanistic information about the amidation reaction, we sought to establish the kinetic rate order for each component.

For the kinetic experiments, we chose the reaction of 2,4-dimethylpivalanilide (**1a**) with ethyl *N*-nosyloxycarbamate (**2aNs**) and $[Pd(OTs)_2(MeCN)_2]$ in *d*-chloroform as model. There are two reasons to justify this choice: (1) the reaction proceeded readily in *d*-chloroform to give **3aa** in 70% yield at 80 ˚C in 4 h; (2) the ^1H NMR signals of the reagents (**1a, 2aNs**) and the product amide (**3aa**) were well

resolved, and thus monitoring of the reaction should be straightforward.

Initial rate method was employed for the kinetic study. We first determined the rate order in **1a** by performing the reactions with fixed concentrations of **2aNs** (100 mM) and [$Pd(OTs)_2(MeCN)_2$] (10 mM), and varying the concentrations of **1a** (50, 100, 150 and 200 mM) in *d*-chloroform (1 mL) at 80 °C. The reaction mixture were pre-heated at 80 °C for 20 seconds to ensure complete dissolution of all the reagents, and the reactions were run for a certain amount of time with **1a** conversion being kept < 25% (see the Experimental Section for details). The reactions were then quenched by immediately cooling to 0 °C. The reaction crude mixtures were spiked with the internal standard (dibromomethane, 0.1 mmol) and were subjected to ^{1}H NMR analysis to determine the quantity of **3aa**. The initial rates were determined by plotting [**3aa**] against time. A plot of the initial rates (*d*[**3aa**] / *d*t) versus [**1a**] gave a straight line (R^2 = 0.99), which is consistent with a first-order dependence on [**1a**] (Figure 3.1). The first-order dependence on [**1a**] was further verified by plotting log (*d*[**3aa**] / *d*t) against log [**1a**], and a linear plot with a slope of 0.78 (R^2 = 0.99) weas obtained (Figure 3.2). This result suggests that one equivalent of **1a** is involved in / before the turnover-limiting step.

Figure 3.1 Plot of the Initial Rate (d[**3aa**] / dt) versus [**1a**]

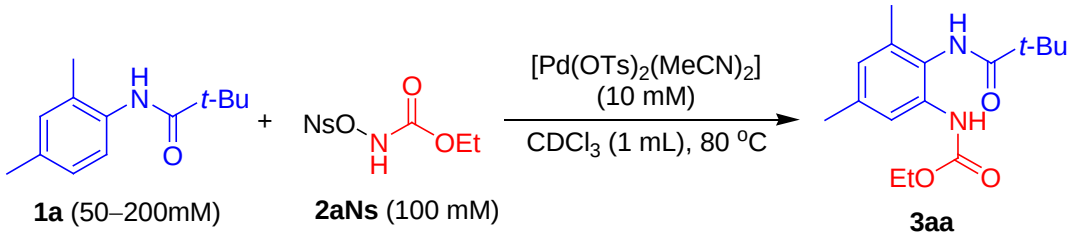

1a (50–200mM) **2aNs** (100 mM) **3aa**

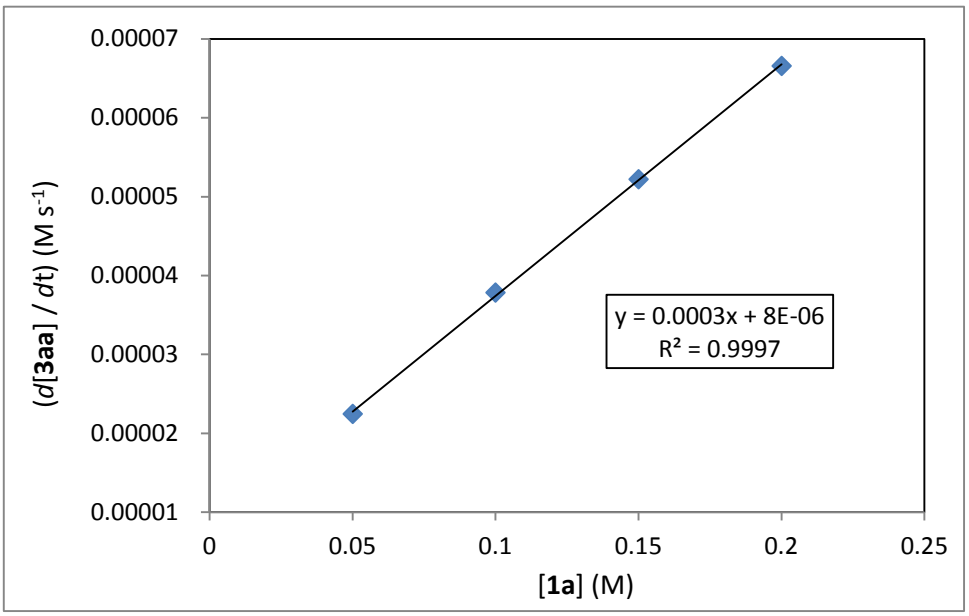

Figure 3.2 Plot of Log (d[**3aa**] / dt) versus Log [**1a**]

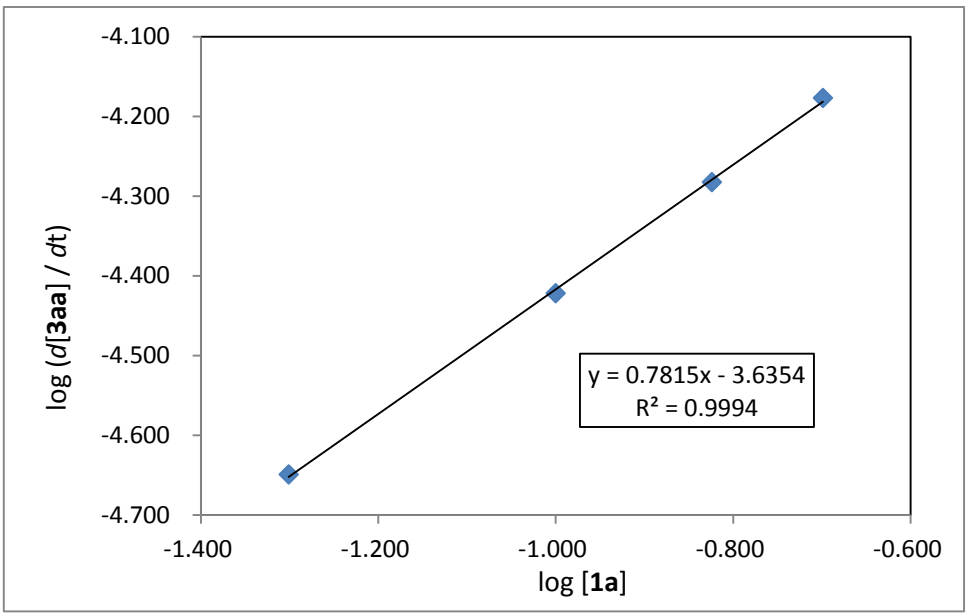

To determine the kinetic order of **2aNs**, the kinetic experiments were performed with fixed concentrations of **1a** (100 mM) and [$Pd(OTs)_2(MeCN)_2$] (10 mM), and varying the concentrations of **2aNs** (50, 75, 100 and 200 mM) in *d*-chloroform (1 mL) at 80 °C. Plotting the initial rates (*d*[**3aa**] / *d*t) against [**2aNs**] provided a linear fit (R^2 = 0.99), revealing a first-order dependence on [**2aNs**] (Figure 3.3). The result was further confirmed by plotting log (*d*[**3aa**] / *d*t) against log [**2aNs**] giving a straight line with a slope of 0.96 (R^2 = 0.99) (Figure 3.4). Therefore, one equivalent of **2aNs** should be involved in / before the turnover-limiting step.

Figure 3.3 Plot of Initial Rate (*d*[**3aa**] / *d*t) versus [**2aNs**]

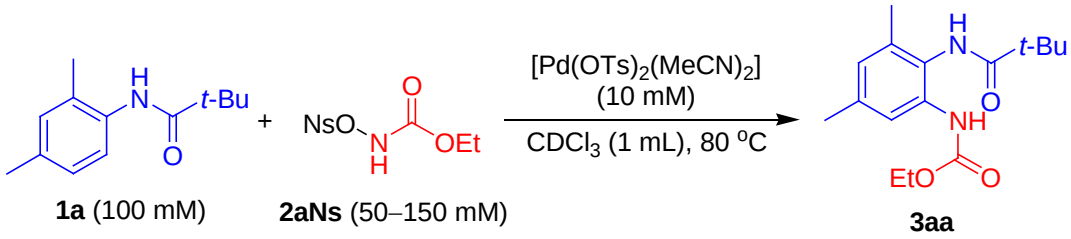

1a (100 mM) **2aNs** (50–150 mM) **3aa**

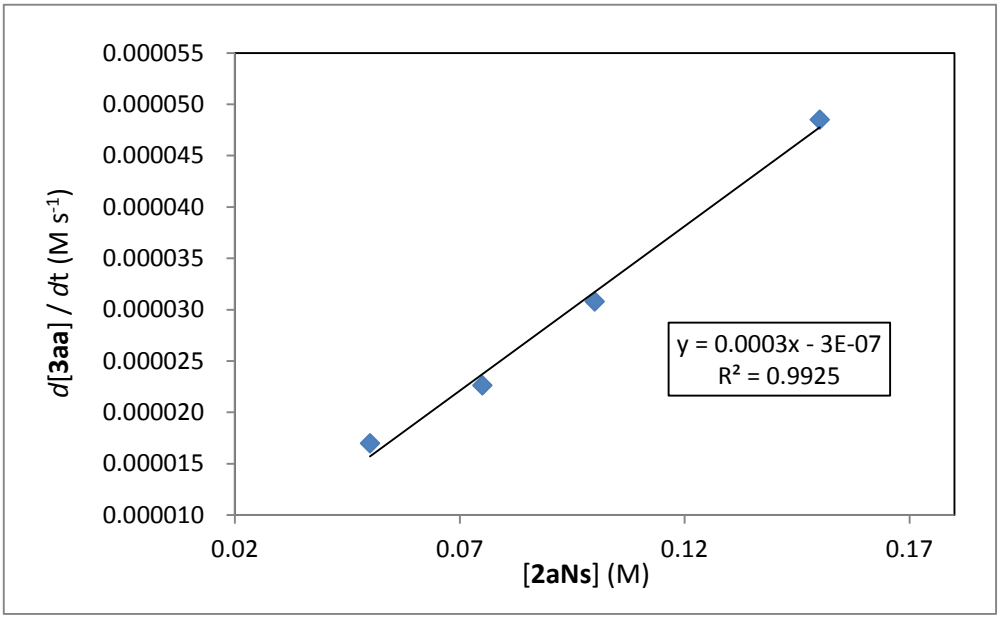

Figure 3.4 Plot of Log (*d*[**3aa**] / *d*t) versus Log [**2aNs**]

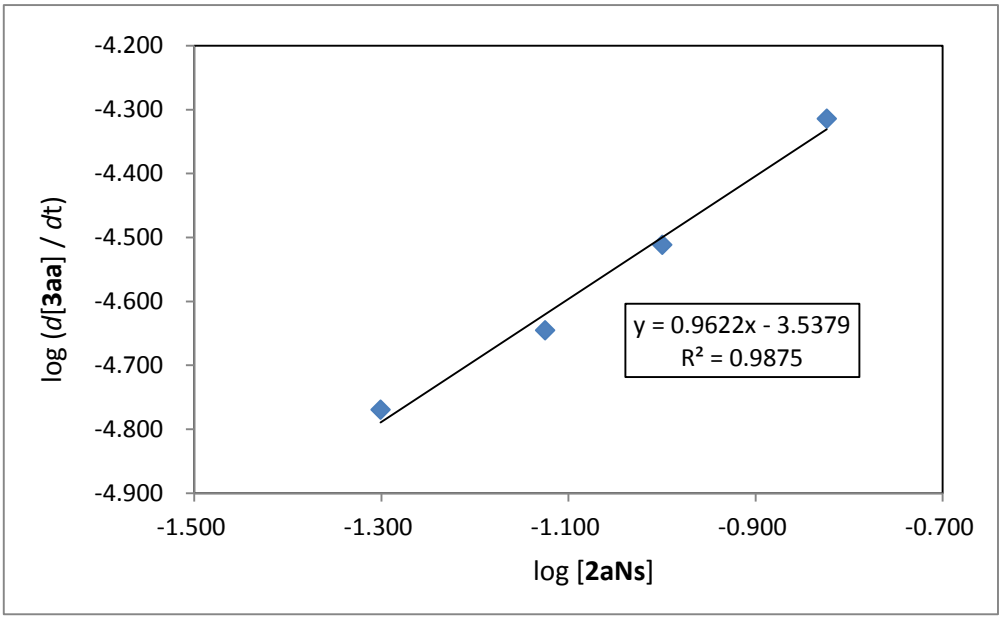

The kinetic rate order of [**Pd**] was determined by performing the kinetic experiments with varying concentrations of [**Pd(OTs)$_2$(MeCN)$_2$**] ([**Pd**], 5, 10, 12.5 and 15 mM) and fixed concentrations of **1a** (100 mM) and **2aNs** (100 mM) in *d*-chloroform (1 mL) at 80 °C. The plot of the initial rates (*d*[**3aa**] / *d*t) against [**Pd(OTs)$_2$(MeCN)$_2$**] revealed a concave curve (Figure 3.5). When plotting (*d*[**3aa**] / *d*t) against [**Pd(OTs)$_2$(MeCN)$_2$**]^2, a linear plot (R^2 = 0.98) was obtained, and that is indicative of a second-order dependence on [**Pd**] (Figure 3.6). The second-order dependence was further verified by the plot of log (*d*[**3aa**] / *d*t) versus log [**Pd(OTs)$_2$(MeCN)$_2$**]; a linear relationship (R^2 = 0.98) with a slope of 1.80 was obtained (Figure 3.7). The second-order kinetics on [**Pd**] implies that the amidation reaction would probably involve a dinuclear palladium intermediate.

Figure 3.5 Plot of Initial Rate (d[**3aa**] / dt) versus [**Pd(OTs)$_2$(MeCN)$_2$**]

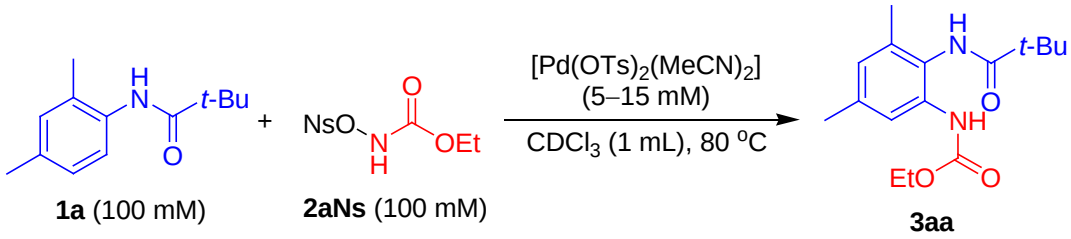

1a (100 mM) **2aNs** (100 mM) **3aa**

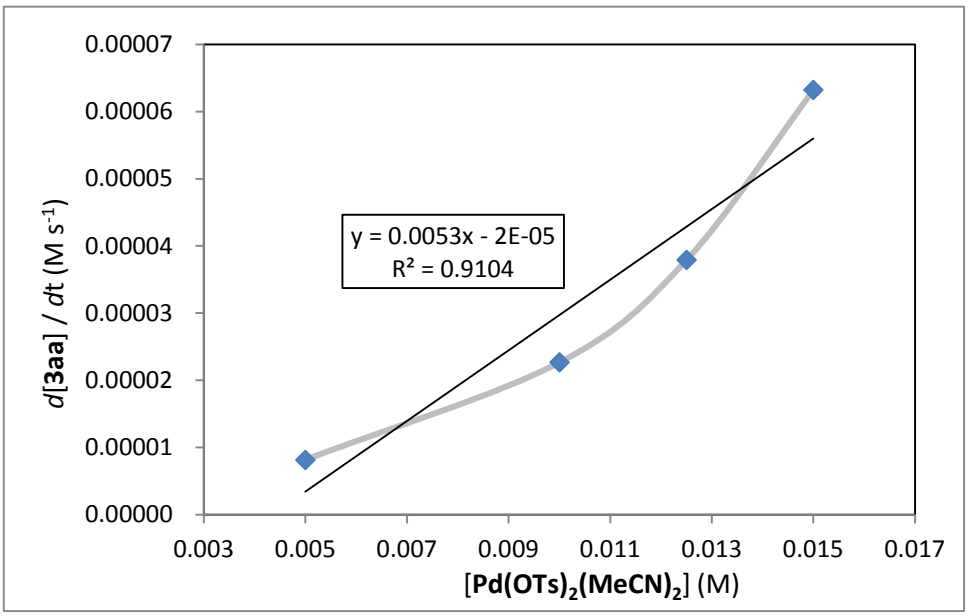

Figure 3.6 Plot of Initial Rate (d[**3aa**] / dt) versus [**Pd(OTs)$_2$(MeCN)$_2$**]^2

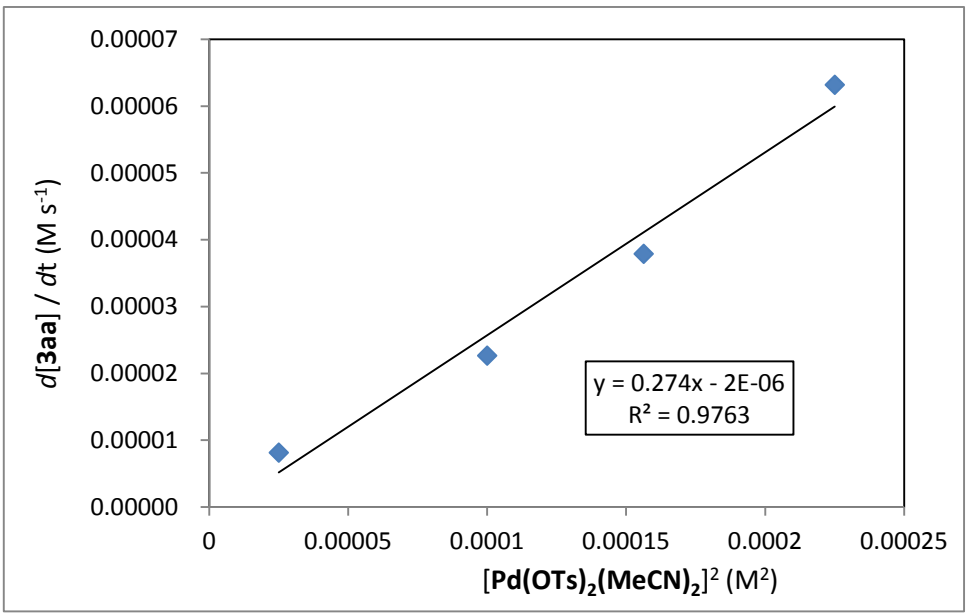

Figure 3.7 Plot of Log (*d*[**3aa**] / *d*t) versus Log [**Pd(OTs)$_2$(MeCN)$_2$**]

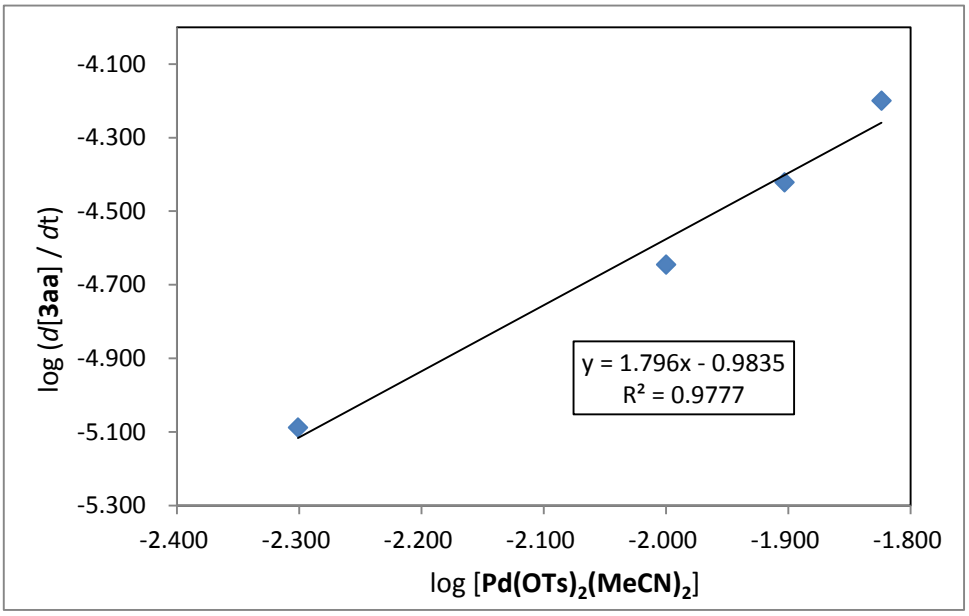

On the basis of the kinetic studies, the following experimental rate law (3.1) was established:

$$rate = k[\mathbf{1a}][\mathbf{2aNs}][\mathbf{Pd}]^2 \qquad (3.1)$$

Thus, one equivalent of **1a**, one equivalent of **2aNs** and two equivalents of a palladium catalyst are involved in / before the turnover-limiting step.

3.2.3 Kinetic Isotope Effect Studies

It has been widely documented that Pd(II)-catalyzed arene C-H functionalizations would exhibit primary kinetic isotope effect (KIE) when deuterated arenes are used as substrates. According to the literature, the intermolecular KIE (k_H / k_D) values were found to range from 2 — 5, and the rate-limiting C-H activation step was proposed.[7b, 41g, 60] In this work, we examined the intermolecular KIE so as to ascertain the nature of the turnover-limiting step.

Our KIE study was performed by determining the initial rates of the amidation of acetanilide (**1t**) and d_5-acetanilide (**1t**-d_5) separately (Scheme 3.3). Anilides **1t** and **1t**-d_5 (0.1 mmol) were treated separately with **2aNs** (1.2 equiv) and [Pd(OTs)$_2$(MeCN)$_2$] (10 mol%) in *d*-chloroform (1 mL) at 80 ˚C. For the amidation of **1t**, the reaction mixtures were pre-heated for 20 seconds for complete reagent dissolution. They were then run for an additional time (180, 360, 600, 900 s). The reactions were quenched by cooling the mixture to 0 °C (the substrate conversions of **1t** were ~10 — 30%). Likewise, for the amidation with **1t**-d_5, the reaction mixtures were pre-heated for 20 seconds for complete reagent dissolution and they were quenched at different time interval (300, 600, 900, 1200 s) by cooling to 0 °C (the substrate conversions of **1t**-d_5 < 20%). The initial rates were determined by measuring

the product yields using ^{1}H NMR with dibromomethane (0.1 mmol) as internal standard. The initial rates for **1t** and **1t**-d_5 were found to be 22.8 × 10^{-6} mol dm^{-3} s^{-1} and 8.1 × 10^{-6} mol dm^{-3} s^{-1}, respectively. Assuming that the amounts of all the reagents at the initial rates remained largely at their initial concentrations, the relative initial rates ((d[**3ta**] / dt) / (d[**3ta**-d_4] / dt)) would be equal to the values of k_H / k_D, and it was then determined to be 2.8. This k_H / k_D value was comparable to the literature reported values (k_H / k_D = 2 — 5) for some related Pd(II)-catalyzed arene C-H functionalizations. Based on this KIE study, the C-H activation should be a turnover-limiting step for the amidation.

Scheme 3.3 KIE Studies on the Parallel Reactions of **1t** and **1t**-d_5 with **2aNs**

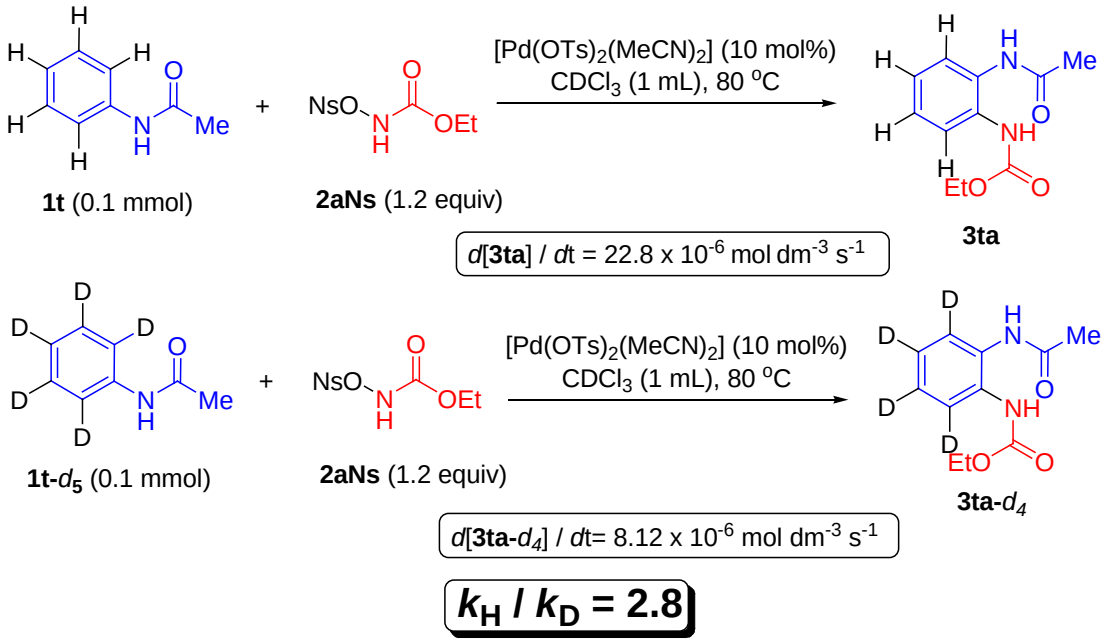

3.2.4 Nature of the C-H Bond Amidation Step

With the established rate law (*rate* = *k* [**1a**][**2aNs**][**Pd**]^2), for gaining insight into the turnover-limiting, we performed linear free energy correlation studies.

3.2.4.1 Hammett Correlation Study for the Amidation of *para*-Substituted Pivalanilides

The reactions of *para*-substituted pivalanilides (**1-Y**) with ethyl *N*-nosyloxycarbamate were examined. In this study, the *para*-substituted pivalanilide (0.1 mmol) was treated with **2aNs** (1 equiv) and [$Pd(OTs)_2(MeCN)_2$] (10 mol%) in *d*-chloroform (1 mL) at 80 °C. The reactions were pre-heated at 80 °C for 20 seconds to ensure complete dissolution of the reagents, and the reactions were run for further 600 s (in all cases, about 10 — 20% of pivalanilide conversion were attained). The reactions were then quenched by quickly cooling the mixture down to 0 °C. A parallel reaction using unsubstituted pivalanilide (**1-H**) as substrate was also performed in the same manner. The reactions were run in triplicate. The initial rates of the amidation were determined by measuring the product formation using ^{1}H NMR with dibromomethane (0.1 mmol) as internal standard. Assuming that the amounts of all

the reagents at the initial rates remained largely at their initial concentrations, the relative initial rates ((*d*[**3-Y**] / *d*t) / (*d*[**3-H**] / *d*t)) would be equal to the values of k_Y / k_H. By plotting log(k_Y / k_H) versus the Hammett σ_{meta} constants, we obtained a straight line (R^2 = 0.98) with ρ value of -0.53 (Figure 3.8).

Figure 3.8 Linear Free Energy Correlation Study for the Pd(II)-Catalyzed Amidation of *para*-Substituted Pivalanilides

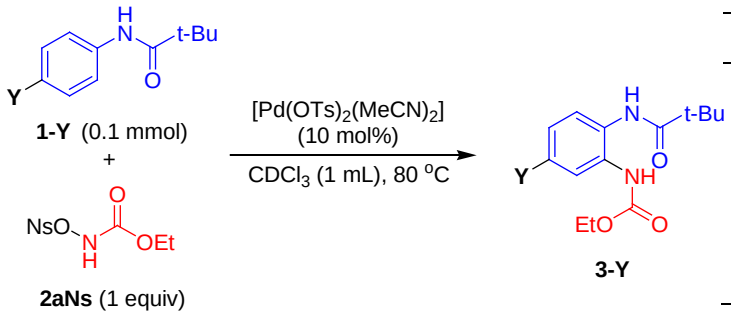

Y	k_Y / k_H	σ_{meta}
Me	1.109	-0.06
H	1.000	0
F	0.719	0.36
Br	0.658	0.37
CF_3	0.556	0.46

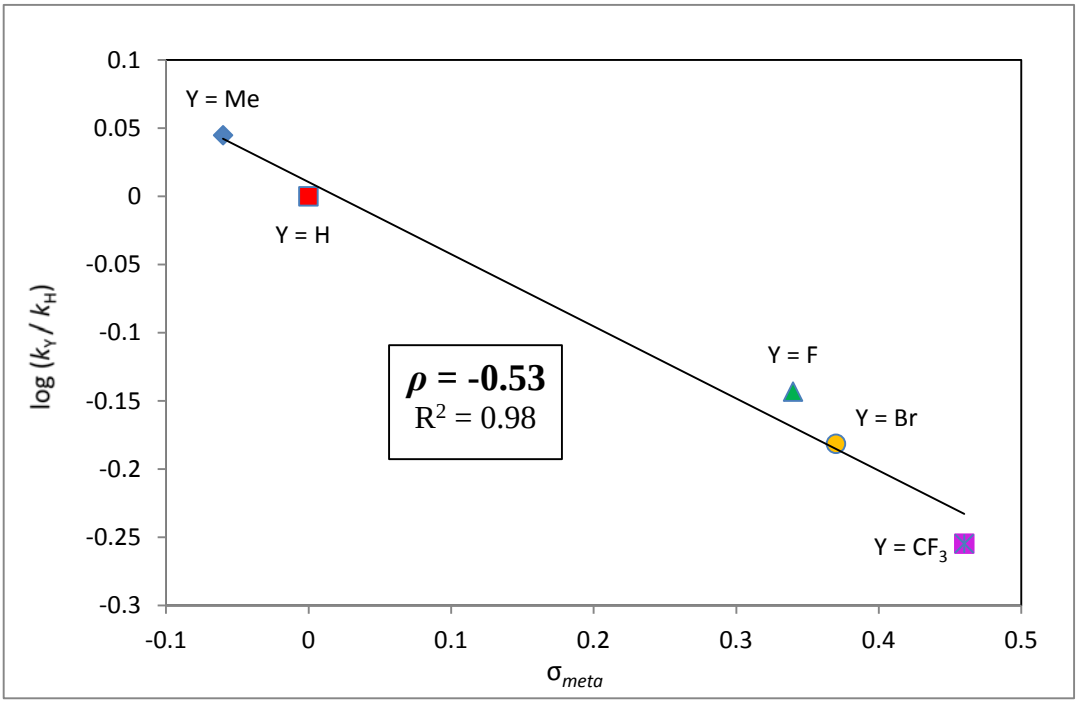

The small negative ρ value suggests the build-up of a partial positive charge at

the C-H activation step. Apparently, the amidation is decelerated by electron-withdrawing *para*-substituents

3.2.4.2 Hammett Correlation Study for *para*-Substituted Ethyl *N*-Arylsulfonyloxycarbamates

We have examined the electronic effect on the *N*-arylsulfonyloxycarbamates for the amidation reaction of **1a**. In this regard, a set of *para*-substituted ethyl *N*-arylsulfonyloxycarbamates (**2-Y**) was employed as reagents under the standard reaction conditions: **1a** (0.1 mmol), ethyl *N*-arylsulfonyloxycarbamate (1 equiv) and $[Pd(OTs)_2(MeCN)_2]$ (10 mol%) in *d*-chloroform (1 mL) at 80 °C. The reaction mixtures were pre-heated at 80 °C for 20 seconds to ensure complete dissolution of all the reagents. The reactions were then run for further 10 min (**1a** conversion being limited to 10 — 20%) and were quenched by quickly cooling down the mixtures to 0 °C. A parallel reaction with ethyl *N*-benzenesulfonyloxycarbamate (**2-H**) as reagent was performed in the same manner. The reactions were run in triplicate. The initial rates of the amidation were determined by measuring the product (**3aa**) formation using ^{1}H NMR with dibromomethane (0.1 mmol) as internal standard. A linear regression analysis (R^2 = 0.97) of log (k_Y / k_H) against the Hammett σ_{para} constants

gave a ρ value of +0.46 (Figure 3.9).

Figure 3.9 Linear Free Energy Correlation Study for the Pd(II)-Catalyzed Amidation of Pivalanilide with *para*-Substituted Ethyl *N*-Arylsufonyloxycarbamates

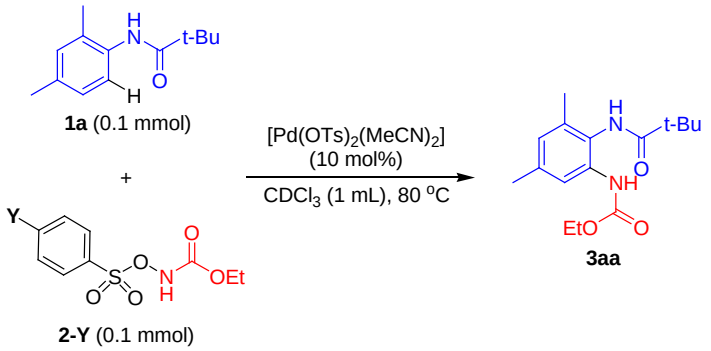

Y	k_Y / k_H	σ_{para}
Me	0.739	-0.14
H	1.000	0
F	1.130	0.36
CF_3	1.713	0.37
NO_2	2.083	0.46

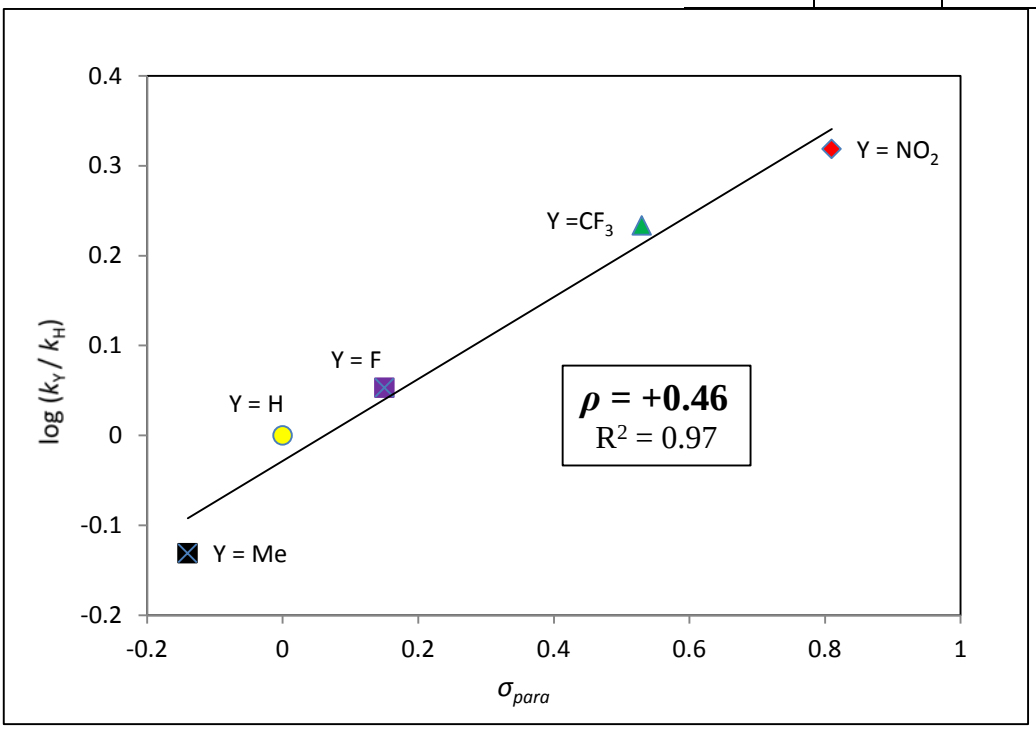

The amidations were promoted by electron-withdrawing *para*-substituents on the arylsulfonates. However, the small positive ρ value indicated a small negative charge build-up at the transition state involving a partial N-O bond cleavage.

3.2.5 Stoichiometric Reactions of Cyclopalladated Complex (1aPd) with *N*-Nosyloxycarbamate

In this work, we have examined the stoichiometric reaction of *N*-nosyloxycarbamate with the cyclopalladated complex of pivalanilide. With reference to a reported procedure,[41a] treating **1a** (1 mmol) and $Pd(OAc)_2$ (1 mmol) with *p*-toluenesulfonic acid (1 equiv) in dichloromethane (10 mL) at 60 ˚C in a vial sealed with a Teflon® liner cap for 30 min produced the dinulcear **1aPd** complex, which was obtained in 80% yield as a brownish yellow solid.

When **1aPd** (0.05 mmol) reacted with **2aNs** (2.4 equiv) in 1,4-dioxane (1 mL) at 80 °C for 2 h, the expected product **3aa** was formed in 45% yield (Table 3.1, entry 1). With two equivalents of **1a** (0.1 mmol) as additive, the stoichiometric reaction of **1aPd** and **2aNs** afforded **3aa** in 75% yield (entry 2). It is plausible that the additional anilide was needed to stabilize the resultant amido-Pd complexes or to release the amide product probably through ligand exchange (see the later sections). It is noteworthy that **1aPd** is a competent catalyst for the C-H amidation. For example, **1aPd** (5 mol%) effectively catalyzed the amidation of **1a** (0.2 mmol) with **2aNs** (2 equiv) in 1,4-dioxane (2 mL) at 80 °C for 2 h to furnish **3aa** in 85% yield (Scheme 3.4).

Table 3.1 Stoichiometric Amidation of **1aPd** with **2aNs**[a]

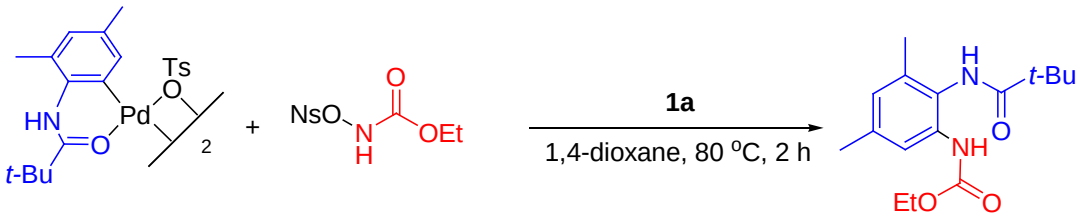

1aPd (0.05mmol) **2aNs** (0.12mmol) **3aa**

entry	**1a**	**3aa** yield(%)[b]
1	--	45
2	0.1 mmol (0.1 mmol)	75

[a]Reaction conditions: **1aPd** (0.05 mmol), **2aNs** (0.12 mmol), 1,4-dioxane (2 mL), 80 °C, 2 h. [b]Yields were determined by ^{1}H NMR with dibromomethane (0.1 mmol) as internal standard.

Scheme 3.4 Cyclometallated **1aPd** Complex is a Competent Catalyst for the Catalytic C-H Amidation

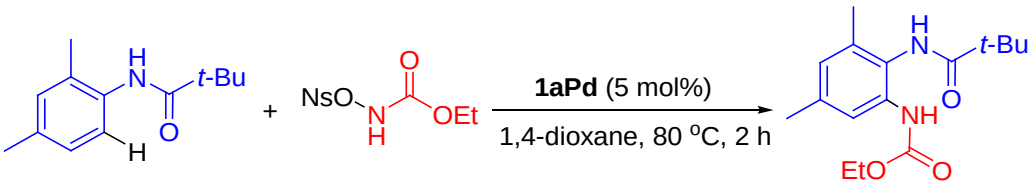

1a (0.2 mmol) **2aNs** (1.2 equiv) **3aa**, 85%

3.2.6 The Impeded Amidation Reaction with *N*-Alkylated Ethyl *N*-Nosyloxycarbamate as Reagent

According to the literature, *N*-arylsulfonyloxycarbamates were known to be nitrene precursors. For example, Maricich and co-workers reported that ethyl *N*-nosyloxycarbamate (25 mmol) reacted with cyclohexane (in excess) in the presence of triethylamine (1 equiv) in dichloromethane at room temperature for 17 h to give cyclohexylurethane in 20% yield. In addition, ethyl *N*-nosyloxycarbamate (30 mmol) was found to react with cyclohexene (in excess) and triethylamine (1 equiv) in dichloromethane for 3 h to afford aziridines in 57% yield (Scheme 3.5).[61b] The nitrene generation mechanism was generally proposed to be *via* sequential deprotonation and α-elimination reactions (Scheme 3.6).[61]

Since nitrene generation must be preceded by N-H deprotonation, the *N*-alkylation should render the nitrenoid formation pathway implausible. Thus, to assess whether a nitrenoid species is an obligatory intermediate in the Pd(II)-catalyzed C-H amidation reaction, we employed ethyl *N*-methyl-*N*-nosyloxycarbamate **2dNs** as probe. The synthesis of **2dNs** is analogous to that of ethyl *N*-nosyloxycarbamate (**2aNs**) with *N*-methylhydroxyamine being used as the starting material, and **2dNs** was obtained in 62% yield.

Scheme 3.5 Reactions of Ethyl *N*-Nosyloxycarbamate with Cyclohexane and Cyclohexene

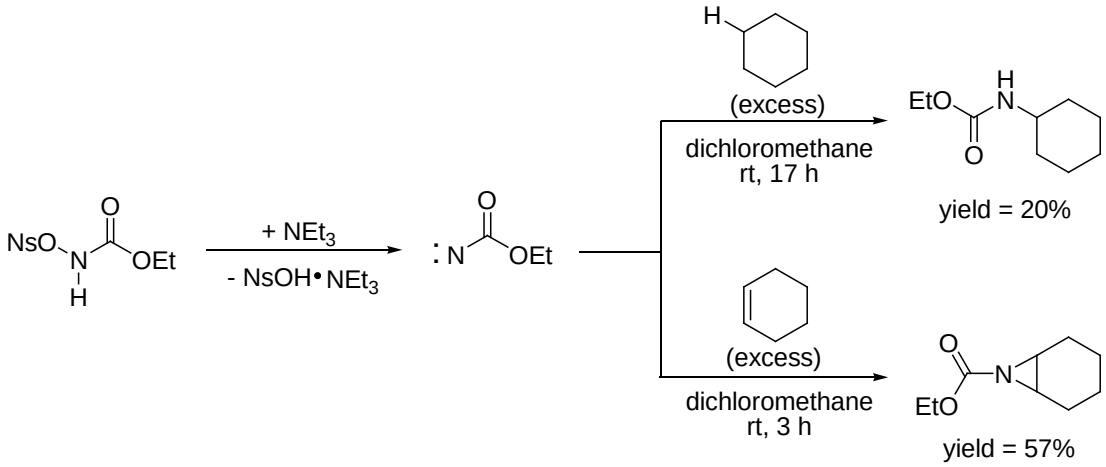

Scheme 3.6 Base-induced Nitrene Generation from *N*-Arylsulfonyloxycarbamate

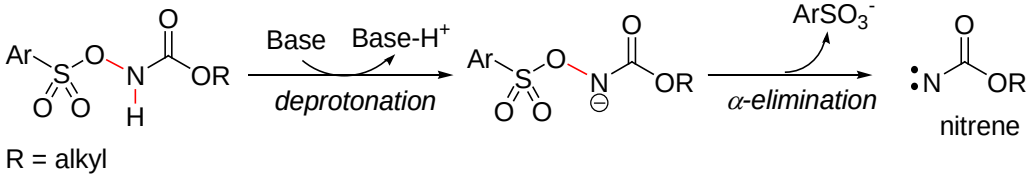

In this work, when **1a** (0.2 mmol) was treated with **2dNs** (1.2 equiv) and $[Pd(OTs)_2(MeCN)_2]$ (10 mol%) in 1,4-dioxane (2 mL) at 80 °C for 6 h, no C-N coupled product **3ad** was produced with **1a** being completely recovered (Table 3.2, entry 1). Notably, performing the reaction at higher temperature (120 °C) also failed to bring about any C-N bond formation with **2dNs** (entry 2). Stoichiometric reaction of the cyclopalladated complex **1aPd** (0.1 mmol) with **2dNs** (2.4 mmol) also failed to produce any **3ad** at 120 ˚C (entry 3).

Table 3.2 *N*-Methyl-*N*-nosyloxycarbamate (**2dNs**) is an Ineffective Amidation Reagent[a]

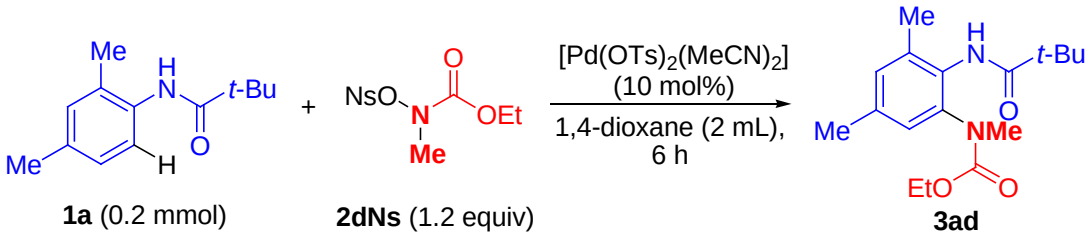

1a (0.2 mmol) **2dNs** (1.2 equiv) **3ad**

entry	temperature (°C)	**3ad** yield (%)[b]
1	80	0
2	120	0
3[c]	120	0

[a]Reaction conditions: **1a** (0.2 mmol), **2aNs** (1.2 equiv), $[Pd(OTs)_2(MeCN)_2]$ (10 mol%), 1,4-dioxane (2 mL), 6 h. [b]Yields were determined by ^{1}H NMR with dibromomethane (0.1 mmol) as internal standard. [c]**1aPd** (0.1 mmol) and **2dNs** (2.4 mmol) were employed for a stoichiometric reaction; no **1a** and $[Pd(OTs)_2(MeCN)_2]$ added.

As *N*-methyl-*N*-nosyloxycarbamate (**2dNs**) is an ineffective reagent for the Pd-catalyzed C-H amidation reaction, this finding implies that the N-H deprotonation is a necessary step for the product turnover and the reaction is likely to go through the nitrenoid formation pathway. In addition, the failure of the amidation reaction of the cyclopalladated complex **1aPd** with **2dNs** to effect C-N bond formation argued against the formation of the possible amido-palladium(IV) intermediate by oxidative addition with the N-O bond (see later sections).

3.3 Discussion

3.3.1 Proposed Mechanism and the Rate Law

Based our kinetic studies, a proposed reaction mechanism that explains the experimental rate law is depicted in Scheme 3.7.

Scheme 3.7 Proposed Catalytic Cycle

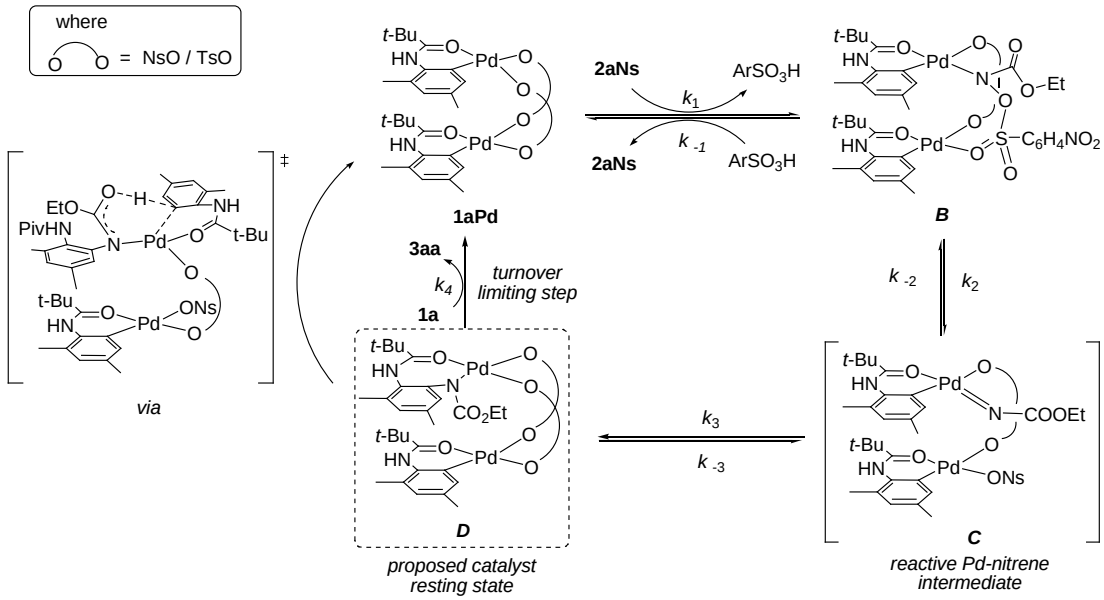

The reaction was probably initiated by the Pd(II)-mediated *ortho*-C-H activation of the pivalanilide (**1a**) to form the dinuclear palladacyclic complex **1aPd**. Initial ligand exchange of **1aPd** with *N*-nosyloxycarbamate (**2aNs**) would afford a palladacycle ***B*** with the elimination of an arylsulfonic acid. Subsequent N-O bond

cleavage would generate a putative Pd-nitrene complex ***C***. Migratory nitrene insertion to the Pd-C(aryl) bond would effect the C-N bond coupling with the concomitant formation of the palladium(II)-amide complex ***D***. A turnover-limiting C-H activation of **1a** by complex ***D*** would release **3aa** and regenerate **1aPd** for another catalytic cycle.

Based on the proposed catalytic cycle, the rate of C-H amidation should exhibit a rate law as shown in equation (3.2):

$$\frac{d[\mathbf{3aa}]}{d\mathrm{t}} = k_4[\boldsymbol{D}][\mathbf{1a}] \qquad (3.2)$$

Assuming: (1) [**1aPd]** = [**Pd**]^2

(2) The formation of a highly energetic Pd-nitrene complex ***C*** should be slow, so that $k_2 < k_1$

(3) The migratory nitrene insertion to Pd-C bond should be fast, so that $k_2 < k_3$

(4) Reverse migratory nitrene insertion to Pd-C bond should be thermodynamically unfavorable; thus, $k_3 > k_{-3}$

Since k_4 should be the turnover-limiting step, [***D***] should be in equilibrium with [***C***]. Applying pre-equilibrium approximation, [***D***] can be expressed in terms of [***C***], and equations (3.3a) and (3.3b) can be obtained:

$$\frac{k_3}{k_{-3}} = \frac{[\boldsymbol{D}]}{[\boldsymbol{C}]} \tag{3.3a}$$

$$[\boldsymbol{D}] = \frac{k_3[\boldsymbol{C}]}{k_{-3}} \tag{3.3b}$$

As mentioned earlier, formation of the putative Pd-nitrene complex ***C*** should be slow, thus steady-state approximation can be applied and equation (3.4a) was obtained. With further manipulation of equation (3.4a), equation (3.4c) that expresses [***C***] in terms of [***B***] and [***D***] was obtained:

$$\frac{d[\mathbf{C}]}{d\mathrm{t}} = k_2[\boldsymbol{B}] - k_{-2}[\boldsymbol{C}] - k_3[\boldsymbol{C}] + k_{-3}[\boldsymbol{D}] = 0 \tag{3.4a}$$

$$k_2[\boldsymbol{B}] + k_{-3}[\boldsymbol{D}] = (k_{-2} + k_3)[\boldsymbol{C}] \tag{3.4b}$$

$$[\boldsymbol{C}] = \frac{k_2[\boldsymbol{B}] + k_{-3}[\boldsymbol{D}]}{(k_{-2} + k_3)} \tag{3.4c}$$

The reverse migratory nitrene insertion should be thermodynamically unfavorable; k_{-3} should be very small and the "$k_{-3}[\boldsymbol{D}]$" term in equation (3.4c) would become negligible comparing to the "$k_2[\boldsymbol{B}]$" term. Thus, equation (3.4c) can be simplified to equation (3.4d):

$$[\boldsymbol{C}] = \frac{k_2[\boldsymbol{B}]}{(k_{-2} + k_3)} \tag{3.4d}$$

Since, the formation of ***C*** should be slow, pre-equilibrium approximation can also be applied to [***B***]. The pre-equilibrium formula of [***B***] can be described by equation (3.5a). After rearrangement, equation (3.5b) was obtained:

$$\frac{k_1}{k_{-1}} = \frac{[\boldsymbol{B}]}{[\mathbf{1aPd}][\mathbf{2aNs}]} \tag{3.5a}$$

$$[\boldsymbol{B}] = \frac{k_1[\mathbf{1aPd}][\mathbf{2aNs}]}{k_{-1}} \tag{3.5b}$$

Based on assumption (1), substituting [**1aPd**] with [**Pd**]^2 would give equations (3.5c):

$$[\boldsymbol{B}] = \frac{k_1[\mathbf{Pd}]^2[\mathbf{2aNs}]}{k_{-1}} \tag{3.5c}$$

Substituting [***B***] in equation (3.5c) into equation (3.4d), equation (3.6) was obtained:

$$[\boldsymbol{C}] = \frac{k_2 k_1[\mathbf{2aNs}][\mathbf{Pd}]^2}{(k_{-2} + k_3)k_{-1}} \tag{3.6}$$

Substituting [***C***] in equation (3.6) into equation (3.3b) would give equation (3.7):

$$[\boldsymbol{D}] = \frac{k_1 k_2 k_3[\mathbf{2aNs}][\mathbf{Pd}]^2}{(k_{-2} + k_3)k_{-1}k_{-3}} \tag{3.7}$$

Finally, expanding [***D***] in equation (3.2) using equation (3.7) would afford the detailed rate expression as shown in equation (3.8):

$$\frac{d[\mathbf{3aa}]}{d\mathrm{t}} = \frac{k_1 k_2 k_3 k_4 [\mathbf{1a}][\mathbf{2aNs}][\mathbf{Pd}]^2}{(k_{-2} + k_3) k_{-1} k_{-3}} \qquad (3.8)$$

Equation (3.8) depicts the first-order dependence to [**1a**], the first-order dependence to [**2aNs**] and the second-order dependence to [**Pd**]. This kinetic expression is consistent to the kinetic data, which showed the same order dependence for each component.

According to our kinetic model, amidopalladium(II) complex ***D*** should be the catalyst resting state. Complex ***D*** would undergo rate-limiting C-H activation of pivalanilide. To give credence to complex ***D*** as catalyst resting state, we investigated the effect of carboxylate / tosylate ligands (**X**) of the palladium catalyst on the initial rate of the amidation reaction. Interestingly, it was found that the plot of log k_x (initial rate constants for Pd$\mathbf{X}_2$; **X** = OTs, TFA, OAc, OPiv) versus pKa of the ligand conjugate acids (i.e., pKa of H**X**) revealed a linear relationship (R^2 = 0.97) with a slope of 0.08 (Figure 3.10; see Experimental Section for detail). Apparently, the rate of amidation is rather insensitive to the nature of the carboxylate / tosylate ligands on

the Pd(II) catalyst. Thus, Pd(II) carboxylates / tosylate are unlikely to be involved in the turnover-limiting C-H activation. The Pd(II) carboxylates / tosylateit is only a precursor for the initial formation of the cyclopalladated complex of pivalanilide. We surmised that amided pivalanilide that remains on the palladium centre would act as a ligand assisting in the turning-limiting C-H bond cleavage step, and we proposed that the catalytic resting state should be complex ***D*** as depicted in Scheme 3.7.

Figure 3.10 Plot of Log k_x versus pKa of H**X**

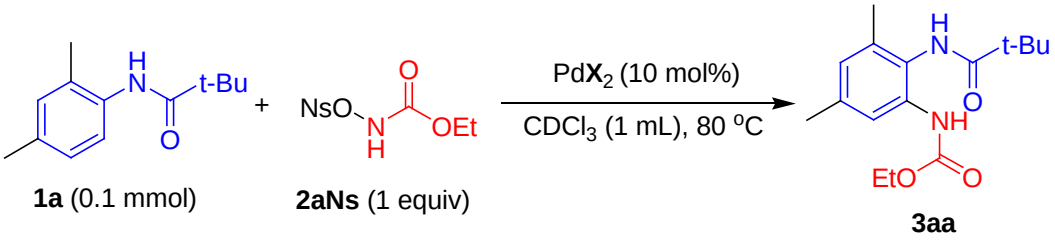

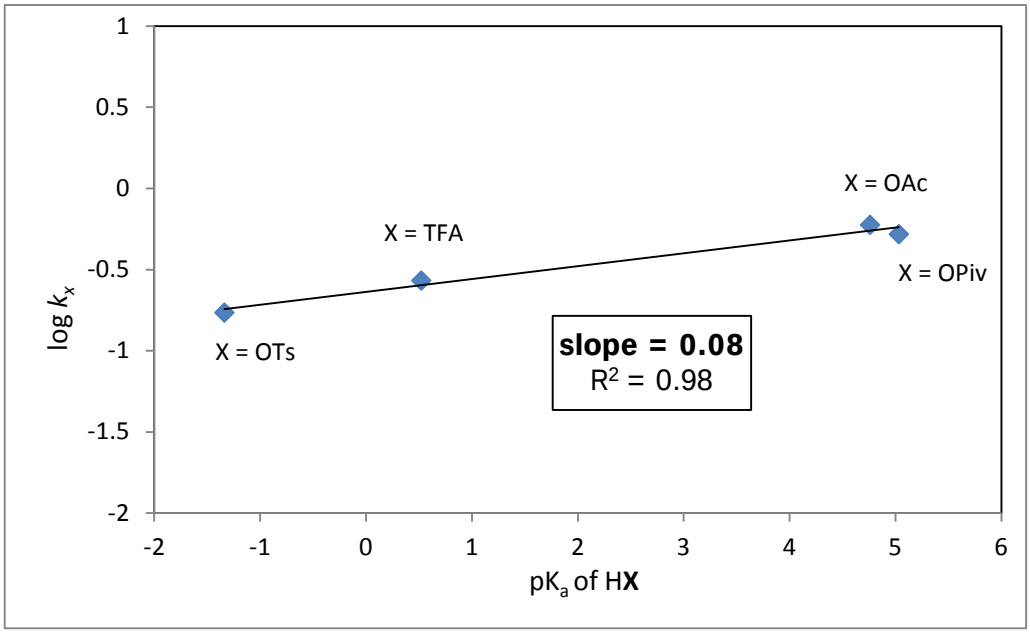

3.3.2 Pd(II)-Mediated *ortho*-C-H Activation of Pivalanilides

According to the literature, the Pd(II)-catalyzed oxidative aromatic C-H bond functionalizations exhibit significant primary kinetic isotope effect with the k_H / k_D values of 2 — 5, which indicates that the turnover-limiting step should involve significant C-H bond cleavage. By directly comparing initial rates of the amidation reaction with the deuterated and non-deuterated anilides, the k_H / k_D value associated with the Pd-catalyzed amidation of pivalanilides was found to be 2.8 (Scheme 3.3). This value is comparable to those related values in the literature. Thus, the Pd(II)-mediated C-H activation of pivalanilide should be involved in the turnover-limiting step for the amidation.

Directing group-assisted Pd(II)-mediated aromatic *ortho*-C-H activation has been a subject of extensive investigation; several mechanistic pathways have been proposed: (1) oxidative addition;[8] (2) electrophilic metalation *via* the Wheland intermediate;[7] (3) concerted metalation deprotonation;[10c,d] and (4) formation of a C-H agostic complex followed by the deprotonation with an coordinated auxiliary ligand[9b] (Scheme 3.8).

Scheme 3.8 Proposed Models for Directing Group-Assisted Aromatic *ortho*-C-H Activation

(1) *Oxidative Addition*

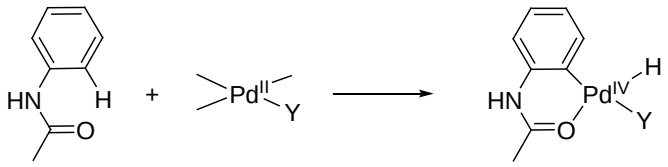

(2) *Electrophilic Metalation via a Wheland Intermediate*

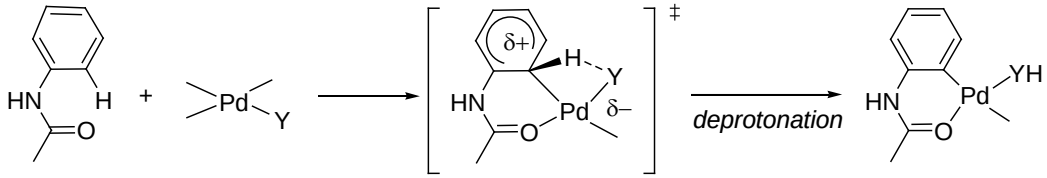

Wheland intermediate

(3) *Concerted Metalation Deprotonation (CMD)*

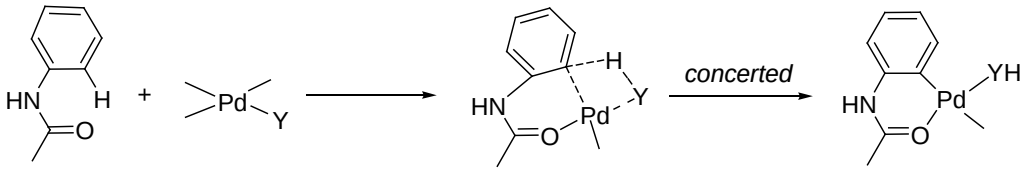

(4) *Formation of Agostic C-H Complex Followed by Deprotonation*

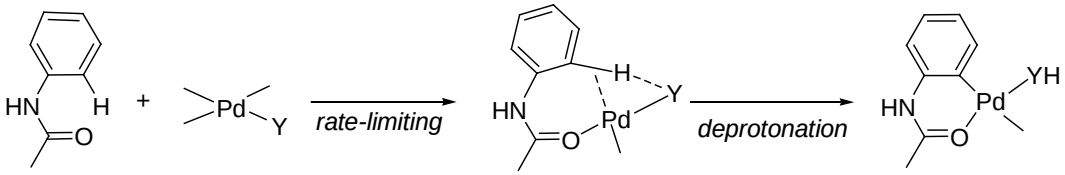

agostic C-H complex

Transition metal catalysts such as Pt(II), Ir(I), Rh(I) and Ru(0) are known to cleave arene C-H bonds *via* oxidative addition.[8, 30, 33, ,62] However, oxidative addition appears implausible for the Pd(II)-mediated arene C-H bond cleavage. In this work, ^{1}H NMR analysis of the cyclopalladated complex of pivalanilide such as **1aPd**

did not reveal the presence of the strongly shielded hydride ligand, which are usually characterized by upfield chemical shifts (δ_H = 0 — -60 ppm). Therefore, C-H activation *via* oxidative addition is not a tenable pathway.

Ryabov and co-workers reported the Hammett correlation study of $Pd(OAc)_2$ mediated *ortho*-C-H activation of *N*,*N*-dimethylbenzylamines; a linear relationship (ρ = -1.6) with Hammett σ_{meta} constants was observed. An electrophilic cyclometalation mechanism with substantial positive charge development on the arene ring (Wheland intermediate) was proposed (Scheme 3.9).[7b]

Scheme 3.9 Electrophilic Cyclometalation of *N*,*N*-Dimethylbenzylamine Proposed by Ryabov and Co-workers

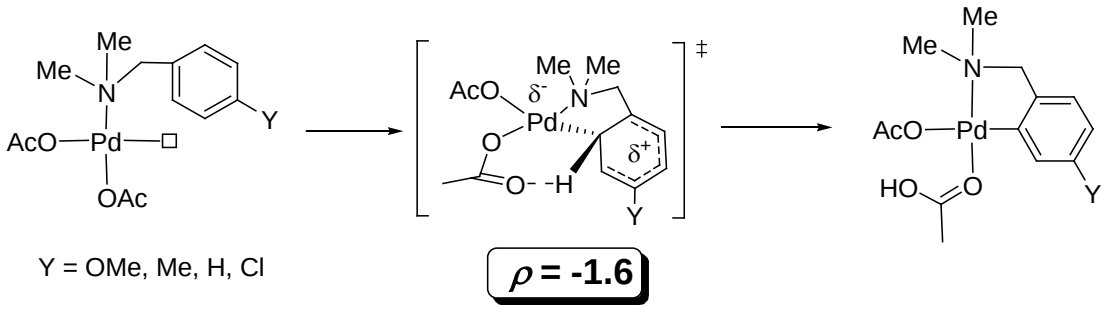

In this work, the Pd(II)-catalyzed C-H amidaions of *para*-substituted pivalanilides were found to be decelerated by electron-withdrawing *para*-substituents; a linear free energy relationship (R^2 = 0.98) with the Hammett σ_{meta} constants giving a ρ value of -0.53 was observed (Figure 3.8). A small negative ρ value observed in this

work (c.f. -1.6 reported by Ryabov and co-workers) is inconsistent with substantial positive charge build-up at the C-H activation transition state. Thus, the Pd(II)-catalyzed C-H activation in the amidation of pivalanilide is unlikely to proceed through a cationic Wheland intermediate. It should be noted that the rate-limiting Wheland intermediate formation in electrophilic aromatic substitution (e.g. chlorination and bromination) reactions are associated with large and negative ρ values (-8 — -12), which is consistent with the rate-limiting formation of the arenium ion.[63]

The concerted metalation deprotonation (CMD) mechanism was proposed by Fagnou and co-workers in their studies of the Pd-catalyzed *ortho*-C-H arylation of simple arenes (i.e., benzene, fluorobenzene and pyridine *N*-oxide) with aryl halides.[10c,d] In particular, it was found that the $Pd(OAc)_2$-catalyzed coupling of pyridine *N*-oxides and aryl bromides exhibited a linear Hammett correlation with a positive slope (ρ = +1.53) for the arylation of C-4 substituted pyridine *N*-oxide (Scheme 3.10).[10c] The observed positive Hammett correlation implied the developing negative charge at the CMD transition state.

Apparently, the negative Hammett correlation observed in this work indicated that the amidation is accelerated by electron-donating substituents on the pivalanilides; our findings are incompatible with Fagnou's study. Thus, the Pd-mediated *ortho*-C-H

bond cleavage of pivalanilides in the amidation reaction is unlikely to proceed *via* the CMD pathway.

Scheme 3.10 Concerted Metalation Deprotonation Mechanism for Pd-Catalyzed Arylation of Pyridine *N*-Oxide Proposed by Fagnou and Co-workers

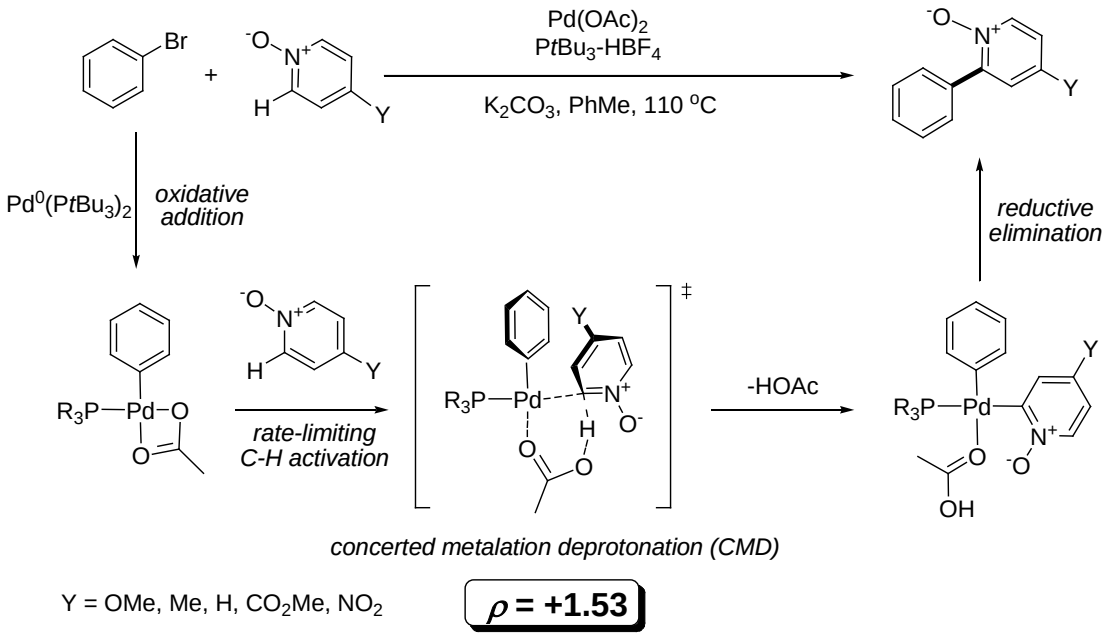

Davies and Macgregor have reported a computational study for the $Pd(OAc)_2$-mediated *ortho*-C-H activation of *N*,*N*-dimethylbenzylamine (DMBA).[9b] According to their density functional calculations (DFT), a pathway for *ortho*-C-H cleavage involving the agostic C-H complex formation is thermodynamically more favorable, when compared to electrophilic cyclometalation *via* a Wheland intermediate and the oxidative addition. The calculation results revealed a

rate-determining formation of an agostic C-H complex, followed by facile deprotonation by the coordinated acetate ligand *via* a highly ordered six-membered cyclic transition state (Scheme 3.11). In addition, the calculated activation energies for cyclopalladation changed when different C-4 substituted DMBA were chosen for calculation (Table 3.3). For example, with 4-chloro-DMBA, the activation barrier was found to be higher (E = +15.0 kcal mol^{-1}) than those for DMBA (E = +14.2 kcal mol^{-1}) and 4-methyl-DMBA (E = +13.2 kcal mol^{-1}). The author suggested that these results should be consistent to a negative slope in Hammett correlation.

Scheme 3.11 DFT Calculated Reaction Profile for Cyclopalladation of *N*,*N*-Dimethylbenzylamine Reported by Davies and Macgregor

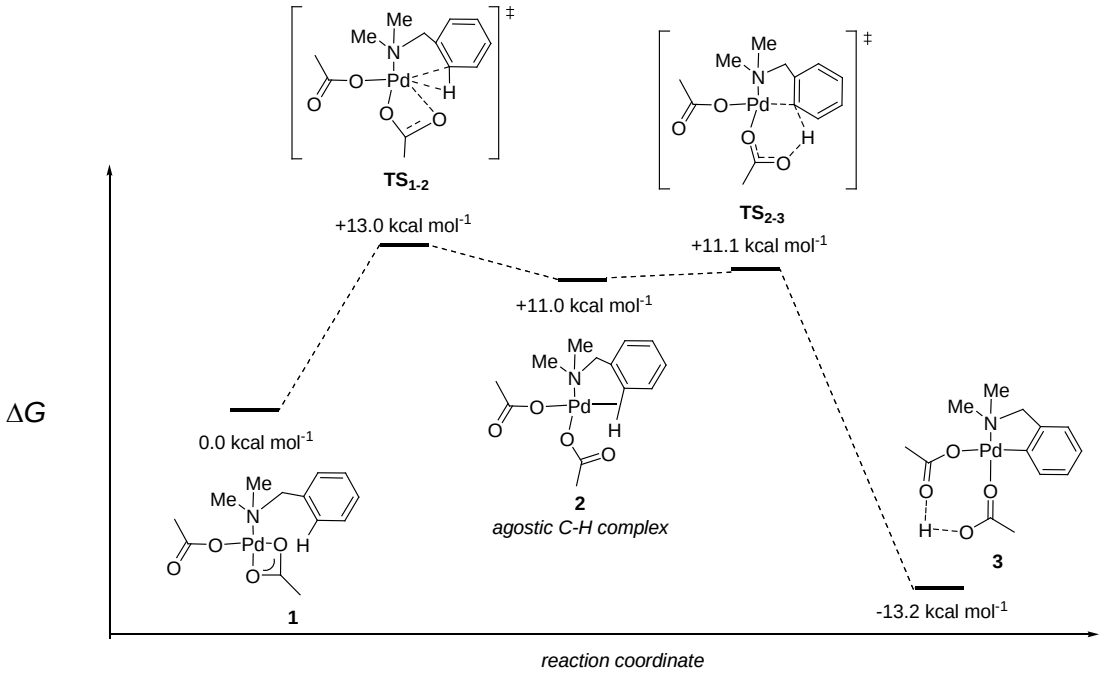

Table 3.3 The Calculated Activation Energies for Agostic C-H Complex Formation with C-4 Substituted *N*,*N*-Dimethylbenzylamines

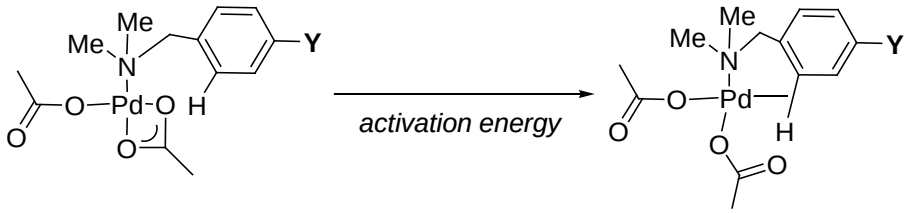

Y	activation energy (kcal mol^{-1})
Cl	15.0
H	14.2
Me	13.2

Apparently, our Hammett correlation results on the Pd-mediated C-H amidation of pivalanilides are compatible with the agostic C-H complex formation pathway. The small negative ρ value in our Hammett correlation study would be consistent with the transition state involving predominant charge-transfer from the aryl C-H bond to the Pd(II) centre with little C-H bond cleavage. Thus, the agostic C-H complex formation should involve small positive charge buildup on the arene ring.

On the basis of our findings, we proposed that the Pd(II)-mediated C-H activation should go through: (1) donor group coordination; (2) agostic C-H complex formation; (3) C-H bond cleavage to afford the dinuclear palladacycle with the concomitant release of the amide product (Scheme 3.12).

Scheme 3.12 Proposed Mechanism for the Turnover-limiting Cyclometalation of Pivalanilide in the Catalytic Cycle

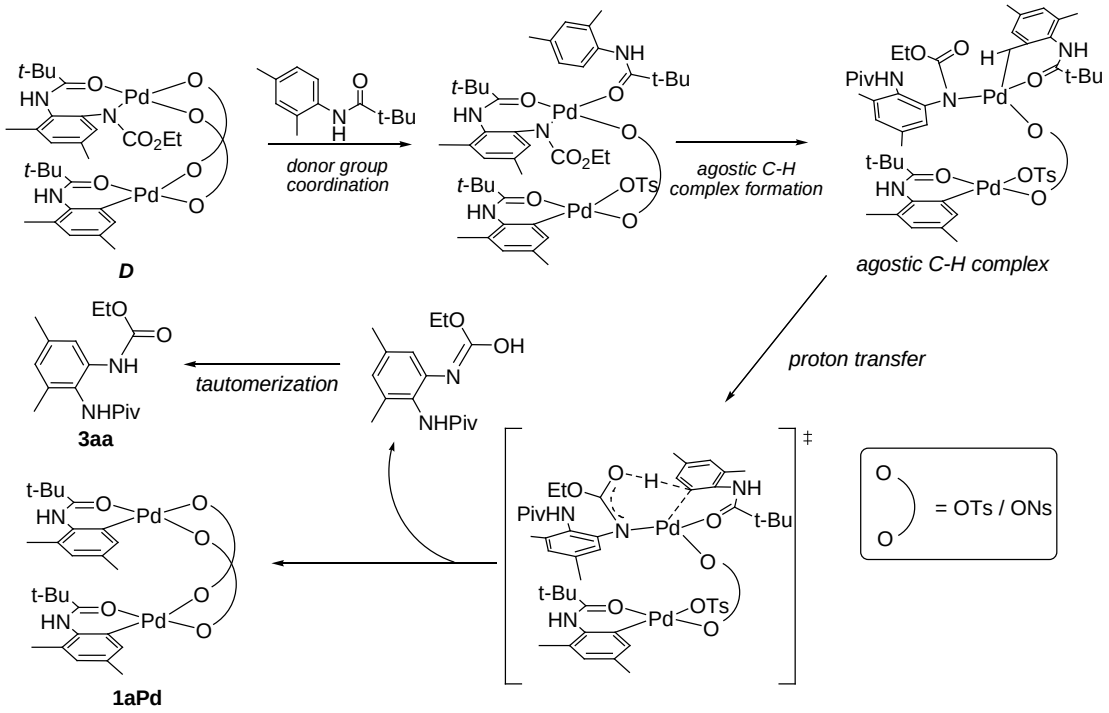

3.3.3 The C-N Bond Formation Step

The use of *N*-arylsulfonyloxycarbamate for transition metal-catalyzed C-N bond formation reaction is sparse in the literature. Prior to our study on the Pd-catalyzed *ortho*-C-H amidation of pivalanilides, the only known example of transition metal-mediated amidation using *N*-arylsulfonyloxycarbamate as reagent was the dirhodium(II, II)-carboxylate-catalyzed sp^3 C-H bond amidation as mentioned in Chapter 1.[21] Unlike the Rh(II)-catalysis which was expected to go through an outer-sphere mechanism, our mechanistic study discussed in earlier sections

implicated an inner-sphere mechanism for the Pd-catalyzed aromatic C-H amidation of pivalanilides. With regard to the inner-sphere C-N bond formation, two plausible pathways were depicted in Scheme 3.13: (1) oxidative addition of the N-O bond across Pd(II) centre to form Pd(IV) species followed by reductive elimination to effect C-N bond formation, and (2) formation a Pd-nitrene complex followed by nitrene insertion.

Scheme 3.13 Two Plausible Mechanisms for the Inner-sphere C-N Bond Formation

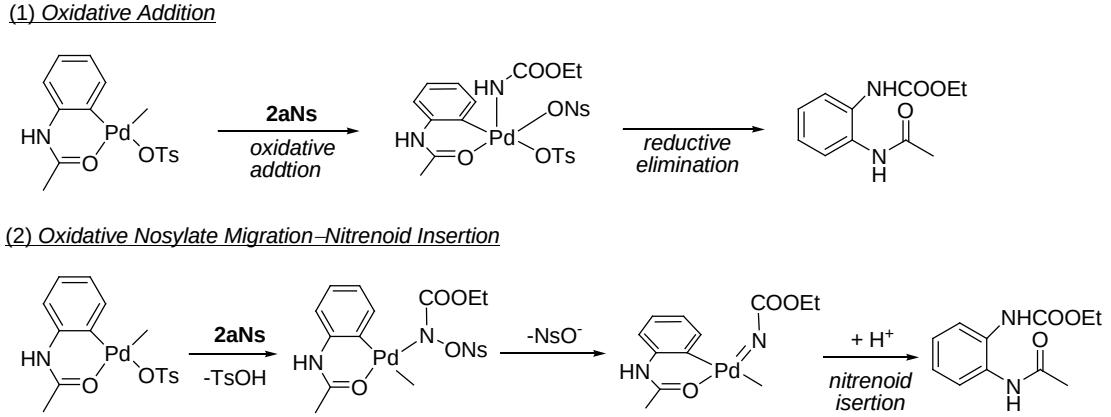

Pd(II)-mediated oxidative addition of C-X bonds (X= halide, OTf) to form reactive Pd(IV) has been thoroughly investigated.[8a,c] Pioneered by the research group of Canty,[8] it was found that (N~N)-dimethylpalladium(II) complexes (N~N = 2,2'-bipyridyl, phenanthroline) can readily react with iodomethane and methyl triflate to furnish isolable Pd(IV) complexes, which were characterized by X-ray crystallography (Scheme 3.14). Notably, those Pd(IV) complexes were only stable at

low temperature (i.e., -60 — -40 °C), and they readily decomposed to give the C-C bond formation product (ethane) *via* reductive elimination upon warming up to room temperature. In 2007, Malinokova and co-workers have also reported an X-ray characterized Pd(IV) complex which was synthesized by reacting methyl 4-bromo-2-butenoate (neat) with a Pd(II) complex ligated with a 2,2'-bipyridyl and a carbon-σ-donor bidentate ligand (Scheme 3.15).[64] The X-ray structure of the Pd(IV) complex revealed an octahedral geometry (a typical geometry for a d^6-complex), and the bromo ligand is *cis* to the η^1-allyl ligand, indicative of a direct oxidative addition of the C-Br bond across the Pd(II) centre. More interestingly, the reductive elimination of that Pd(IV) complex at 0 °C afforded mainly the C(aryl)-C(allyl) bond formation product that remained bonded to the Pd(II)-centre, and no carbon-halogen bond formation was observed.

Scheme 3.14 The Isolable Pd(IV) Complexes Produced by the Reactions of (N~N)-Dimethylpalladium(II) with Iodomethane and Methyl Triflate

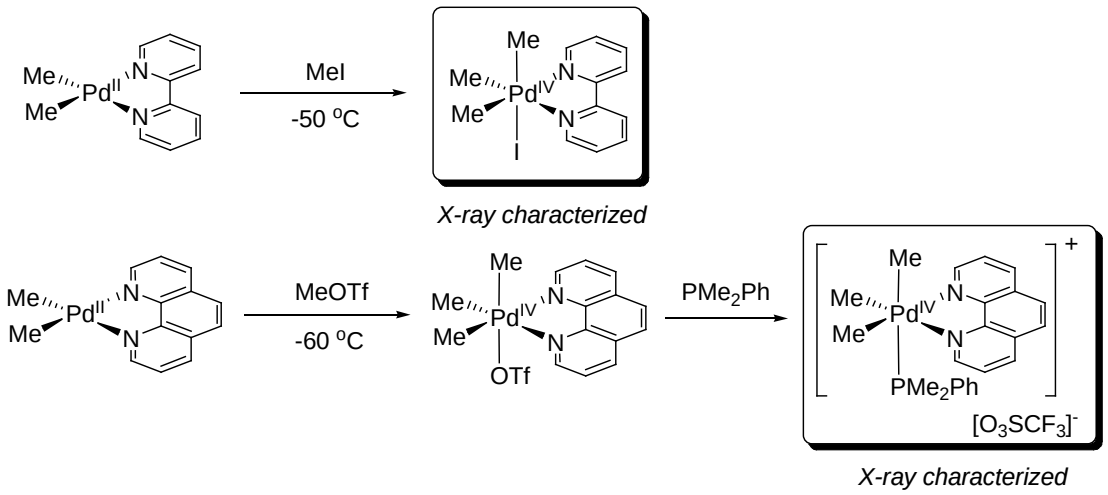

Scheme 3.15 The Isolable Pd(IV) Complex Reported by Malinakova and Co-workers

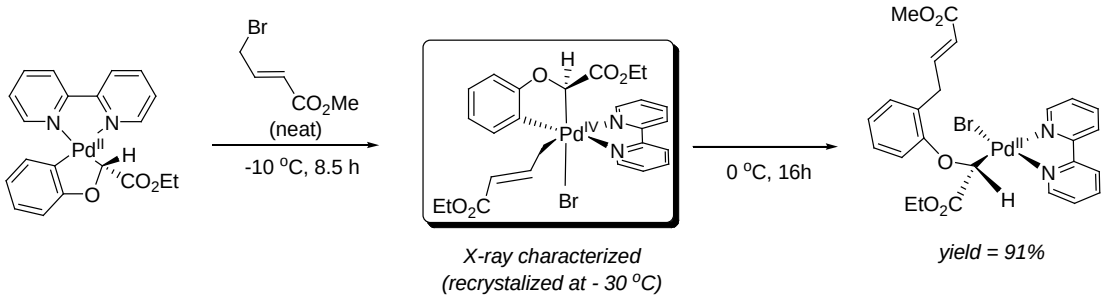

The formation of amido-Pd(IV) species has been proposed in some Pd-catalyzed intramolecular arene C-H amidation reactions. For example, in Yu (J.-Q.)'s report on the $Pd(OAc)_2$-catalyzed cyclization of *N*-trifuoromethylsulfonyl-2-phenylethyamines (Ar~NHTf), the cyclometalated aryl-amido-Pd(II) complex was proposed to be oxidized to generate a Pd(IV) intermediate by 2,4,6-trimethylpyridium fluoride trifate,

and the Pd(IV) complex would reductively eliminate to afford the C-N bond coupled product (Scheme 3.16**)**.[49b]

Scheme 3.16 $Pd(OAc)_2$-Catalyzed Cyclization of Ar~NHTf and the Proposed Mechanism *via* Pd(IV) Intermediate Formation

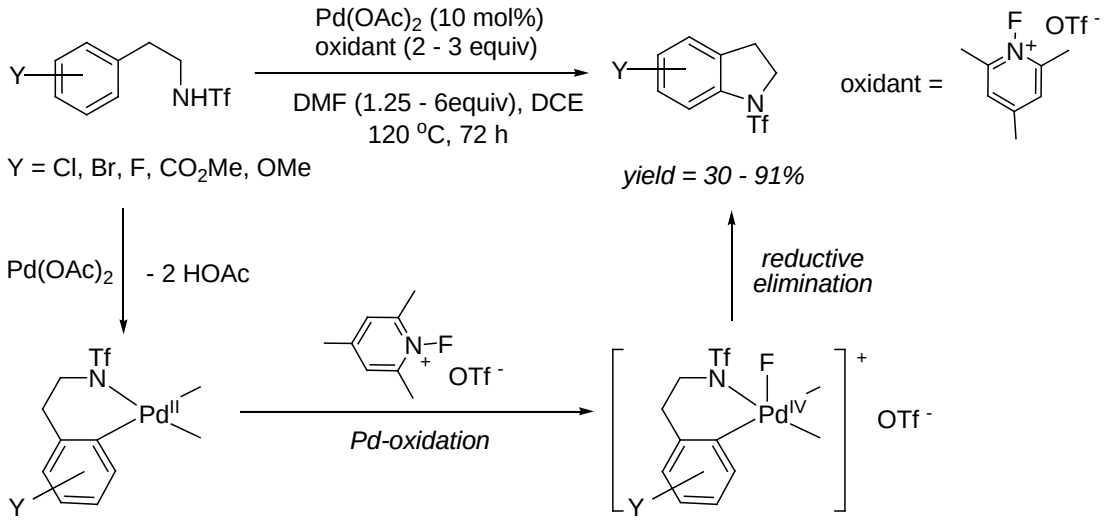

The first stable (at room temperature) amido-Pd(IV) species has been isolated and characterized by Sanford and co-workers in 2007.[65] According to Sanford's study, the reaction of bis(2-phenylpyridine)palladium(II) complex with *N*-chlorosuccinimide (NCS) afforded an amido-Pd(VI) complex in 67% yield (Scheme 3.17). The X-ray crystallography study revealed that the complex is octahedral, typical to a d^6-complex, and the chloro ligand is *cis* to the succinimido ligand. This unique *cis*-coordination is a likely characteristic of the direct oxidative addition across the N-Cl bond. Reductive elimination of the complex at 80 ˚C gave C-C bond, C-Cl bond and C-N bond

formation products in a solvent-dependent manner (Table 3.4). When the reaction was carried out in a donor solvent such as pyridine, the homo-coupling product (C-C bond formation) of 2-phenylpyrdine was formed pre-dominantly (entry 1). In acetic acid, the major product was the C-2 chlorination product (entry 2). It is noteworthy that in both cases, the formation of the C-N coupled product was rather unfavorable.

Scheme 3.17 Formation a Pd(IV) Complex by Oxidative Addition of *N*-Chlorosuccinimide

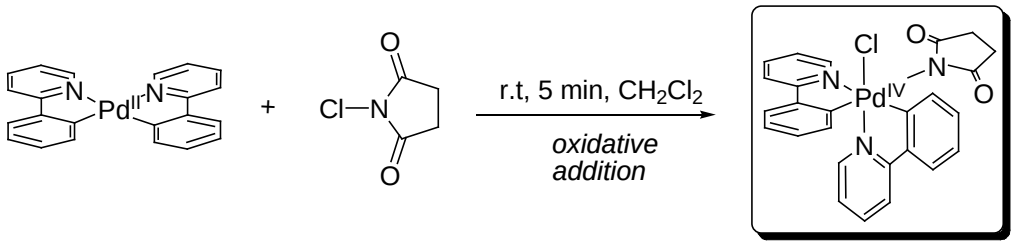

X-ray characterized
yield = 67%

Table 3.4 Bis(2-phenylpyridine)chlorosuccimindo Pd(VI) Complex Reductive Elimination Reaction

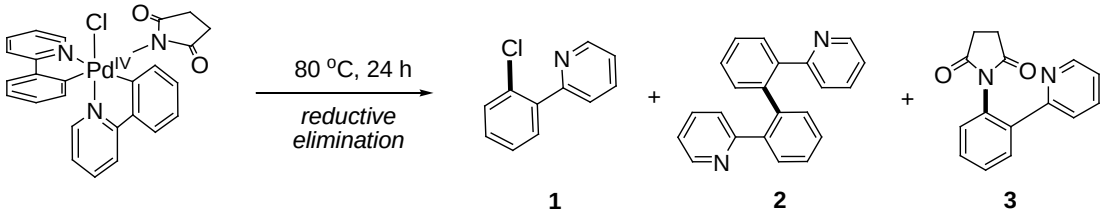

1 **2** **3**

entry	solvent	**1** yield%	**2** yield%	**3** yield%
1	pyridine	6	81	8
2	AcOH	67	5	<1

Oxidative addition of an N-O bond across transition metal complexes has been proposed in several studies on Pd-[66, 72b] or Rh-catalyzed[10a,b, 67, 68] C-N bond formation reactions involving reagents containing N-O bond. Among those studies, Hartwig and co-workers provided more solid evidence for the oxidative addition of N-O bond on a Pd(0) metal centre. In their study on Pd-catalyzed cyclization of *O*-acetyl 2-phenylpropanone oxime derivatives, the Pd(II) complex generated from direct N-O bond oxidative addition was isolated and characterized by X-ray crystallography (Scheme 3.18).[49a] When the Pd(II) complex was heated at 150 ˚C in the presence of Cs_2CO_3 (1 equiv) in toluene for 2 h, the corresponding indole was produced in 31% yield.

Scheme 3.18 Pd-Catalyzed Cyclization of *O*-Acetyl 2-Phenylpropanone Oxime and the Isolation of the Pd(II) Complex Generated from N-O Bond Oxidative Addtion

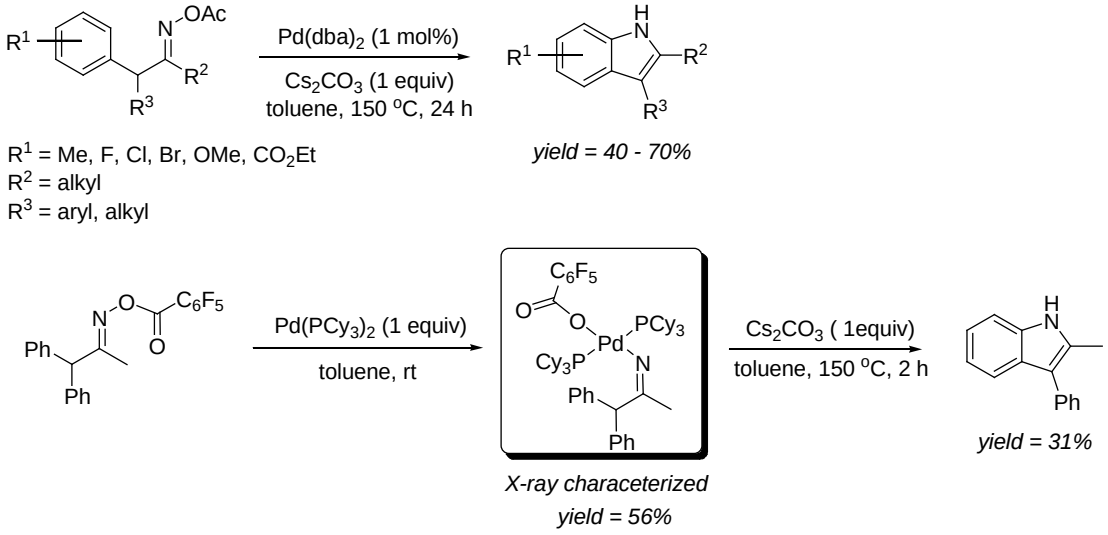

In this work, to evaluate the viability of the oxidative addition pathway, we examined the amidation using *N*-alkylated *N*-nosyloxycarbamate (i.e., **2dNs**) as probe reagent. Treating the cyclopalladated complex of 2,4-dimethylpivalanilide (**1aPd**) with ethyl **2dNs** at 120 °C for 6 h failed to afford the expected amide or the possible C-O bond formation products (Table 3.2). More importantly, **1aPd** and **2dNs** were completely recovered without decomposition. This result argued against the oxidative addition of the N-O bond across a palladacyclic complex for the C-N bond formation.

Alternatively, a pathway involving the metal-nitrene formation was also considered. In 2007, Sanford and co-workers demonstrated palladacycles would react with (*N*-(*p*-tolylsulfonyl)imino)phenyliodinane (PhINTs) in the presence of pyridine to afford the "NTs" insertion products. It was believed that the reaction would involve the formation of a Pd(IV)-nitrene intermediate **(**Scheme 3.19).

Scheme 3.19 Stoichiometric Amidation of Palladacycle with PhINTs and the Corresponding Proposed Mechanism Involving a Pd(IV)-Nitrene Intermediate

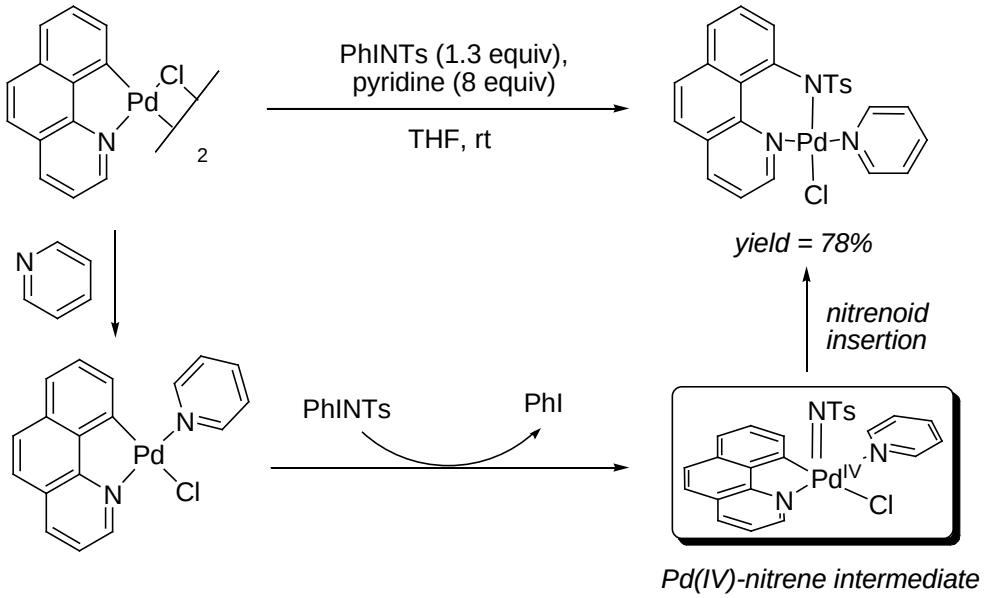

The Pd(IV)-nitrene complex was later supported by a computational study reported by Cundari and co-workers. Their studies revealed that the formation of a Pd(IV)-tosylimido intermediate is a thermodynamically feasible pathway for the reaction of the cyclopalladated complex of benzo[*h*]quinoline with PhINTs as reagent.[50b] According to this model, PhINTs should coordinate to the Pd(II) center with its nitrogen and sulfonyl oxygen to form an octahedral complex, and upon the coordination, the nitrogen-iodine bond was significantly weakened. The facile N-I bond heterolytic cleavage afforded the Pd(IV)-imido complex (Scheme 3.20)

Scheme 3.20 Formation of the Cyclometalated Pd(IV)-Tosylimido Proposed by Cundari and Co-workers

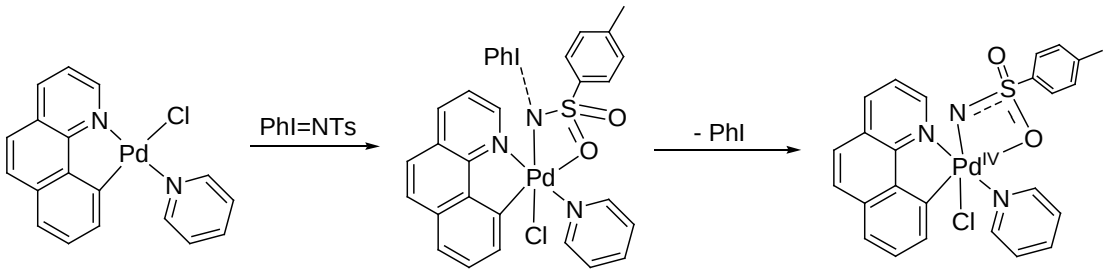

Since *N*-nosyloxycarbamates were known to be nitrene precursors, which form nitrenes *via* a sequential deprotonation—α-elimination pathway, and *N*-alkylated *N*-nosyloxycarbamate is an ineffective reagent for the amidation, we surmised that ethyl *N*-nosyloxycarbamates would react with the cyclopalladated complex to form a Pd-nitrenoid intermediate as depicted in Scheme 3.21.

Scheme 3.21 Proposed Mechanism for C-N Bond Formation

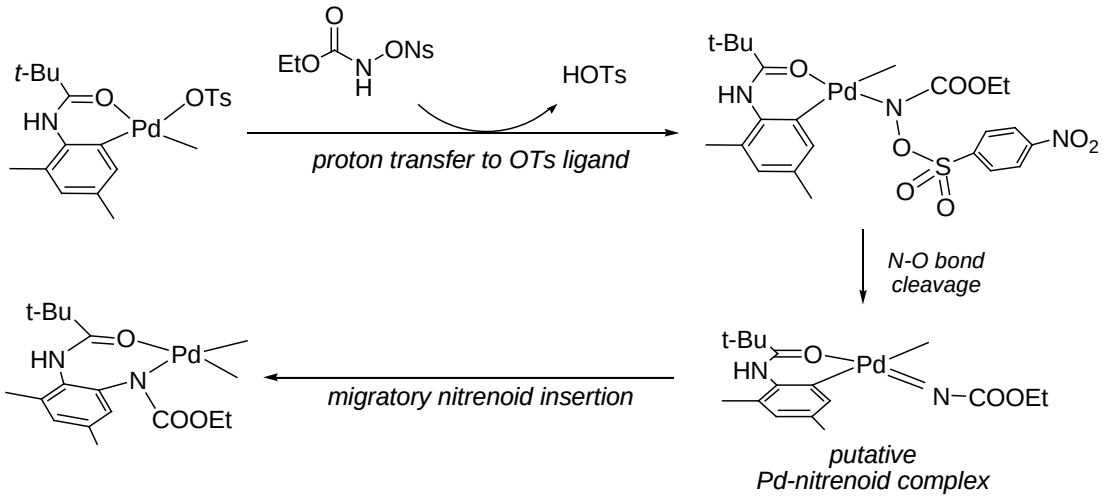

N-Nosyloxycarbamate would first coordinate to the cyclopalladated complex followed by deprotonation by the adjacent tosylate ligand forming a bicyclic Pd(II) complex. Oxidative nosylate migration would generate a putative Pd-nitrenoid complex, and subsequent migratory nitrene insertion would effect the C-N bond formation.

A similar metal-nitrene formation mechanism involving N-O bond cleavage was previously proposed in a computational study by Xia and co-workers on the Rh(III)-catalyzed annulations of *N*-acyloxybenzamides with alkenes.[68] In that study, the oxidative carboxylate migration pathway proceeding through a Rh(V)-imido intermediate was found to be the most accessible route leading to the cyclization product (Scheme 3.22).

Scheme 3.22 Oxidative Carboxylate Migration Reported By Xia and Co-workers in the Computational Study of Rh(III)-Catalyzed Annulation of *N*-Acyloxybenzamides

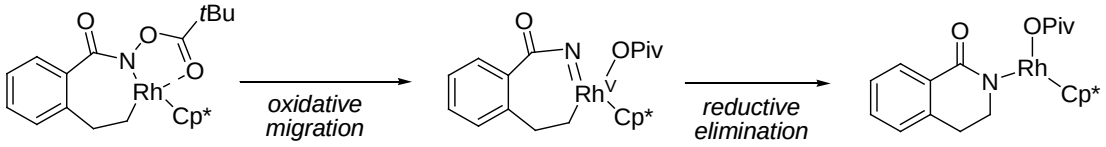

Apart from the oxidative nosylate migration mechanism, concerted aryl migration — nosylate elimination can also be a plausible pathway after the

coordination and deprotonation of **2aNs** (Scheme 3.23). However, the two pathways are difficult to be distinguished by performing kinetic experiments; computational studies may be necessary for further mechanistic elucidation.

Scheme 3.23 Possible Concerted Aryl Migration—Nosylate Elimination Mechanism

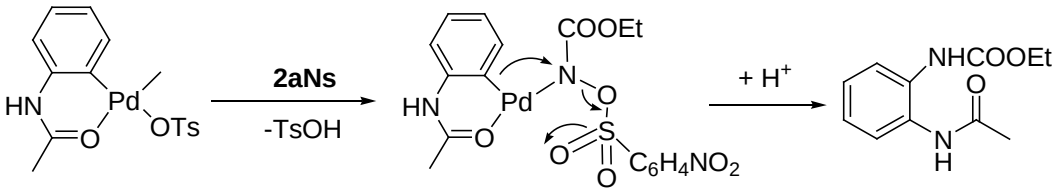

3.4 Summary on Mechanistic Results

The Pd(II)-catalyzed C-H amidation of pivalanilides using *N*-nosyloxycarbamate exhibited first-order dependence on [**1a**], first-order dependence on [**2aNs**] and second-order dependence on [**Pd**]. The rate law was determined to be:

$$rate = k\,[\mathbf{1a}][\mathbf{2aNs}][\mathbf{Pd}]^2$$

The kinetic isotope effect studies (k_H / k_D = 2.8) revealed that the C-H activation is a turnover-limting step. The cyclopalladated complex **1aPd** is competent to both the catalytic and stoichiometric amidation reactions. The Hammett correlation study on *para*-substituted pivalanilides gave a small negative slope (ρ = -0.53), and the C-H activation step was proposed to proceed *via* an agostic C-H complex formation. The failure of amidation reaction of **1aPd** with *N*-alkylated *N*-nosyloxycarbamate implied a mechanism of N-H deprotonation followed by oxidative nosylate migration to generate a putative Pd-nitrenoid intermediate.

3.5 Experimental Section

All solvents and reagents were obtained from commercial sources and were used as received. d_5-Acetanilide(**1t**-d_5), pivalanilides,[41g] ethyl *N*-arylsulfonyloxycarbamates,[21] $[Pd(OTs)_2(MeCN)_2]$[59c] and $Pd(OPiv)_2$[59d] were prepared according to the literature. All the reactions were performed in 8 mL-vials equipped with Teflon® liner caps. The kinetic experiments were performed on a temperature controlled silicon oil bath. (The fume hood air flow rate would profoundly influence the oil bath temperature; therefore, the shielding glass of the fume hood was fixed at a height 30 centimeters from the bench. The temperature (80 ± 1 ˚C) of the oil bath was closely monitored while the kinetic experiments were underway.) 1,4-Dioxane was sodium-dried and freshly distilled before use.

Thin layer chromatography was performed on silica gel plates. Flash column chromatography was performed on 230-400 mesh silica gel (NA Chemical). ^{1}H, ^{13}C, DEPT 135^o NMR analyses were performed on a Bruker (400 MHz) spectrometer. Chemical shifts (δ) were given in ppm, and the signals were referenced with the solvent residual peak(s). NMR yields and conversions were determined with dibromomethane (0.1 mmol) as internal standard, which has a singlet signal (2H) at 4.9 ppm in *d*-chloroform or 5.3 ppm in d_6-acetone. IR spectra were obtained by a Nicolet-380 FT-IR spectrometer. Melting points were recorded on a BÜCHI-B-545 instrument and were uncorrected. High resolution mass spectra were obtained using a VG MICROMASS Fison VG platform and with an electrospray ionization mode.

3.5.1 Experimental Procedures and Characterizations

3.5.1.1 Procedures for the Preparation of 1aPd

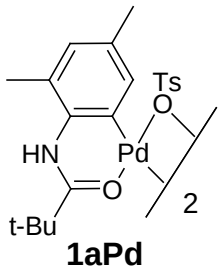

1aPd

To mixture of $Pd(OAc)_2$ (1 mmol) and *p*-toluenesulfonic acid (1 equiv) in DCM (10 mL), 2,4-dimethylpivalanilide (1 equiv) was added in one portion, and the reaction mixture was brought to reflux for 0.5 h. After cooling to room temperature, the solution was concentrated *in vacuo* followed by the addition of Et_2O. The mixture was shaken until a slightly turbid solution was observed, and the solvent was completely removed by rotary evaporation. To the gummy semi-solid, 5 mL of Et_2O was added and the gummy crude product would start to solidify upon scratching with a spetula for about 10 min. The light yellow supernatant was removed, and the residue was washed twice with Et_2O (10 mL × 2). The residue was dried *in vacuo* yielding **1aPd** as a brownish-yellow solid. **1aPd** was characterized by ^1H and ^{13}C NMR (384.8 mg, 80% yield); mp = 175-176 ^oC; ^1H NMR (CD_2Cl_2, 400 MHz): δ_H 8.29 (br.s, 1H), 7.83 (d, J = 8Hz, 2H), 7.22 (d, J = 8Hz, 1H), 6.75 (s, 1H), 6.72 (s, 1H), 2.39 (s, 3H), 2.27 (s, 3H), 2.14 (s, 3H), 1.27 (s, 9H); ^{13}C NMR (CD_2Cl_2, 100 MHz) δ_C 173.97 (C), 141.30 (C), 140.06 (C), 132.53 (CH), 132.33 (C), 128.71 (CH), 128.51 (CH), 126.33 (CH), 125.49 (C), 121.73 (C), 112.75 (C), 39.09 (C), 26.98 (CH_3), 21.00 (CH_3), 20.43 (CH_3), 17.22 (CH_3); IR (KBr, cm^{-1}): 3437, 3390, 2965, 1606, 1592, 1529, 1244, 1226, 1152, 1117, 1033, 1010, 681.

3.5.1.2 Procedures for the Preparation of 3ta

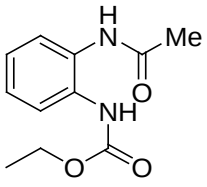

3ta

3ta was prepared by the Pd(II)-catalyzed amidation of **1t** with **2aNs** at 80 ˚C in 1,4-dioxane for 6 h, and it was isolated as a pink solid by flash column chromatography on silica gel (26.6 mg, 60% yield). R_f = 0.3 (1 : 1 hexane : EtOAc); mp = 119-120 ºC; ^{1}H NMR ($CDCl_3$, 400MHz): δ_H 8.17 (br.s, 1H), 7.47 (d, *J* = 8Hz, 1H), 7.35 (br.s, 1H), 7.26 (d, *J* = 7.2Hz, 1H), 7.16 (t, *J* = 7.6Hz, 1H), 7.10-7.06 (m, 1H), 4.21 (q, *J* = 7.2Hz, 2H), 2.11 (s, 3H), 1.30 (t, *J* = 7.2Hz, 3H); ^{13}C NMR ($CDCl_3$, 100 MHz) δ_C 169.65 (C), 154.97 (C), 130.89 (C), 129.51 (C), 126.40 (CH), 125.23 (CH), 125.09 (CH), 124.43 (CH), 61.52 (CH_2), 23.69 (CH_3), 14.48 (CH_3); IR (KBr, cm^{-1}): 3308, 1720, 1676, 1522, 1456, 1248, 1059; HRMS m/z (ESI): calculated for $C_{11}H_{14}N_2O_3Na^+$: 245.0902, found: 245.0914.

3.5.1.3 Kinetic Experiments on Reaction Rate Order

General Procedures for the Kinetic Experiments on Rate Order

To an 8-mL vial equipped with a magnetic stir bar, **2aNs** and [$Pd(OTs)_2(MeCN)_2$] were added. A stock solution of **1a** in *d*-chloroform (1 mL) was added *via* a 1-mL syringe. The reaction mixture was pre-heated at 80 ˚C for 20 seconds for complete reagent dissolution, and the reaction was stirred for additional time. At the designated time interval, the reaction was stopped quickly by cooling in an ice-bath (the substrate conversion of **1a** was kept < 25% for determination of rate order of [**2aNs**] and

[**Pd(OTs)$_2$(MeCN)$_2$**]; the substrate conversion of **2aNs** was kept < 25% for determination of rate order of [**1a]**). The crude mixtures were spiked with dibromomethane (0.1 mmol), and were then subjected to ^{1}H NMR analysis to determine the product (**3aa**) yield. The initial rates of product formation (*d*[**3aa**] / *d*t) were determined by plotting [**3aa**] (M) versus time (s).

To determine the yield of **3aa** in the reaction mixture, the ^{1}H NMR signal of a singlet (1H) at 6.89 ppm was chosen for quantification with reference to the singlet signal of dibromomethane (2H) at 4.95 ppm.

A representative example of initial rate determination:

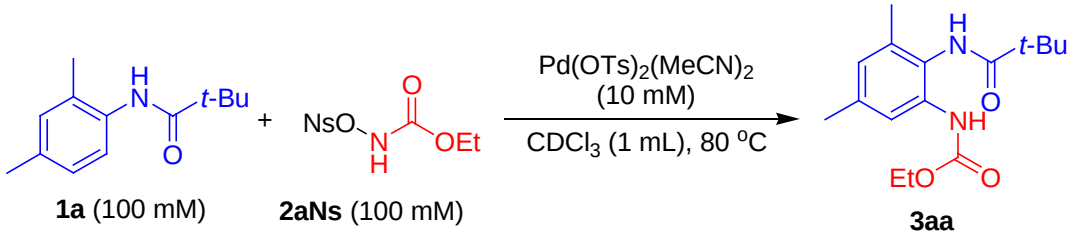

1a (100 mM) **2aNs** (100 mM) **3aa**

time (s)	[**3aa**] (M)
120	0.00874
240	0.01348
360	0.01751
480	0.02254

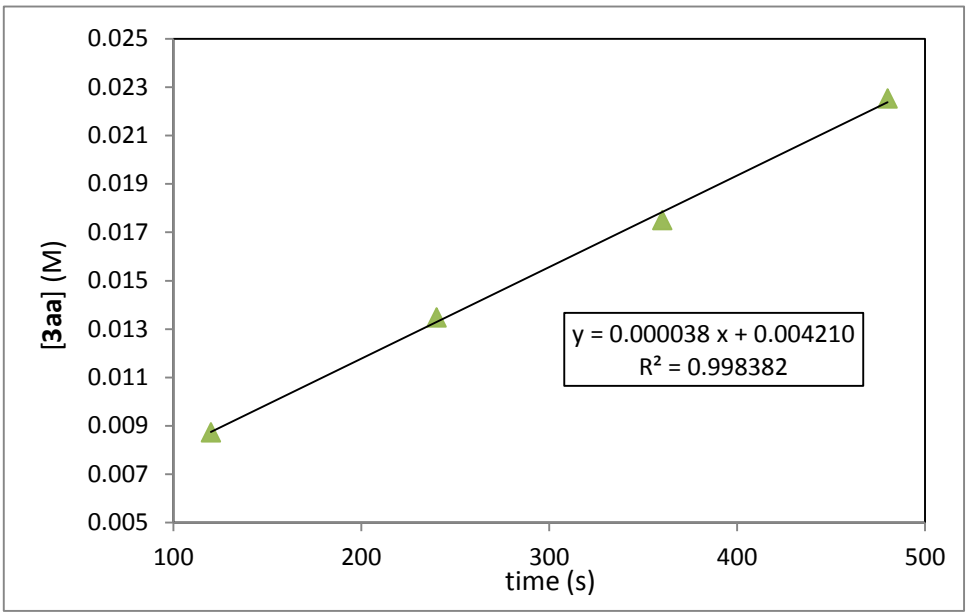

^{1}H NMR spectrum for the determination of **3aa**

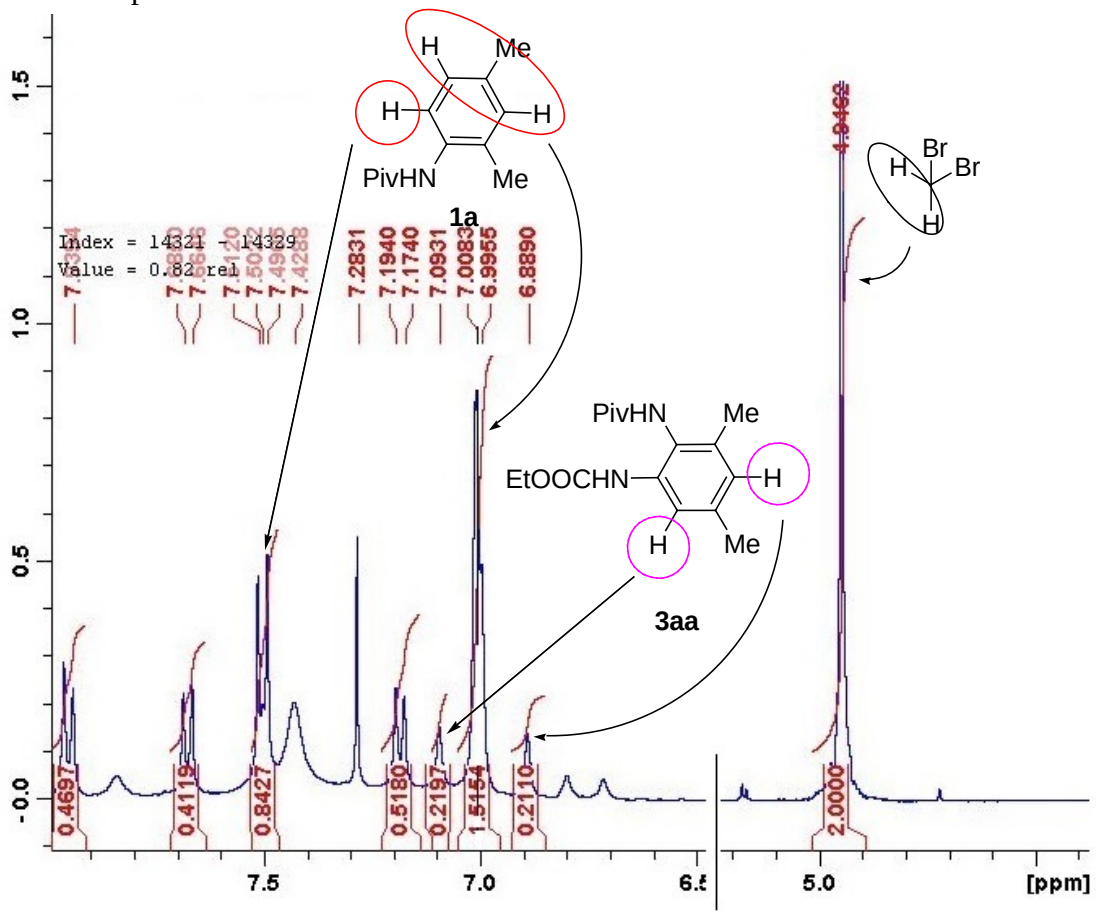

Rate Order for [**1a**]

The reactions were performed according to the general procedures with varying concentrations of **1a** (50 mM, 100 mM, 150 mM, 200 mM) and fixed concentrations of **2aNs** (100 mM) and [$Pd(OTs)_2(MeCN)_2$] (10 mM) in 1 mL of *d*-chloroform.

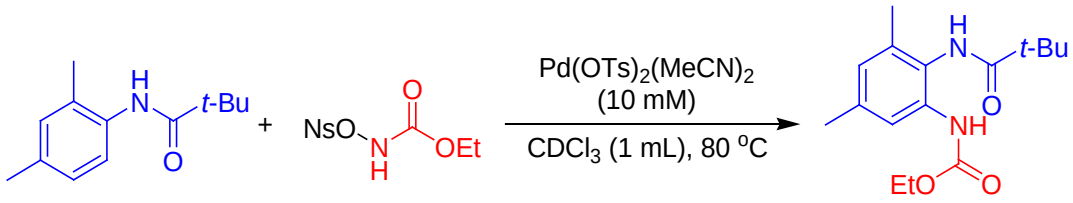

1a (50–200mM) **2aNs** (100 mM) **3aa**

[**1a**] (M)	[**3aa**] (M) at the designated time						rate ($M\ s^{-1}$)	R^2
	60 s	120 s	180 s	240 s	360s	480 s		
0.05	--	0.00687	--	0.01126	0.01356	0.01508	2.24×10^{-5}	0.944
0.10	--	0.00874	--	0.01348	0.01751	0.02254	3.79×10^{-5}	0.998
0.15	0.00743	0.01114	0.01315	0.01720	--	--	5.22×10^{-5}	0.985
0.20	0.00695	0.01204	0.01479	0.01935	--	--	6.66×10^{-5}	0.988

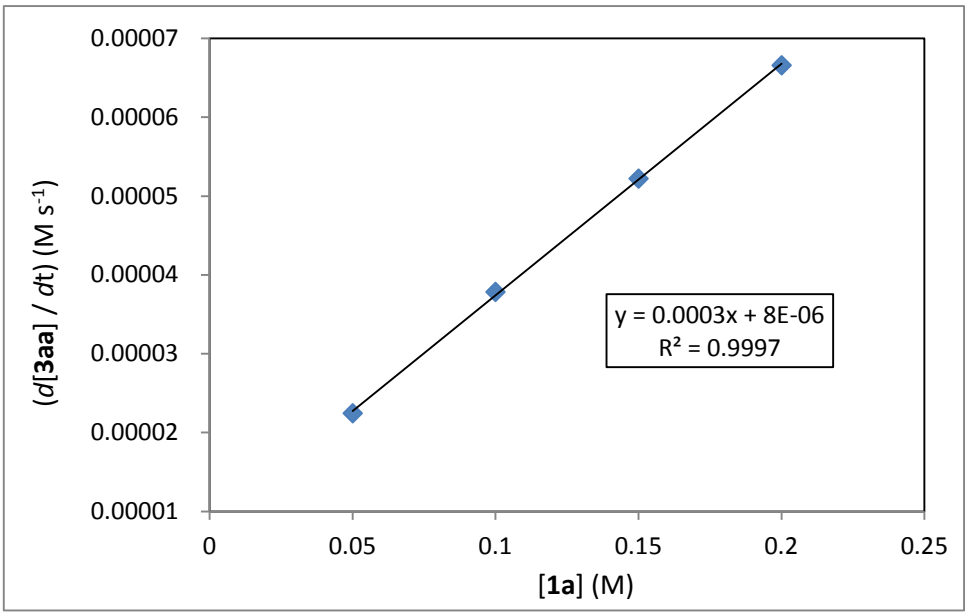

The first-order kinetic of [**1a**] was further verified by plotting the log of (*d*[**3aa**] / *d*t) versus the log of [**1a**].

Log plot of (d[**3aa**] / dt) versus [**1a**]

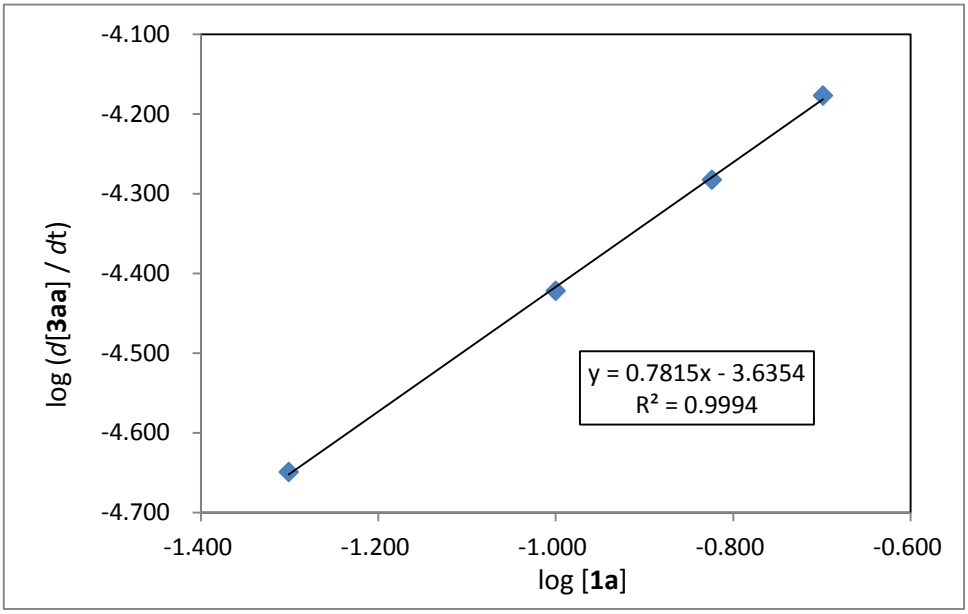

Rate Order for [**2aNs**]

The reactions were performed according to the general procedures with varying concentrations of **2aNs** (50 mM, 75 mM, 100 mM, 200 mM) and fixed concentrations of **1a** (100 mM) and [$Pd(OTs)_2(MeCN)_2$] (10 mM) in 1 mL of *d*-chloroform.

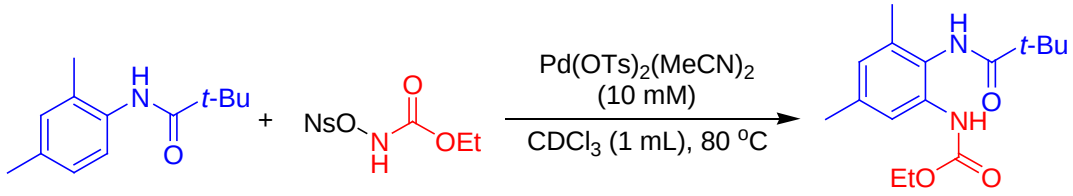

1a (100 mM) **2aNs** (50–150mM) **3aa**

[**2aNs**] (M)	[**3aa**] (M) at the designated time								rate ($M\ s^{-1}$)	R^2
	180 s	240 s	300 s	360 s	420 s	540 s	600 s	900 s		
0.05	0.0104	--	0.0153	--	--	--	0.0205	0.0232	1.70×10^{-5}	0.93
0.075	0.0136	--	0.0167	--	0.0195	0.0218	--	--	2.26×10^{-5}	0.99
0.10	0.0142	--	0.0208	--	0.0239	0.0254	--	--	3.08×10^{-5}	0.91
0.15	0.0173	0.0209	0.0234	0.0261	--	--	--	--	4.85×10^{-5}	0.99

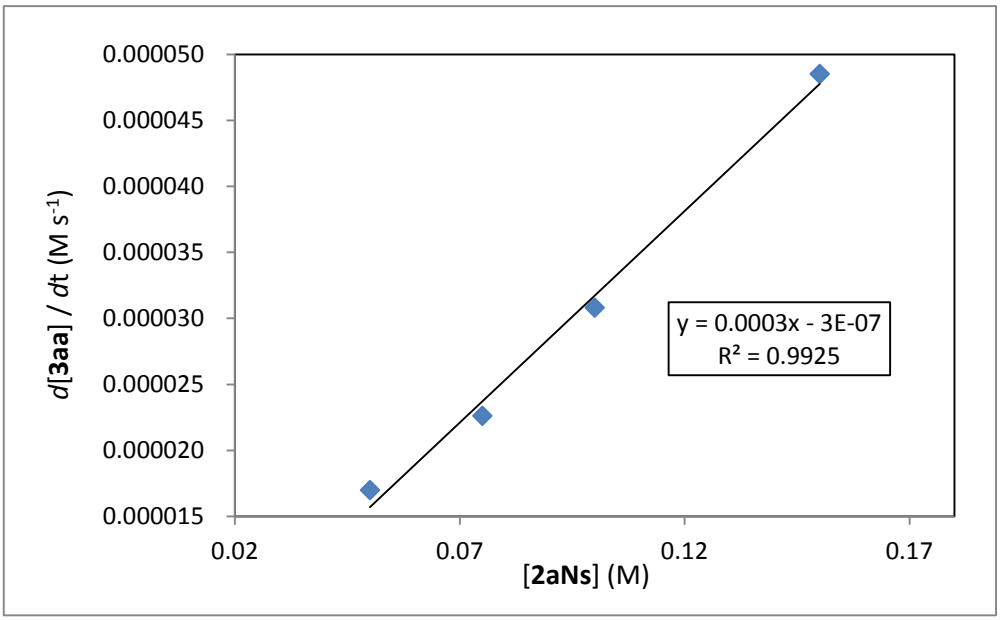

The first-order kinetic of [**2aNs**] was further verified by plotting the log of (*d*[**3aa**] / *d*t) versus the log of [**2aNs**].

Log plot of (*d*[**3aa**] / *d*t) versus [**2aNs**]

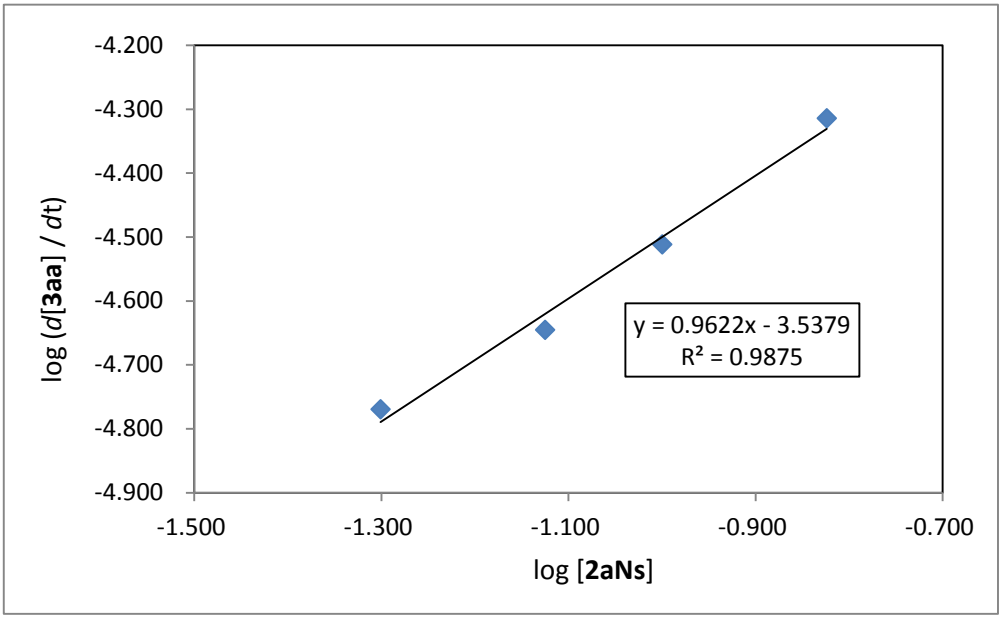

Rate Order for[**Pd(OTs)$_2$(MeCN)$_2$**]

The reactions were performed according to the general procedures with varying concentrations of [Pd(OTs)$_2$(MeCN)$_2$] (5 mM, 10 mM, 12.5 mM, 15 mM) and fixed concentrations of **1a** (100 mM) and **2aNs** (100 mM) at 1 mL of *d*-chloroform.

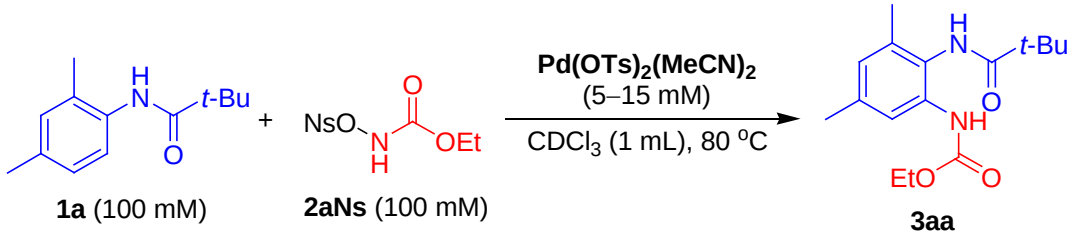

1a (100 mM) **2aNs** (100 mM) **3aa**

[**Pd**] (mM)	[**3aa**] (M) at the designated time								rate (M s^{-1})	R^2
	120 s	240 s	300 s	360 s	480 s	540 s	900 s	1200 s		
5	--	--	0.0165	--	--	0.0203	0.0229	0.0241	0.82x10^{-5}	0.93
10	0.0171	0.0198	--	0.0229	0.0252	--	--	--	2.27x10^{-5}	0.99
[**Pd**] (mM)	60 s		120 s	180 s		240 s	300 s		rate (M s^{-1})	R^2
12.5	0.00745		--	0.01215		0.01434	0.01654		3.79x10^{-5}	0.99
15	0.00943		0.01577	0.01881		0.02106	--		6.32x10^{-5}	0.94

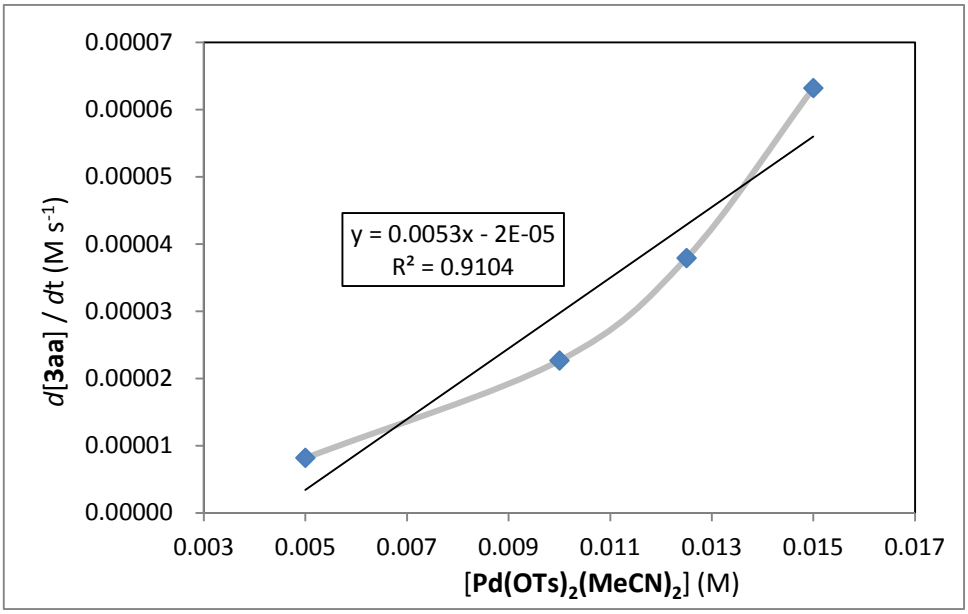

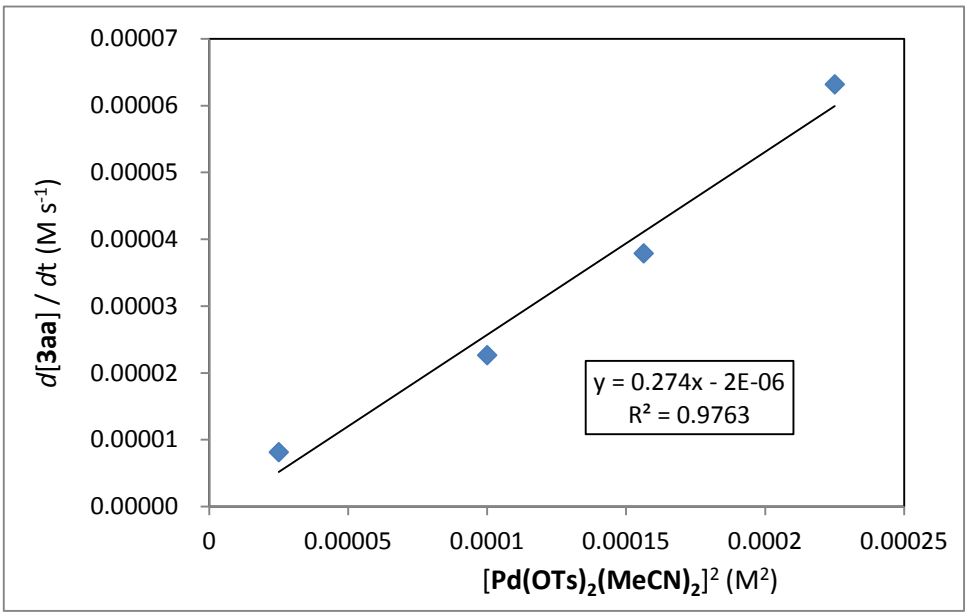

The second-order kinetic of [**Pd(OTs)$_2$(MeCN)$_2$**] was further verified by plotting the log of (*d*[**3aa**] / *d*t) versus the log of [**Pd(OTs)$_2$(MeCN)$_2$**].

Log plot of (*d*[**3aa**] / *d*t) versus [**2aNs**]

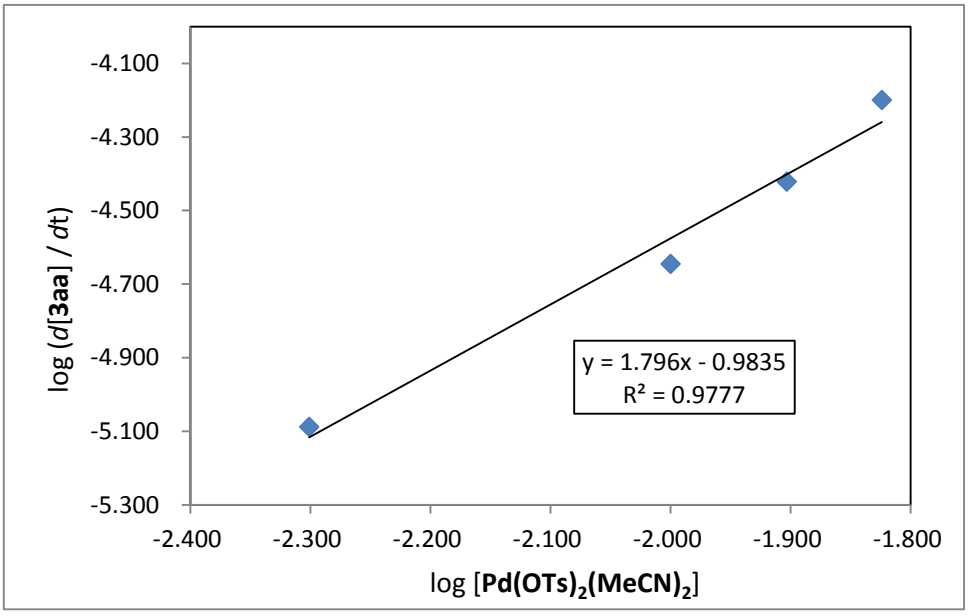

3.5.1.4 Kinetic Isotope Effect Experiments

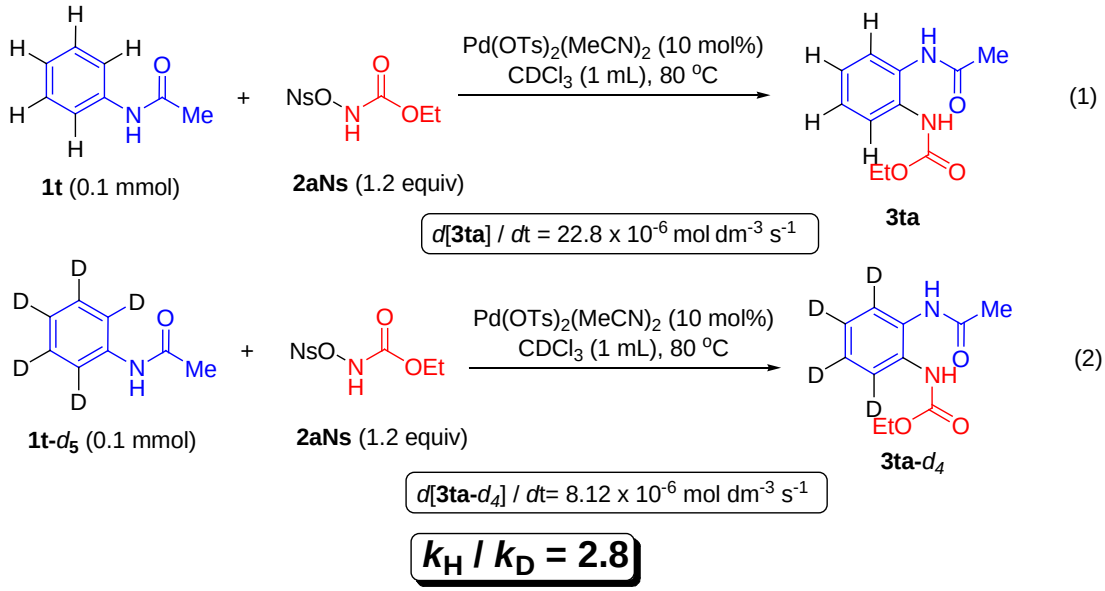

In each reaction, to a mixture of **1t** (0.1 mmol) and $[Pd(OTs)_2(MeCN)_2]$ (0.01 mmol) in *d*-chloroform (1 mL) in an 8 mL-vial, **2aNs** (0.12 mmol) was added in one portion, and the vial was sealed with a Teflon® liner cap. The reaction mixture was pre-heated at 80 °C for 20 seconds for complete dissolution of reagents, and was run for additional time. At the designated time interval (see below), the reaction was quickly removed from the oil bath and cooled in an ice-water bath. The reaction crude mixtures were analyzed by ^{1}H NMR for product (**3ta**) yields determination with dibromomethane (0.1 mmol) as the internal standard. The same procedures were repeated using **1t**-d_5 as substrate. The initial rates were determined by plotting [**3ta**] or [**3ta**-d_4] (M) versus time (s).

Determination and Calculations of the k_H / k_D Value:

With reference to the singlet signal of dibromomethane (2H) at 4.90 ppm (in *d*-chloroform), the ^{1}H NMR signals of a singlet (3H) at 2.11 ppm was chosen for product (**3ta** or **3ta**-d_4) yields quantification. The k_H / k_D value was determined based on the initial rates of **3ta** and **3ta**-d_4 formation (Assuming all reagent concentrations remain unchanged at the initial rate expressions). The results were listed below:

time (s)	[**3ta**] (M)	[**3ta**-d_4] (M)
180	0.0098	--
300	--	0.0117
360	0.0146	--
600	0.0173	0.0146
900	0.0270	0.0166
1200	--	0.0191

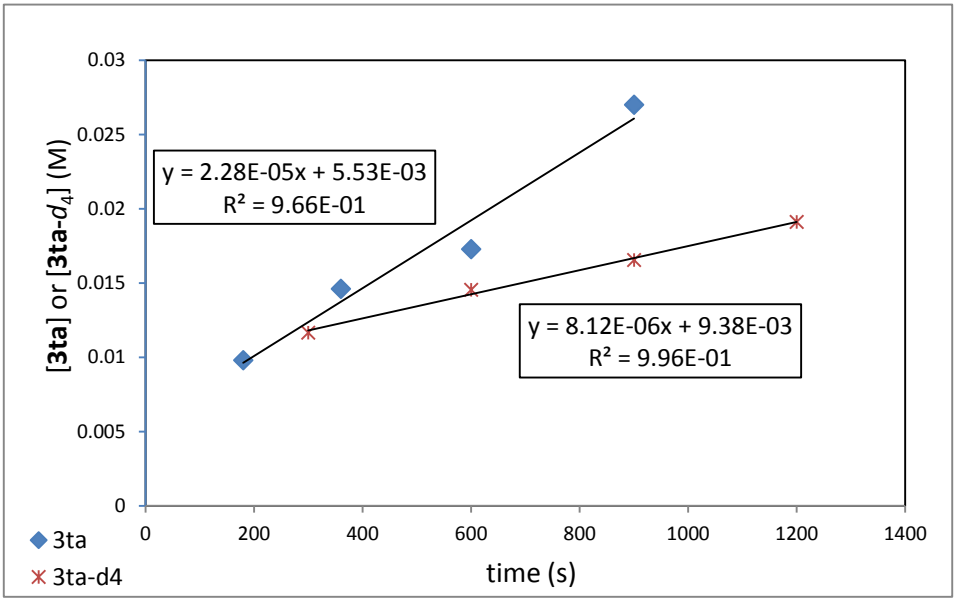

k_H / k_D = (22.8 × 10^{-6}) / (8.1 × 10^{-6}) = **2.81**

3.5.1.5 General Procedures for Stoichiometric Amidation with 1aPd

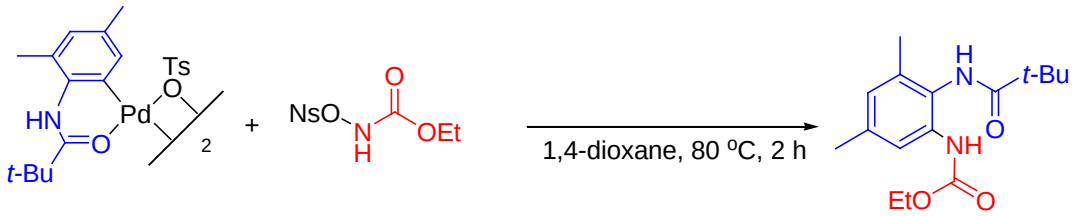

1aPd (0.05mmol) **2aNs** (0.12mmol) **3aa**

To an 8-mL vial, 1aPd (0.05 mmol), 2aNs (2.4 equiv) and 1,4-dioxane (2 mL) were added, and the mixture was sealed with a Teflon® liner cap. The mixture was stirred at 80 °C for 2 hours. After cooling to room temperature, the reaction mixture was diluted with about 4 mL of EtOAc. The diluted mixture was washed with 5 mL of a sat. $NaHCO_3$ solution, and the aqueous layer was extracted with EtOAc (5 mL × 3). The combined organic extract was dried over anhydrous Na_2SO_4 and then filtered through a short plug of silica gel. The silica gel was washed with EtOAc (40 mL) and the filtrate was evaporated to dryness by rotary evaporation. The residue was redissolved with small amount of *d*-chloroform, and it was analyzed by ^1H NMR to determine the yield of 3aa with dibromomethane (0.1 mmol) as internal standard.

3.5.1.6 Hammett Correlation Studies

3.5.1.6.1 Hammett Correlation for Amidation of *p*ara-Substituted Pivalanilides

To an 8 mL-vial, the *para*-substituted pivalanilide (0.1 mmol), **2aNs** (1 equiv), $[Pd(OTs)_2(MeCN)_2]$ (10 mol%) and *d*-chloroform (1 mL) were added, and the vial was sealed with a Teflon® liner cap. The reaction was heated at 80 °C for 20 seconds for complete dissolution of reagents, and was further run for additional 10 min

(conversions based on pivalanilides were < 20%). The reaction was stopped by cooling at an ice-water bath. The reaction mixture was analyzed by ^{1}H NMR to determine the amidation product yield with dibromomethane (0.1 mmol) as internal standard.

Determination and Calculations of the k_Y / k_H Value:

With reference to the singlet signal of dibromomethane (2H) at 4.90 ppm (in *d*-chloroform), the ^{1}H NMR signals of a quartet (4.20 ppm, 2 H) was chosen for product yields quantification. The k_Y / k_H value was determined based on the initial rates of product formation (Assuming all reagent concentrations remain unchanged at the initial rate expressions). The experiment was run in triplicate, and the results were listed below:

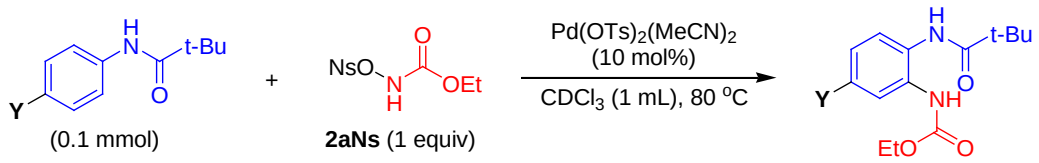

Y	σ_{meta}	time (s)	yield 1st (mmol)	yield 2nd (mmol)	yield 3rd (mmol)	average yield (mmol)	product formation rate (M s^{-1})	k_Y / k_H
-Me	-0.06	600	0.0118	0.0113	0.0117	0.0116	19.0×10^{-6}	1.109
-H	0	600	0.0106	0.0106	0.0096	0.0102	17.3×10^{-6}	1
-F	0.34	600	0.0070	0.0075	0.0077	0.0074	12.3×10^{-6}	0.719
-Br	0.37	600	0.0070	0.0070	0.0063	0.0068	11.3×10^{-6}	0.658
-CF_3	0.46	600	0.0056	0.0063	0.0053	0.0057	9.5×10^{-6}	0.556

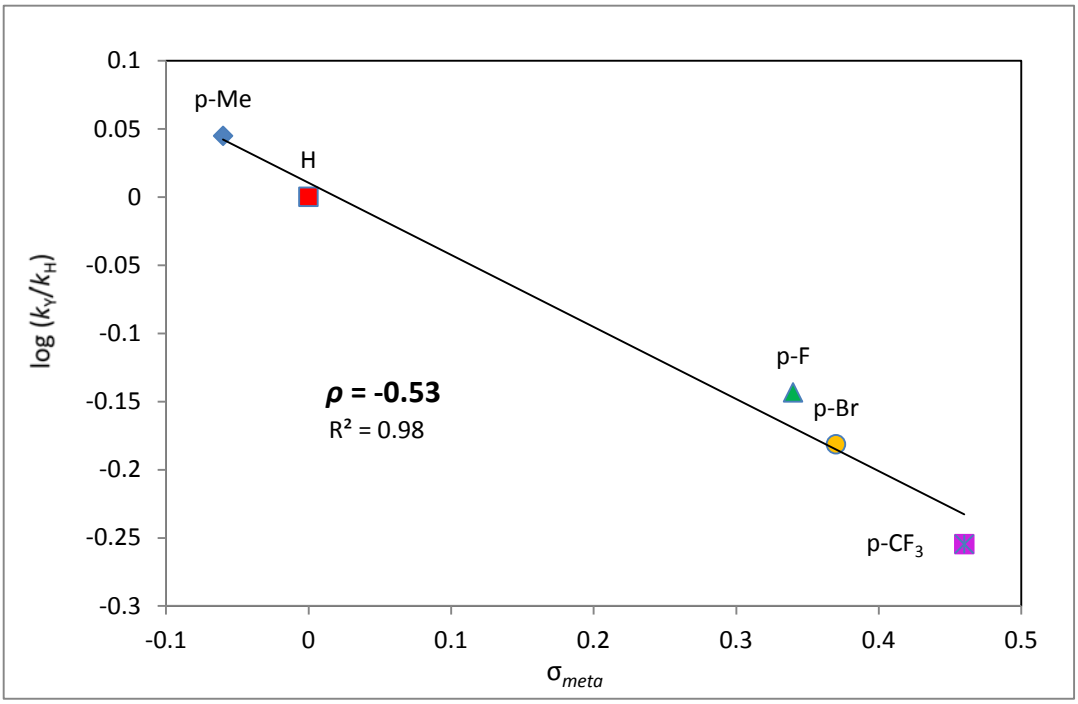

3.5.1.6.2 Hammett Correlation for Amidation with *para*-Substituted Ethyl *N*-Arylsulfonyloxycarbamates

To an 8 mL-vial, the **1a** (0.1 mmol), ethyl *N*-arylsulfonyloxycarbamate (0.1 mmol), [Pd(OTs)$_2$(MeCN)$_2$] (10 mol%) and *d*-chloroform (1 mL) were added, and the vial was sealed with a Teflon® liner cap. The reaction was pre-heated at 80 ˚C for 20 seconds for complete dissolution of reagents, and was further run for additional 10 min (conversions based on **1a** were < 20%). The reaction was stopped by cooling at an ice-water bath. The reaction mixture was analyzed by ^{1}H NMR to determine the amidation product yield with dibromomethane (0.1 mmol) as internal standard.

Determination and Calculations of the k_Y / k_H Value:

With reference to the singlet signal of dibromomethane (2H) at 4.90 ppm (in *d*-chloroform), the ^{1}H NMR signals of a quartet (4.20 ppm, 2 H) was chosen for

product yields quantification. The k_Y / k_H value was determined based on the initial rates of product formation (Assuming all reagent concentrations remain unchanged at the initial rate expressions). The experiment was run in triplicate, and the results were listed below:

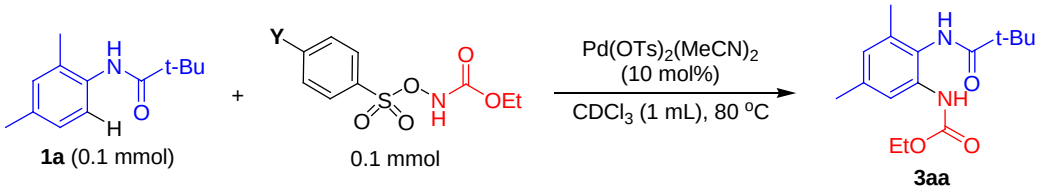

1a (0.1 mmol) + 0.1 mmol → **3aa**

Y	σ_{para}	time (s)	yield 1st (mmol)	yield 2nd (mmol)	yield 3rd (mmol)	average yield (mmol)	product formation rate (M s^{-1})	k_Y / k_H
-Me	-0.06	600	0.0057	0.0053	0.0050	0.0053	8.8×10^{-6}	0.739
-H	0	600	0.0071	0.0070	0.0075	0.0072	12.0×10^{-6}	1
-F	0.34	600	0.0076	0.0087	0.080	0.0081	13.5×10^{-6}	1.130
$-CF_3$	0.37	600	0.0118	0.0124	0.0126	0.0123	20.5×10^{-6}	1.713
$-NO_2$	0.46	600	0.0146	0.0158	0.0144	0.0149	24.8×10^{-6}	2.083

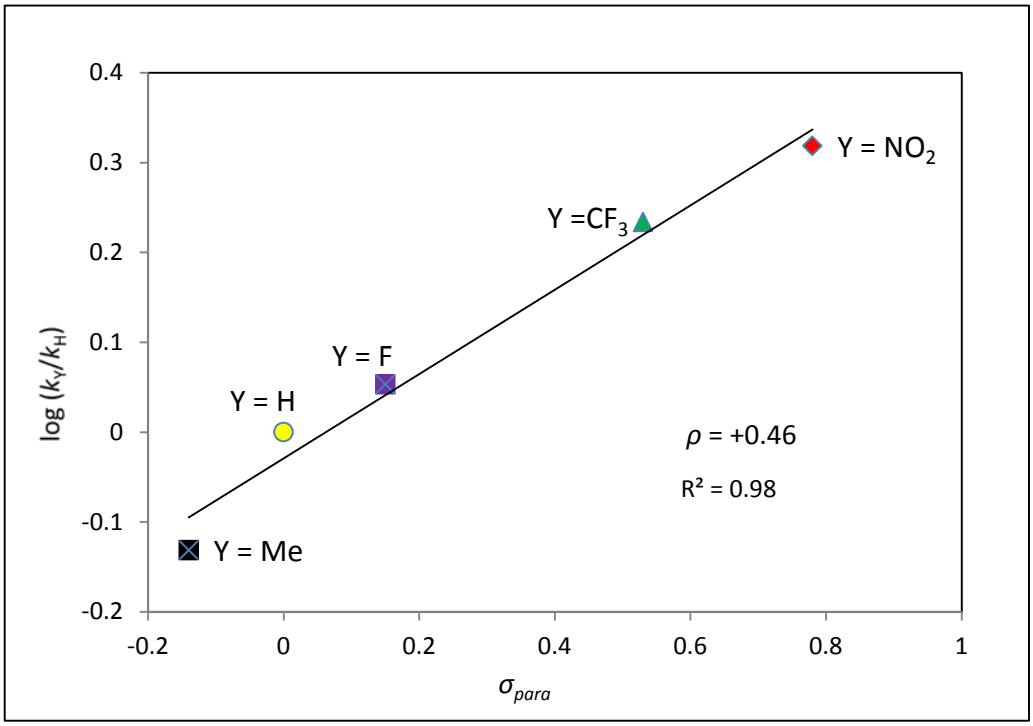

3.5.1.7 Ligand Effect of PdX_2 on the Rate of Amidation

In each reaction, to a mixture of **1a** (0.1 mmol) and PdX_2 (0.01 mmol) in *d*-chloroform (1 mL) in an 8 mL-vial, **2aNs** (0.12 mmol) was added in one portion, and the vial was sealed with a Teflon® liner cap. The reaction mixture was stirred at 80 °C for 20 minutes for complete dissolution of reagents, and was run for additional time (see below). At the designated time interval, the reaction was quickly removed from the oil bath and cooled in an ice-water bath (conversions based on **1a** were < 25%). The reaction mixtures were analyzed by ^{1}H NMR to determine yields of **3aa** with dibromomethane (0.1 mmol) as the internal standard. The initial rates of product formation (d[**3aa**] / dt) were determined by plotting [**3aa**] (M) versus time (s)

Determination and Calculations of the k_x Value:

With reference to the singlet signal of dibromomethane (2H) at 4.90 ppm (in *d*-chloroform), the ^{1}H NMR signals of a singlet (6.89 ppm, 1 H) was chosen for product (**3aa**) yields quantification. The k_x values were determined based on the initial rates of product formation (assuming all components at initial rate remained constant at it original concentration) with the following equation:

$$k_x = v_x / [\mathbf{1a}]_o[\mathbf{2aNs}]_o[\mathbf{PdX_2}]_o^2$$

Where v_x is the rate of product (**3aa**) formation with PdX_2 as catalyst; $[\mathbf{1a}]_o$, $[\mathbf{2aNs}]_o$ and $[\mathbf{PdX_2}]_o$ are the original concentrations of **1a**, **2aNs** and PdX_2.

The results were listed below:

time (s)	$Pd(OPiv)_2$ [**3aa**] (M)	$Pd(OAc)_2$ [**3aa**] (M)	$Pd(TFA)_2$ [**3aa**] (M)	$Pd(OTs)_2(MeCN)_2$ [**3aa**] (M)
120	--	0.0064	--	0.0092
180	--	0.0097	--	--
300	0.0026	0.0167	0.0033	0.0119
360	--	0.0208	--	--
450	0.0112	--	0.0060	--
600	0.0183	--	0.0114	0.0165
900	--	--	--	0.0227
v_x (M s^{-1})	5.23×10^{-5}	5.96×10^{-5}	2.70×10^{-5}	1.72×10^{-5}
R^2	0.997	0.999	0.964	0.999

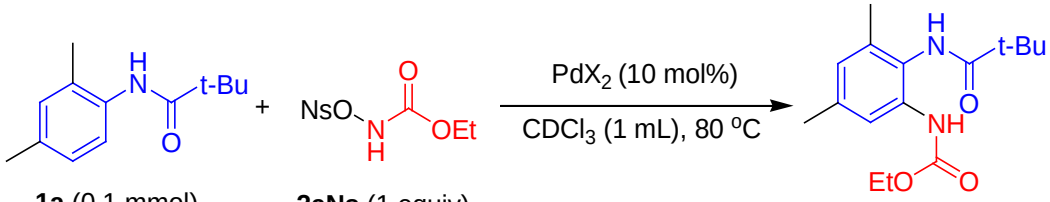

1a (0.1 mmol) **2aNs** (1 equiv) **3aa**

X	pK_a of H**X**	v_x	[**1a**]$_o$ (M)	[**2aNs**]$_o$ (M)	[**PdX$_2$**]$_o^2$ $(M)^2$	k_x	log k_x
OPiv	5.03	5.23×10^{-5}	0.1	0.1	0.001	0.523	-0.281
OAc	4.76	5.96×10^{-5}	0.1	0.1	0.001	0.597	-0.224
TFA	0.52	2.70×10^{-5}	0.1	0.1	0.001	0.270	-0.569
OTs	-1.34	1.72×10^{-5}	0.1	0.1	0.001	0.172	-0.765

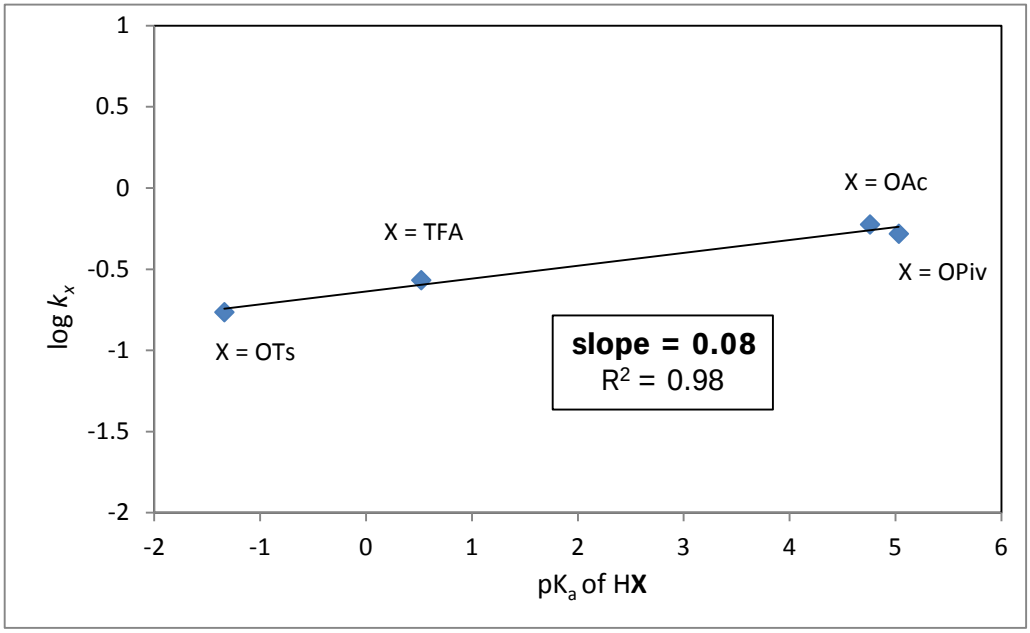
1
0.5
0
-0.5
-1
-1.5
-2
log k_x
-2
-1
0
1
2
3
4
5
6
pK$_a$ of H**X**
X = OAc
X = TFA
X = OPiv
X = OTs
slope = 0.08
R^2 = 0.98

3.5.1.8 Derivation of Rate Expression

Proposed Mechanism:

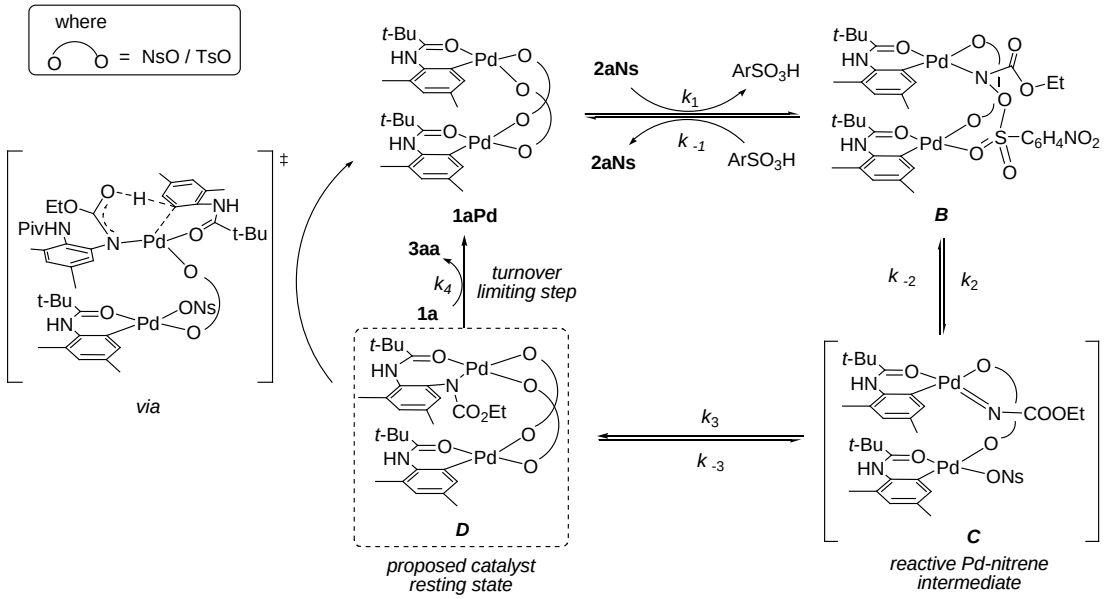

Assumptions:

(1) $[\mathbf{1aPd}] = [\mathbf{Pd}]^2$

(2) $k_2 < k_1$ and k_3; formation of the highly energetic Pd(IV)-imido should be slow.

(3) k_{-3} is very small; reverse migratory nitrene insertion is a thermodynamically unfavorable reaction.

Rate equation (1):

$$\frac{d[\mathbf{3aa}]}{d\mathrm{t}} = k_4[\boldsymbol{D}][\mathbf{1a}] \qquad (1)$$

Equation (2) for **[*D*]***:*

$\because$ $k_4 < k_3$

$\therefore$ pre-equilibrium approximation was applied to [***D***]:

$$\frac{k_3}{k_{-3}} = \frac{[\boldsymbol{D}]}{[\boldsymbol{C}]}$$

$$[\boldsymbol{D}] = \frac{k_3[\boldsymbol{C}]}{k_{-3}} \quad (2)$$

Equation (3) for **[*C*]**:

$\because$ $k_2 < k_3$

$\therefore$ steady state approximation was applied to ***C***

$$\frac{d[\mathbf{C}]}{d\mathrm{t}} = k_2[\boldsymbol{B}] - k_{-2}[\boldsymbol{C}] - k_3[\boldsymbol{C}] + k_{-3}[\boldsymbol{D}] = 0$$

$$k_2[\boldsymbol{B}] + k_{-3}[\boldsymbol{D}] = (k_{-2} + k_3)[\boldsymbol{C}]$$

$$[\boldsymbol{C}] = \frac{k_2[\boldsymbol{B}] + k_{-3}[\boldsymbol{D}]}{(k_{-2} + k_3)}$$

$\because$ k_{-3} is very small

$\therefore$ $k_{-3}[\boldsymbol{D}]$ is negligible

$$[\boldsymbol{C}] = \frac{k_2[\boldsymbol{B}]}{(k_{-2} + k_3)} \quad (3)$$

Equation (4) for **[*B*]**:

$\because$ $k_2 < k_1$

$\therefore$ pre-equilibrium approximation was applied to [***B***]

$$\frac{k_1}{k_{-1}} = \frac{[\boldsymbol{B}]}{[\mathbf{1aPd}][\mathbf{2aNs}]}$$

$$[\boldsymbol{B}] = \frac{k_1[\mathbf{1aPd}][\mathbf{2aNs}]}{k_{-1}}$$

Assuming [**1aPd**] = [**Pd**]^2:

$$[\boldsymbol{B}] = \frac{k_1[\mathbf{Pd}]^2[\mathbf{2aNs}]}{k_{-1}} \tag{4}$$

Derivation of the Overall Rate Expression:

Equation (5):

Substituting [$\boldsymbol{B}$] in the equation (4) to equation (3):

$$[\boldsymbol{C}] = \frac{k_2[\boldsymbol{B}]}{(k_{-2} + k_3)}$$

$$[\boldsymbol{C}] = \frac{k_2 k_1[\mathbf{2aNs}][\mathbf{Pd}]^2}{(k_{-2} + k_3)k_{-1}} \tag{5}$$

Equation (6):

Substituting [$\boldsymbol{C}$] in the equation (5) to equation (2):

$$[\boldsymbol{D}] = \frac{k_3[\boldsymbol{C}]}{k_{-3}}$$

$$[\boldsymbol{D}] = \frac{k_1 k_2 k_3[\mathbf{2aNs}][\mathbf{Pd}]^2}{(k_{-2} + k_3)k_{-1}k_{-3}} \tag{6}$$

Overall Rate Expression:

Substituting [$\boldsymbol{E}$] in the equation (6) to equation (1):

$$\frac{d[\mathbf{3aa}]}{d\mathrm{t}} = k_4[\boldsymbol{D}][\mathbf{1a}]$$

$$\frac{d[\mathbf{3aa}]}{d\mathrm{t}} = \frac{k_1 k_2 k_3 k_4[\mathbf{1a}][\mathbf{2aNs}][\mathbf{Pd}]^2}{(k_{-2} + k_3)k_{-1}k_{-3}}$$

Chapter 4

Rhodium-Catalyzed Intermolecular Aromatic C-H Bond Amination with *N*-Chloroamines

4.1 Introduction

Dehydrogenative coupling of arene C-H bond and amine N-H bond is a straightforward and attractive approach to access a variety of anilines. However, examples of direct arene C-H amination with N-H amines are very rare.

Recently, the research groups of Davies[28c] and Jones[28a,b] reported donor group-assisted Cp*Rh(III)-mediated *ortho*-C-H activation of arenes leading to the formation of a series of cyclometalated Rh(III) complexes. The cyclorhodated complexes were reported the couple with alkenes, alkynes, aldehydes and imines resulting in new C-C bond formation (Scheme 4.1).[33,69] For the couplings with aldehydes and imines, the Cp*Rh(III)Ar complexes can be understood as an aryl anion equivalent, which then react with the electrophilic carbon of the imine / carbonyl groups. We thus surmised that the Cp*Rh(III)Ar complexes would be regarded “nucleophilic” with respect to its reactivity.

Thus, coupling of the Cp*Rh(III)Ar with amine would involve a

nucleophile-to-nucleophile reaction, which is exceedingly challenging.

Scheme 4.1 Rh(III)-Catalyzed Arene C-H Bond Functionalizations

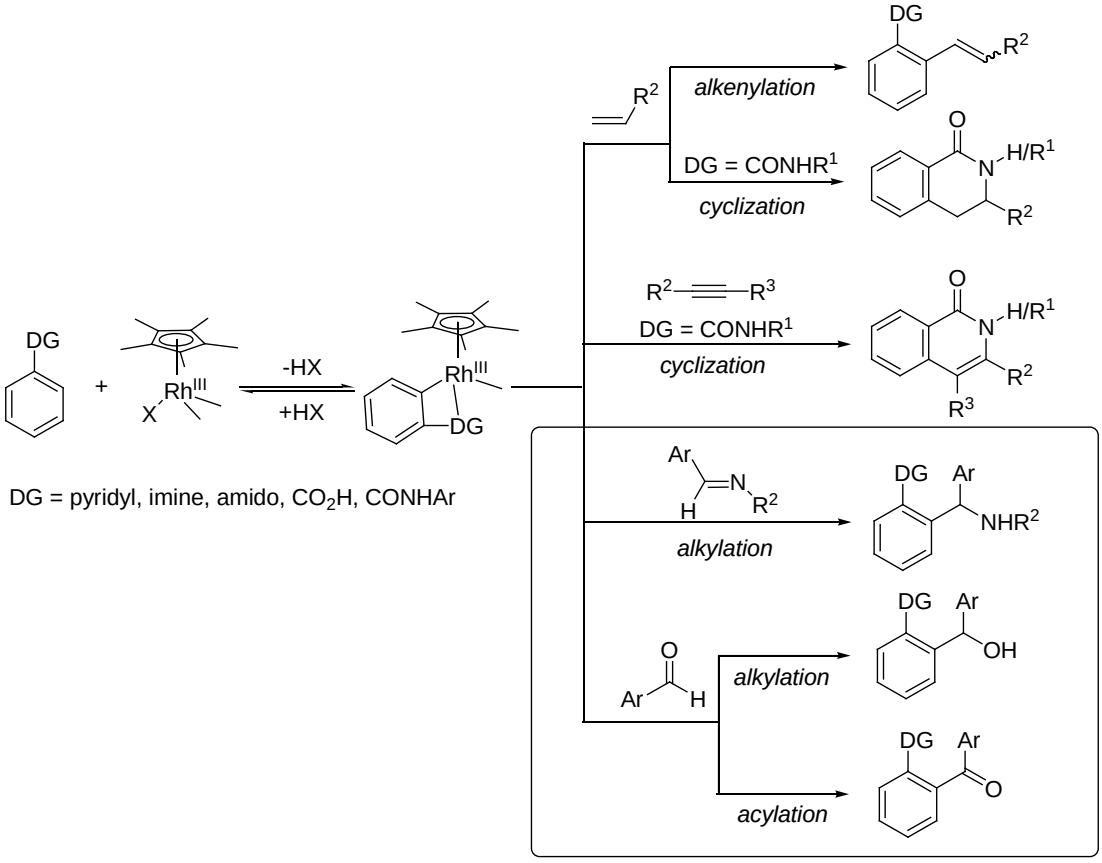

To overcome the "nucleophile-to-nucleophile" challenge, we considered an umpolung strategy for amine activation. According to the literature, N-H amines were known to be readily oxidized (activated) by bleach or NCS to produce *N*-chloroamines.[70] These activated amines would react with carbanions reagents (i.e. organolithium, Grignard reagents) and organoboranes by electrophilic amination (Scheme 4.2).[70, 71]

Thus, it is of interest to examine the reaction of Cp*Rh(III)Ar with *N*-haloamines for C-N bond formation. The success of this reaction should provide a foundation for developing facile catalytic C-H / N-H coupling reactions (Scheme 4.3).

Scheme 4.2 Electrophilic Amination of Carbanion Equivalents with *N*-Chloroamines

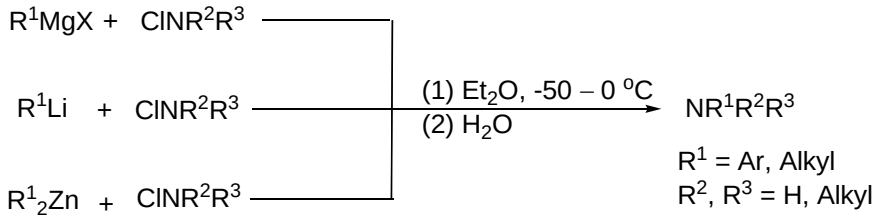

Scheme 4.3 Umpolung Strategy for C-H / N-H Bond Coupling

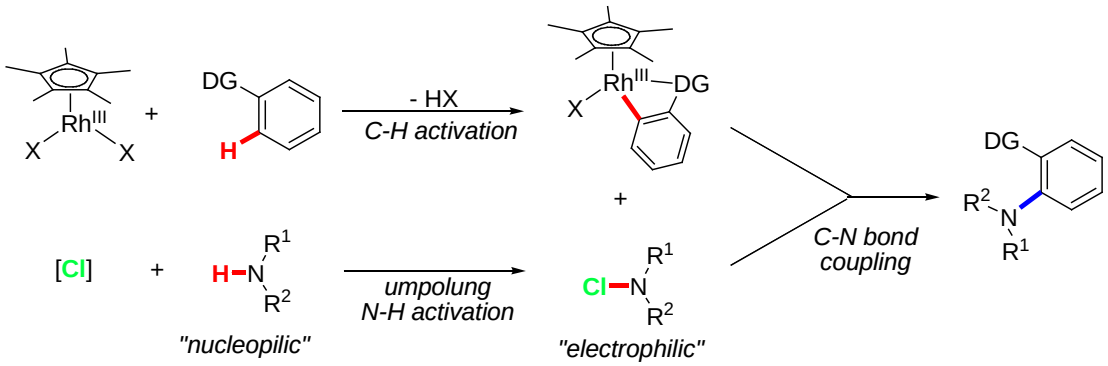

4.2 Rh-Catalyzed Direct Aromatic C-H Bond Amination Using *N*-Chloromorpholine

Table 4.1 Initial Studies on Rh(III)-Catalyzed Acetopheone *O*-Methyloxime Amination with *N*-Chloromorpholine[a]

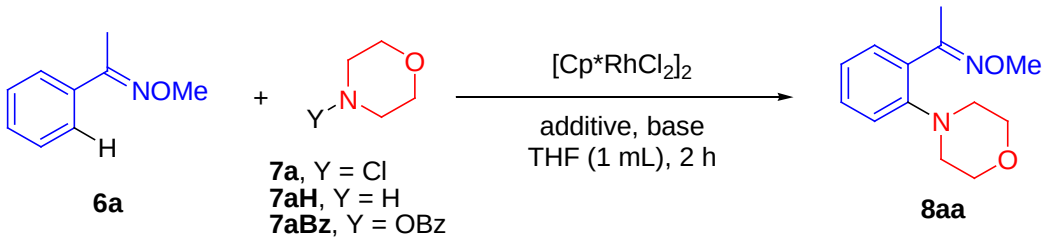

entry	reagent (equiv)	additive (equiv)	base (equiv)	temp (°C)	yield[b] (%)
1	**7a** (1.5)	--	CsOAc (1.2)	80	0
2	**7a** (1.5)	AgOAc (1.2)	--	80	< 5
3	**7a** (1.5)	$AgSbF_6$ (1.2)	--	80	< 5
4	**7a** (1.5)	$AgSbF_6$ (1.5)	CsOAc (1.5)	80	38[c]
5[d]	**7a** (1.5)	$AgSbF_6$ (1.5)	CsOAc (1.5)	80	0
6	**7aH** (1.5)	$AgSbF_6$ (1.5)	CsOAc (1.5)	80	0
7	**7aBz** (1.2)	$AgSbF_6$ (1.5)	CsOAc (1.5)	80	< 5
8	**7aBz** (1.2)	$AgSbF_6$ (1.5)	CsOAc (1.5)	40	< 5

[a]Reaction conditions: **6a** (0.2 mmol), morpholine reagent, $[Cp^*RhCl_2]_2$ (2.5 mol %), additive, base, THF (1 mL), 2 h. [b]Yields were determined by ^1H NMR with dibromomethane as internal standard. [c]Isolated yield. [d]Without $[Cp^*RhCl_2]_2$.

At the outset, we tested the reaction of acetophenone *O*-methyloxime (**6a**, 0.2 mmol) with *N*-chloromorpholine (**7a**, 1.2 equiv) as the amination reagent in the

presence of CsOAc (1.2 equiv) and $[Cp^*RhCl_2]_2$ (2.5 mol%) in THF at 80 °C for 2 h. No amine product (**8aa**) was observed (Table 4.1, entry 1). However, when only AgOAc (1.2 equiv) was used (entry 2), a trace amount of **8aa** (<5%) was obtained. The poor solubility of AgOAc in THF may have limited its ability for halide abstraction and ligand exchange for acetate. However, using $AgSbF_6$ alone produced a less than 5% of **8aa** (entry 3). Gratifyingly, using a combination of $AgSbF_6$ (1.5 equiv) and CsOAc (1.5 equiv) afforded **8aa** in 38% yield (entry 4). This result suggested that a carboxylate ligand is required for effective Rh(III)-catalyzed C-H amination. The molecular structure of **8aa** HCl-hydrate has been characterized by X-ray crystallography (Figure 4.1). It should be noted that no **8aa** was produced in the absence of $[Cp^*RhCl_2]_2$ catalyst (entry 5). The reaction with morpholine alone in the absence of any oxidizing agent (entry 6) failed to give any **8aa**. As reported by Yu and co-workers, *N*-benzoyloxymorpholine (**7aBz**) is an effective reagent for Pd-catalyzed arene C-H amination,[72b] In this work, employing **7aBz** as reagent afforded **8aa** in less than 5% yield (entries 7 — 8).

Figure 4.1 Molecular Structure for **8aa**·HCl-hydrate

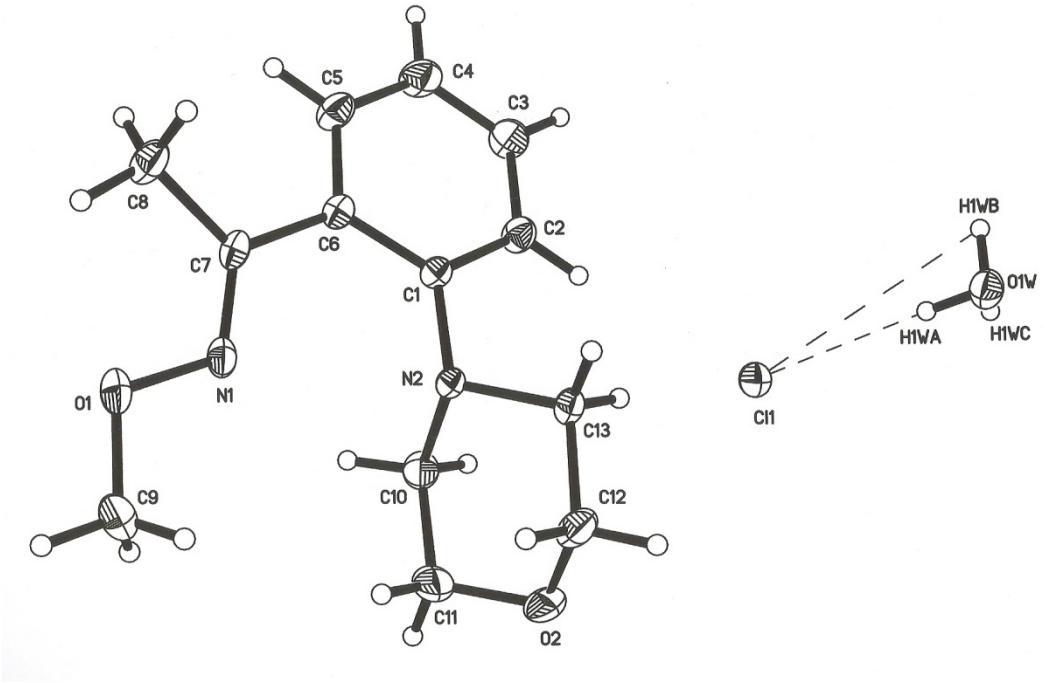

Table 4.2 Selected Bond Distances [Å] and Angles[°]

Bond distances	
N(2)-C(1)	1.4791(14)
N(2)-C(10)	1.5030(17)
N(2)-C(13)	1.5099(16)
Bond angles	
C(1)-N(2)-C(10)	112.22(10)
C(1)-N(2)-C(13)	114.08(9)
C(10)-N(2)-C(13)	108.37(10)
C(2)-C(1)-N(2)	118.10(11)
C(6)-C(1)-N(2)	120.48(11)

Table 4.3 Crystal Data and Structure Refinement for **8aa**·HCl-hydrate

Empirical formula	$(C_{13}H_{17}N_2O_2)\cdot(H_3O\cdot Cl)$	
Formula weight	288.77	
Temperature	296(2) K	
Wavelength	0.71073 Å	
Crystal system	Triclinic	
Space group	P-1	
Unit cell dimensions	*a* = 8.3927(4) Å	α = 82.796(2)°.
	b = 9.5793(5) Å	β = 68.217(2)°.
	c = 10.0117(5) Å	γ = 89.920(2)°.
Volume	740.64(6) $Å^3$	
Z	2	
Density (calculated)	1.295 mg/m^3	
Absorption coefficient	0.264 mm^{-1}	
F(000)	308	
Crystal size	0.50 x 0.50 x 0.50 mm^3	
Theta range for data collection	2.21 to 27.48°.	
Index ranges	-10<=h<=10, -12<=k<=12, -12<=l<=12	
Reflections collected	15230	
Independent reflections	3369 [R(int) = 0.0249]	
Completeness to theta = 27.48°	99.2 %	
Absorption correction	Semi-empirical from equivalents	
Max. and min. transmission	0.7456 and 0.6533	
Refinement method	Full-matrix least-squares on F^2	
Data / restraints / parameters	3369 / 0 / 173	
Goodness-of-fit on F^2	1.001	
Final R indices [I>2sigma(I)]	R1 = 0.0413, wR2 = 0.1236	
R indices (all data)	R1 = 0.0490, wR2 = 0.1314	
Extinction coefficient	0.008(4)	
Largest diff. peak and hole	0.693 and -0.399 $e.Å^{-3}$	

4.2.1 Reaction Optimization

With the preliminary results in hand, we turned to examine different experimental conditions for optimization. Table 4.4 depicts the effect of temperature on the amination reaction.

Table 4.4 Temperature Effect[a]

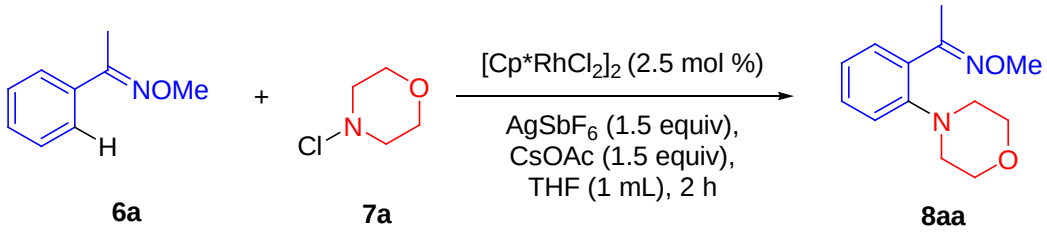

6a **7a** **8aa**

entry	temp. (°C)	yield[b] (%)
1[c]	80	38[d]
2	60	67
3	40	73, 72[d]
4	rt	68

[a]Reaction conditions: **6a** (0.2 mmol), **7a** (1.2 equiv), $[Cp^*RhCl_2]_2$ (2.5 mol %), $AgSbF_6$ (1.5 equiv), CsOAc (1.5 equiv), THF (1 mL), 2 h. [b]Yields were determined by ^1H NMR with dibromomethane as internal standard. [c]**7a** (1.5 equiv) was used. [d]Isolated yields.

As described earlier, treating **6a** (0.2 mmol) with *N*-chloromorpholine (**7a**, 1.5 equiv), $[Cp^*RhCl_2]_2$ (2.5 mol%), $AgSbF_6$ (1.5 equiv) and CsOAc (1.5 equiv) in THF at 80 °C for 2 h afforded **8aa** in 38% isolated yield (Table 4.4, entry 1). When the

temperature was lowered to 60 °C, the yield improved to 67% (entry 2). Lower temperature may slow down the self-decomposition of **7a**. The reaction was best performed at 40 °C, and **8aa** was obtained in 72% isolated yield (entry 3). It is noteworthy that effective amination was also observed at room temperature with **8aa** being formed in 68% yield (entry 4).

Table 4.5 Solvent Effect[a]

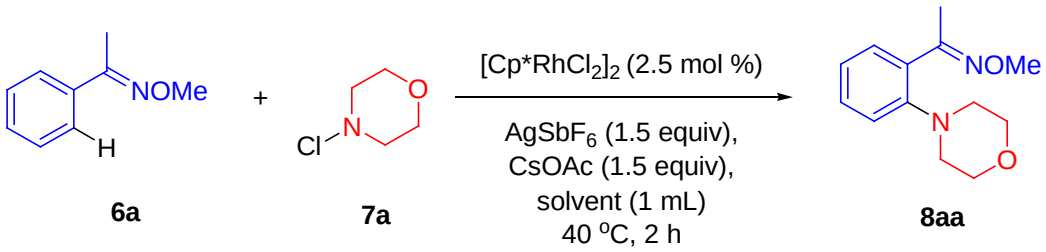

6a + **7a** → **8aa**

entry	solvent	yield[b] (%)
1	THF	73, 72[c]
2	1,4-dioxane	< 5
3	*tert*-amyl alcohol	< 5
4	toluene	0
5	DCE	12
6	DMF	15
7	MeCN	8

[a]Reaction conditions: **6a** (0.2 mmol), **7a** (1.2 equiv), $[Cp^*RhCl_2]_2$ (2.5 mol %), $AgSbF_6$ (1.5 equiv), CsOAc (1.5 equiv), solvent (1 mL), 2 h. [b]Yields were determined by ^1H NMR with dibromomethane as internal standard. [c]Isolated yields.

We studied the solvent effect, and THF was found to be the best solvent for this

reaction (Table 4.5, entry 1). Employing 1,4-dioxane as solvent resulted in the formation of less than 5% of **8aa** (entry 2). While *tert*-amyl alcohol was reported to be a suitable solvent for many Rh(III)-catalyzed aromatic C-H activation / C-C bond formations; however, less than 5% product yield was observed when *tert*-amyl alcohol was the solvent (entry 3). No product formation with full recovery of **6a** was observed, when toluene was used (entries 4). 1,2-Dichloroethane was a less effective solvent (entry 5, 12% yield). Donor solvents such as DMF and acetonitrile were poor solvents for the amination with product yields of 15% and 8% were observed, respectively (entries 6 — 7).

Table 4.6 Additive Screening[a]

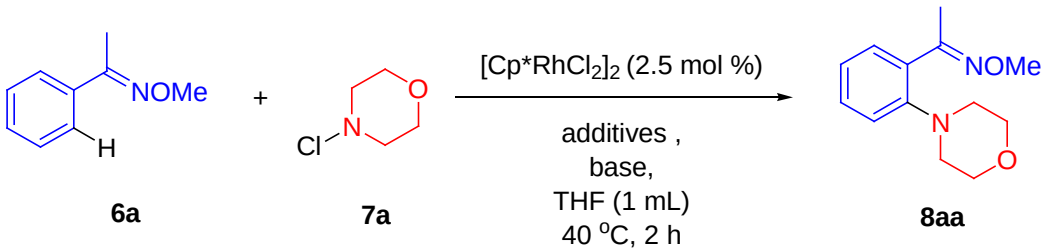

6a **7a** **8aa**

entry	silver additive (equiv)	other additive (equiv)	base (equiv)	yield (%)[b]
1	$AgSbF_6$ (1.5)	--	CsOAc (1.5)	73, 72[c]
2	$AgPF_6$ (1.5)	--	CsOAc (1.5)	64
3	$AgBF_4$ (1.5)	--	CsOAc (1.5)	21
4	AgOTf (1.5)	--	CsOAc (1.5)	40
5	$AgSbF_6$ (1.5)	--	KOAc (1.5)	43
6	$AgSbF_6$ (1.5)	--	Cs_2CO_3 (1.5)	40
7	$AgSbF_6$ (1.5)	AcOH (0.3)	Cs_2CO_3 (1.5)	36
8	$AgSbF_6$ (1.5)	AcOH (0.3)	K_3PO_4 (1.5)	43

9	$AgSbF_6$ (1.5)	AcOH (0.3)	K_2CO_3 (1.5)	38
10	$AgSbF_6$ (1.5)	AcOH (0.3)	KOtBu (1.5)	<5
11[d]	$AgSbF_6$ (1.5)	AcOH (0.3)	--	52
12[e]	$AgSbF_6$ (1.5)	--	--	77

[a]Reaction conditions: **6a** (0.2 mmol), **7a** (1.2 equiv), $[Cp^*RhCl_2]_2$ (2.5 mol %), additives, base, THF (1 mL), 2 h. [b]Yields were determined by ^1H NMR with dibromomethane as internal standard. [c]Isolated yield. [d]Reaction run for 1 h. [e]$[Cp^*Rh(OAc)_2]$ (5 mol %) was used instead of $[Cp^*RhCl_2]_2$ (2.5 mol%).

Different combinations of additives were also examined (Table 4.6). Among the silver salts with non-coordinating anions such as SbF_6^- PF_6^-, BF_4^- and OTf^-, $AgSbF_6$ in combination with CsOAc (1.5 equiv) gave the best result (entries 1 — 4). Replacing CsOAc with KOAc (1.5 equiv) or Cs_2CO_3 (1.5 equiv) resulted in lower product yields of 43% and 40%, respectively (entries 5-6). The use of other bases (1.5 equiv) such as Cs_2CO_3, K_3PO_4 and K_2CO_3 in combination with AcOH (0.3 equiv) did not improve the product yields, and only **8aa** was obtained in 36-43% yields (entries 7 — 9). With KtOBu (1.5 equiv) as base, less than 5% product was produced (entry 10). When AcOH (0.3 equiv) was used in the absence of a base, **8aa** was produced in 52% yield (entry 11). It is noteworthy that $[Cp^*Rh(OAc)_2]$ (5 mol%) is an effective catalyst for the amination reaction, and **8aa** was furnished in 77% yield in the absence of CsOAc (entry 12).

Based on the results of our screening study, we adjusted the quantity of $AgSbF_6$,

CsOAc and the catalyst for better results (Table 4.7). When the amounts of $AgSbF_6$ and CsOAc were reduced to 1.1 equiv, the product yield dropped to 53% (entry 2). With 0.3 equivalent of $AgSbF_6$, **8aa** was produced in <5% yield (entry 3). This indicated that $AgSbF_6$ is a crucial reagent for effective catalytic turnovers. The product yield was significantly improved when the amount of CsOAc was reduced to 0.3 equivalent (entry 4, 87% yield). Probably, a lower acetate concentration would favor ligand dissociation from the Rh(III) centre, rendering vacant sites more available for C-H activation.[9] It is also noteworthy that 1 mol% of $[Cp^*RhCl_2]_2$ was equally effective (entry 5, 81%), further reduction of the catalyst loading to 0.5 mol% resulted in diminished yields (61 — 64%) of **8aa** even after 18 h reaction (entries 6 and 7).

Table 4.7 Effect of Additives Amount, Catalyst Loading and Reaction Time[a]

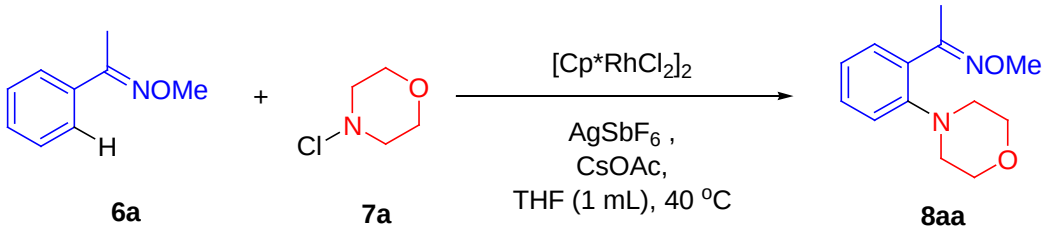

entry	$AgSbF_6$ (equiv)	CsOAc (equiv)	$[Cp^*RhCl_2]_2$ (mol %)	time	yield[b] (%)
1	1.5	1.5	2.5	2 h	73, 72[c]
2	1.1	1.1	2.5	2 h	53
3	0.3	1.5	2.5	2 h	< 5
4	1.5	0.3	2.5	1 h	87, 85[c]
5	1.5	0.3	1	2 h	83, 81[c]
6	1.5	0.3	0.5	3 h	61
7	1.5	0.3	0.5	18 h	64

[a]Reaction conditions: **6a** (0.2 mmol), **7a** (1.2 equiv), $[Cp^*RhCl_2]_2$, $AgSbF_6$, CsOAc, THF (1 mL), 2 h. [b]Yields were determined by ^1H NMR with dibromomethane as internal standard. [c]Isolated yields.

The optimal reaction conditions were found to be: **6a** (0.2 mmol), **7a** (1.2 equiv), $[Cp^*RhCl_2]_2$ (2.5 mol%), $AgAbF_6$ (1.5 equiv) and CsOAc (0.3 equiv) in THF (1 mL) at 40 °C for 1 h **(**entry 4, 87% yield).

4.2.2 Scopes and Limitations

With the optimized reaction conditions in hand, we turned to examine the scope of the amination reaction (Table 4.8). Firstly, we studied the substrate scope of *O*-methyloxime using **7a** as coupling partner. In general, functionalized oximes can be transformed to their respective arylamines **8ba** — **8ga** in 43 — 73% yields with excellent *ortho*-selectivity. Although substrates with electron-donating groups and electron-withdrawing groups can be aminated under the Rh(III)-catalysis, slightly lower yields were obtained with electron-deficient arenes (**8da** : 52%, **8ea** : 43%). Tolerance to the bromine and ester substituents is especially noteworthy since they are useful functional groups for subsequent cross coupling reactions.

Table 4.8 Substrate Scope[a,b]

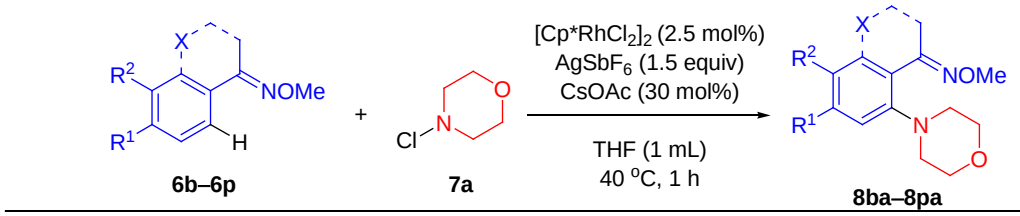

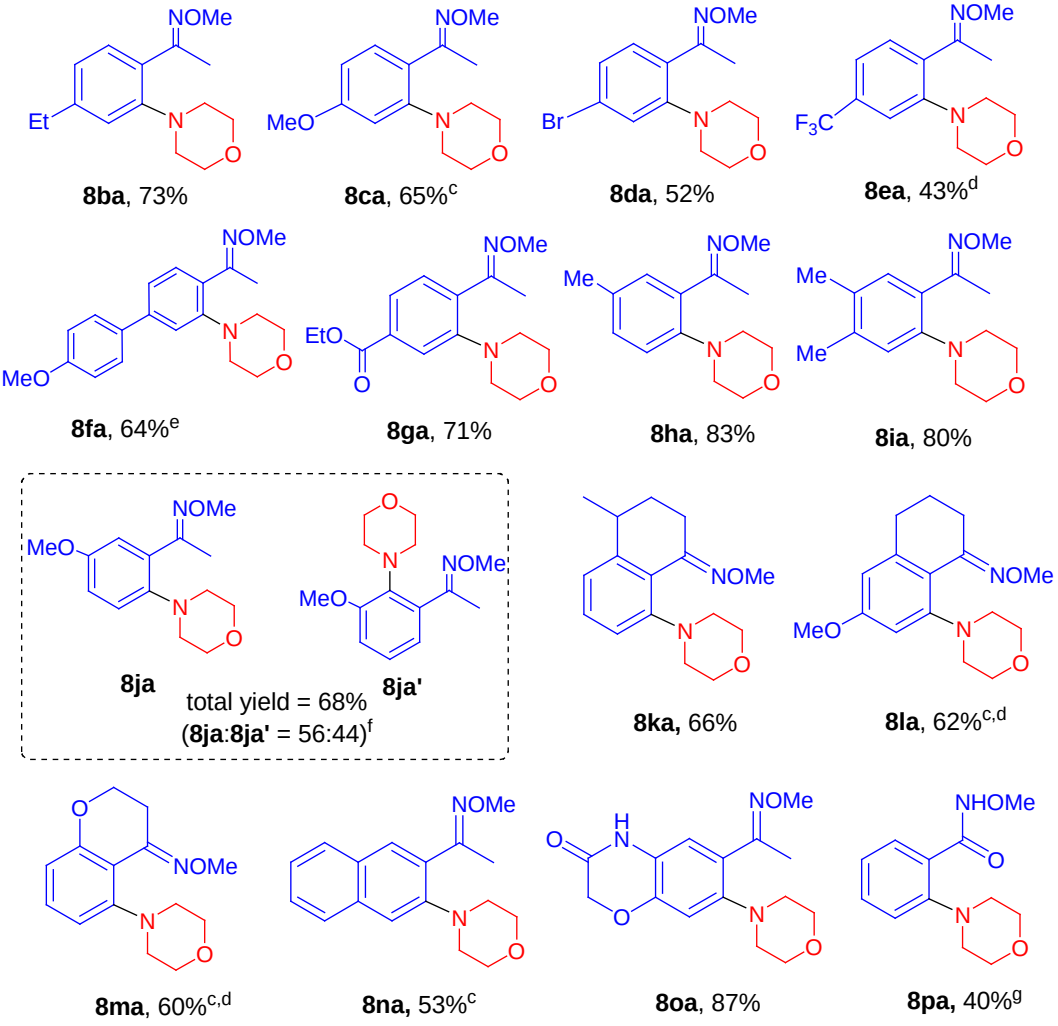

[a]Reaction conditons: substrate (0.2 mmol), **7a** (1.2 equiv), $[Cp^*RhCl_2]_2$ (2.5 mol%), CsOAc (30 mol%), $AgSbF_6$ (1.5 equiv), THF (1 mL), 40 °C, 1h. [b]Isolated yields. [c]N-Chloromorpholine in THF was slowly added with a syringe pump over 30 minutes, 1.5 mL THF used. [d]Reaction run at 60 °C. [e]THF (3 mL) was used. [f]The isomeric ratio was determined by ^1H NMR with dibromomethane as internal standard. [g] CsOAc (1.5 equiv) used.

Regarding to the regioselectivity, the amination reaction of *meta*-substituted oxime **6h** occurred exclusively to the less hindered C-H bond (**8ha**: 83%). Likewise, **6i** bearing two methyl substituents was converted to **8ia** selectively in 80% yield. However, the analogous reaction of the 3-methoxyacetophenone oxime **6j** produced inseparable regioisomeric products **8ja** and **8ja′** in a ratio of 56 : 44 based on ^{1}H NMR analysis. Assuming the aryl-Rh(III) complexes as the intermediate, our findings are compatible with an earlier report by Jones and co-workers that C-H rhodation by $[Cp^*RhCl_2]_2$ occurred with lower regioselectivies with *meta*-substituted arenes such as *m*-OMe and *m*-F substituted phenyl benzaldimine.[28a] In this work, other bicyclic oximes such as those containing tetralone (**6k** — **6l**) and chromalone (**6m**) scaffolds are effective substrates for the direct amination reactions. Amination of oximes with fused ring systems such as naphthalene and *2H*-1,4-bezoxazin-3(*4H*)-one was also achieved to afford **8na** and **8oa** in 53% and 87% yields. It was also found that *N*-methoxybenzamide can be aminated to furnish **8pa** in 40% yield using 1.5 equiv of CsOAc. When 0.3 equivalent of CsOAc was used for the reaction with *N*-methoxybenzamide, only 12% of **8pa** was produced. Extra CsOAc may function as a base for NH deprotonation so that the substrate could coordinate to the Cp*Rh complex for rhodacyclic complex formation. Glorius and coworkers reported a similar amination reaction using *N*-pivaloyloxy benzamides as substrates.[72a]

Table 4.9 Amine Scope[a,b]

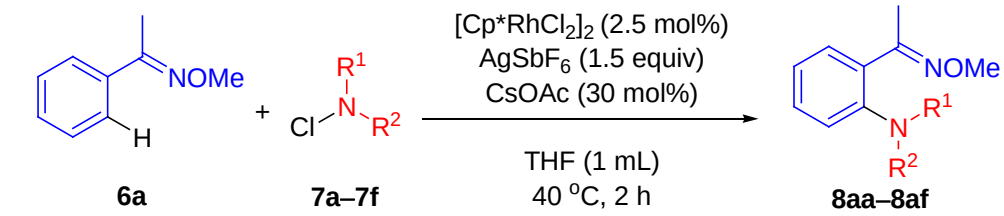

6a **7a–7f** **8aa–8af**

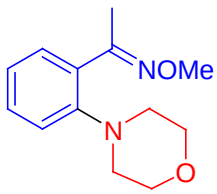

8aa, 85%

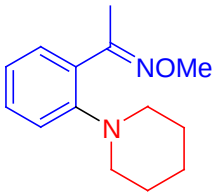

8ab, 87%

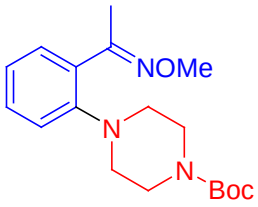

8ac, 63%

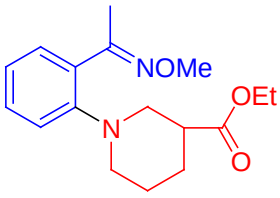

8ad, 53%[c]

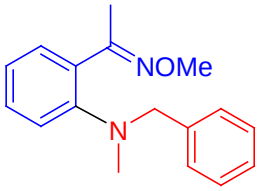

8ae, 44%[d]

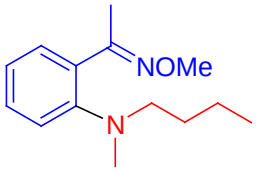

8af, 35%[e]

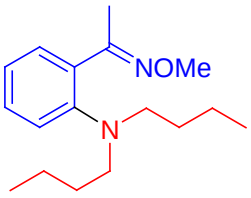

8ag, ~9%[f]

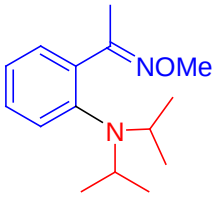

8ah, 0%[f]

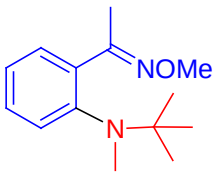

8ai, <5%[f]

[a]Reaction conditions: **6a** (0.2 mmol), *N*-chloroamine (1.2 equiv), $[Cp^*RhCl_2]_2$ (2.5 mol %), CsOAc (30 mol%), $AgSbF_6$ (1.5 equiv), THF (1 mL), 40 °C, 2 h. [b]Isolated yield. [c]Reaction was carried out at room temperature for 15 h. [d]$[Cp^*RhCl_2]_2$ (5 mol%) was used. [e]*N*-Chloro-*N*-methylbutylamine (**7f**, 1.2 equiv) was added dropwise at a rate of 2.4 equiv / h. [f]Yields were determined by ^{1}H NMR.

Employing **6a** as substrate, the amine scope was investigated (Table 4.9). Analogous to **7a**, the Rh-catalyzed coupling of *N*-chloropiperidine and 4-Boc-*N*-chloropiperazine gave **8ab** (87%) and **8ac** (63%) effectively. The analogous

reaction of *N*-chloroethyl nipecotate afforded **8ad** in 53% yield. Yet, the reactions with the *N*-chloroamines of *N*-methylbutylamine and *N*-methylbenzylamine afforded **8ae** and **8af** in moderate yields (35 — 44%). When compared with cyclic *N*,*N*-dialkylamines, it is possible that increased steric hindrance of the aliphatic acyclic amines rendered them less effective for the amination reactions. Consistent with this notion, more sterically demanding dialkylamines such as *N*,*N*-dibutylamine, *N*,*N*-diisopropylamine and *N*-methyl-*tert*-butylamine were all ineffective coupling partners (**8ag** — **8ai**).

Having established the catalytic arene C-H / *N*-chloroamine coupling reactions, we then pursued a one-pot direct amination method based on *in situ* generation of *N*-chloroamines. In this work, *N*-chloromorpholine was generated by treating morpholine with NCS (1:1) in THF for 20 min in the dark (Scheme 4.4). When this mixture was treated with **6a** (0.2 mmol), $[Cp^*RhCl_2]_2$ (2.5 mol%), $AgSbF_6$ (0.3 mmol) and CsOAc (0.06 mmol) in THF at 40 °C for 1 h, **8aa** was obtained 80% yields. With the same procedure, piperadine and *N*-Boc piperazine also effectively coupled to **6a** to afford **8ab** and **8ac** in 79% and 53%, respectively.

Scheme 4.4 One-pot Direct Amination

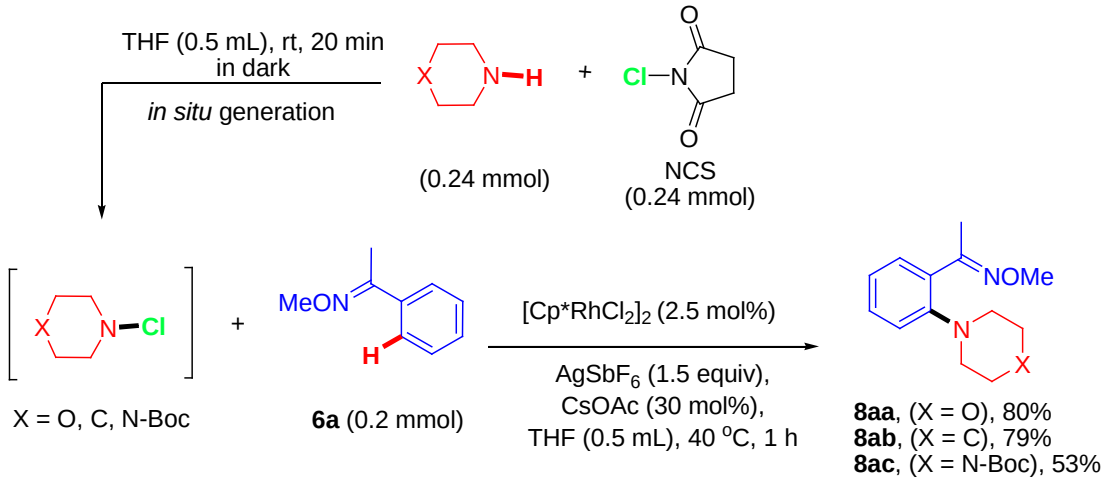

4.3 Rh-Catalyzed Direct Aromatic C-H Bond Amination Using Primary *N*-Chloroalkylamines

Having developed the Rh-catalyzed arene C-H amination with secondary *N*-chloroamine, we were eager to extend the current method to the coupling of primary *N*-chloroalkylamines. Apparently, the direct *ortho*-C-H amination of acetophenone *O*-methyloximes with primary *N*-chloroalkylamines should furnish 2-acyl-*N*-alkylaniline derivatives in one step. According to the literature, 2-acyl-*N*-alkylaniline is a common intermediate for the synthesis of some pharmaceutically important heterocycles, which are frequently embedded in some medicinal products (Figure 4.2).[73]

Figure 4.2 Examples of Pharmaceutical Products Containing 2-Acyl-*N*-alkylaniline Scaffold

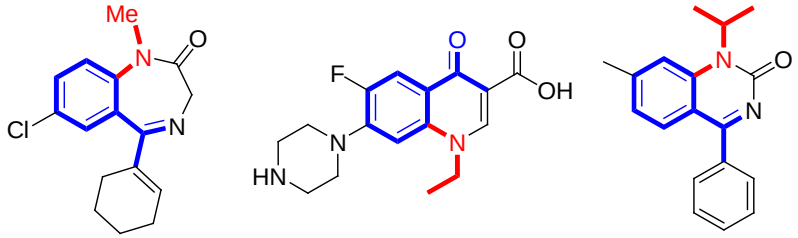

Tetrazepam Norfloxacin Proquazone

Although the synthesis of primary *N*-chloroalkylamines were commonly employed for converting the parent amine to the corresponding aldehyde / ketone, primary *N*-chloroalkylamines are poor reagents for amination reactions (Scheme 4.5).[70c, 74b,c] With regard to the earlier success on aromatic C-H amination with secondary *N*-chloroamines, we hypothesized that with suitable reaction conditions, primary *N*-chloroalkylamines would be competent coupling partners. In this work, we investigated the direct arene C-H amination with primary *N*-chloroalkylamines.

Scheme 4.5 Use of Primary *N*-Chloroalkylamines for Functional Group Transformation ($-NH_2$ to C=O)

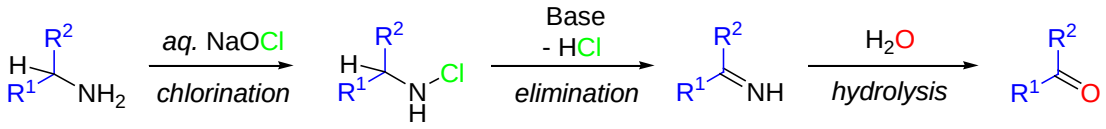

Initially, we examined the coupling reaction of acetophenone *O*-methyloxime (**6a**)

with *N*-chlorocyclopentylamine (**9a**) with the optimal conditions for the secondary amine coupling: *O*-methyloxime (**6a**, 0.2 mmol), *N*-chlorocyclopentylamine (**9a**, 1.1 equiv, *in situ* generated), $[Cp^*RhCl_2]_2$ (2.5 mol%), $AgSbF_6$ (1.5 equiv), CsOAc (0.3 equiv) in THF at 40 °C for 1 h (Table 4.10, entry 1), and the amination product **10aa** was obtained in 10% yield. Apart from the amination product, two chlorinated amine products **10ua** and **10ua'** were also isolated in 29% and 10% yields, respectively. Without $[Cp^*RhCl_2]_2$, no amination product or chlorination products were formed (entry 2). Slow addition of **9a** with a syringe pump at a rate of 1.1 equiv / h improved the product yield of **10aa** to 33%. Notably, the yields of the chlorination products of **10ua** and **10ua'** were lowered to 15% and 6% (entry 3). This observation indicated that the chlorination reaction would be probably associated with the reaction between **10aa** and **9a**; the slow addition of **9a** should avoid prolonged exposure of **10aa** to the chlorination reagent. When the amount of **9a** was increased to 2.2 equivalent (slow addition at 1.1 equiv / h), the substrate conversion increased to 90%. However, the yield of **10aa** (28%) was not improved. More chlorination products **10ua** (40%) and **10ua'** (22%) were obtained.

Table 4.10 Initial Studies on Rh(III)-Catalyzed Amination of **6a** with *N*-Chlorocyclopentylamine[a]

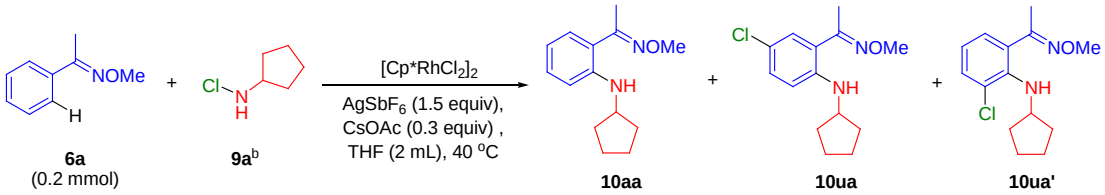

entry	$[Cp^*RhCl_2]_2$ (mol%)	addition of **9a** (equiv)	time	conv. of **6a** (%)[c]	**10aa** (%)[c]	**10ua** (%)[c]	**10ua'** (%)[c]
1	2.5	one-pot (1.1)	1 h	50	10	25	10
2	--	one-pot (1.1)	1 h	<5	--	--	--
3[d]	5	1.1 equiv / h (1.1)	2 h	60	33	15	6
4[d]	5	1.1 equiv / h (2.2)	3 h	90	28[e]	40[e]	22[e]

[a]Reaction conditions: **6a** (0.2 mmol), $[Cp^*RhCl_2]_2$, $AgSbF_6$ (1.5 equiv), CsOAc (0.3 equiv), **9a**, THF (2 mL), at 40 °C. [b]**9a** was freshly prepared by reacting cyclopentylamine and *N*-chlorosuccinimide (1:1) at room temperature for 10 min in the dark. [c]Yields and conversions were determined by ^1H NMR with dibromomethane as internal standard. [d]**9a** was added slowly via a syringe pump. [e]Isolated yields.

According to the literature, *N*-chloroamines become electrophilic chlorinating agents in the presence of a strong acid (i.e. aq. HCl).[74a,e] Amino groups are known to be *para*- and *ortho*-directing activators for electrophilic substitution reactions.[1a] Since the chlorination only occurred on the *meta*-positions to **10aa**, it is plausible that the chlorination products **10ua** and **10ua'** were produced by electrophilic chlorination of **10aa** with *N*-chlorocyclopentylamine **9a**.

To examine this possibility, we performed the reactions between **10aa** and **9a** (Table 4.11). Treating **10aa** with **9a** (1.1 equiv) in THF at 40 °C for 1 h did not result in any chlorination product, and **10aa** was completely recovered (entry 1). With the addition of 1.2 equivalent of AcOH, formation of a trace amount of **10ua** was observed (entry 2). However, when TsOH·H_2O (1.2 equiv) was added, spontaneous chlorination of **10aa** occurred to give the corresponding chlorination products **10ua** (75%) and **10ua'** (21%) in 1 h at 40 °C (entry 3). These results agreed with the literature that *N*-chlorocyclopentylamine could be a potent electrophilic chlorination reagent in the presence of a strong acid. Regarding to the catalytic amination reaction, we were aware that $HSbF_6$ would be generated as a side product in each catalytic cycle (see later section). Thus, $HSbF_6$ would be accumulated in the catalytic reaction.

Table 4.11 Chlorination Reactions of **10aa** with **9a** as Reagent[a]

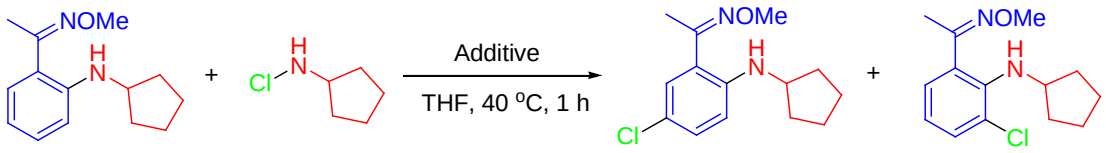

10aa **9a**[b] **10ua** **10ua'**

entry	additive	**10ua** yield (%)[c]	**10ua'** yield (%)[c]
1	--	--	--
2	AcOH (1.2 equiv)	trace	--
3	TsOH·H_2O (1.2 equiv)	75%	21%

[a]Reaction conditions: **10aa** (0.2 mmol), **9a** (1.1 equiv) in THF (1.5 mL) at 40 °C for 1 h. [b]**9a** was generated *in situ* by combining cyclopentylamine and *N*-chlorosuccinimide

(1:1) in THF (1 mL) at room temperature for 10 min in the dark. [c]Yields were determined by ^{1}H NMR with dibromomethane as internal standard.

4.3.1 Reaction Optimization

Aiming to minimize the acid-promoted chlorination, we employed a base to remove the $HSbF_6$ side-product generated *in situ* (Table 4.12).

Table 4.12 Effect of the Base Additives[a]

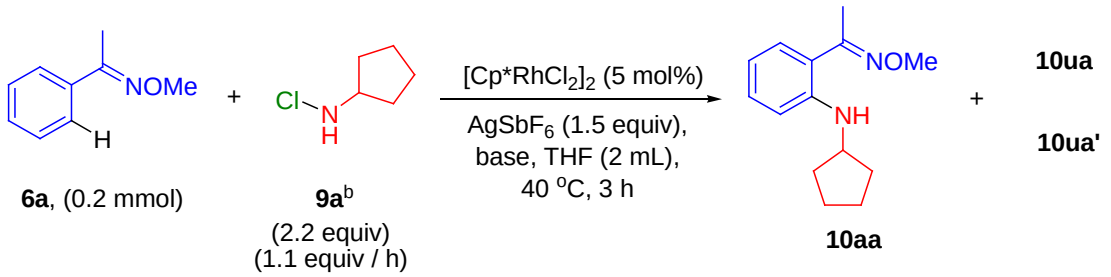

entry	base (equiv)	CsOAc (equiv)	conv. of **6a** (%)[c]	**10aa** yield(%)[c]	**10ua** yield(%)[c]	**10ua'** yield(%)[c]
1	KO*t*Bu 1.3	0.3	10	<5	--	--
2	K_2CO_3 1.3	0.3	50	35	--	--
3	$KHCO_3$ 1.3	0.3	42	28	--	--
4	K_3PO_4 1.3	0.3	48	33	trace	--
5	K_2HPO_4 1.3	0.3	52	18	17	8
6	NEt_3 1.3	0.3	50	39	trace	--
7	pyridine 1.3	0.3	<5	<5	--	--
8[d]	AgOAc 1.5	--	<5	<5	--	--
9	KOAc 1.3	--	79	77	trace	--
10	--	1.3	77	73	trace	--
11	--	0.6	74	20	25	17
12	--	2.0	30	18	--	--

[a]Reaction conditions: **6a** (0.2 mmol), $[Cp^*RhCl_2]_2$ (5 mol%), $AgSbF_6$ (1.5 equiv), CsOAc, THF (1 mL), at 40 °C for 3 h and **9a** (2.2 equiv in 1 mL THF) was added via a syringe pump at a rate of 1.1 equiv / h [b]**9a** was freshly prepared by reacting cyclopentylamine and *N*-chlorosuccinimide (1:1) room temperature for 10 min in the dark. [c]Yields and conversions were determined by ^{1}H NMR with dibromomethane as internal standard. [d]No $AgSbF_6$ was added.

In the presence of KO*t*Bu (1.3 equiv), reacting **6a** (0.2 mmol) with **9a** (2.2 equiv), $[Cp^*RhCl_2]_2$ (5 mol%), $AgSbF_6$ (1.5 equiv) in THF, at 40 °C for 3 h only afforded **10aa** in <5% yield (entry 1), and **6a** was almost completely recovered. Probably, the strongly basic KO*t*Bu might have decomposed **9a** by dehydrochlorination.[74d] Inorganic bases such as K_2CO_3, $KHCO_3$, K_3PO_4 and K_2HPO_4 also gave inferior results (entries 2 — 5). Organic bases were not suitable for the amination reaction. For example, when triethylamine was used as base, **10aa** was obtained in only 39% yield. Pyridine was found to terminate the catalytic reaction (entries 6 — 7). Similar to the earlier results, AgOAc is ineffective for the amination reaction with <5% yield of **10aa** being formed (entry 8). Gratifyingly, when KOAc (1.3 equiv) or CsOAc (1.3 equiv) was used, **10aa** was formed in 77% and 73% yields (entries 9 — 10), and only a trace amount of chlorination product **10ua** was detected. It is likely that acetate could react with the $HSbF_6$ to form the weaker HOAc, which has been shown to exhibit little promotional effect for the aromatic chlorination reaction. For the ease of

handling, CsOAc was employed for further screening study. As expected, when CsOAc was reduced to 0.6 equivalent, chlorination products **10ua** and **10ua'** were obtained in 25% and 17% yields (entry 11). When 2.0 equivalent of CsOAc was employed, **10aa** was obtained in only 18% yield (entry 12). Probably, increasing the acetate concentration would slow down the C-H activation since acetate dissociation from the rhodium metal centre is a pre-requisite.[9]

We turned to test the effect of solvents (Table 4.13). Empolying *tert*-amyl alcohol, 1,2-dichloroethane, toluene and 1,4-dioxane as solvents gave poor results for the amination reaction, and THF was the solvent of choice.

Table 4.13 Solvent Effect[a]

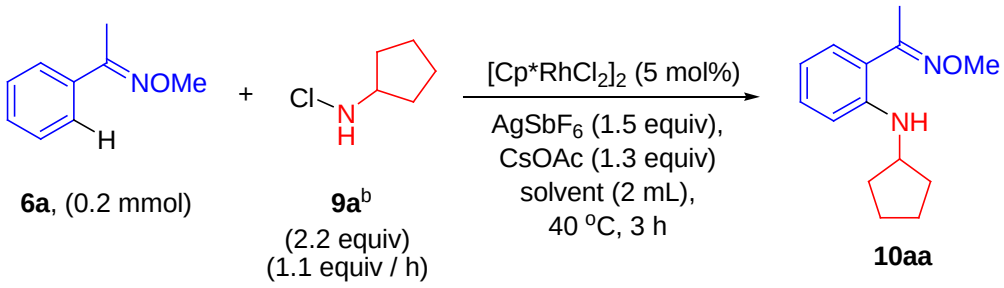

6a, (0.2 mmol) **9a**[b] (2.2 equiv) (1.1 equiv / h) **10aa**

entry	solvent	yield (%)[c]
1	THF	73
2	*tert*-amyl alcohol	< 5
3	1,2-dichloroethane	9
4	toluene	0
5	1,4-dioxane	< 5

[a]Reaction conditions: **6a** (0.2 mmol), $[Cp^*RhCl_2]_2$ (5 mol%), $AgSbF_6$ (1.5 equiv), CsOAc (1.3 equiv), solvent (1 mL), at 40 °C for 3 h and **9a** (2.2 equiv in 1 mL solvent)

was added via a syringe pump at a rate of 1.1 equiv / h [b]**9a** was freshly prepared by reacting cyclopentylamine and *N*-chlorosuccinimide (1:1) at room temperature for 10 min in the dark. [c]Yields were determined by ^{1}H NMR with dibromomethane as internal standard.

The effect of reaction temperature was examined (Table 4.14). At room temperature, **10aa** was obtained in 76% yield with a negligible amount of chlorination product being formed (entry 1). A comparable result was observed when the reaction was performed at 40 °C (entry 2). However, at 60 °C, the yield for **10aa** significantly dropped to 27% (entry 3); a small amount of chlorination products (~15%) was produced. Possibly, higher reaction temperature would promote the decomposition of the chloroamine **10a**, thereby lowering the yield of the amination product. Based on the temperature study, 40 °C was chosen for further optimization.

Table 4.14 Effect of Temperature[a]

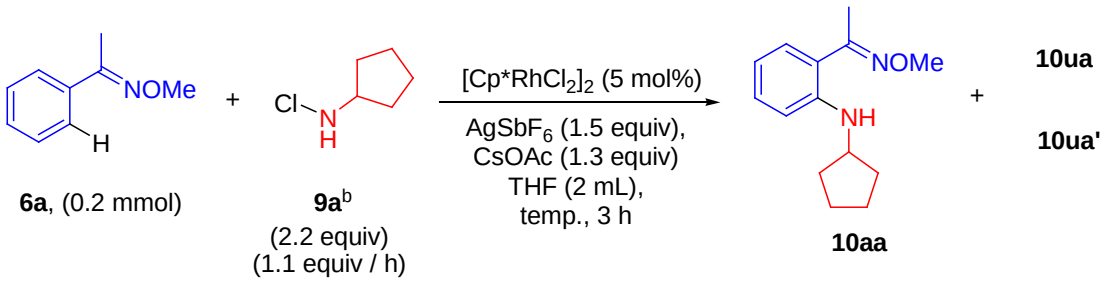

entry	temp.	conversion of **6a** (%)[c]	**10aa** yield(%)[c]	**10ua** yield(%)[c]	**10ua'** yield(%)[c]
1	rt	83	76	trace	--
2	40°C	77	73	trace	--
3	60°C	66	27	10	<5

[a]Reaction conditions: **6a** (0.2 mmol), $[Cp^*RhCl_2]_2$ (5 mol%), $AgSbF_6$ (1.5 equiv), CsOAc (1.3 equiv), THF (1 mL) for 3 h and **9a** (2.2 equiv in 1 mL THF) was added via a syringe pump at a rate of 1.1 equiv / h [b]**9a** was freshly prepared by reacting cyclopentylamine and *N*-chlorosuccinimide (1:1) at room temperature for 10 min in the dark. [c]Yields and conversions were determined by ^{1}H NMR with dibromomethane as internal standard.

Table 4.15 depicts the effect of the concentration and the addition rate of **9a**. The addition rates of **9a** were first tested (entries 1 — 3). We found that by adding **9a** (2.2 equiv) dropwise over 1 h with a syringe pump (total reaction time = 2 h), **10aa** was furnished in 80% yield (entry 3). Increasing the amount of **9a** to 2.5 equivalent or 3.0 equivalent did not give better results (entries 4 — 5). Addition of 1.8 equivalent of **9a** over 1 h produced **10aa** in 59% yield (entry 6).

The best conditions for the amination reaction was found to be: **6a** (0.2 mmol) with $[Cp^*RhCl_2]_2$ (5 mol%), $AgSbF_6$ (1.5 equiv), CsOAc (1.3 equiv) and **9a** (2.2 equiv, in 1 mL THF, addition rate = 2.2 equiv / h) at 40 °C for 3 h; **10aa** was obtained in 80% yield.

Table 4.15 Effect of **9a** Amount and the Addition Rate[a]

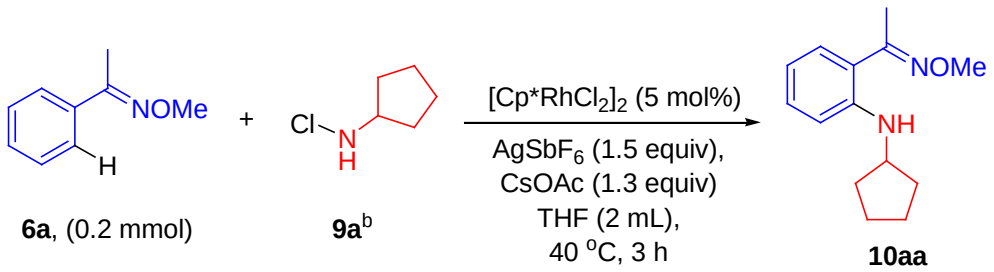

6a, (0.2 mmol) **9a**[b] **10aa**

entry	**9a** (equiv)	rate of addition	time	conversion (%)[c]	**10aa** yield(%)[c]
1	2.2	0.7 equiv / h	5 h	66	65
2	2.2	1.1 equiv / h	3 h	77	73
3	2.2	2.2 equiv / h	2 h	83	80[d]
4	2.5	2.2 equiv / h	2 h	64	65
5	3.0	3.0 equiv / h	2 h	55	43
6	1.8	1.8 equiv / h	2 h	61	59

[a]Reaction conditions: **6a** (0.2 mmol), $[Cp^*RhCl_2]_2$ (5 mol%), $AgSbF_6$ (1.5 equiv), CsOAc (1.3 equiv), THF (1 mL) for 3 h and **9a** (in 1 mL THF) was added via a syringe pump. [b]**9a** was freshly prepared by reacting cyclopentylamine and *N*-chlorosuccinimide (1:1) at room temperature for 10 min in the dark. [c]Yields and conversions were determined by ^1H NMR with dibromomethane as internal standard. [d]Isolated yield.

4.3.2 Scopes and Limitations

Table 4.16 depicts the substrate scope of the direct aminations of acetophenone oximes with primary *N*-chloroamines. In general, *O*-methyloximes bearing electron-withdrawing or electron-donating groups at the *para*-position were successfully aminated (**10ba** — **10ga**, **10qa**, **10ra** and **10sa**). Initially, we found that the reactions of *O*-methyloximes bearing electron-withdrawing groups at the

para-position such as –Br, -CF_3, -COOEt, -Cl, -SO_2Me and –NO_2 gave moderate yields (**10da**, **10ea**, **10ga**, **10qa**, **10ra**, **10sa**; 23 — 52%) when 1.3 equivalent of CsOAc was used as additive. Gratifyingly, when 1.0 equivalent of CsOAc was employed, a significant improvement in the product yields (77 — 92%) was achieved with negligible chlorination. The aminations of the arenes bearing electron-donating *para*-substituents such as –OMe, -Et and –C_6H_4(*p*-OMe) gave moderate product yields (**10ba**, **10ca** and **10fa**; 36 — 64%) accompanied with formation of the chlorination product. However, when 1.5 equivalent of CsOAc was employed, the yields for the amination products dropped significantly to 14 — 23%, albeit without chlorination product being formed. Oximes having *meta*-substituents such as –Me, -Cl and –CF_3 were aminated at the less hindered *ortho*-C-H bond in moderate to good yields (**10ha**, **10ta**, **10ua**; 44 — 78%). Amination of the arenes having fused ring scaffolds such as 4-methyltetralone (**6k**) and 1-acetylnaphthalene (**6n**) were also examined. While the reaction of 4-methyltetralone oxime (**6k**) furnished **10ka** in 60% yield, the analogous reaction of **6n** with 1.3 equivalent of CsOAc did not give the expected product **10na**. Yet, only a small amount of chlorinated amination product **10na-3Cl** (<5%) was obtained. When 1.0 equivalent of CsOAc was used, **10na-3Cl** was produced as an exclusive product in 43% yield.

Table 4.16 Substrate Scope[a,b]

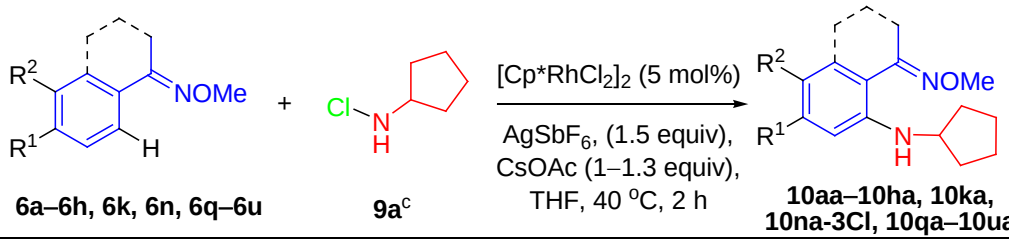

6a–6h, 6k, 6n, 6q–6u | **9a**[c] | **10aa–10ha, 10ka, 10na-3Cl, 10qa–10ua**

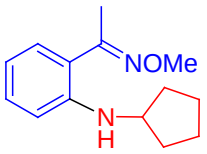

10aa, 80%

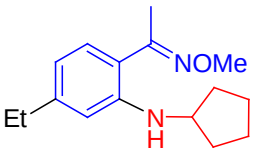

10ba, 64%[d]

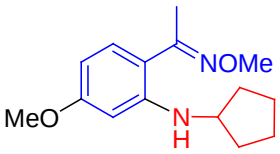

10ca, 36%[d]

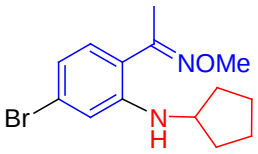

10da, 52% (78%)[e]

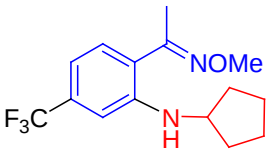

10ea, 28% (81%)[e]

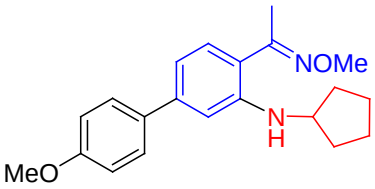

10fa, 49%[d]

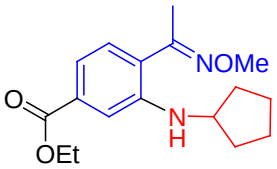

10ga, 43% (81%)[e]

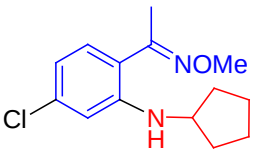

10qa, 48% (76%)[e]

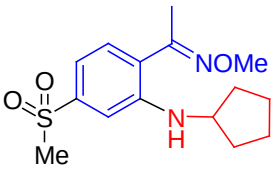

10ra, 32% (77%)[e]

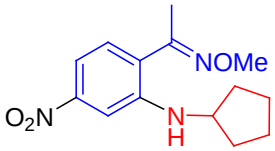

10sa, 23% (92%)[e]

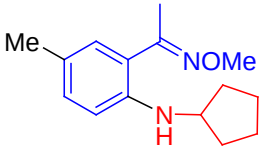

10ha, 55%

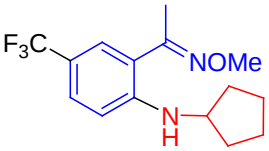

10ta, 46% (78%)[e]

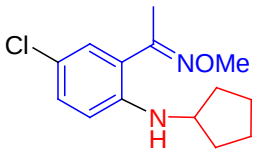

10ua, 44%

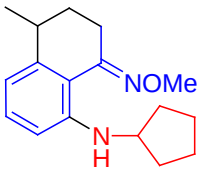

10ka, 60%

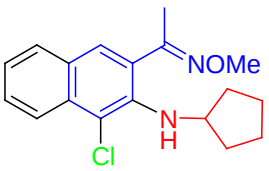

10na-3Cl, <5% (43%)[e]

[a]Reaction conditions: *O*-methyloxime (0.2 mmol), $[Cp^*RhCl_2]_2$ (5 mol%), CsOAc (1.3 equiv), $AgSbF_6$ (1.5 equiv) in THF (1 mL) at 40 °C, 2 h, **9a** (2.2 equiv, in 1 mL THF) was added dropwise using a syringe pump at a rate of 2.2 equiv / h. [b]Isolated yields. [c]**9a** was generated *in situ* by combining cyclopentylamine and

N-chlorosuccinimide (1:1) in THF(1 mL) at room temperature for 10 min in the dark. [d]C-5 Chlorination products were detected by ^{1}H NMR. [e]CsOAc (1.0 equiv) was used and isolated yields.

Table 4.17 depicts the amine scope of the C-H coupling reaction. With 4-nitroacetophenone oxime **6s** as substrate, coupling of *N*-chlorocyclohexylamine produced **10sb** in 86% yield, and its structure was characterized by X-ray crystallography (Figure 4.3). *N*-Chloroalkylamines of 4-aminotetrahydropyran and *exo*-2-aminonorbornane reacted with **6s** to give **10sc** (66%) and **10sd** (75%), respectively. Apart from cycloalkylamines, *N*-chloroamines derived from *sec*-butylamine and isopropylamine containing a branched alkyl group were also effective coupling partners, and **10se** and **10sf** were obtained in 85% and 84% yields. However, the reactions with *N*-chloroamines of α-methylbenzylamine and 1-cyclohexylethylamine only led to moderate yields (**10sg**: 55% and **10sh**: 42%). It is probably due to increase in steric hindrance of the amine skeletons. Consistent with this notion, *N*-chloro-*tert*-butylamine (**9i**) and *N*-chloro-1-adamantylamine (**9j**) are ineffective coupling partners for the direct C-H amination reaction.

Table 4.17 Amine Scope[a,b]

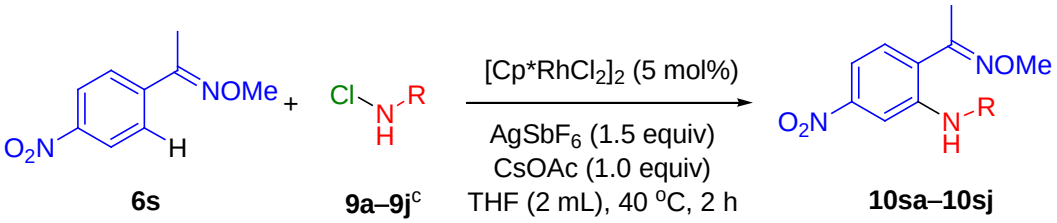

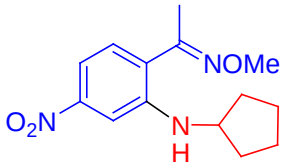

10sa, 92%

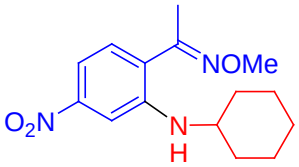

10sb, 86%[d]

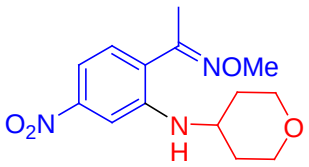

10sc, 66%[d]

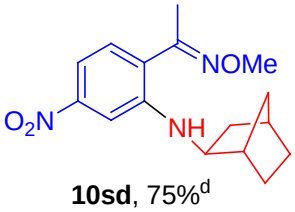

10sd, 75%[d]

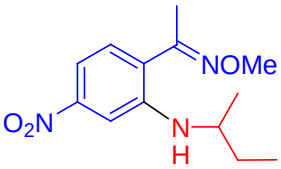

10se, 85%[d]

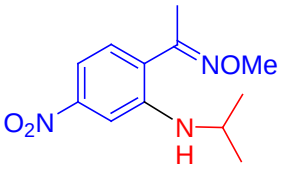

10sf, 84%

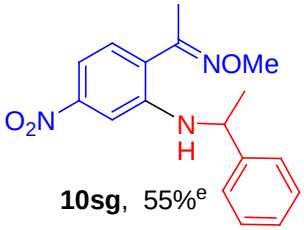

10sg, 55%[e]

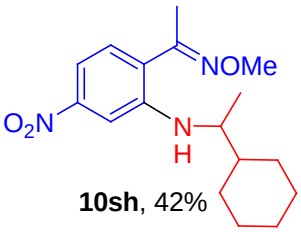

10sh, 42%

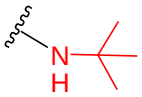

10si, 0%

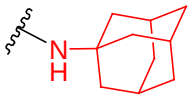

10sj, 0%

[a]Reaction conditions: **6s** (0.2 mmol), $[Cp^*RhCl_2]_2$ (5 mol%), $AgSbF_6$ (1.5 equiv), CsOAc (1.0 equiv), THF (1 mL) at 40 °C, 2 h, **9a — 9j** (2.2 equiv, in 1 mL THF) was added dropwise using a syringe pump at a rate of 2.2 equiv / h. [b]Isolated yields. [c]**9a—9j** were generated *in situ* by combining *N*-chlorosuccinimide and the suitable primary amine (1:1) in THF (1 mL) for at room temperature for 10 min in the dark. [d]CsOAc (1.1equiv) was used. [e]Yield was determined by ^1H NMR with dibromomethane as internal standard; similar product **10ag** from *O*-methyloxime (**6a**) was isolated in 66% yield.

Figure 4.3 Molecular Structure of **10sb**

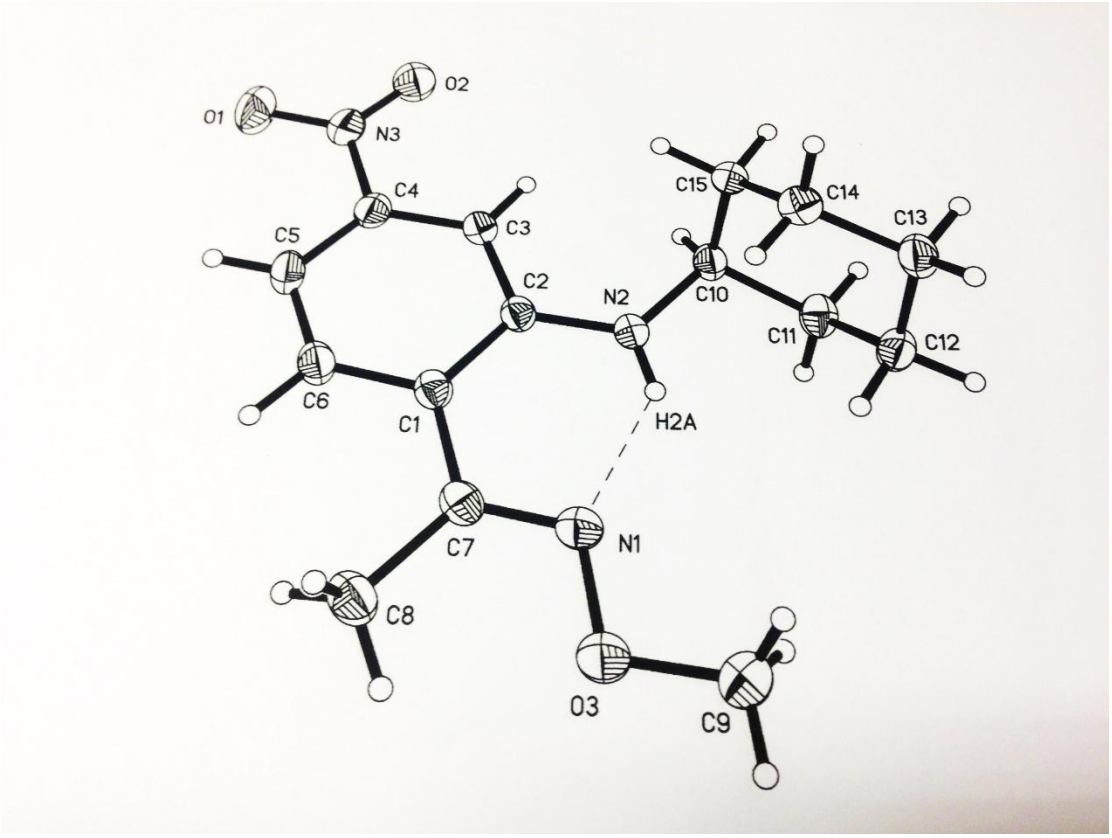

Table 4.18 Selected Bond Distances [Å] and Angles[°] for **10sb**

Bond distances	
N(2)-C(2)	1.3583(11)
N(2)-C(10)	1.4594(12)
N(2)-C(13)	1.5099(16)
N(2)-H(2A)	0.851 (11)
H(2A)…N(1)	1.973 (11)
N(2)-N(1)	2.6554(11)
Bond angles	
C(2)-N(2)-C(10)	123.77(7)
N(2)-C(10)-C(11)	109.45(8)
N(2)-C(10)-C(15)	112.00(8)

C(3)-C(2)-N(2)	119.96(8)
C(1)-C(2)-N(2)	122.10(7)
N(2)-H(2A)…N(1)	136.5(10)

Table 4.19 Crystal Data and Structure Refinement for **10sb**

Empirical formula	$C_{15}\ H_{21}\ N_3\ O_3$
Formula weight	351.40
Temperature	296(2) K
Wavelength	0.71073 Å
Crystal system	Triclinic
Space group	P-1
Unit cell dimensions	*a* = 7.2262(2) Å α = 102.1500(10)°.
	b = 9.2507(2) Å β = 92.3590(10)°.
	c = 11.4120(3) Å γ = 92.3670(10)°.
Volume	744.17(3) $Å^3$
Z	2
Density (calculated)	1.568 mg/m^3
Absorption coefficient	0.107 mm^{-1}
F(000)	372
Crystal size	0.50 x 0.46 x 0.40 mm^3
Theta range for data collection	1.83 to 27.66°.
Index ranges	-9<=h<=9, -11<=k<=12, -14<=l<=14
Reflections collected	19566
Independent reflections	3394 [R(int) = 0.0318]
Completeness to theta = 27.66°	98.0 %
Absorption correction	Semi-empirical from equivalents
Max. and min. transmission	0.7456 and 0.6671
Refinement method	Full-matrix least-squares on F^2
Data / restraints / parameters	3394 / 0 / 275
Goodness-of-fit on F^2	1.004
Final R indices [I>2sigma(I)]	R1 = 0.0423, wR2 = 0.1067
R indices (all data)	R1 = 0.0591, wR2 = 0.1186
Extinction coefficient	0.097(4)
Largest diff. peak and hole	0.165 and -0.170 $e.Å^{-3}$

Table 4.20 Amination with *N*-Chloro-*n*-hexylamine[a,b]

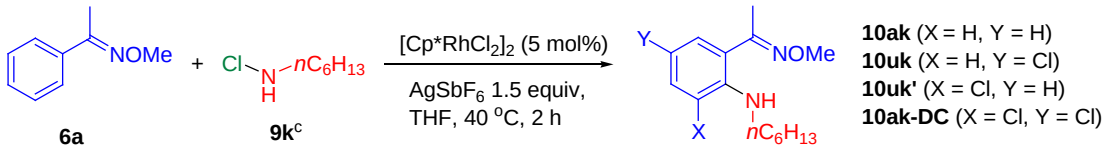

6a **9k**[c]

entry	CsOAc (equiv)	additive (equiv)	**10ak** yield(%)	**10uk** yield(%)	**10uk'** yield(%)	**10ak-DC** yield(%)
1	1.3	--	--	trace	--	--
2	0.3	--	trace	20	17	trace
3[d]	--	--	trace	10[e]	20[e]	12%[e]

[a]Reaction conditions: **6a** (0.2 mmol), $[Cp^*RhCl_2]_2$ (5 mol%), $AgSbF_6$ (1.5 equiv), CsOAc, THF (1 mL) at 40 °C, 2 h, **9k** (2.2 equiv, in 1 mL THF) was added dropwise using a syringe pump at a rate of 2.2 equiv / h. [b]Yields were determined by ^{1}H NMR with dibromomethane as internal standard. [c]**9k** were generated *in situ* by combining *N*-chlorosuccinimide and *n*-hexylamine (1:1) in THF (1 mL) at room temperature for 10 min in the dark. [d]$[Cp^*Rh(OAc)_2]$ (10 mol%) was used instead. [e]Isolated yields.

Apart from cycloalkyl and branched alkylamines, we also examined the coupling reaction with primary *N*-chloro-*n*-alkylamine. Employing *N*-chloro-*n*-hexylamine (**9k**) as the reagent under the optimized conditions, the reaction produced a trace amount of chlorindated product **10uk** (Table 4.20, entry 1). When 0.3 equivalent of CsOAc was used, the chlorinated arylamine products **10uk** (20%) and **10uk'** (17%) were obtained (entry 2). Employing $[Cp^*Rh(OAc)_2]$ (10 mol%) alone as catalyst without CsOAc resulted in formation of chlorination products (**10uk** and **10uk'**; 10% and 20%) and the double chlorination product (**10ak-DC**; 12% yield) (entry 3). It is possible that *N*-chloro-*n*-hexylamine is not stable in the presence of base. However, without any added base, acid-promoted arene chlorination occurred.

2-Aminoacetophenone is a privileged scaffold in medicinally important heterocycles. Therefore, deprotection of the oxime function in the arylamine products is an essential part for further manipulations. Table 4.21 depicts the scope of oxime deprotection. In this work, treating **8ab** (0.1 mmol) with 6 M HCl (1 mL) at reflux for 2 h afforded **8ab2** in 89% yield. Arylamines bearing mono-alkylamino groups: isopropylamino (**10sf**) and cyclopentylamino (**10sa**) were also effectively deprotected to furnish **10sf2** and **10sa2** in 81% yields. 2-(cyclopentylamino)acetophenone *O*-methyloximes with 4-Br (**10da**) and 4-CF_3 (**10ea**) substituents remained intact after deprotection giving **10da2** and **10ea2** in 89% and 75% yields, respectively.

Table 4.21 Deprotection of *O*-Methyloxime Arylamine Products[a,b]

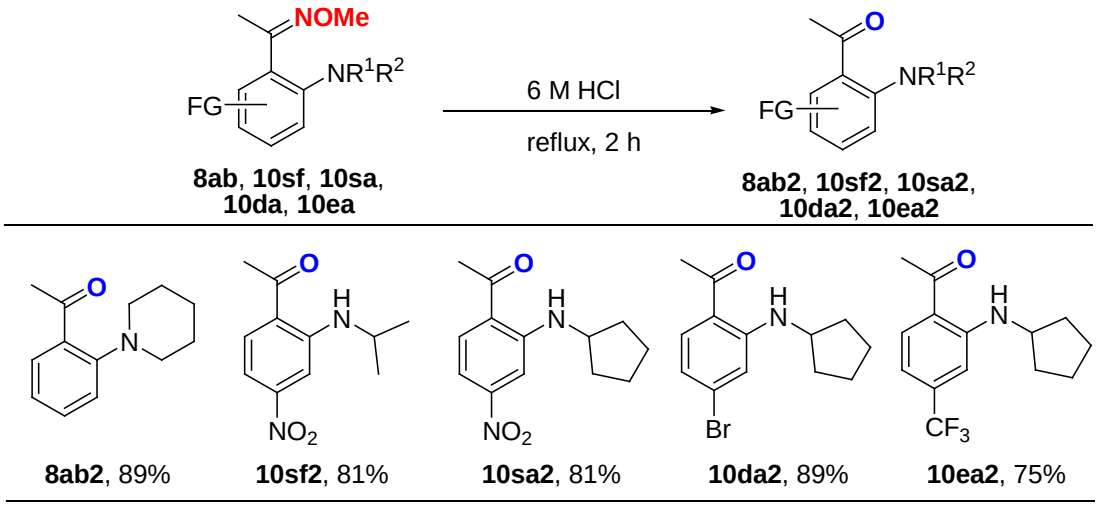

[a]Reaction conditions: *O*-methyloxime arylamine (0.1 mmol) in 6 M HCl (1 mL) reflux (~130 °C), 2 h. [b]Isolated yields.

4.4 Mechanistic Investigation

4.4.1 Deuterium-Labeled Experiments

To gain insight on the nature of the turnover limiting step, we performed deuterium-labeled experiments. According to the works of Fagnou[69d,e] and Rovis,[69b] the Rh-mediated arene C-H activation is reversible in the cycloaddition of acetanilides and benzamides with alkynes. In this work, treating **6a**-d_5 with $[Cp^*RhCl_2]_2$ (5 mol %), $AgSbF_6$ (1.5 equiv) and CsOAc (0.3 equiv) in MeOH at 40 °C for 20 min in the absence of *N*-chloroamine led to 47% loss of *ortho*-deuterium (Scheme 4.6). This result is compatible with the findings of Fagnou and Rovis that Rh(III)-mediated C-H bond activation is a reversible reaction.

Scheme 4.6 H / D Exchange Reactions

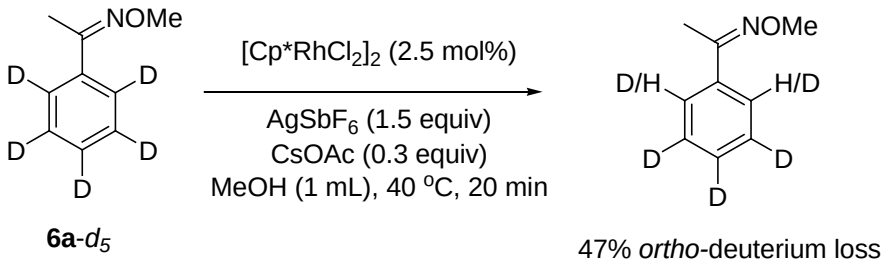

6a-d_5

47% *ortho*-deuterium loss

However, when the H / D exchange reaction was performed using **6a** as substrate in the presence of *N*-chloromorpholine (**7a**, 1.2 equiv) in d_4-methanol and was quenched at 63% conversion, less than 5% *ortho*-deuteration of **6a** was detected and

8aa was produced in 60% yield. This result indicated that C-H activation is irreversible in the presence of *N*-chloroamine, and the C-N bond formation step could be fast and irreversible.

To investigate the kinetic isotope effect of the amination reactions, we performed two parallel reactions of **6a** and **6a**-d_5 with **9a** (Scheme 4.7). The substrate (**6a** or **6a**-d_5, 0.2 mmol) was treated with **10a** (1.2 equiv, in 1 mL THF), $[Cp^*RhCl_2]_2$ (10 mol%), $AgSbF_6$ (1.5 equiv) and CsOAc (1.3 equiv) in 1 mL THF at 0 °C for 5 min. The reactions were quenched by 30% aqueous ammonia at ~10 — 20% conversion of **6a** / **6a**-d_5, and they were run in duplicate. The initial rates were determined by measuring the product yields of **10aa** and **10aa**-d_4 by ^{1}H NMR, and the k_H / k_D value was determined to be 2.1 (initial rate for **6a** = 27×10^{-6} mol dm^{-3} s^{-1}; initial rate for **6a**-d_5 = 13×10^{-6} mol dm^{-3} s^{-1}). According to the literature, the k_H / k_D values of Rh(III)-catalyzed arene *ortho*-C-H functionalizations were found to be in a range of 2.2 — 4.2;[37a,b, 69d,e] our results are comparable to those reported values. Based on the primary kinetic isotope effect observed, we proposed that the Rh-mediated C-H activation would be the rate-limiting step.

Scheme 4.7 Parallel Reactions of **6a** and **6a-d_5** with **9a**

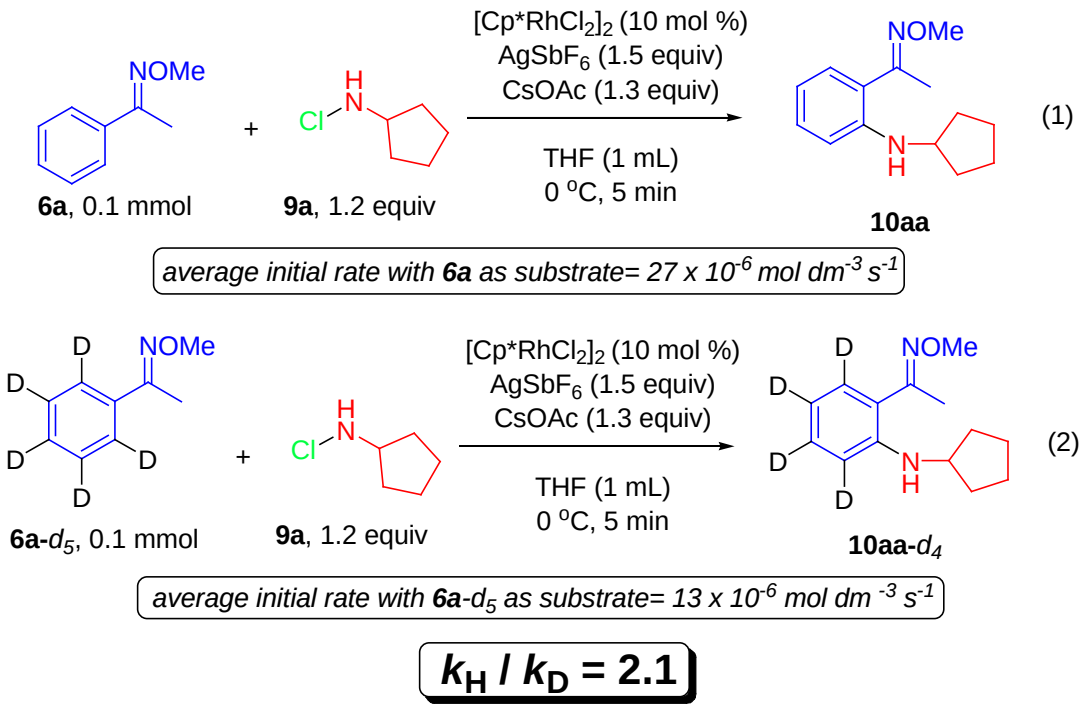

4.4.2 Hammett Correlation Study

To gain further insight into the nature of the Rh(III)-catalyzed C-H activation, a Hammett correlation study was performed. In this work, the relative reaction rates of a series of *para*-substituted acetophenone oxime versus **6a** were determined; a plot of logarithm of the relative rates versus the σ_{meta} substituent constants (Hammett plot) was obtained. In each reaction, the substituted acetophenone *O*-methyloximes (0.1 mmol) were treated with **9a** (1.2 equiv), $[Cp^*RhCl_2]_2$ (10 mol%), $AgSbF_6$ (1.5 equiv) and CsOAc (1.3 equiv) in THF (2 mL) at 0 °C for 5 — 8 min. The reactions were quenched with 30% aqueous ammonia at ~10 — 25% substrate conversions, and the

initial rates were determined by measuring the product yields by ^{1}H NMR. Each reaction was run in duplicate. The plot of relative rates (log k_Y / k_H) versus the σ_{meta} constants gave a linear fit (R^2 = 0.92), and the ρ value of -0.69 (Figure 4.4). The negative ρ value suggests that the transition state associated with the C-H bond cleavage mediated by the Rh(III) centre should be electrophilic in character.

Figure 4.4 Linear Free Energy Correlation for the Rh(III)-catalyzed C-H Amination of Acetophenone *O*-Methyloximes

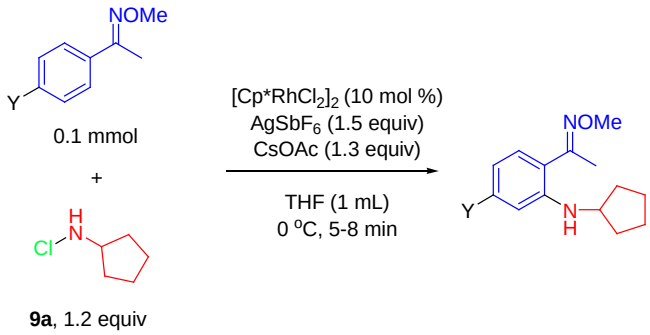

Y =	k_Y / k_H	σ_{meta}
H	1.000	0
OMe	0.686	0.12
Cl	0.530	0.37
CF_3	0.357	0.46
NO_2	0.329	0.71

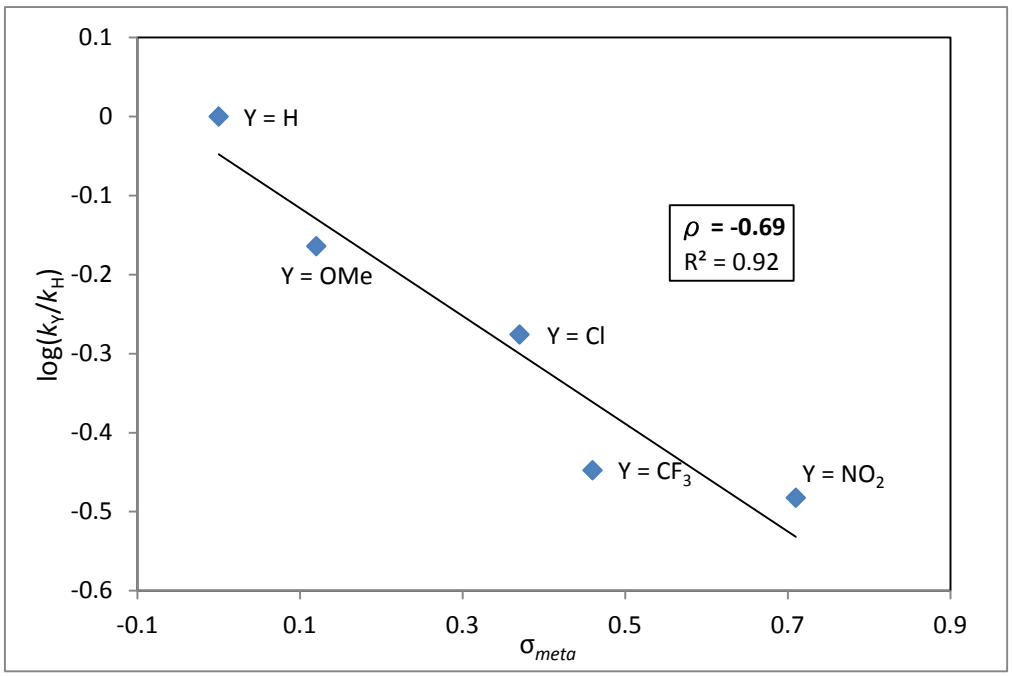

4.4.3 Stoichiometric Reactions of the Cyclorhodated Complex

As indicated earlier, the reaction would be initiated by C-H bond activation to form cyclorhodated complexes, which are likely the active intermediates for the amination reactions. To examine this possibility, a rhodacyclic complex of 2-phenylpyridine (**11aRh**) was prepared for stoichiometric amination reactions. The complex was synthesized by reacting $[Cp^*RhCl_2]_2$ (0.1 mmol) with NaOAc (2.2 equiv) and 2-phenylpyrindine (2.4 equiv) in dichloromethane (20 mL) at room temperature for 24 h, and the product complex was obtained in 78% yield.

When **11aRh** was treated with **7a** (1.1 equiv) and $AgSbF_6$ (2.2 equiv) in THF at 40 °C for 2 h, **12aa** was produced in 52% yield (Table 4.22). Primary *N*-chloroalkylamines were also effective coupling partners; the coupling of **11aRh** with **9a** and **9c** furnished the corresponding **13aa** and **13ac** in 79% and 93% yields. Similarly, the aminations with α-branched *N*-chloroalkylamines such as **9h** and **9l** gave **13ah** (81%) and **13al** (86%) in good yields. Based on these findings, we proposed that cyclorhodated complex should be the active intermediate in the catalytic cycle, and the C-N bond formation step should proceed by the coupling of Cp*Rh(III)Ar with *N*-chloroamines.

Table 4.22 Stoichiometric Aminations with **11aRh**[a,b]

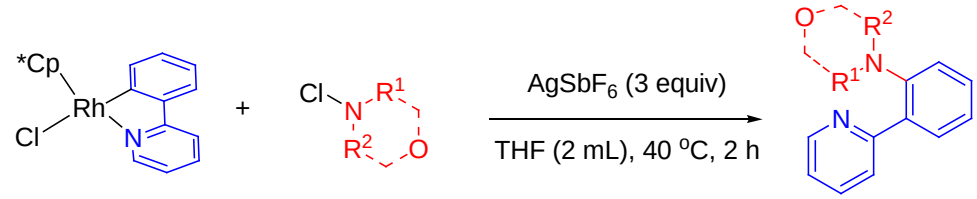

11aRh, 0.1 mmol

7a, **9a**, **9c**, **9h**, **9l**, 1.2 equiv[c]

12aa, **13aa**, **13ac**, **13ah**, **13al**

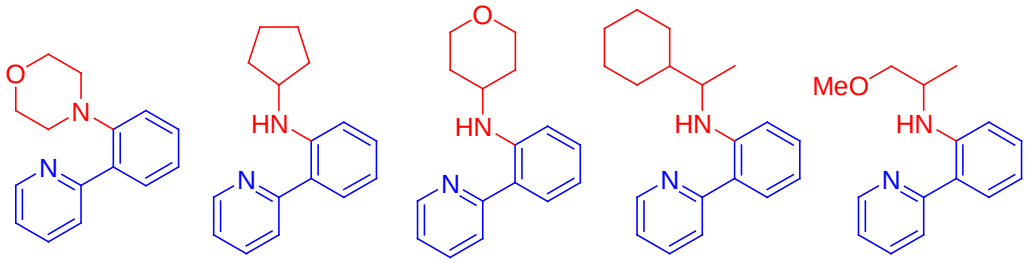

12aa, 52% **13aa**, 79% **13ac**, 93% **13ah**, 81% **13al**, 86%

[a]Reaction conditions: **11aRh** (0.1 mmol), $AgSbF_6$ (3.0 equiv), *N*-chloroamine (1.2 equiv in 1 mL THF) in THF (1 mL) at 40 °C for 2 h. [b]Isolated yields. [c]*N*-Chloroamines were generated *in situ* by combining *N*-chlorosuccinimide and the suitable amine (1:1) in THF (1 mL) at room temperature for 10 min.

While the stoichiometric reactions of **11aRh** with *N*-chloroamines were found to be successful, we were also interested to gain more insights into the nature of the C-N bond formation step. In this work, we carried out two independent stoichiometric reactions of **11aRh** with **9a** as reagent, with an objective to examine whether a vacant site on the Rh(III) centre is required for the C-N bond formation (Scheme 4.8). Treating **11aRh** alone with **9a** (1.2 equiv) in THF (1 mL) at 40 °C for 2 h did not lead to **13aa** formation. In contrast, when **11aRh** was pre-treated with $AgSbF_6$ (0.95 equiv) at room temperature for 10 min and with the removal of the AgCl precipitate, the

reaction with **9a** (1.2 equiv) in the same condition gave **13aa** in 72% yield. These results implied that a vacant site is required for the C-N bond formation.

Scheme 4.8 Two Stoichiometric Reactions of **11aRh** with **9a** Under Different Conditions

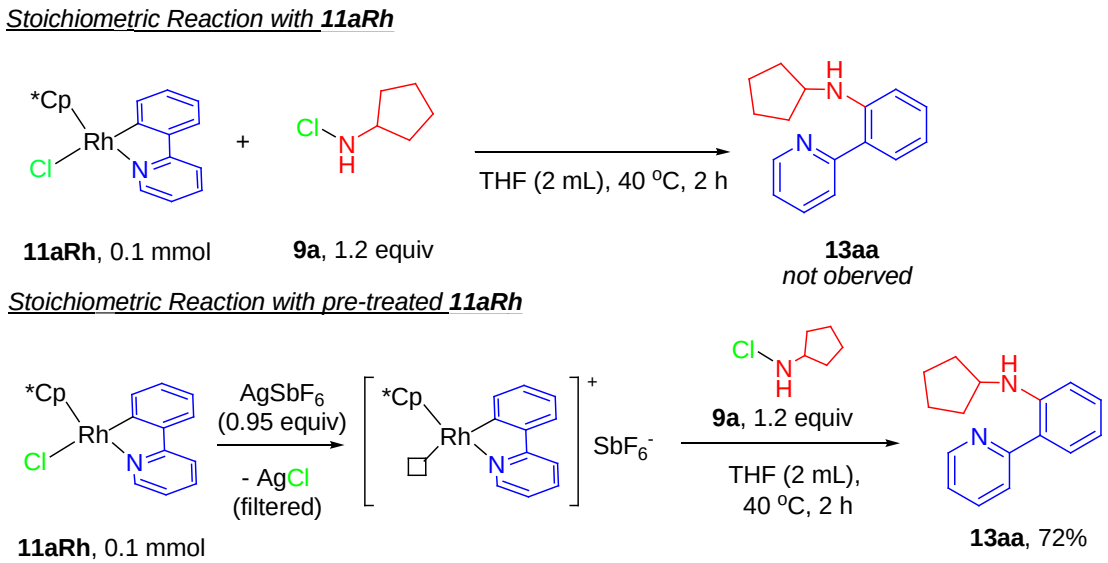

4.4.4 Discussion on Reaction Mechanism

4.4.4.1 Rh(III)-Catalyzed *ortho*-C-H Activation of Oximes

In the H / D exchange experiments, we found that the Rh(III)-mediated *ortho*-C-H activation of acetophenone *O*-methyloximes is reversible in the absence of any *N*-chloroamine reagent (Scheme 4.6). However, the *ortho*-H / D scrambling was not observed in both the substrate **6a** and the product **8aa** (yield = 60%) when

N-chloromorpholine was added. This finding suggested that the coupling of the Cp*Rh(III)Ar complex with *N*-chloromorpholine for C-N bond formation should be a faster step than the C-H activation.

In the kinetic isotope effect experiments, primary KIE was observed for the Rh(III)-catalyzed arene *ortho*-C-H amination, and the k_H / k_D values were determined to be 2.1 for direct comparison of the initial rates for amination of **6a** and **6a**-d_5 (Schemes 4.7). As mentioned earlier, the reported k_H / k_D values for Cp*Rh(III)-catalyzed arene *ortho*-C-H functionalizations were within a range of 2.2 — 4.2; our k_H / k_D values are comparable to the report values.[37a,b, 69d,e] Based on these results, C-H activation is likely to be the rate-limiting step.

The Hammett correlation study with *para*-substituted acetophenone oximes revealed a linear free energy relationship with the Hammett σ_{meta} constants providing a ρ value of -0.69 (Figure 4.4). The ρ value is comparable to Fagnou's finding on the Rh(III)-catalyzed acetanilide cyclization with alkynes.[69d,e] In Fagnou's study, the acetanilide cyclization revealed a linear free energy relationship with Hammett σ_{meta} constants with a ρ value of -1.04. These negative values indicated buildup of a partial positive charge in the transition state of the C-H bond cleavage, which is consistent with the electrophilic cyclometalation mechanism. However, when compared with electrophilic aromatic substitution such as bromination (ρ = -12.1)[63b] and chlorination

(ρ = -8.1),[63a] the small negative ρ value observed in arene cyclorhodation implies only a small extent of positive charge build up. Thus, the C-H activation should not proceed through a Wheland intermediate as proposed for the electrophilic aromatic substitution. A computational study of $[Cp^*Ir(\kappa^2\text{-OAc})]^+$ mediated *ortho*-C-H bond activation of *N,N*-dimethylbenzylamine reported by Davies and coworkers[9a] suggested that the reaction should occur *via* electrophilic activation with an involvement of intramolecular hydrogen transfer to the coordinated acetate (ambiphilic activation) in a six-membered transition state. Based on these studies, the mechanism for Rh(III)-medated C-H activation was proposed (Scheme 4.9). In the presence of CsOAc and $AgSbF_6$, chloride abstraction and ligand exchange of $[Cp^*RhCl_2]_2$ would generate $[Cp^*Rh(\kappa^1\text{-OAc})(\kappa^2\text{-OAc})]$. The κ^1-OAc ligand should dissociate to generate $[Cp^*Rh(\kappa^2\text{-OAc})]^+$ and the nitrogen-donor ligand of the oxime would then coordinate to the Rh(III) centre. With one of the acetate arm dissociated, the complex would undergo electrophilic activation with the assistance of intramolecular acetate deprotonation through a six-membered transition state resulting in the cyclorhodated complex of acetophenone *O*-methyloxime.

Scheme 4.9 Proposed Mechanism for Rh(III)-Catalyzed C-H Activation

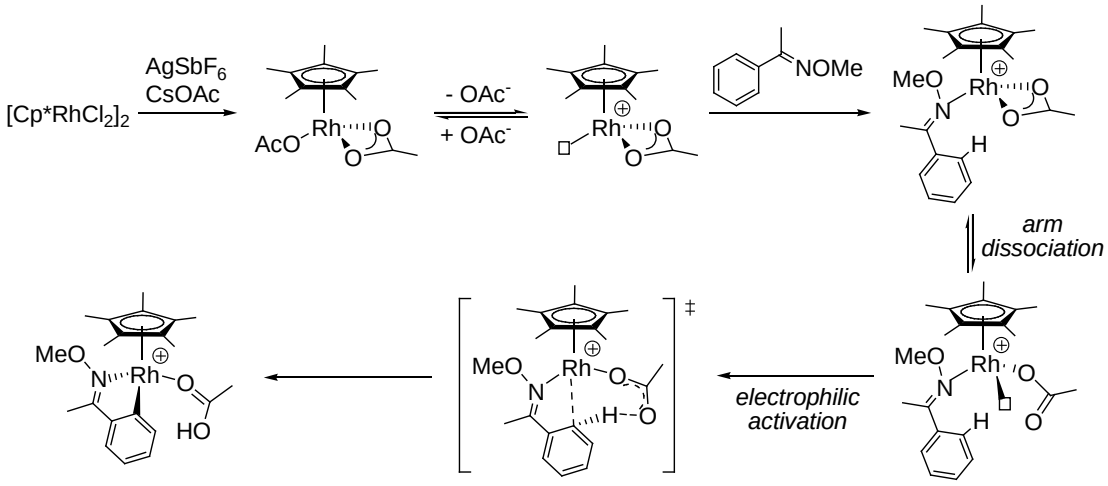

4.4.4.2 The C-N Bond Formation Step

In our earlier findings, the cyclorhodated complex of 2-phenylpyridine **11aRh** was able to couple with primary and secondary amines to give the corresponding amine products in good yields (Table 4.22, 52 — 93%). These results indicated that the Cp*Rh(III)Ar complex should be the key intermediate that it reacts with *N*-chloroamines for C-N bond formation.

Literature examples of electrophilic amination using *N*-chloroamines usually involve common reactants such as organometallic compounds such as Grignard reagents, organolithium and organozincs; similar reactions with trialkylboranes as substrates were also reported.[71,75]

Although Coleman and co-workers have extensively studied the amination of

Grignard reagents with *N*-chloroamines as reagents,[75] the mechanim of those coupling reactions remained unknown. However, the analogous mechanism for reactions of *O*-alkylhydroxyamines or *N*-arylsulfonyloxyamines with carbanion reagents were thoroughly studied by the research groups of Beak[76] and Erdick.[77] In Erdick's studies. It was found that the electrophilic aminations of aryl Grignard reagents with *O*-alkylhydroxyamines / *N*-arylsulfonyloxyamines followed second-order kinetics. The Hammett correlation between substituted aryl Grignard reagents with Hammett σ constants revealed negative ρ values indicating that the reactions are accelerated by electron-donating substituents. In addition, the activation entropy ($\Delta S^{\neq}$) for the reaction of phenylmagnesium bromide with *N*,*N*-dimethyl-*N*-sulfonyloxyamine was determined to be -135.3 ± 9.0 J mol^{-1} K^{-1} implying an association mechanism during the transition state.[77a] The data supported a S_N2-type nucleophilic substitution mechanism for the amination of carbanion equivalent reagents. More recently, a DFT calculation performed by Nakamura and co-workers also suggested a similar S_N2-type transition state for the electrophilic amination of aryl Grignard reagents with *N*-chloroamines (Scheme 4.10).[71a]

Scheme 4.10 Proposed Mechanism for Electrophilic Amination of Aryl Gragnard Reagents with *N*-Chloroamines

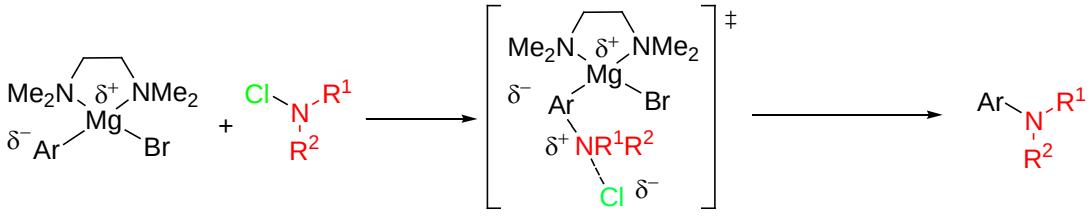

For the coupling of trialkylboranes with *N*-chloroamines, the related mechanistic studies were sparse. In general, the reactions were believed to proceed *via* an adduct formation—anionotropic migration sequence (Scheme 4.11)[71d-f, 78]

Scheme 4.11 Proposed Mechanism for Electrophilic Amination of Trialkylboranes with *N*-Chloroamines

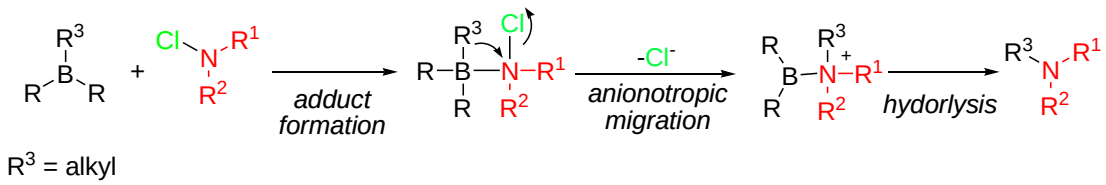

R^3 = alkyl

It is noticeable that the two mechanisms with distinct pathways are possible for the Rh(III)-catalyzed arene amination (Scheme 4.12): an outer-sphere pathway (no prior reagent coordination needed) for the S_N2-type nucleophilic substitution and an inner-sphere pathway for the anionotropic migration. For the outer-sphere pathway, the metal-carbon bond would directly "substitute" a chloride on the electrophilic

nitrogen for the C-N bond formation. However, for the inner-sphere pathway, prior coordination of *N*-chloroamine to the metal centre is required for the subsequent migration.

Scheme 4.12 Two Possible Pathways for C-N Bond Formation

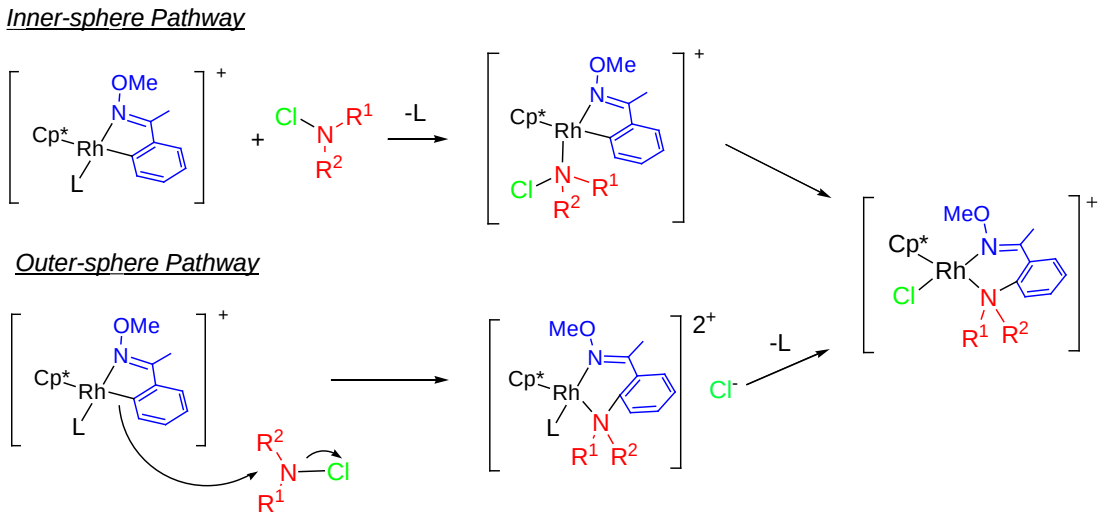

To test which pathway is more likely, we performed two stoichiometric reactions of **11aRh** with **9a** under different conditions (Scheme 4.8). In the first experiment, **11aRh** (0.1 mmol) was treated with **9a** (1.2 equiv) in the absence of a silver salt at 40 °C in THF (2 mL) for 2 h, and no **13aa** was formed. In the next reaction, **11aRh** was first reacted with 0.95 equivalent of $AgSbF_6$ for 15 min to remove the chloride from Rh(III), and then the mixture (AgCl filered) was treated with **9a** in THF at 40 °C for 2 h. In this case, **13aa** was produced in 72% yield. These results suggested that a vacant site on the Rh(III)-centre for *N*-chloroamine coordination should be necessary for

effective amination because the coordinatively saturated **11aRh** could not directly react with **9a**; the reaction between a Cp*Rh(III)Ar and the *N*-chloroamine is not likely to go through the outer-sphere pathway. In addition, it is noteworthy that no extra $AgSbF_6$ was needed for the amination with the chloride-abstracted **11aRh**. Therefore, the silver salt may only act as a chloride abstraction agent to remove chloride from Rh(III) centre for catalytic turnover.

4.4.5 Proposed Mechanism

Scheme 4.13 depicts a plausible mechanism for the amination. Firstly, $[Cp^*RhCl_2]_2$ would react with $AgSbF_6$ and CsOAc by chloride abstraction and ligand exchange to generate $[Cp^*Rh(OAc)_2]$. Dissociation of the κ^1-OAc and coordination of the oxime would result in complex ***I***. The reaction would proceed by a rate-limiting electrophilic *ortho*-C-H activation of acetophenone *O*-methyloxime to furnish arylrhodium(III) species ***II***. It should be noted that the C-H activation step could be a reversible reaction. *N*-Chloroamine coordination would result in the intermediate ***III***, and the following anionotropic migration would furnish the arylamine product, which would remain to the metal centre as complex ***IV***. Finally, protonation of the arylamine by HOAc and chloride abstraction from complex ***IV*** by $AgSbF_6$ would release the

arylamine·$HSbF_6$ salt and regenerate [Cp*Rh $(OAc)_2$].

Scheme 4.13 Proposed Mechanism

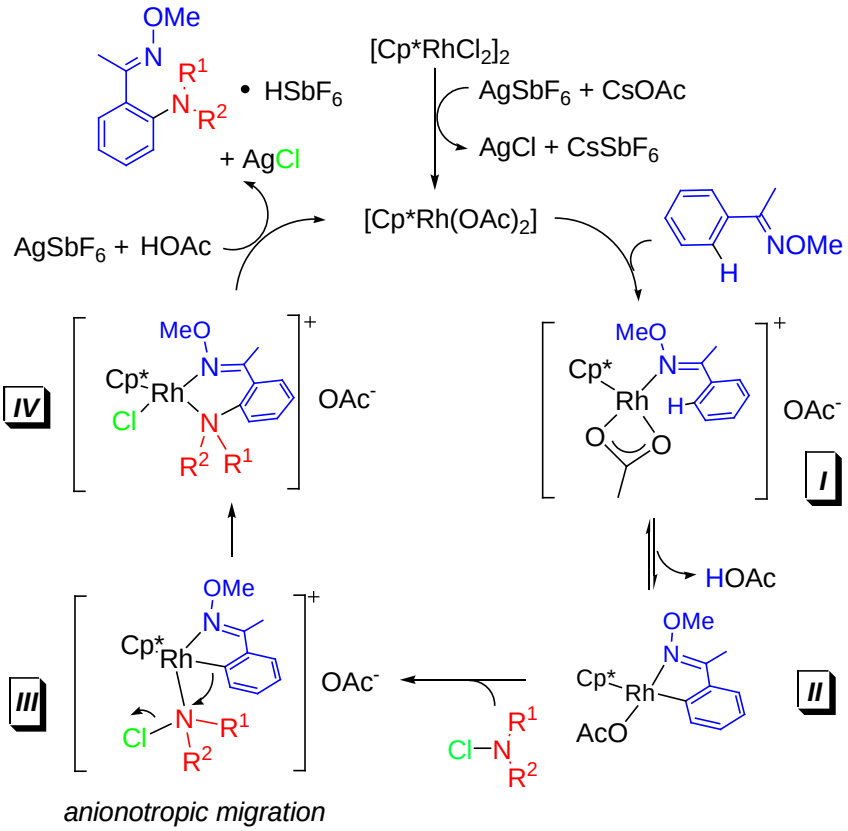

4.5 Concluding Summary

In conclusion, we have demonstrated that the dehydrogenative coupling of arene C-H bonds and amine N-H bonds can be achieved by combining C-H activation through Rh(III)-catalysis and N-H oxidation *via N*-chloroamine generation. In this work, with acetophenone *O*-methyloximes as substrates, secondary and primary *N*-chloroalkylamines were selectively coupled the arene *ortho*-C-H bonds in up to 92% yields. Acetophenone *O*-methyloximes bearing functional groups such as halogens, methoxy, -CF_3 and –NO_2 were well tolerated. *N*-chloroamines from cyclic *N*,*N*-dialkylamines such as morpholine, piperidine and *N*-Boc piperazine were coupled in excellent yields, despite moderate yields for the couplings with acyclic secondary *N*-chloroamines. With *N*-chlorosuccinimide as N-H chlorination reagent, the *N*-chloroamines generated *in situ* such as *N*-chloromorpholine, *N*-chloropiperidine and 4-Boc-*N*-chloro-piperazine coupled to give good yields of arylamine products. The *in situ* generation method also applied in primary amine coupling. Various α-branched primary amines were installed in good yields. Nonetheless, couplings with *n*-alkylamines remained a challenge, and the aminations with tertiary alkylamines were unsuccessful. Simple deprotection of the arylamine *O*-methyloximes using 6 M HCl under reflux effectively furnished 2-aminoacetophenones in 52 — 93% yields.

The results of the KIE studies hinted on a rate-limiting C-H activation step. The effective stoichiometric reactions of **11aRh** with *N*-chloroamines also suggested that cyclorhodated complexes could be the active intermediate for amination. The reaction of **11aRh** with *N*-chloroamine requires a vacant site from the Rh(III) centre of **11aRh**; the C-N bond formation step may involve an inner-sphere pathway. The reaction would be initiated by a rate-limiting reversible C-H activation to generate a cyclorhodated complex of *O*-methyloxime followed by *N*-chloroamine coordination, and the subsequent aniontropic migration would furnish the arylamine products, which would be released by protonation. Chloride abstraction by $AgSbF_6$ would regenerate the active rhodium catalyst for the next catalytic cycle.

4.6 Experimental Section

All solvents and reagents were obtained from commercial sources, and were used as received. *O*-Methyloximes,[79] 4-(4-Methoxyphenyl)acetophenone,[80] 4-*N*-Boc-piperazine,[81] $[Cp^*RhCl_2]_2$,[82] $[Cp^*Rh(OAc)_2]$[82] and [Cp*RhCl(2-phenylpyridine)][28a] (**11aRh**) were prepared according to literature. All the Rh-catalyzed amination reactions were performed in amber 8 mL-vials equipped with Teflon® liner caps under an atmosphere of nitrogen. THF was dried with metallic sodium wire and distilled before use.

Thin layer chromatography was performed on silica gel plates. Flash column chromatography was performed on 230-400 mesh silica gel (NA Chemical). GC-MS analyses were performed on a 6890N-GC (Agilent Technology) with 5973Network-MS (Agilent Technology). ^1H, ^{13}C, DEPT 135° NMR analyses were performed on a Bruker (400 MHz) spectrometer. Chemical shifts (δ) were given in ppm, and the signals were referenced with the solvent residual peak(s). NMR yields and conversions were determined with dibromomethane (0.1 mmol) as internal standard, which has a singlet signal (2H) at 4.9 ppm (in *d*-chloroform) (5.3 ppm in d_6-acetone). IR spectra were obtained by a Nicolet-380 FT-IR spectrometer. Melting points were recorded on a BÜCHI-B-545 instrument and were uncorrected. High resolution mass spectra were obtained using a VG MICROMASS Fison VG platform and with an electrospray ionization mode.

4.6.1 General Experimental Procedures and Characterizations

4.6.1.1 General Procedures for the Preparation of *N*,*N*-Dialkyl-*N*-Chloroamines

N-H amine (10 mmol) and *tert*-butanol (5 mmol) were added to a 100 mL round-bottom flask containing 40 mL of EtOAc. The mixture was cooled to 0 °C and 14% sodium hypochlorite solution (15 mmol) and AcOH (15 mmol) were added dropwise at the same time. The reaction was stirred at 0 °C for 1 h. The reaction was diluted with EtOAc (~20 mL) and washed with a saturated $NaHCO_3$ solution (10 mL × 2) and finally with brine (~10 mL). The organic layer was dried with Na_2SO_4, filtered, and concentrated by rotary evaporation (at room temperature). The EtOAc residue was removed by addition and evaporation with chloroform (~10 mL) three times. The *N*-chloroamines was isolated as a pale yellow oil (yield = ~60%) and the characterization data were consistent with literature report.[53] it was used for amination reaction without further purifications.

(**Precautions**: (1) *N*-chloroamines such as **7b** and **7f** are relatively volatile, and the solvents were removed by rotary evaporation at ~0 °C. (2) *N*-chloroamines were stored at -20 °C and they can be kept for approximately one week.)

4.6.1.2 General Procedures for Rh-Catalyzed C-H Amination of *O*-Methyloximes with *N*,*N*-Dialkyl-*N*-chloroamines

Method A:

To an amber 8 mL-vial, $[Cp^*RhCl_2]_2$ (2.5 mol %, 3.1 mg), CsOAc (30 mol %, 11.5 mg) and $AgSbF_6$ (1.5 equiv, 103 mg) were added, and the vial was sealed with a Teflon® liner cap. The vial was evacuated and back filled with N_2 for three times. Freshly distilled THF (1 mL) was added to the reaction vial, followed by the addition of *O*-methyloxime (0.2 mmol) with a 50-μL syringe. The reaction was pre-heated at 40 °C for 5 min, followed by the addition of *N*,*N*-dialkyl-*N*-chloroamine (1.2 equiv) with a 50-μL syringe in one portion. The reaction was stirred at 40 °C for 1 h. After cooling to room temperature, 30% aqueous ammonia (2 mL) and 5 mL of EtOAc were added. The organic layer was collected, and the aqueous layer was washed with EtOAc (5 mL × 2). The combined organic fraction was dried over Na_2SO_4 and then filtered through a short plug of Celite®. Solvents were removed by rotary evaporation, and the residue was re-dissolved in a small amount of dichloromethane (DCM). The dissolved mixture was subjected to flash column chromatography with silica gel as stationary phase and hexanes-EtOAc mixture as mobile phase for the separation of the amination product(s).

Method B *(Slow addition method)**:***

To an amber 8 mL-vial (vial **A**), $[Cp^*RhCl_2]_2$ (2.5 mol %, 3.1 mg), CsOAc (30 mol %, 11.5 mg) and $AgSbF_6$ (1.5 equiv, 103 mg) were added, and the vial was sealed with a Teflon® liner cap. Another empty amber 4-mL vial was also sealed with a Teflon® liner cap (vial **B**). Both vials were evacuated and back filled with N_2 for

three times. Freshly distilled THF (0.5 mL) was added to the vial **A**, followed by the addition of the *O*-methyloxime (0.2 mmol) with a 50-μL syringe. The reaction was pre-heated at 40 °C for 5 min. *N*,*N*-dialkyl-*N*-chloroamine (1.2 equiv) and THF (1 mL) were added to the vial **B**, and they were well mixed. The mixture was taken up by a 2.5-mL syringe equipped with a long needle, and it was then fitted onto a syringe-pump. The THF solution of *N*,*N*-dialkyl-*N*-chloroamine was added dropwise to the reaction (vial **A**) over 30 min, and the reaction was stirred at 40 °C for 1 h. After cooling to room temperature, 30% aqueous ammonia (2 mL) and EtOAc (5 mL) were added. The organic layer was collected, and the aqueous layer was washed with EtOAc (5 mL × 2). The combined organic fractions were dried over Na_2SO_4 and then filtered through a short plug of Celite®. Solvents were removed by rotary evaporation, and the residue was re-dissolved in a small amount of dichloromethane (DCM). The dissolved mixture was subjected to flash column chromatography with silica gel as stationary phase and hexanes-ethyl acetate mixture as mobile phase for the separation of the amination product(s).

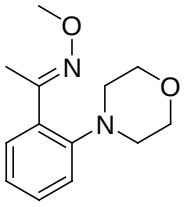

8aa was synthesized using ***Method A*** and was isolated by flash column chromatography as a light yellow oil (39.8 mg, 85% yield). R_f = 0.3 (10% EtOAc in hexanes); ^{1}H NMR ($CDCl_3$, 400 MHz): δ_H 7.35-7.28 (m, 2H), 7.06-7.02 (m, 2H), 3.96 (s, 3H), 3.81 (bt, *J* = 4.8 Hz, 4H), 2.99 (bt, *J* = 4.8 Hz, 4H), 2.25 (s, 3H); ^{13}C NMR ($CDCl_3$, 100 MHz) δ_C 158.41 (C), 150.45 (C), 132.00 (C), 130.29 (CH), 129.76 (CH), 123.02 (CH), 118.48 (CH), 67.20 (CH_2), 61.63 (CH_3), 52.21 (CH_2), 15.11

(CH_3); IR (neat, cm^{-1}): 2959, 2852, 2817, 1487, 1447, 1225, 1119, 1054, 1039, 881; HRMS m/z (ESI): calculated for $C_{13}H_{19}N_2O_2^+$: 235.1447, found: 235.1437.

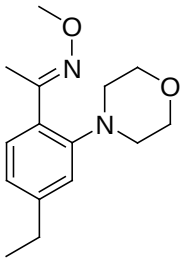

8ba was synthesized using ***Method A*** and was isolated by flash column chromatography as a colorless oil (38.3 mg, 73% yield). R_f = 0.2 (5% EtOAc in hexanes); ^{1}H NMR ($CDCl_3$, 400 MHz): δ_H 7.20 (d, *J* = 7.6 Hz, 1H), 6.89 (d, *J* = 8 Hz, 1H), 6.85 (s, 1H), 3.95 (s, 3H), 3.80 (bt, *J* = 4.4 Hz, 4H), 2.99 (bt, *J* = 4.4 Hz, 4H), 2.63 (q, *J* = 7.6 Hz, 2H), 2.24 (s, 3H), 1.23 (t, *J* = 7.6 Hz, 3H); ^{13}C NMR ($CDCl_3$, 100 MHz) δ_C 158.38 (C), 150.42 (C), 146.19 (C), 130.22 (CH), 129.26 (C), 122.38 (CH), 118.03 (CH), 67.24 (CH_2), 61.57 (CH_3), 52.24 (CH_2), 28.83 (CH_2), 15.45 (CH_3), 15.12 (CH_3); IR (neat, cm^{-1}): 2962, 2935, 2852, 2816, 1607, 1451, 1420, 1119, 1051, 880; HRMS m/z (ESI): calculated for $C_{15}H_{23}N_2O_2^+$: 263.1760, found: 263.1748.

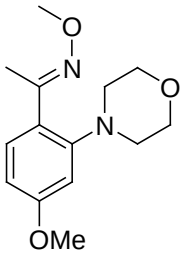

8ca was synthesized using ***Method B*** and was isolated by flash column chromatography as a colorless semi-solid (38.3 mg, 73% yield). R_f = 0.2 (10% EtOAc in hexanes); ^{1}H NMR ($CDCl_3$, 400 MHz): δ_H 7.22 (d, *J* = 8.8 Hz, 1H), 6.57-6.55 (m,

2H), 3.95 (s, 3H), 3.81-3.78 (m, 7H), 2.97 (bt, J = 4.4 Hz, 4H), 2.22 (s, 3H); ^{13}C NMR ($CDCl_3$, 100 MHz) δ_C 160.97 (C), 158.13 (C), 151.77 (C), 131.33 (CH), 124.41 (C), 106.77 (CH), 105.41 (CH), 67.12 (CH_2), 61.54 (CH_3), 55.26 (CH_3), 52.05 (CH_2), 15.11 (CH_3); IR (neat, cm^{-1}): 2958, 2852, 2817, 1611, 1599, 1499, 1453, 1264, 1199, 1171, 1118, 1048, 880; HRMS m/z (ESI): calculated for $C_{14}H_{21}N_2O_3^+$: 265.1552, found: 265.1542.

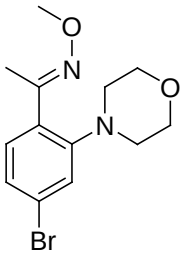

8da was synthesized using ***Method A*** and was isolated by flash column chromatography as a white solid (32.4 mg, 52% yield). R_f = 0.3 (10% EtOAc in hexanes); mp = 76.6-78.0 °C; ^{1}H NMR ($CDCl_3$, 400 MHz): δ_H 7.16-7.12 (m, 3H), 3.95 (s, 3H), 3.80 (bt, J = 4. 4Hz, 4H), 2.98 (bt, J = 4.4 Hz, 4H), 2.21 (s, 3H); ^{13}C NMR ($CDCl_3$, 100 MHz) δ_C 157.41 (C), 151.50 (C), 131.68 (CH), 130.51 (C), 125.78 (CH), 123.67 (C), 123.56 (C), 121.81 (CH), 66.97 (CH_2), 61.74 (CH_3), 51.95 (CH_2), 14.79 (CH_3); IR (KBr, cm^{-1}): 2847, 2828, 1577, 1480, 1443, 1362, 1220, 1116, 1048, 942, 879, 817; HRMS m/z (ESI): calculated for $C_{13}H_{18}N_2O_2Br^+$: 313.0552, found: 313.0544.

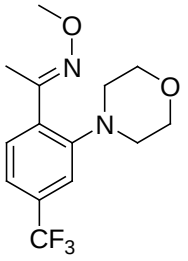

8ea was synthesized using ***Method A*** at 60 °C and was isolated by flash column chromatography as a pale yellow oil (26.0 mg, 43% yield). R_f = 0.2 (5% EtOAc in hexanes); ^{1}H NMR ($CDCl_3$, 400 MHz): δ_H 7.39 (d, *J* = 8.0 Hz, 1H), 7.29 (d, *J* = 8.0 Hz, 1H), 7.22 (s, 1H), 3.98 (s, 3H), 3.82 (bt, *J* = 4.8 Hz, 4H), 3.02 (bt, *J* = 4.8 Hz, 4H), 2.23 (s, 3H); ^{13}C NMR ($CDCl_3$, 100 MHz) δ_C 157.21 (C), 150.71 (C), 134.90 (C), 130.96 (CH), 119.46 (CH), 119.42 (C), 115.15 (CH), 66.95 (CH_2), 61.85 (CH_3), 51.90 (CH_2), 14.65 (CH_3); IR (neat, cm^{-1}): 2962, 2941, 2855, 2823, 1422, 1343, 1313, 1298, 1168, 1122, 1094, 1050, 881; HRMS m/z (ESI): calculated for $C_{14}H_{18}N_2O_2F_3^+$: 303.1320, found: 303.1311.

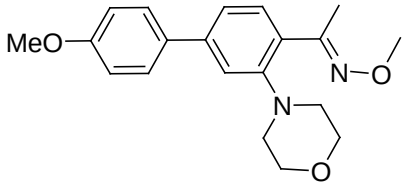

8fa was synthesized using ***Method A*** with 3 mL of THF and was isolated by flash column chromatography as a white solid (43.5 mg, 64% yield). R_f = 0.2 (10% EtOAc in hexanes); mp = 155.6-156.3 °C; ^{1}H NMR ($CDCl_3$, 400 MHz): δ_H 7.51 (d, *J* = 8.4 Hz, 2H), 7.34 (d, *J* = 8.0 Hz, 1H), 7.24-7.21 (m, 1H), 7.18 (d, *J* = 1.2 Hz, 1H), 6.98 (d, *J* = 8.8 Hz, 2H), 3.98 (s, 3H), 3.85-3.82 (m, 7H), 3.05 (bt, *J* = 4.8 Hz, 4H), 2.28 (s, 3H); ^{13}C NMR ($CDCl_3$, 100 MHz) δ_C 159.34 (C), 158.14 (C), 150.77 (C), 142.49 (C), 133.31 (C), 130.72 (CH), 130.12 (C), 128.11 (CH), 121.28 (CH), 116.94 (CH), 114.18 (CH), 67.21 (CH_2), 61.67 (CH_3), 55.31 (CH_3), 52.24 (CH_2), 15.07 (CH_3); IR

(KBr, cm^{-1}): 2962, 1604, 1492, 1252, 1185, 1118, 1054, 1041, 887, 820; HRMS m/z (ESI): calculated for $C_{20}H_{25}N_2O_3^+$: 341.1865, found: 341.1878.

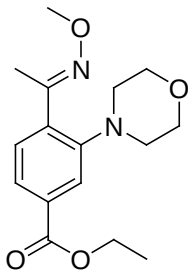

8ga was synthesized using ***Method A*** (2 mL of saturated $NaHCO_3$ was used to quench the reaction instead of 30% aq ammonia) and was isolated by flash column chromatography as a pale yellow viscous oil (43.5 mg, 71% yield). R_f = 0.2 (10% EtOAc in hexanes); ^{1}H NMR ($CDCl_3$, 400 MHz): δ_H 7.71-7.68 (m, 2H), 7.34 (d, *J* = 7.6 Hz, 1H), 4.37 (q, *J* = 7.2 Hz), 3.97 (s, 3H), 3.81 (bt, *J* = 4.4 Hz, 4H), 3.02 (bt, *J* = 4.4 Hz, 4H), 2.23 (s, 3H), 1.39 (t, *J* = 7.2 Hz, 3H); ^{13}C NMR ($CDCl_3$, 100 MHz) δ_C 166.25 (C), 157.64 (C), 150.42 (C), 136.03 (C), 131.66 (C), 130.43 (CH), 123.99 (CH), 119.50 (CH), 67.05 (CH_2), 61.80 (CH_3), 52.05 (CH_2), 14.80 (CH_3), 14.26 (CH_3); IR (neat, cm^{-1}): 2961, 2939, 2853, 2820, 1716, 1452, 1415, 1365, 1277, 1244, 1216, 1119, 1050, 1025, 881; HRMS m/z (ESI): calculated for $C_{16}H_{23}N_2O_4^+$: 307.1658, found: 307.1652.

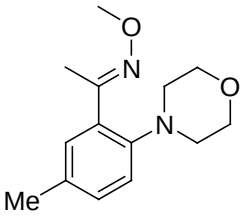

8ha was synthesized using ***Method A*** and was isolated by flash column chromatography as a white solid (41.2 mg, 83% yield). R_f = 0.25 (5% EtOAc in

hexanes); mp = 80.5-81.3 °C; ^{1}H NMR ($CDCl_3$, 400 MHz): δ_H 7.14-7.11 (m, 2H), 6.94 (d, *J* = 8.0 Hz, 1H), 3.96 (s, 3H), 3.79 (bt, *J* = 4.4 Hz, 4H), 2.94 (bt, *J* = 4.4 Hz, 4H), 2.30 (s, 3H), 2.24 (s, 3H); ^{13}C NMR ($CDCl_3$, 100 MHz) δ_C 158.57 (C), 148.16 (C), 132.65 (C), 132.02 (C), 130.73 (CH), 130.24 (CH), 118.61 (CH), 67.27 (CH_2), 61.62 (CH_3), 52.42 (CH_2), 20.46 (CH_3), 15.27 (CH_3); IR (KBr, cm^{-1}): 2967, 2851, 2823, 1499, 1448, 1227, 1113, 1053, 938, 900, 862, 815; HRMS m/z (ESI): calculated for $C_{14}H_{21}N_2O_2^+$: 249.1603, found: 249.1614.

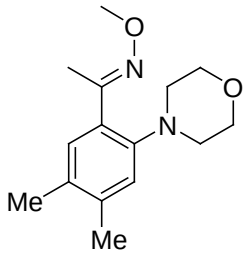

8ia was synthesized using ***Method A*** and was isolated by flash column chromatography as a white solid (41.92 mg, 80% yield). R_f = 0.35 (10% EtOAc in hexanes); mp = 77.3-78.6 °C; ^{1}H NMR ($CDCl_3$, 400 MHz): δ_H 7.06 (s, 1H), 6.81 (s, 1H), 3.96 (s, 3H), 3.79 (bt, *J* = 4.4 Hz, 4H), 2.95 (bt, *J* = 4.4 Hz, 4H), 2.25 (s, 3H), 2.24 (s, 3H), 2.20 (s, 3H); ^{13}C NMR ($CDCl_3$, 100 MHz) δ_C 158.40 (C), 148.29 (C), 138.09 (C), 131.23 (CH), 131.15 (C), 129.50 (C), 120.02 (CH), 67.29 (CH_2), 61.56 (CH_3), 52.44 (CH_2), 19.78 (CH_3), 18.74 (CH_3), 15.29 (CH_3); IR (KBr, cm^{-1}): 2958, 2849, 2824, 1443, 1372, 1251, 1202, 1110, 1048, 907, 869; HRMS m/z (ESI): calculated for $C_{15}H_{23}N_2O_2^+$: 263.1760, found: 263.1750.

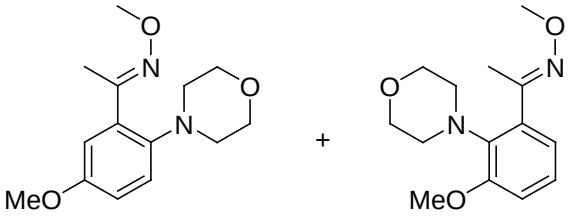

8ja and **8ja'** were synthesized using ***Method A*** and were separated from the reaction crude mixture by flash column chromatography as a colorless oil (35.9 mg, 68% total yield). R_f = 0.25 (5% EtOAc in hexanes); The two compounds are having the same R_f values and they were obtained as an inseparable mixture with a ratio of 56:44 (**8ja**:**8ja'**, NMR ratio); (*The following ^1H NMR data are not complete due to overlapping of some of the peaks*) ^{1}H NMR for **8ja** ($CDCl_3$, 400 MHz): δ_H 7.01 (d, *J* = 8.8 Hz, 1H), 3.96 (s, 3H), 3.79-3.77 (m, 7H), 2.90 (bt, *J* = 4.4 Hz, 4H), 2.25 (s, 3H); ^{1}H NMR for **8ja'** ($CDCl_3$, 400 MHz) : δ_H 7.12 (t, *J* = 8, 1H), 3.93 (s, 3H), 3.82 (s, 3H), 3.73 (bt, *J* = 4.4 Hz, 4H), 3.12 (bs, 4H), 2.20 (s, 3H).

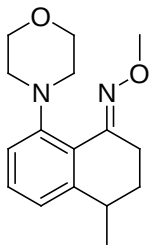

8ka was synthesized using ***Method A*** and was isolated by flash column chromatography as a pale yellow viscous oil (36.2 mg, 66% yield). R_f = 0.4 (20% EtOAc in hexanes); ^{1}H NMR ($CDCl_3$, 400 MHz): δ_H 7.21 (t, *J* = 8.0 Hz, 1H), 6.92 (d, *J* = 7.6 Hz, 1H), 6.88 (d, *J* = 7.2 Hz, 1H), 4.01 (s, 3H), 3.85 (t, *J* = 4.8 Hz, 4H), 3.09-3.00 (m, 4H), 2.84-2.75 (m, 3H), 1.84-1.76 (m, 1H), 1.60-1.53 (m, 1H), 1.23 (d, *J* = 7.2 Hz, 3H); ^{13}C NMR ($CDCl_3$, 100 MHz) δ_C 154.22 (C), 150.66 (C), 148.09 (C), 129.24 (CH), 122.85 (C), 120.64 (CH), 117.26 (CH), 67.01 (CH_2), 61.77 (CH_3),

52.56 (CH_2), 34.30 (CH_3), 27.76 (CH_2), 22.53 (CH_2), 19.43 (CH_3); IR (neat, cm^{-1}):2957, 2933, 2844, 2858, 2812, 1584, 1467, 1443, 1257, 1236, 1115, 1051, 966, 913, 866; HRMS m/z (ESI): calculated for $C_{16}H_{23}N_2O_2^+$: 275.1760, found: 275.1747.

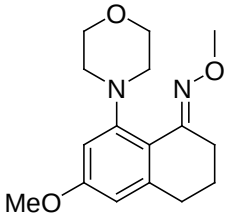

8la was synthesized using ***Method B*** at 60°C and was isolated by flash column chromatography as a pale yellow semi-solid (37.1 mg, 64% yield). R_f = 0.3 (20% EtOAc in hexanes); ^{1}H NMR ($CDCl_3$, 400 MHz): δ_H 6.45 (d, *J* = 2.4 Hz, 1H), 6.36 (d, *J* = 2.4 Hz, 1H), 3.97 (s, 3H), 3.86 (bt, *J* = 4.4 Hz, 4H), 3.79 (s, 3H), 3.04 (bt, *J* = 4.4 Hz, 4H), 2.75 (t, *J* = 6.8 Hz, 2H), 2.59 (t, *J* = 6.0 Hz, 2H), 1.73-1.67 (m, 2H); ^{13}C NMR ($CDCl_3$, 100 MHz) δ_C 160.02 (C), 154.38 (C), 152.61 (C), 145.27 (C), 116.16 (C), 106.62 (CH), 104.06 (CH), 66.96 (CH_2), 61.61 (CH_3), 55.08 (CH_3), 52.38 (CH_2), 31.88 (CH_2), 25.51 (CH_2), 20.97 (CH_2); IR (neat, cm^{-1}): 2938, 2894, 2858, 2812, 1598, 1468, 1439, 1358, 1270, 1195, 1167, 1115, 1049, 866; HRMS m/z (ESI): calculated for $C_{16}H_{23}N_2O_3^+$: 291.1709, found: 291.1700.

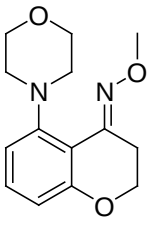

8ma was synthesized using ***Method B*** at 60 °C and was isolated by flash column chromatography as a white solid (31.4 mg, 60% yield). R_f = 0.25 (10% EtOAc in hexanes); mp = 76.8-78.8 °C; ^{1}H NMR ($CDCl_3$, 400 MHz): δ_H 7.20 (t, *J* = 8.0 Hz,

1H), 6.66-6.62 (m, 2H), 4.14 (t, J = 6.4 Hz, 2H), 4.05 (s, 3H), 3.92 (bt, J = 4.4 Hz, 4H), 3.10 (bt, J = 4.4 Hz, 4H), 2.99 (t, J = 6.4 Hz, 2H); ^{13}C NMR ($CDCl_3$, 100 MHz) δ_C 159.28 (C), 151.72 (C), 149.53 (C), 130.74 (CH), 112.00 (CH), 111.28 (CH), 111.19 (C), 66.97 (CH_2), 64.11 (CH_2), 61.86 (CH_3), 52.46 (CH_2), 25.08 (CH_2); IR (KBr, cm^{-1}): 2957, 2815, 1582, 1440, 1228, 1114, 1099, 1057, 1048, 1004, 949, 857, 800; HRMS m/z (ESI): calculated for $C_{14}H_{19}N_2O_3^+$: 263.1396, found: 263.1400.

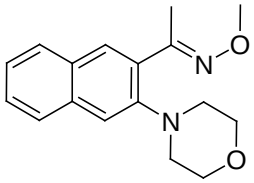

8na was synthesized using ***Method B*** and was isolated by flash column chromatography as a white solid (30.1 mg, 53% yield). R_f = 0.1 (5% EtOAc in hexanes); mp = 101.5-104.4 °C; ^{1}H NMR ($CDCl_3$, 400 MHz): δ_H 7.79-7.76 (m, 2H), 7.73 (d, J = 8.4 Hz, 1H), 7.45 (td, J = 8.0Hz, 1.2 Hz, 1H), 7.37 (td, J = 7.6 Hz, 0.8 Hz, 1H), 7.33 (s, 3H), 4.02 (s, 3H), 3.86 (bt, J = 4.4 Hz, 4H), 3.10 (bt, J = 4.4 Hz, 4H), 2.30 (s, 3H); ^{13}C NMR ($CDCl_3$, 100 MHz) δ_C 158.56 (C), 148.25 (C), 134.20 (C), 132.16 (C), 129.84 (CH), 129.70 (C), 127.97 (CH), 126.66 (CH x 2), 124.75 (CH), 115.09 (CH), 67.19 (CH_2), 61.72 (CH_3), 52.45 (CH_2), 15.55 (CH_3); IR (KBr, cm^{-1}): 2961, 2850, 2814, 1448, 1211, 1183, 1112, 1049, 874, 753; HRMS m/z (ESI): calculated for $C_{17}H_{21}N_2O_2^+$: 285.1603, found: 285.1602.

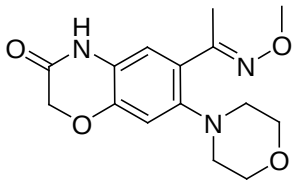

8oa was synthesized using ***Method A*** and was isolated by flash column chromatography as a white solid (53.1 mg, 87% yield). R_f = 0.45 (50% EtOAc in hexanes); mp = 229.0-230.6 °C; ^{1}H NMR ($CDCl_3$, 400 MHz): δ_H 9.18 (s, 1H), 6.80 (s, 1H), 6.66 (s, 1H), 4.58 (s, 2H), 3.94 (s, 3H), 3.78 (bt, *J* = 4.4 Hz, 4H), 2.90 (bt, *J* = 4.4 Hz, 4H), 2.21 (s, 3H); ^{13}C NMR ($CDCl_3$, 100 MHz) δ_C 165.37 (C), 157.41 (C), 147.34 (C), 144.58 (C), 126.51 (C), 121.16 (C), 117.67 (CH), 107.67 (CH), 67.15 (CH_2), 67.06 (CH_2), 61.68 (CH_3), 52.34 (CH_2), 15.20 (CH_3); IR (KBr, cm^{-1}): 2974, 1693, 1509, 1185, 1121, 1048, 872; HRMS m/z (ESI): calculated for $C_{15}H_{20}N_3O_4^+$: 306.1454, found: 306.1445.

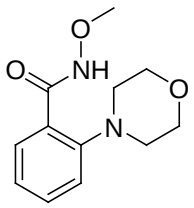

8pa was synthesized using ***Method A*** with 1.5 equiv of CsOAc (Saturated $NaHCO_3$ solution (2 mL) was used to quench the reaction instead of 30% aqueous ammonia) and was isolated by flash column chromatography as a white solid (18.9 mg, 40% yield). R_f = 0.25 (50% EtOAc in hexanes); mp = 72.6-77.0 °C; ^{1}H NMR ($CDCl_3$, 400 MHz): δ_H 11.88 (bs, 1H), 8.08 (dd, *J* = 8.0 Hz, 1.6 Hz, 1H), 7.49-7.45 (m, 1H), 7.28-7.25 (m, 1H), 7.20 (d, *J* = 8.0 Hz, 1H), 3.91-3.89 (m, 7H), 3.01 (bt, *J* = 4.4 Hz, 4H); ^{13}C NMR ($CDCl_3$, 100 MHz) δ_C 165.57 (C), 149.96 (C), 132.51 (CH), 131.38 (CH), 126.45 (C), 125.53 (CH), 120.28 (CH), 67.13 (CH_2), 64.39 (CH_3), 53.43 (CH_2);

IR (KBr, cm^{-1}): 2964, 2850, 1665, 1478, 1458, 1114, 1043, 1032, 927, 918; HRMS m/z (ESI): calculated for $C_{12}H_{17}N_2O_3^+$: 237.1239, found: 237.1230.

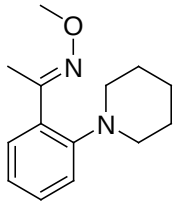

8ab was synthesized using ***Method A*** and was isolated by flash column chromatography as a colorless oil (40.4 mg, 87% yield). R_f = 0.55 (10% EtOAc in hexanes); ^{1}H NMR ($CDCl_3$, 400 MHz): δ_H 7.32-7.27 (m, 2H), 7.04-6.97 (m, 2H), 3.98 (s, 3H), 2.93 (bt, *J* = 5.2 Hz, 4H), 2.25 (s, 3H), 1.70-1.65 (m, 4H), 1.56-1.52 (m, 2H); ^{13}C NMR ($CDCl_3$, 100 MHz) δ_C 159.11 (C), 152.06 (C), 131.95 (C), 130.05 (CH), 129.54 (CH), 122.19 (CH), 118.81 (CH), 61.55 (CH_3), 53.29 (CH_2), 26.40 (CH_2), 24.22 (CH_2), 14.86 (CH_3); IR (neat, cm^{-1}): 2935, 1487, 1447, 1448, 1381, 1228, 1053, 1042, 881; HRMS m/z (ESI): calculated for $C_{14}H_{21}N_2O^+$: 233.1654, found: 233.1646.

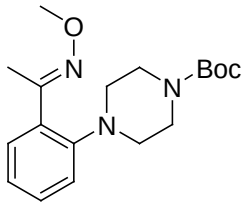

8ac was synthesized using ***Method A*** and was isolated by flash column chromatography as a white solid (42.0 mg, 63% yield). R_f = 0.3 (10% EtOAc in hexanes); mp = 74.2-80.0 °C; ^{1}H NMR ($CDCl_3$, 400 MHz): δ_H 7.33-7.26 (m, 2H), 7.06-6.99 (m, 2H), 3.96 (s, 3H), 3.52 (bt, *J* = 4.4 Hz, 4H), 2.93 (bs, 4H), 2.22 (s, 3H) 1.47 (s, 9H); ^{13}C NMR ($CDCl_3$, 100 MHz) δ_C 158.30 (C), 154.71 (C), 150.52 (C),

132.39 (C), 130.20 (CH), 129.70 (CH), 123.23 (CH), 118.92 (CH), 79.72 (C), 61.62 (CH_3), 51.83 (CH_2), 50.14 (CH_2), 28.36 (CH_3), 15.29 (CH_3); IR (KBr, cm^{-1}): 29742, 1702, 1488, 1463, 1424, 1366, 1265, 1249, 1225, 1175, 1055, 1041; HRMS m/z (ESI): calculated for $C_{18}H_{28}N_3O_3^+$: 334.2131, found: 334.2134.

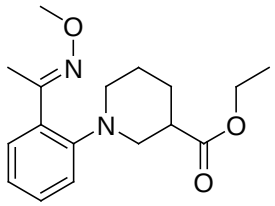

8ad was synthesized using ***Method A*** at room temperature for 15 h and was isolated by flash column chromatography as a pale yellow viscous oil (32.2 mg, 53% yield). R_f = 0.3 (5% EtOAc in hexanes); ^{1}H NMR ($CDCl_3$, 400 MHz): δ_H 7.33-7.26 (m, 2H), 7.07-7.01 (m, 2H), 4.16-4.09 (m, 2H), 3.97 (s, 3H), 3.44 (d, *J* = 11.2 Hz, 1H), 3.13 (d, *J* = 11.6 Hz, 1H), 2.89 (t, *J* = 10.4 Hz, 1H), 2.70-2.65 (m, 2H), 2.19 (s, 3H) 1.99 (bd, *J* = 9.6 Hz, 1H), 1.81-1.80 (m, 1H), 1.66-1.61 (m, 2H), 1.24 (t, *J* =7.2 Hz, 3H); ^{13}C NMR ($CDCl_3$, 100 MHz) δ_C 173.77 (C), 158.58 (C), 151.26 (C), 132.58 (C), 130.00 (CH), 129.60 (CH), 122.97 (CH), 119.36 (CH), 61.55 (CH_3), 60.32 (CH_2), 54.03 (CH_2), 53.38 (CH_2), 42.18 (CH_3), 26.62 (CH_2), 24.96 (CH_2), 15.19 (CH_3), 14.13 (CH_3); IR (neat, cm^{-1}): 2939, 1732, 1448, 1219, 1178, 1052, 1041, 884; HRMS m/z (ESI): calculated for $C_{17}H_{25}N_2O_3^+$: 305.1865, found: 305.1862.

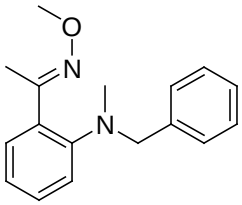

8ae was synthesized using ***Method A*** with 5% $[Cp^*RhCl_2]_2$ and was isolated by flash column chromatography as a light yellow oil (23.6 mg, 44% yield). R_f = 0.55 (10% EtOAc in hexanes); ^{1}H NMR ($CDCl_3$, 400 MHz): δ_H 7.31-7.22 (m, 7H), 7.04-7.00 (m, 2H), 4.14 (s, 2H), 3.95 (s, 3H), 2.61 (s, 3H), 2.27 (s, 3H), 2.27 (s, 3H); ^{13}C NMR ($CDCl_3$, 100 MHz) δ_C 158.65 (C), 151.12 (C), 138.10 (C), 131.99 (C), 130.15 (CH), 129.39 (CH), 128.63 (CH), 128.15 (CH), 126.99 (CH), 122.20 (CH), 119.63 (CH), 61.51 (CH_3), 60.43 (CH_2), 40.49 (CH_3), 15.53 (CH_3); IR (neat, cm^{-1}): 2936, 1489, 1450, 1363, 1051, 1042, 883; HRMS m/z (ESI): calculated for $C_{17}H_{21}N_2O^+$: 269.1654, found: 269.1652.

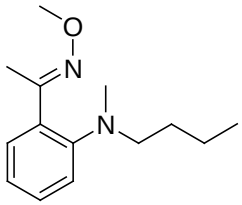

8af was synthesized using ***Method B*** with **7f** (1.2 equiv) added at a rate of 2.4 equiv / h and was isolated by flash column chromatography as a light yellow oil (16.4 mg, 35% yield). R_f = 0.4 (5% Et_2O in hexanes); ^{1}H NMR ($CDCl_3$, 400 MHz): δ_H 7.29-7.23 (m, 2H), 7.01 (d, *J* = 8.0 Hz, 1H), 6.96 (t, *J* =7.2 Hz, 1H), 3.97 (s, 3H), 2.96 (t, *J* = 8.8 Hz, 2H), 2.71 (s, 3H), 2.18 (s, 3H), 1.51-1.43 (m, 2H), 1.30-1.24 (m, 2H), 0.90 (t, *J* = 8.0 Hz, 3H); ^{13}C NMR ($CDCl_3$, 100 MHz) δ_C 159.06 (C), 151.33 (C), 131.70 (C), 130.06 (CH), 129.27 (CH), 121.60 (CH), 119.11 (CH), 61.50 (CH_3), 55.52 (CH_2), 40.91 (CH_3), 29.14 (CH_2), 20.26 (CH_2), 14.99 (CH_3), 13.84 (CH_3); IR

(neat, cm^{-1}): 2958, 2930, 1643, 1489, 1053, 1042, 881; HRMS m/z (ESI): calculated for $C_{14}H_{23}N_2O^+$: 235.1810, found: 235.1803.

4.6.1.3 General Procedures for Rh-Catalyzed C-H Amination of *O*-Methyloximes with Primary *N*-Chloroamines

To an amber 8 mL-vial (vial **A**), $[Cp^*RhCl_2]_2$ (5 mol %, 6.2 mg), CsOAc (1.3 equiv, 49.7 mg) and $AgSbF_6$ (1.5 equiv, 103 mg) were added, and the vial was sealed with a Teflon® liner cap. To another amber 4-mL vial (vial **B**), *N*-chlorosuccinimide (2.2 equiv, 58.7 mg) was added, and the vial was sealed with a Teflon® liner cap. Both vials were evacuated and filled back with N_2 for three times. Freshly distilled THF (1 mL) was added to the vial **A**, followed by the addition of the *O*-methyloxime (0.2 mmol) with a 50-μL syringe. Vial **A** was pre-heated at 40°C. THF (1 mL) and primary amine (2.2 equiv) were added to the vial **B**, and they were mixed and stirred for 10 min. The mixture in Vial **B** was taken up by a 2.5-mL syringe equipped with a long needle (L 6 in, size 22 gauge), and it was then fitted onto a syringe-pump. The THF solution of *N*-chloroamine was added dropwise to the reaction (vial **A**) over 1 h in dark, and the reaction was stirred at 40 °C for a total of 2 h. After cooling to room temperature, the reaction was quenched by 30% aqueous ammonia (2 mL) and was extracted by EtOAc (5 mL). The organic layer was collected, and the aqueous layer was washed with EtOAc (5 mL × 2). The combined organic fractions were dried over Na_2SO_4 and then filtered through a short plug of Celite®. Solvents were removed by rotary evaporation, and the residue was re-dissolved in a small amount of dichloromethane (DCM). The dissolved mixture was subjected to flash column

chromatography / preparative TLC with silica gel as stationary phase and hexanes-DCM mixture as mobile phase for the separation of the amination product(s).

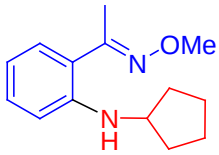

10aa was synthesized using the general procedure and it was isolated as a yellowish green oil (37.1 mg, 80%) by flash column chromatography followed by high vacuum evacuation overnight (0.5 mmHg, ~18 h, for removal of **6a** residue). R_f = 0.2 (2% Et_2O in hexanes); ^1H NMR ($CDCl_3$, 400 MHz): δ_H 7.87 (bs, 1H), 7.38 (dd, *J* = 8.0 Hz, 1.2 Hz, 1H), 7.20 (td, *J* = 8.0 Hz, 1.6 Hz, 1H), 6.72 (d, *J* = 8.4 Hz, 1H), 6.64 (t, *J* = 8.0 Hz, 1H), 3.98 (s, 3H), 3.90 (bs, 1H), 2.30 (s, 3H), 2.04-2.01 (m, 2H), 1.79-1.77 (m, 2H), 1.68-1.60 (m, 4H); ^{13}C NMR ($CDCl_3$, 100 MHz) δ_C 157.48 (C), 146.72 (C), 129.70 (CH), 128.96 (CH), 116.87 (C), 114.40 (CH), 111.55 (CH), 61.74 (CH_3), 53.99 (CH), 33.46 (CH_2), 23.99 (CH_2), 12.76 (CH_3); IR (thin-film, cm^{-1}): 3293, 2955, 2869, 1734, 1604, 1568, 1521, 1453, 1337, 1272, 1184, 1052, 900, 743; HRMS m/z (ESI): calculated for $C_{14}H_{21}N_2O^+$: 233.1654, found: 233.1647.

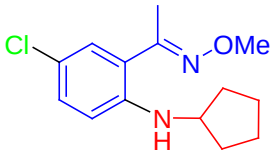

10ua was synthesized using the general procedure and it was isolated as a lightly brown oil (23.4 mg, 44%) by flash column chromatography followed by high vacuum evacuation overnight (0.5 mmHg, ~18 h, for removal of **6m** residue) R_f = 0.3 (2% Et_2O in hexanes); ^1H NMR ($CDCl_3$, 400 MHz): δ_H 7.88 (bs, 1H), 7.31 (d, *J* = 2.4 Hz,

1H), 7.12 (dd, *J* = 9.2 Hz, 2.4 Hz, 1H), 6.64 (d, *J* = 9.4 Hz, 1H), 3.97 (s, 3H), 3.84 (bs, 1H), 2.25 (s, 3H), 2.03-1.98 (m, 2H), 1.76-1.74 (m, 2H), 1.67-1.64 (m, 2H), 1.60-1.56 (m, 2H); ^{13}C NMR ($CDCl_3$, 100 MHz) δ_C 156.54 (C), 145.25 (C), 129.32 (CH), 128.41 (CH), 119.04 (C), 118.01 (C), 112.76 (CH), 61.88 (CH_3), 54.13 (CH), 33.33 (CH_2), 23.95 (CH_2), 12.67 (CH_3); IR (thin-film, cm^{-1}): 3290, 2956, 2869, 1735, 1600, 1566, 1512, 1449, 1409, 1325, 1262, 1183, 1040, 913, 804; HRMS m/z (ESI): calculated for $C_{14}H_{20}N_2OCl^+$: 267.1264, found: 267.1266.

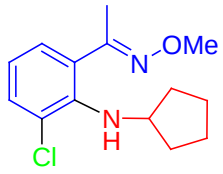

10ua' was isolated as a light brown oil (22% yield based on Table 4.10, entry 4) (*chlorination side product)* by flash column chromatography. R_f = 0.1 (2% Et_2O in hexanes); ^{1}H NMR ($CDCl_3$, 400 MHz): δ_H 7.29 (dd, *J* = 8.0 Hz, 1.2 Hz, 1H), 7.15 (dd, *J* = 7.6 Hz, 1.2 Hz, 1H), 6.82 (t, *J* = 8.0 Hz, 1H), ~5.3 (bs, 1H), 3.98 (s, 3H), 3.89-3.84 (m, 1H), 2.20 (s, 3H), 1.80-1.77 (m, 2H), 1.70-1.66 (m, 2H), 1.58-1.54 (m, 2H), 1.46-1.44 (m, 2H); ^{13}C NMR ($CDCl_3$, 100 MHz) δ_C 156.75 (C), 143.18 (C), 130.04 (CH), 128.66 (C), 128.38 (CH), 125.70 (C), 120.43 (CH), 61.82 (CH_3), 58.96 (CH), 33.39 (CH_2), 23.36 (CH_2), 14.48 (CH_3); IR (thin-film, cm^{-1}): 3360, 3313, 2957, 2870, 1592, 1453, 1439, 1253, 1079, 1048, 891, 779, 743; HRMS m/z (ESI): calculated for $C_{14}H_{20}N_2OCl^+$: 267.1264, found: 267.1262.

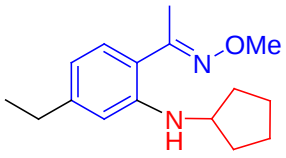

10ba was synthesized using the general procedure and it was isolated as a pale yellow oil (33.3 mg, 64% yield) by flash column chromatography. R_f = 0.15 (10% DCM in hexanes); ^{1}H NMR ($CDCl_3$, 400 MHz): δ_H 7.88(bs, 1H), 7.30 (d, *J* = 8.0 Hz, 1H), 6.56-6.51 (bm, 2H), 3.95 (s, 3H), 3.93-3.89 (m, 1H), 2.60 (q, *J* = 7.6 Hz, 2H), 2.27 (s, 3H), 2.04-2.00 (m, 2H), 1.78-1.76 (m, 2H), 1.67-1.64 (m, 4H), 1.24 (t, *J* = 7.6 Hz, 3H); ^{13}C NMR ($CDCl_3$, 100 MHz) δ_C 157.38 (C), 146.19 (C), 128.99 (CH), 114.27 (C), 110.91 (C), 61.68 (CH_3), 54.07 (CH), 33.39 (CH_2), 29.03 (CH_2), 23.95 (CH_2), 15.32 (CH_3), 12.67 (CH_3) (2 CH signals missing); IR (thin-film, cm^{-1}): 3292, 2959, 2869, 1612, 1596, 1562, 1438, 1274, 1062, 1045, 894; HRMS m/z (ESI): calculated for $C_{16}H_{25}N_2O^+$: 261.1955, found: 261.1967.

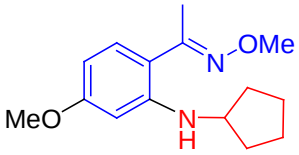

10ca was synthesized using the general procedure and it was isolated as a brown oil (18.8 mg, 36% yield) by flash column chromatography. R_f = 0.2 (20% DCM in hexanes); ^{1}H NMR ($CDCl_3$, 400 MHz): δ_H 8.10 (bs, 1H), 7.30 (d, *J* = 8.4 Hz, 1H), 6.23-6.21 (m, 2H), 3.94 (s, 3H), 3.84-3.81 (m, 4H), 2.25 (s, 3H), 2.04-2.00 (m, 2H), 1.78-1.77 (m, 2H), 1.67-1.58 (m, 4H); ^{13}C NMR ($CDCl_3$, 100 MHz) δ_C 160.95 (C), 157.18 (C), 130.36 (CH), 61.61 (CH_3), 55.01 (CH_3), 54.28 (CH), 33.24 (CH_2), 23.98 (CH_2), 12.62 (CH_3) (2 CH, 2 C signals missing); IR (thin-film, cm^{-1}): 3285, 2954,

2869, 1613, 1567, 1528, 1463, 1288, 1222, 1050, 894; HRMS m/z (ESI): calculated for $C_{15}H_{23}N_2O_2^+$: 263.1760, found: 263.1748.

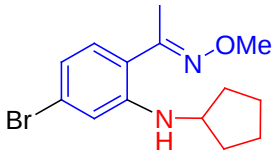

10da was synthesized using the general procedure with 1.0 equiv of CsOAc and it was isolated as a light brown oil (48.5 mg, 78% yield) (with 1.3 equiv of CsOAc, ^{1}H NMR yield = 52%) by preparative TLC. R_f = 0.4 (10% DCM in hexanes); ^{1}H NMR ($CDCl_3$, 400 MHz): δ_H 8.08 (bs, 1H), 7.19 (d, *J* = 8.4 Hz, 1H), 6.83 (d, *J* = 2 Hz, 1H), 6.72 (dd, *J* = 8.4 Hz, 1.6 Hz, 1H), 3.96 (s, 3H), 3.83-3.82 (bm, 1H), 2.24 (s, 3H), 2.05-2.00 (m, 2H), 1.76-1.75 (m, 2H), 1.68-1.65 (m, 2H), 1.61-1.56 (m, 2H); ^{13}C NMR ($CDCl_3$, 100 MHz) δ_C 156.93 (C), 147.57 (C), 130.19 (CH), 124.15 (C), 117.34 (CH), 115.80 (C), 114.13 (CH), 61.84 (CH_3), 54.05 (CH), 33.25 (CH_2), 23.91 (CH_2), 12.66 (CH_3); IR (thin-film, cm^{-1}): 3275, 2956, 2869, 1597, 1563, 1509, 1425, 1273, 1061, 1044, 905; HRMS m/z (ESI): calculated for $C_{14}H_{20}N_2OBr^+$: 311.0759, found: 311.0763.

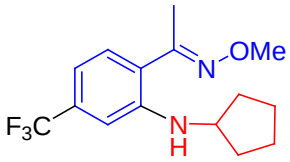

10ea was synthesized using the general procedure with 1.0 equiv of CsOAc and it was isolated as a pale yellow oil (48.6 mg, 81% yield) (with 1.3 equiv of CsOAc, ^{1}H NMR yield = 28%) by preparative TLC. R_f = 0.4 (10% DCM in hexanes); ^{1}H NMR ($CDCl_3$, 400 MHz): δ_H 8.10 (bs, 1H), 7.44 (d, *J* = 8.4 Hz, 1H), 6.90 (s, 1H), 6.84 (d, *J* = 8.0

Hz, 1H), 4.00 (s, 3H), 3.91 (bs, 1H), 2.29 (s, 3H), 2.08-2.03 (m, 2H), 1.78-1.69 (m, 4H), 1.62-1.58 (m, 2H); ^{13}C NMR ($CDCl_3$, 100 MHz) δ_C 156.72 (C), 146.62 (C), 131.72, 131.41, 131.09, 130.77 (q, J = 31 Hz, C), 129.26 (CH), 128.35, 125.61, 122.90, 120.24 (q, J = 266 Hz, C), 110.54, 110.50, 110.46, 110.43 (q, J = 4 Hz, CH), 107.93, 107.89, 107,85, 107.81 (q, J = 4 Hz, CH), 61.94 (CH_3), 53.97 (CH), 33.28 (CH_2), 23.91 (CH_2), 12.75 (CH_3); IR (thin-film, cm^{-1}): 3285, 2959, 2872, 1619, 1600, 1569, 1535, 1444, 1338, 1278, 1168, 1123, 1097, 1060, 1045, 923, 853, 803; HRMS m/z (ESI): calculated for $C_{15}H_{20}N_2OF_3^+$: 301.1528, found: 301.1540.

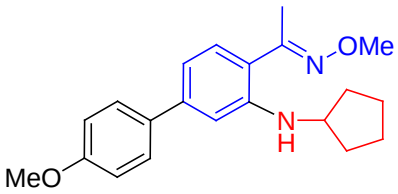

10fa was synthesized using the general procedure and it was isolated as a light brown solid (33.1 mg, 49% yield) by flash column chromatography. R_f = 0.3 (30% DCM in hexanes); mp = 73.2-75.0 °C; ^{1}H NMR ($CDCl_3$, 400 MHz): δ_H 8.01 (bs, 1H), 7.56 (d, J = 8.8 Hz, 2H), 7.43 (d, J = 8.0 Hz, 1H), 6.98 (d, J = 8.4 Hz, 2H), 6.90-6.83 (bm, 2H), 3.99 (m, 4H), 3.86 (s, 3H), 2.31 (s, 3H), 2.07-2.06 (bm, 2H), 1.80 (bs, 2H), 1.67 (bs, 4H); ^{13}C NMR ($CDCl_3$, 100 MHz) δ_C 159.23 (C), 157.28 (C), 142.01 (C), 133.90 (C), 129.38 (CH), 128.11 (2CH), 114.04 (2CH), 113.48 (C), 109.73 (C), 61.78 (CH_3), 55.29 (CH_3), 54.13 (CH), 33.41 (CH_2), 24.01 (CH_2), 12.70 (CH_3) (2 CH signals missing); IR (KBr, cm^{-1}): 3268, 2952, 2933, 1594, 1556, 1506, 1436, 1285, 1246, 1179, 1049, 1027, 912, 827; HRMS m/z (ESI): calculated for $C_{21}H_{27}N_2O_2^+$: 339.2073, found: 339.2074.

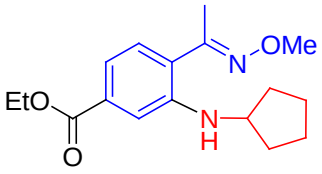

10ga was synthesized using the general procedure with 1.0 equiv of CsOAc and it was isolated as a brown oil (49.2 mg, 81% yield) (with 1.3 equiv of CsOAc, ^{1}H NMR yield = 43%) by preparative TLC. R_f = 0.55 (50% DCM in hexane); ^{1}H NMR ($CDCl_3$, 400 MHz): δ_H 7.95 (bs, 1H), 7.41-7.39 (m, 2H), 7.257 (dd, *J* = 8.4 Hz, 1.2 Hz, 1H), 4.36 (q, *J* = 7.2 Hz, 2H), 3.99-3.97 (m, 4H), 2.23 (s, 3H), 2.09-2.05 (m, 2H), 1.77-1.75 (m, 2H), 1.69-1.65 (m, 2H), 1.60-1.56 (m, 2H), 1.39 (t, *J* = 7.2 Hz, 3H); ^{13}C NMR ($CDCl_3$, 100 MHz) δ_C 166.86 (C), 156.97 (C), 146.43 (C), 131.05 (C), 128.77 (CH), 120.47 (C), 115.20 (CH), 112.65 (CH), 61.91 (CH_3), 60.75 (CH_2), 54.08 (CH), 33.39 (CH_2), 23.96 (CH_2), 14.24 (CH_3), 12.76 (CH_3); IR (thin-film, cm^{-1}): 3294, 2957, 2870, 1716, 1597, 1561, 1435, 1306, 1248, 1111, 1045, 901, 763; HRMS m/z (ESI): calculated for $C_{17}H_{25}N_2O_3^+$: 305.1865, found: 305.1852.

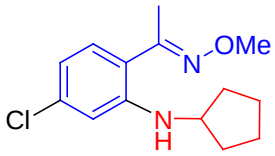

10qa was synthesized using the general procedure with 1.0 equiv of CsOAc and it was isolated as a light brown oil (40.5 mg, 76% yield) (with 1.3 equiv of CsOAc, ^{1}H NMR yield = 48%) by preparative TLC. R_f = 0.4 (10% DCM in hexanes); ^{1}H NMR ($CDCl_3$, 400 MHz): δ_H 8.13 (bs, 1H), 7.27 (d, *J* = 8.4 Hz, 1H), 6.69 (d, *J* = 1.6 Hz, 1H), 6.59 (dd, *J* = 8.4 Hz, 2 Hz, 1H), 3.96 (s, 3H), 3.86-3.82 (bm, 1H), 2.25 (s, 3H), 2.06-1.99 (m, 2H), 1.78-1.75 (m, 2H), 1.68-1.64 (m, 2H) 1.62-1.59 (m, 2H); ^{13}C NMR ($CDCl_3$, 100 MHz) δ_C 156.85 (C), 147.45 (C), 135.62 (C), 130.02 (CH), 115.48

(C), 114.50 (CH), 111.22 (CH), 61.82 (CH_3), 54.11 (CH), 33.24 (CH_2), 23.91 (CH_2), 12.69 (CH_3); IR (thin-film, cm^{-1}): 3289, 2957, 2869, 1600, 1512, 1409, 1325, 1262, 1183, 1046, 913, 804; HRMS m/z (ESI): calculated for $C_{14}H_{20}N_2OCl^+$: 267.1264, found: 267.1257.

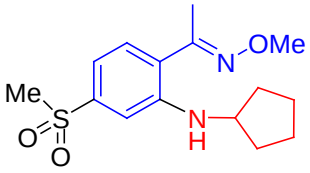

10ra was synthesized using the general procedure with 1.0 equiv of CsOAc and it was isolated as a yellow oil (47.7 mg, 77% yield) (with 1.3 equiv of CsOAc, ^1H NMR yield = 32%) by preparative TLC (30% EtOAc in hexane) followed by flash column chromatography (30% hexane in DCM). R_f = 0.5 (10% hexane in DCM); ^1H NMR ($CDCl_3$, 400 MHz): δ_H 8.22 (bs, 1H), 7.50 (d, J = 8.4 Hz, 1H), 7.20 (s, 1H), 7.10 (d, J = 8.0 Hz, 1H), 4.00 (s, 3H), 3.94-3.92 (bm, 1H), 3.04 (s, 3H), 2.29 (s, 3H), 2.09-2.04 (m, 2H), 1.78-1.68 (m, 4H), 1.59-1.55 (m, 2H); ^{13}C NMR ($CDCl_3$, 100 MHz) δ_C 156.48 (C), 146.91 (C), 140.75 (C), 129.79 (CH), 120.86 (C), 112.05 (CH), 109.59 (CH), 62.11 (CH_3), 54.07 (CH), 44.31 (CH_3), 33.21 (CH_2), 23.85 (CH_2), 12.88 (CH_3); IR (thin-film, cm^{-1}): 3280, 2957, 2870, 1597, 1561, 1517, 1429, 1310, 1279, 1154, 1058, 1043, 899, 760, 546; HRMS m/z (ESI): calculated for $C_{15}H_{23}N_2O_3S^+$: 311.1429, found: 311.1417.

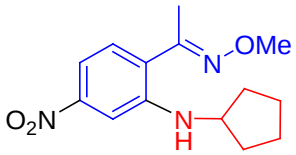

10sa was synthesized using the general procedure with 1.0 equiv of CsOAc and it was isolated as an orange solid (50.9 mg, 92% yield) (with 1.3 equiv of CsOAc, ^{1}H NMR yield = 23%) by flash column chromatography. R_f = 0.25 (20% DCM in hexanes); mp = 99.0-100.5 °C; ^{1}H NMR ($CDCl_3$, 400 MHz): δ_H 8.25 (bs, 1H), 7.51 (d, *J* = 2.0 Hz, 1H), 7.47 (d, *J* = 8.8 Hz, 1H), 7.41 (dd, *J* = 8.8 Hz, 2.0 Hz, 1H), 4.01 (s, 3H), 3.95-3.92 (bm, 1H), 2.30 (s, 3H), 2.12-2.07 (m, 2H), 1.80-1.68 (m, 4H), 1.62-1.59 (m, 2H); ^{13}C NMR ($CDCl_3$, 100 MHz) δ_C 156.38 (C), 148.45 (C), 147.01 (C), 129.47 (CH), 121.83 (C), 108.71 (CH), 105.79 (CH), 61.18 (CH_3), 54.19 (CH), 33.20 (CH_2), 23.91 (CH_2), 12.92 (CH_3); IR (KBr, cm^{-1}): 3256, 2956, 2934, 1621, 1527, 1505, 1434, 1342, 1284, 1056, 1042, 907; HRMS m/z (ESI): calculated for $C_{14}H_{20}N_3O_3^+$: 278.1505, found: 278.1495.

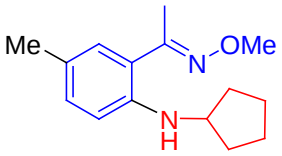

10ha was synthesized using the general procedure and it was isolated as a light brown oil (27.0 mg, 55% yield) by flash column chromatography followed by high vacuum evacuation overnight (0.5 mmHg, ~18 h, for removal of **1k** residue). R_f = 0.2 (2% Et_2O in hexanes); ^{1}H NMR ($CDCl_3$, 400 MHz): δ_H 7.58 (bs, 1H), 7.17 (s, 1H), 7.02 (d, *J* = 8.0 Hz, 1H), 6.68 (bs, 1H), 3.96 (s, 3H), 3.86-3.85 (bm, 1H), 2.27 (s, 3H), 2.26 (s, 3H), 2.02-1.96 (m, 2H), 1.77-1.74 (bm, 2H), 1.66-1.60 (m, 4H); ^{13}C NMR ($CDCl_3$, 100 MHz) δ_C 157.29 (C), 130.45 (CH), 129.27 (CH), 112.59 (bs, C), 61.76 (CH_3),

54.48 (bs, CH), 33.25 (CH_2), 23.95 (CH_2), 20.42 (CH_3), 12.87 (CH_3) (1 CH, 2 C signals missing); IR (thin-film, cm^{-1}): 3300, 2954, 2868, 1620, 1521, 1325, 1273, 1182, 1047, 925, 879, 805; HRMS m/z (ESI): calculated for $C_{15}H_{23}N_2O^+$: 247.1810, found: 247.1800.

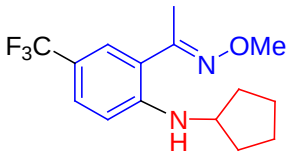

10ta was synthesized using the general procedure with 1.0 equiv of CsOAc and it was isolated as a light brown oil (46.8 mg, 78% yield) (with 1.3 equiv of CsOAc, ^1H NMR yield = 46%) by preparative TLC. R_f = 0.45 (10% DCM in hexanes); ^1H NMR ($CDCl_3$, 400 MHz): δ_H 8.37 (bs, 1H), 7.59 (s, 1H), 7.39 (d, *J* = 8.8 Hz, 1H), 6.73 (d, *J* = 8.8 Hz, 1H), 3.99 (s, 3H), 3.92-3.91 (bm, 1H), 2.31 (s, 3H), 2.06-2.02 (m, 2H), 1.78-1.76 (m, 2H), 1.70-1.66 (m, 2H), 1.64-1.59 (m, 2H); ^{13}C NMR ($CDCl_3$, 100 MHz) δ_C 156.82 (C), 148.81 (C), 129.08, ~126.4, 123.71, 121.03 (q, *J* = 268 Hz, C), 126.49-126.37 (m, CH), 126.23, 126.19, 126.15, 126.11 (q, *J* = 4 Hz, CH), 116.37, 116.06, 115.73, 115.40 (q, *J* = 33 Hz, C), 116.06 (C), 111.01 (CH), 61.89 (CH_3), 53.96 (CH), 33.28 (CH_2), 23.91 (CH_2), 12.52 (CH_3); IR (thin-film, cm^{-1}): 3273, 2959, 2873, 1619, 1599, 1535, 1337, 1317, 1269, 1108, 1047, 898, 814, 647; HRMS m/z (ESI): calculated for $C_{15}H_{20}N_2OF_3^+$: 301.1528, found: 301.1519.

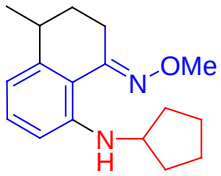

10ka was synthesized using the general procedure and it was isolated as a greenish brown semi-solid (32.6 mg, 60% yield) by preparative TLC. R_f = 0.6 (20% DCM in hexanes); ^{1}H NMR ($CDCl_3$, 400 MHz): δ_H 8.37 (bs, 1H), 7.12 (t, *J* = 8.0 Hz, 1H), 6.59 (d, *J* = 8.0 Hz, 1H), 6.48 (d, *J* = 8 Hz, 1H), 3.97 (s, 3H), 3.89 (bs, 1H), 2.91-2,80 (m, 3H), 2.04-2.01 (m, 2H), 1.87-1.82 (m, 1H), 1.78 (bs, 2H), 1.67-1.62 (m, 5H), 1.24 (d, *J* = 7.2 Hz, 3H); ^{13}C NMR ($CDCl_3$, 100 MHz) δ_C 158.26 (C), 147.39 (C), 146.63 (C), 129.68 (CH), 113.81 (CH), 110.93 (CH), 109.44 (C), 61.75 (CH_3), 54.11 (CH), 34.06 (CH), 33.51 (CH_2), 33.48 (CH_3), 27.53 (CH_2), 24.02 (CH_2), 21.63 (CH_2), 20.67 (CH_3); IR (thin-film, cm^{-1}): 3277, 2956, 2866, 1593, 1519, 1464, 1335, 1181, 1053, 900, 790, 741; HRMS m/z (ESI): calculated for $C_{17}H_{25}N_2O^+$: 273.1967, found: 273.1955.

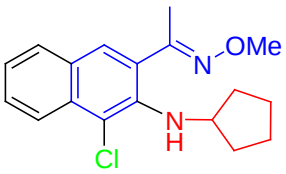

10na-3Cl was synthesized using the general procedure with 1.0 equiv of CsOAc and it was isolated as a brown oil (27.2 mg, 43% yield) by preparative TLC. R_f = 0.2 (20% DCM in hexanes); ^{1}H NMR ($CDCl_3$, 400 MHz): δ_H 8.10 (d, *J* = 8.4 Hz, 1H), 7.74 (d, *J* = 8.0 Hz, 1H), 7.68 (s, 1H), 7.53 (t, *J* = 7.6 Hz, 1H), 7.35 (t, *J* = 7.6 Hz, 1H), 4.81 (bs, 1H), 4.03 (s, 3H), 3.90-3.85 (m, 1H), 2.28 (s, 3H), 1.84-1.78 (m, 2H), 1.74-1.71 (m, 2H), 1.59-1.57 (m, 2H), 1.49-1.45 (m, 2H); ^{13}C NMR ($CDCl_3$, 100 MHz) δ_C 157.23 (C), 140.87 (C), 131.41 (C), 129.70 (C), 128.89 (C), 128.39 (CH),

128.34 (CH), 127.72 (CH), 124.11 (CH), 123.15 (CH), 119.71 (C), 61.88 (CH_3), 59.32 (CH), 33.46 (CH_2), 23.44 (CH_2), 14.73 (CH_3); IR (thin-film, cm^{-1}): 3358, 2858, 2870, 1625, 1473, 1438, 1047, 884, 747; HRMS m/z (ESI): calculated for $C_{18}H_{22}N_2OCl^+$: 317.1421, found: 317.1420.

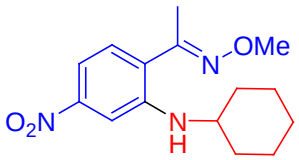

10sb was synthesized using the general procedure with 1.1 equiv of CsOAc and it was isolated as an orange solid (50.0 mg, 86% yield) by preparative TLC. R_f = 0.35 (30% DCM in hexanes); mp = 98.2-99.0 °C; ^{1}H NMR ($CDCl_3$, 400 MHz): δ_H 8.20 (bs, 1H), 7.48-7.45 (m, 2H), 7.38 (dd, *J* = 8.8 Hz, 2.0 Hz, 1H), 4.02 (s, 3H), 3.50 (bs, 1H), 2.30 (s, 3H), 2.06-2.03 (m, 2H), 1.78-1.74 (m, 2H), 1.66-1.62 (m, 1H), 1.52-1.46 (m, 2H), 1.44-1.35 (m, 3H); ^{13}C NMR ($CDCl_3$, 100 MHz) δ_C 156.44 (C), 148.55 (C), 146.51 (C), 129.66 (CH), 121.80 (C), 108.52 (CH), 105.46 (CH), 62.22 (CH_3), 50.81 (CH), 32.42 (CH_2), 25.77 (CH_2), 24.25 (CH_2), 13.01 (CH_3); IR (KBr, cm^{-1}): 3269, 2930, 2856, 1621, 1531, 1510, 1342, 1283, 1058, 1043, 903, 857; HRMS m/z (ESI): calculated for $C_{15}H_{22}N_3O_3^+$: 292.1661, found: 292.1653.

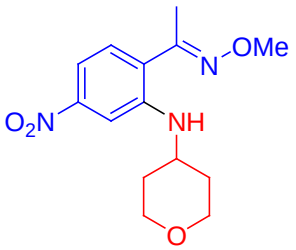

10sc was synthesized using the general procedure with 1.1 equiv of CsOAc and it was isolated as an orange solid (38.7 mg, 66% yield) by flash column chromatography. R_f

= 0.2 (50% DCM in hexanes); mp = 151.5-153.5 °C ^{1}H NMR ($CDCl_3$, 400 MHz): δ_H 8.29 (bd, *J* = 6.0 Hz, 1H), 7.50-7.48 (m, 2H), 7.43 (d, *J* = 8.4 Hz, 1H), 4.02-3.97 (m, 5H), 3.73-3.72 (bm, 1H), 3.62 (t, *J* = 10 Hz, 2H), 2.31 (s, 3H), 2.12-2.09 (m, 2H), 1.65-1.57 (m, 2H); ^{13}C NMR ($CDCl_3$, 100 MHz) δ_C 156.47 (C), 148.51 (C), 146.20 (C), 129.80 (CH), 122.13 (C), 109.14 (CH), 105.23 (CH), 66.20 (CH_2), 62.28 (CH), 48.08 (CH_3), 32.65 (CH_2), 13.03 (CH_3); IR (KBr, cm^{-1}): 3225, 2937, 2861, 1531, 1504, 1434, 1340, 1135, 1035, 909, 859, 824; HRMS m/z (ESI): calculated for $C_{14}H_{19}N_3O_4^+$: 294.1454, found: 294.1455.

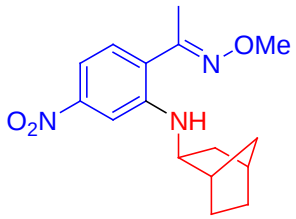

10sd was synthesized using the general procedure with 1.1 equiv of CsOAc and it was isolated as an orange gum (45.6 mg, 75% yield) by preparative TLC. R_f = 0.3 (20% DCM in hexanes); ^{1}H NMR ($CDCl_3$, 400 MHz): δ_H 8.18 (bd, *J* = 4.0 Hz, 1H), 7.47-7.39 (m, 3H), 4.01 (s, 3H), 3.39 (bs, 1H), 2.35-1.96 (m, 5H), 1.93-1.91 (m, 1H), 1.64-1.52 (m, 3H), 1.32-1.25 (m, 4H); ^{13}C NMR ($CDCl_3$, 100 MHz) δ_C 156.36 (C), 148.44 (C), 146.59 (C), 129.44 (CH), 121.76 (C), 108.65 (CH), 105.61 (CH), 62.20 (CH), 56.15 (CH), 41.49 (CH_3), 40.90 (CH_2), 35.74 (CH), 35.68 (CH_2), 28.39 (CH_2), 26.30 (CH_2), 12.87 (CH_3); IR (thin-film, cm^{-1}): 3281, 2953, 2870, 1618, 1538, 1434, 1345, 1284, 1060, 1044, 904, 857, 818, 742; HRMS m/z (ESI): calculated for $C_{16}H_{22}N_3O_3^+$: 304.1661, found: 304.1667.

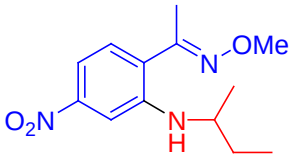

10se was synthesized using the general procedure with 1.1 equiv of CsOAc and it was isolated as an orange solid (45.1 mg, 85% yield) by preparative TLC. R_f = 0.35 (30% DCM in hexanes); mp = 62.8-64.5 °C; ^{1}H NMR ($CDCl_3$, 400 MHz): δ_H 8.14 (bs, 1H), 7.48-7.45 (m, 2H), 7.39 (dd, *J* = 8.8 Hz, 2.0 Hz, 1H), 4.01 (s, 3H), 3.62-3.57 (m, 1H), 2.31 (s, 3H), 1.69-1.60 (m, 2H), 1.26 (d, *J* = 6.4 Hz, 3H) 1.01 (t, *J* = 7.6 Hz, 2H); ^{13}C NMR ($CDCl_3$, 100 MHz) δ_C 156.42 (C), 148.56 (C), 146.84 (C), 129.63 (CH), 121.87 (C), 108.56 (CH), 105.44 (CH), 62.16 (CH_3), 49.55 (CH), 29.26 (CH_2), 19.75 (CH_3), 12.99 (CH_3) 10.10 (CH_3); IR (KBr, cm^{-1}): 3251, 2963, 2930, 1621, 1531, 1506, 1436, 1342, 1283, 1062, 1045, 901, 863, 819; HRMS m/z (ESI): calculated for $C_{13}H_{20}N_3O_3^+$: 266.1513, found: 266.1505.

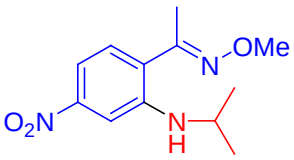

10sf was synthesized using the general procedure with 1.0 equiv of CsOAc and it was isolated as an orange solid (42.2 mg, 84% yield) by flash column chromatography. R_f = 0.4 (30% DCM in hexanes); mp = 79.5-81.5 °C; ^{1}H NMR ($CDCl_3$, 400 MHz): δ_H 8.12 (bs, 1H), 7.47-7.45 (m, 2H), 7.40 (d, *J* = 8.8 Hz, 1H), 4.02 (s, 3H), 3.79-3.76 (bm, 1H), 2.30 (s, 3H), 1.30 (d, *J* = 6.4 Hz, 2H); ^{13}C NMR ($CDCl_3$, 100 MHz) δ_C 156.34 (C), 148.54 (C), 146.59 (C), 129.62 (CH), 121.83 (C), 108.63 (CH), 105.43 (CH), 62.17 (CH_3), 43.96 (CH), 22.52 (CH_3), 13.01 (CH_3); IR (KBr, cm^{-1}): 3255, 2977,

2966, 2928, 1621, 1536, 1512, 1436, 1342, 1284, 1060, 1044, 902; HRMS m/z (ESI): calculated for $C_{12}H_{18}N_3O_3^+$: 252.1348, found: 252.1336.

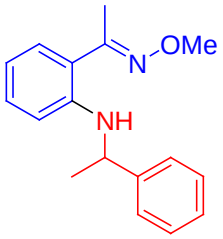

10ag was isolated as a yellow solid (35.4 mg, 66% yield) by flash column chromatography. R_f = 0.3 (20% DCM in hexanes); mp = 71.0-72.4 °C; ^{1}H NMR ($CDCl_3$, 400 MHz): δ_H 8.35 (bd, *J* = 3.2, 1H), 7.42-7.38 (m, 3H), 7.35-7.31 (m, 2H), 7.26-7.22 (m, 1H), 7.05 (t, *J* = 7.2 Hz, 1H), 6.63 (t, *J* = 7.2 Hz, 1H), 6.47 (d, *J* = 8.0 Hz, 1H), 4.65-4.59 (m, 1H), 4.03 (s, 3H), 2.36 (s, 3H), 1.60 (d, *J* = 6.8 Hz, 3H); ^{13}C NMR ($CDCl_3$, 100 MHz) δ_C 157.62 (C), 146.15 (C), 145.40 (C), 129.67 (CH), 128.83 (CH), 128.56 (CH), 126.71 (CH), 125.79 (CH), 117.07 (C), 114.97 (CH), 112.22 (CH), 61.86 (CH_3), 53.14 (CH), 24.98 (CH_3), 12.85 (CH_3); IR (KBr, cm^{-1}): 3275, 2962, 2930, 1598, 1521, 1450, 1275, 1049, 1036, 899, 762, 740, 702; HRMS m/z (ESI): calculated for $C_{17}H_{21}N_2O^+$: 269.1654, found: 269.1653.

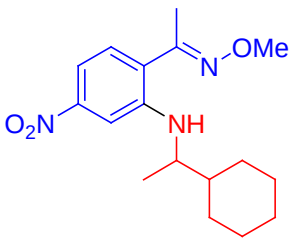

10sh was synthesized using the general procedure with 1.0 equiv of CsOAc and it was isolated as an orange oil (26.8 mg, 42% yield) by flash column chromatography. R_f =

0.4 (30% DCM in hexanes); ^{1}H NMR ($CDCl_3$, 400 MHz): δ_H 8.20 (bd, J = 6.4 Hz, 1H), 7.47-7.45 (m, 2H), 7.37 (d, J = 8.4 Hz, 1H), 4.01 (s, 3H), 3.53-3.49 (bm, 1H), 2.31 (s, 3H), 1.92-1.89 (m, 1H), 1.77-1.68 (m, 4H), 1.57-1.52 (m, 1H), 1.25-1.13 (m, 8H); ^{13}C NMR ($CDCl_3$, 100 MHz) δ_C 156.62 (C), 148.62 (C), 147.16 (C), 129.69 (CH), 121.60 (C), 108.16 (CH), 105.15 (CH), 62.18 (CH_3), 52.91 (CH), 43.28 (CH), 29.24 (CH_2), 28.91 (CH_2), 26.47 (CH_2), 26.35 (CH_2), 26.26 (CH_2), 17.13 (CH_3), 12.92 (CH_3); IR (thin-film, cm^{-1}): 3281, 2929, 2852, 1618, 1533, 1437, 1344, 1281, 1059, 1044, 906, 821; HRMS m/z (ESI): calculated for $C_{17}H_{26}N_3O_3^+$: 320.1974, found: 320.1976.

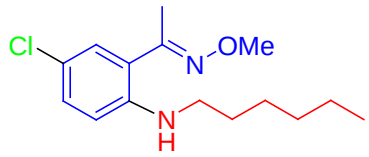

10uk was produced as indicated in Table 4.20 (entry 3) and it was isolated as a white solid (9.6 mg, 17% yield) by flash column chromatography. R_f = 0.3 (20% DCM in hexanes); mp = 52.0-53.5 °C; ^{1}H NMR ($CDCl_3$, 400 MHz): δ_H 7.68 (bs, 1H), 7.32 (d, J = 2.4 Hz, 1H), 7.13 (dd, J = 8.8 Hz, 2.4 Hz, 1H), 7.59 (d, J = 8.8 Hz, 1H), 3.98 (s, 3H), 3.17-3.12 (m, 2H), 2.26 (s, 3H), 1.68 (p, J = 7.2 Hz, 2H), 1.48-1.44 (m, 2H), 1.36-1.32 (m, 4H), 0.90 (t, J = 6.8 Hz, 3H); ^{13}C NMR ($CDCl_3$, 100 MHz) δ_C 156.60 (C), 145.84 (C), 129.44 (CH), 128.35 (CH), 119.16 (C), 118.03 (C), 111.87 (CH), 61.92 (CH_3), 43.37 (CH_2), 31.57 (CH_2), 29.01 (CH_2), 26.97 (CH_2), 22.57 (CH_2), 13.96 (CH_3), 12.73 (CH_3); IR (KBr, cm^{-1}): 3284, 2953, 2928, 2855, 1602, 1560, 1516, 1412, 1251, 1045, 916, 798; HRMS m/z (ESI): calculated for $C_{15}H_{24}N_2OCl^+$: 283.1577, found: 283.1579.

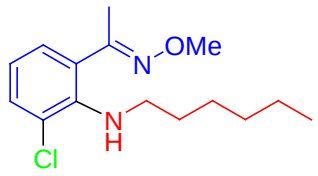

10uk' was produced as indicated in Table 4.20 (entry 3) and it was isolated as an colourless oil (11.3 mg, 20% yield) by flash column chromatography. R_f = 0.1 (20% DCM in hexanes); ^{1}H NMR ($CDCl_3$, 400 MHz): δ_H 7.28 (dd, *J* = 8.0 Hz, 1.6 Hz, 1H), 7.12 (dd, *J* = 8.0 Hz, 1.6 Hz, 1H), 6.78 (t, *J* = 8.0 Hz, 1H), 4.96 (bs, 1H), 3.98 (s, 3H), 3.09 (t, *J* = 7.2 Hz, 2H), 2.19 (s, 3H), 1.52-1.49 (m, 2H), 1.34-1.25 (bm, 6H), 0.87 (t, *J* = 6.8 Hz, 3H); ^{13}C NMR ($CDCl_3$, 100 MHz) δ_C 156.66 (C), 144.02 (C), 129.99 (CH), 128.46 (CH), 127.75 (C), 124.90 (C), 119.97 (CH), 61.80 (CH_3), 48.19 (CH_2), 31.49 (CH_2), 30.66 (CH_2), 26.50 (CH_2), 22.51 (CH_2), 14.68 (CH_3), 13.92 (CH_3); IR (thin-film, cm^{-1}): 3377, 3306, 2956, 2929, 2856, 1593, 1492, 1456, 1441, 1365, 1253, 1048, 889, 779, 741; HRMS m/z (ESI): calculated for $C_{15}H_{24}N_2OCl^+$: 283.1577, found: 283.1584.

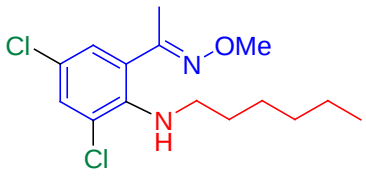

10ak-DC was produced as indicated in Table 4.20 (entry 3) and it was isolated as an white gummy paste (6.3 mg, 12% yield) by flash column chromatography followed by high vacuum evacuation overnight (0.5 mmHg, ~18 h, for removal of **1a** residue). R_f = 0.2 (20% DCM in hexanes). ^{1}H NMR ($CDCl_3$, 400 MHz): δ_H 7.28 (d, *J* = 2.4 Hz, 1H), 7.12 (d, *J* = 2.4 Hz, 1H), 4.95 (bs, 1H), 3.98 (s, 3H), 3.07 (t, *J* = 6.8 Hz, 2H), 2.17 (s, 3H), 1.51-1.47 (m, 2H), 1.33-1.27 (m, 6H), 0.87 (t, *J* = 6.4 Hz, 3H); ^{13}C NMR ($CDCl_3$, 100 MHz) δ_C 155.62 (C), 142.84 (C), 129.42 (CH), 128.34 (CH), 125.30 (C),

124.11 (C), 61.96 (CH_3), 48.14 (CH_2), 31.45 (CH_2), 30.60 (CH_2), 26.45 (CH_2), 22.50 (CH_2), 14.50 (CH_3), 13.91 (CH_3); IR (thin-film, cm^{-1}): 3379, 3306, 2956, 2930, 2856, 1479, 1466, 1440, 1366, 1242, 1050, 863, 817, 743; HRMS m/z (ESI): calculated for $C_{15}H_{23}N_2OCl_2^+$: 317.1187, found: 317.1181.

4.6.1.4 General Procedures for Stoichiometric Amination with 11aRh

To an amber 8 mL-vial (vial **A**), **4** (0.05 mmol, 21.4 mg) and $AgSbF_6$ (3 equiv, 51.45 mg) were added, and the vial was sealed with a Teflon® liner cap. To another amber 4-mL vial (vial **B**), *N*-chlorosuccinimide (1.5 equiv, 10.0 mg) was added, and the vial was sealed with a Teflon® liner cap. Both vials were evacuated and back filled with N_2 for three times. Freshly distilled THF (1 mL) was added to the vial **A**, the mixture was pre-heated and stirred at 40 °C for 10 min. THF (1 mL) and primary amine (1.2 equiv) were added to the vial **B**, and they were mixed and stirred for 10 min. The mixture in Vial **B** was transferred to the reaction (vial **A**) in one portion, and stirred at 40 °C for 2 h. To work-up, 30% aqueous ammonia (2 mL) and EtOAc (5 mL) were added. The organic layer was collected, and the aqueous layer was washed with EtOAc (5 mL × 2). The combined organic fractions were dried over Na_2SO_4 and then filtered through a short plug of silica gel. Solvents were removed by rotary evaporation, and the residue was re-dissolved in a small amount of dichloromethane (DCM). The mixture was subjected to flash column chromatography / preparative TLC with silica gel as stationary phase with hexane-Et_2O as mobile phase for the separation of the amination products.

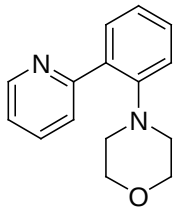

12aa was isolated as a pale yellow solid by flash column chromatography (5.5 mg, 52% yield). R_f = 0.2 (20% EtOAc in hexanes); mp = 105-106.6 °C; ^{1}H NMR ($CDCl_3$, 400 MHz): δ_H 8.69 (d, *J* = 4.8 Hz, 1H), 8.01 (d, *J* = 8 Hz, 1H), 7.69 (td, *J* = 8 Hz, 2 Hz, 2H), 7.56 (dd, *J* = 7.6 Hz, 1.6 Hz, 1H) 7.35 (td, *J* = 7.2 Hz, 1.2 Hz, 1H), 7.21-7.18 (m, 1H), 7.14 (td, *J* = 7.2 Hz, 0.8 Hz, 1H), 7.06 (d, *J* = 8 Hz, 1H), 3.62 (bt, *J* = 4 Hz, 4H), 2.84 (bt, *J* = 4 Hz, 4H); ^{13}C NMR ($CDCl_3$, 100 MHz) δ_C 158.71 (C), 150.14 (C), 149.74 (CH), 135.45 (CH), 133.82 (C), 131.61 (CH), 129.45 (CH), 124.26 (CH), 123.16 (CH), 121.62 (CH), 118.01 (CH), 66.86 (CH_2), 52.04 (CH_2); IR (KBr, cm^{-1}): 2964, 2856, 2814, 1597, 1503, 1492, 1463, 1440, 1220, 1118, 935, 757, 748; HRMS m/z (ESI): calculated for $C_{15}H_{17}N_2O^+$: 241.1341, found: 241.1334.

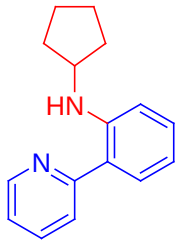

13aa was isolated as a pale yellow oil by preparative TLC (9.4 mg, 79% yield). R_f = 0.7 (20% EtOAc in hexanes); ^{1}H NMR ($CDCl_3$, 400 MHz): δ_H 8.57 (d, *J* = 4.4 Hz, 1H), 8.18 (bs, 1H), 7.74 (t, *J* = 7.2 Hz, 1H), 7.67 (d, *J* = 8.0 Hz, 1H) 7.53 (d, *J* = 7.6 Hz, 1H), 7.27-7.24 (m, 1H), 7.16 (td, *J* = 6.0 Hz, 1H), 6.81 (bd, 1H), 6.71-6.69 (bm, 1), 3.87 (bt, *J* = 5.2 Hz, 1H), 2.06-2.03 (m, 2H), 1.75-1.73 (m, 2H), 1.64-1.58 (m, 4H); ^{13}C NMR ($CDCl_3$, 100 MHz) δ_C 159.61 (C), 147.22 (CH), 136.80 (CH), 130.16 (CH), 129.34 (CH), 122.22 (CH), 121.45 (C), 120.69 (CH), 115.82 (bs, CH), 115.27

(C), 112.85 (bs, CH), 54.54 (CH), 33.27 (CH_2), 24.04 (CH_2); IR (thin-film, cm^{-1}): 3291, 2954, 2867, 1604, 1584, 1515, 1478, 1442, 1332, 1240, 745; HRMS m/z (ESI): calculated for $C_{16}H_{19}N_2^+$: 239.1538, found: 239.1548.

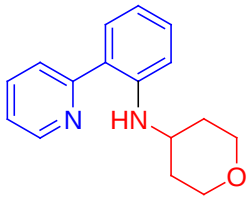

13ac was isolated as a yellow semi-solid by preparative TLC (11.6 mg, 93% yield). R_f = 0.55 (20% EtOAc in hexanes); ^{1}H NMR ($CDCl_3$, 400 MHz): δ_H 8.58 (d, *J* = 4.8 Hz, 1H),7.77 (t, *J* = 7.2 Hz, 1H), 7.70 (d, *J* = 8.4 Hz, 1H), 7.58 (d, *J* = 7.6 Hz, 1H) 7.27 (t, *J* = 7.6 Hz, 1H), 7.19 (t, *J* = 6.0 Hz, 1H), 6.87 (bs, 1H), 6.78 (bs, 1H), 4.00-3.95 (m, 2H), 3.66-3.63 (m, 1H), 3.58-3.52 (m, 2H), 2.09-2.04 (m, 2H), 1.66-1.57 (m, 2H); ^{13}C NMR ($CDCl_3$, 100 MHz) δ_C 159.36 (C), 147.21 (CH), 136.94 (CH), 130.24 (CH), 129.59 (CH), 122.25 (CH), 121.72 (bs, C), 120.86 (CH), 116.37 (bs, CH), 112.68 (bs, CH), 66.37 (CH_2), 48.38 (bs, CH), 32.77 (CH_2) (1 arene-C missing); IR (thin-film, cm^{-1}): 3276, 2952, 2847, 1604, 1584, 1518, 1478, 1443, 1422, 1329, 1259, 1239, 1160, 1138, 1087, 748; HRMS m/z (ESI): calculated for $C_{16}H_{19}N_2O^+$: 255.1497, found: 255.1494.

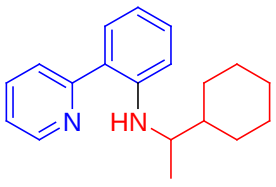

13ah was isolated as a pale yellow oil by preparative TLC (11.4 mg, 81% yield). R_f = 0.5 (5% EtOAc in hexanes); ^{1}H NMR ($CDCl_3$, 400 MHz): δ_H 8.57 (d, *J* = 4.4 Hz, 1H), 7.74 (t, *J* = 7.2 Hz, 1H), 7.69 (d, *J* = 8.0 Hz, 1H), 7.56 (d, *J* = 7.6 Hz, 1H) 7.24 (t, *J* = 7.6 Hz, 1H), 7.16 (t, *J* = 6.0 Hz, 1H), 6.81 (bs, 1H), 6.68 (bm, 1H), 3.46-3.43 (m,

1H), 1.87-1.57 (m, 6H), 1.26-1.15 (m, 8H); ^{13}C NMR ($CDCl_3$, 100 MHz) δ_C 159.64 (C), 147.11 (CH), 136.70 (CH), 130.23 (CH), 129.58 (C), 129.45 (CH), 122.08 (CH), 121.06 (bs, C), 120.52 (CH), 115.15 (bs, CH), 112.17 (bs, CH), 53.06 (bs, CH), 42.93 (CH), 29.48 (CH_2), 28.60 (CH_2), 26.67 (CH_2), 26.54 (CH_2), 26.37 (CH_2), 16.97 (CH); IR (think-film, cm^{-1}): 3302, 2924, 2850, 1605, 1584, 1518, 1478, 1445, 1330, 1163, 744; HRMS m/z (ESI): calculated for $C_{19}H_{25}N_2^+$: 281.2018, found: 281.2010.

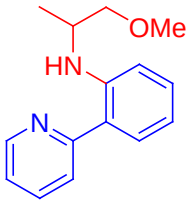

13al was isolated as a pale yellow oil by flash column chromatography (10.45 mg, 86% yield). R_f = 0.3 (60% DCM in hexanes); ^{1}H NMR ($CDCl_3$, 400 MHz): δ_H 8.58 (d, J = 4.8 Hz, 1H), 8.17 (bs, 1H), 7.74 (t, J = 7.6 Hz, 1H), 7.66 (d, J = 8.0 Hz, 1H) 7.53 (d, J = 7.6 Hz, 1H), 7.27-7.24 (m, 1H), 7.16 (t, J = 76.0 Hz, 1H), 6.84 (bs, 1H), 6.72 (bs, 1H), 3.77-3.73 (m, 1H), 3.58-3.54 (m, 1H), 3.39-3.32 (m, 4H), 1.29 (d, J = 6.4); ^{13}C NMR ($CDCl_3$, 100 MHz) δ_C 157.37 (C), 147.29 (CH), 139.56 (C), 136.78 (CH), 130.20 (CH), 129.58 (CH), 123.63 (C), 122.29 (CH), 120.74 (CH), 115.78 (CH), 77.14 (CH), 59.04 (CH_3), 17.91 (CH_3) (1 arene-CH, 1 alkyl-CH_2 missing); IR (thin-film, cm^{-1}): 3270, 2973, 2924, 1064, 1585, 1517, 1478, 1443, 1389, 1239, 1168, 1110, 747; HRMS m/z (ESI): calculated for $C_{15}H_{19}N_2O^+$: 243.1497, found: 243.1508.

4.6.1.5 General Procedures for Oxime Deprotection

To an 8-mL vial containing *O*-methyloxime arylamine product (0.1 mmol) 6 M HCl (0.5 mL) was added, and the vial was tightly sealed with a Teflon® liner cap. The mixture was stirred vigorously at reflux (oil bath temp. = 120 °C) for 2 h. To

work-up, the solution was diluted with DI water (5 mL) and it was neutralized with saturated $NaHCO_3$ solution followed by the addition ethyl acetate (10 mL). The organic fraction was collected, and the aqueous fraction was washed with ethyl acetate (10 mL) twice. The combined organic fractions were washed with brine, dried over Na_2SO_4, and filtered through a short plug of Celite®. The solution was dried using a rotary evaporator, and the resulting residue was dissolved in a small amount of dichloromethane followed by a flash column chromatography using silica gel as the stationary phase for isolation of the 2-acetyl-*N*-alkylaniline products.

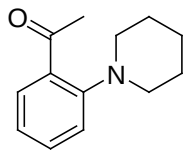

8ab2 was prepared by the deprotection of **8ab**, and was isolated as a pale yellow oil (18.1 mg, 89% yield). R_f = 0.15 (2% EtOAc in hexanes); ^{1}H NMR ($CDCl_3$, 400 MHz): δ_H 7.40-7.36 (m, 2H), 7.05 (d, J = 8.0 Hz, 1H), 7.01 (t, J =7.6 Hz, 1H), 2.94 (t, J = 5.2 Hz, 2H), 2.66 (s, 3H), 1.74-1.69 (m, 4H), 1.59-1.55 (m, 2H); ^{13}C NMR ($CDCl_3$, 100 MHz) δ_C 204.79 (C), 152.55 (C), 135.28 (C), 131.75 (CH), 129.05 (CH), 121.88 (CH), 118.59 (CH), 54.48 (CH_2), 28.94 (CH_3), 26.15 (CH_2), 23.96 (CH_2); IR (neat, cm^{-1}): 2935, 1679, 1593, 1484, 1446, 1287, 1243, 1227; HRMS m/z (ESI): calculated for $C_{13}H_{18}NO^+$: 204.1388, found: 204.1395.

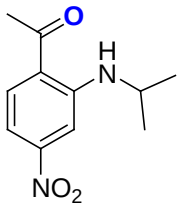

10sf2 was prepared by the deprotection of **10sf**, and was isolated as an orange solid (20.1 mg, 81% yield) by flash column chromatography. R_f = 0.35 (30% DCM in hexanes); mp = 54.0-55.0 ° C; ^{1}H NMR ($CDCl_3$, 400 MHz): δ_H 8.98 (bs, 1H), 7.86 (d, *J* = 8.8 Hz, 1H), 7.52 (d, *J* = 2.0 Hz, 1H), 7.30 (dd, *J* = 8.8 Hz, 1.6 Hz, 1H), 3.83-3.74 (m, 1H), 2.62 (s, 3H), 1.31 (d, *J* = 6.4 Hz, 6H); ^{13}C NMR ($CDCl_3$, 100 MHz) δ_C 200.26 (C), 151.65 (C), 150.24 (C), 133.94 (CH), 120.36 (C), 107.21 (CH), 106.84 (CH), 43.71 (CH), 28.33 (CH_3), 22.46 (CH_3); IR (KBr, cm^{-1}): 3287, 2983, 2928, 1647, 1529, 1346, 1231, 1169, 1130; HRMS m/z (ESI): calculated for $C_{11}H_{15}N_2O_3^+$: 223.1083, found: 223.1080.

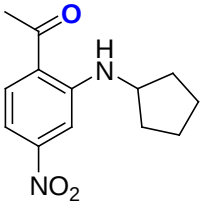

10sa2 was prepared by the deprotection of **10sa**, and was isolated as an orange solid (20.1 mg, 81% yield) by flash column chromatography. R_f = 0.20 (20% DCM in hexanes); mp = 66.0-68.5 ° C; ^{1}H NMR ($CDCl_3$, 400 MHz): δ_H 9.07 (bs, 1H), 7.85 (d, *J* = 8.8 Hz, 1H), 7.54 (d, *J* = 2.0 Hz, 1H), 7.24 (dd, *J* = 8.8 Hz, 2.4 Hz, 1H), 3.95-3.89 (m, 1H), 2.62 (s, 3H), 2.12-2.08 (m, 2H), 1.79-1.77 (m, 2H), 1.71-1.67 (m, 2H), 1.62-1.56 (m, 2H); ^{13}C NMR ($CDCl_3$, 100 MHz) δ_C 200.21 (C), 151.52 (C), 150.67 (C), 133.79 (CH), 120.43 (C), 107.28 (CH), 53.80 (CH), 33.22 (CH_2), 28.28 (CH_3), 23.92 (CH_2) (1 CH missing); IR (KBr, cm^{-1}): 3305, 2960, 2872, 1650, 1537, 1350,

1264, 1232; HRMS m/z (ESI): calculated for $C_{13}H_{17}N_2O_3^+$: 249.1239, found: 249.1243.

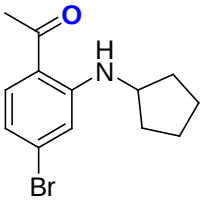

10da2 was synthesized by the deprotection of **10da,** and was isolated as a yellow oil (25.0 mg, 89% yield) by flash column chromatography. R_f = 0.35 (10% DCM in hexanes); ^{1}H NMR ($CDCl_3$, 400 MHz): δ_H 8.99 (bs, 1H), 7.50 (d, *J* = 8.8 Hz, 1H), 6.87 (d, *J* = 2.0 Hz, 1H), 6.65 (dd, *J* = 8.4 Hz, 2.0 Hz, 1H), 3.84-3.79 (m, 1H), 2.52 (s, 3H), 2.06-1.78 (m, 2H), 1.77-1.75 (m, 2H), 1.66-1.63 (m, 2H), 1.62-1.61 (m, 2H); ^{13}C NMR ($CDCl_3$, 100 MHz) δ_C 199.98 (C), 151.20 (C), 133.88 (CH), 129.91 (C), 116.69 (CH), 116.12 (C), 115.06 (CH), 53.50 (CH), 33.26 (CH_2), 27.79 (CH_3), 23.92 (CH_2); IR (thin-film, cm^{-1}): 3284, 2958, 2869, 1639, 1594, 1563, 1504, 1439, 1358, 1239, 954; HRMS m/z (ESI): calculated for $C_{13}H_{17}NOBr^+$: 282.0494, found: 282.0506.

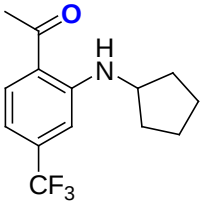

10ea2 was prepared by the deprotection of **10ea**, and was isolated as a yellow oil (20.3 mg, 75% yield) by flash column chromatography. R_f = 0.35 (10% DCM in hexanes); ^{1}H NMR ($CDCl_3$, 400 MHz): δ_H 9.04 (bs, 1H), 7.81 (d, *J* = 8.4 Hz, 1H), 6.94 (s, 1H), 6.75 (d, *J* = 8.4 Hz, 1H), 3.91-3.87 (m, 1H), 2.59 (s, 3H), 2.08-2.04 (m, 2H), 1.79-1.76 (m, 2H), 1.68-1.65 (m, 2H), 1.64-1.61 (m, 2H); ^{13}C NMR ($CDCl_3$, 100 MHz) δ_C 200.39 (C), 150.21 (C), 136.22-135.24 (q, *J* = 31 Hz, C), 133.31 (CH), 127.70-119.77 (q, *J* = 260 Hz, CF_3), 118.91 (C), 109.43-109.28 (m, CH) (1 CH

missing); IR (thin-film, cm^{-1}): 3297, 2960, 2872, 1650, 1577, 1524, 1464, 1337, 1240, 1171, 1128, 1089, 962; HRMS m/z (ESI): calculated for $C_{14}H_{17}NOF_3^+$: 272.1262, found: 272.1253.

4.6.1.6 Kinetic Isotope Effect Experiments

4.6.1.6.1 H/D Scrambling Experiments

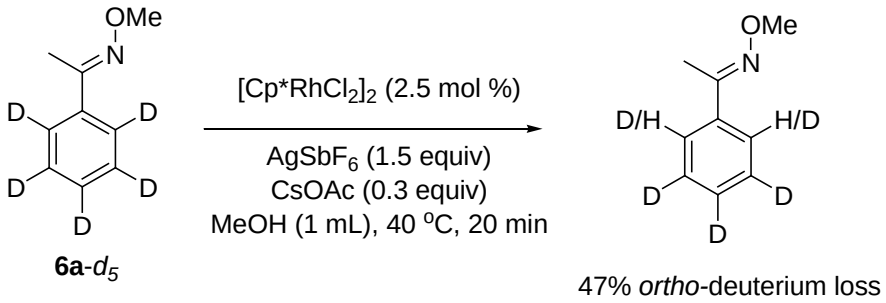

6a-d_5

To an amber 8 mL-vial, $[Cp^*RhCl_2]_2$ (2.5 mol %, 1.5 mg), CsOAc (30 mol %, 5.7 mg) and $AgSbF_6$ (1.5 equiv, 52 mg) were added, and the vial was sealed with a Teflon® liner cap. The vial was evacuated and filled back with N_2 for three times. Freshly distilled MeOH (1 mL) was added to the reaction vial, followed by the addition of **6a**-d_5 (0.1 mmol, 15.5 μL) with a 50-μL syringe. The reaction was stirred at 40 °C for 20 min. The reaction mixture was diluted with EtOAc and filtered through a short plug of silica gel washing with EtOAc. The solvents were removed by rotary evaporation and the residue was redissolved in *d*-chloroform followed by the addition of the internal standard (DBM, 0.1 mmol). The mixture was analyzed by ^1H NMR and 47% H-incorporation on *ortho*-positions was observed (47% deuterium loss).

Figure 4.5 ^{1}H NMR Spectrum Indicating the Occurrence of H/D Scramble

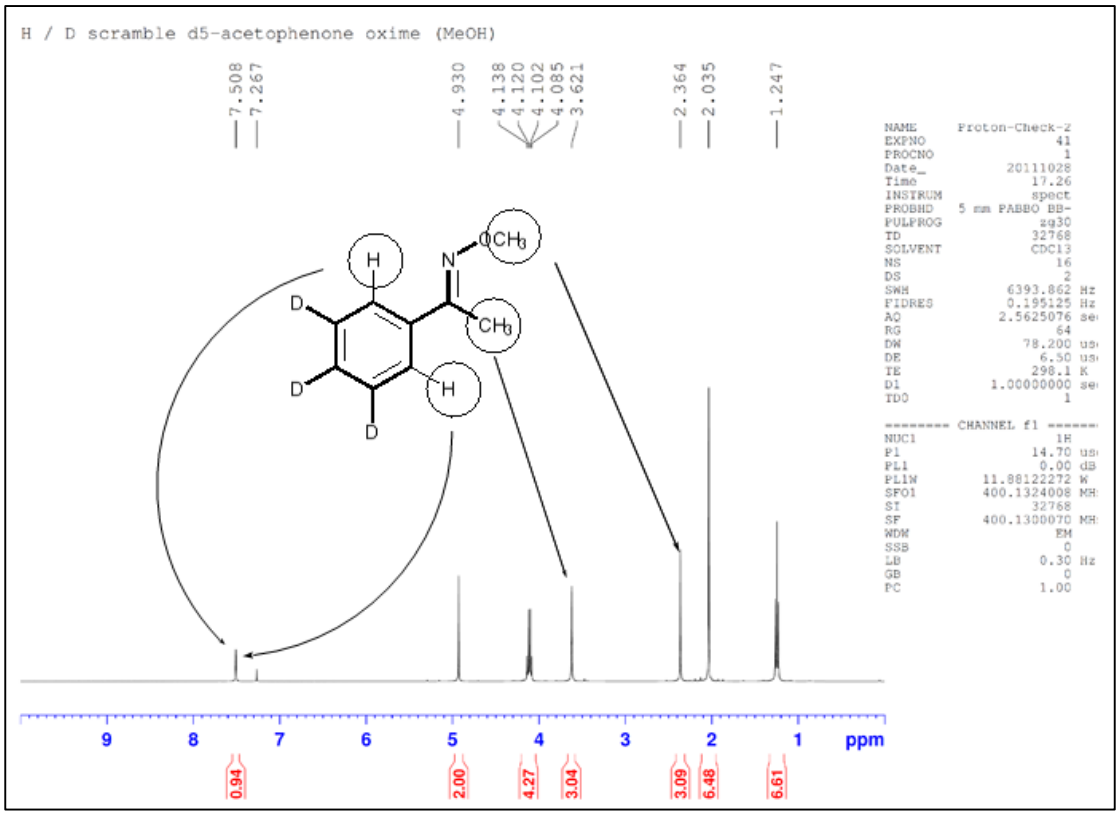

4.6.1.6.2 Direct Comparison of Initial Rates

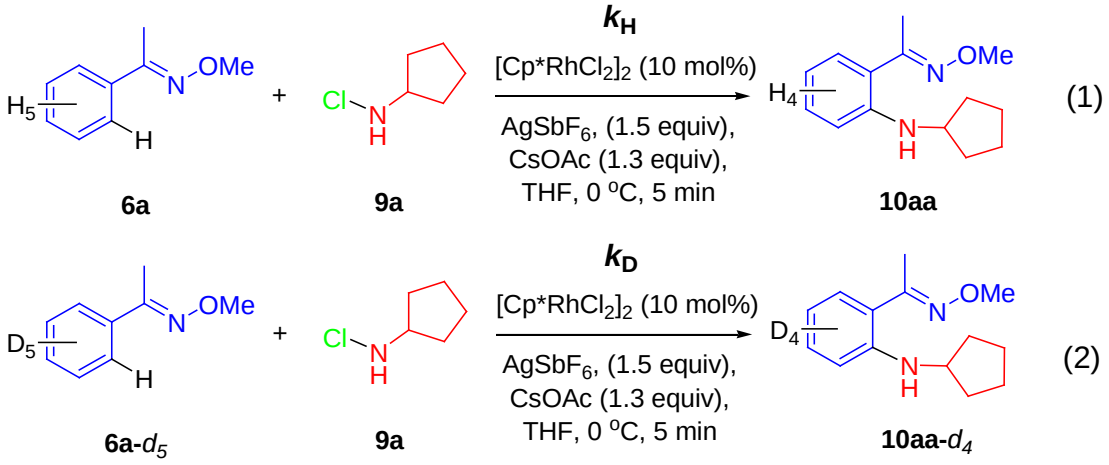

To an amber 8 mL-vial (vial **A**), $[Cp^*RhCl_2]_2$ (10 mol %, 6.2 mg), CsOAc (1.3 equiv, 24.8 mg) and $AgSbF_6$ (1.5 equiv, 51.5 mg) were added, and the vial was sealed with a Teflon® liner cap. To another amber 4-mL vial (vial **B**), *N*-chlorosuccinimide (2.2 equiv, 58.7 mg) was added, and the vial was sealed with a Teflon® liner cap. Both vials were evacuated and filled back with N_2 for three times. Freshly distilled THF (1 mL) was added to the vial **A**, followed by the addition of the **6a** (0.1 mmol) using a 50-µL syringe. Vial **A** was pre-cooled at 0°C. THF (1 mL) and cyclopentylamine (2.2 equiv, 22 µL) were added to the vial **B**, and they were mixed and stirred for 10 min. The mixture in Vial **B** was taken up by a 1-mL syringe, and added to the reaction (vial **A**) in one portion, and the reaction was stirred at 0 °C for 5 min. The reaction was quenched by adding 30% aqueous ammonia (2 mL). EtOAc (5 mL) were added for extraction. The organic layer was collected, and the aqueous layer was washed with EtOAc (5 mL × 2). The combined organic fractions were dried over Na_2SO_4 and then filtered through a short plug of Celite®. Solvent was removed by rotary evaporation, and the residue was subjected to ^{1}H NMR analysis to determine the substrate conversions.

A parallel reaction was run at the same time with **6a**-d_5 as substrate. The reactions were run in duplicate.

Determination and Calculations of the k_H / k_D Value:

To determine rates of product (**10aa** and **10aa**-d_4) formation, with reference to the singlet signal of dibromoethane (2H) at 4.90 ppm (in *d*-chloroform), the ^{1}H NMR signal of a singlet (3H) at 2.30 ppm was chosen for product yields quantification. k_H /

k_D was determined based on the initial rates of **10aa** and **10aa-d_4** fomration (Assuming all reagent concentrations remain unchanged at the initial rate expressions). The experiment was run in duplicate, and the results were listed below:

runs	amount for **10aa** **(**mmol)	amount for **10aa-d_4** (mmol)	reaction time (s)	THF (dm^3)
1st	0.0179	0.00787	300	0.002
2nd	0.0144	0.00780	300	0.002
average	0.0162	0.00784		

Initial rate of with **6a** as substrate = 0.0162 / (1000 × 0.002 × 300) mol dm^{-3} s^{-1}

= $\underline{27 \times 10^{-6}}$ $\underline{mol\ dm^{-3}}$ $\underline{s^{-1}}$

Initial rate of with **6a-d_5** as substrate= 0.00784 / (1000 × 0.002 × 300) mol dm^{-3} s^{-1}

= $\underline{13 \times 10^{-6}}$ $\underline{mol\ dm^{-3}}$ $\underline{s^{-1}}$

$k_H / k_D = (27 \times 10^{-6}) / (13 \times 10^{-6}) =$ **$\underline{2.08}$**

4.6.1.7 Hammett Correlation Study

To an amber 8 mL-vial (vial **A**), $[Cp^*RhCl_2]_2$ (10 mol %, 6.2 mg), CsOAc (1.3 equiv, 24.8 mg) and $AgSbF_6$ (1.5 equiv, 51.5 mg) were added, and the vial was sealed with a Teflon® liner cap. To another amber 4-mL vial (vial **B**), *N*-chlorosuccinimide (2.2 equiv, 58.7 mg) was added, and the vial was sealed with a Teflon® liner cap. Both vials were evacuated and filled back with N_2 for three times. Freshly distilled

THF (1 mL) was added to the vial **A**, followed by the addition of a suitable *para*-substituted acetophenone *O*-methyloxime (0.1 mmol) using a 50-μL syringe. Vial **A** was pre-cooled at 0°C. THF (1 mL) and cyclopentylamine (2.2 equiv, 22 μL) were added to the vial **B**, and they were mixed and stirred for 10 min. The mixture in Vial **B** was taken up by a 1-mL syringe, and added to the reaction (vial **A**) in one portion, and the reaction was stirred at 0 °C for 5 - 8 min. The reaction was quenched by adding 30% aqueous ammonia (2 mL). EtOAc (5 mL) were added for extraction. The organic layer was collected, and the aqueous layer was washed with EtOAc (5 mL × 2). The combined organic fractions were dried over Na_2SO_4 and then filtered through a short plug of Celite®. Solvent was removed by rotary evaporation, and the residue was subjected to ^{1}H NMR analysis to determine the product yields.

Determination and Calculations of the k_Y / k_H Value:

To determinate the rate of product formation, with reference to the singlet signal of dibromoethane (2H) at 4.90 ppm (in *d*-chloroform), the ^{1}H NMR signals of products as listed below was chosen for product yields quantification. The k_Y / k_H value was determined based on the initial rates of product fomration (Assuming all reagent concentrations remain unchanged at the initial rate expressions). The experiment was run in duplicate, and the results were listed below:

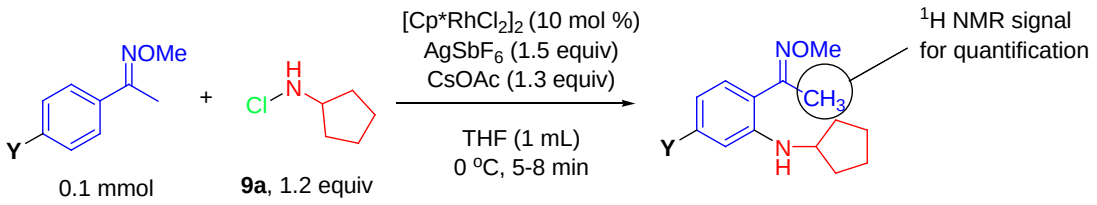

Y	σ_{meta}	chemical shifts (ppm)	yield 1st (mmol)	yield 2nd (mmol)	average yield (mmol)	time (s)	product formation rate ($M\ s^{-1}$)	k_Y / k_H
-H	0	2.27 (3H, s)	0.0122	0.0100	0.0111	300	18.5×10^{-6}	1
-OMe	0.12	2.23 (3H, s)	0.0071	0.0082	0.0076	300	12.7×10^{-6}	0.686
-Cl	0.37	2.27 (3H, s)	0.0095	0.0093	0.0094	480	9.8×10^{-6}	0.530
$-CF_3$	0.46	2.27 (3H, s)	0.0057	0.0070	0.0063	480	6.6×10^{-6}	0.357
$-NO_2$	0.71	2.27 (3H, s)	0.0058	--	0.0058	480	6.0×10^{-6}	0.327

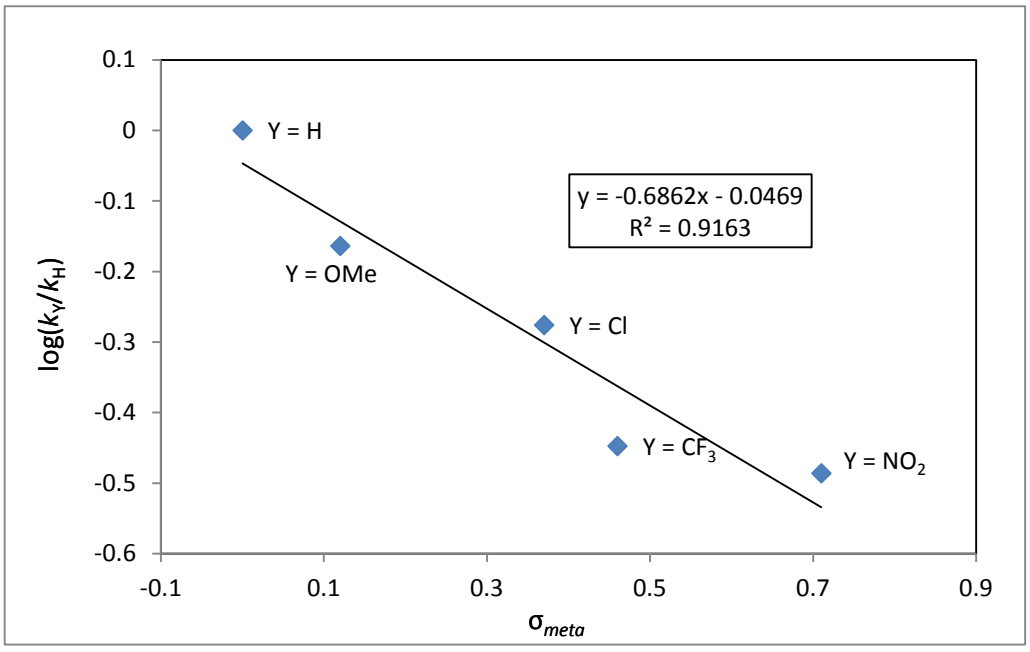

Chapter 5

Conclusion

Transition-metal catalyzed regioselective aromatic C-N bond cross coupling reactions *via* C-H activation have been explored. With the use of electrophilic nitrogen reagents such as *N*-arylsulfonyloxycarbamates and *N*-chloroamines, we developed the Pd(II)- and Cp*Rh(III)-catalyzed direct arene C-H amidation / amination. In our study, cyclopalladated and cyclorhodated complexes were found to be competent catalyst for the corresponding C-N bond coupling reactions and thus verifying the involvement of the metal-aryl complexes.

In *Chapter 2*, we developed the Pd(II)-catalyzed direct *ortho*-selective amidation of pivalanilides with ethyl *N*-nosyloxycarbamates to afford 2-aminoanilines in up to 87% yields. Apart from good functional group tolerance, benzyl and vinyl groups known to be susceptible to nitrene C-H insertion and aziridination reactions were also tolerated. The Pd-catalyzed reaction was also successfully extended to the amidation of benzoic acids to furnish anthranilic acids. The reactions of lithium benzoates with $Pd(OAc)_2$ as catalyst and *N*-mesitylsulfonyloxycarbamates as reagents afforded the anticipated anthranilic acids in up to 73% yields, but benzoic acid alone is an

ineffective substrate. Strong dependence on the counter ion of the benzoates was observed; counter ions such as Na^+, K^+ and $NnBu_4^+$ were less effective than Li^+. Probably harder counter ions would induce stronger binding to the benzoate, and this would favor the formation of a κ^1-benzoate-palladium(II) complex which has an *ortho*-C-H bond in close proximity to the Pd-metal centre. Similar to the amidation of pivalanilides, lithium benzoates bearing halogens, $-CF_3$, benzyl and methoxy group were effectively transformed to the corresponding anthranilic acids.

Transition-metal catalyzed direct amidation of arenes was scarce in the literature, and the reaction mechanism was poorly understood. In *Chapter 3*, we pursued the reaction mechanism for the Pd(II)-catalyzed amidation of pivalanilide with *N*-nosyloxycarbamates. We employed the reaction of 2,4-dimethylpivalanilide (**1a**) with ethyl *N*-nosyloxycarbamate (**2aNs**) and $[Pd(OTs)_2(MeCN)_2]$ (**Pd**) in *d*-chloroform as a model for kinetic experiments. The rate law was determined to be:

$$rate = k\,[\mathbf{1a}][\mathbf{2aNs}][\mathbf{Pd}]^2$$

Primary kinetic isotope effect (k_H / k_D = 2.8) was observed; this indicates that substantial C-H bond cleavage is involved in the turnover-limiting step. A linear Hammett correlation for the amidations with *para*-substituted pivalanilide was

established, and the ρ value was found to be -0.53, whereas the analogous Hammett correlation study with *para*-substituted ethyl *N*-arylsulfonyloxycarbamates revealed ρ value of +0.46. Ethyl *N*-methyl-*N*-nosyloxycarbamate was found to be an ineffective reagent for the amidation, and the metal-nitrenoid pathway appears to be obligatory for the Pd-catalyzed C-H amidation reaction. Based on our results, a proposed mechanism involves: (1) initial Pd(II)-mediated C-H activation of pivalanilide (**1a**) to give **1aPd**; (2) ligand exchange of **1aPd** with *N*-nosyloxycarbamate (**2aNs**) would afford the palladacycle ***B***; (3) N-O bond cleavage would generate a Pd-nitrene complex ***C***; (4) migratory nitrene insertion to the Pd-C(aryl) bond would effect the C-N bond coupling with the concomitant formation of the palladium(II)-amide complex ***D***; (5) turnover-limiting C-H activation of **1a** would release **3aa** and regenerate **1aPd** for another catalytic cycle. On the basis of the proposed mechanism, the detailed rate expression was derived:

$$\frac{d[\mathbf{3aa}]}{d\mathrm{t}} = \frac{k_1 k_2 k_3 k_4 [\mathbf{1a}][\mathbf{2aNs}][\mathbf{Pd}]^2}{(k_{-2} + k_3) k_{-1} k_{-3}}$$

Apart from the amidation of arenes, efficient methods for direct coupling of arene C-H bonds with N-H amine remained very rare. In *chapter 4*, we demonstrated dehydrogenative coupling of arene C-H bond with amine N-H bond by combining the

Cp*Rh(III)-catalyzed arene C-H activation and the amine N-H oxidation. To begin, Cp*Rh(III)-catalyzed direct amination of acetophenone *O*-methyloximes with secondary *N*-chloroamines was investigated. The reaction showed good functional group tolerance; *O*-methyloximes bearing halogens, $-CF_3$, $-NO_2$ and methoxy were effectively aminated in up to 87% yields. Cyclic *N*,*N*-dialkylamines such as morpholine, piperidine and *N*-Boc piperazine were installed in excellent yields, but acyclic secondary *N*-chloroamines were coupled in moderate yields. In this work, we found *N*-chloroamines can be generated *in situ* by reacting the amines with *N*-chlorosuccinimide; this N-H / C-H dehydrogenative approach is applicable to both secondary and primary amines. Various α-branched primary amines were effectively coupled to acetophenone *O*-methyloximes affording the *N*-alkylarylamines in good yield. However, *n*-alkylamines remained challenging for the C-N coupling reaction, and coupling of tertiary alkylamines was unsuccessful. Primary KIE (k_H / k_D = 2.1) was observed indicating a rate-limiting C-H activation step. Stoichiometic reaction of **11aRh** with *N*-chloroamines produced the amine products in quantitative yields. This indicated that cyclorhodated complexes should be the active intermediate for the amination. Without $AgSbF_6$, **11aRh** failed to react with *N*-chloroamine to give the expected amine product. Thus, it is believed that the *N*-chloroamine should first coordinate to the Rh metal centre prior to the C-N bond formation. The reaction

should be initiated by a turnover-limiting C-H activation to generate a cyclorhodated complex of *O*-methyloxime, followed by *N*-chloroamine coordination, and the subsequent anionotropic migration to furnish the arylamine products. Chloride abstraction by $AgSbF_6$ would regenerate the active rhodium catalyst.

APPENDICES

Figure A1. ^{1}H NMR of **1r**

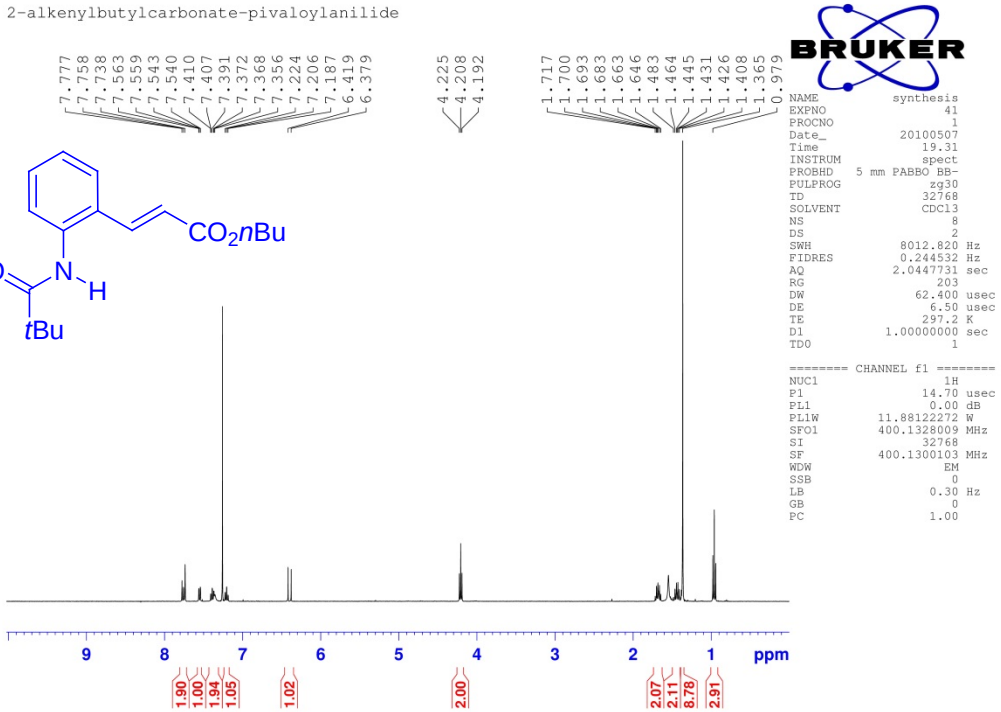

Figure A2. ^{13}C NMR of **1r**

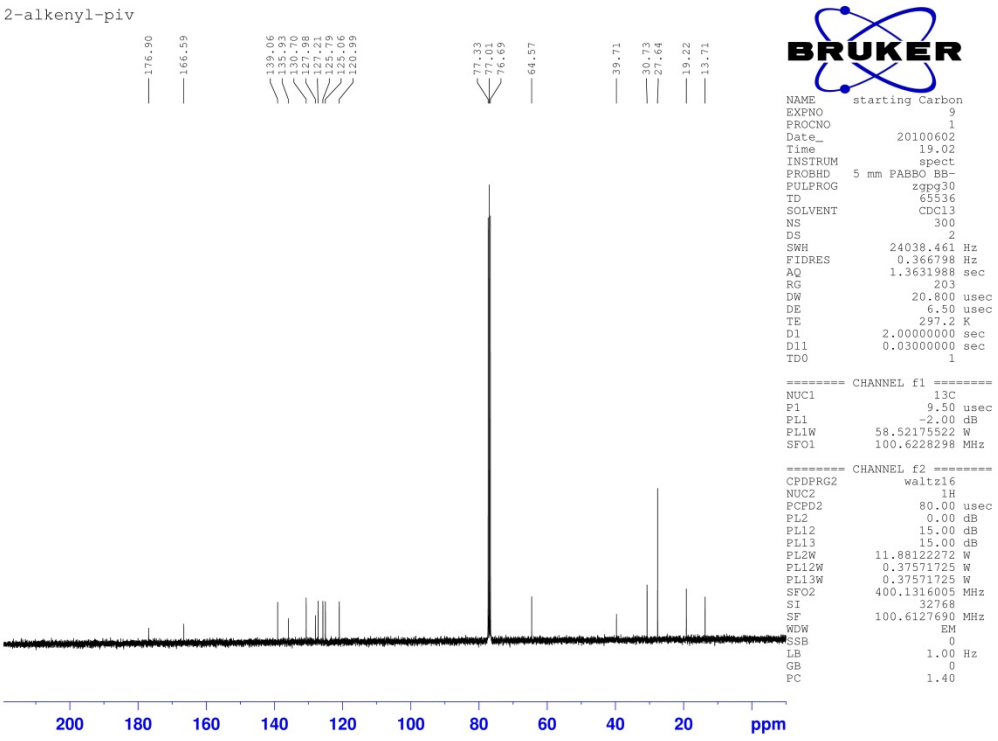

Figure A3. ^{1}H NMR of **1s**

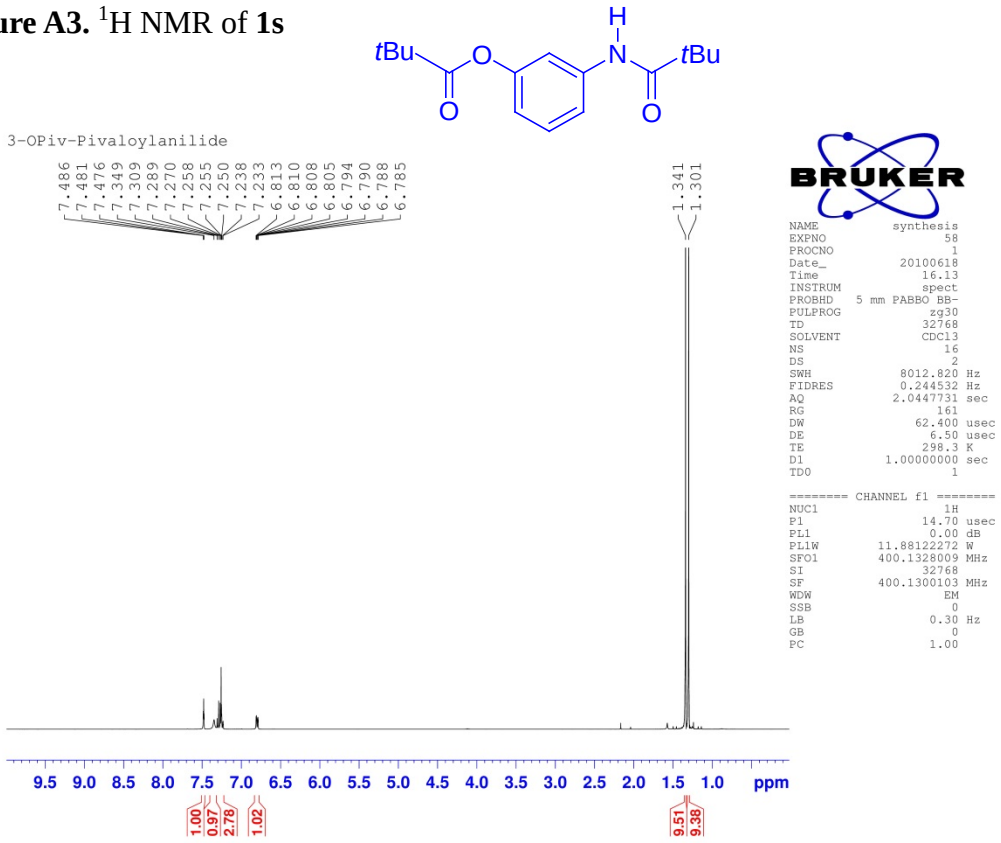

Figure A4. ^{13}C NMR of **1s**

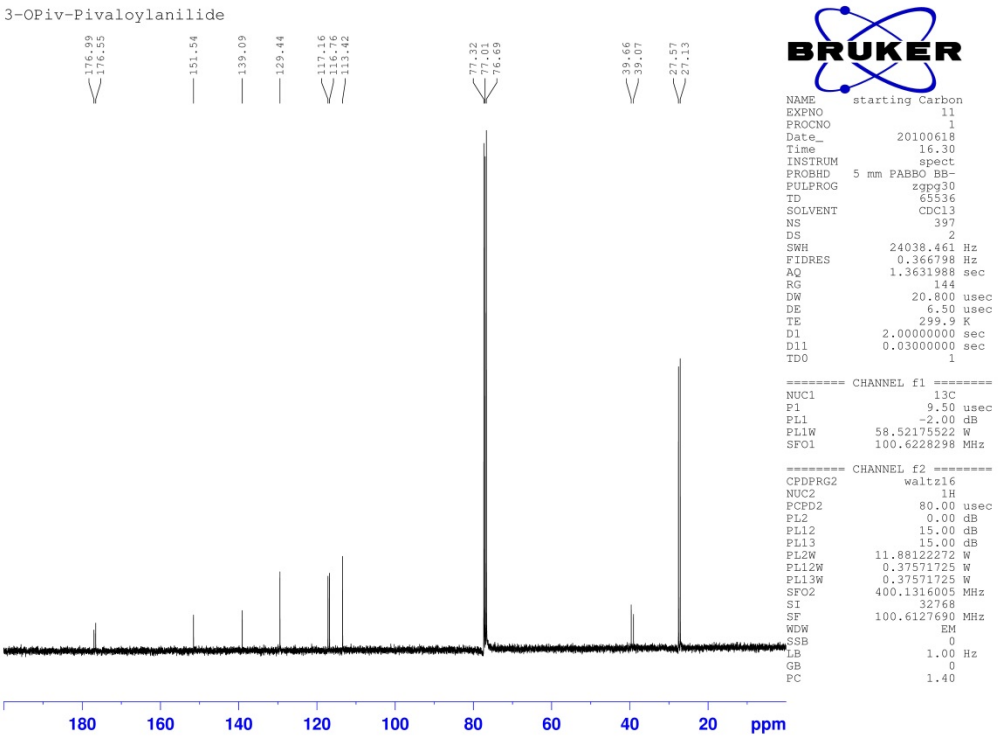

Figure A5. ^{1}H NMR of **2aNs**

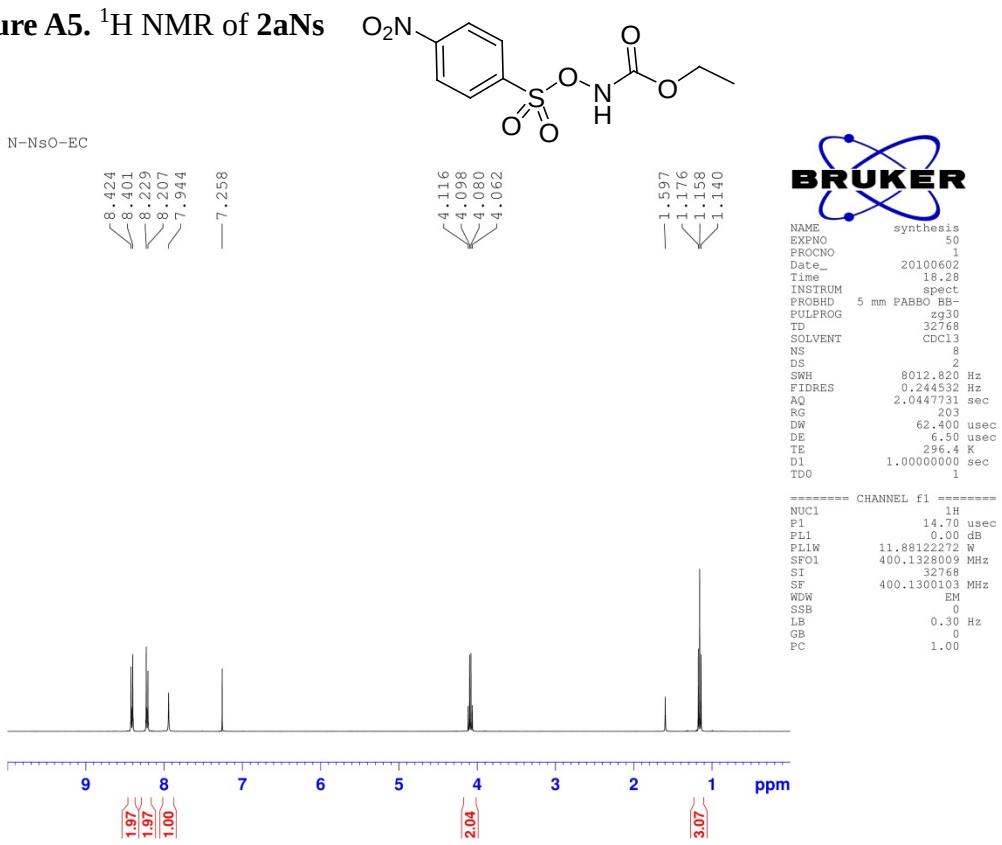

Figure A6. ^{13}C NMR of **2aNs**

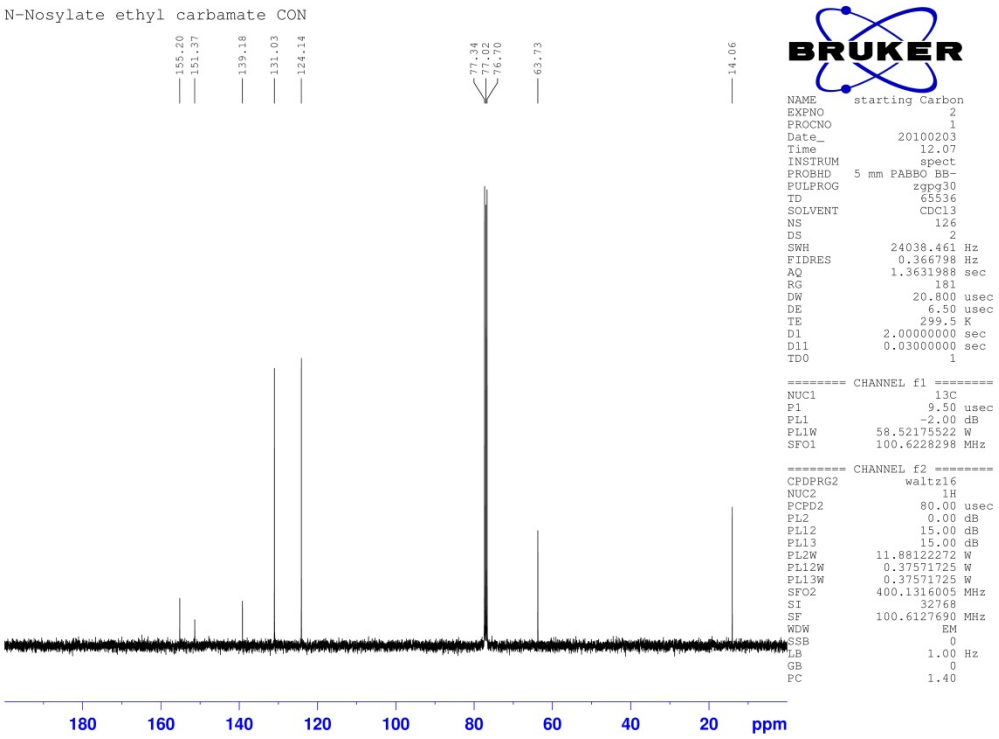

Figure A7. ^{1}H NMR of **2bNs**

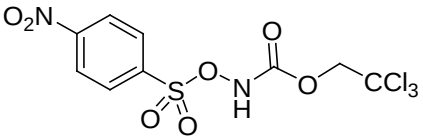

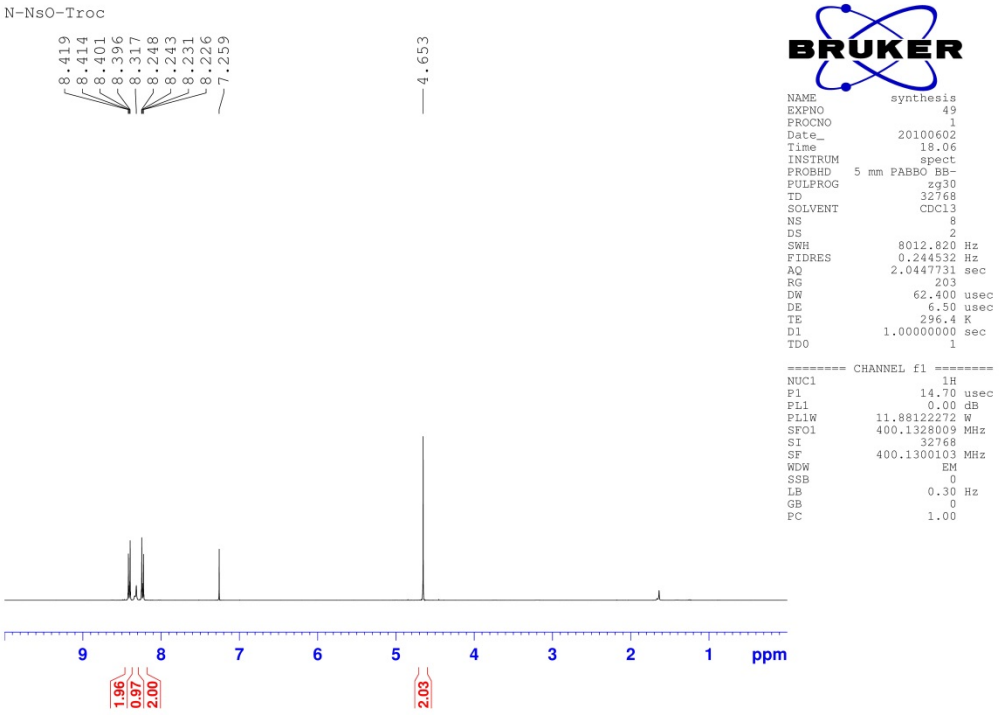

Figure A8. ^{13}C NMR of **2bNs**

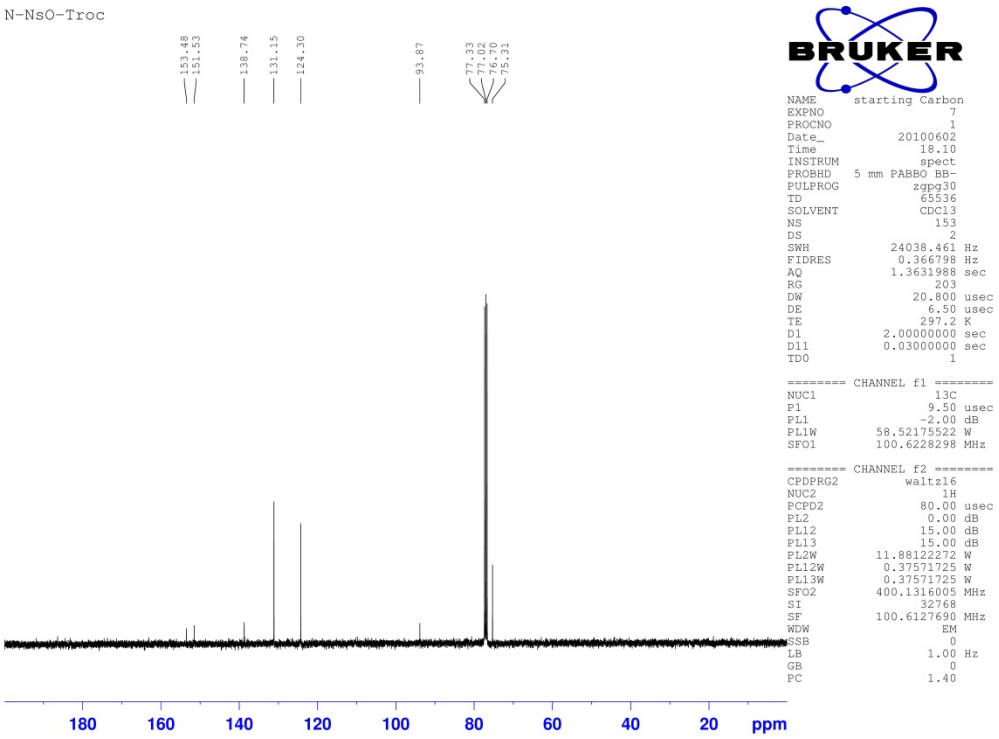

Figure A9. ^{1}H NMR of **2cNs**

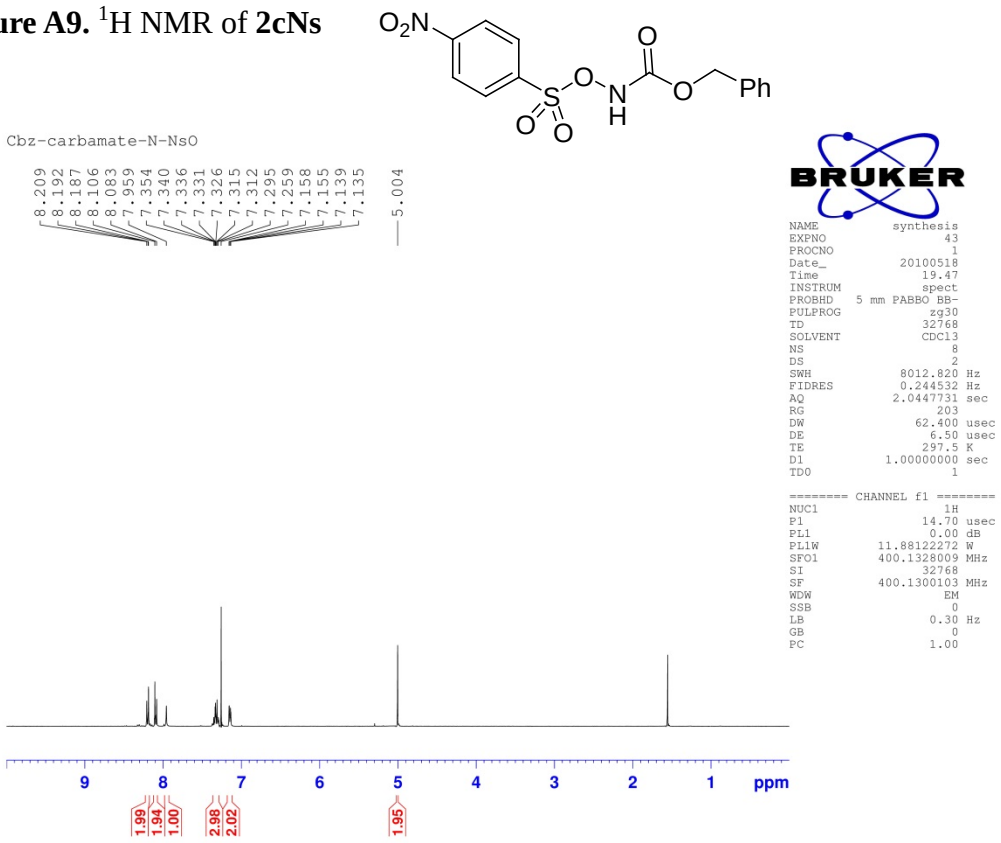

Figure A10. ^{13}C NMR of **2cNs**

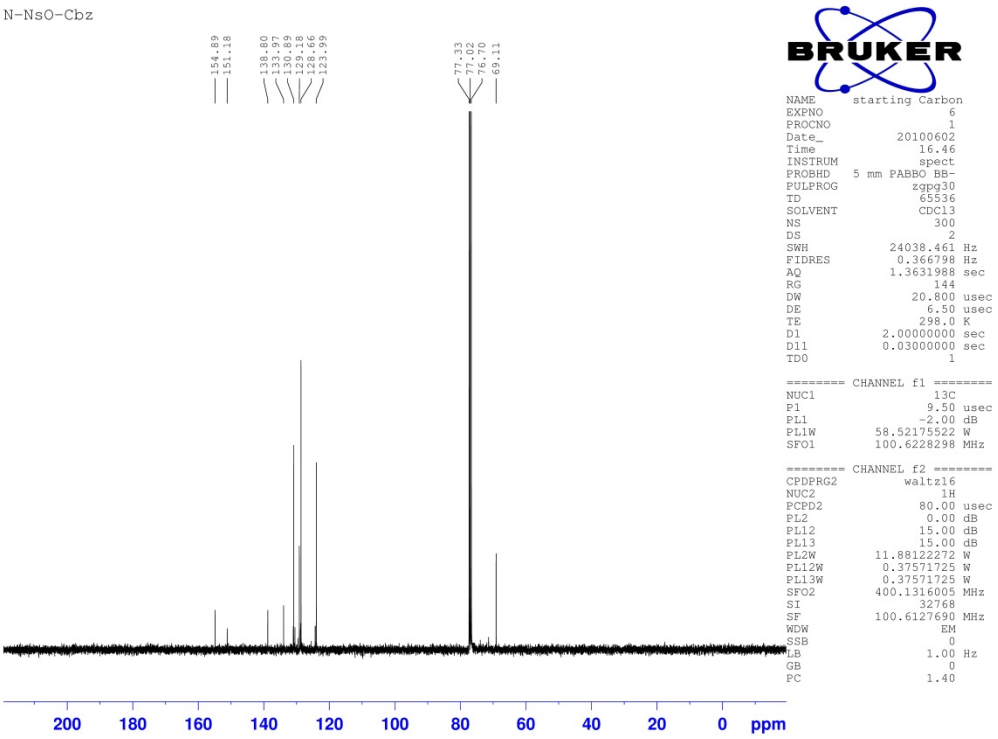

Figure A11. ^{1}H NMR of **3aa**

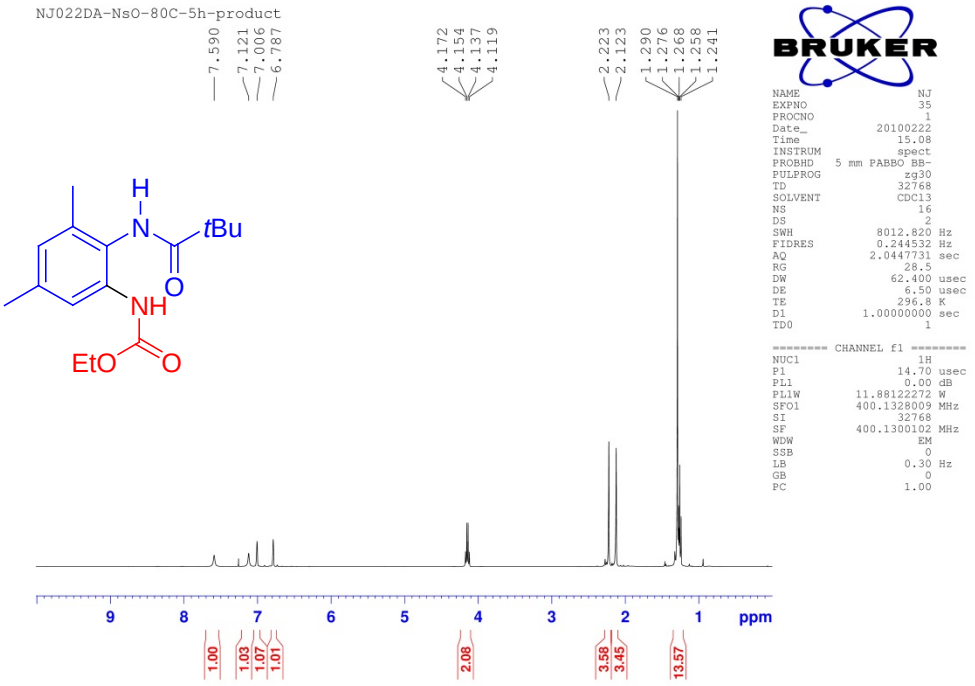

Figure A12. ^{13}C NMR of **3aa**

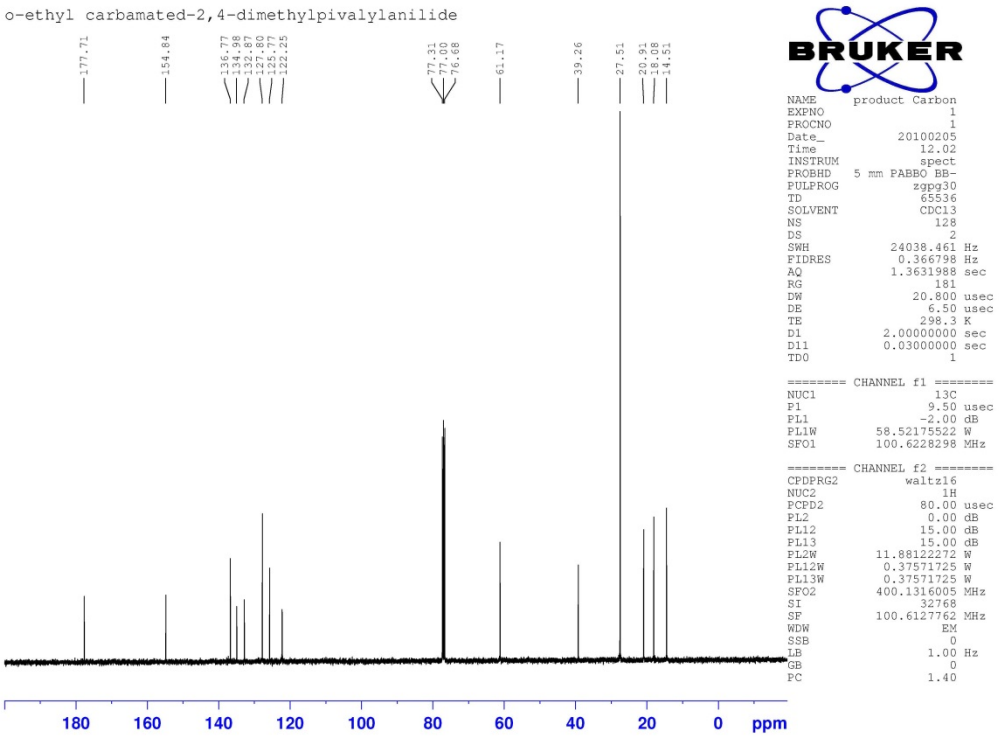

Figure A13. ^{1}H NMR of **3ba**

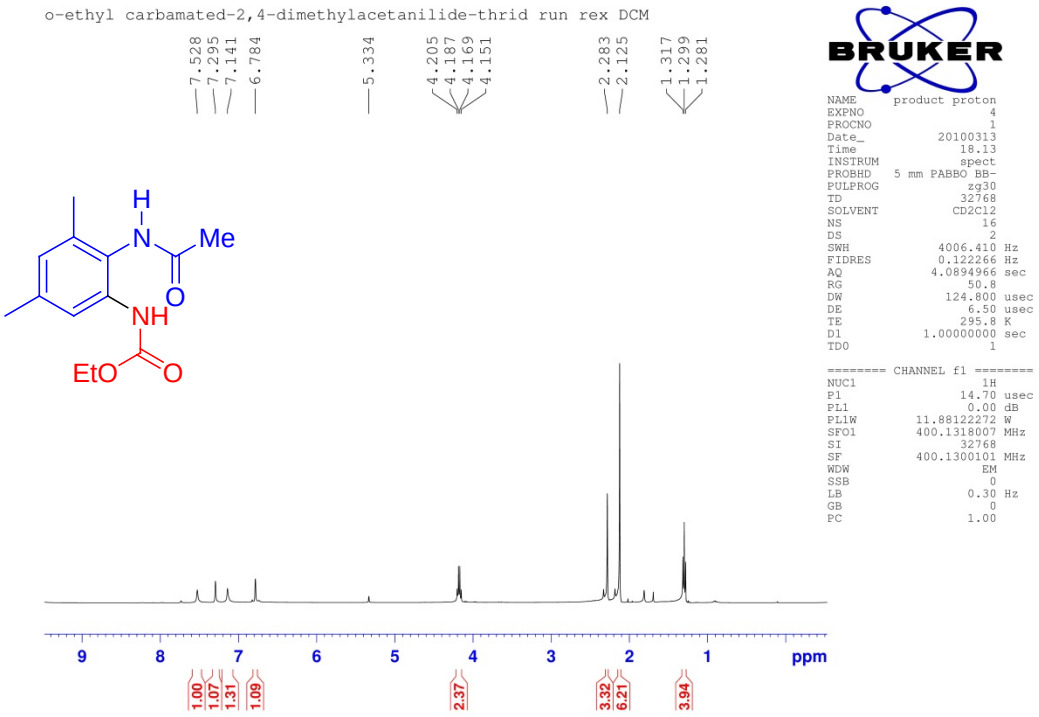

Figure A14. ^{13}C NMR of **3ba**

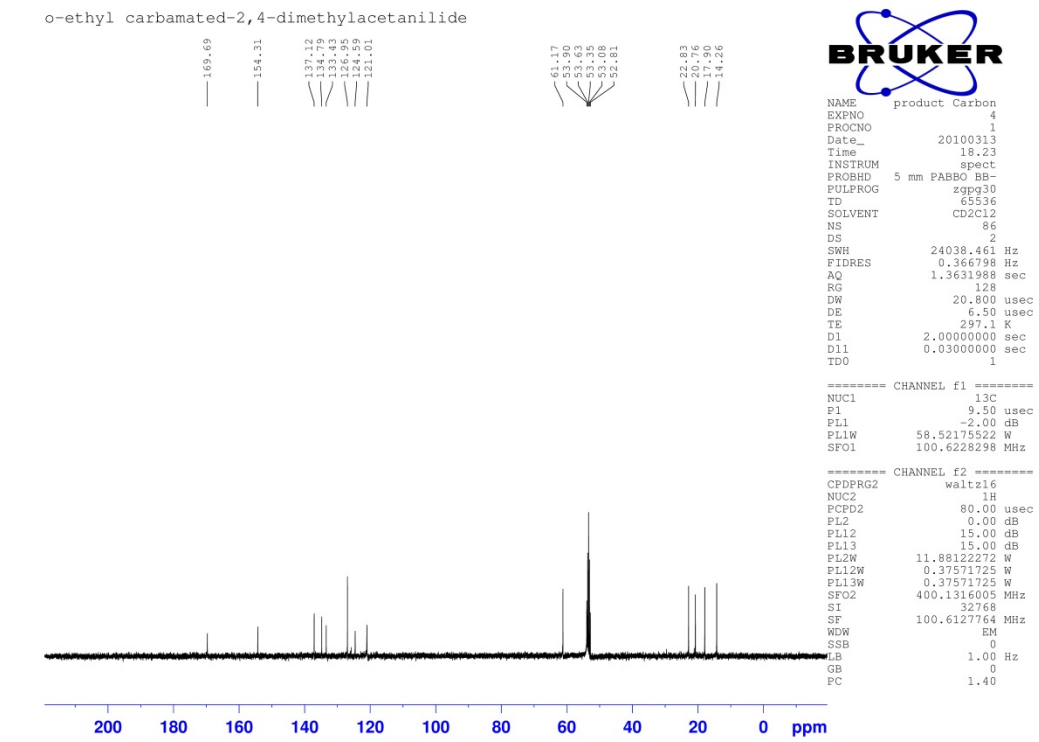

Figure A15. ^{1}H NMR of **3ca**

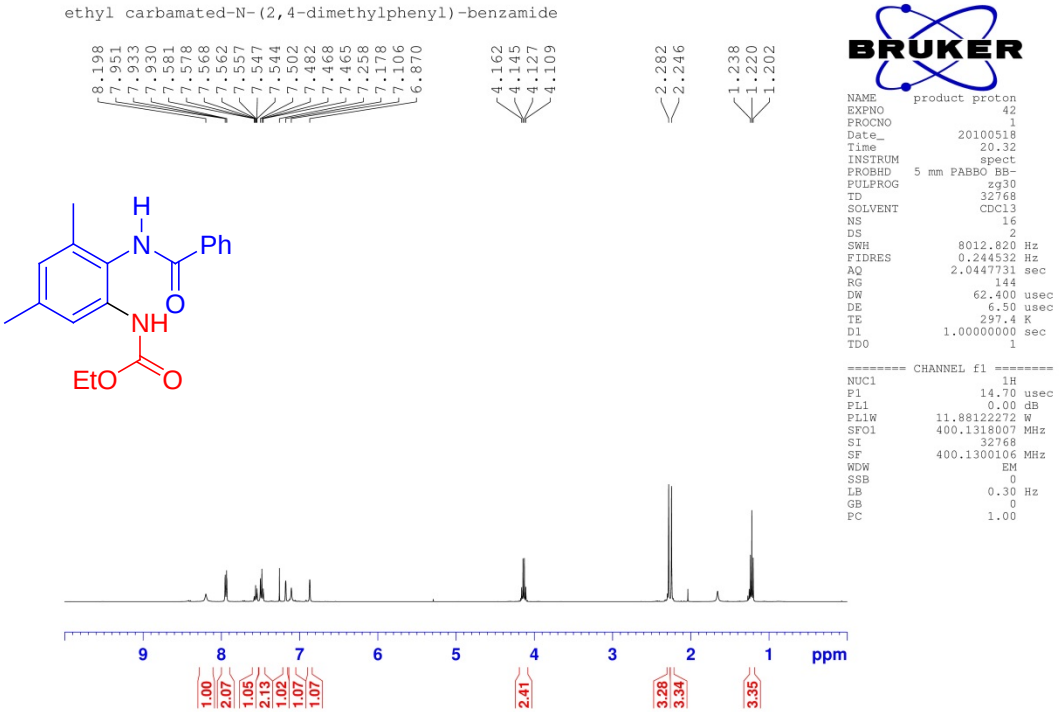

Figure A16. ^{13}C NMR of **3ca**

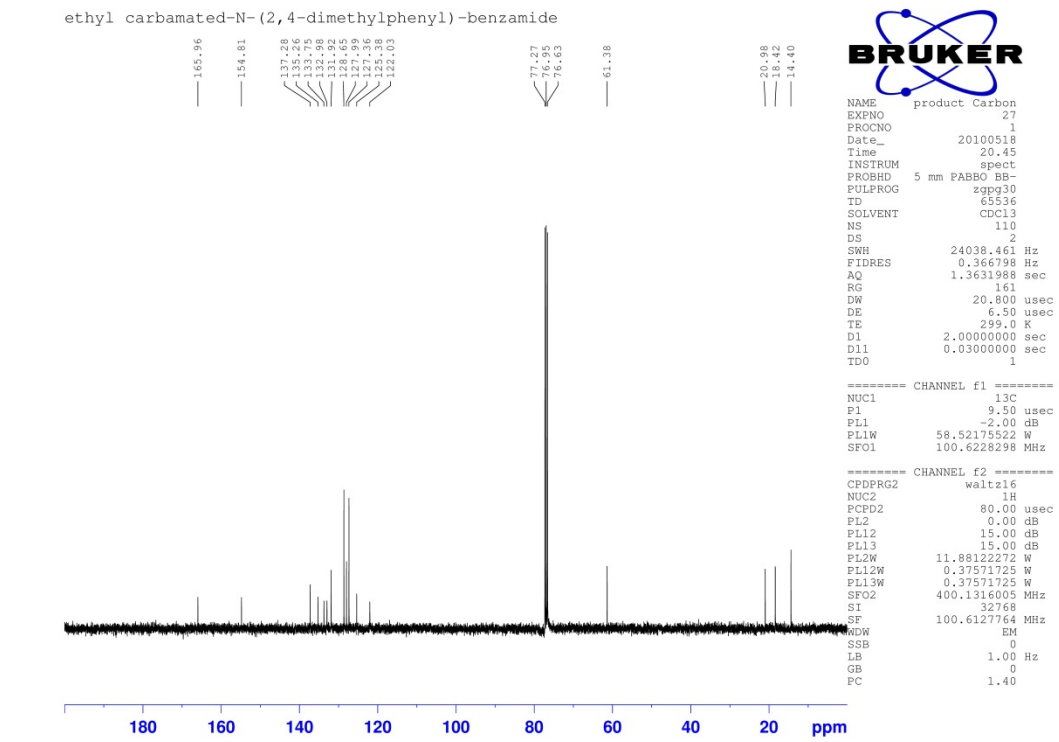

Figure A17. ^{1}H NMR of **3da**

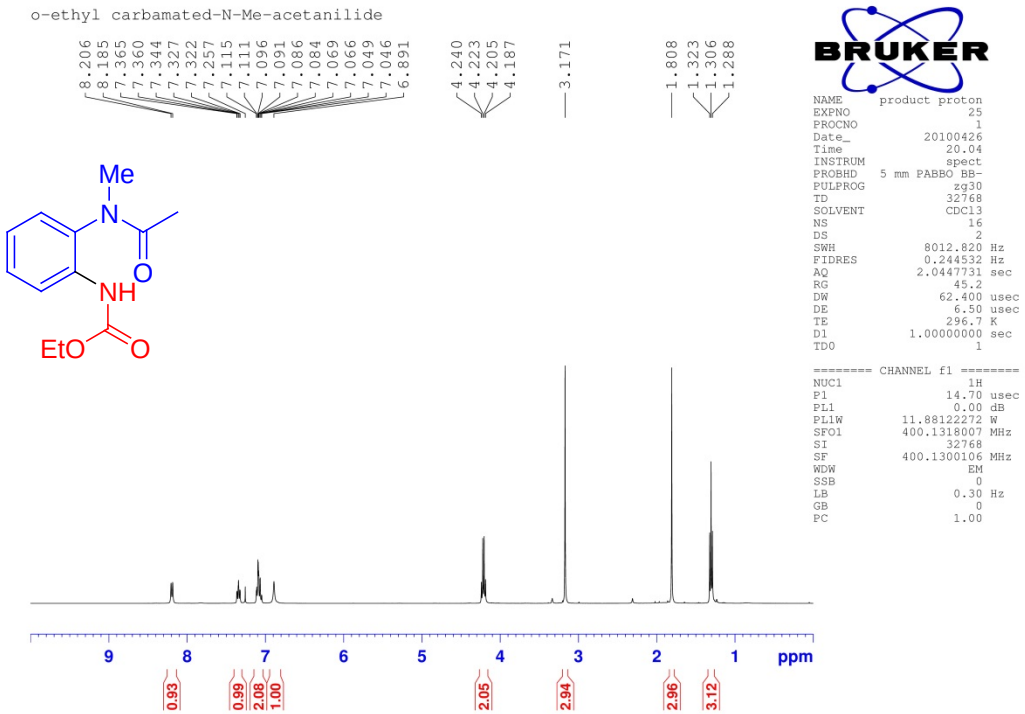

Figure A18. ^{13}C NMR of **3da**

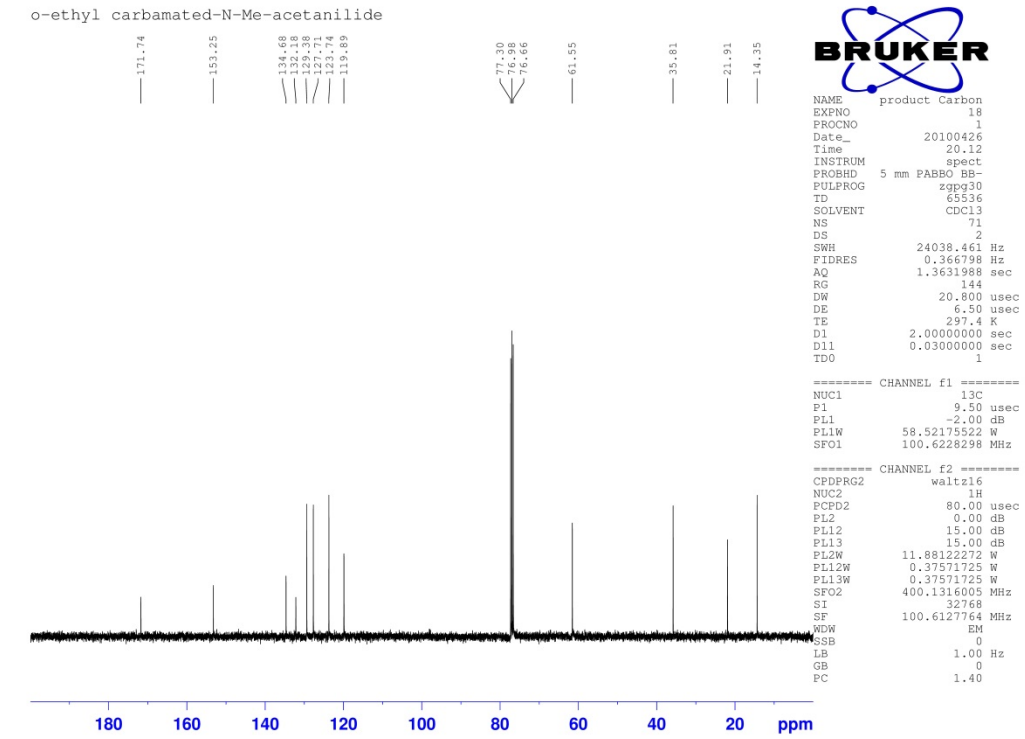

Figure A19. ^{1}H NMR of **3ea**

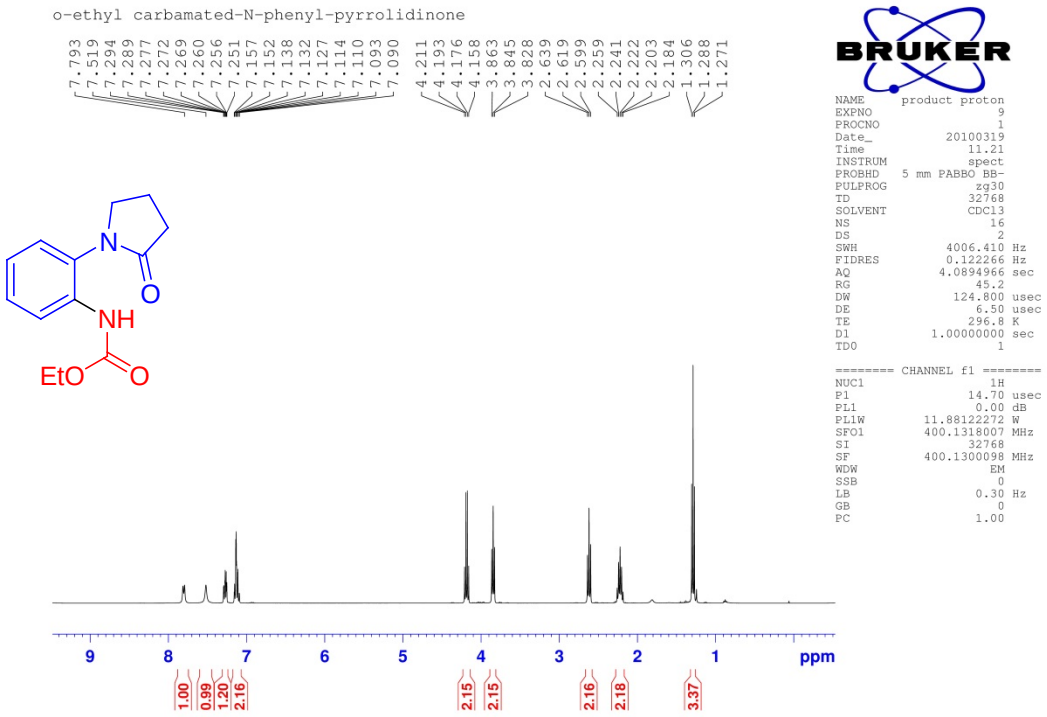

Figure A20. ^{13}C NMR of **3ea**

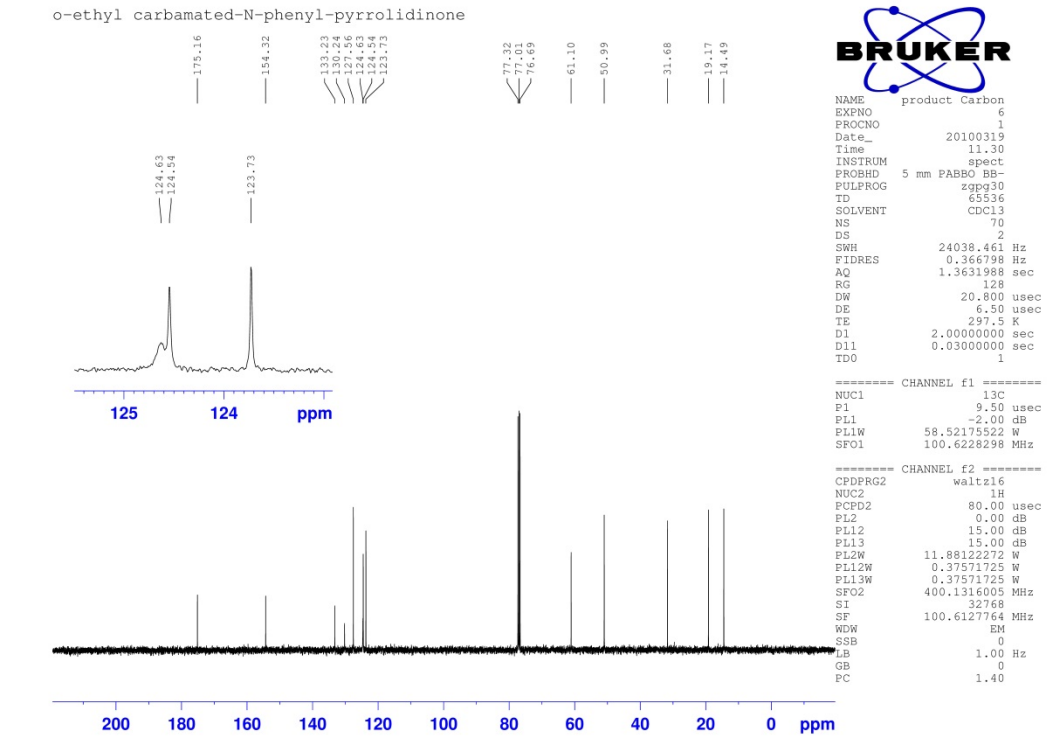

Figure A21. ^{1}H NMR of **3fa**

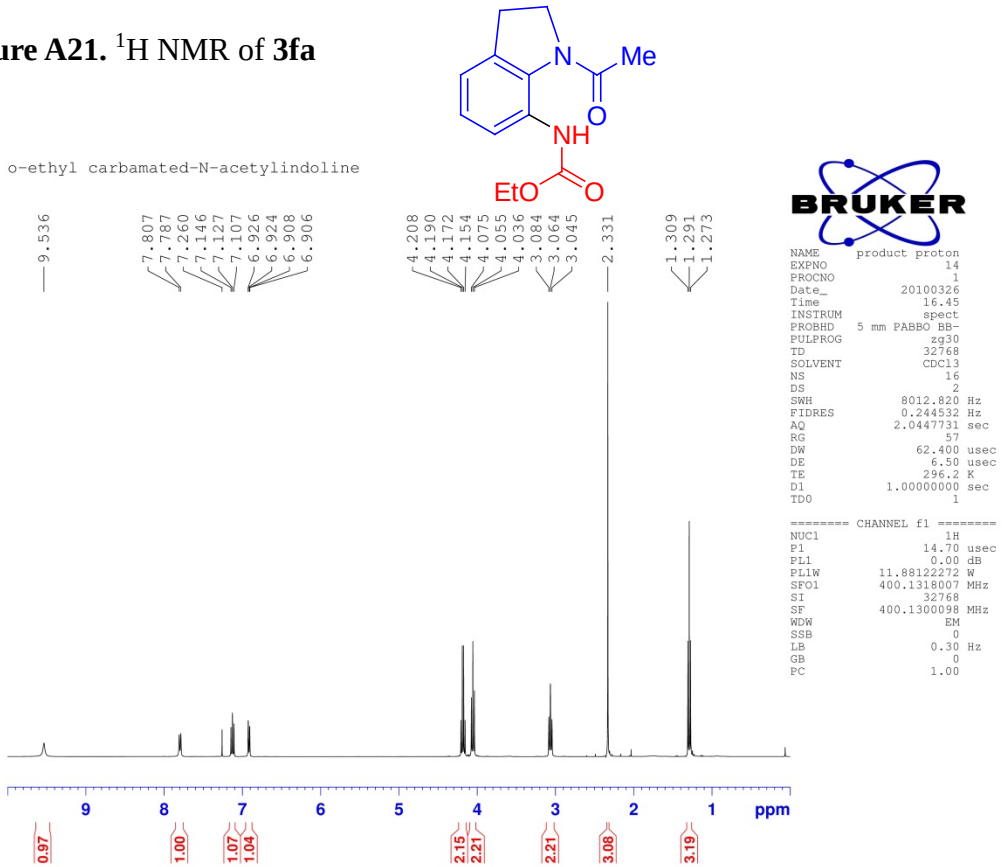

Figure A22. ^{13}C NMR of **3fa**

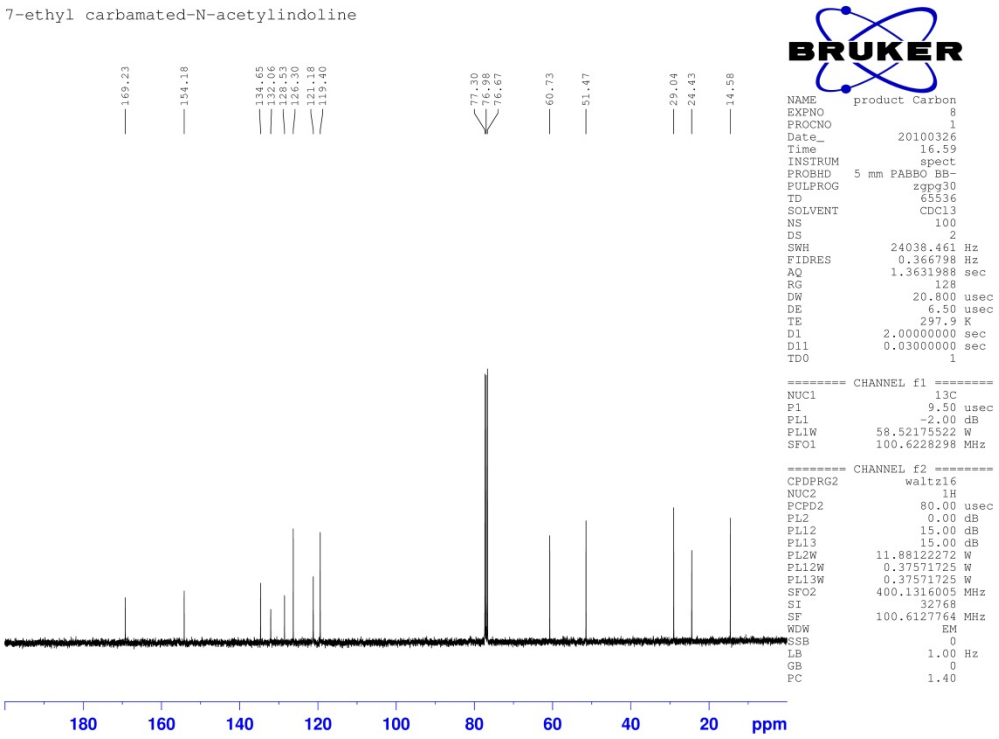

Figure A23. ^{1}H NMR of **3ab**

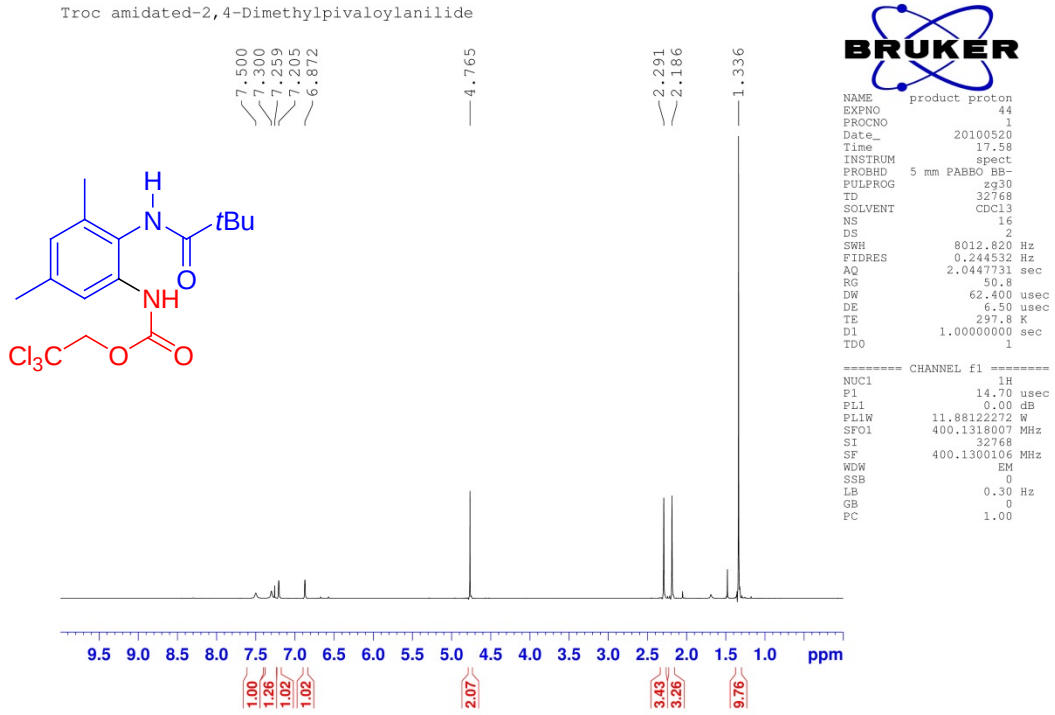

Figure A24. ^{13}C NMR of **3ab**

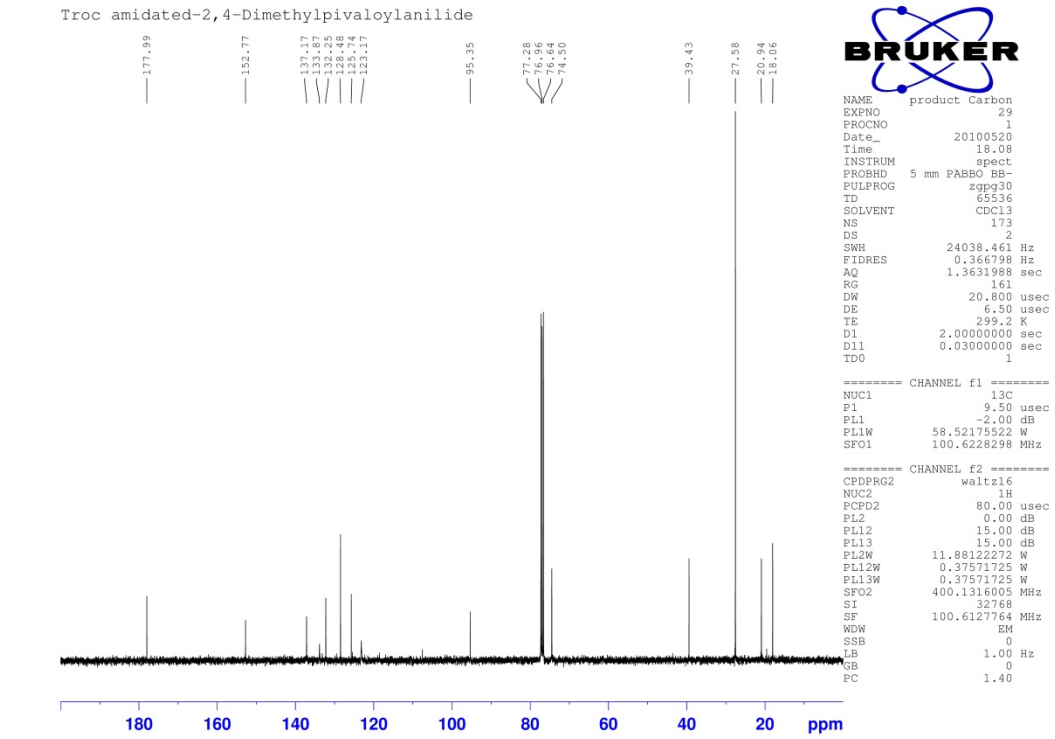

Figure A25 ^{1}H NMR of **3ac**

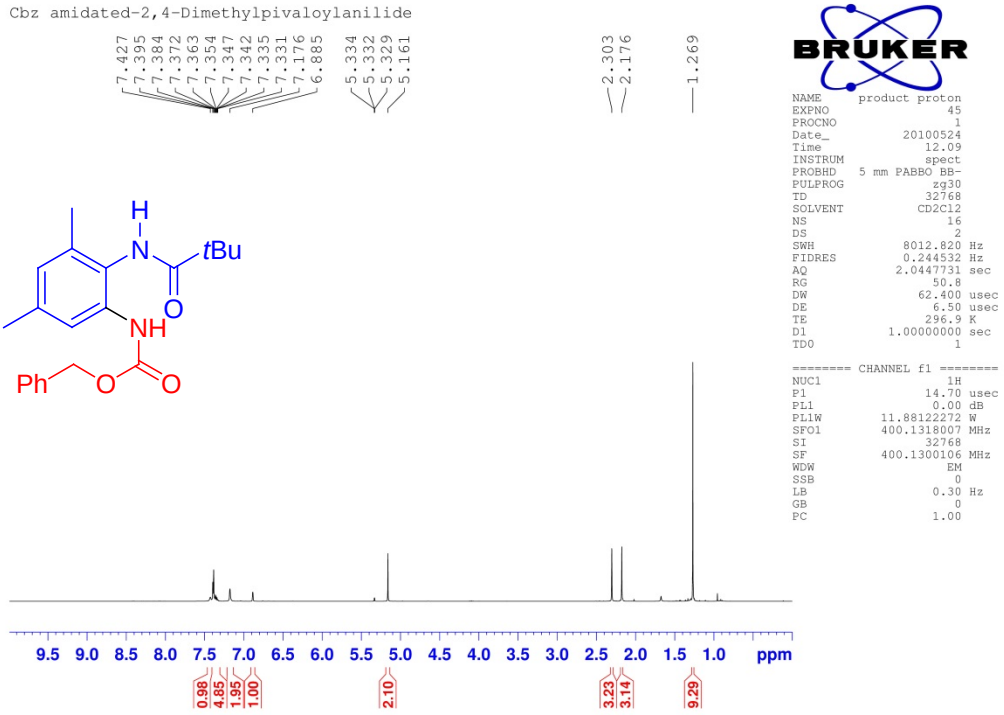

Figure A26. ^{13}C NMR of **3ac**

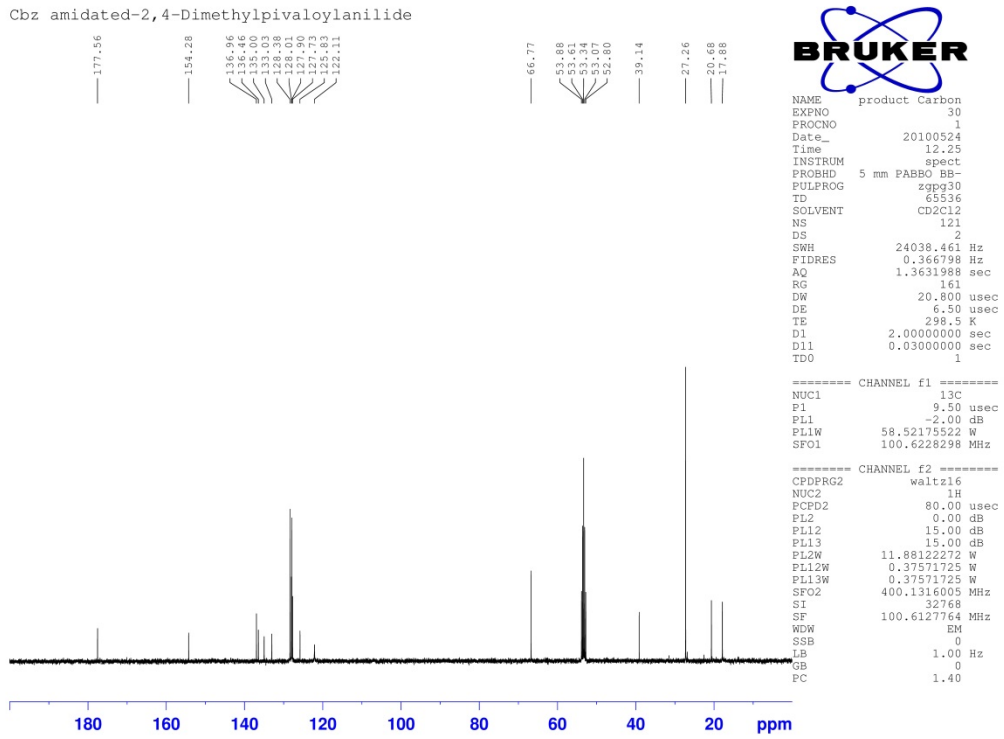

Figure A27. ^{1}H NMR of **3ga**

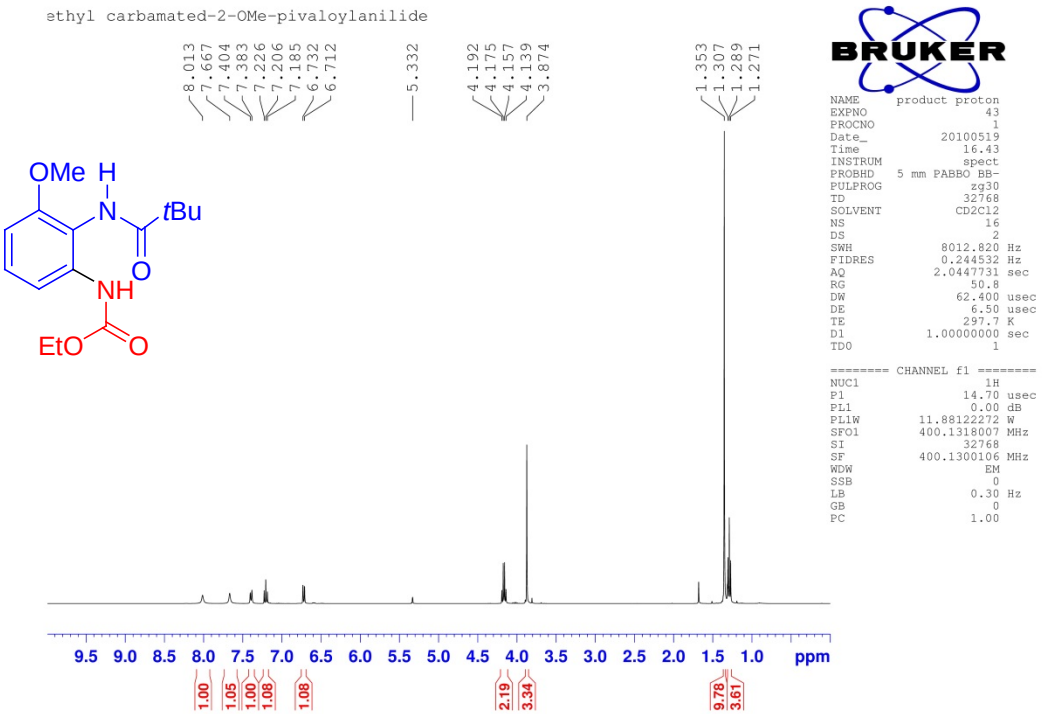

Figure A28. ^{13}C NMR of **3ga**

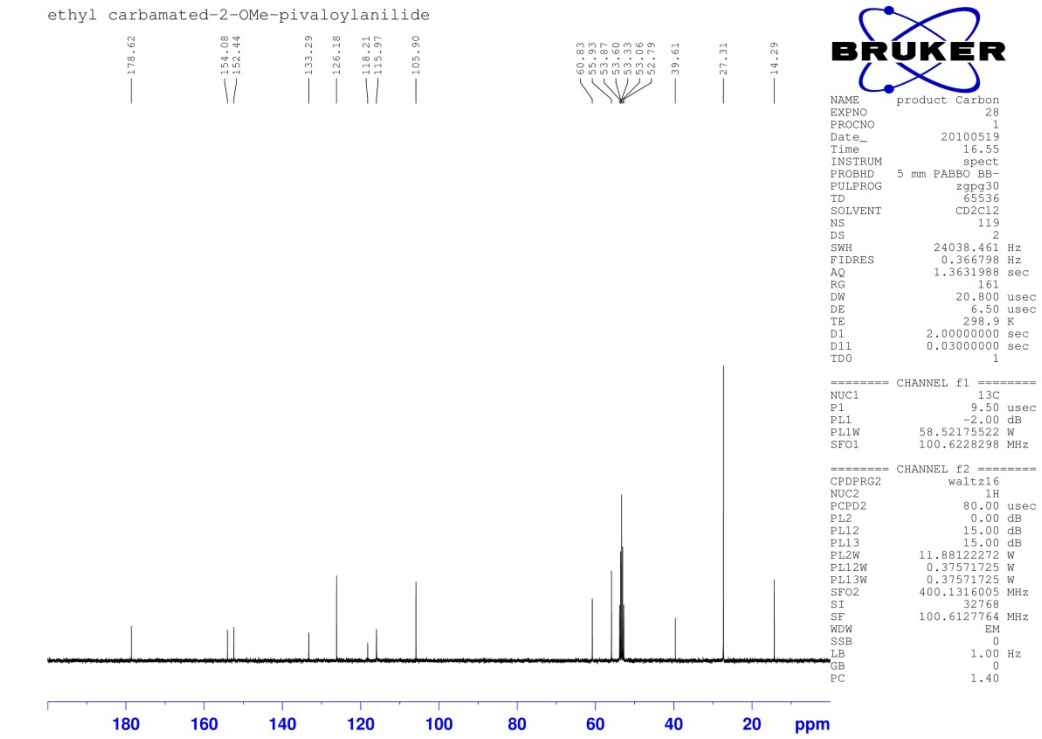

Figure A29. ^{1}H NMR of **3ha**

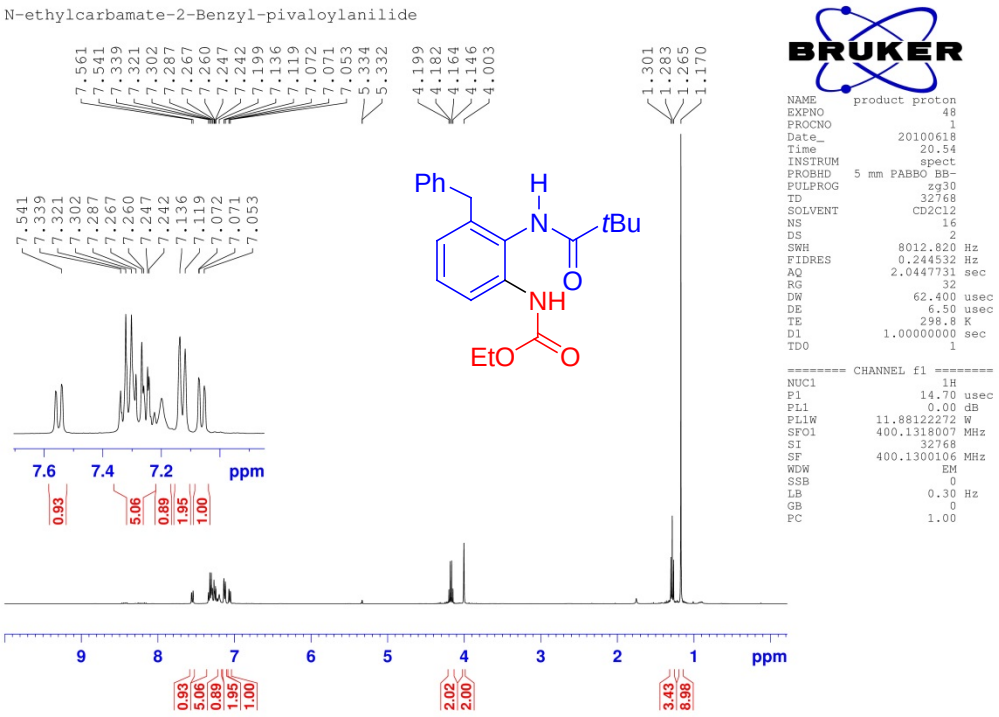

Figure A30. ^{13}C NMR of **3ha**

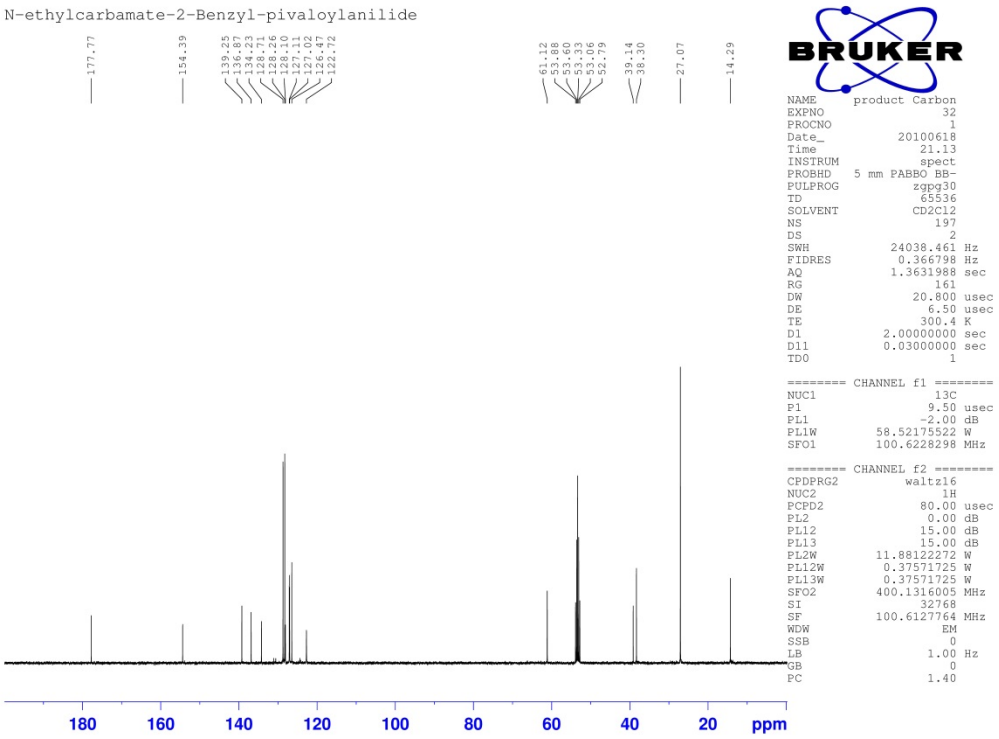

Figure A31. ^{1}H NMR of **3ia**

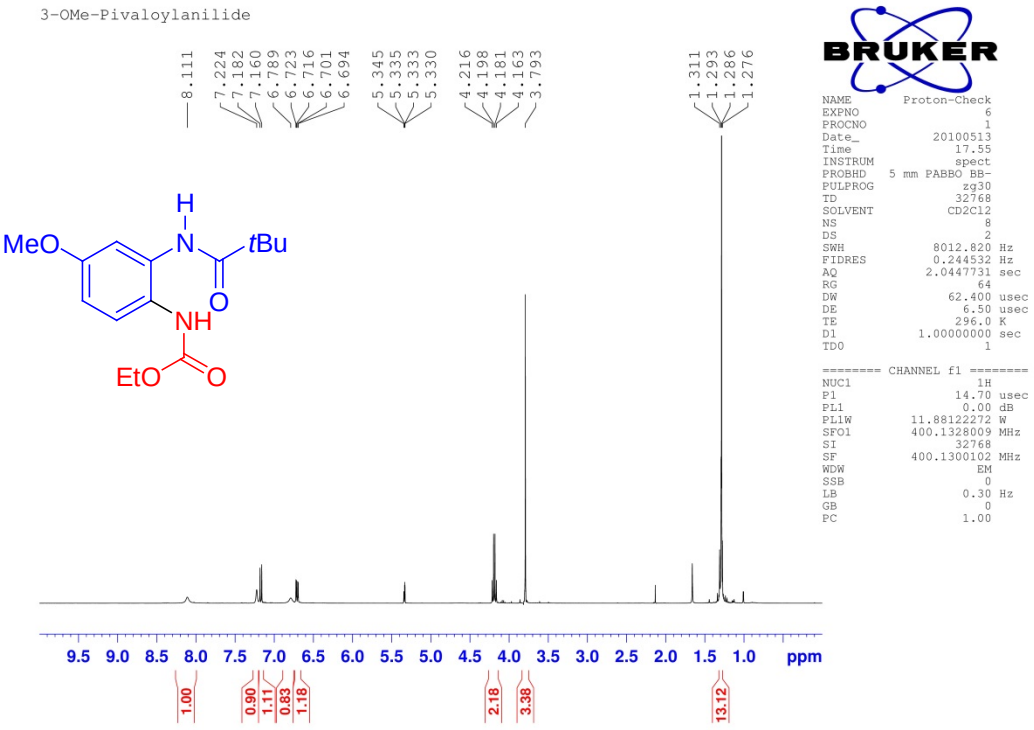

Figure A32. ^{13}C NMR of **3ia**

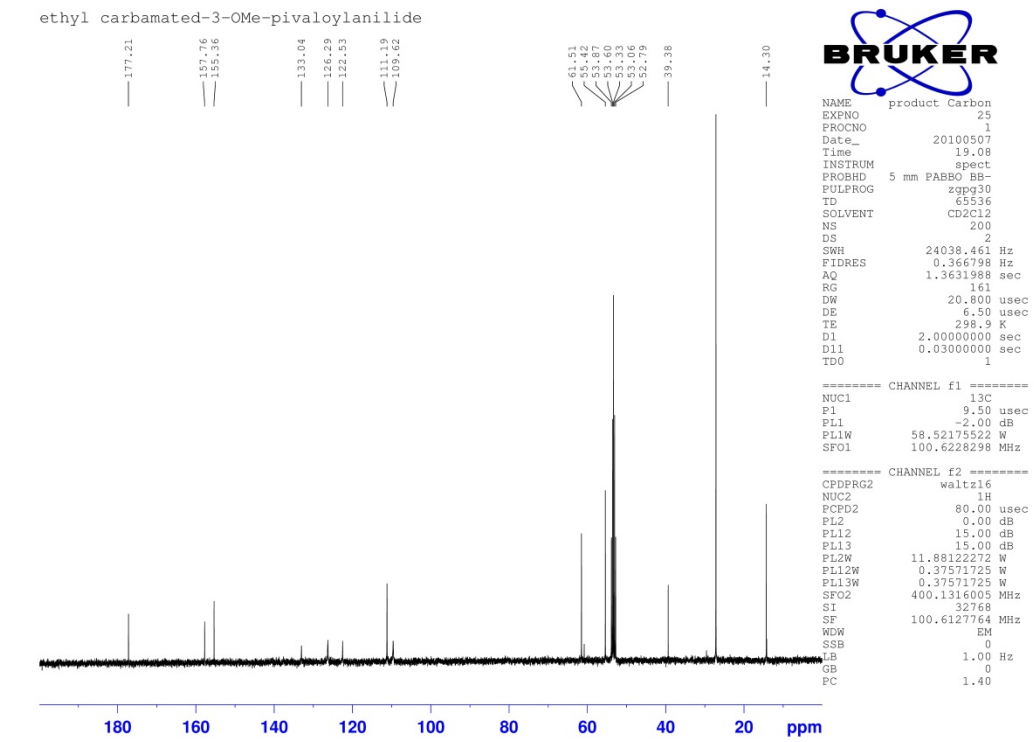

Figure A33. ^{1}H NMR of **3ja**

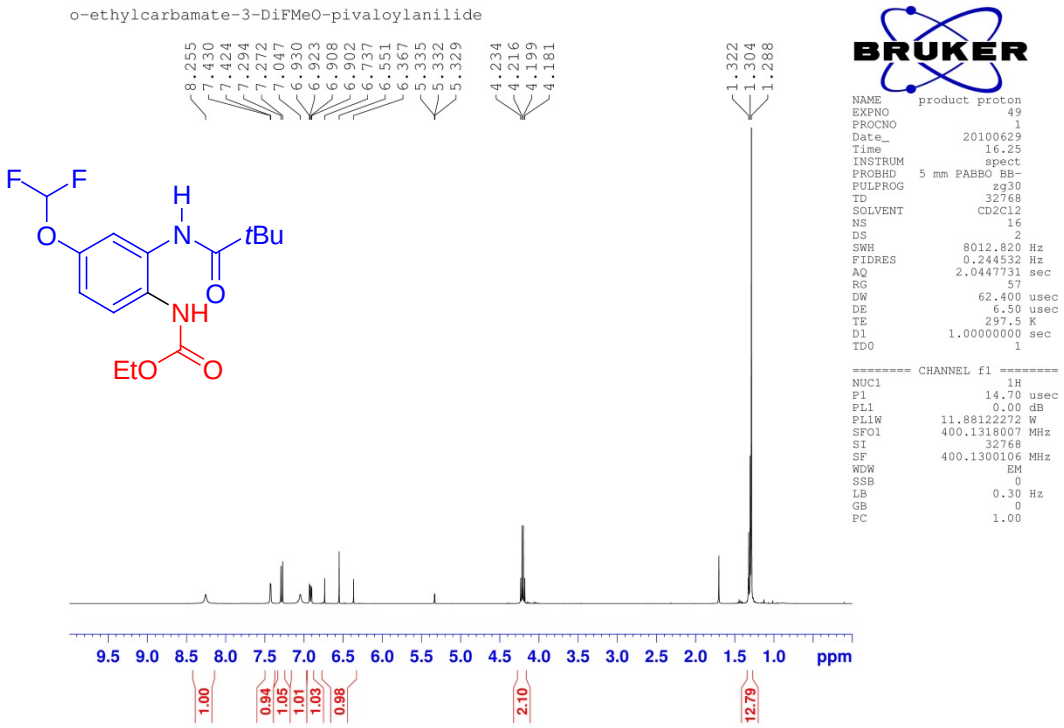

Figure A34. ^{13}C NMR of **3ja**

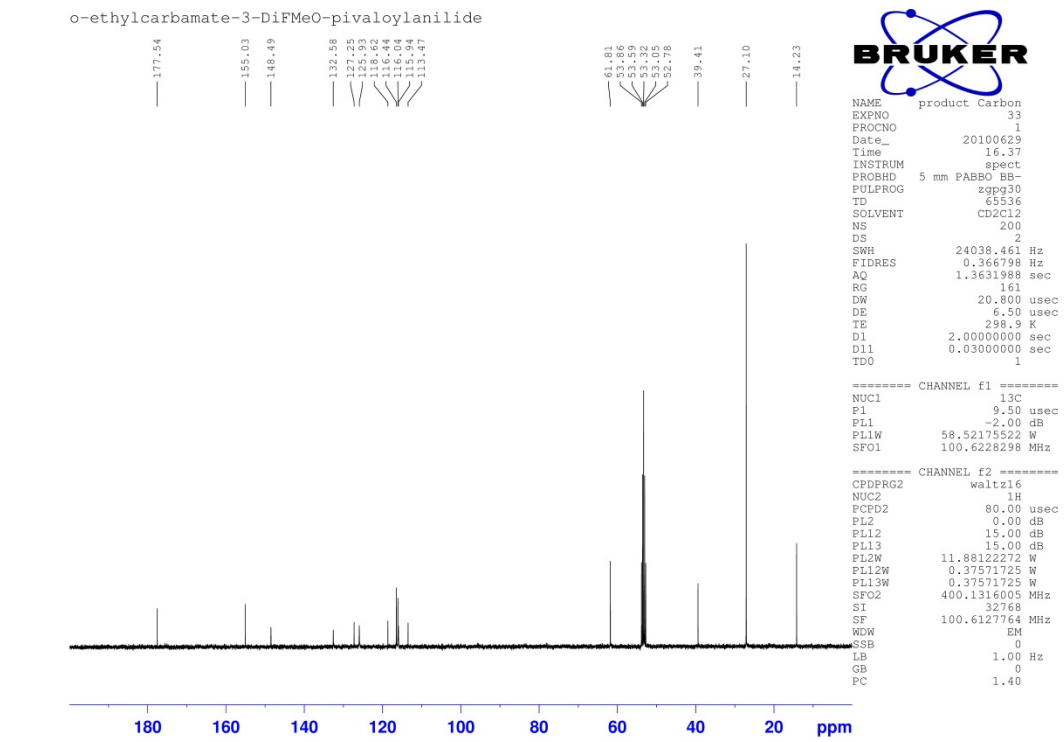

Figure A35. ^{1}H NMR of **3ka**

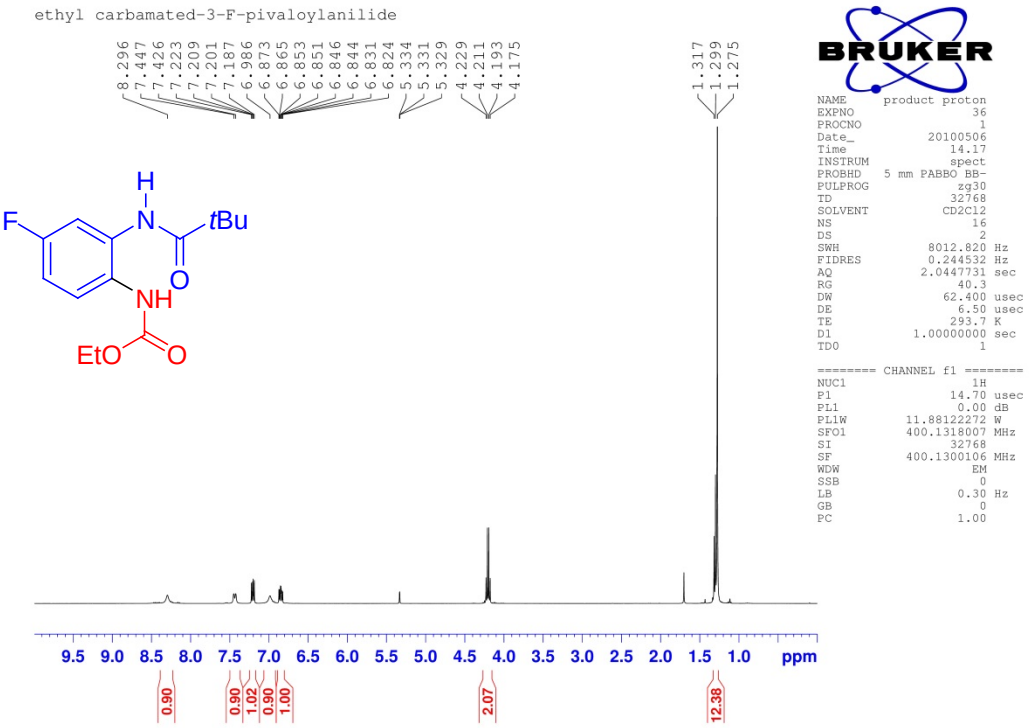

Figure A36. ^{13}C NMR of **3ka**

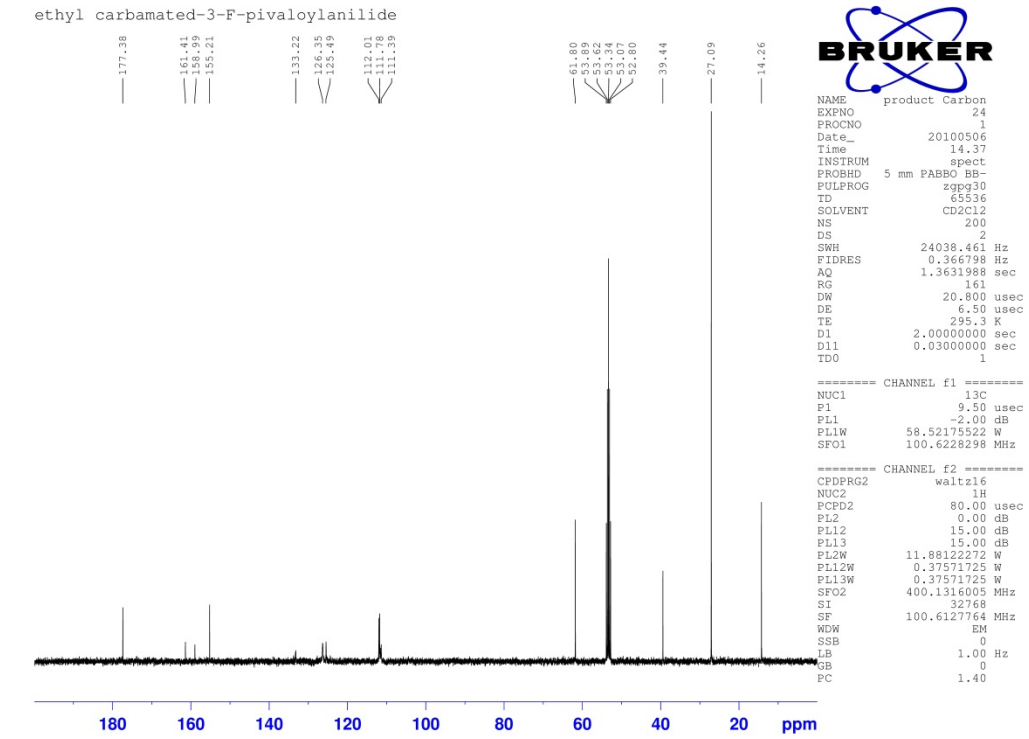

Figure A37. ^{1}H NMR of **3la**

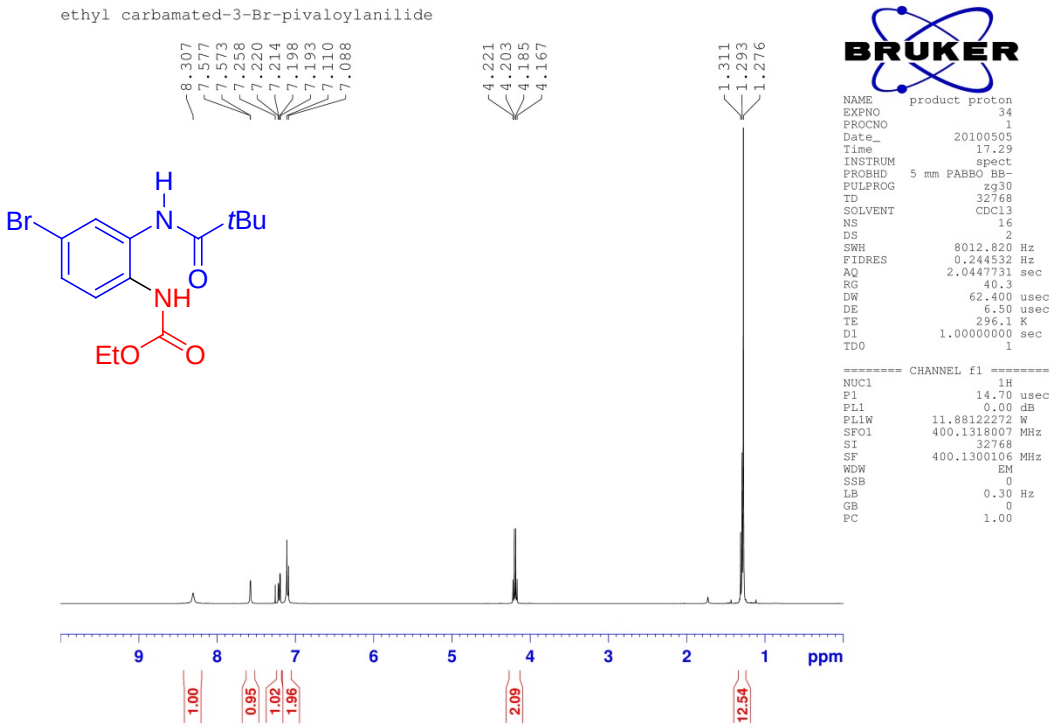

Figure A38. ^{13}C NMR of **3la**

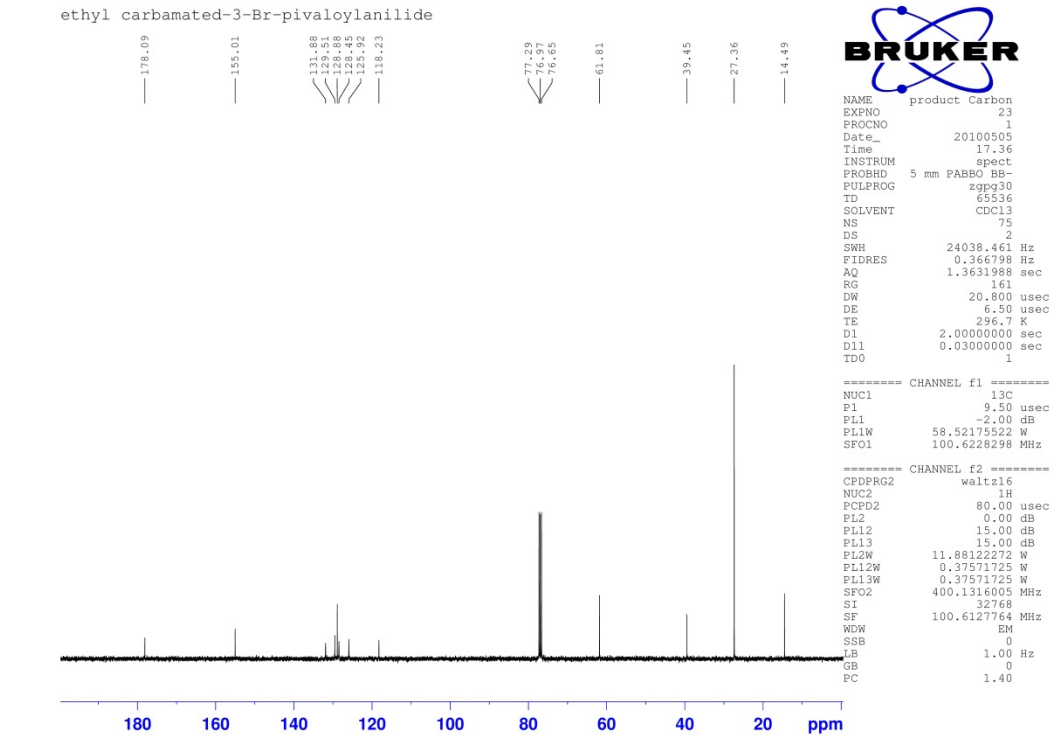

Figure A39. ^{1}H NMR of **3ma**

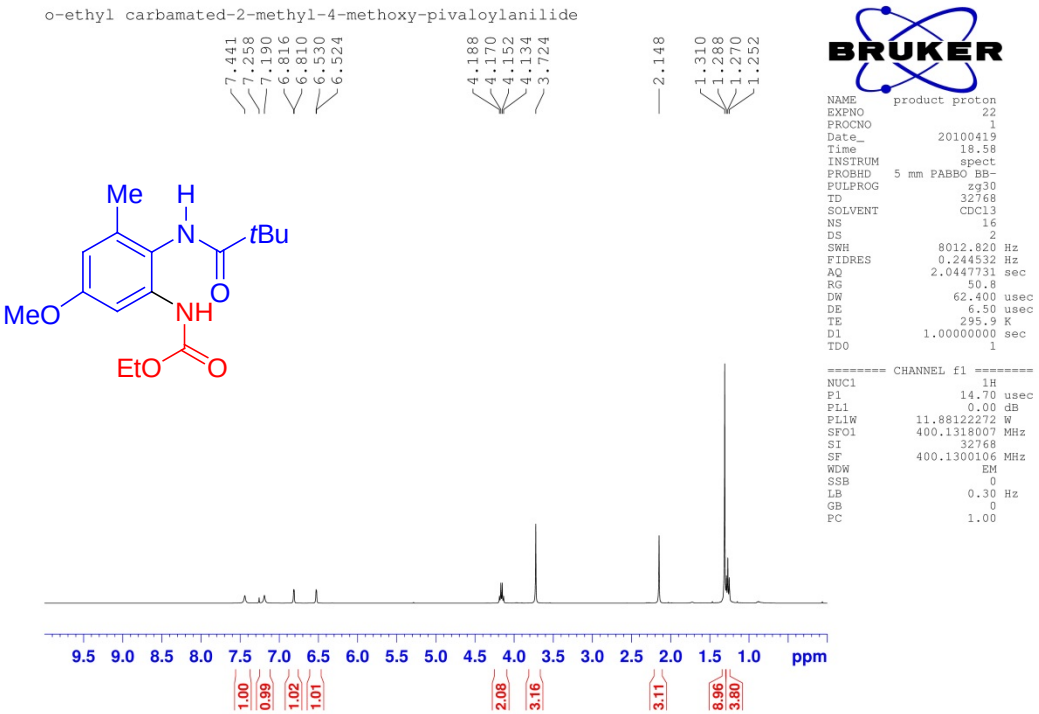

Figure A40. ^{13}C NMR of **3ma**

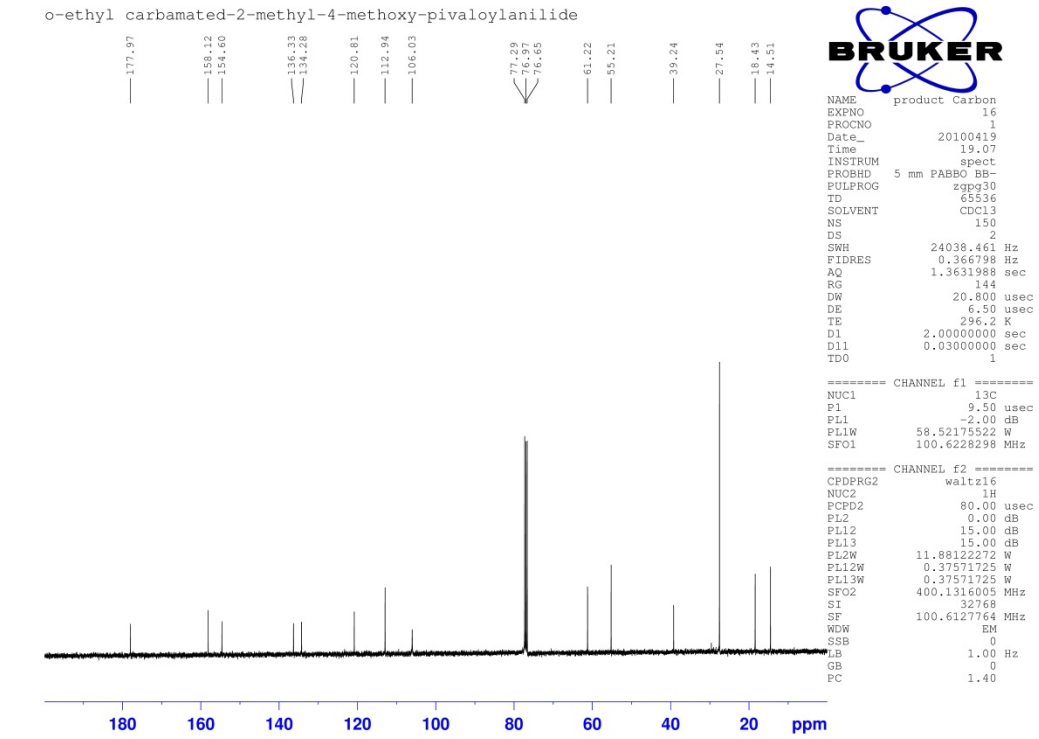

Figure A41. ^{1}H NMR of **3na**

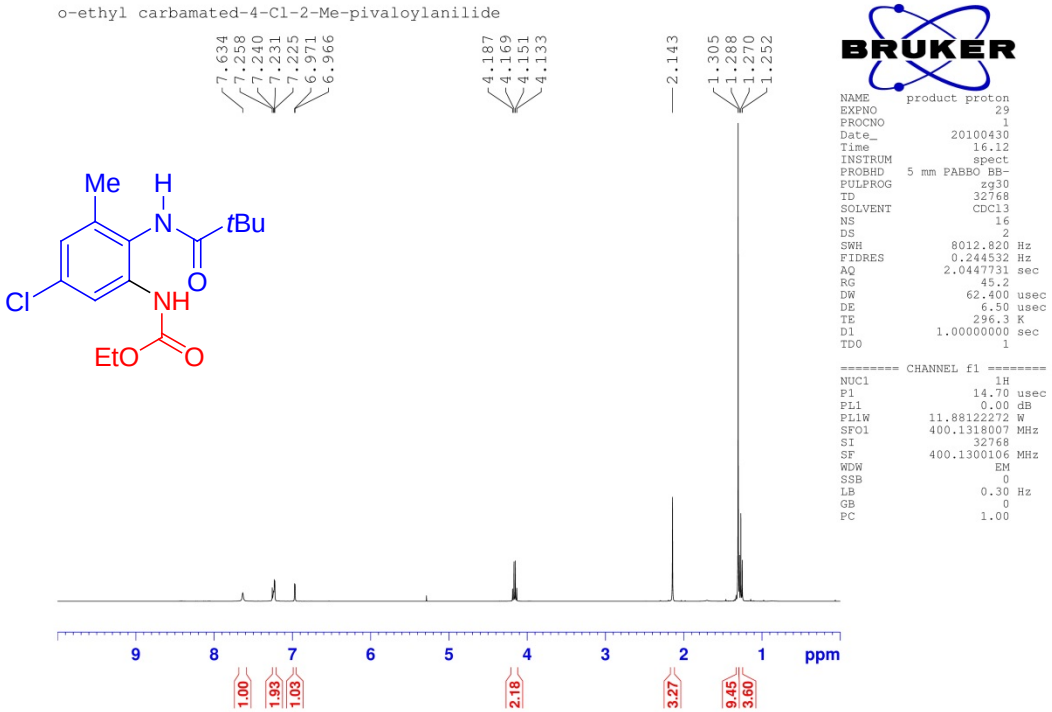

Figure A42. ^{13}C NMR of **3na**

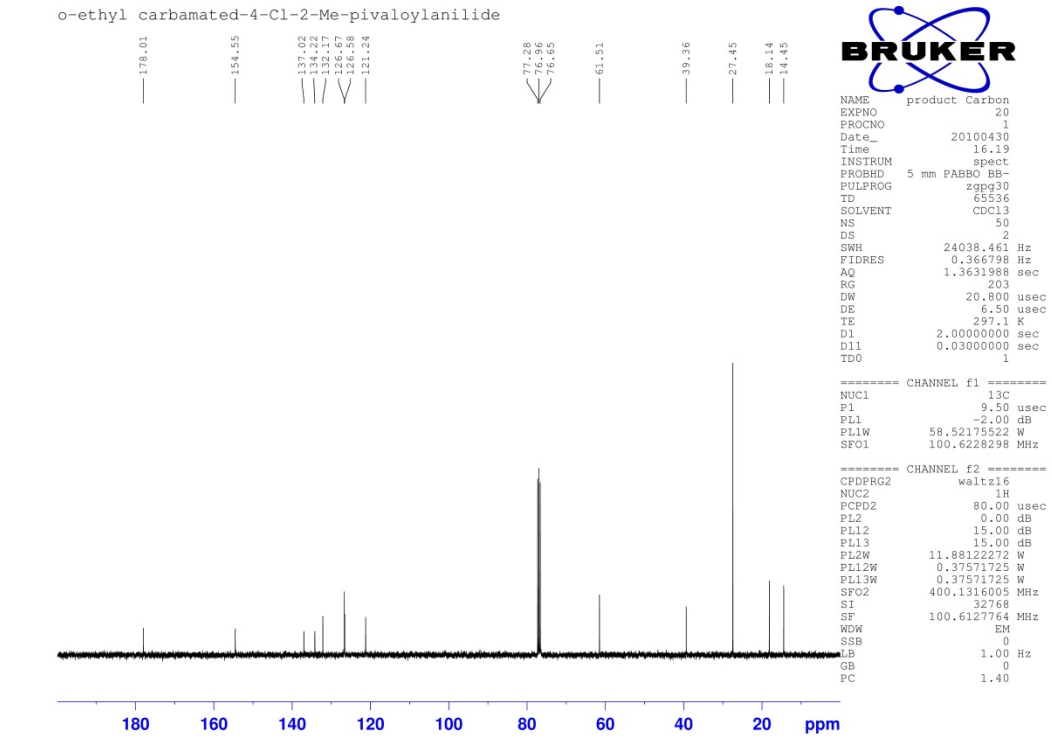

Figure A43. ^{1}H NMR of **3oa**

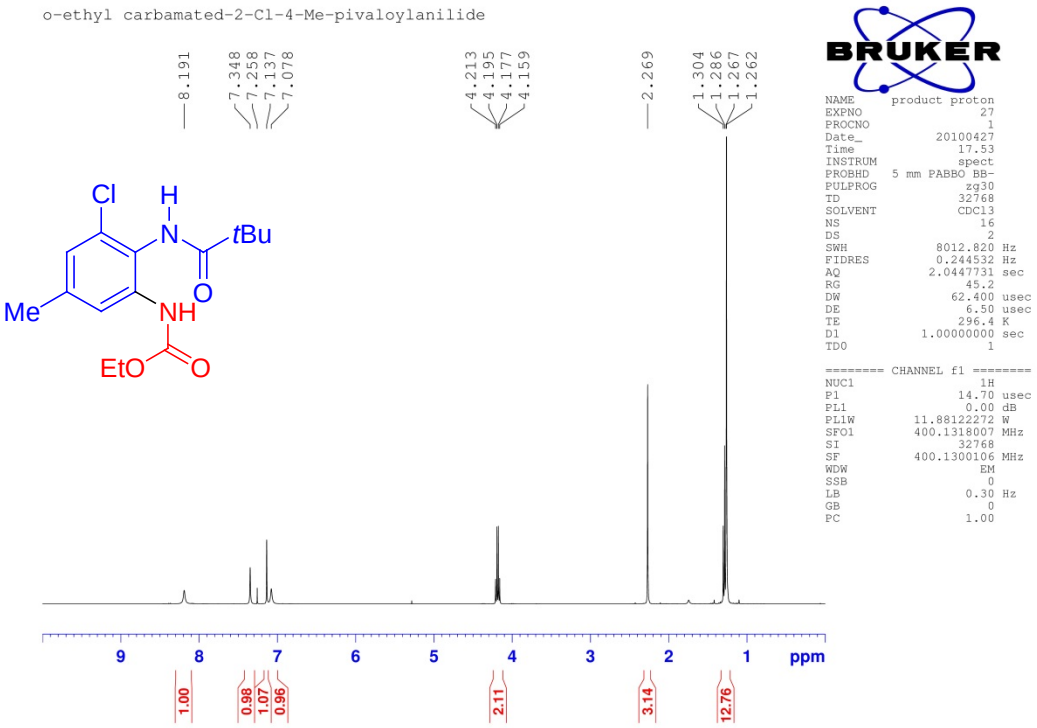

Figure A44. ^{13}C NMR of **3oa**

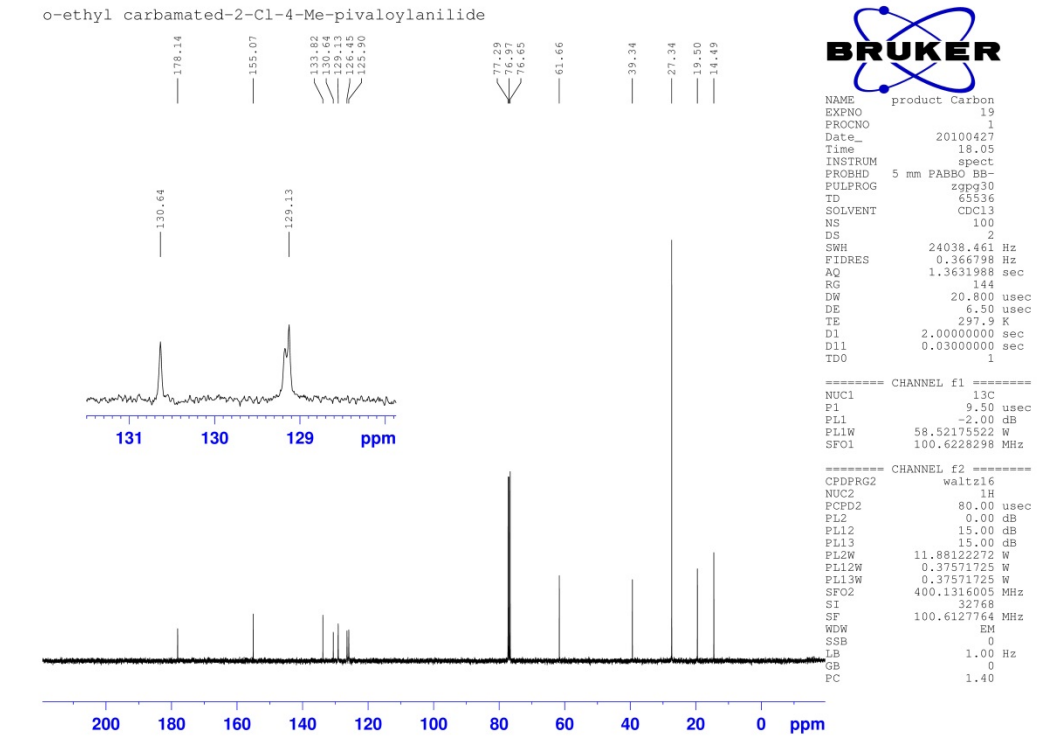

Figure A45. ^{1}H NMR of **3pa**

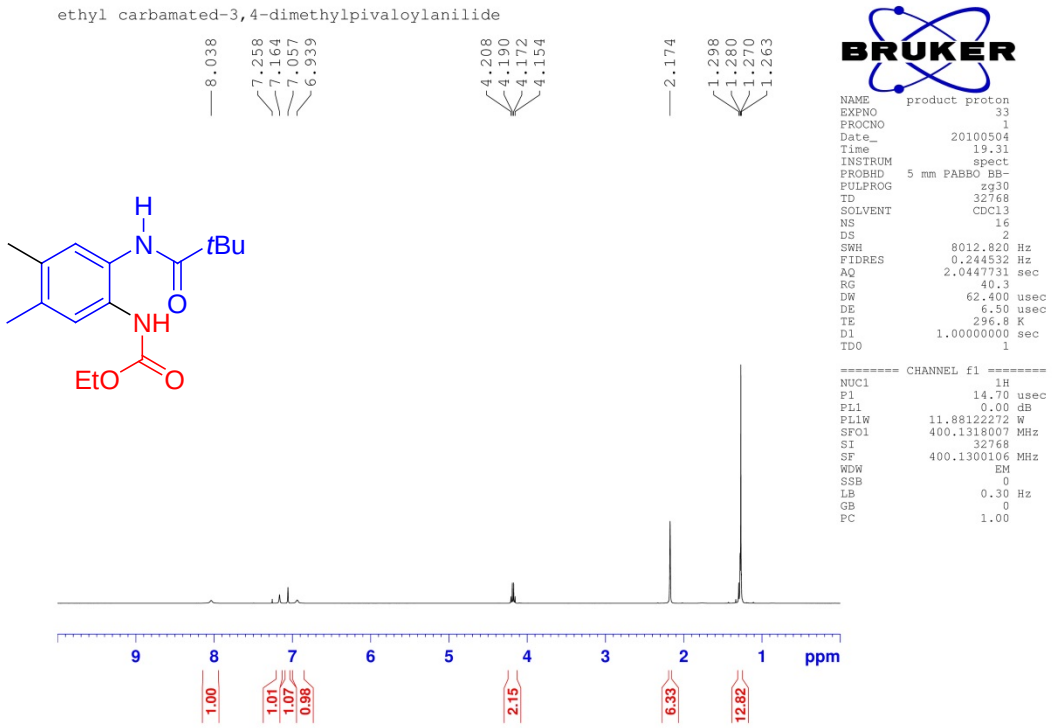

Figure A46. ^{13}C NMR of **3pa**

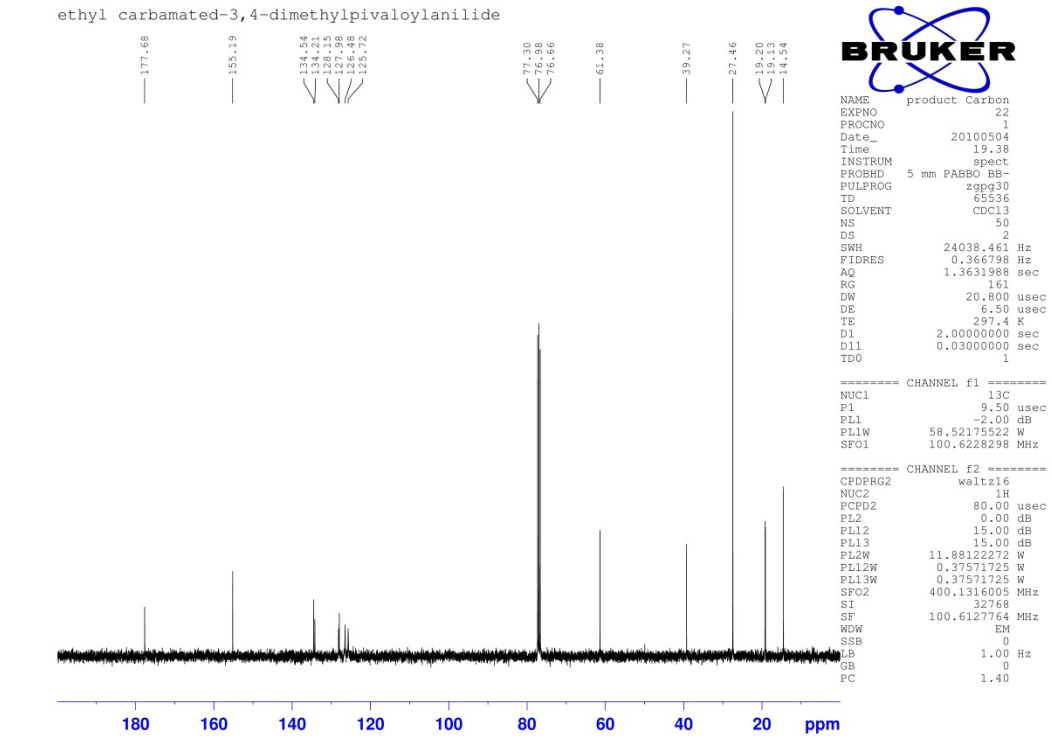

Figure A47. ^{1}H NMR of **3qa**

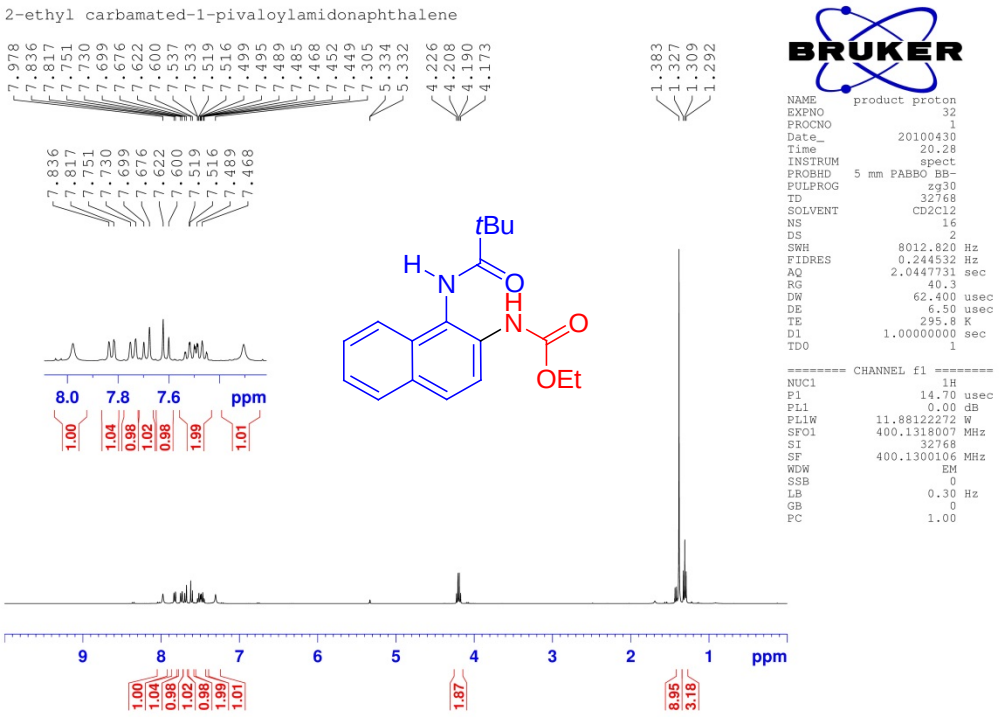

Figure A48. ^{13}C NMR of **3qa**

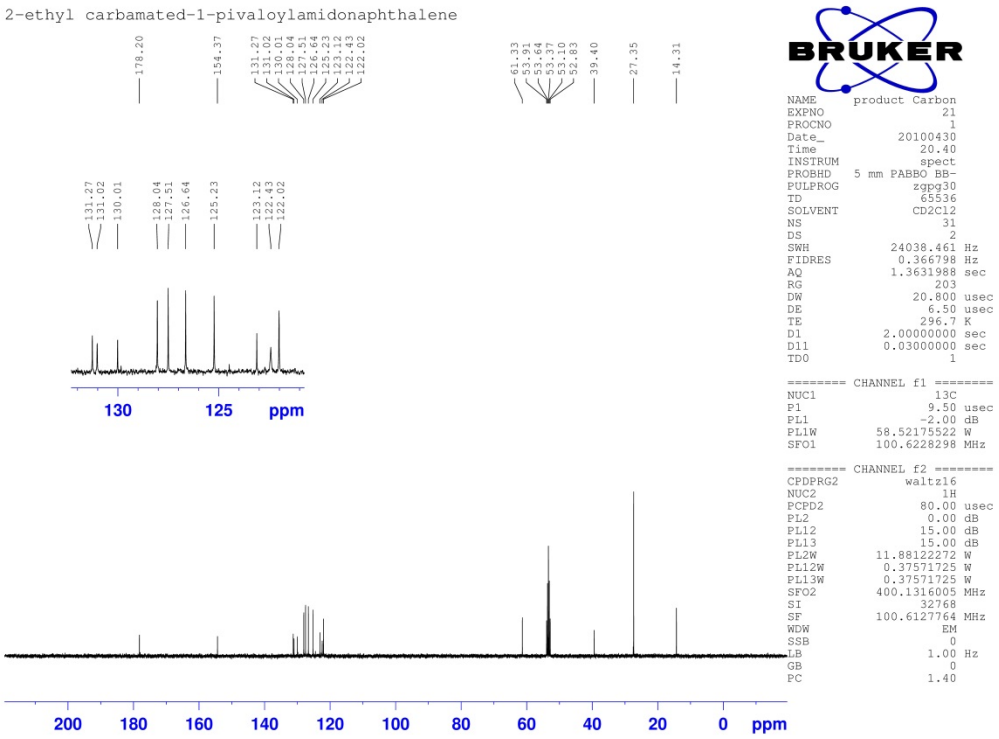

Figure A49. ^{1}H NMR of **3ra**

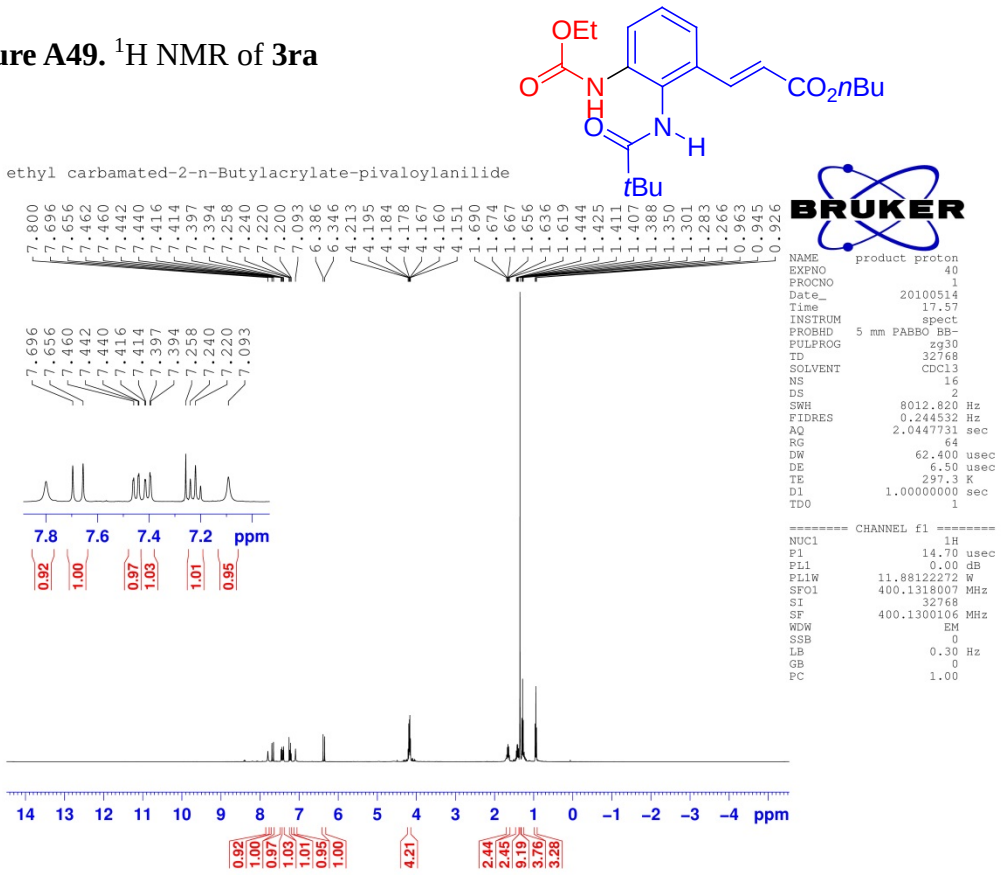

Figure A50. ^{13}C NMR of **3ra**

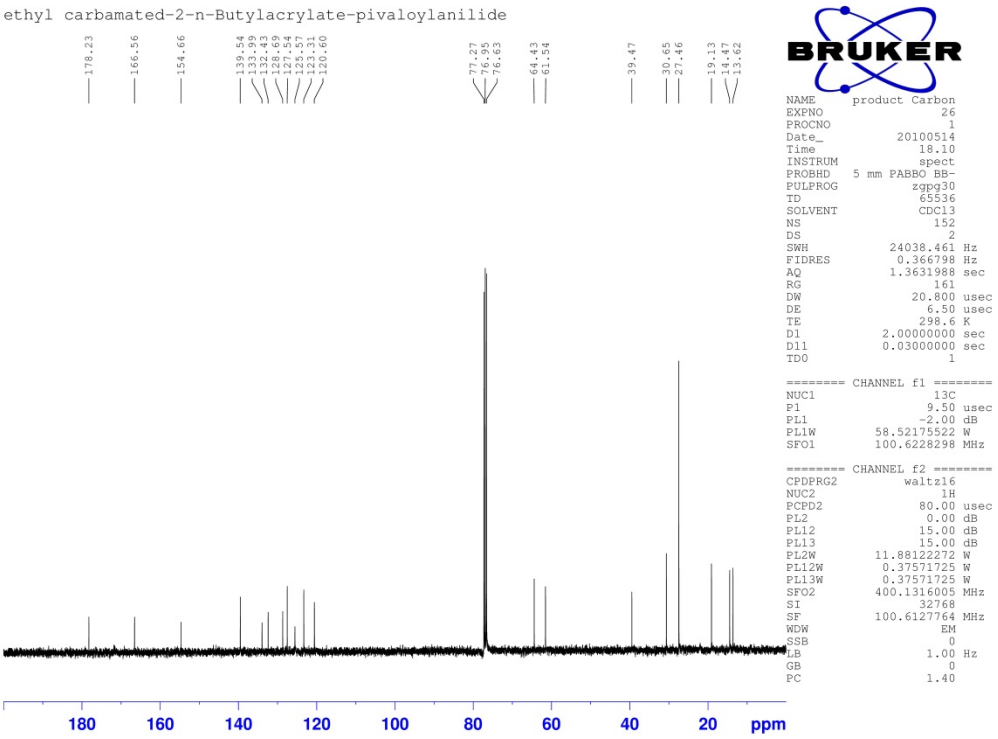

Figure A51. ^{1}H NMR of **3sa**

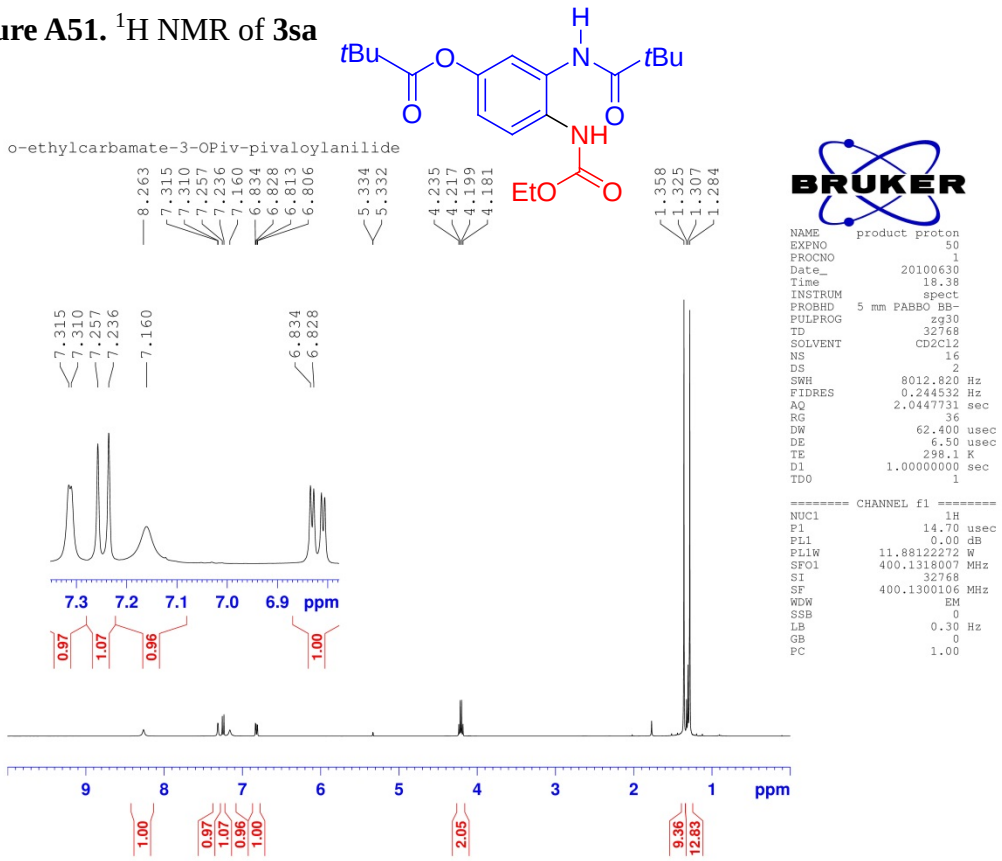

Figure A52. ^{13}C NMR of **3sa**

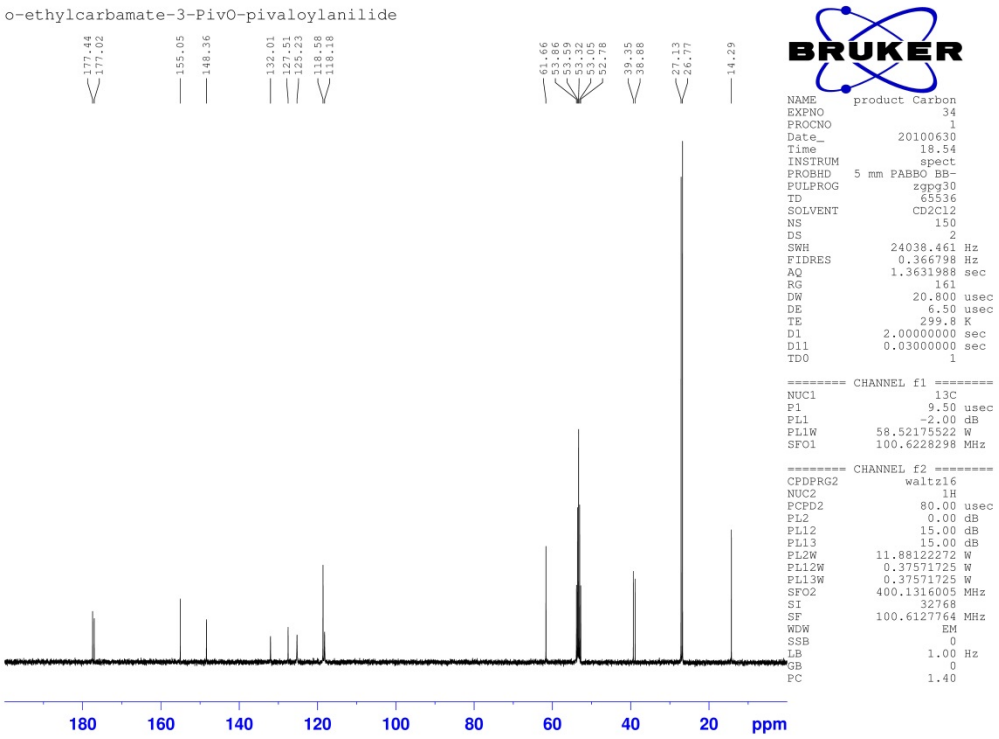

Figure A53. ^{1}H NMR of **5aa**

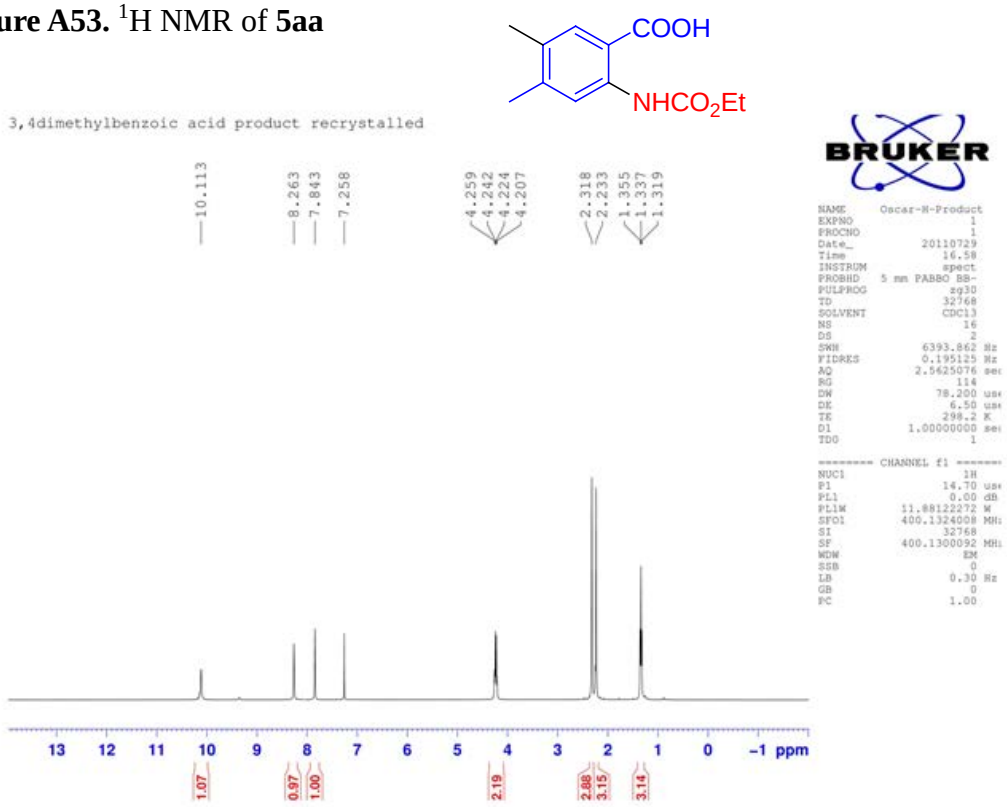

Figure A54. ^{13}C NMR of **5aa**

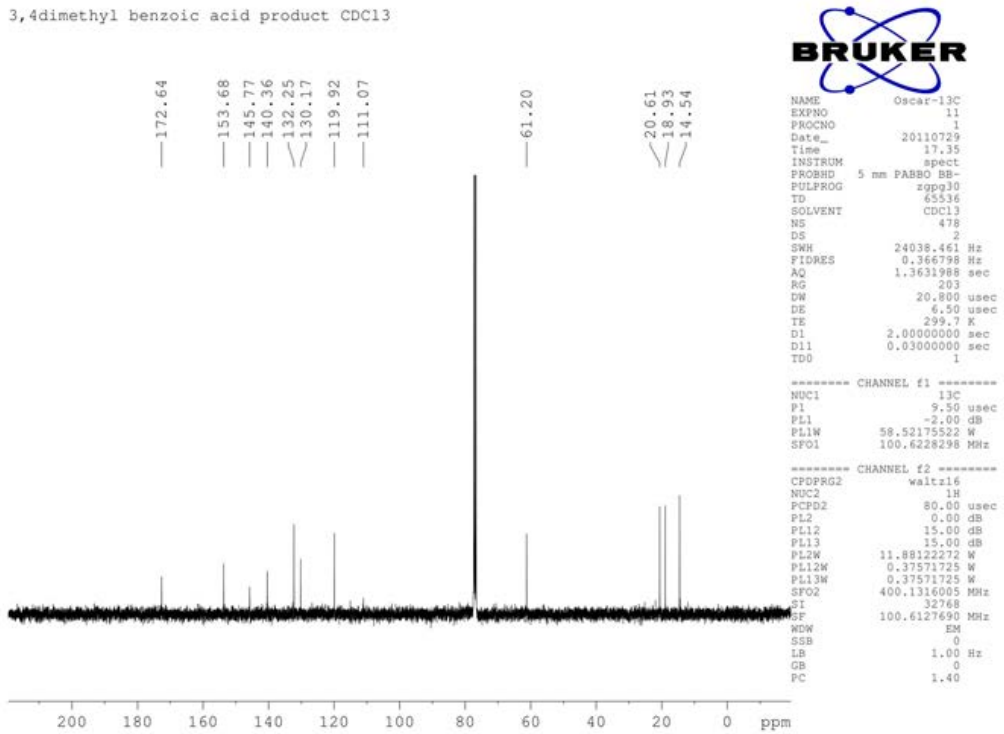

Figure A55. ^{1}H NMR of **5ba**

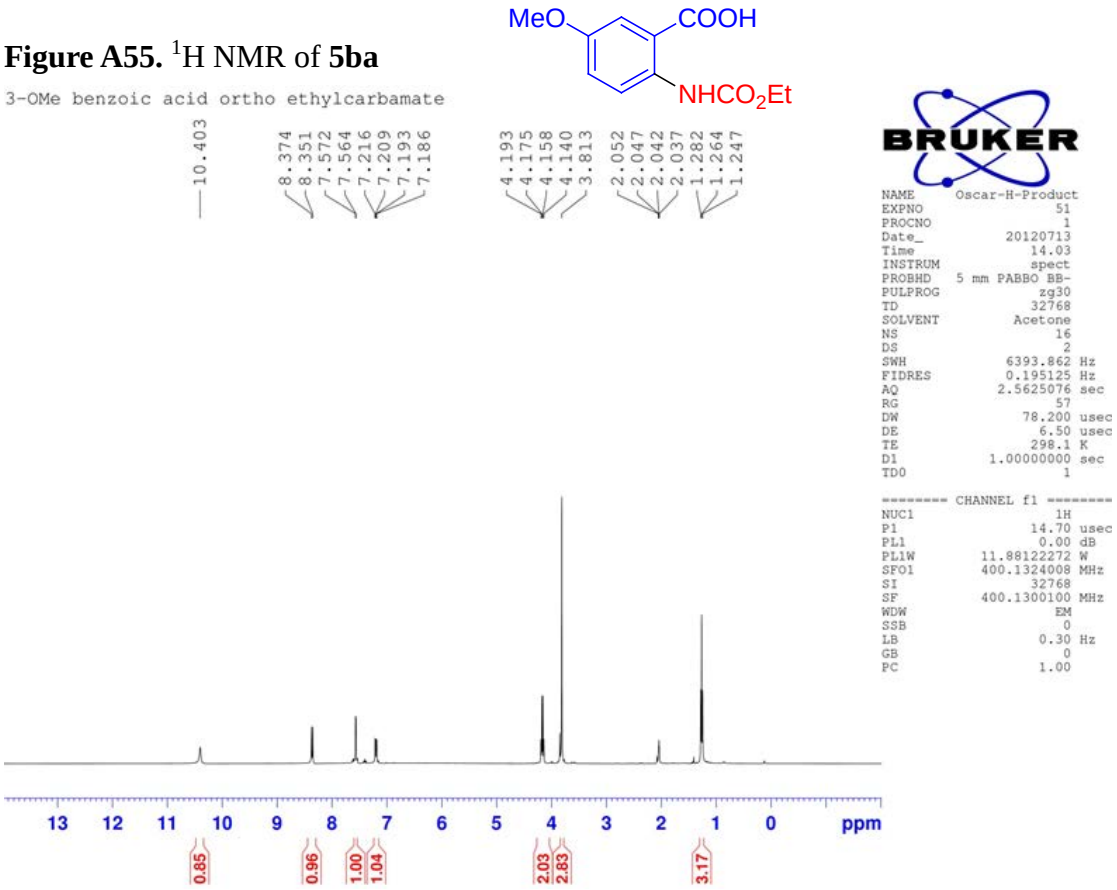

Figure A56. ^{13}C NMR of **5ba**

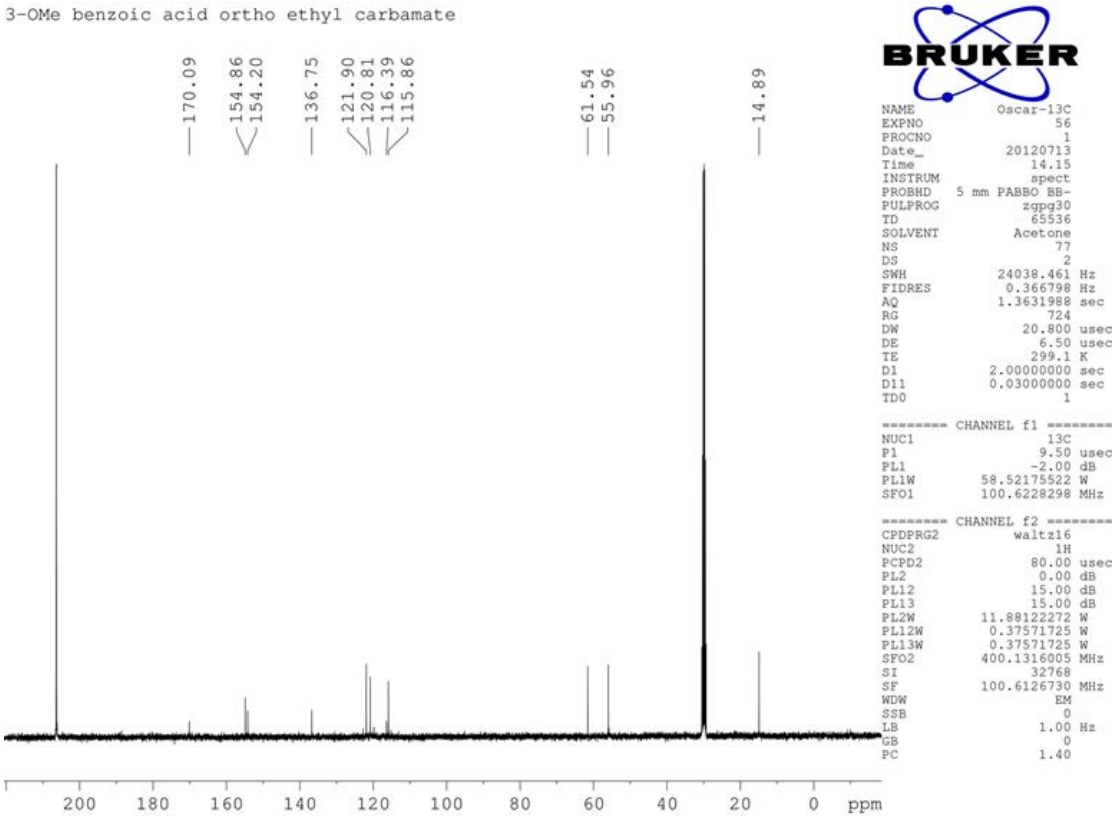

Figure A57. ^{1}H NMR of **5ca**

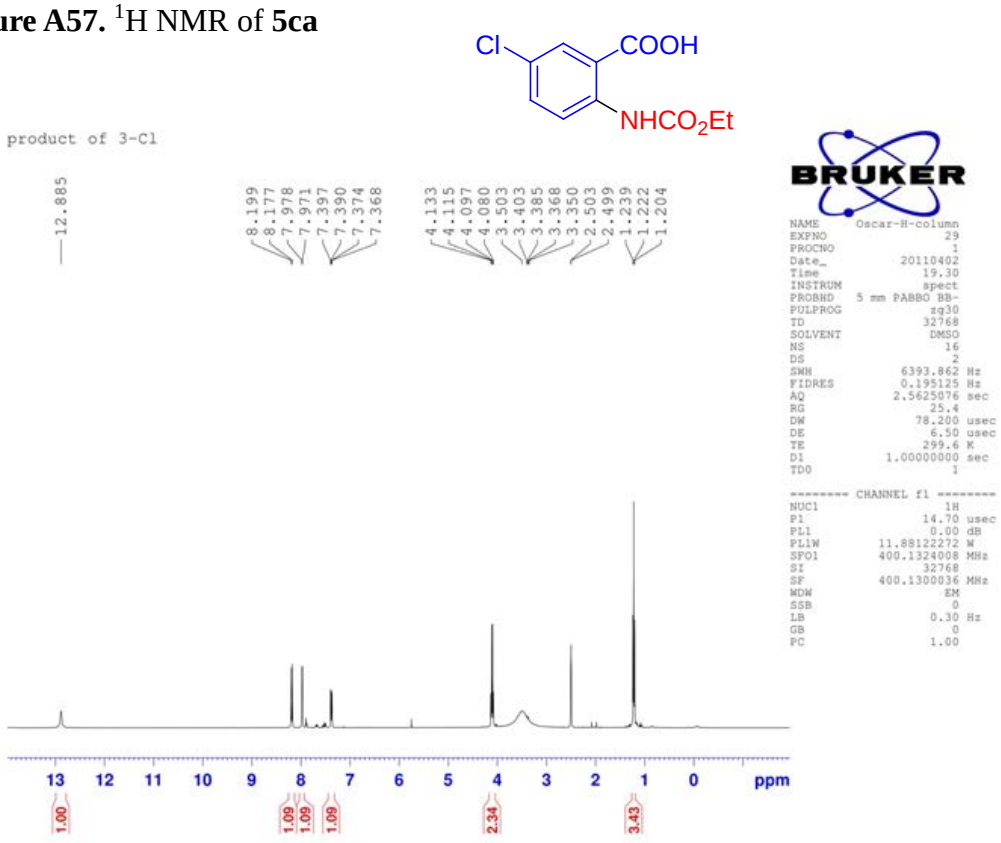

Figure A58. ^{13}C NMR of **5ca**

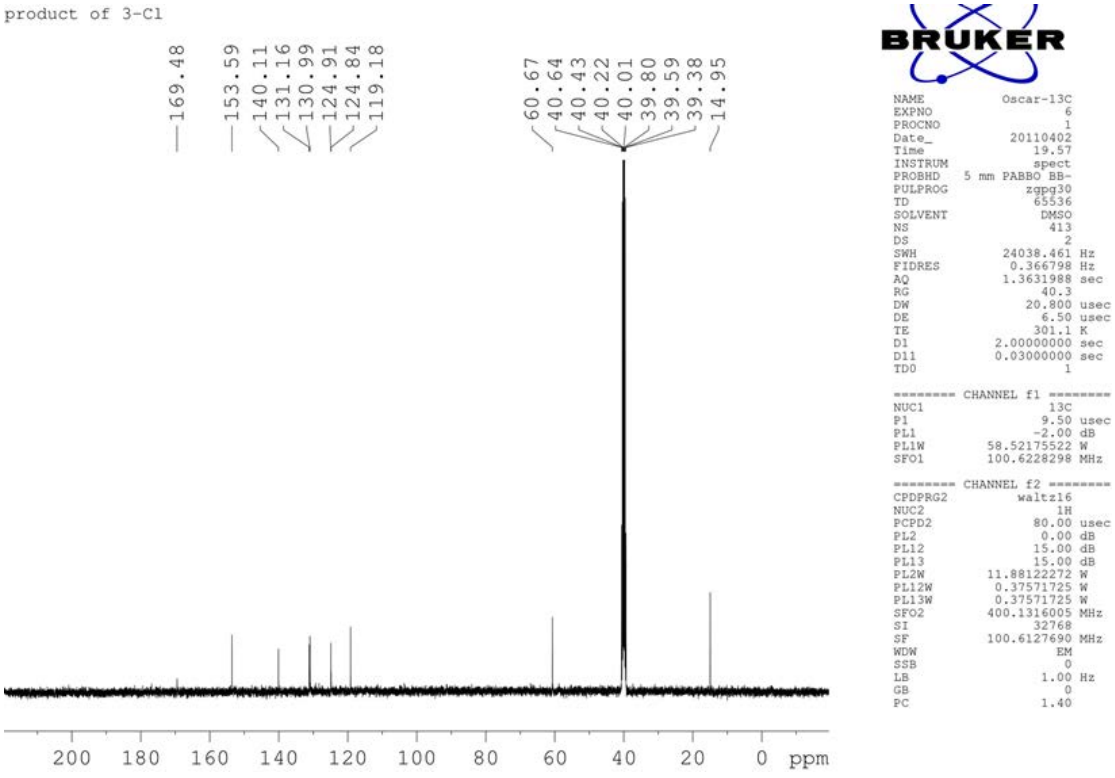

Figure A59. ^{1}H NMR of **5da**

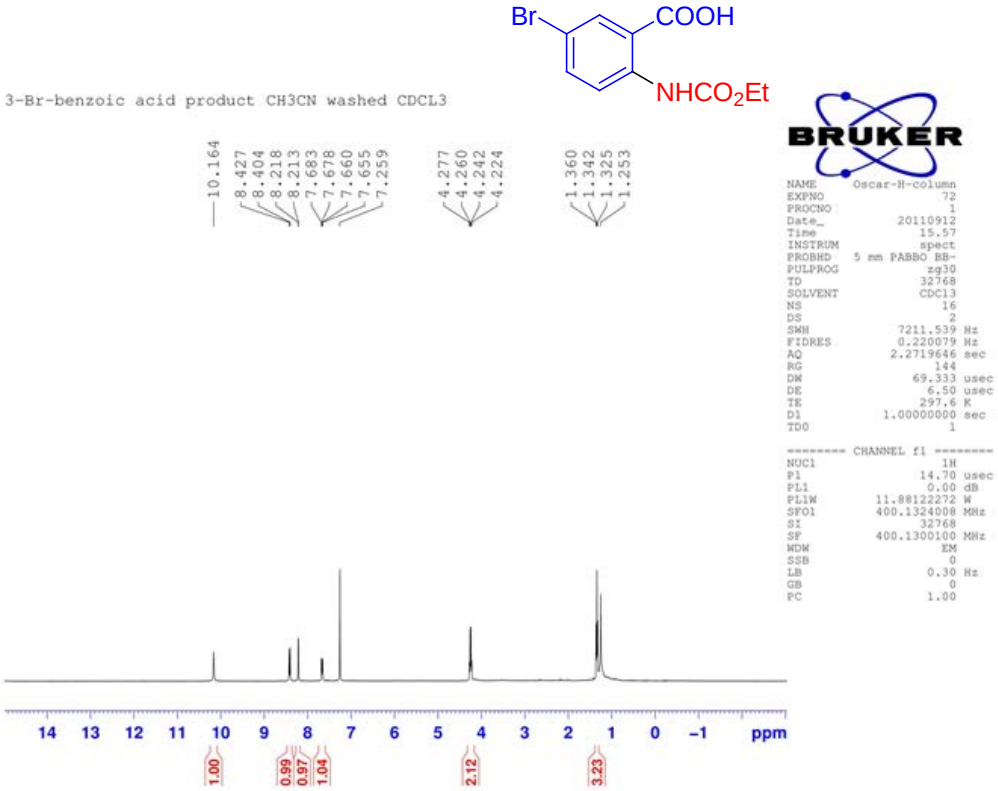

Figure A60. ^{13}C NMR of **5da**

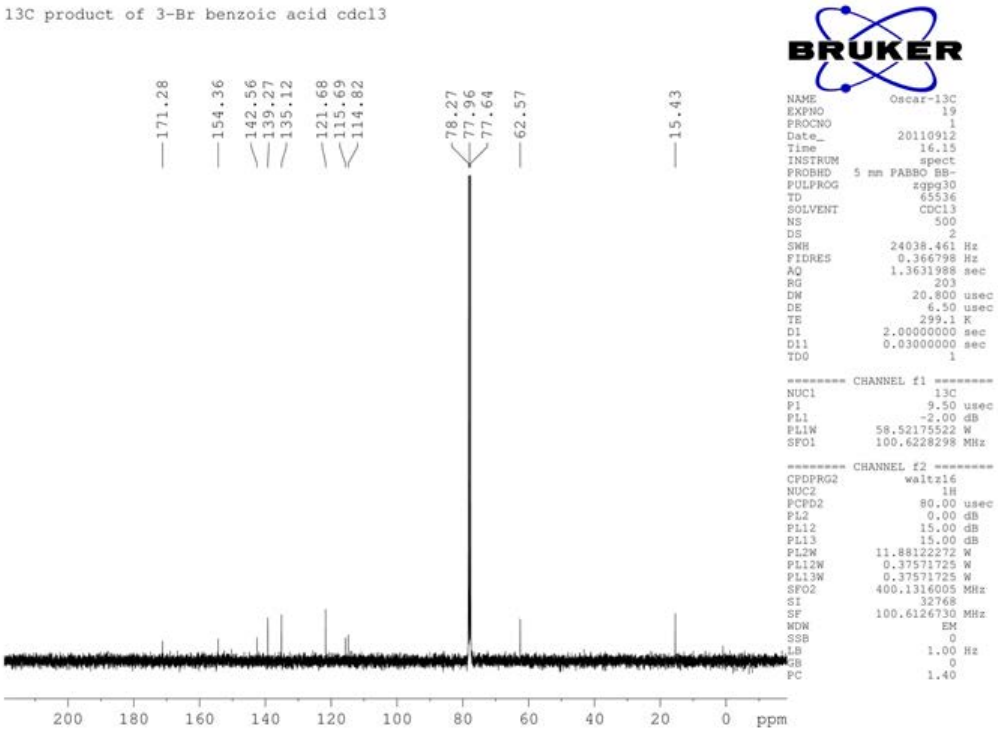

Figure A61. ^{1}H NMR of **5ea**

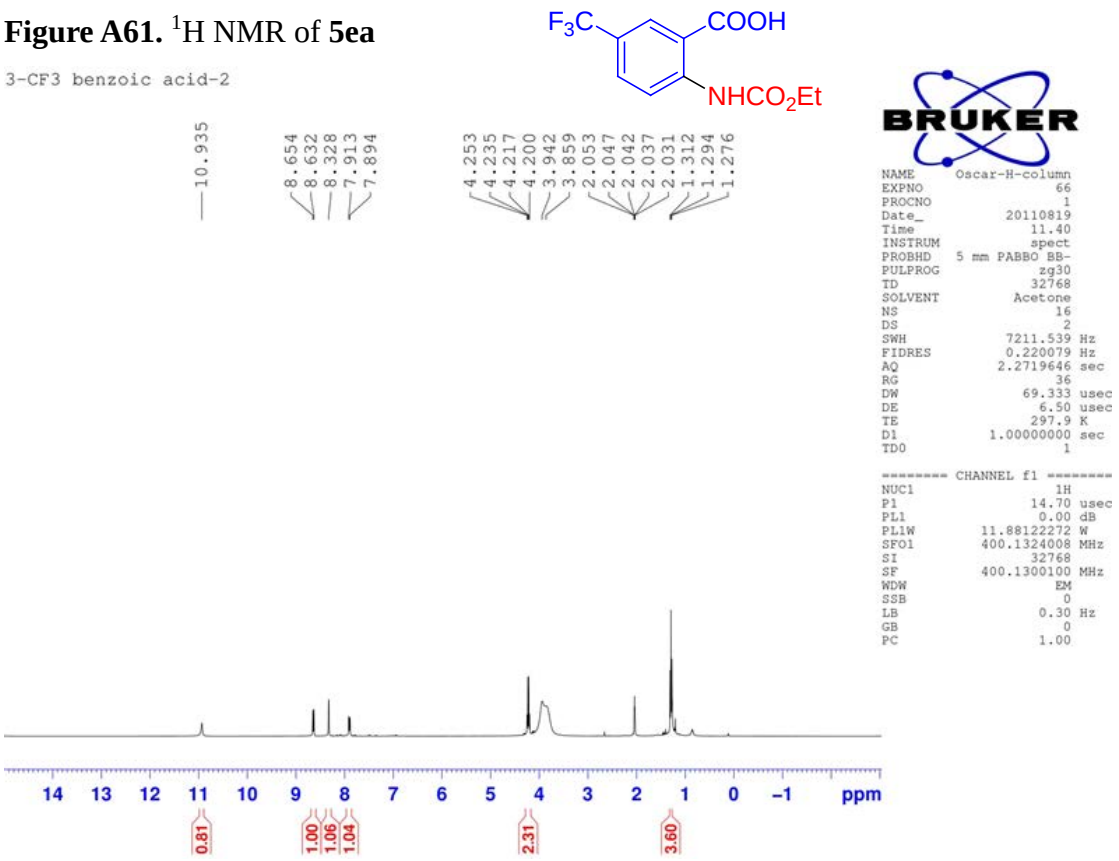

Figure A62. ^{13}C NMR of **5ea**

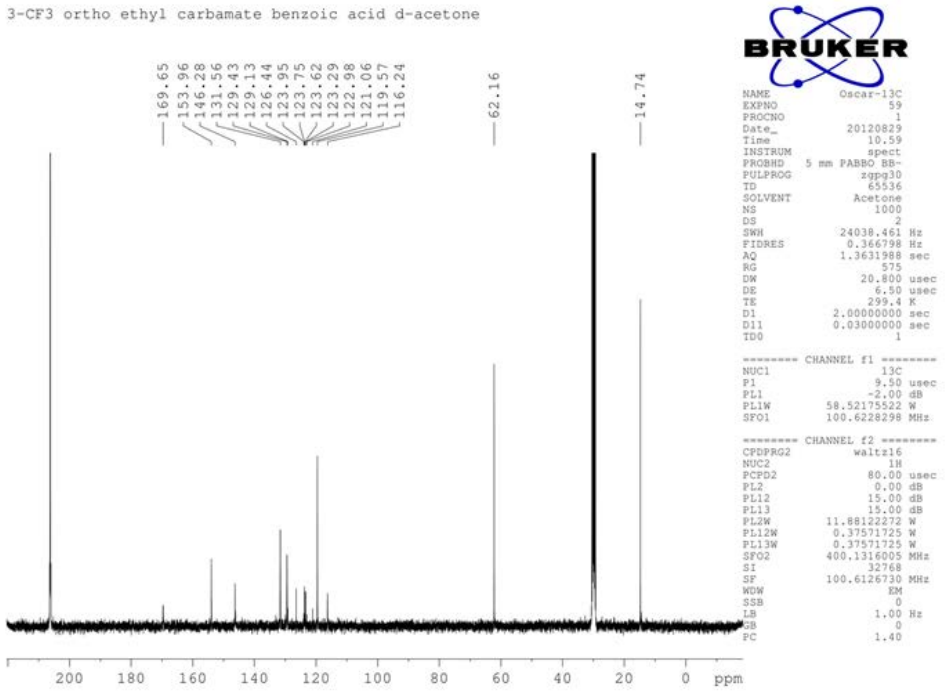

Figure A63. ^{1}H NMR of **5fa**

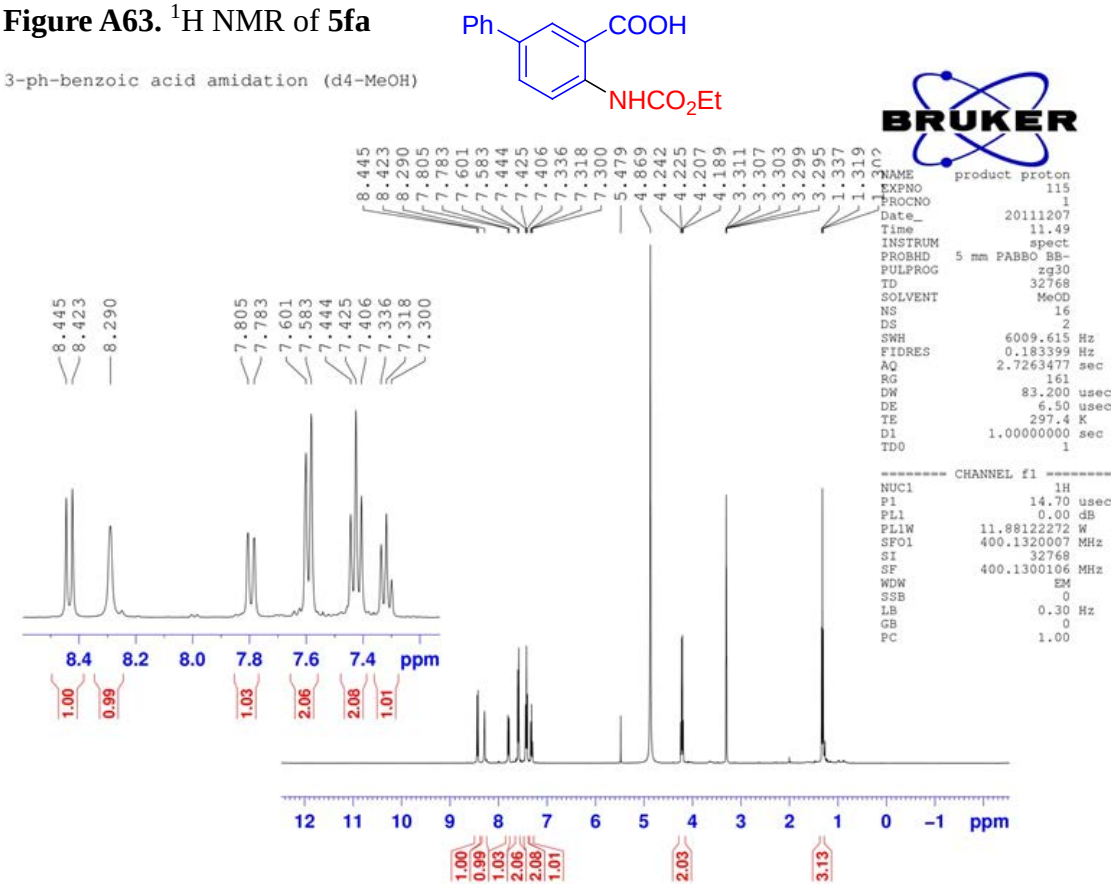

Figure A64. ^{13}C NMR of **5fa**

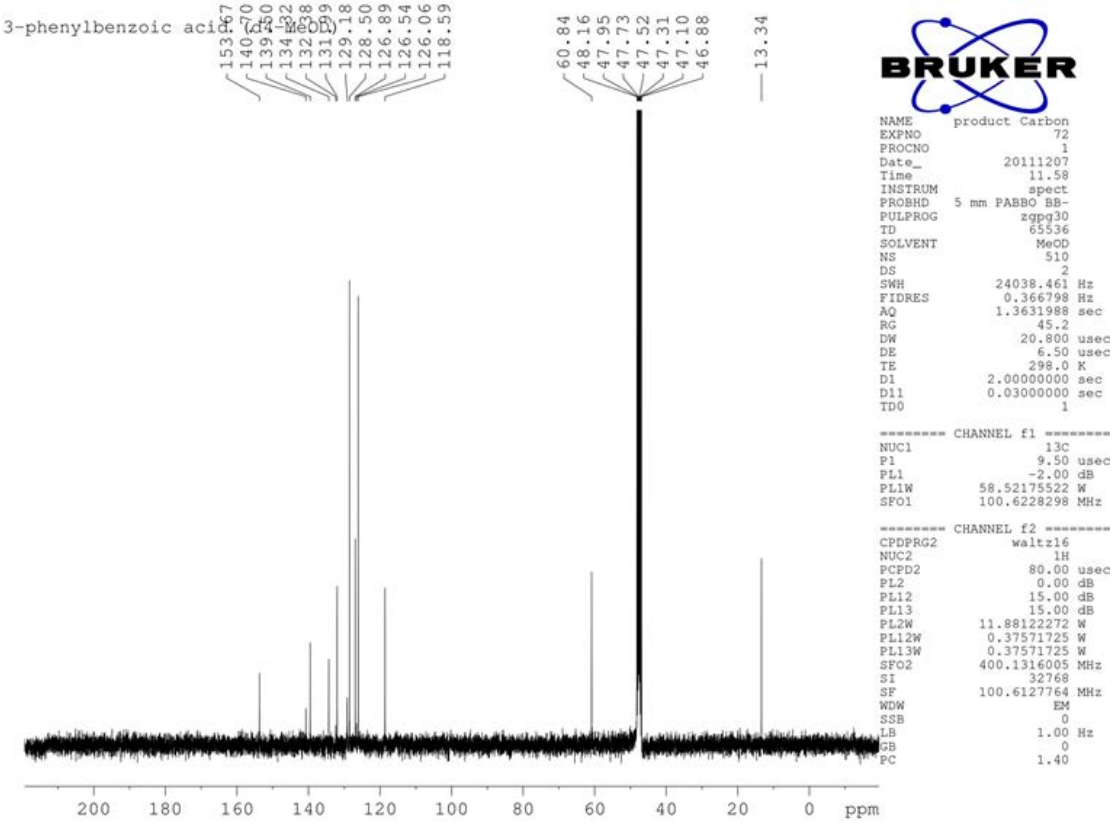

Figure A65. ^{1}H NMR of **5ga**

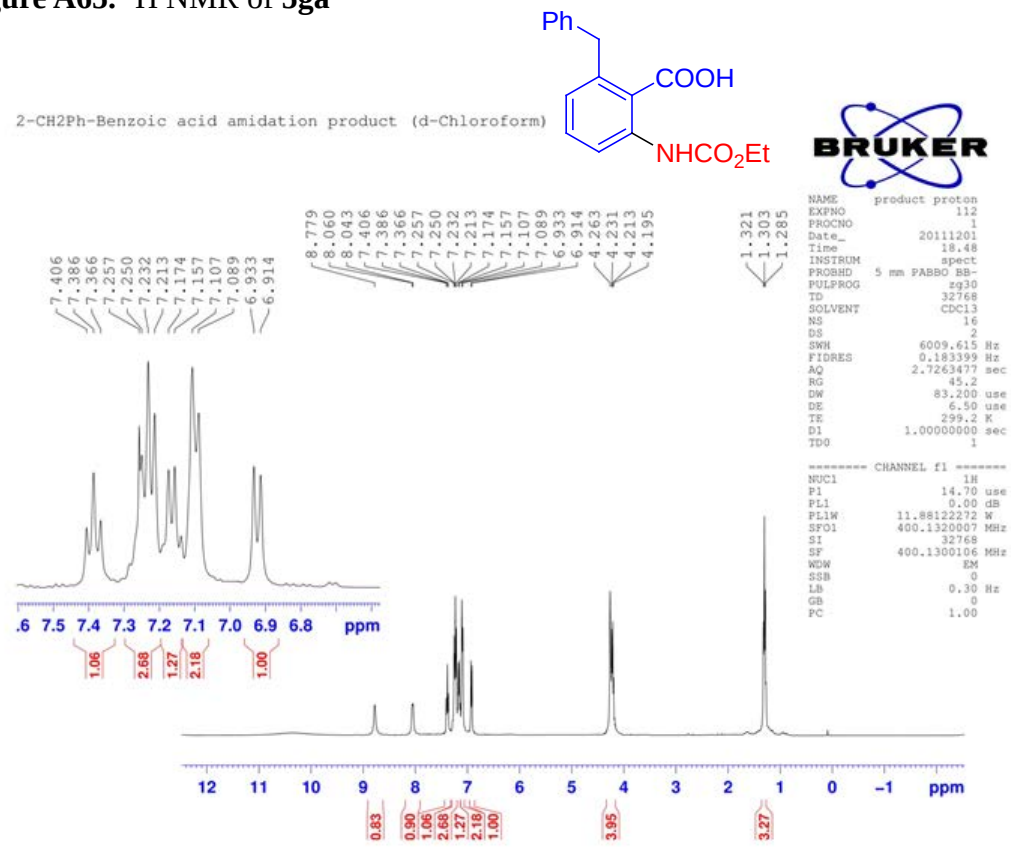

Figure A66. ^{13}C NMR of **5ga**

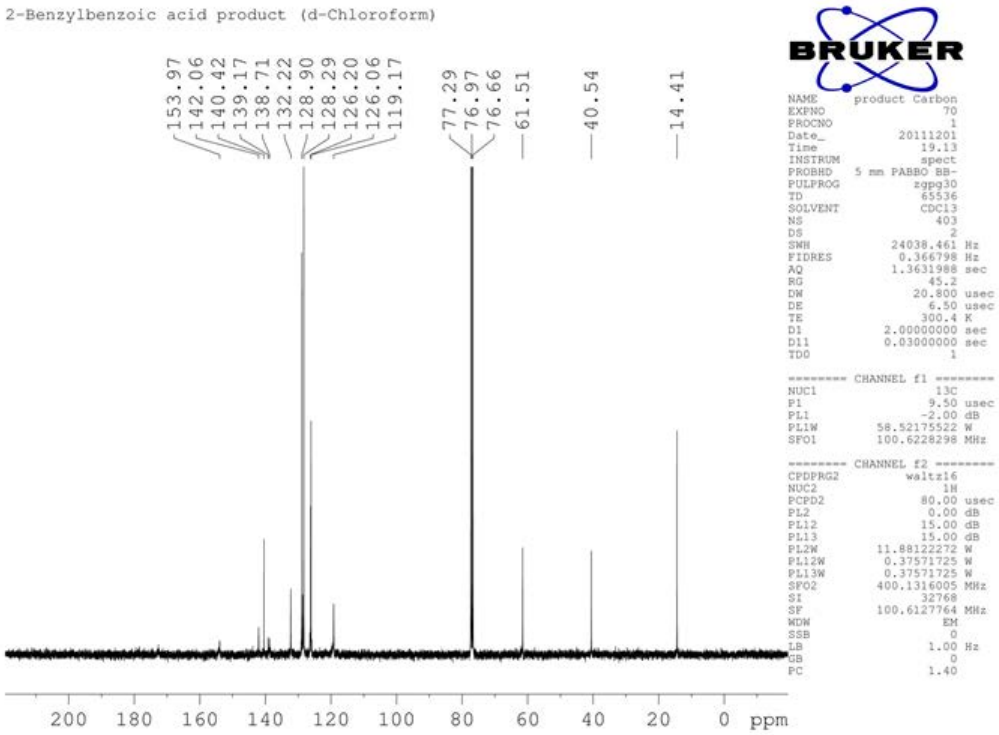

Figure A67. ^{1}H NMR of **5ha**

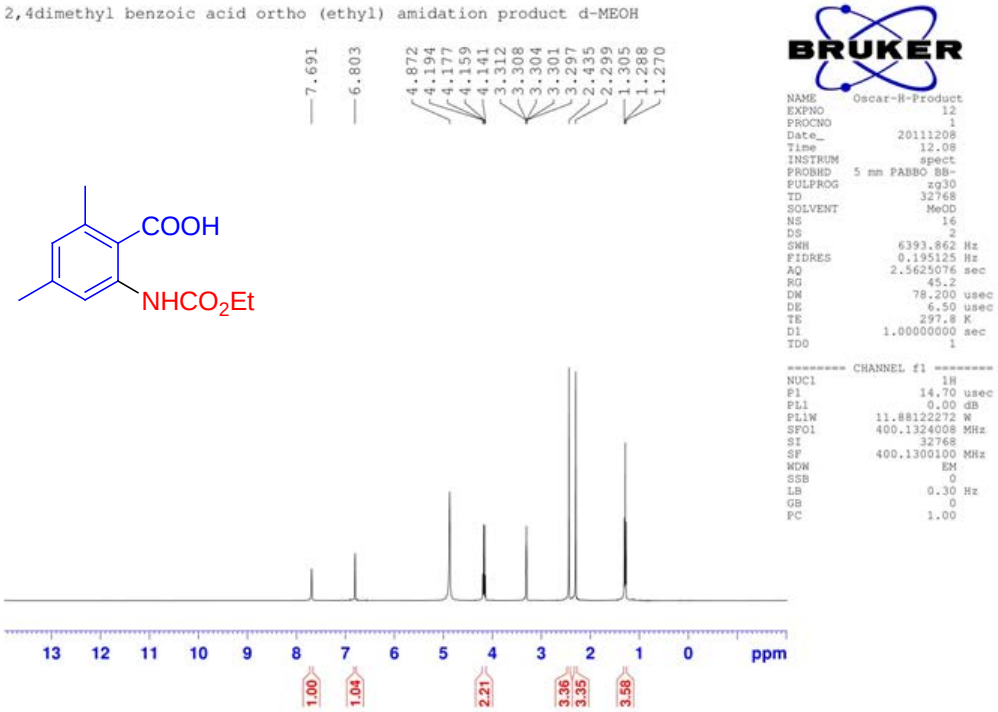

Figure A68. ^{13}C NMR of **5ha**

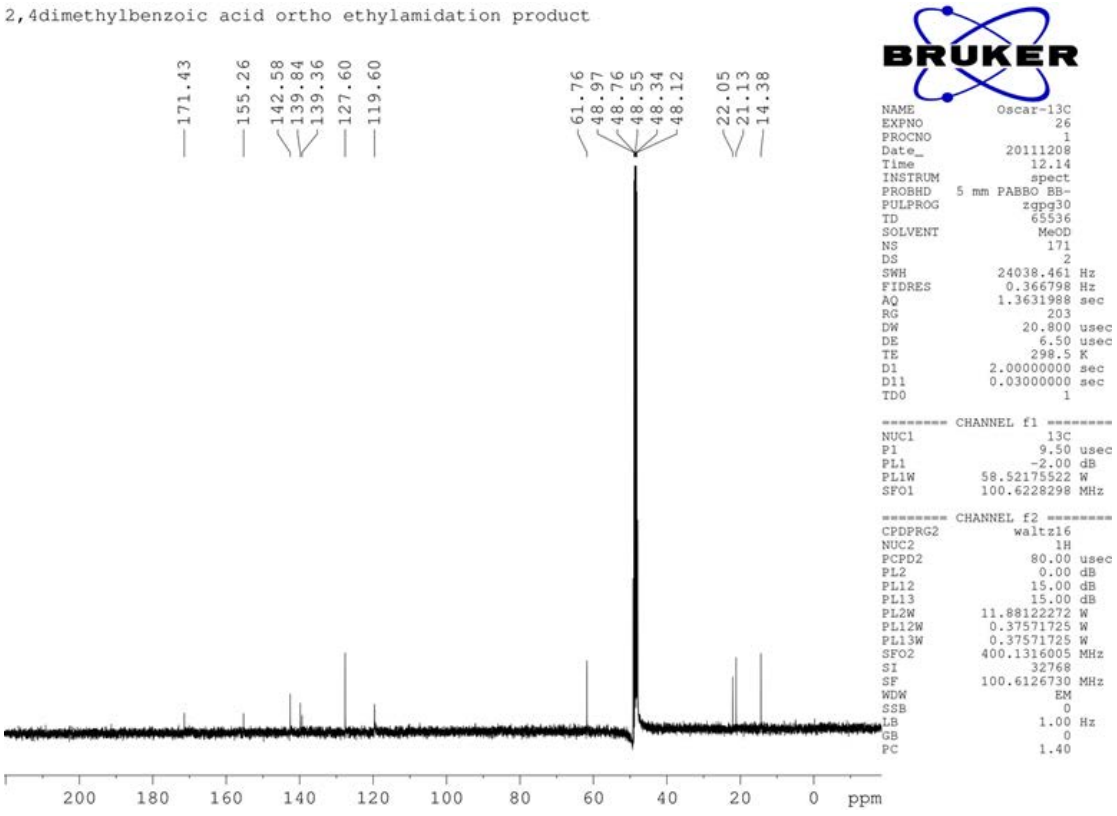

Figure A69. ^{1}H NMR of **5ia**

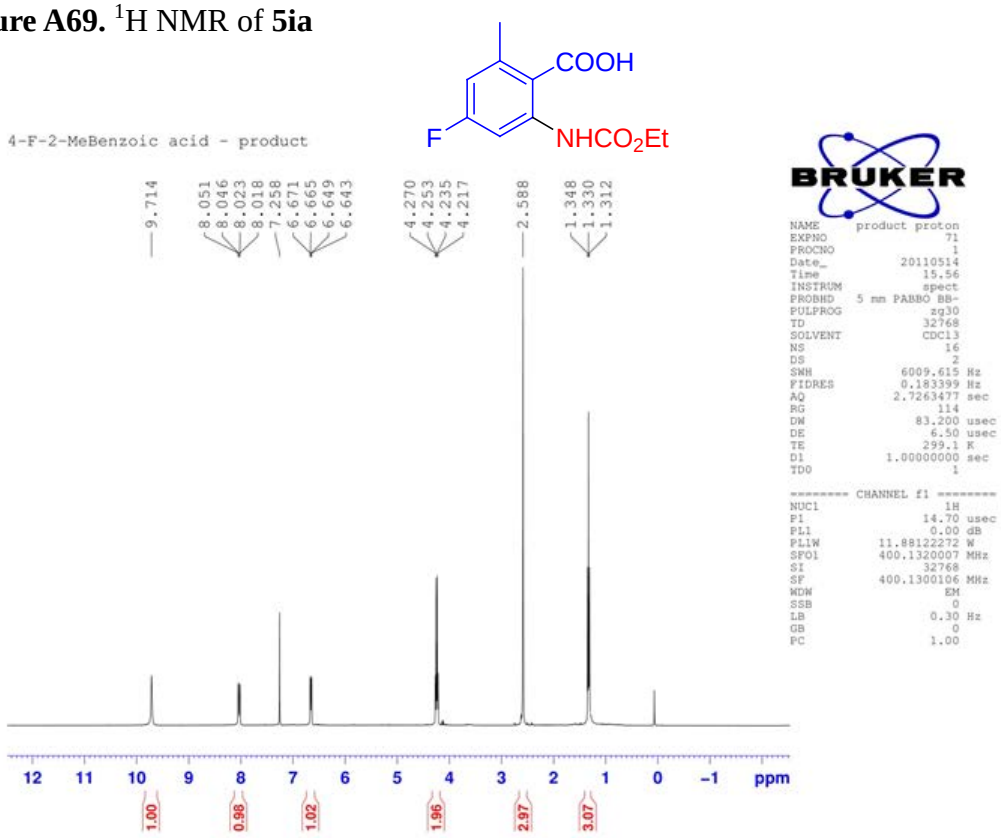

Figure A70. ^{13}C NMR of **5ia**

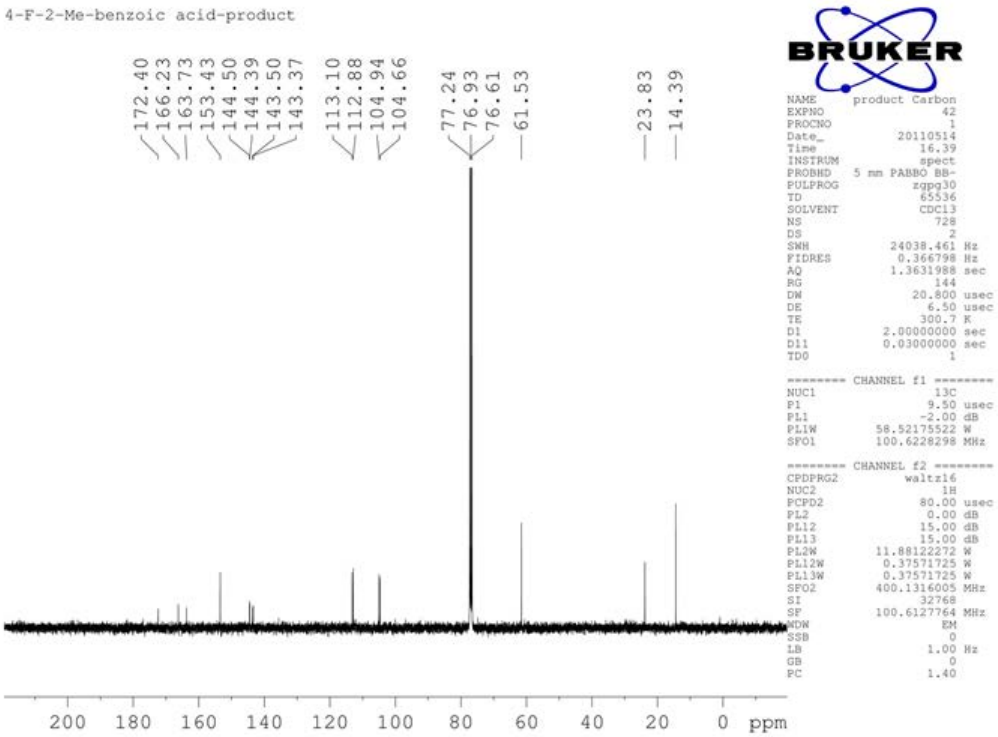

Figure A71. ^{1}H NMR of **5ja**

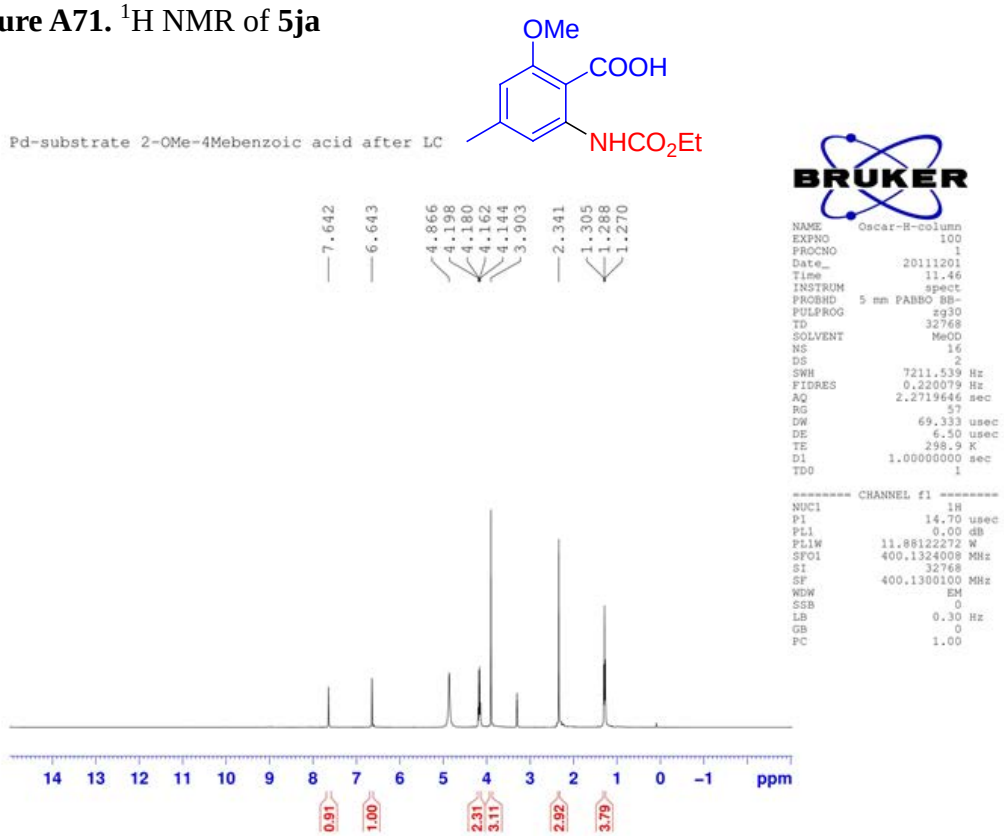

Figure A72. ^{13}C NMR of **5ja**

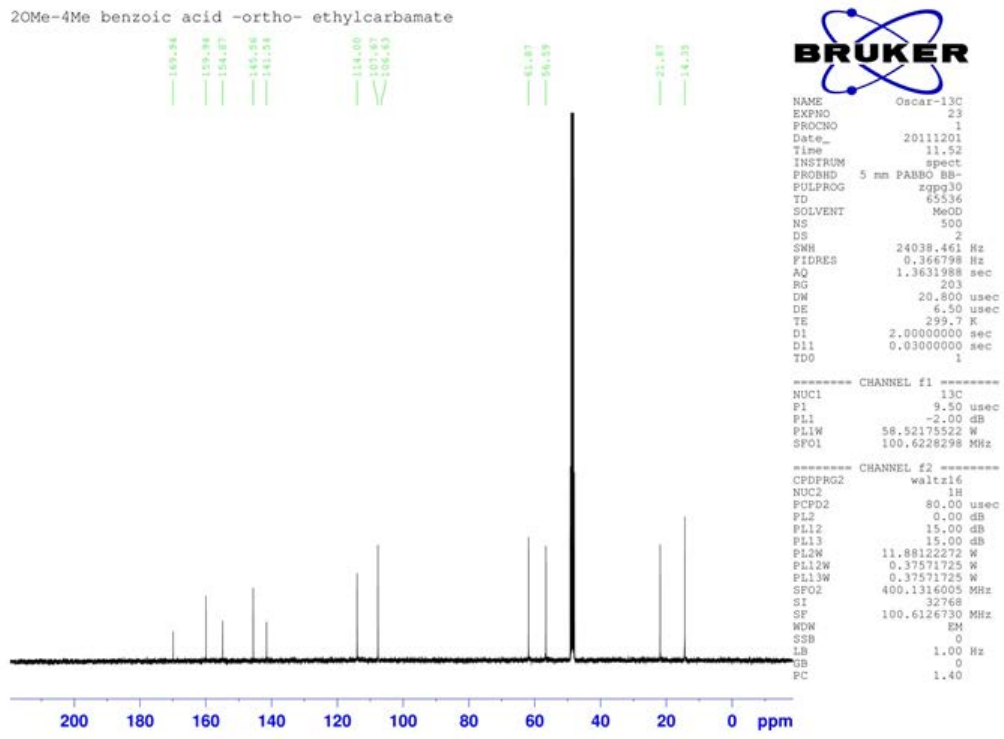

Figure A73. ^{1}H NMR of **5ka**

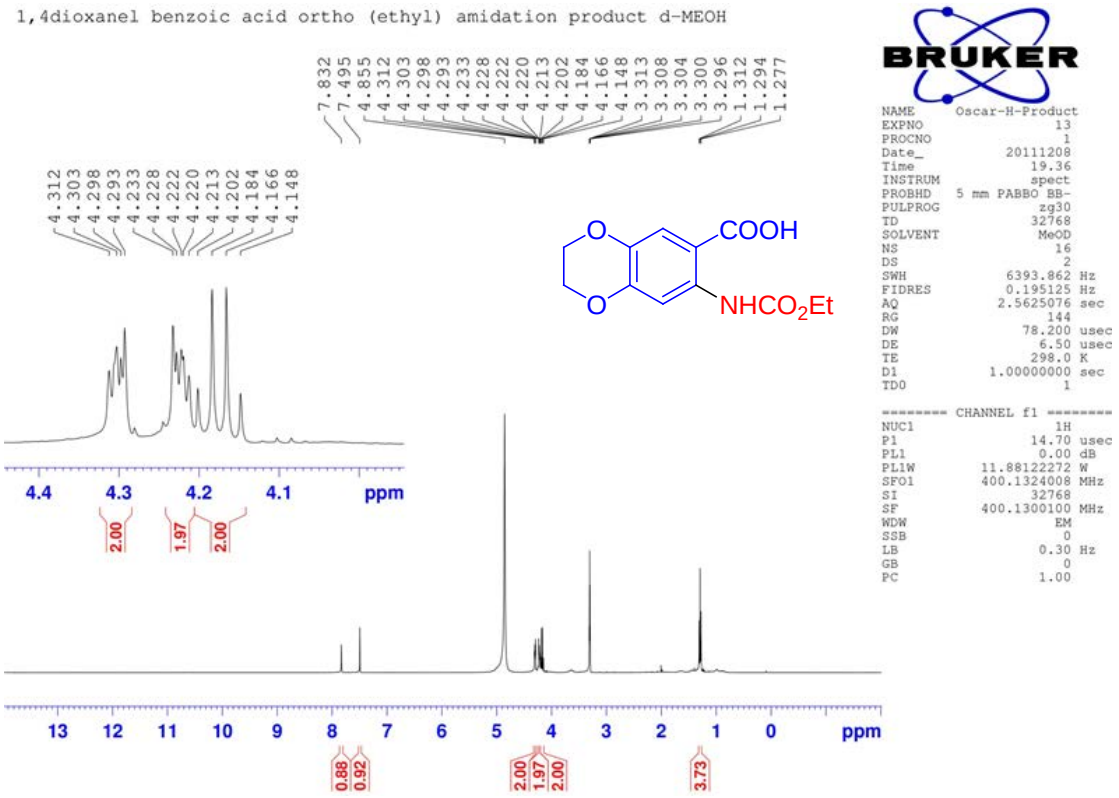

Figure A74. ^{13}C NMR of **5ka**

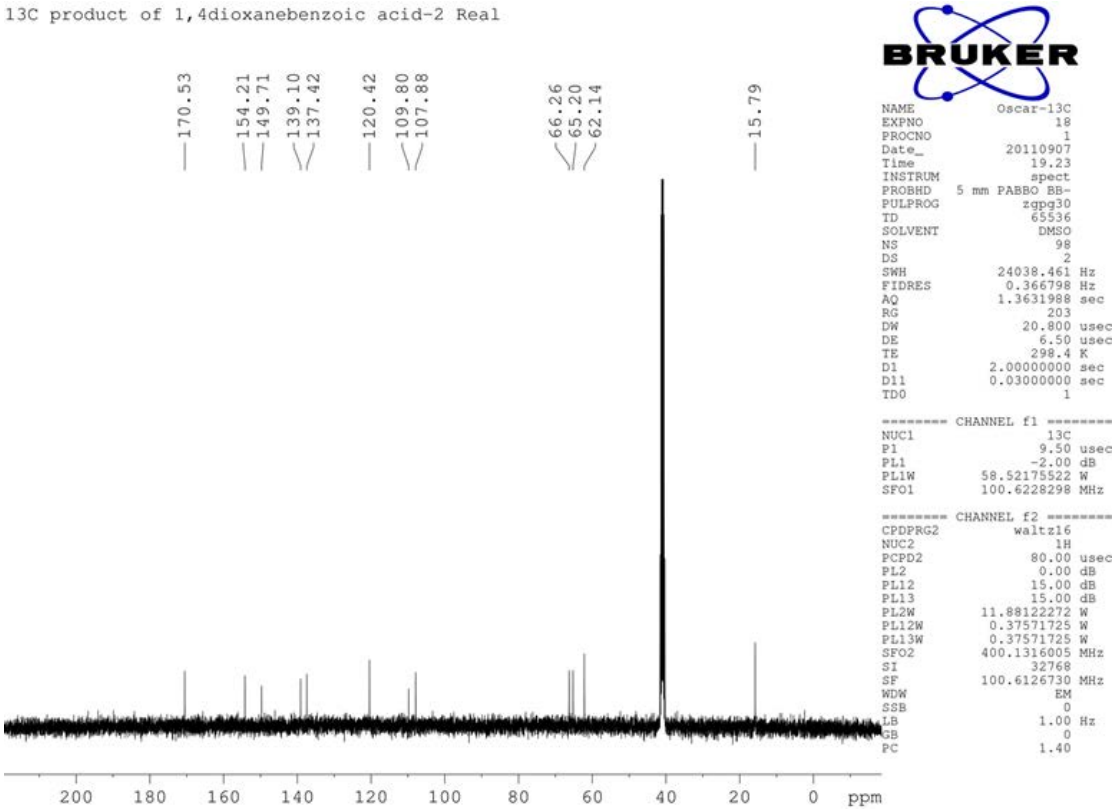

Figure A75. ^{1}H NMR of **5la**

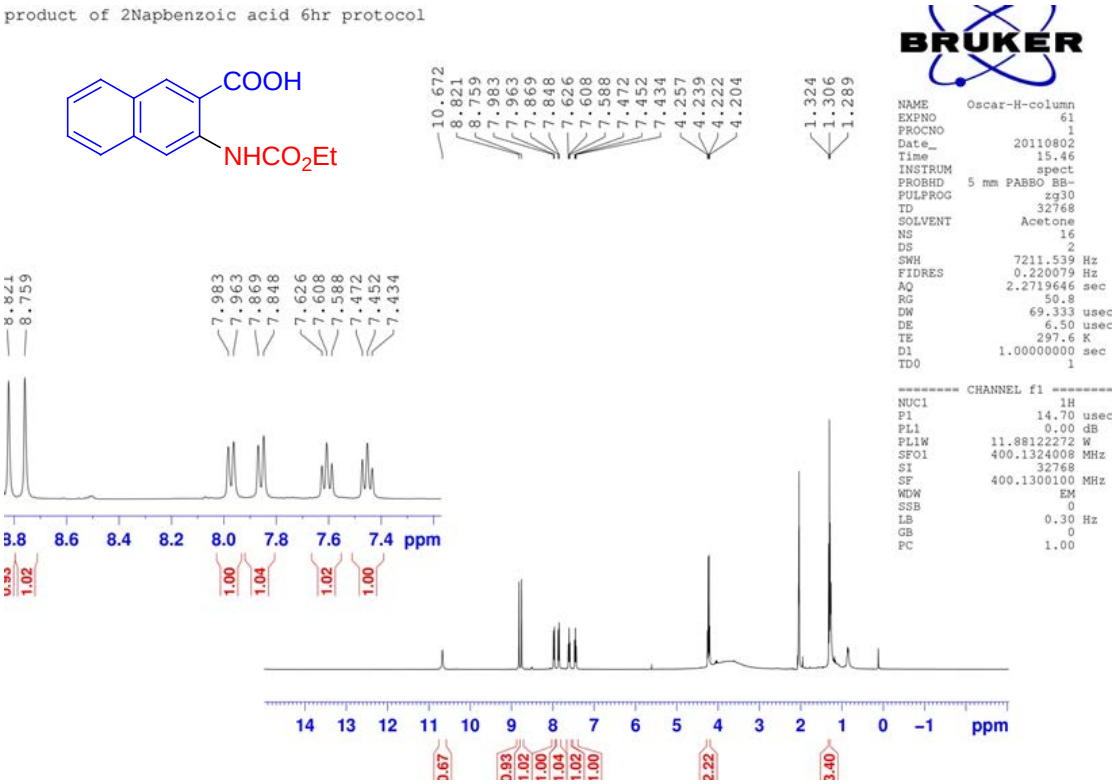

Figure A76. ^{13}C NMR of **5la**

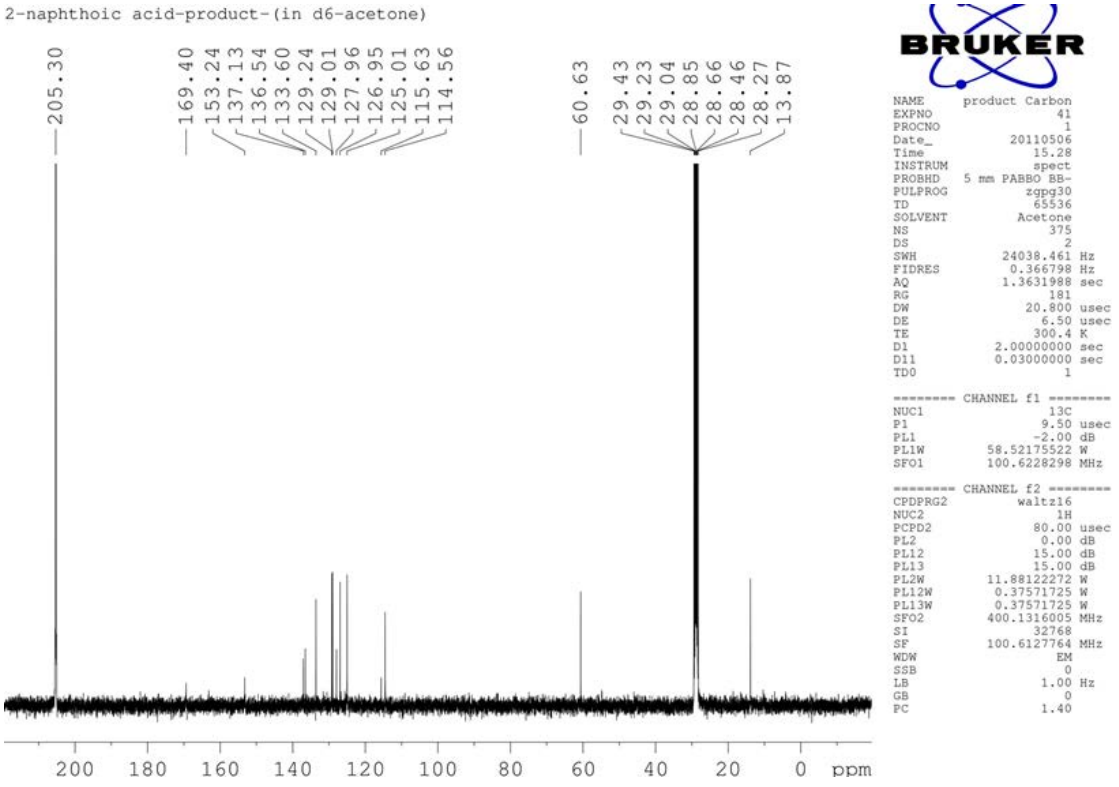

Figure A77. ^{1}H NMR of **5ma**

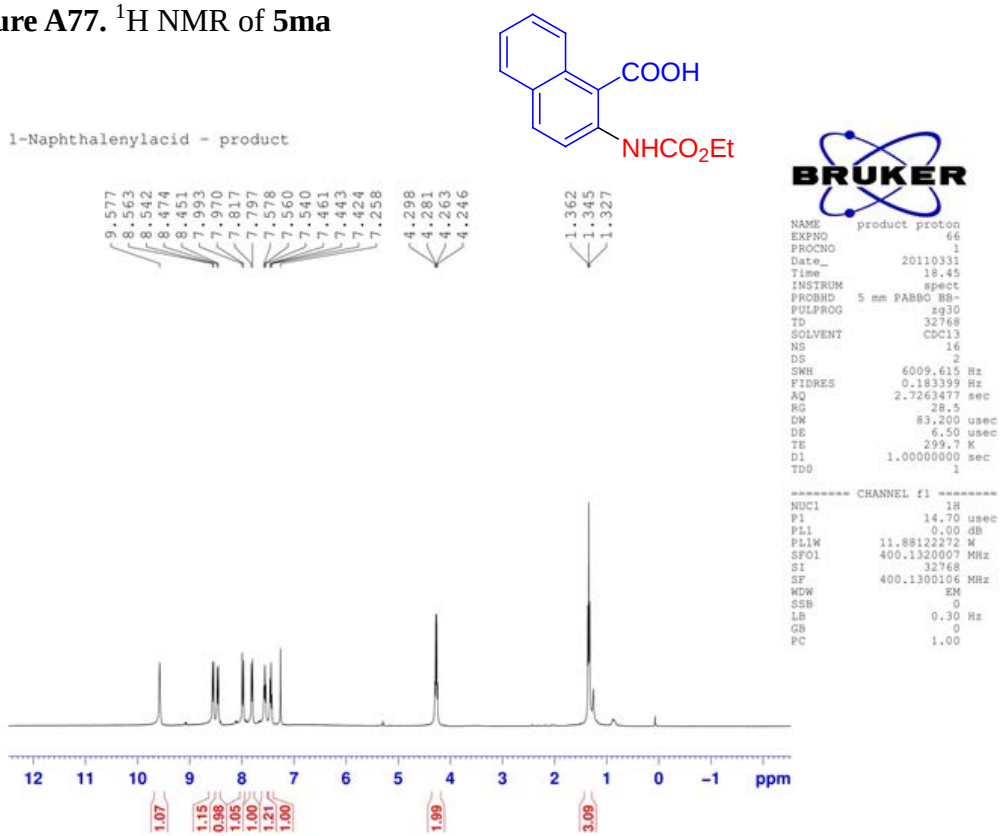

Figure A78. ^{13}C NMR of **5ma**

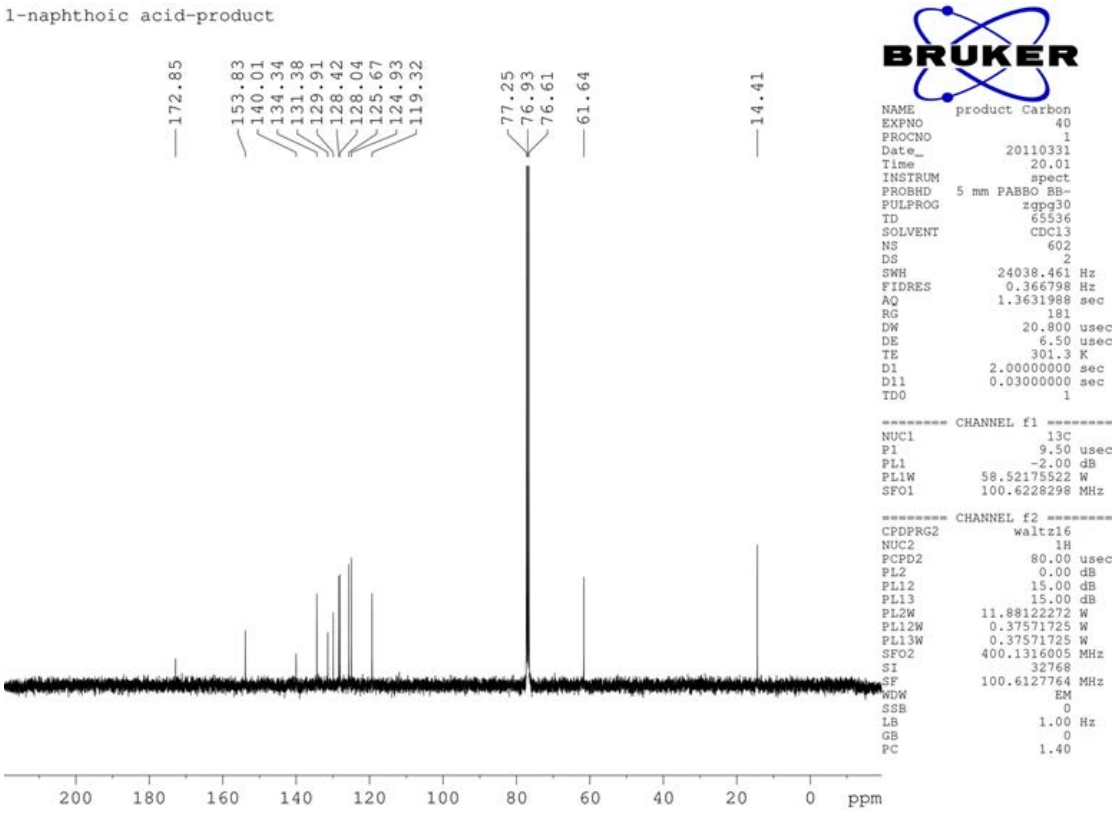

Figure A79. ^{1}H NMR of **3ta**

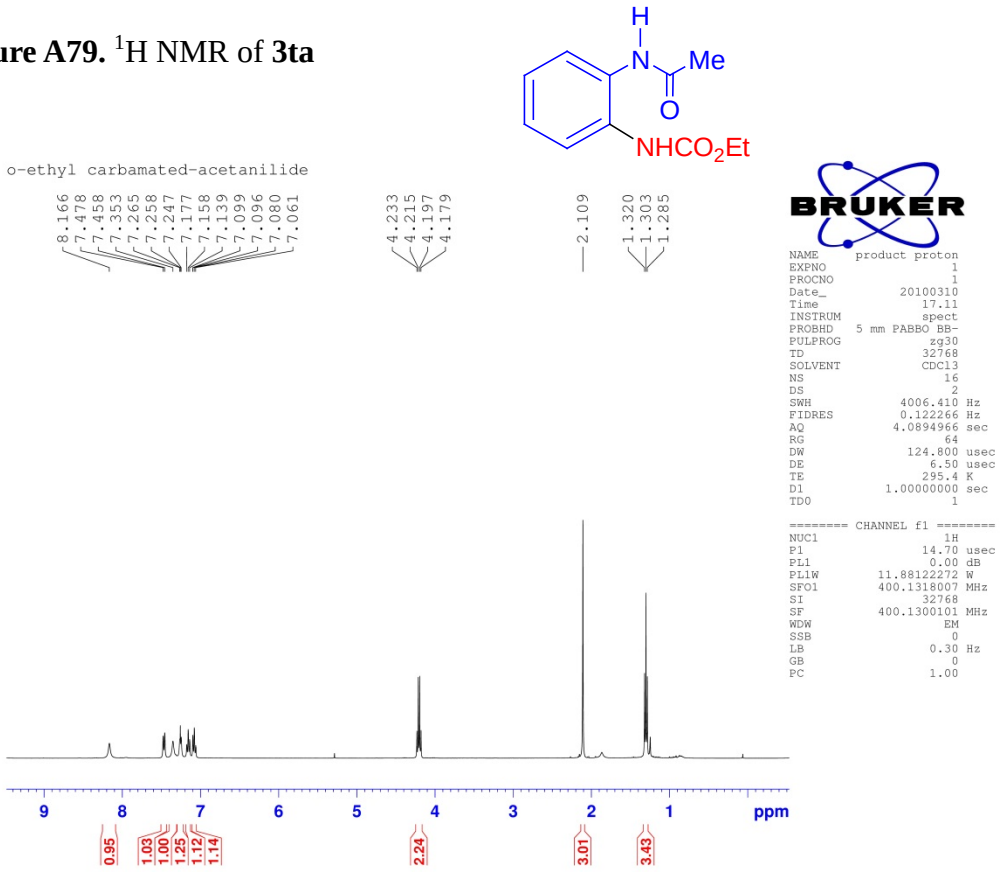

Figure A80. ^{13}C NMR of **3ta**

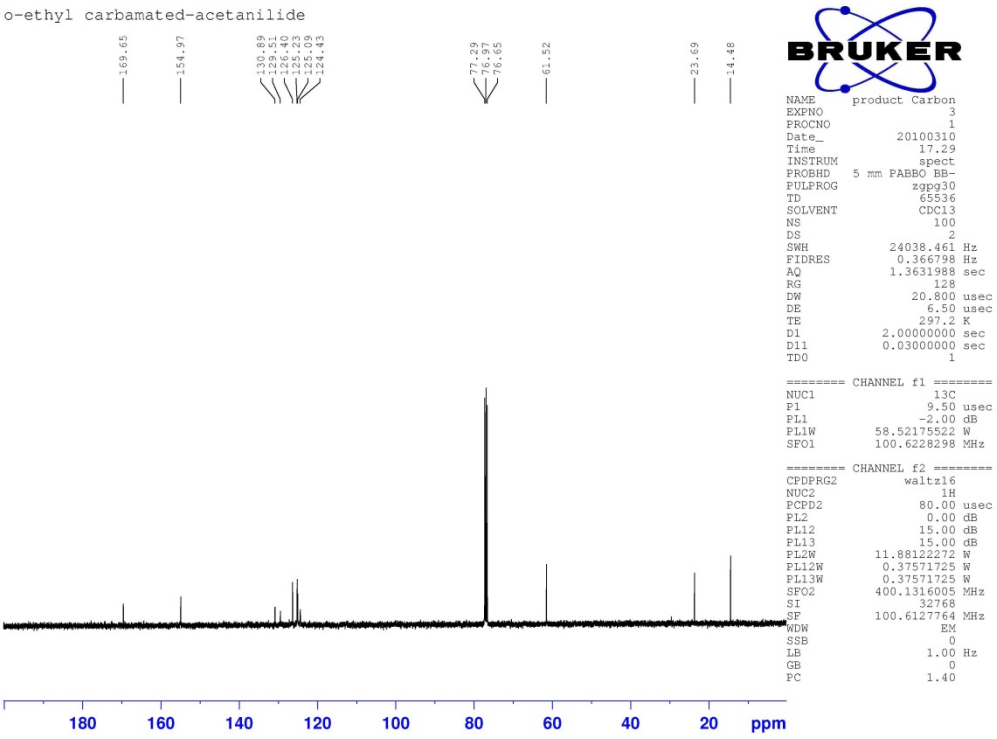

Figure A81. ^{1}H NMR of **1aPd**

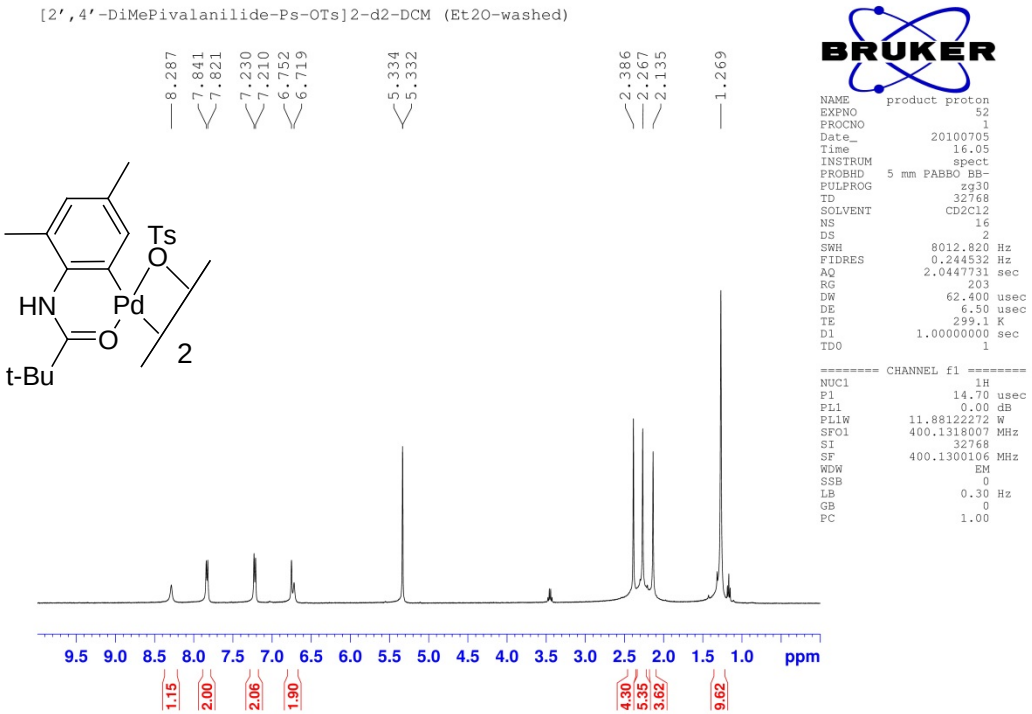

Figure A82. ^{13}C NMR of **1aPd**

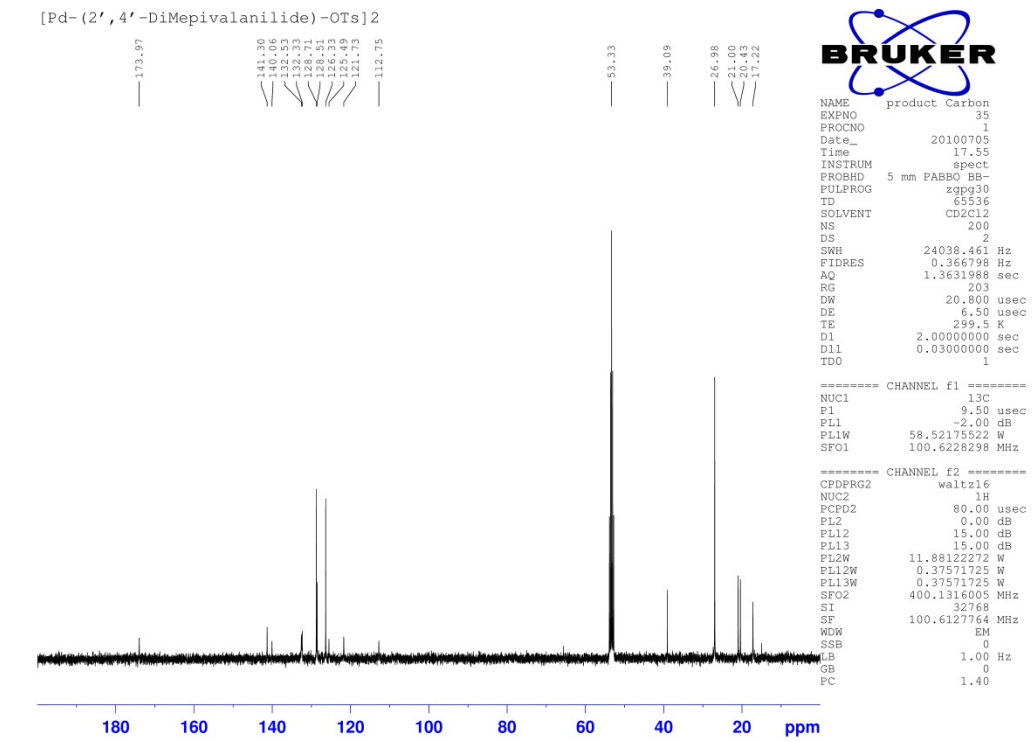

Figure A83. ^{1}H NMR of **8aa**

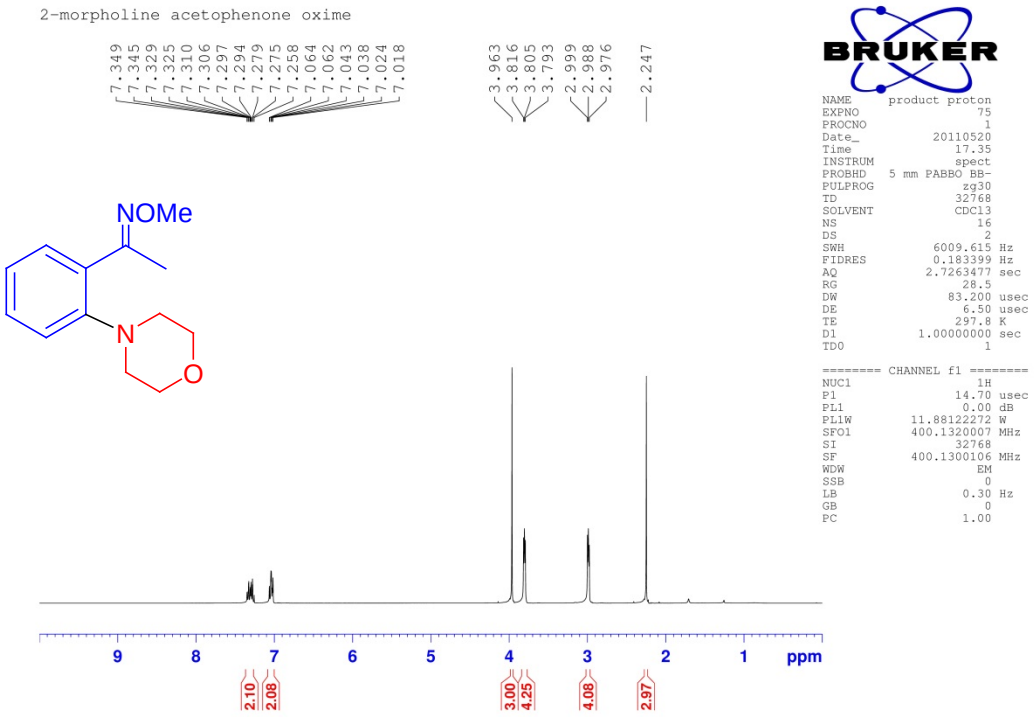

Figure A84. ^{13}C NMR of **8aa**

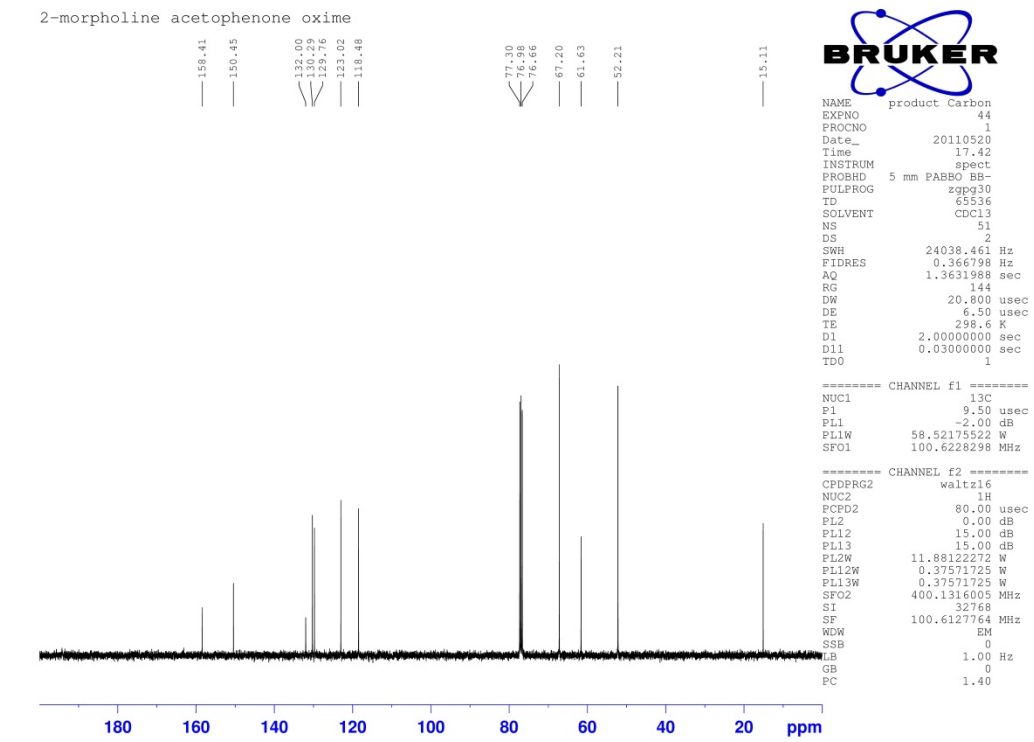

Figure A85. ^{1}H NMR of **8ba**

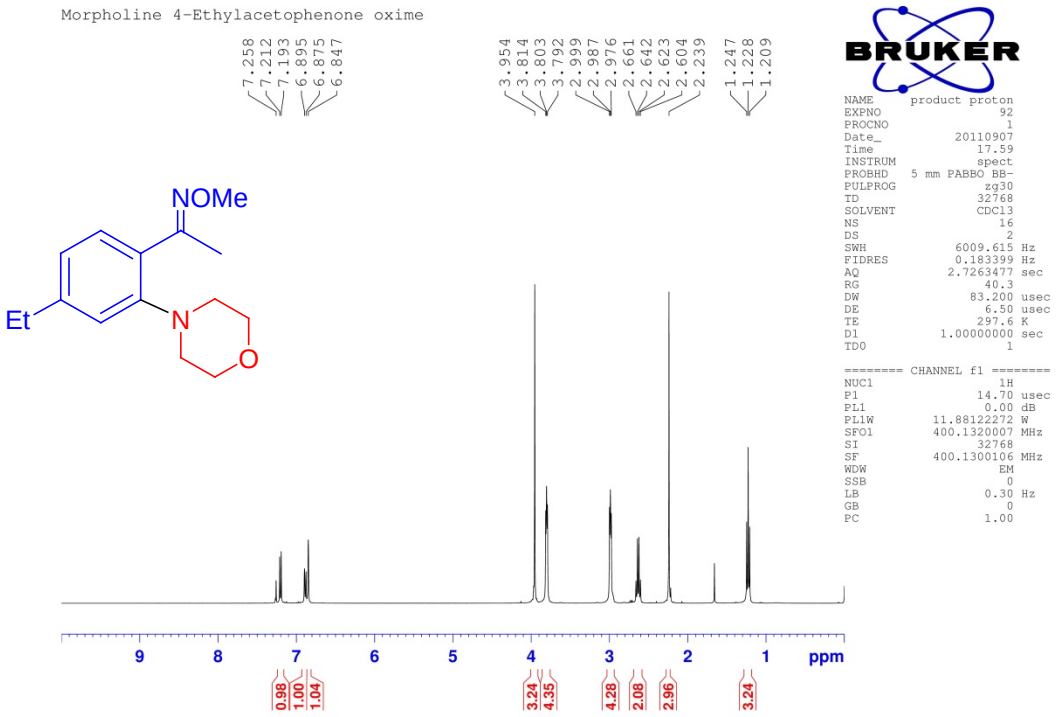

Figure A86. ^{13}C NMR of **8ba**

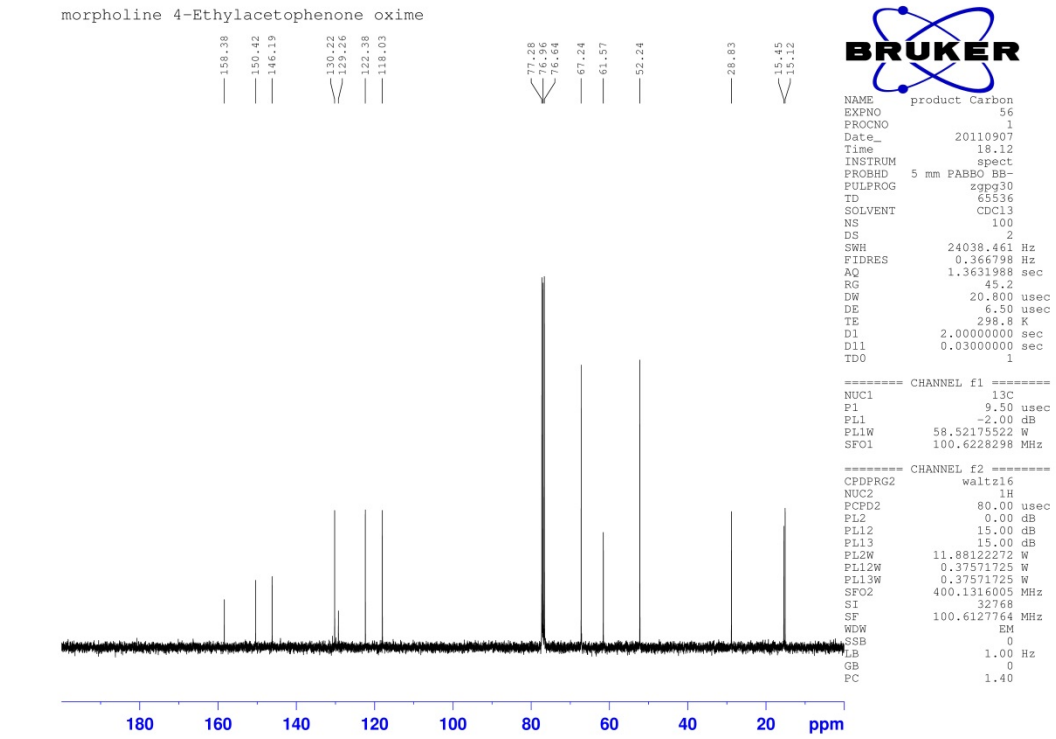

Figure A87. ^{1}H NMR of **8ca**

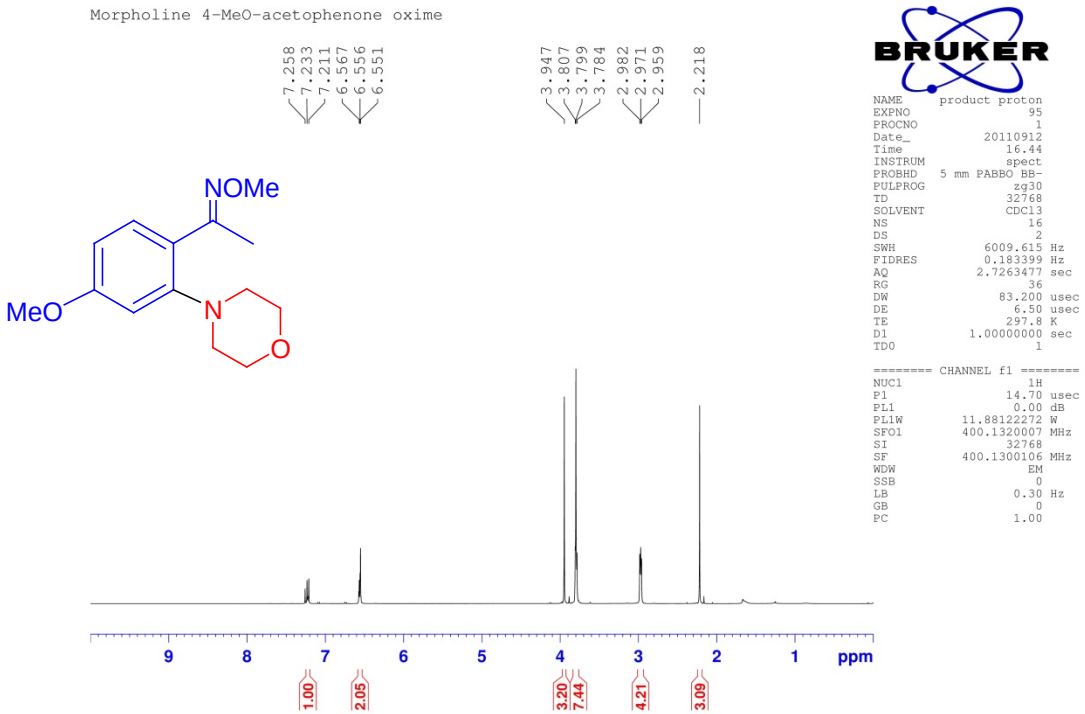

Figure A88. ^{13}C NMR of **8ca**

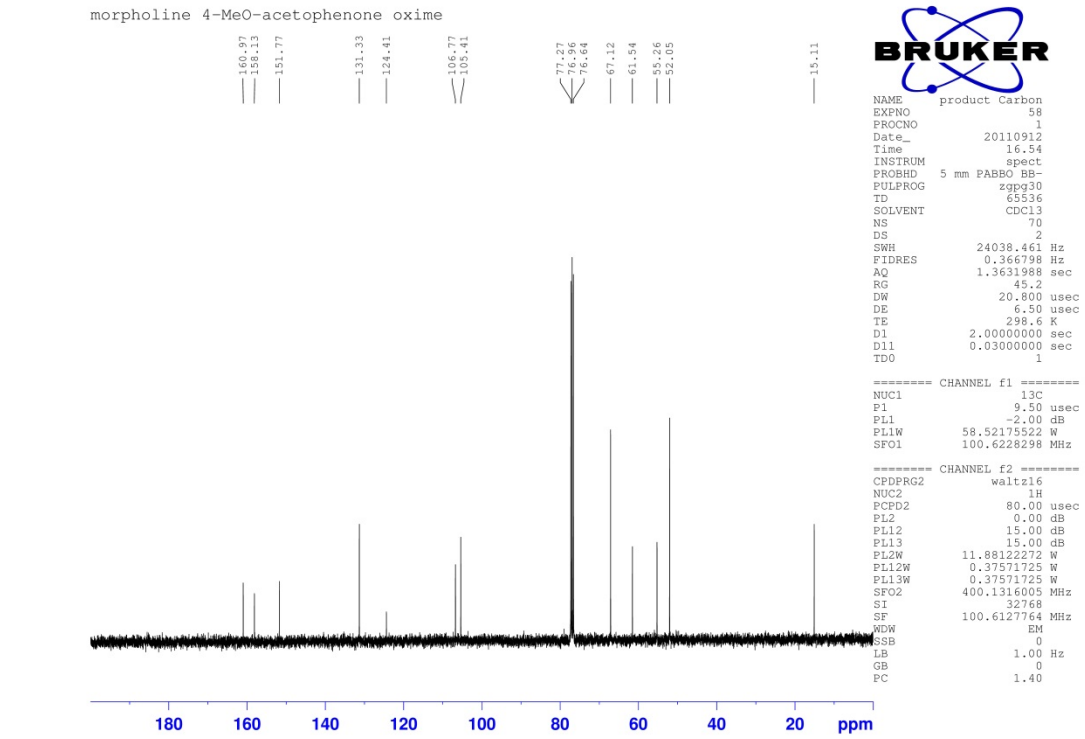

Figure A89. ^{1}H NMR of **8da**

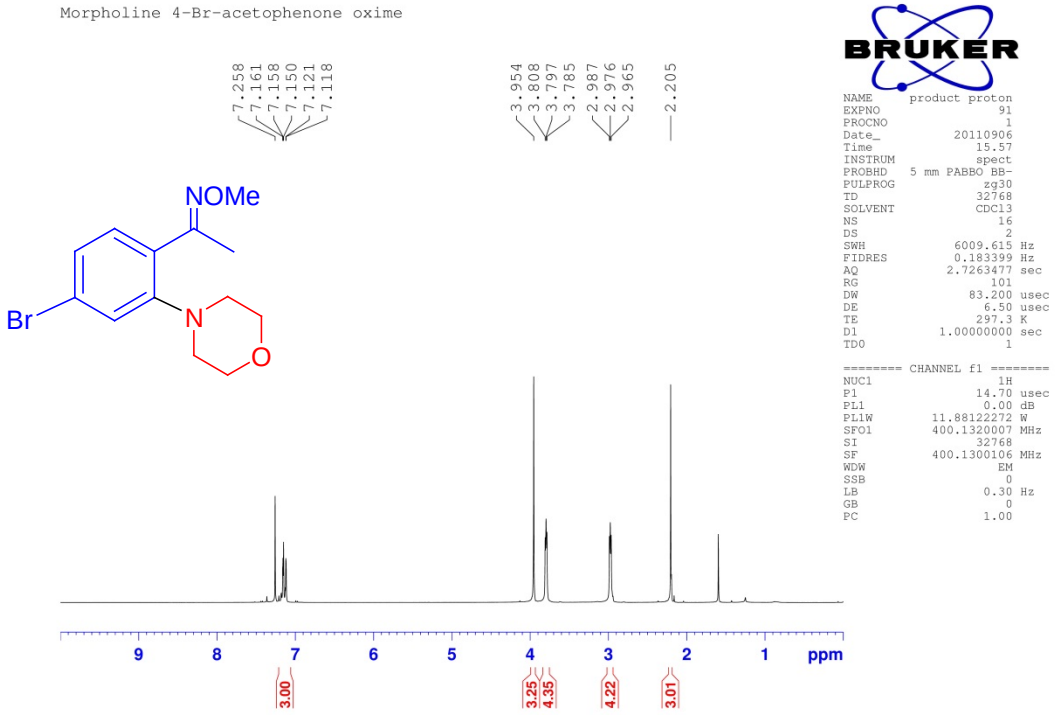

Figure A90. ^{13}C NMR of **8da**

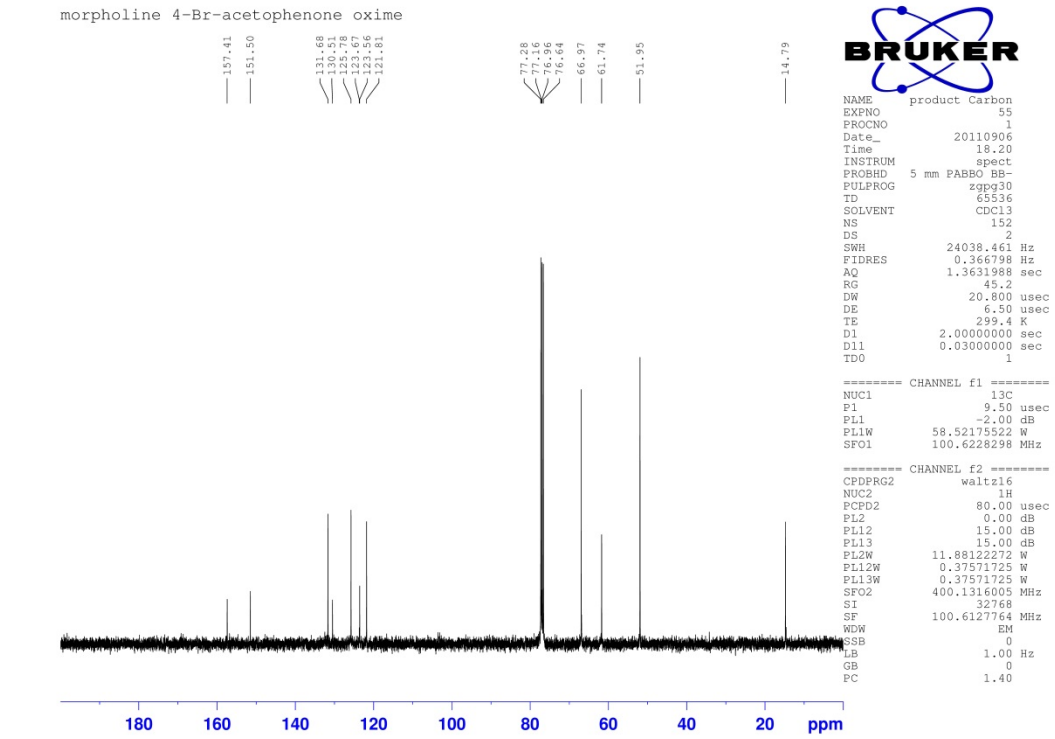

Figure A91. ^{1}H NMR of **8ea**

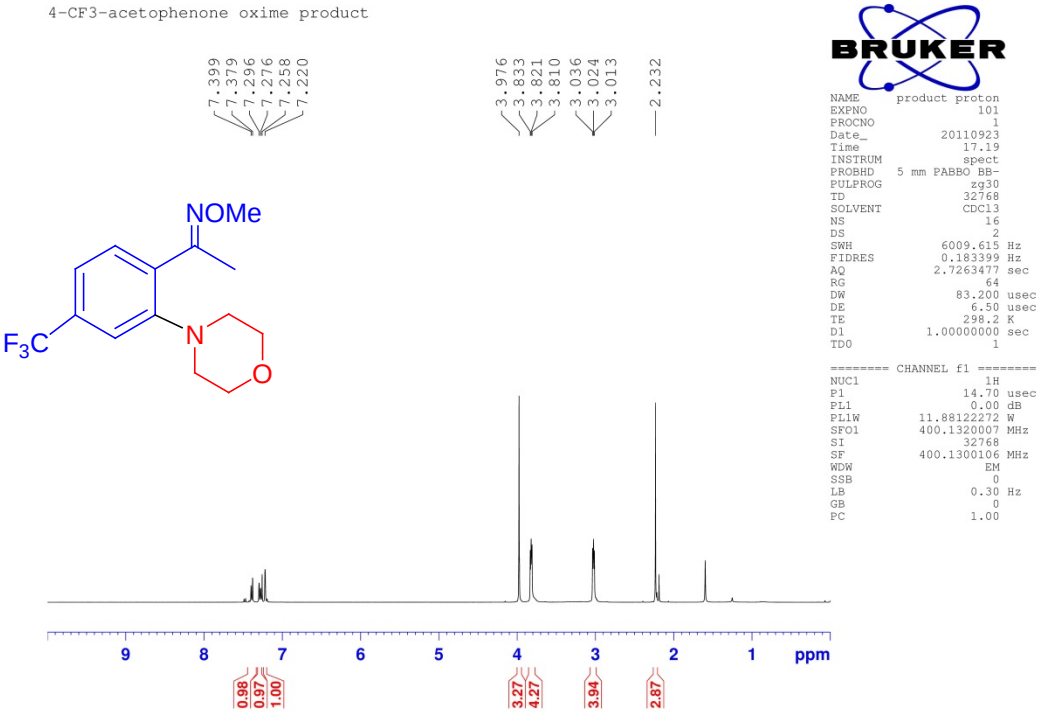

Figure A92. ^{13}C NMR of **8ea**

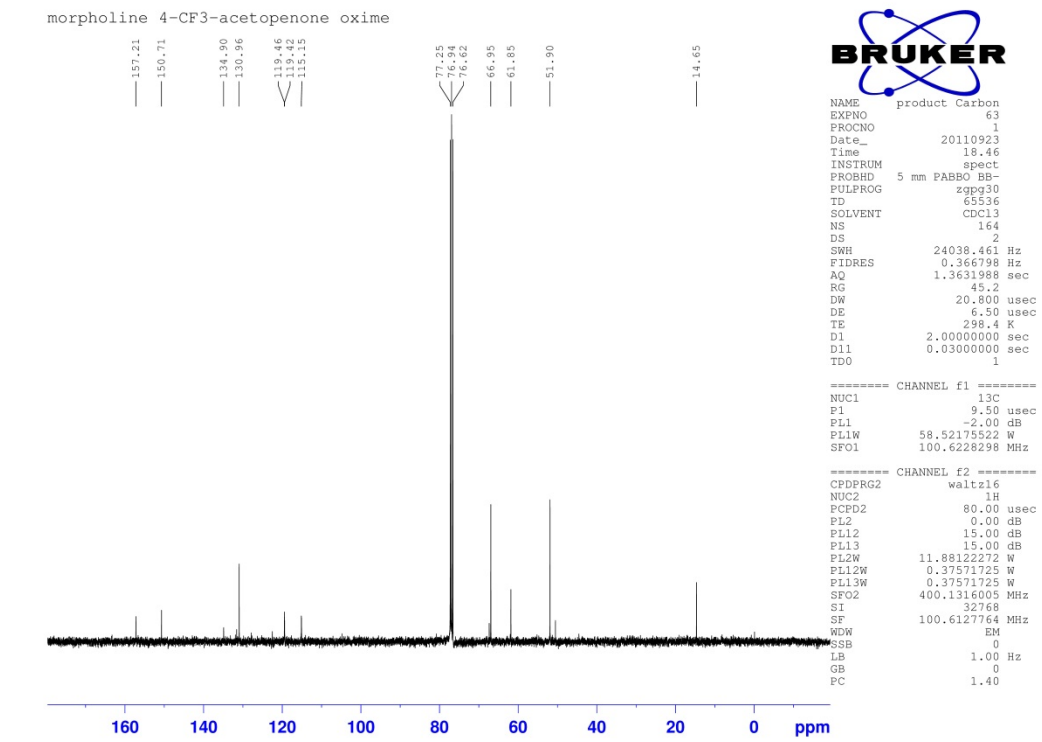

Figure A93. ^{1}H NMR of **8fa**

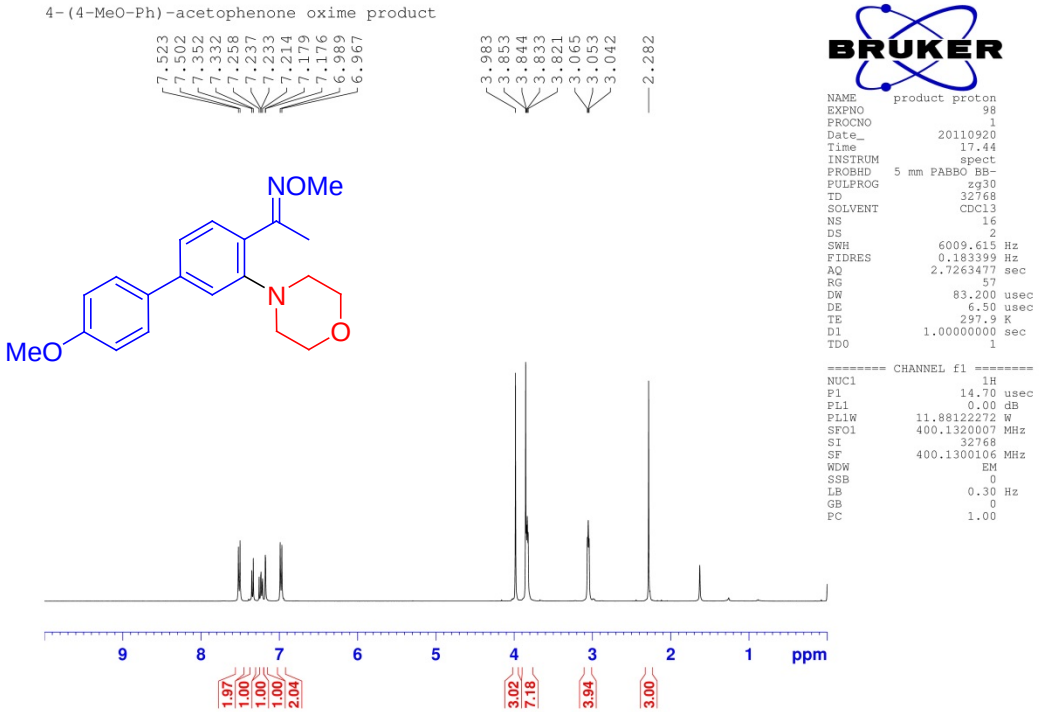

Figure A94. ^{13}C NMR of **8fa**

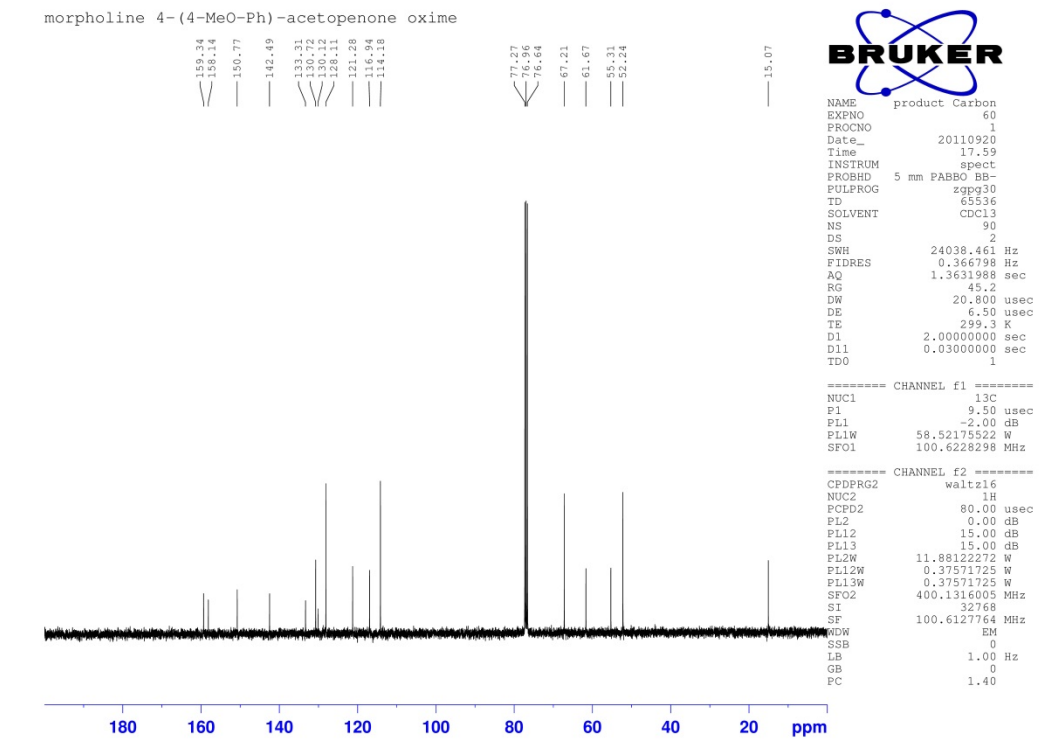

Figure A95. ^{1}H NMR of **8ga**

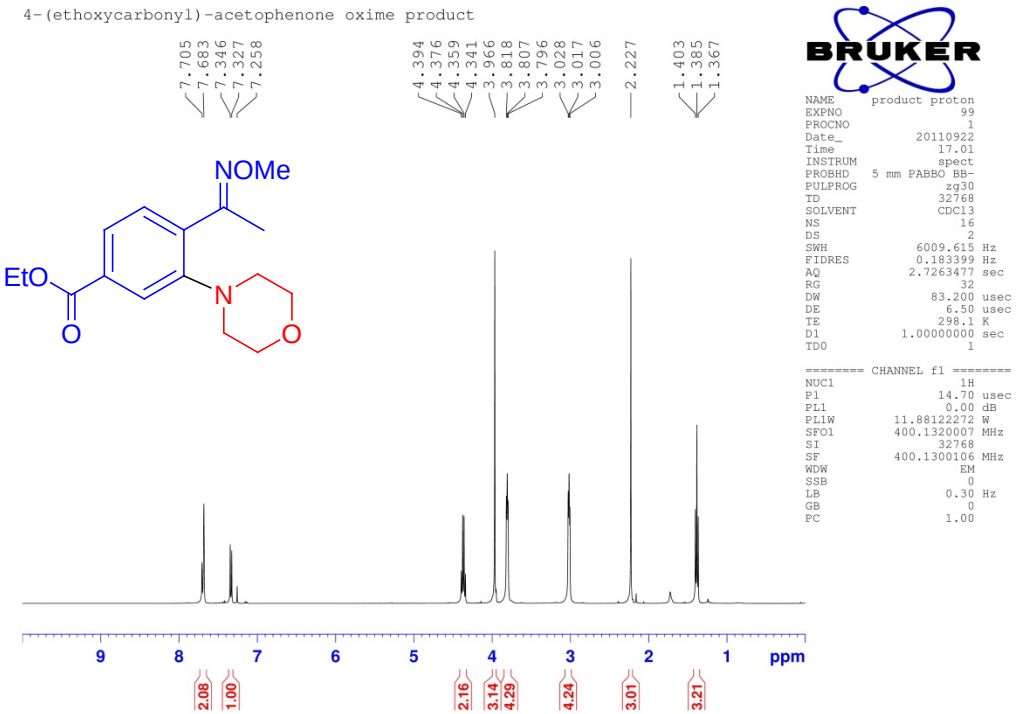

Figure A96. ^{13}C NMR of **8ga**

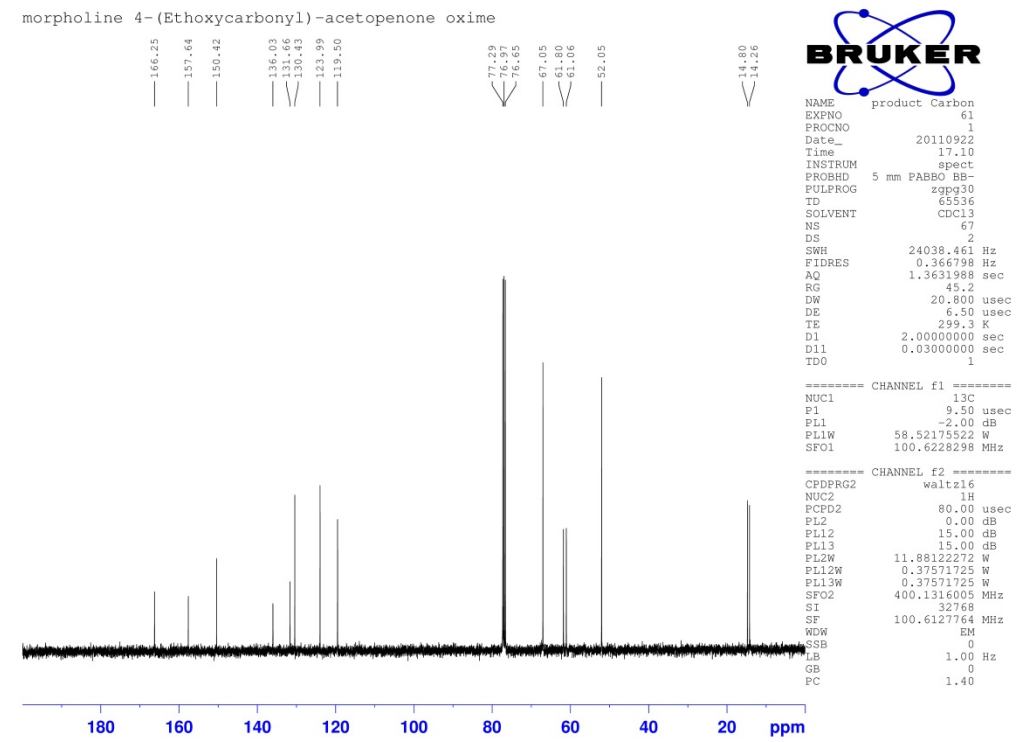

Figure A97. ^{1}H NMR of **8ha**

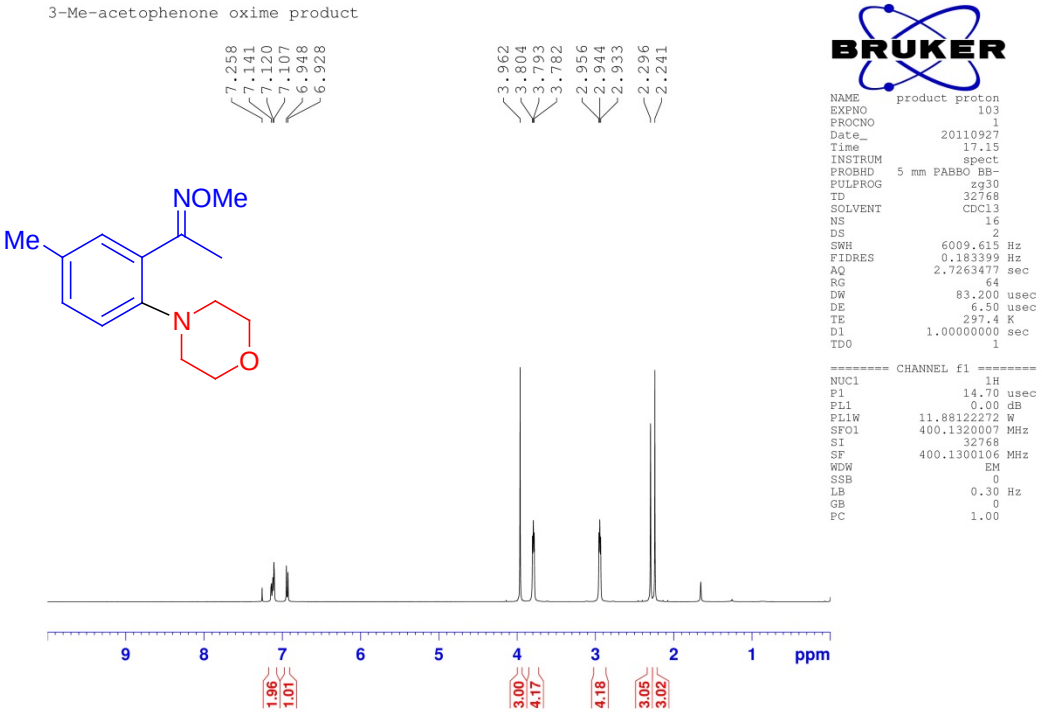

Figure A98. ^{13}C NMR of **8ha**

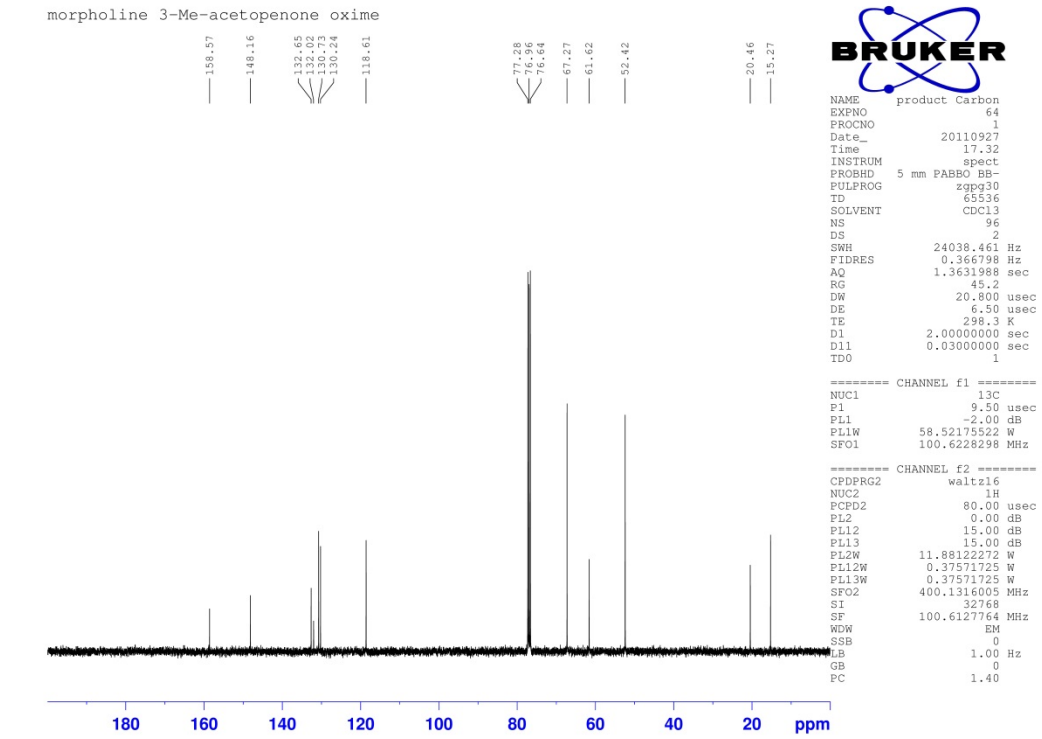

Figure A99. ^{1}H NMR of **8ia**

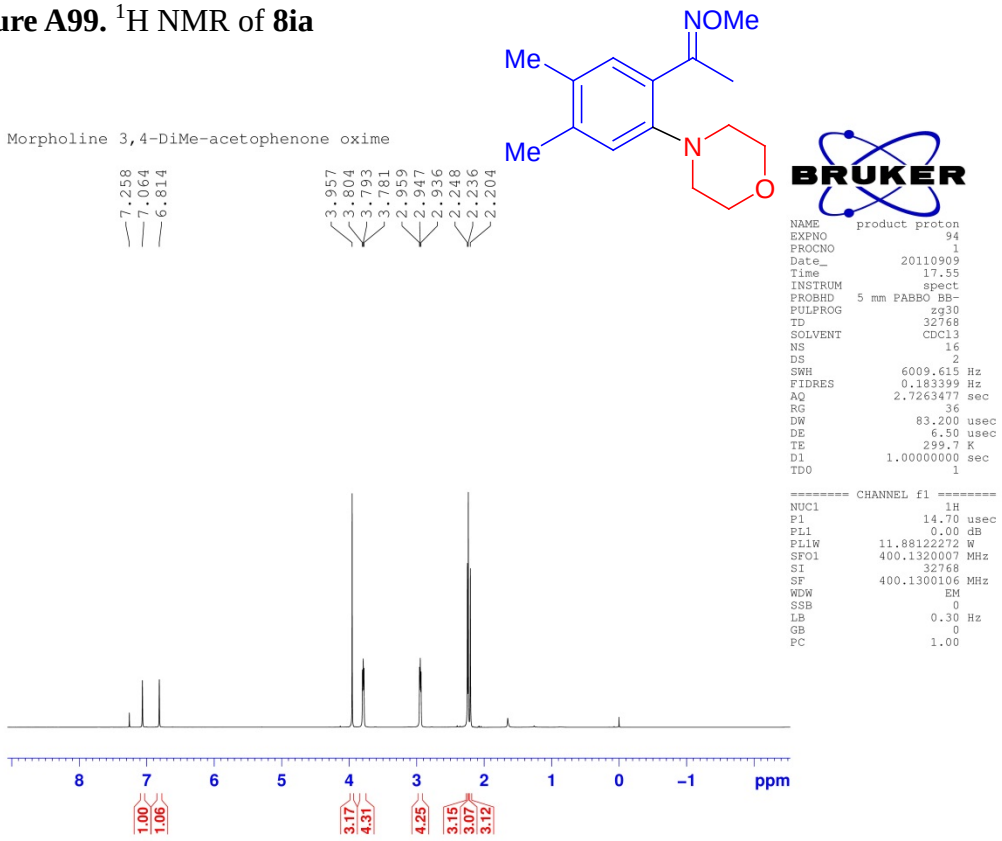

Figure A100. ^{13}C NMR of **8ia**

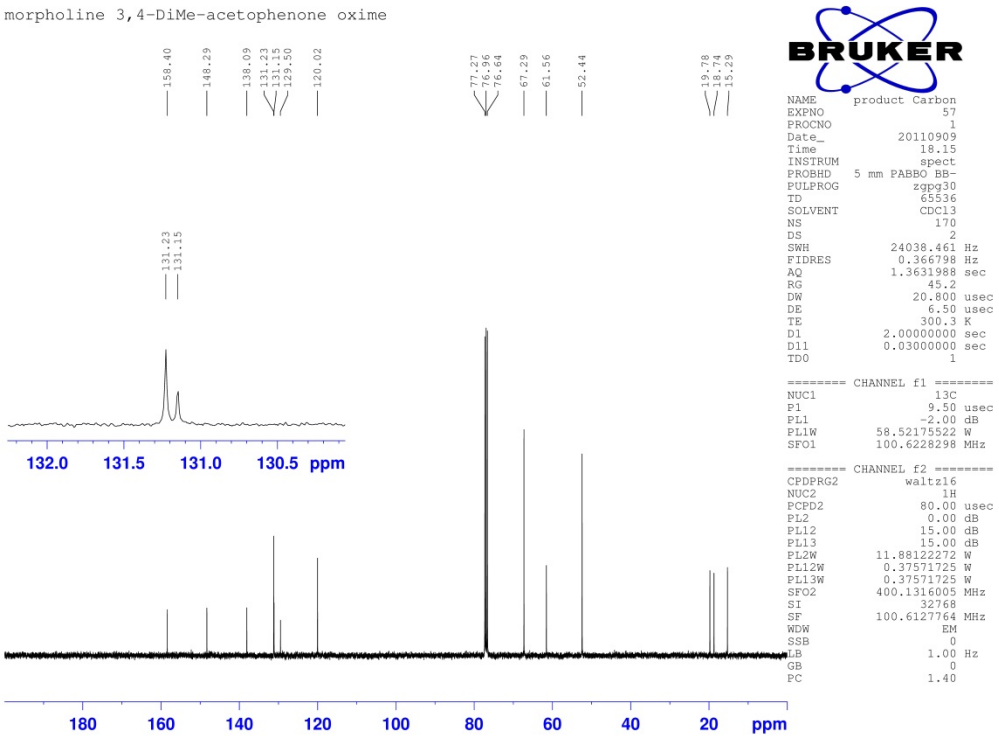

Figure A101. ^{1}H NMR of **8ja + 8ja'**

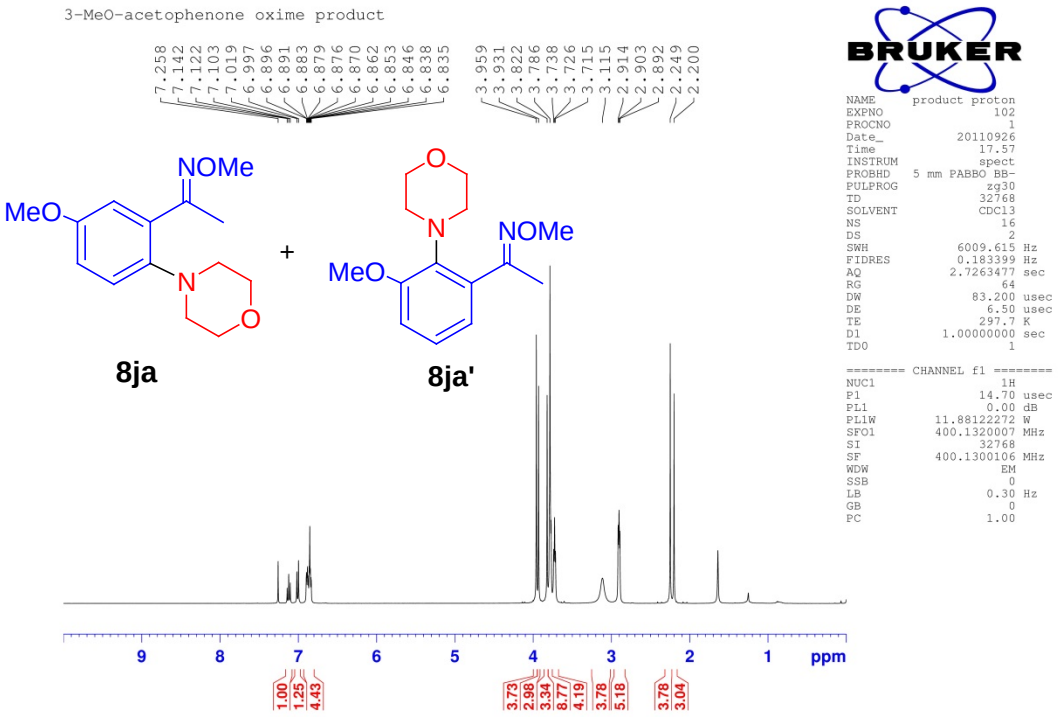

Figure A102. ^{1}H NMR of **8ja** (Partial Integration)

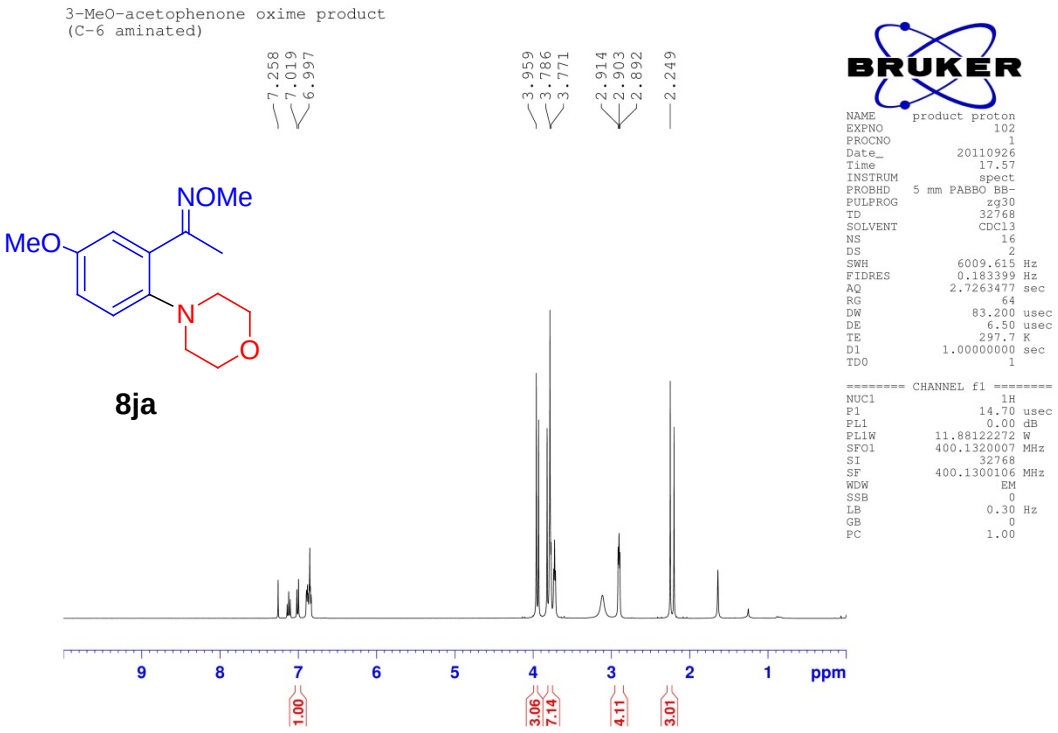

Figure A103. ^{1}H NMR of **8ja'** (Partial Integration)

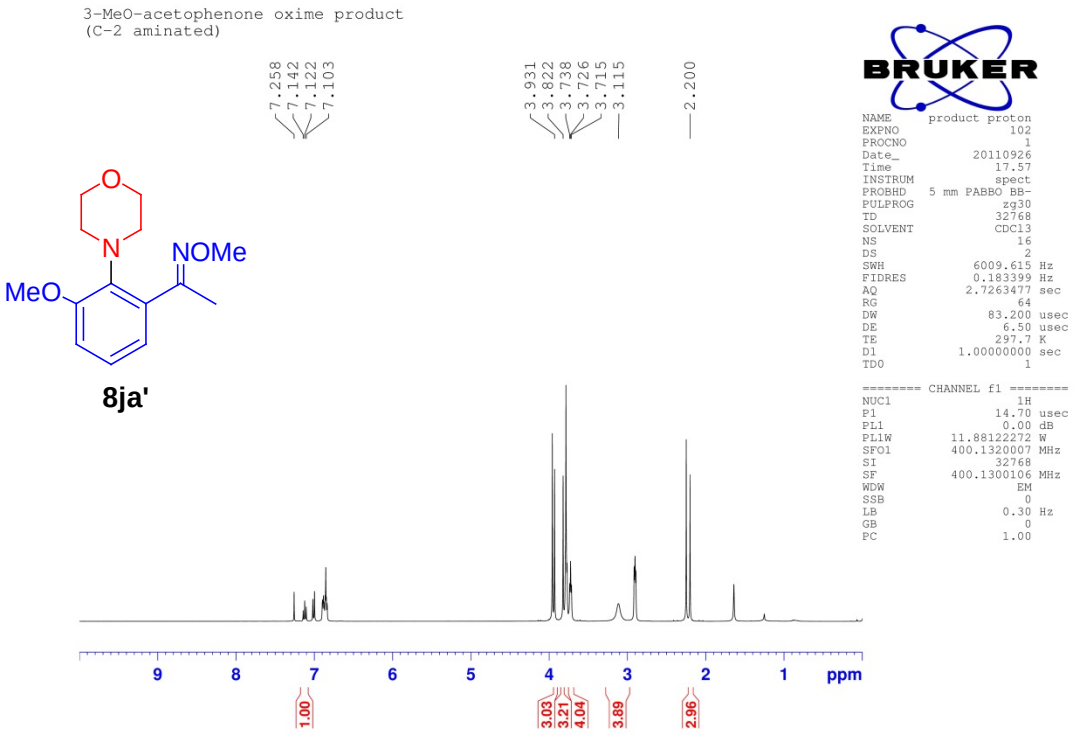

Figure A104. ^{1}H NMR of **8ka**

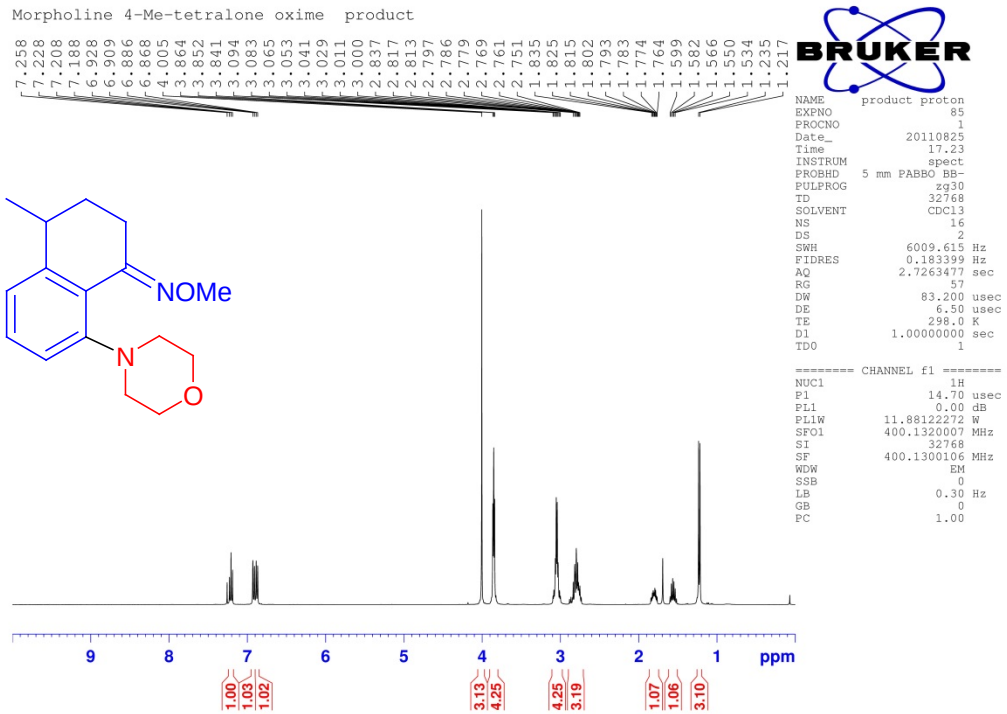

Figure A105. ^{13}C NMR of **8ka**

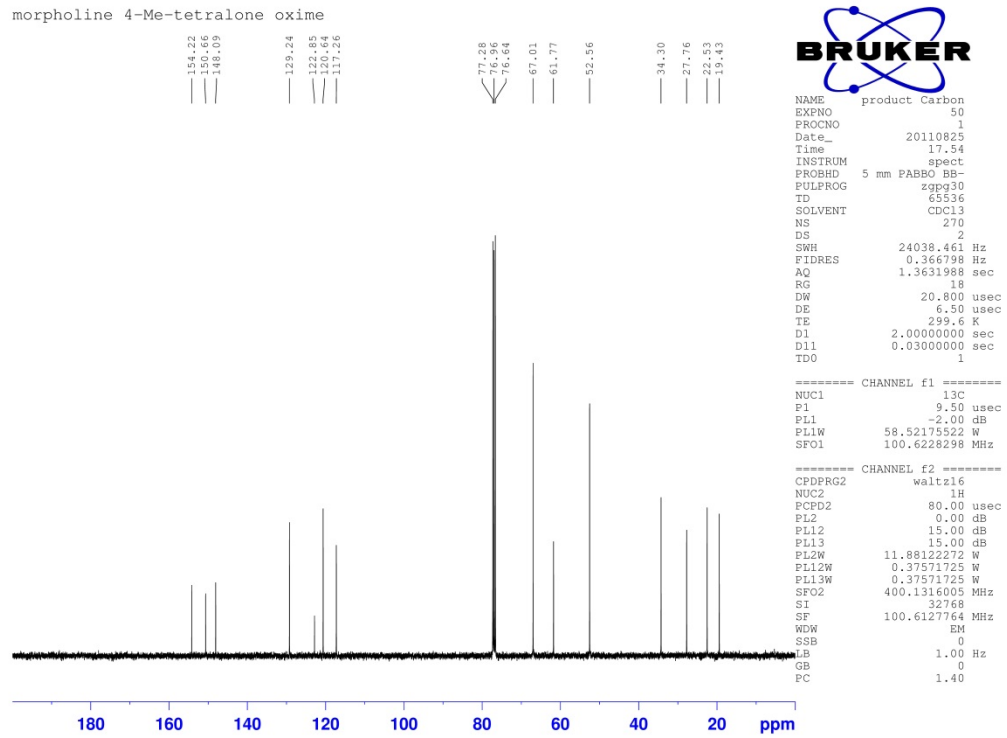

Figure A106. ^{1}H NMR of **8la**

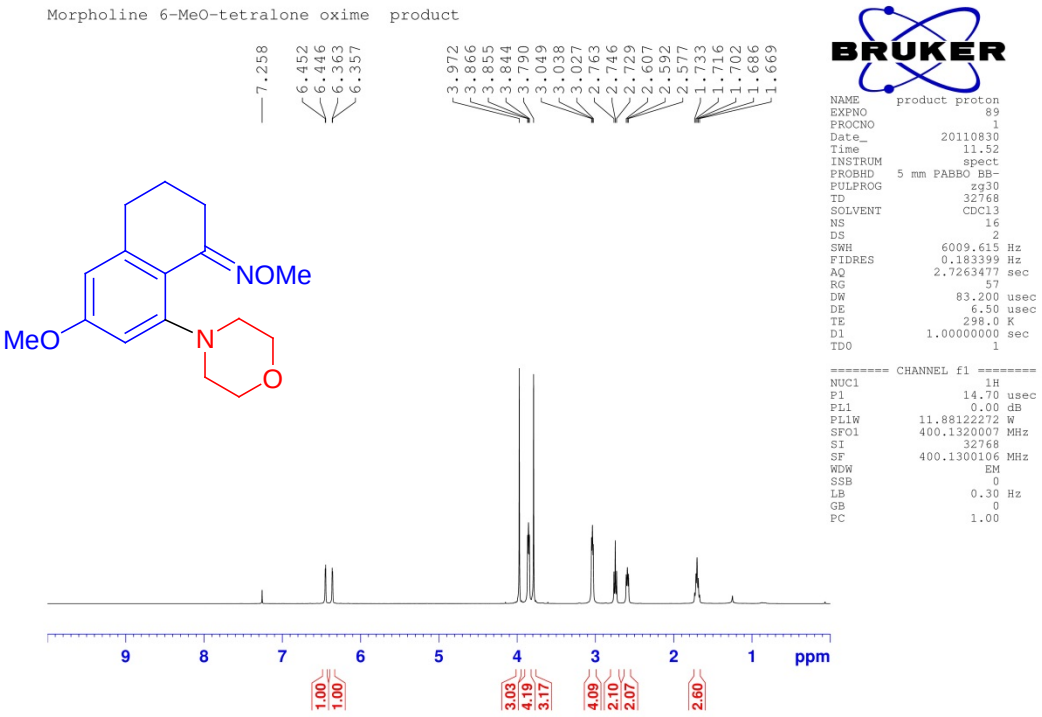

Figure A107^{13}C NMR of **8la**

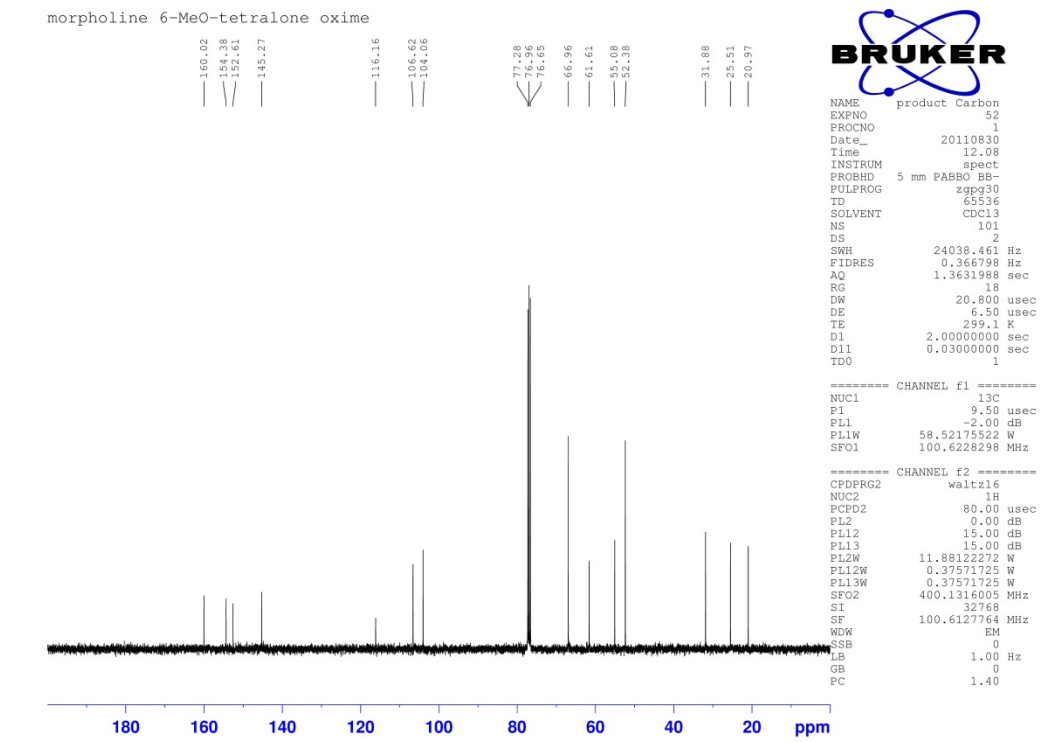

Figure A108. ^{1}H NMR of **8ma**

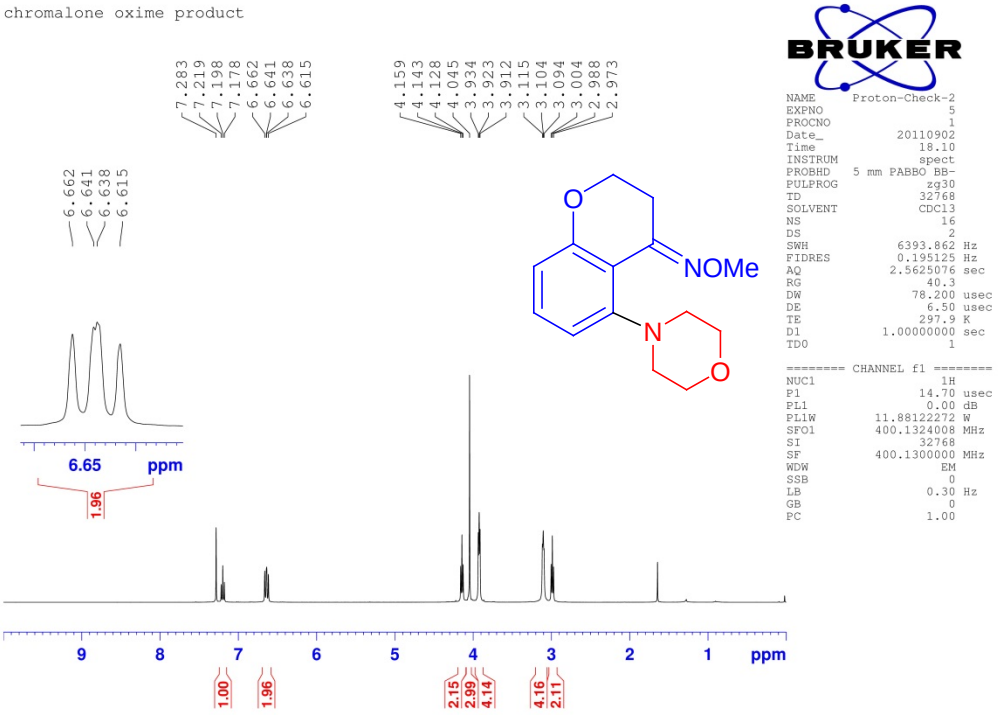

Figure A109. ^{13}C NMR of **8ma**

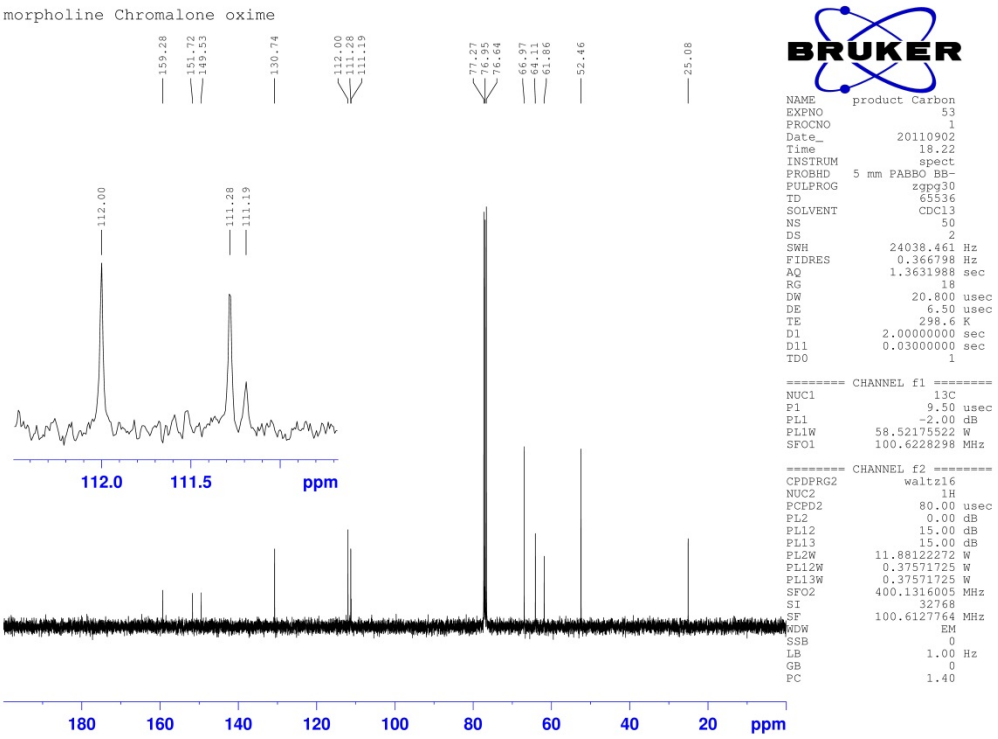

Figure A110. ^{1}H NMR of **8na**

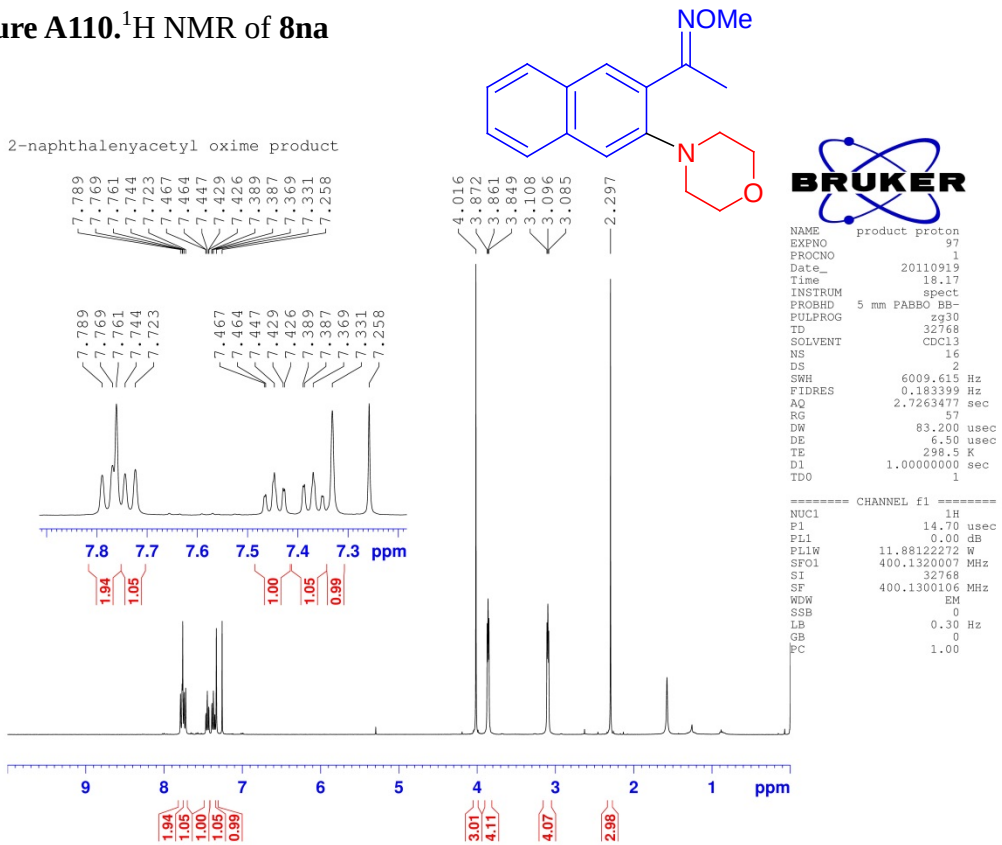

Figure A111. ^{13}C NMR of **8na**

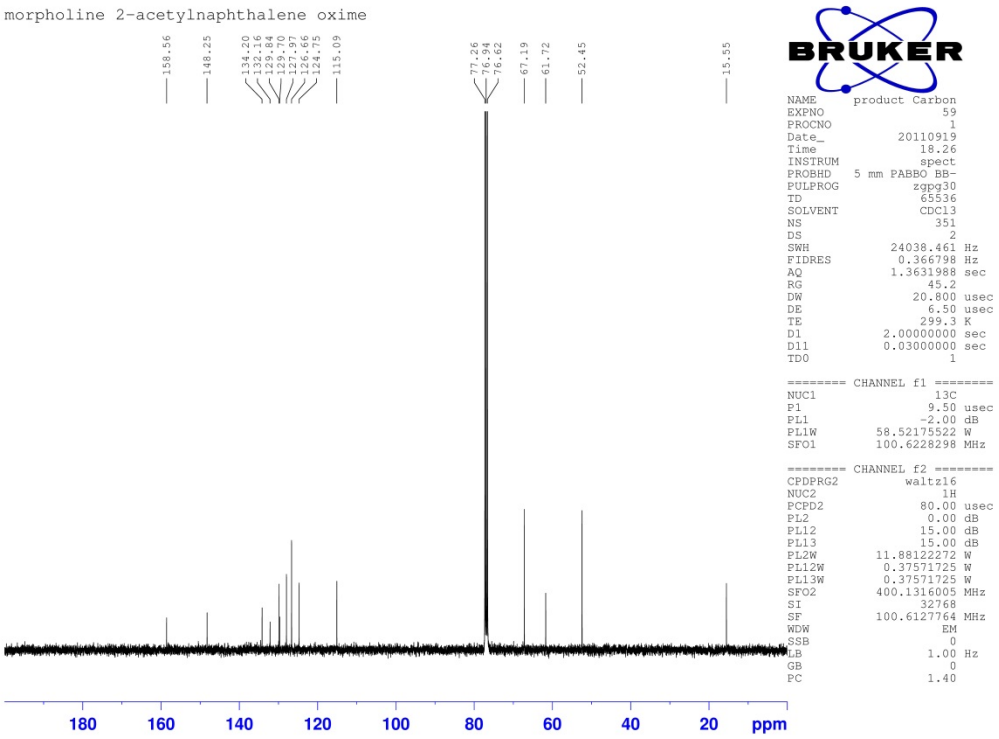

Figure A112. ^{1}H NMR of **8oa**

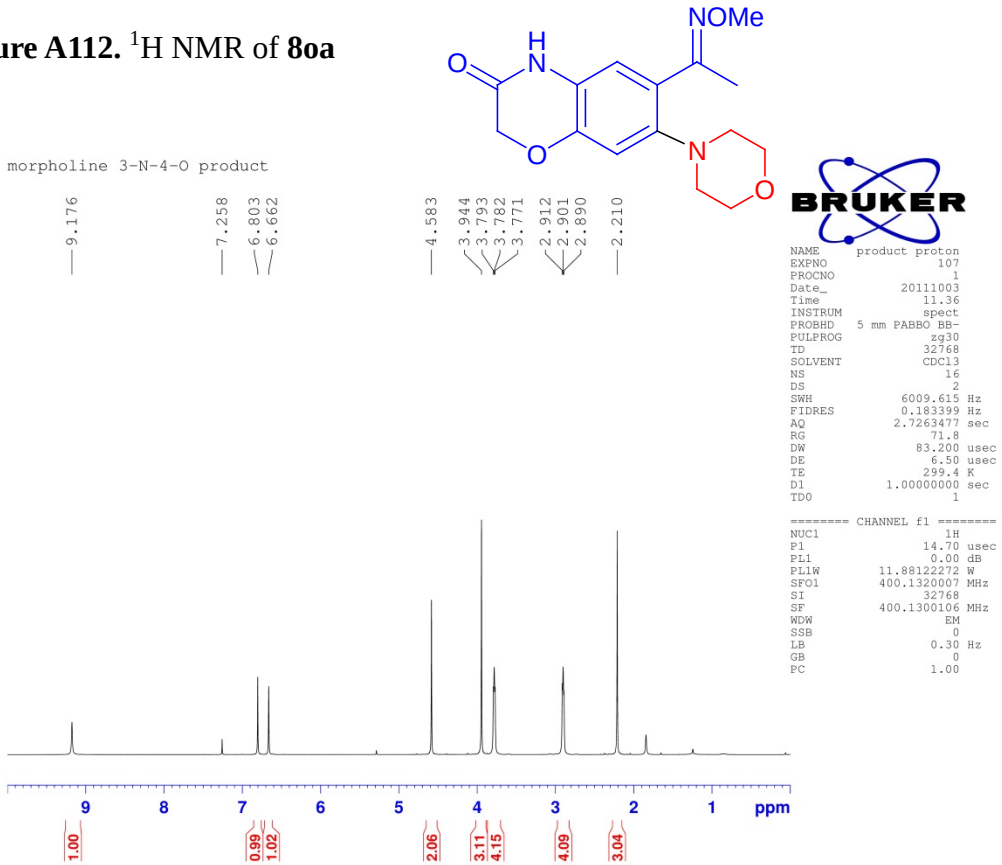

Figure A113. ^{13}C NMR of **8oa**

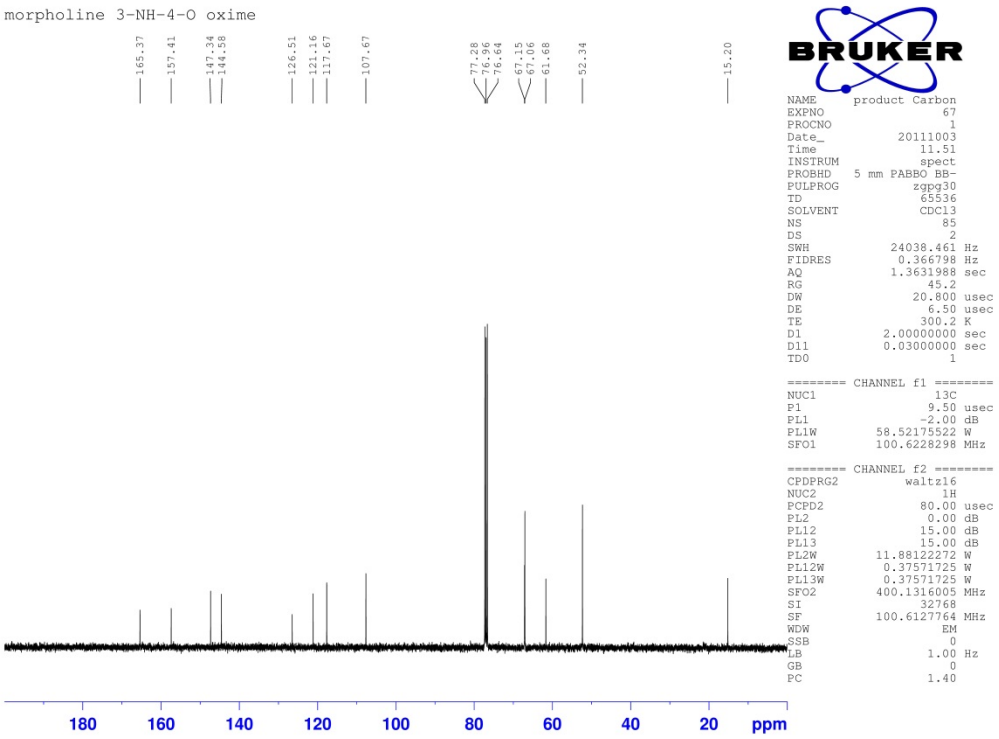

Figure A114. ^{1}H NMR of **8pa**

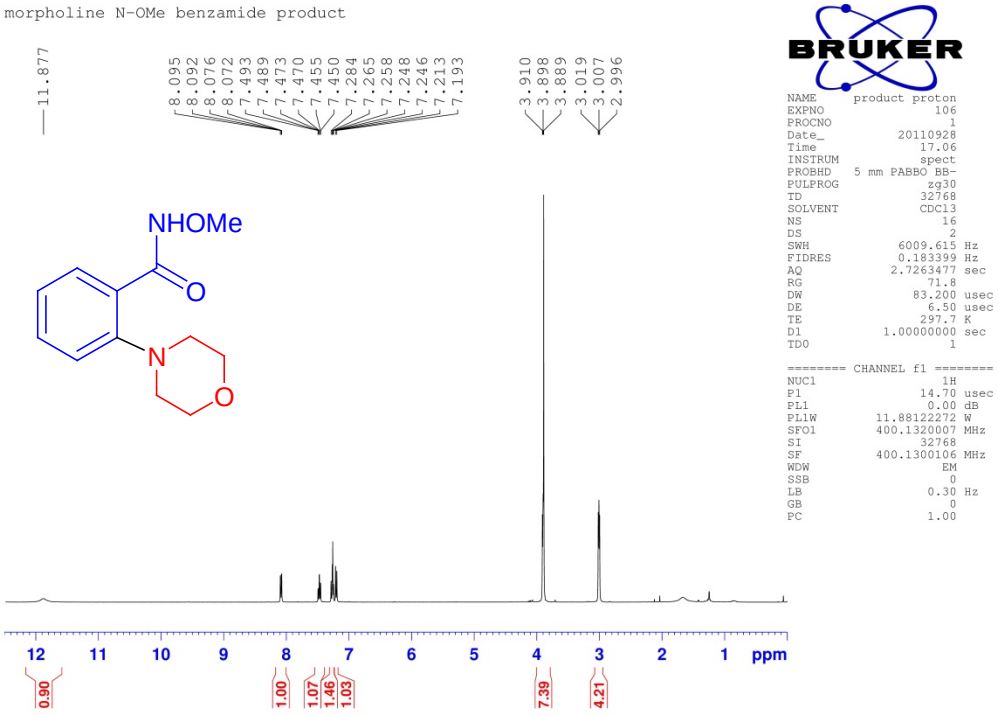

Figure A115. ^{13}C NMR of **8pa**

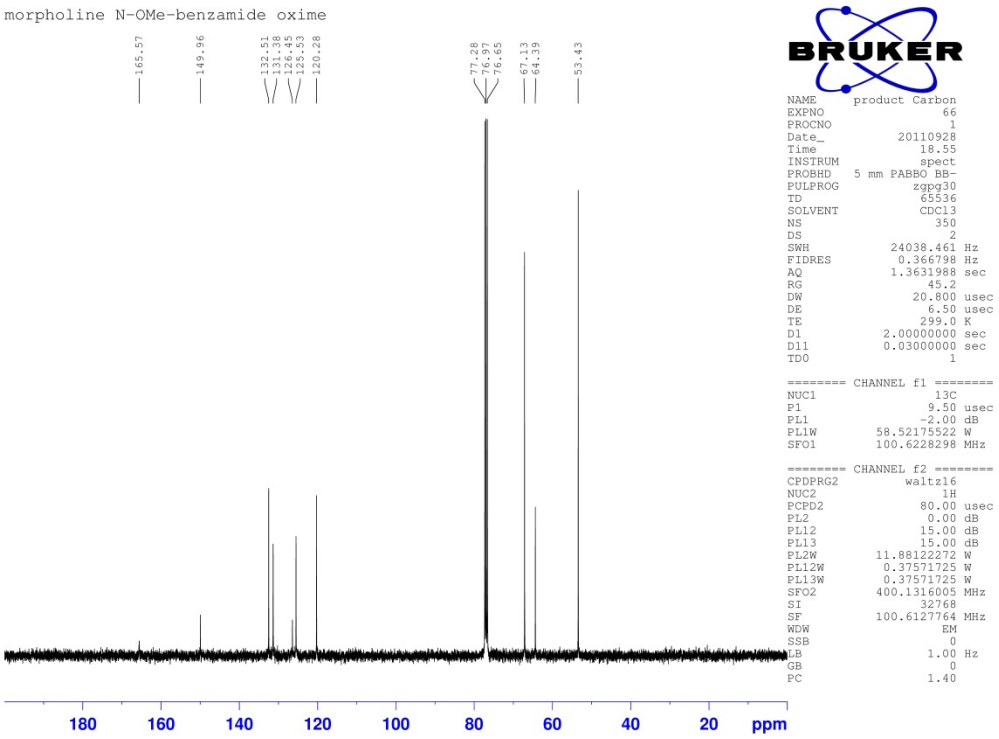

Figure A116. ^{1}H NMR of **8ab**

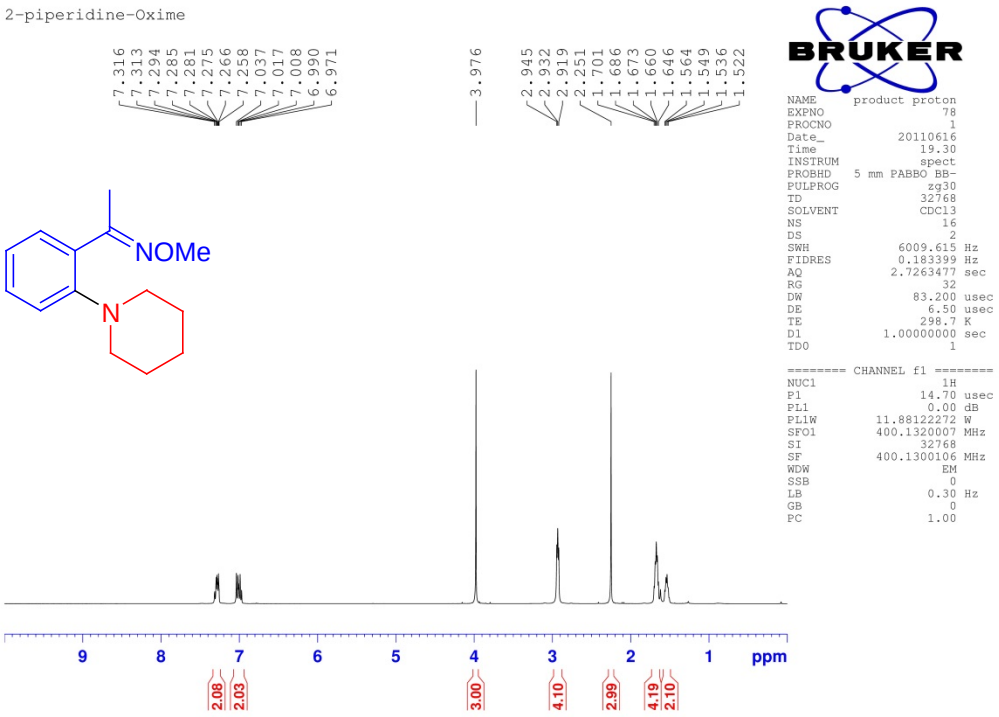

Figure A117. ^{13}C NMR of **8ab**

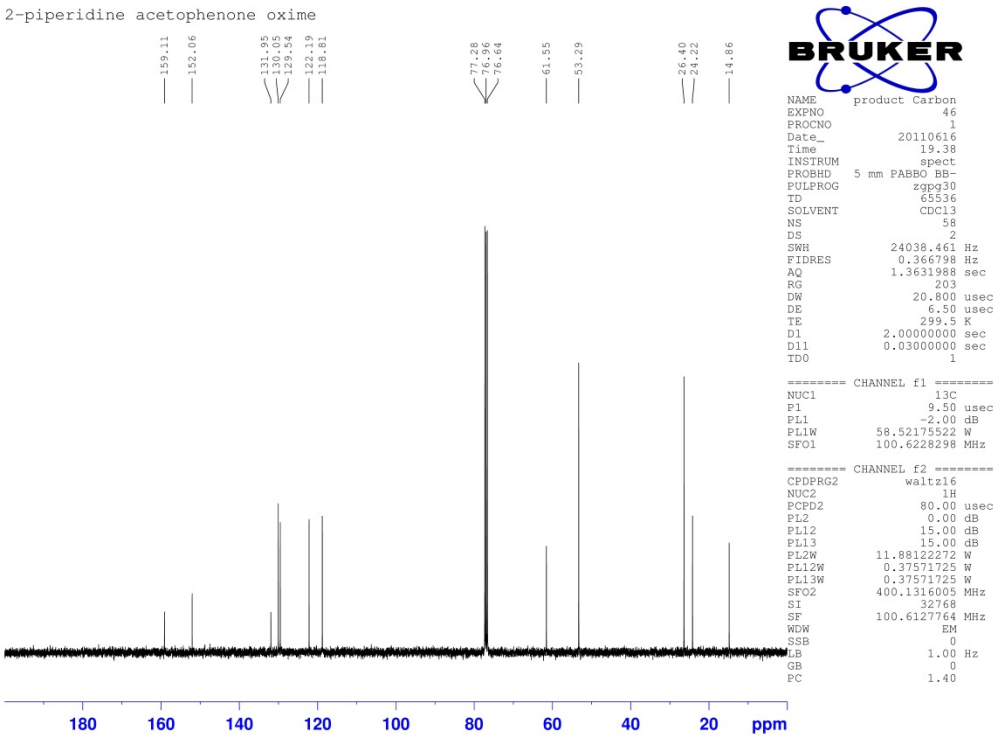

Figure A118. ^{1}H NMR of **8ac**

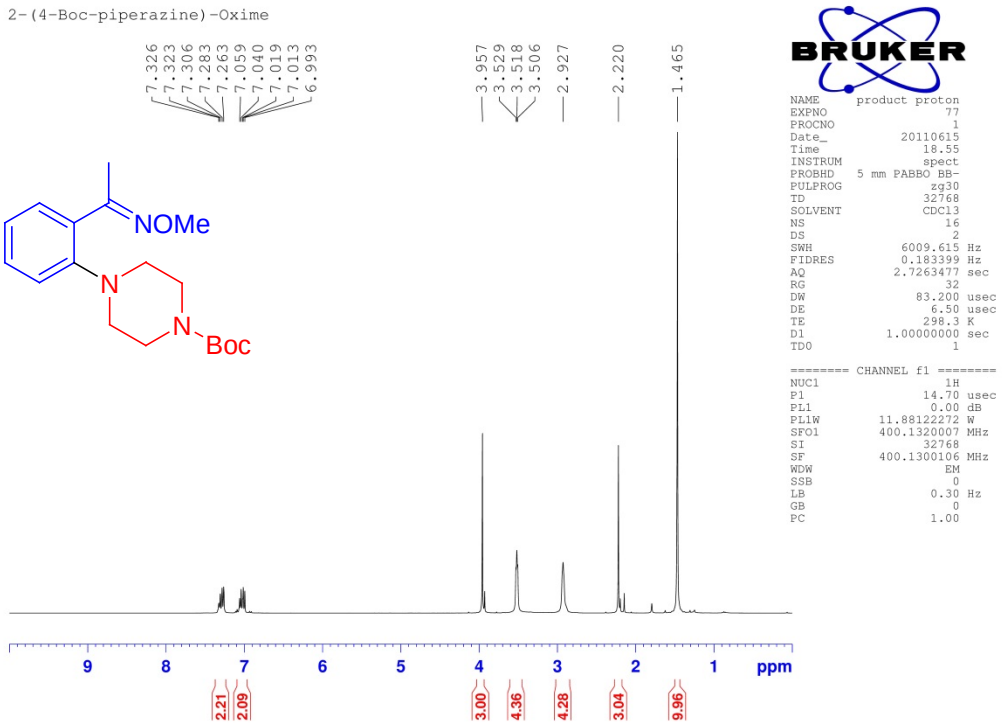

Figure A119 ^{13}C NMR of **8ac**

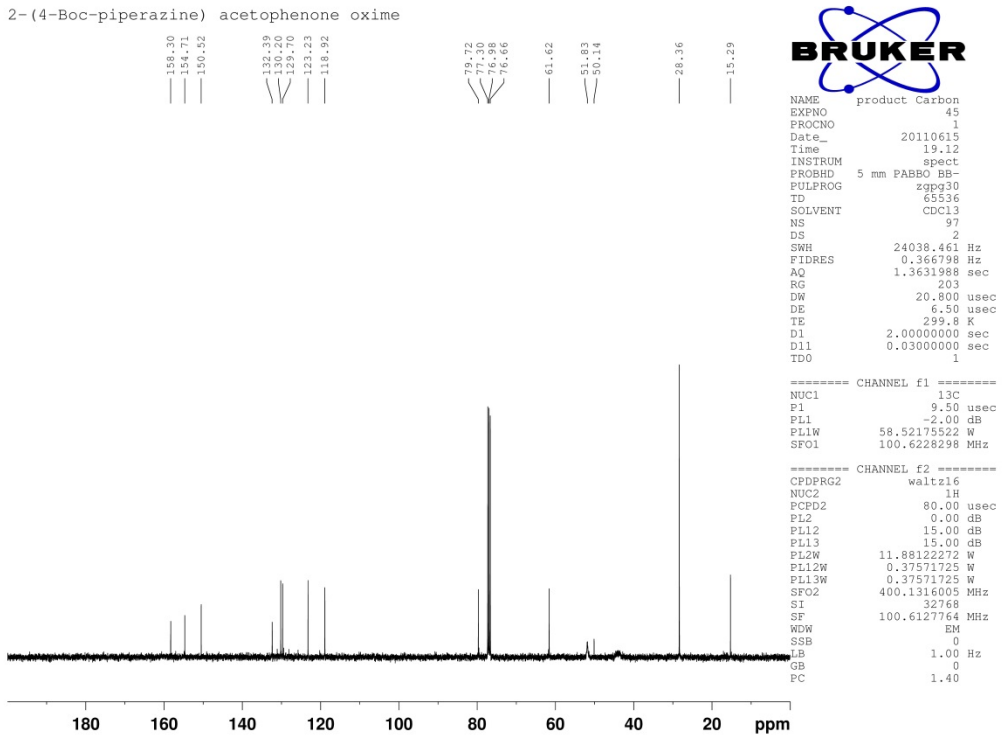

Figure A120. ^{1}H NMR of **8ad**

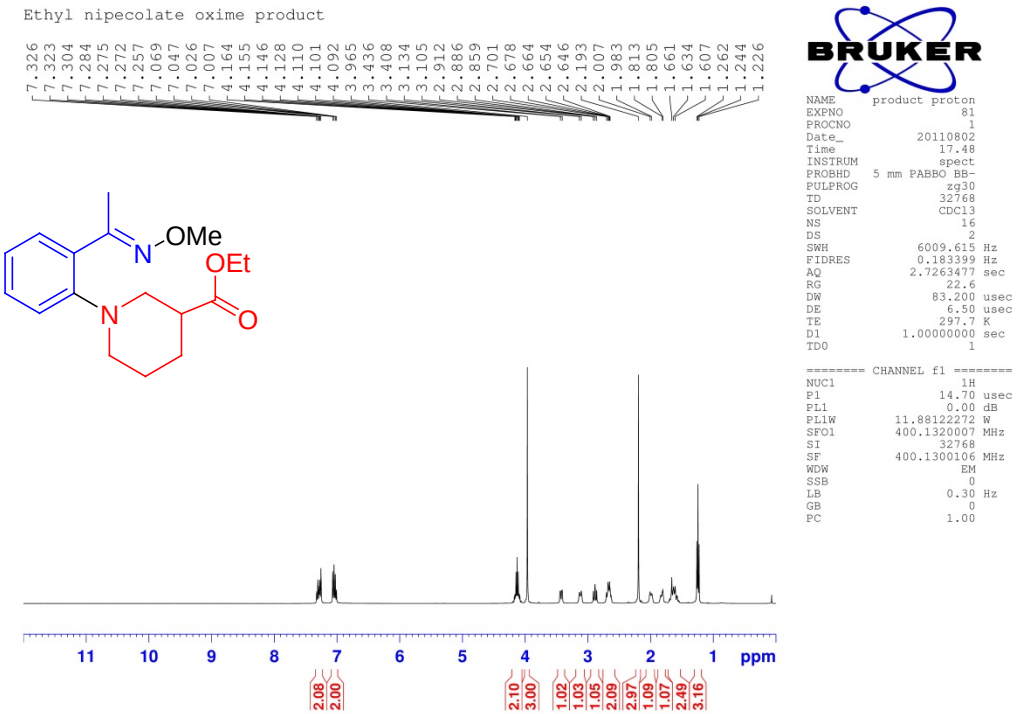

Figure A121. ^{13}C NMR of **8ad**

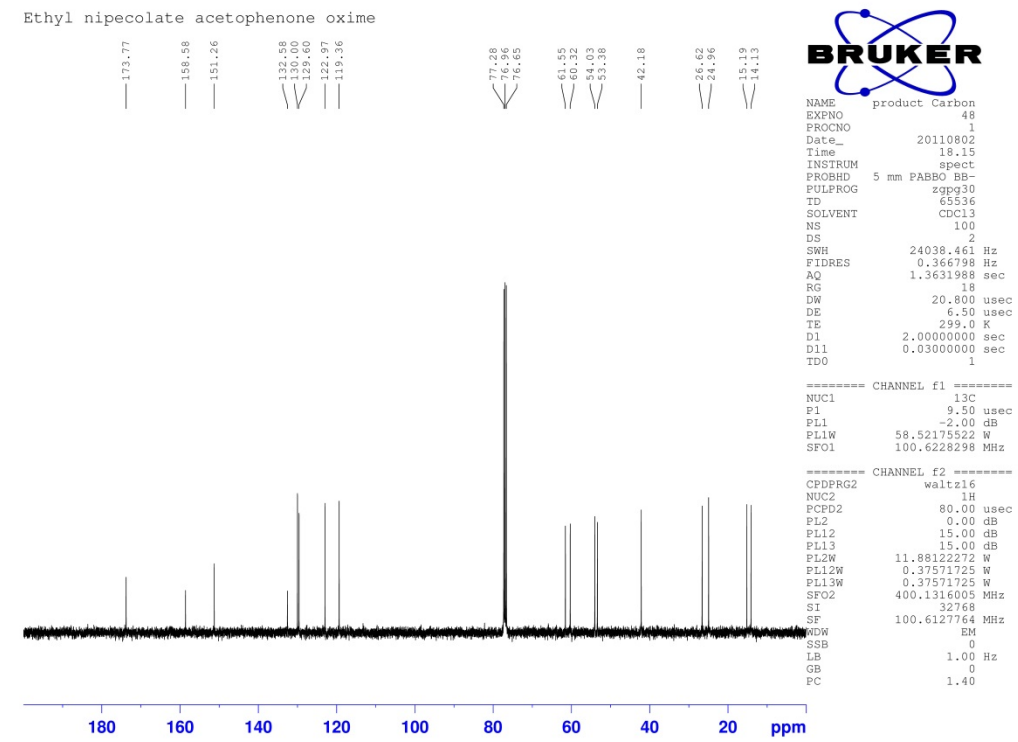

Figure A122. ^{1}H NMR of **8ae**

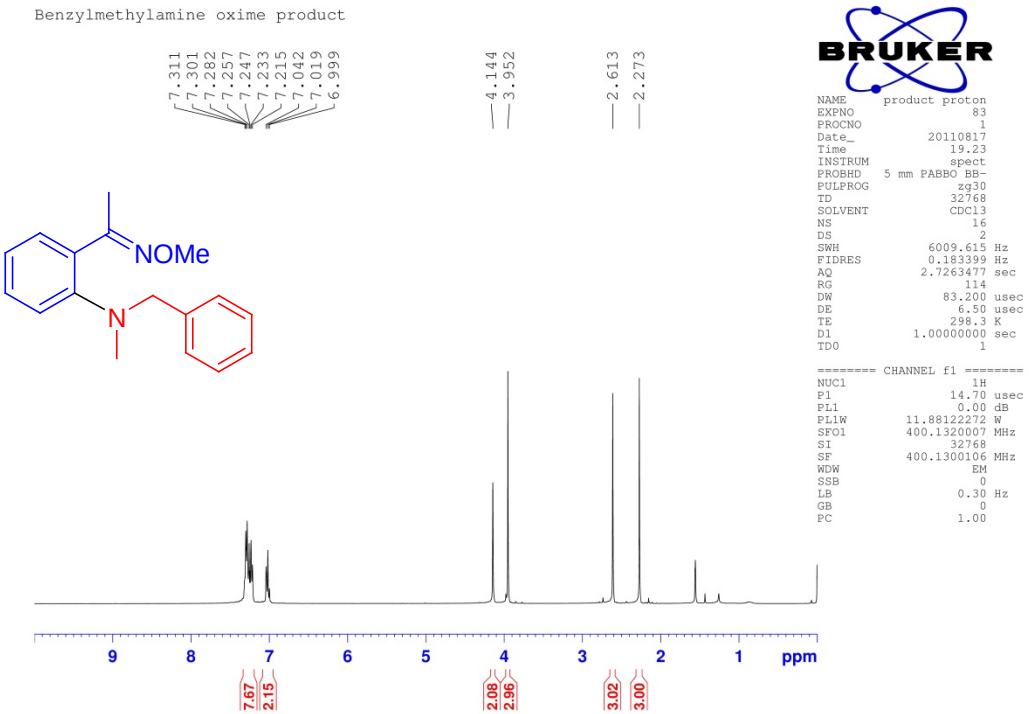

Figure A123. ^{13}C NMR of **8ae**

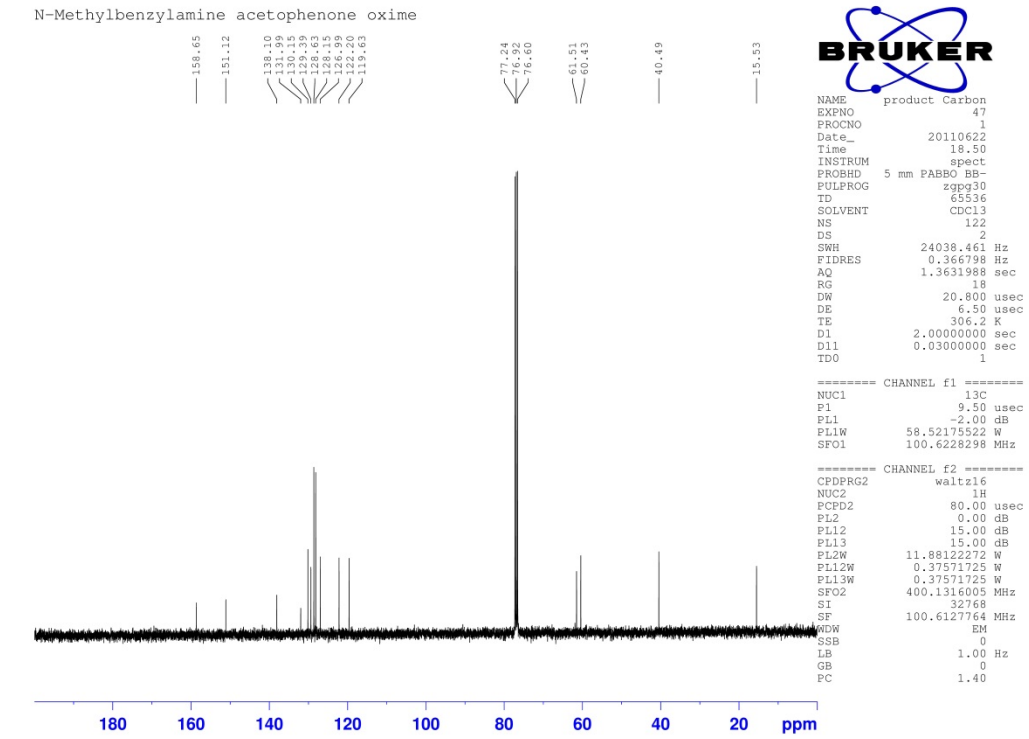

Figure A124[1]H NMR of **8af**

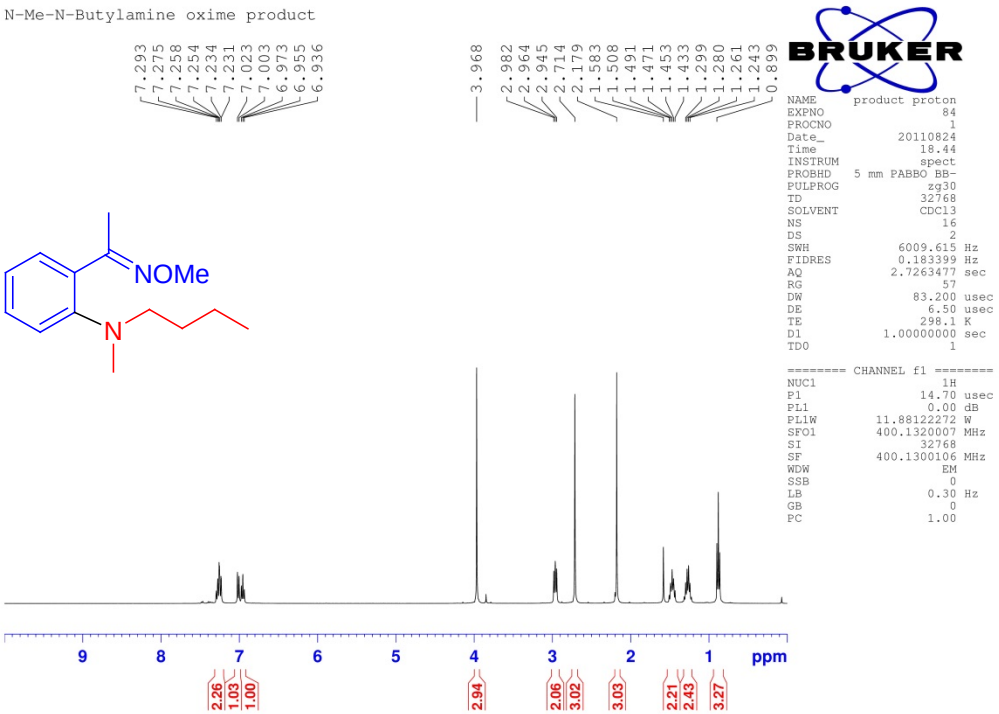

Figure A125[13]C NMR of **8af**

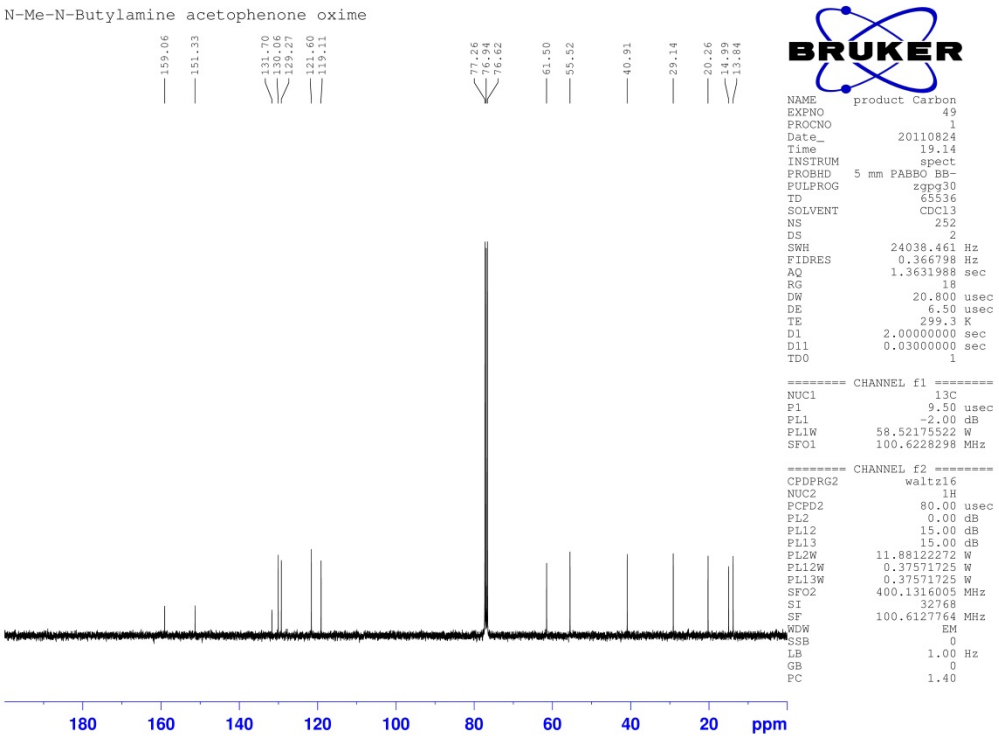

Figure A126. ^{1}H NMR of **10aa**

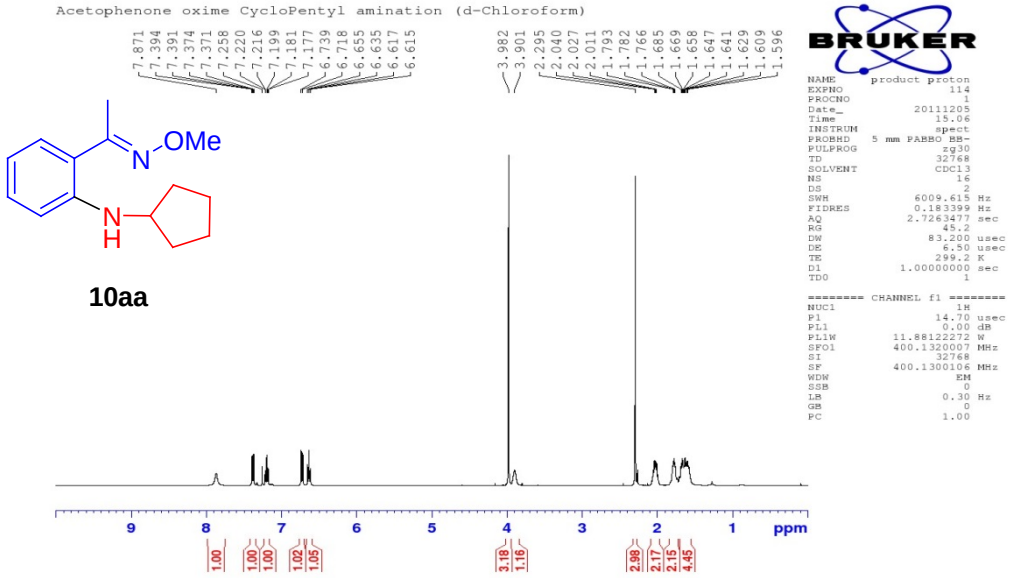

Figure A127. ^{13}C NMR of **10aa**

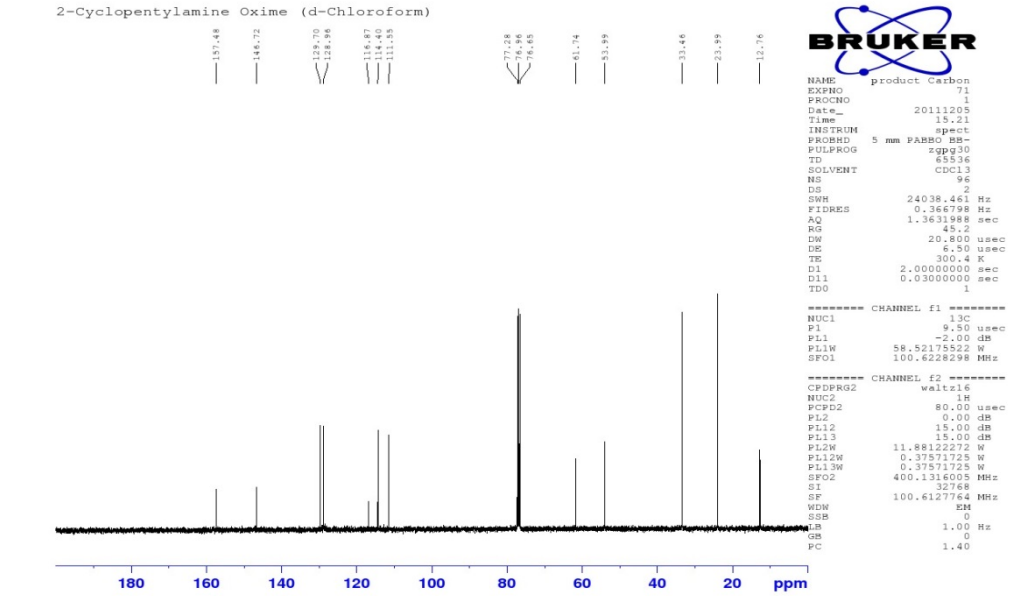

Figure A128. ^{1}H NMR of **10ua**

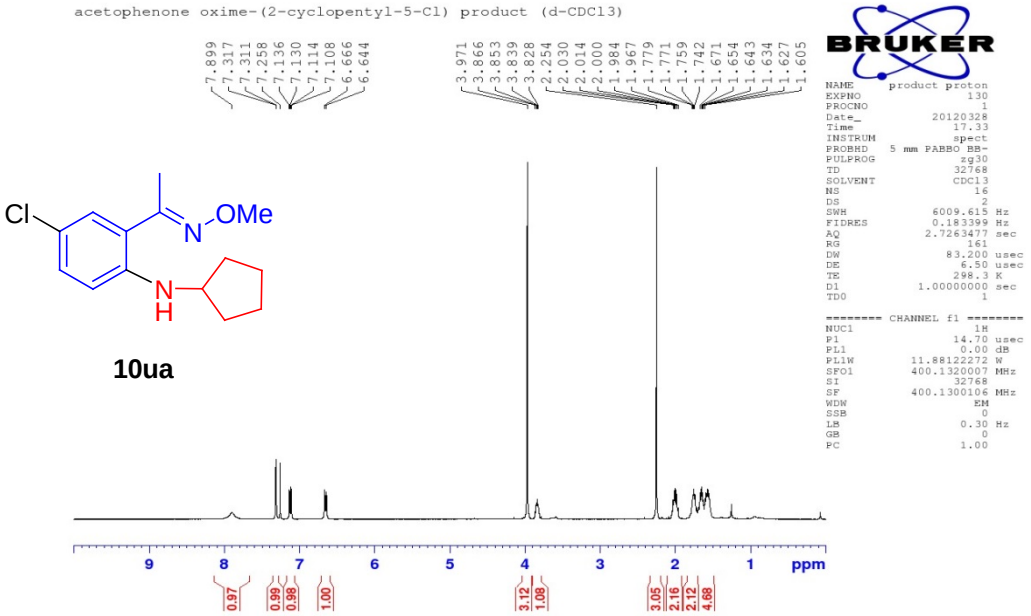

Figure A129. ^{13}C NMR of **10ua**

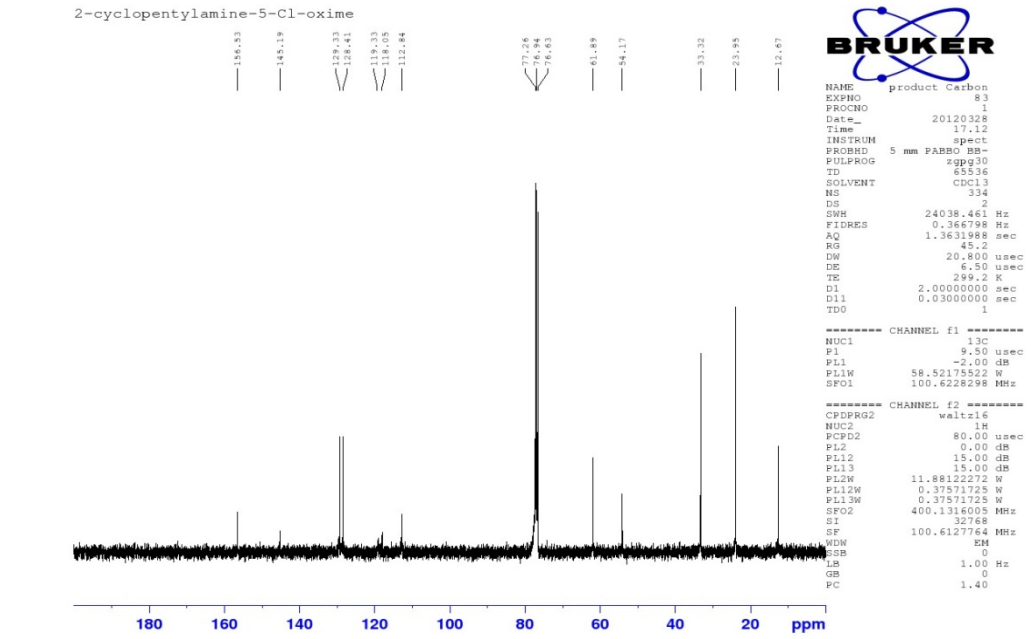

Figure A130. ^{1}H NMR of **10ua'**

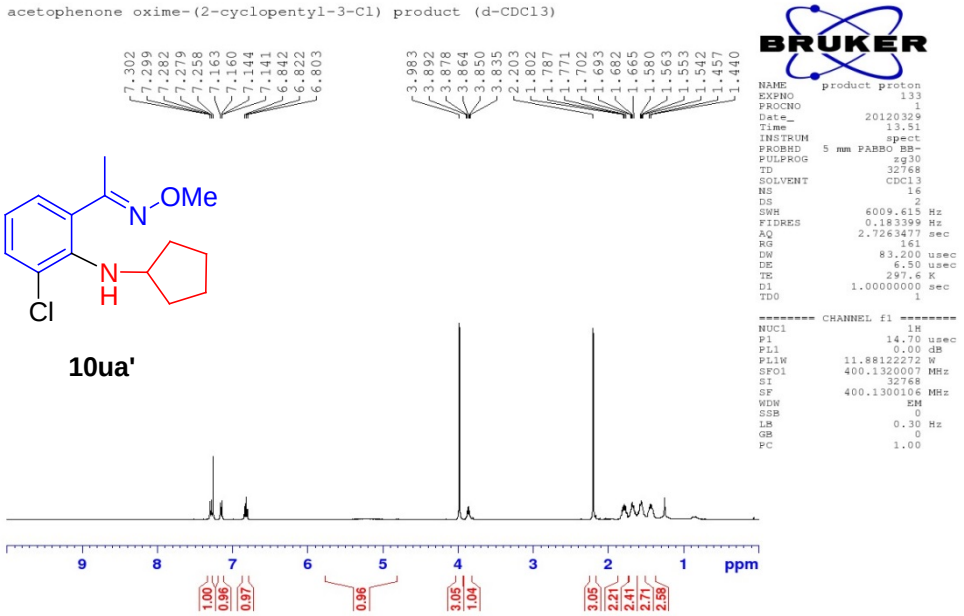

Figure A131. ^{13}C NMR of **10ua'**

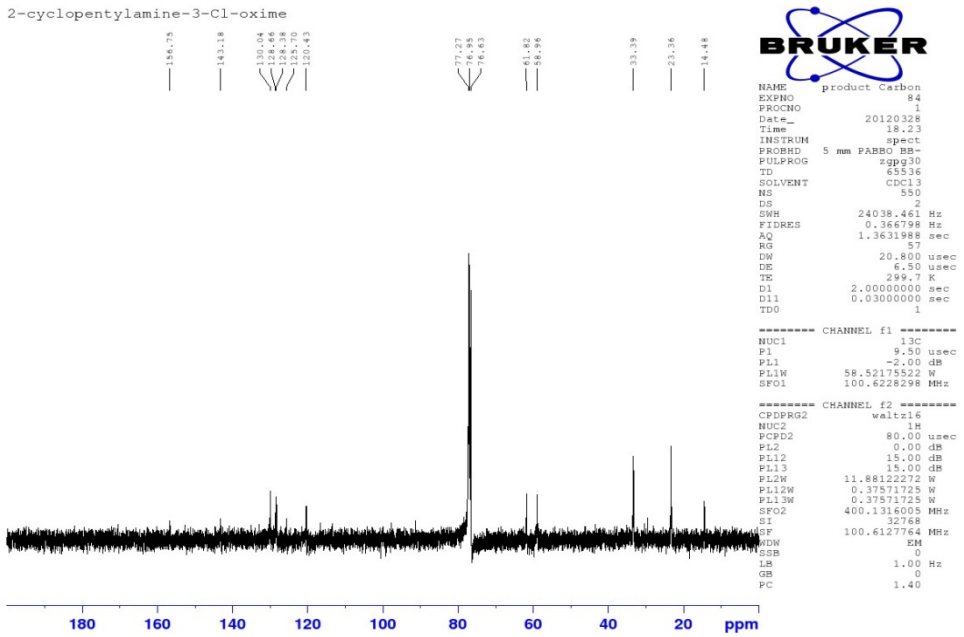

Figure A132. ^{1}H NMR of **10ba**

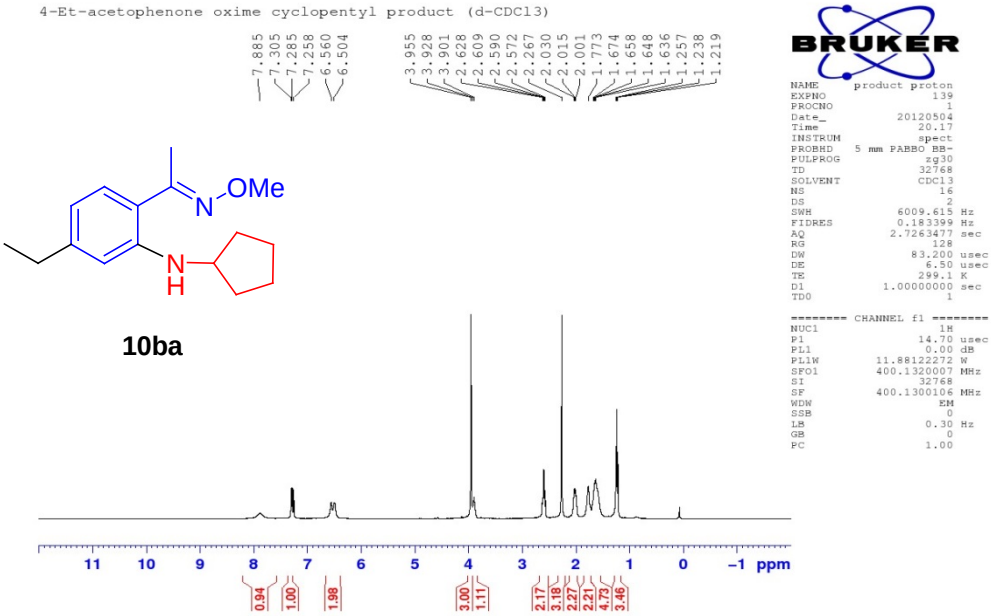

Figure A133. ^{13}C NMR of **10ba**

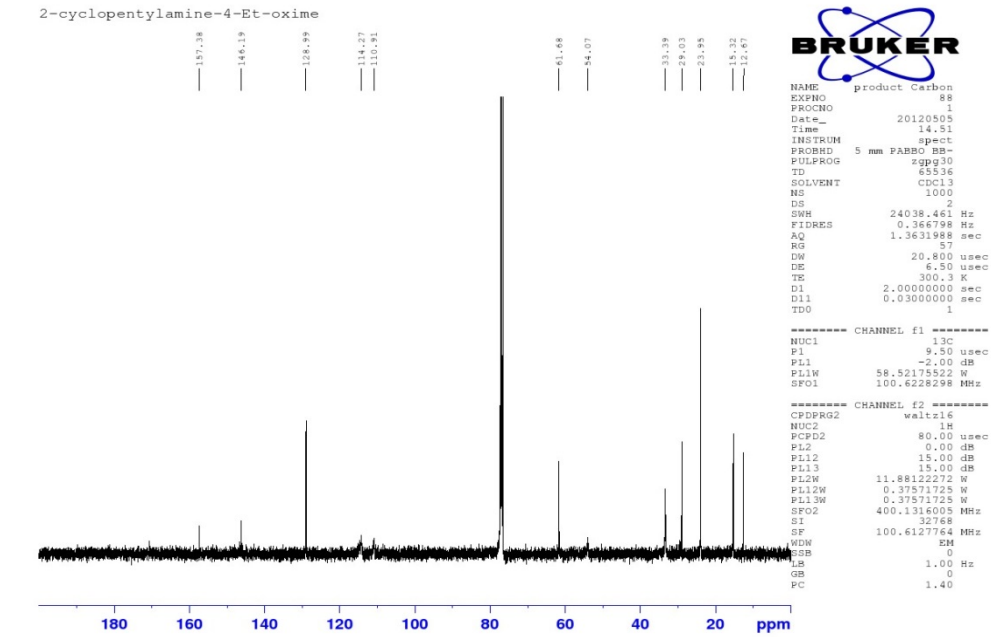

Figure A134. ^{1}H NMR of **10ca**

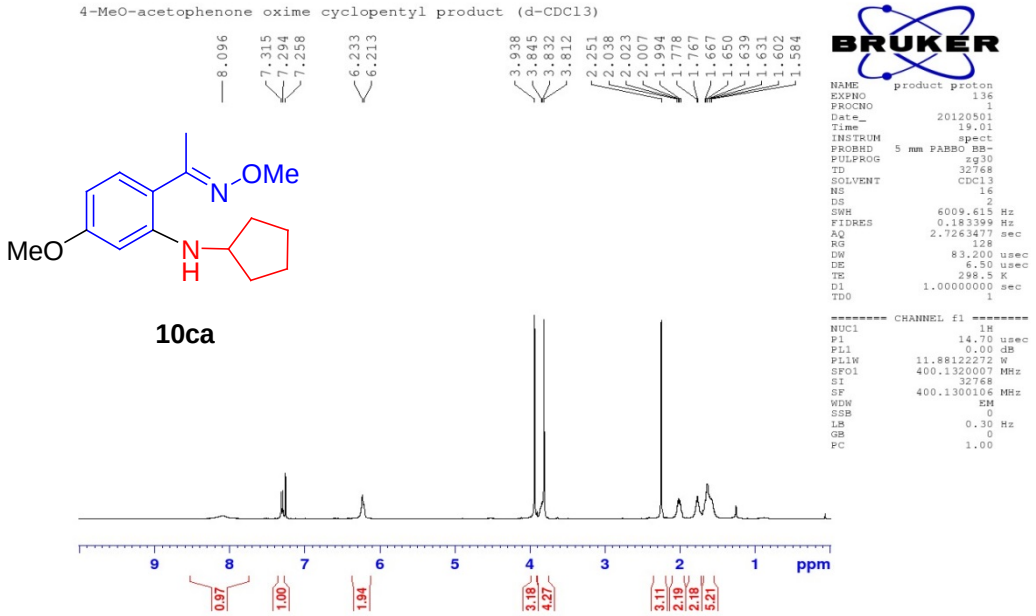

Figure A135. ^{13}C NMR of **10ca**

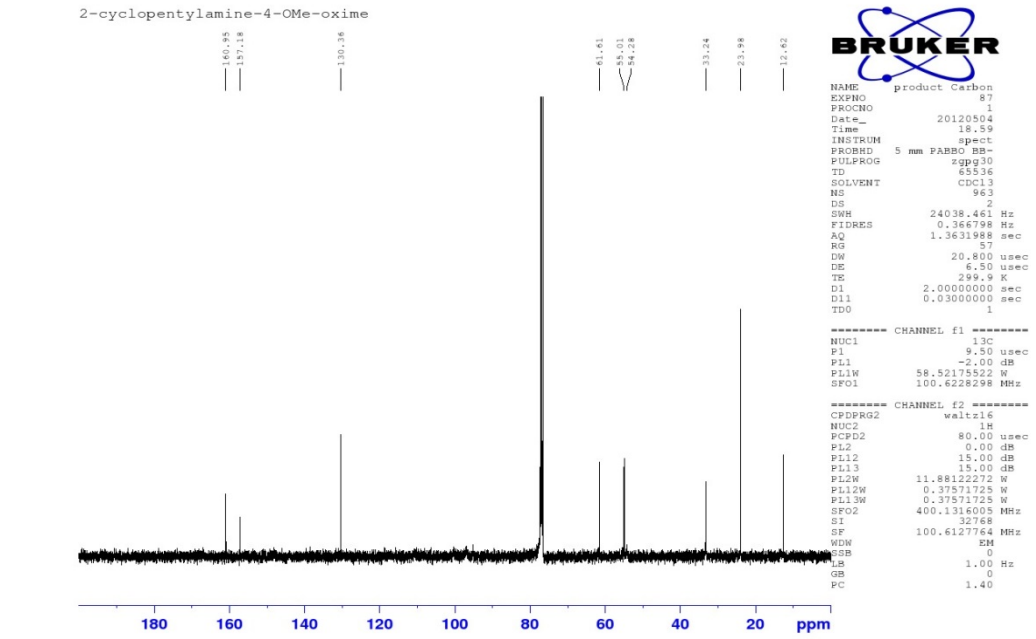

Figure A136. ^{1}H NMR of **10da**

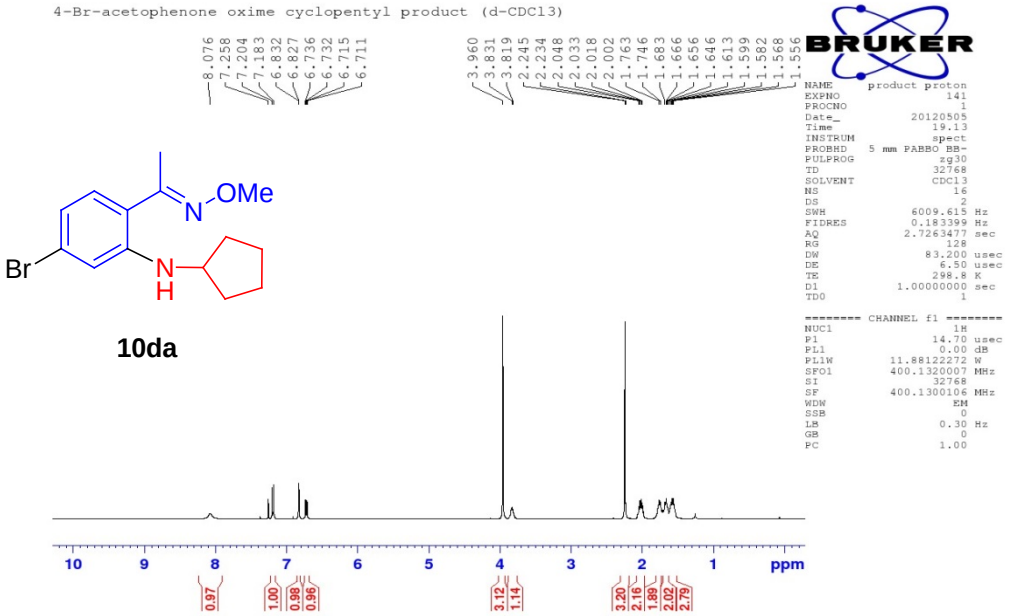

Figure A137. ^{13}C NMR of **10da**

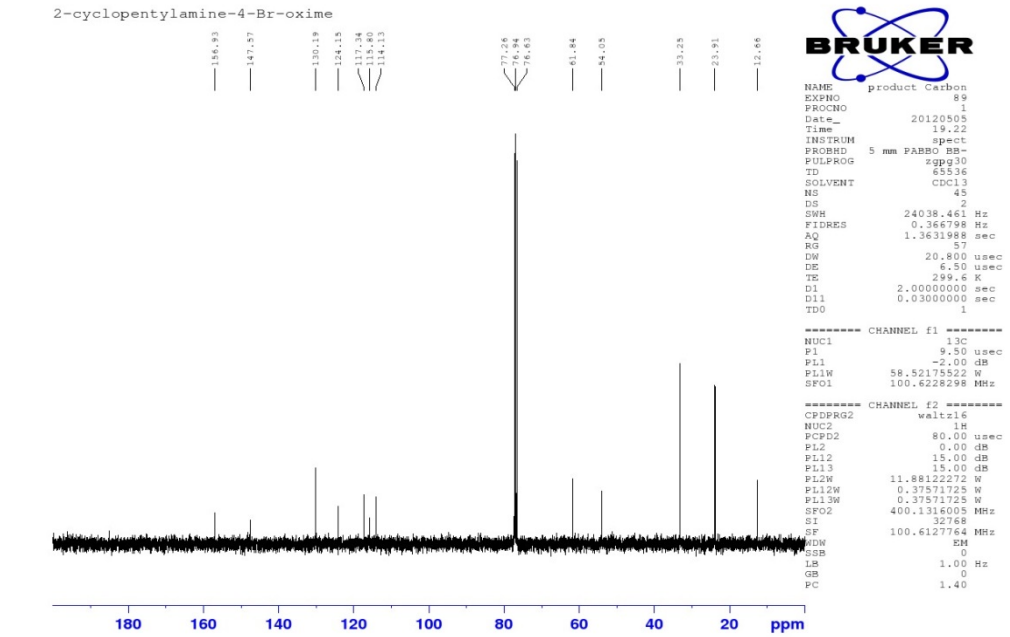

Figure A138. ^{1}H NMR of **10ea**

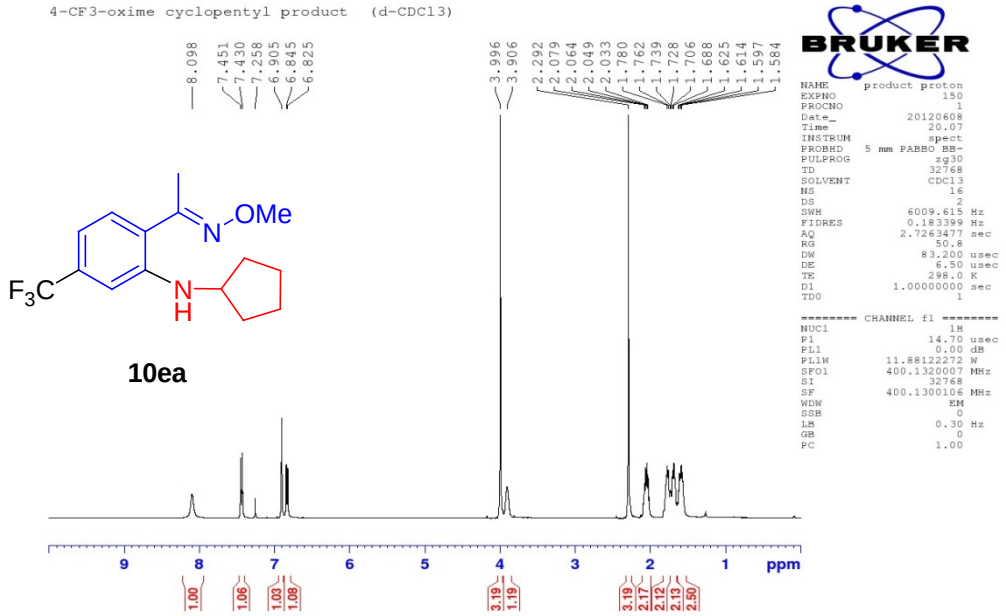

Figure A139. ^{13}C NMR of **10ea**

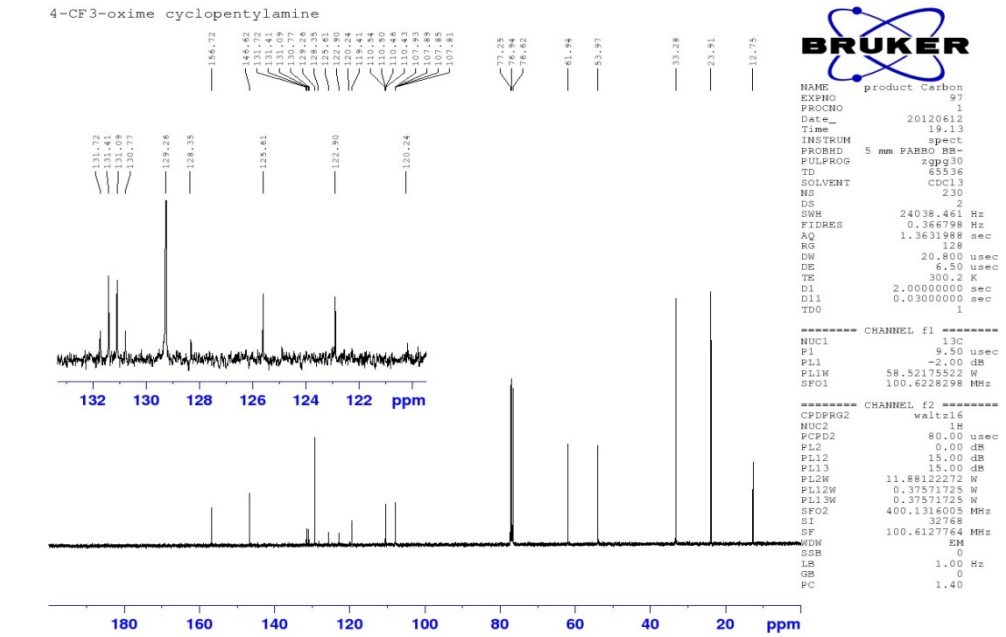

Figure A140. ^{1}H NMR of **10fa**

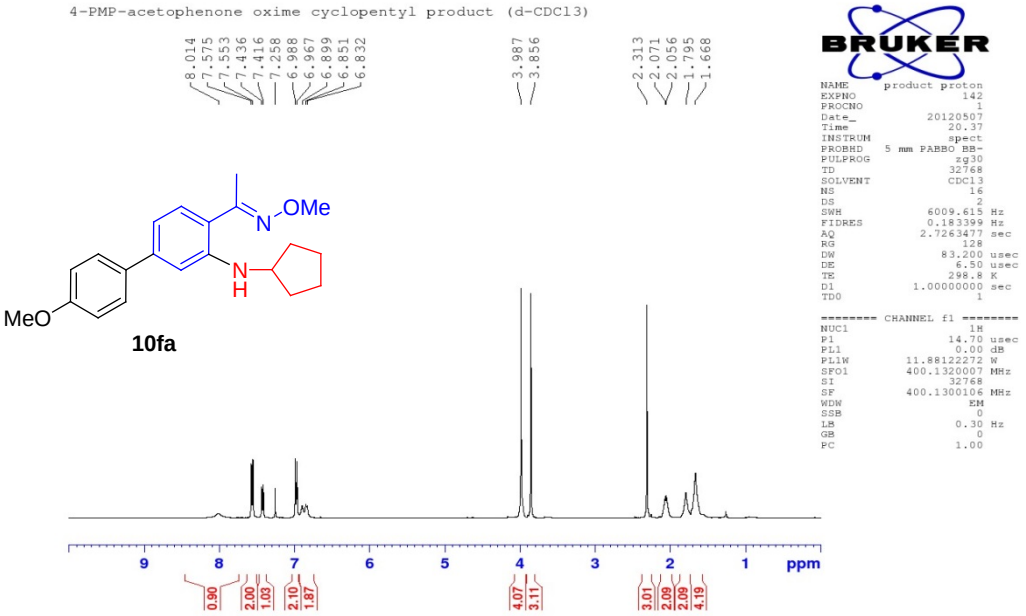

Figure A141. ^{13}C NMR of **10fa**

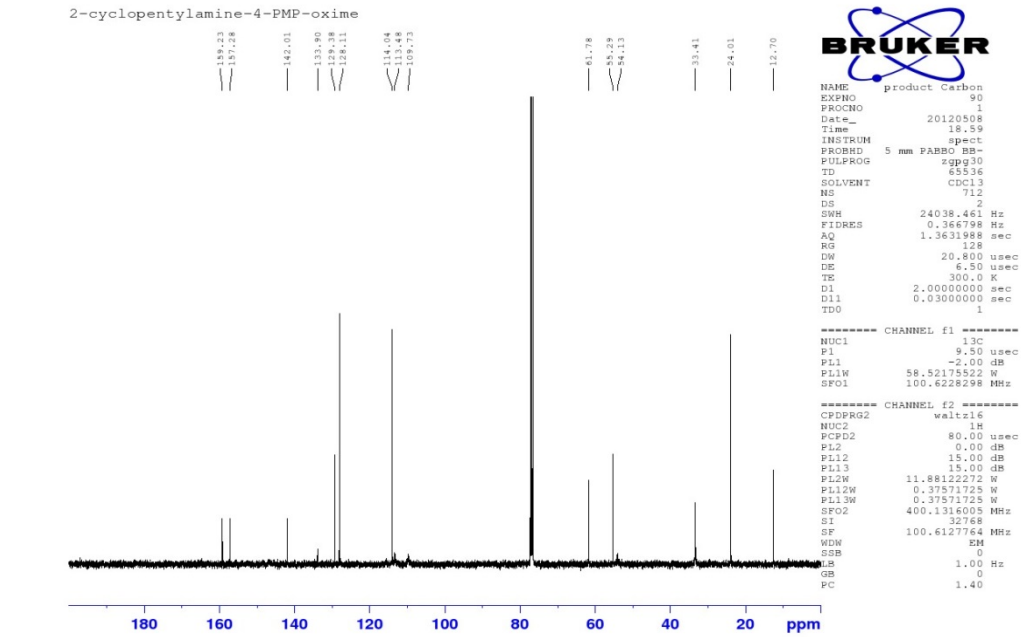

Figure A142. ^{1}H NMR of **10ga**

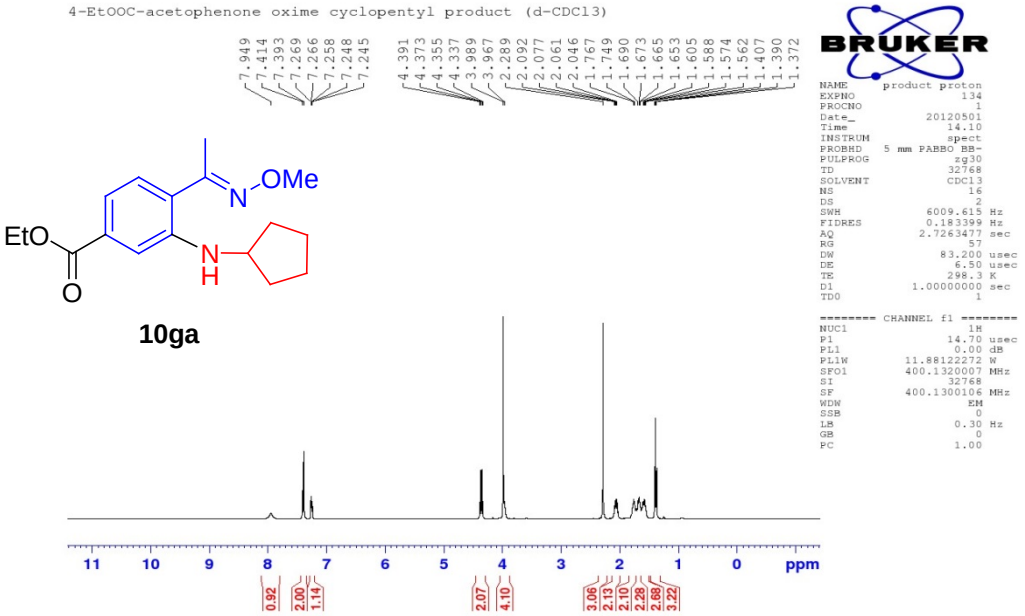

Figure A143. ^{13}C NMR of **10ga**

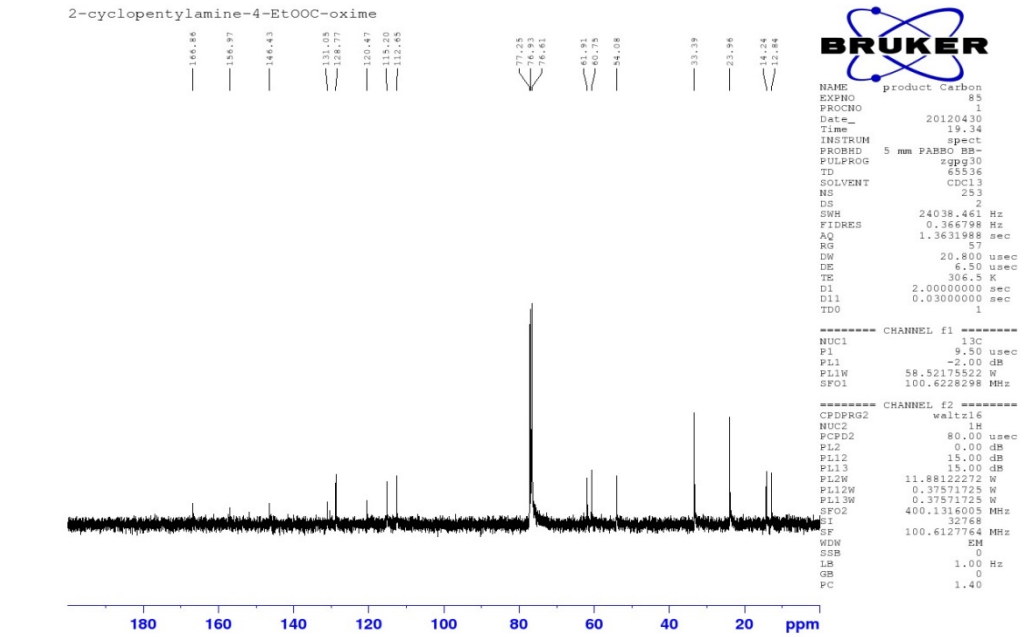

Figure A144 ^{1}H NMR of **10qa**

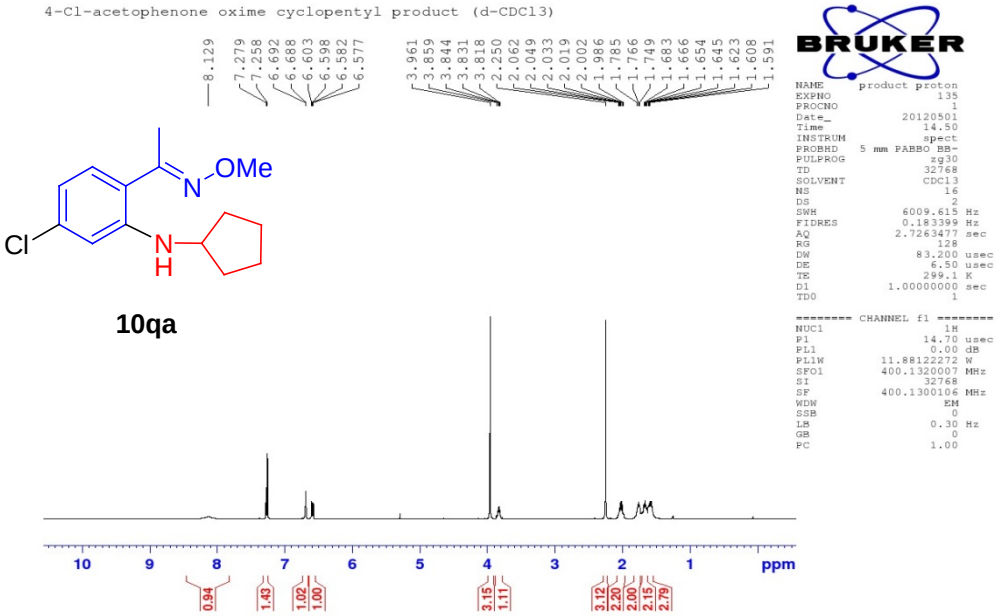

Figure A145. ^{13}C NMR of **10qa**

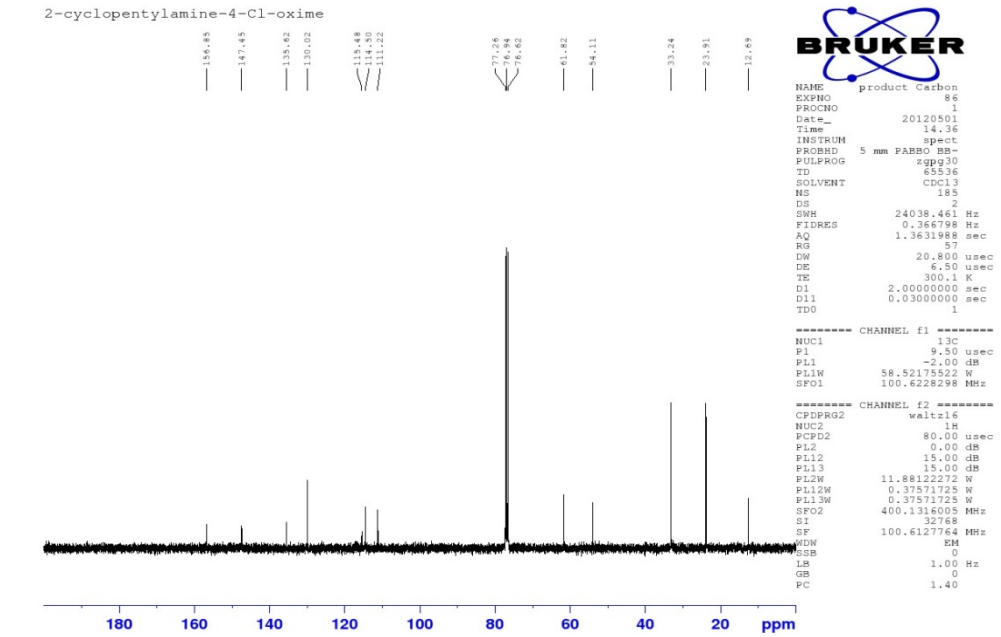

Figure A146. ^{1}H NMR of **10ra**

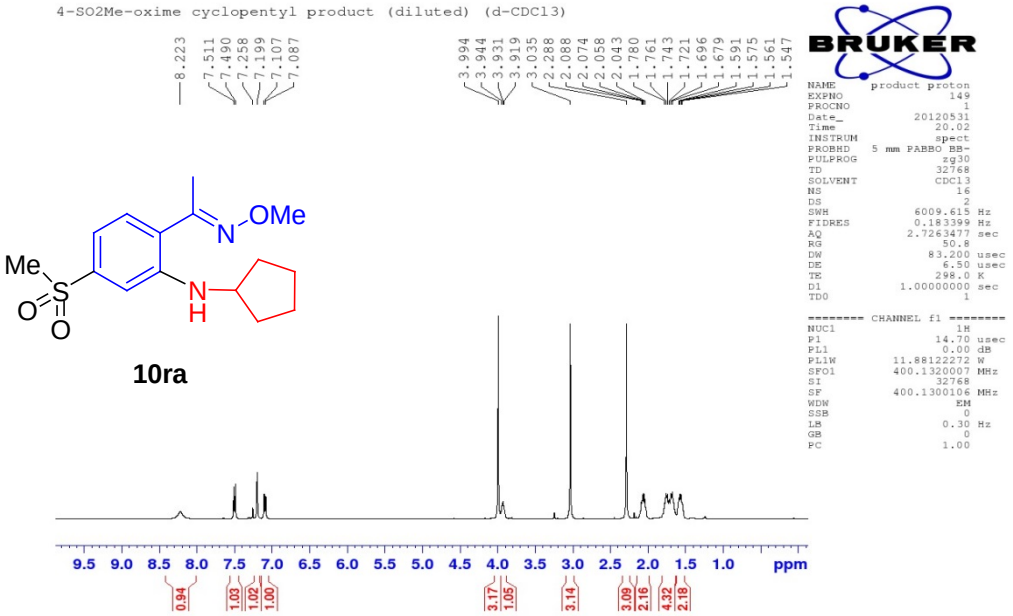

Figure A147. ^{13}C NMR of **10ra**

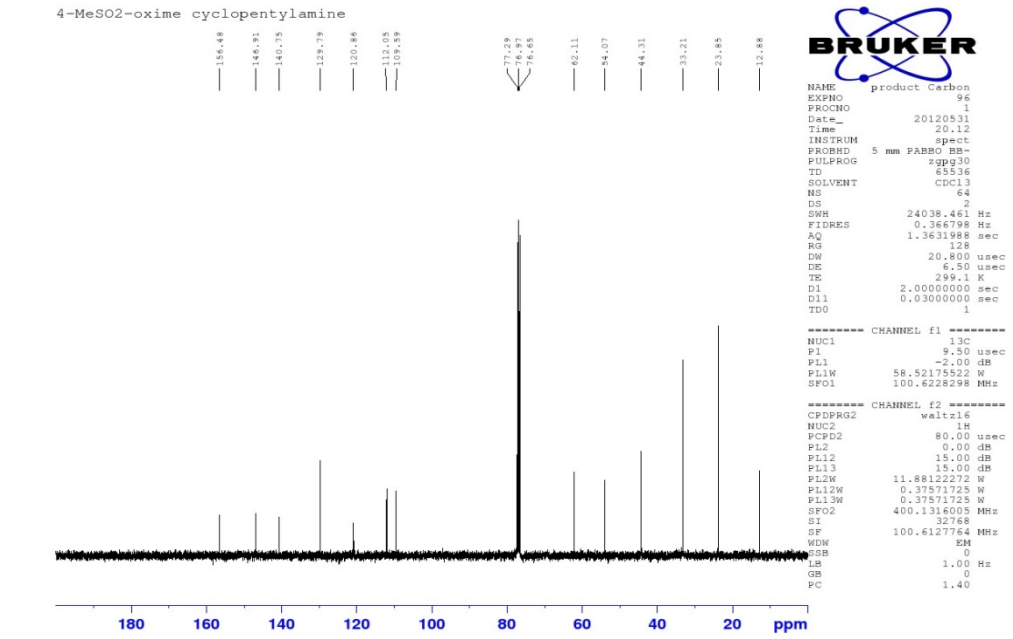

Figure A148. ^{1}H NMR of **10sa**

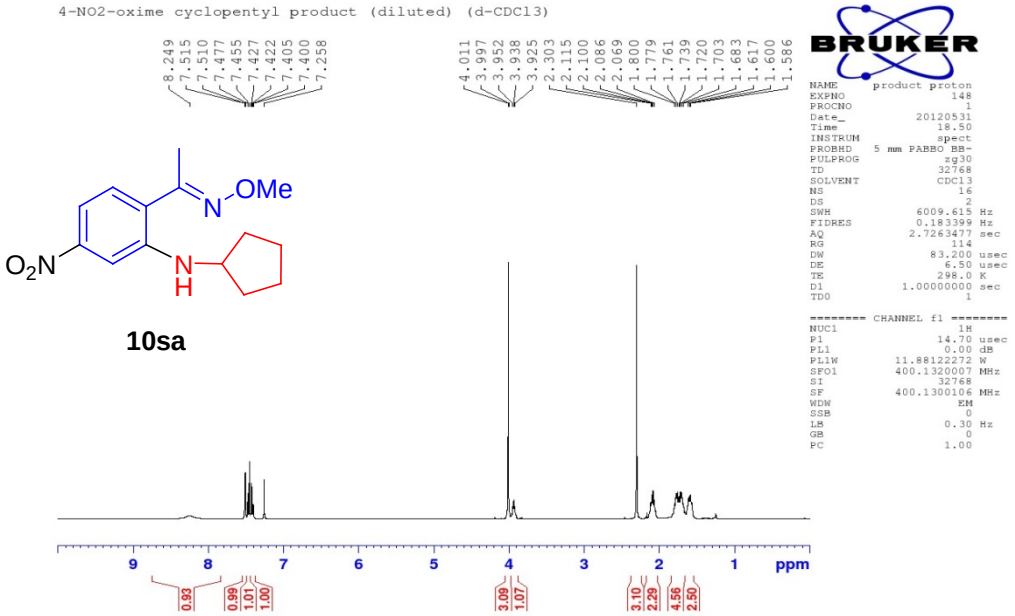

Figure A149. ^{13}C NMR of **10sa**

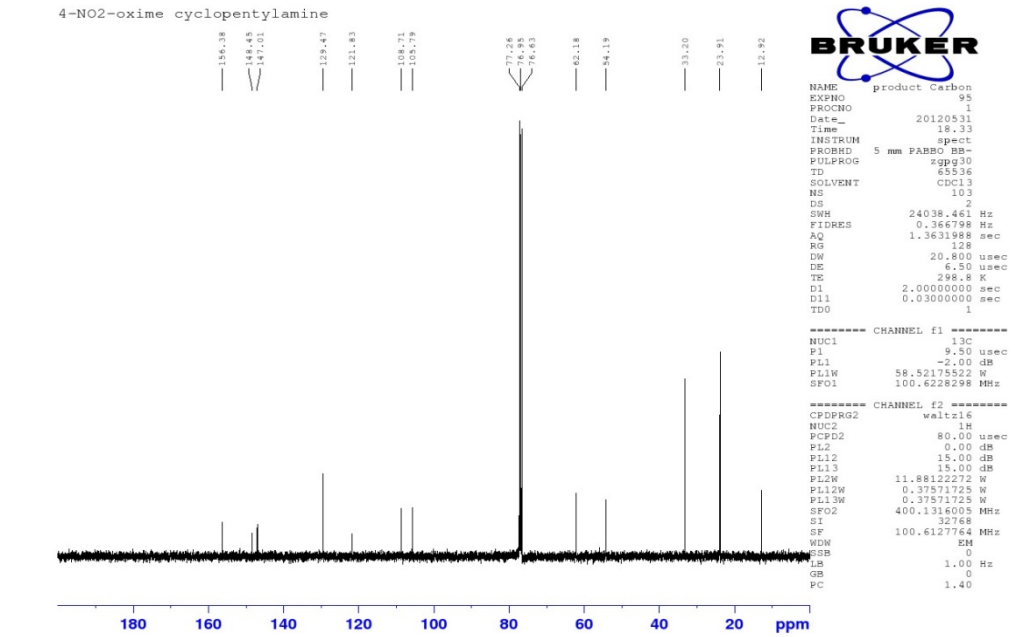

Figure A150. ^{1}H NMR of **10ha**

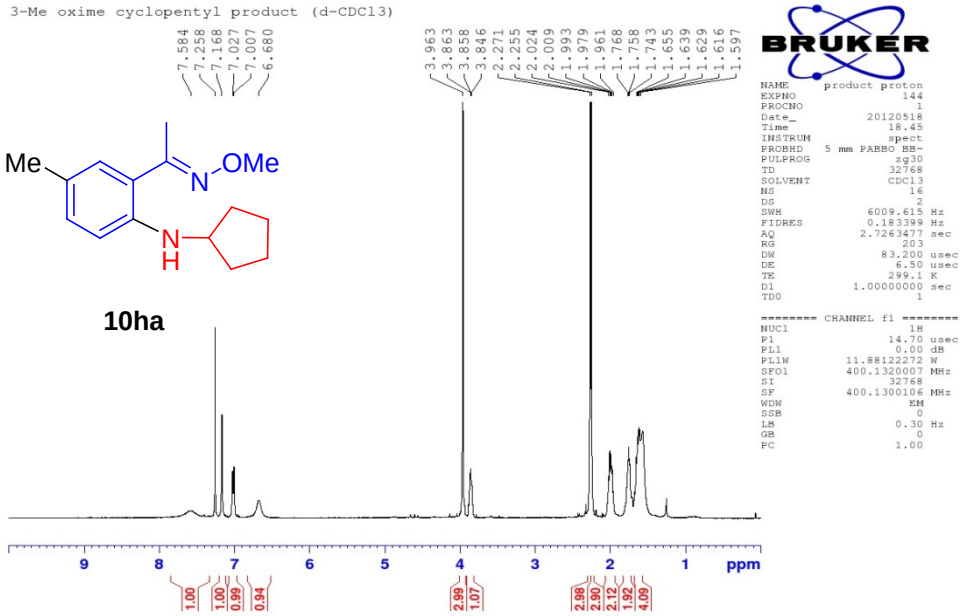

Figure A151. ^{13}C NMR of **10ha**

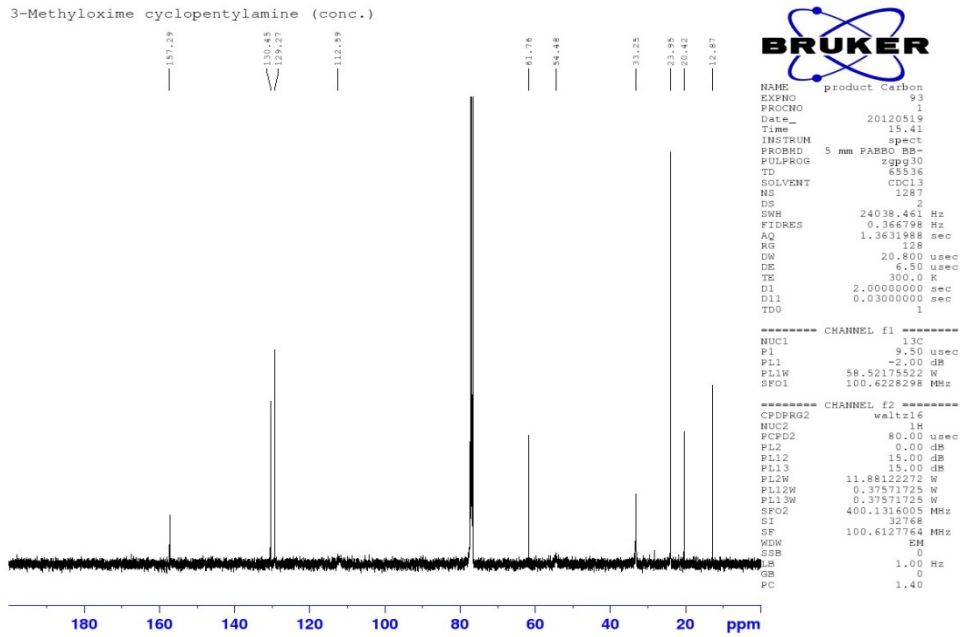

Figure A152. ^{1}H NMR of **10ta**

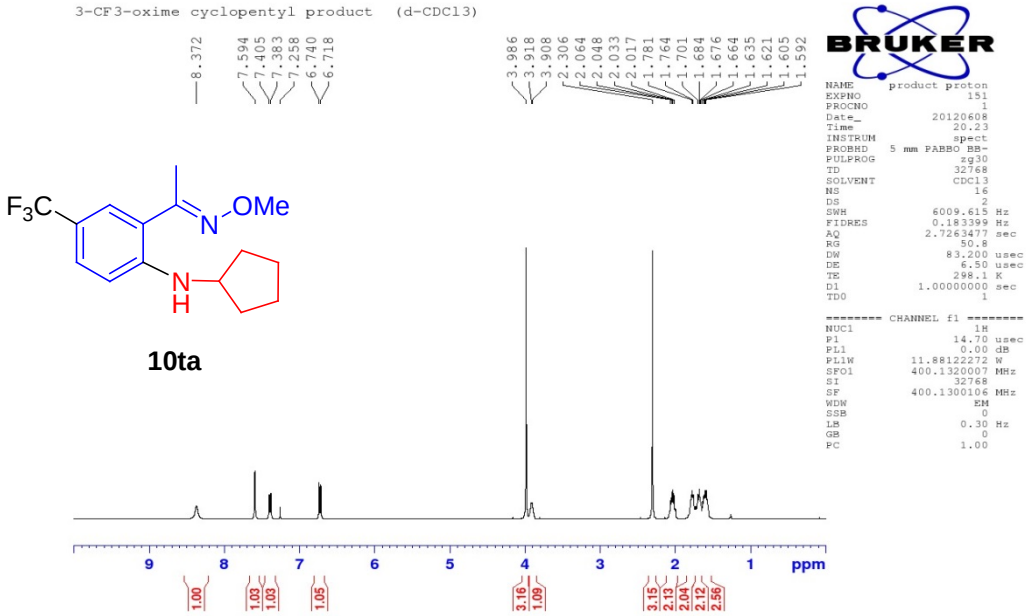

Figure A153. ^{13}C NMR of **10ta**

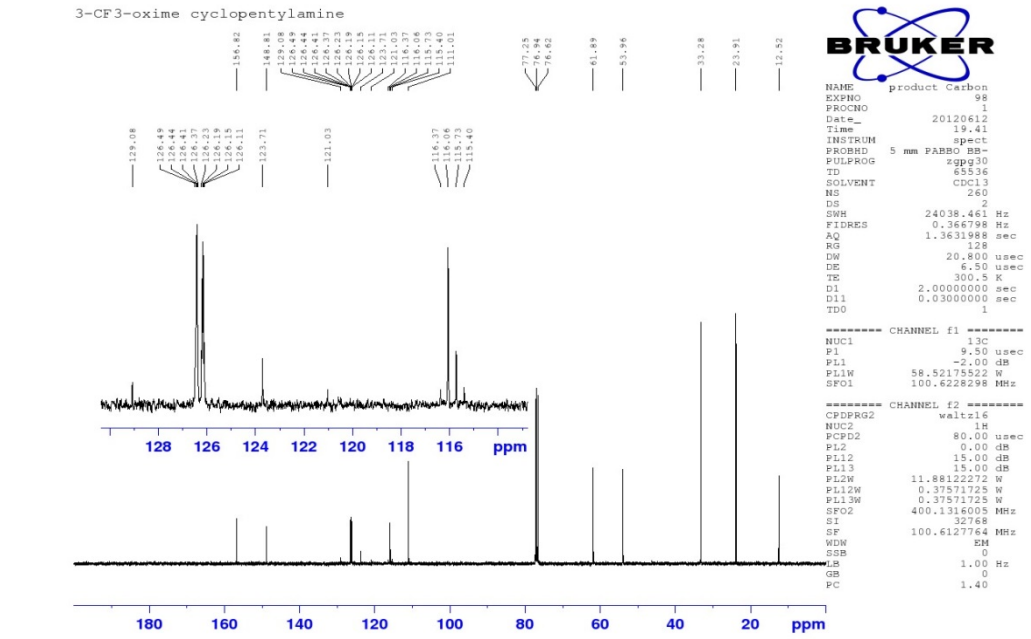

Figure A154. ^{1}H NMR of **10ka**

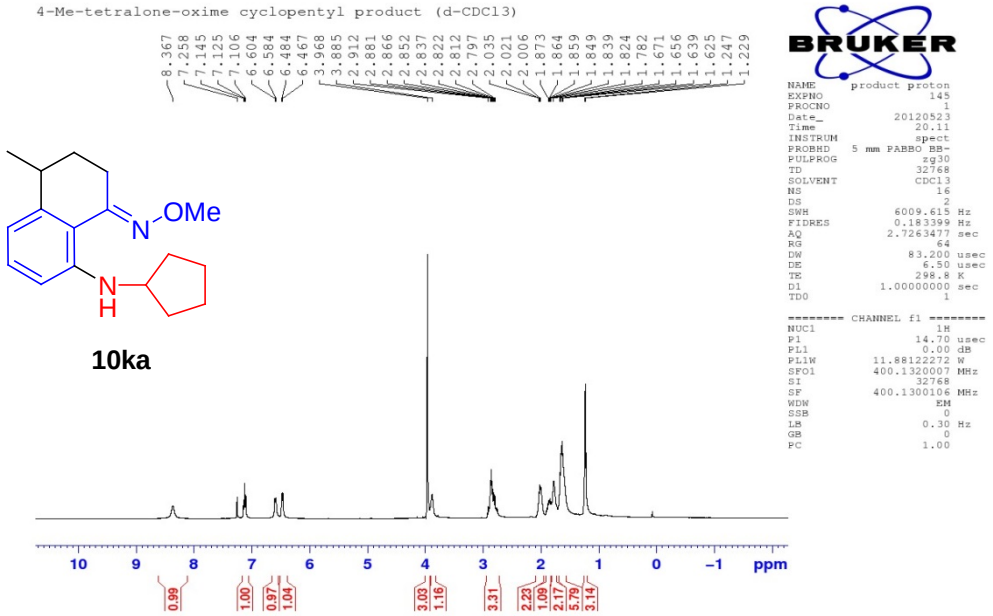

Figure A155. ^{13}C NMR of **10ka**

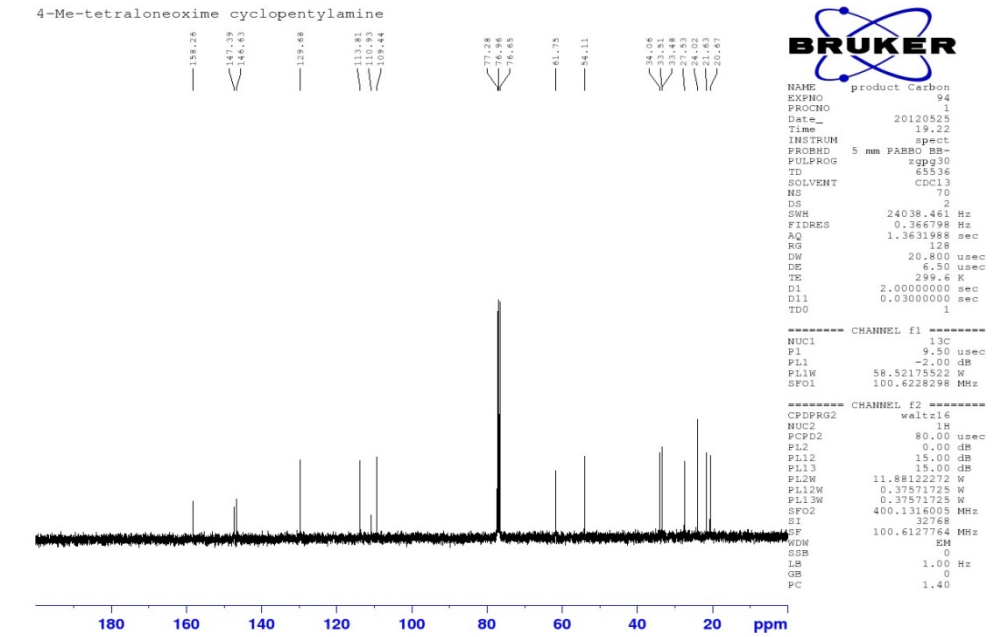

Figure A156[1]H NMR of **10na-3Cl**

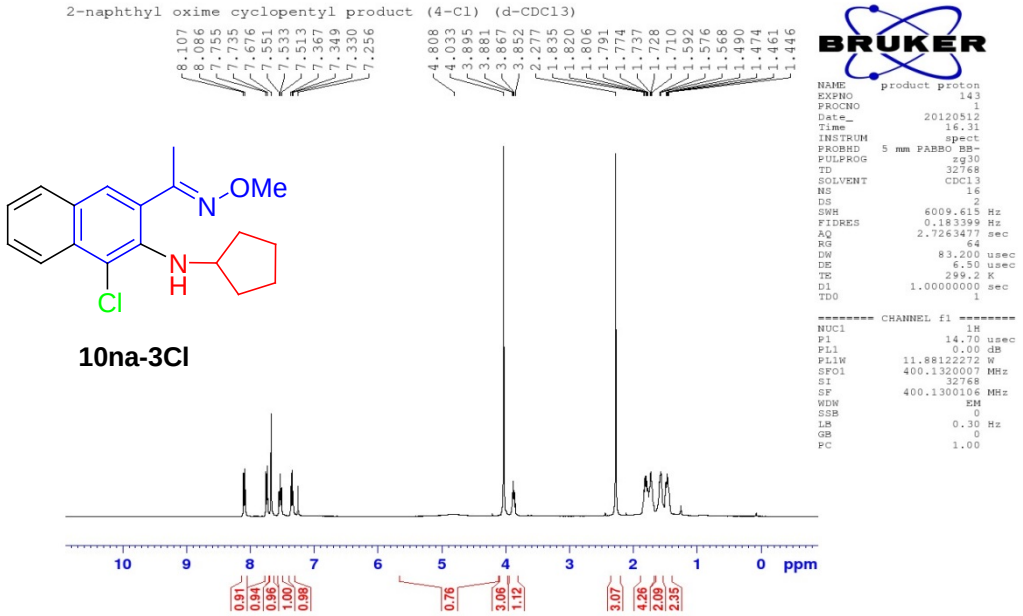

Figure A157. [13]C NMR of **10na-3Cl**

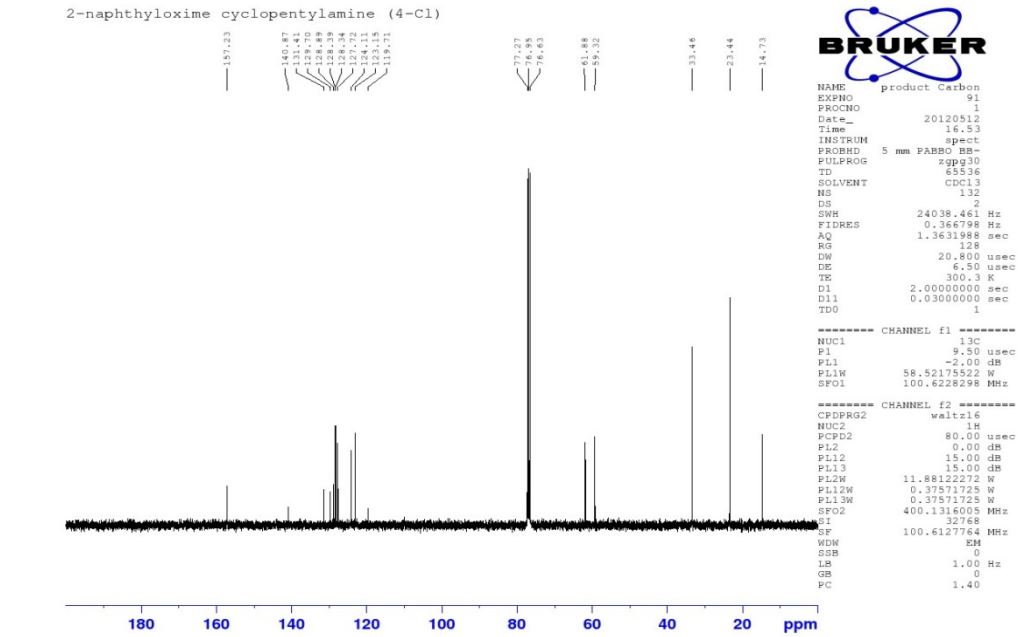

Figure A158. COSY NMR of **10na-3Cl**

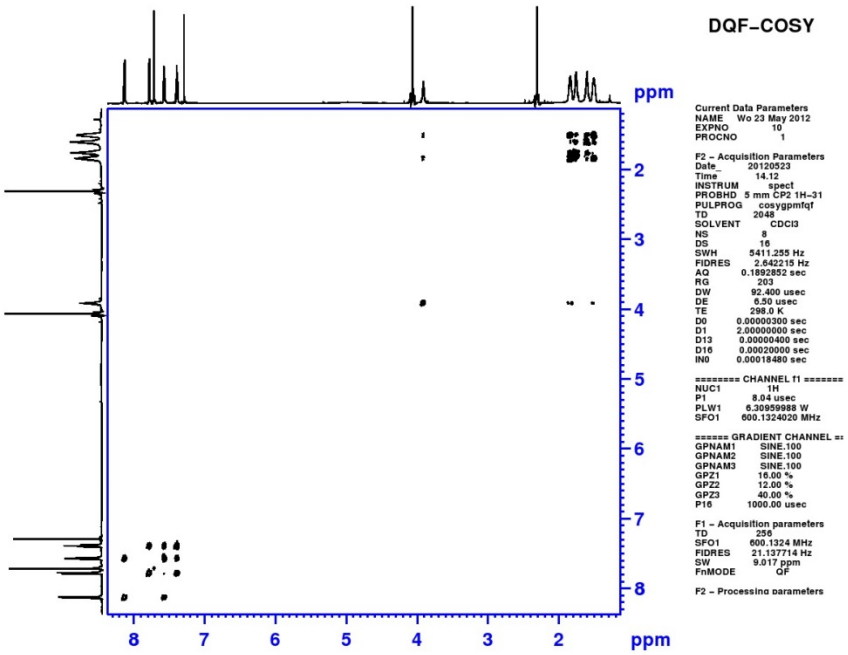

(Original)

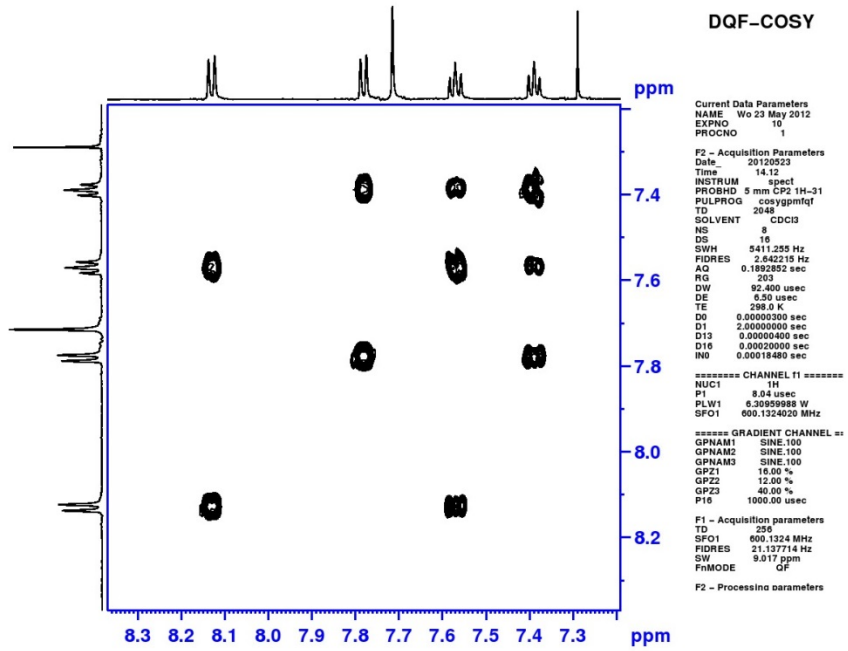

(Magnified at 8.4-7.2 ppm)

Figure A159. NOSY NMR of **10na-3Cl**

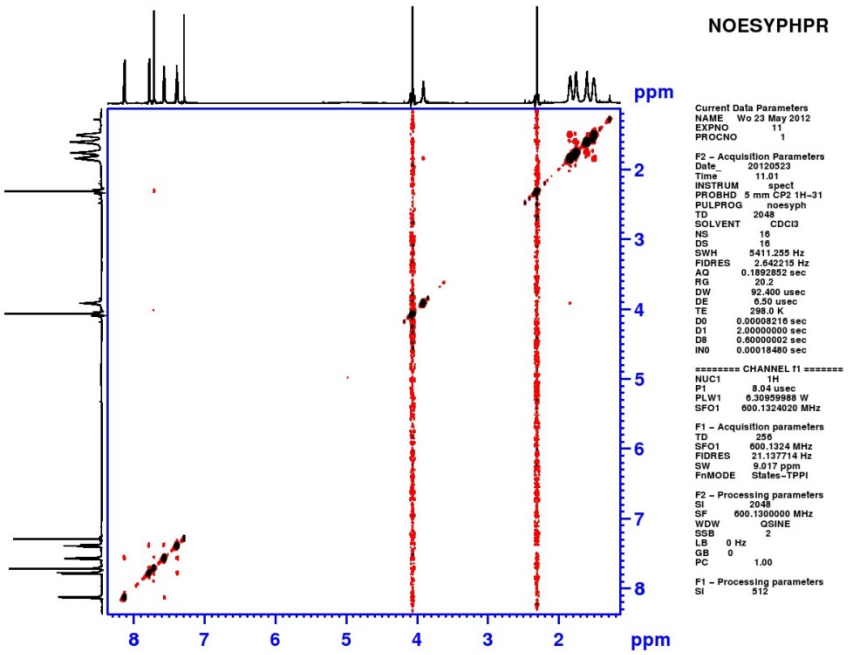

(Original)

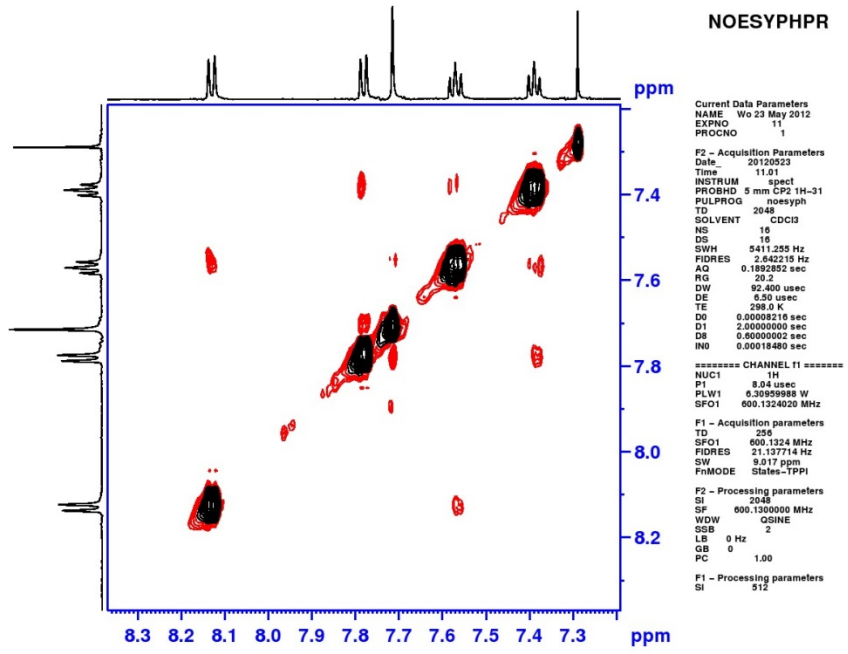

(Magnified at 8.4-7.2 ppm)

Figure A160. ^{1}H NMR of**10sb**

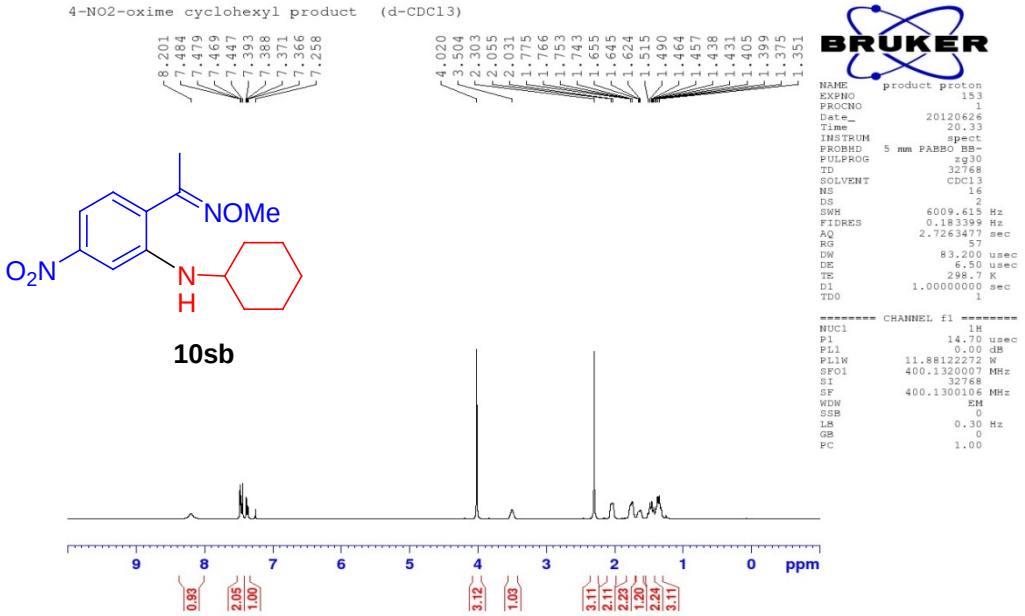

Figure A161. ^{13}C NMR of **10sb**

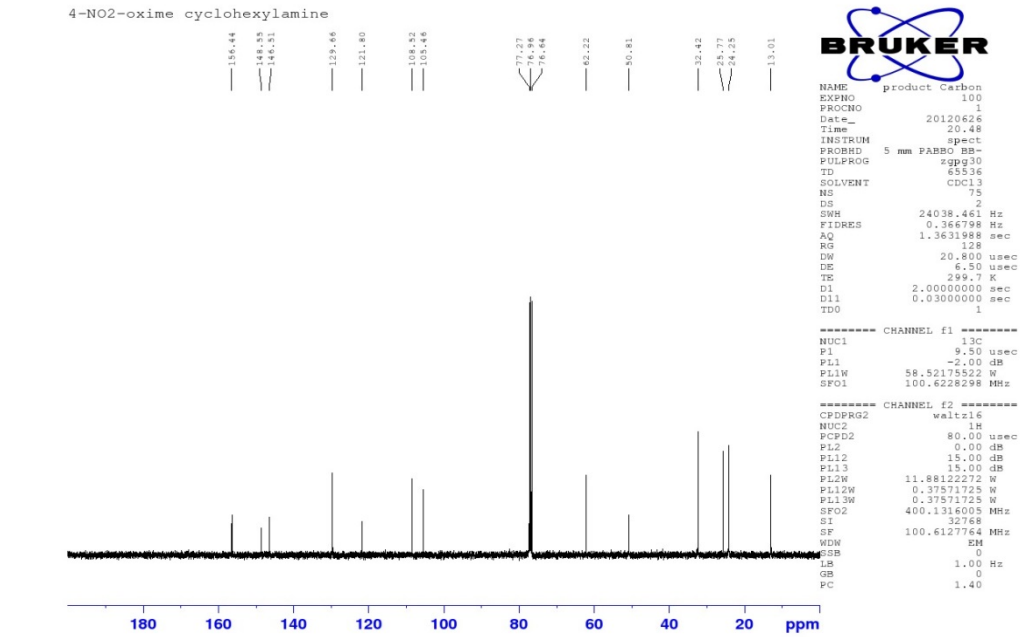

Figure A162. ^{1}H NMR of **10sc**

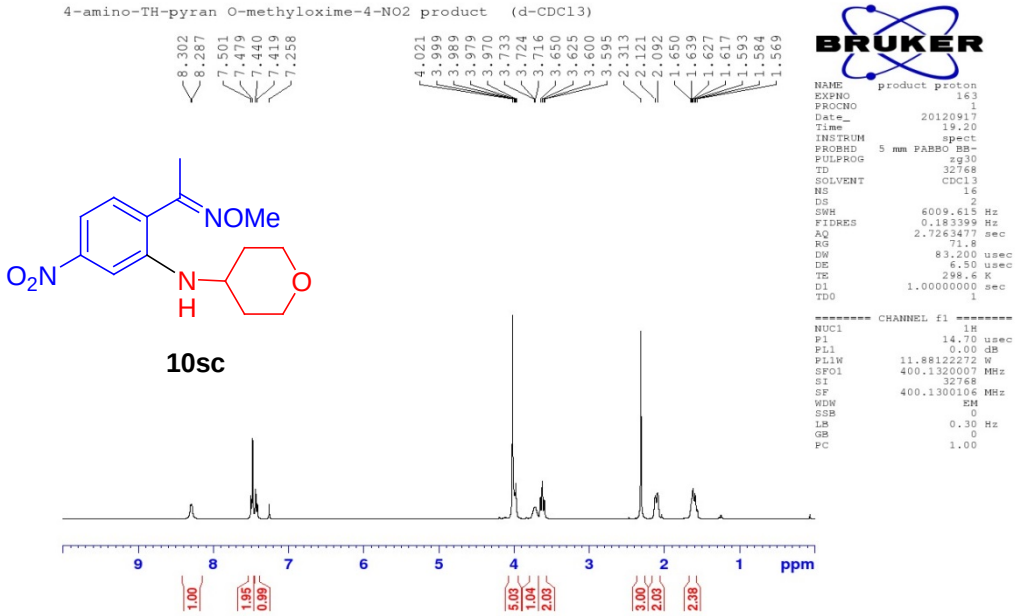

Figure A163. ^{13}C NMR of **10sc**

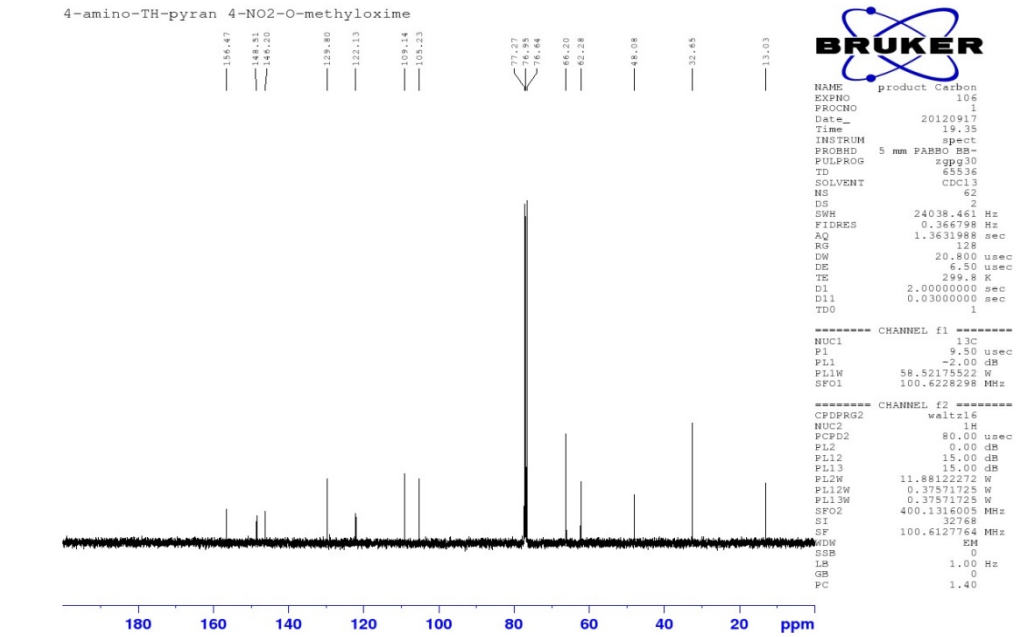

Figure A164. ^{1}H NMR of **10sd**

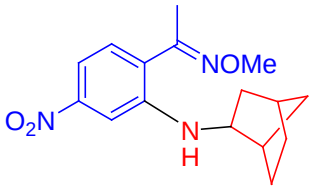

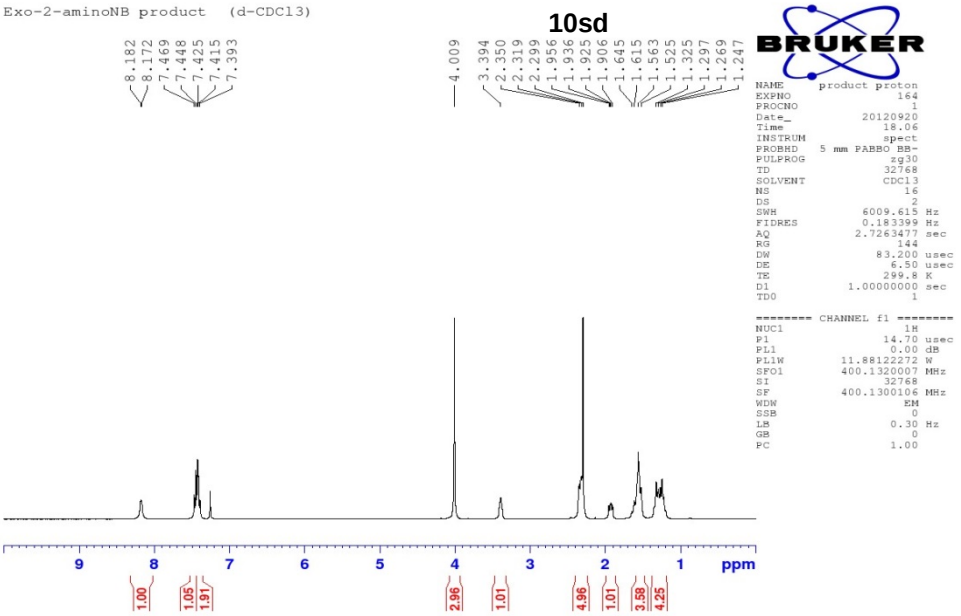

Figure A165. ^{13}C NMR of **10sd**

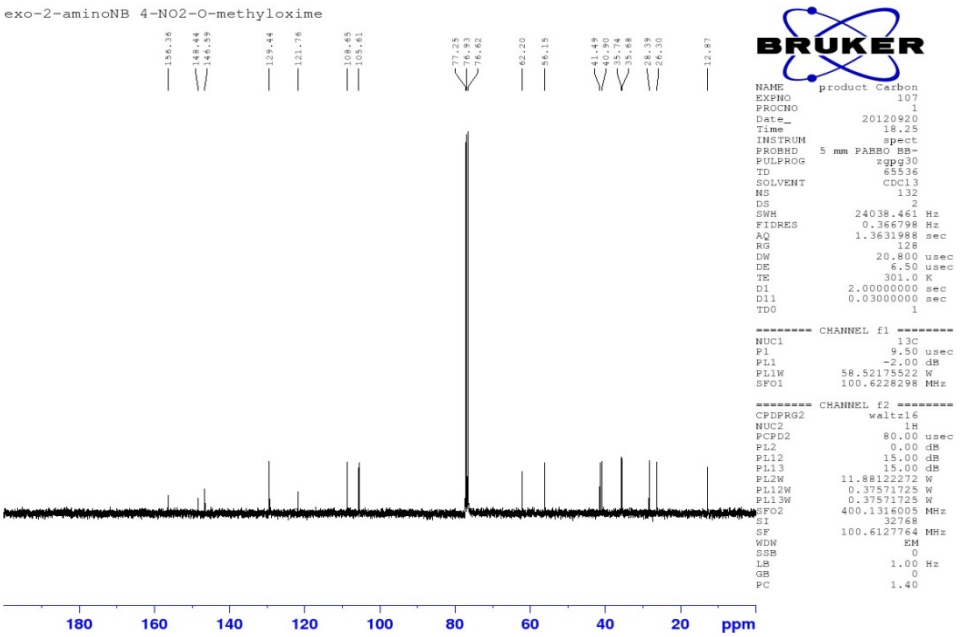

Figure A166. ^{1}H NMR of **10se**

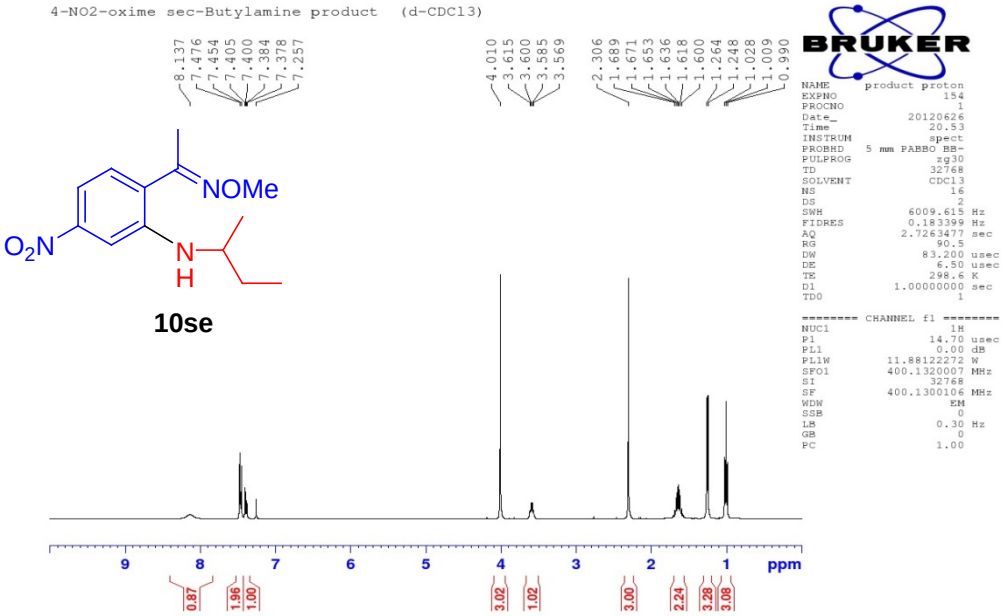

Figure A167. ^{13}C NMR of **10se**

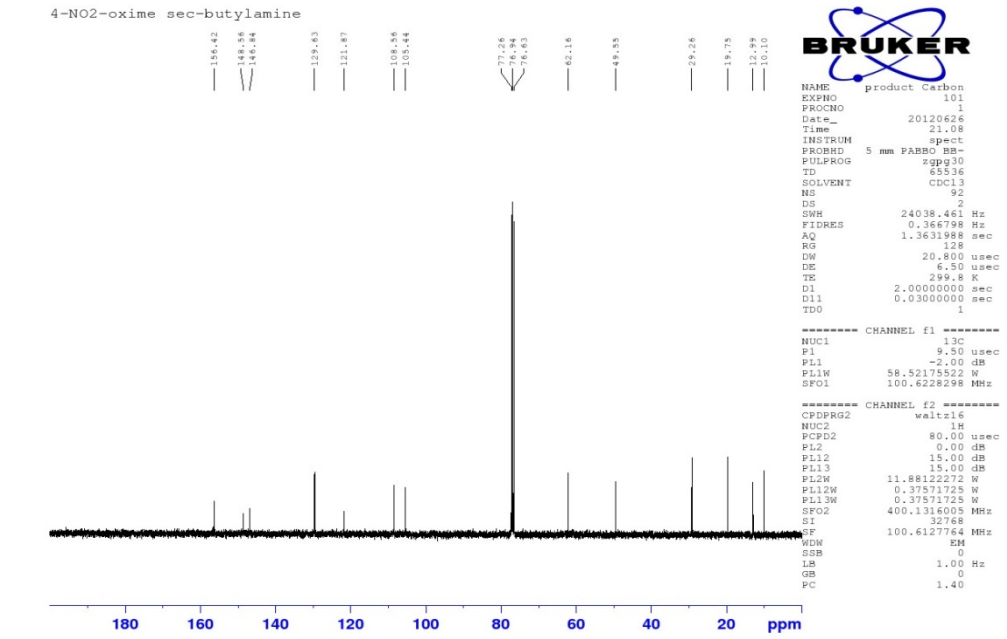

Figure A168. ^{1}H NMR of **10sf**

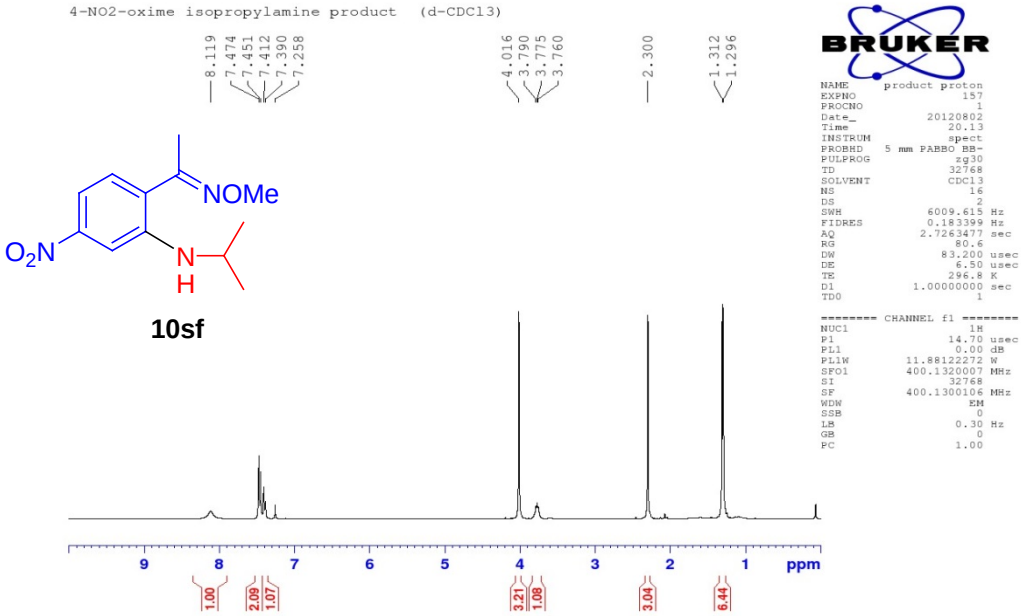

Figure A169. ^{13}C NMR of **10sf**

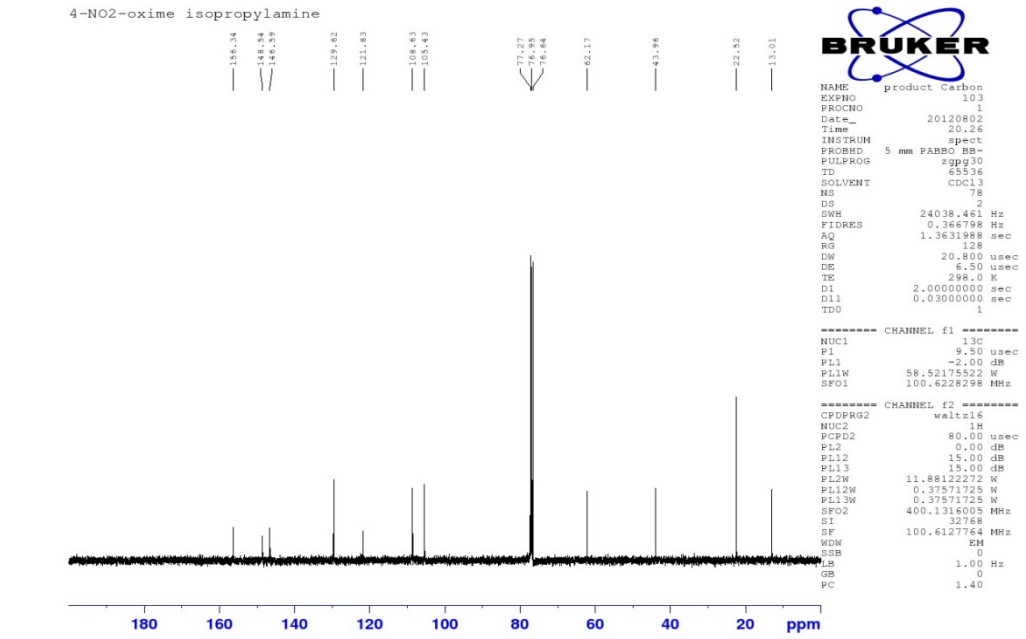

Figure A170. ^{1}H NMR of **10sg**

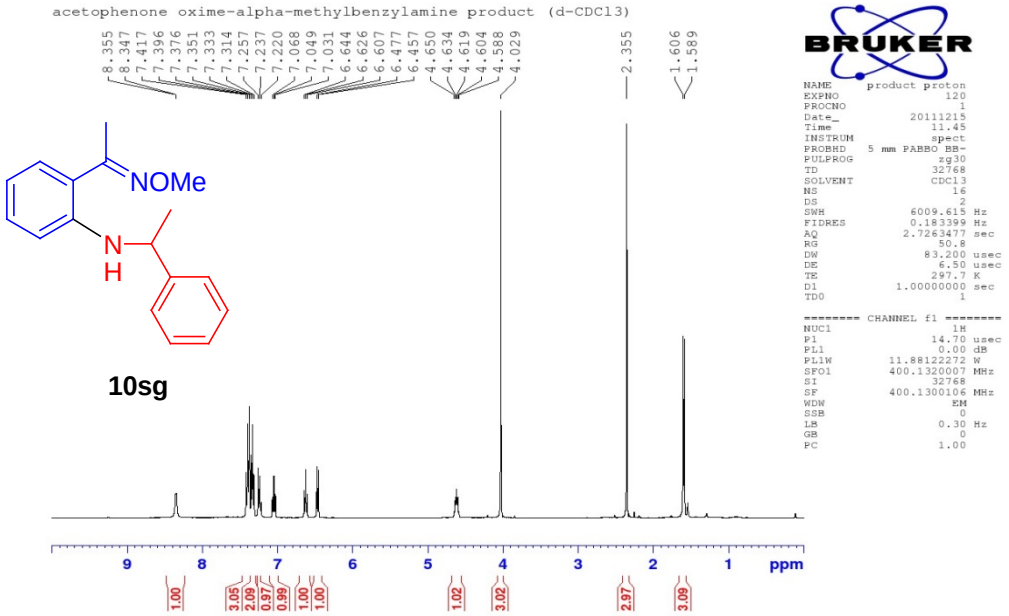

Figure A171. ^{13}C NMR of **10sg**

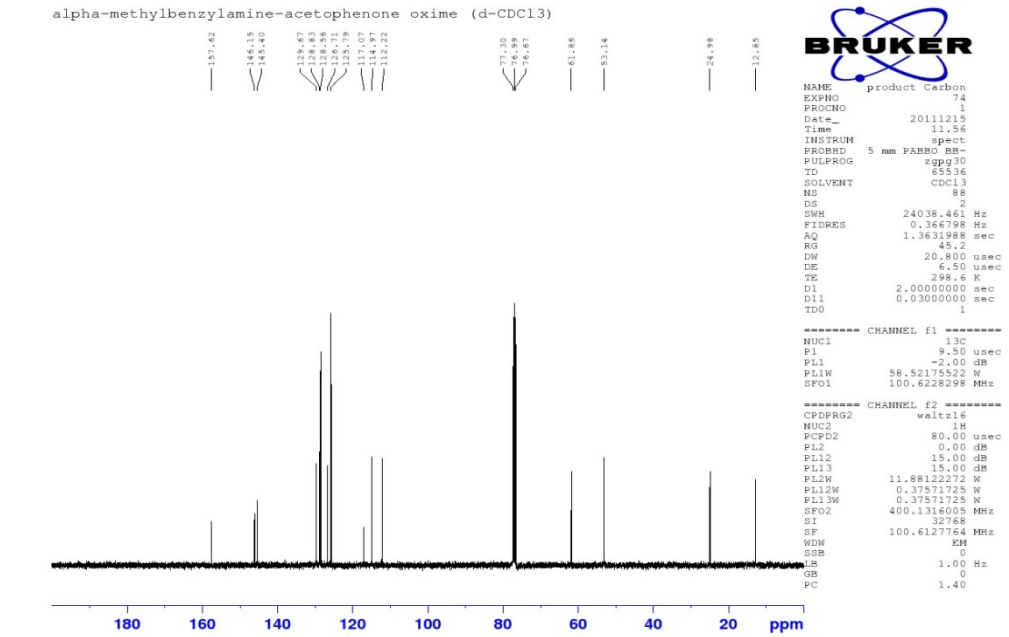

Figure A172. ^{1}H NMR of **10sh**

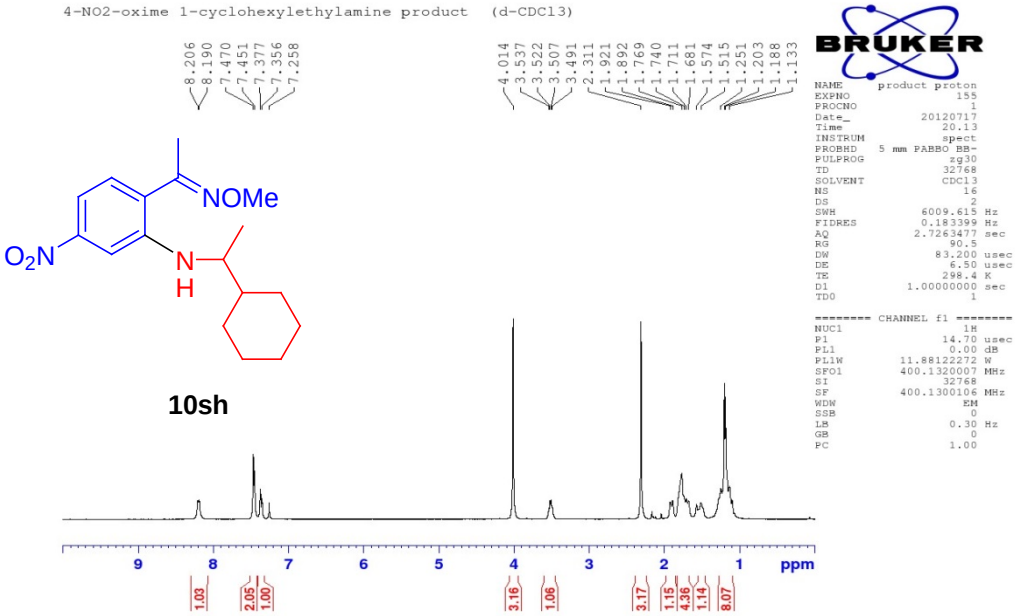

Figure A173. ^{13}C NMR of **10sh**

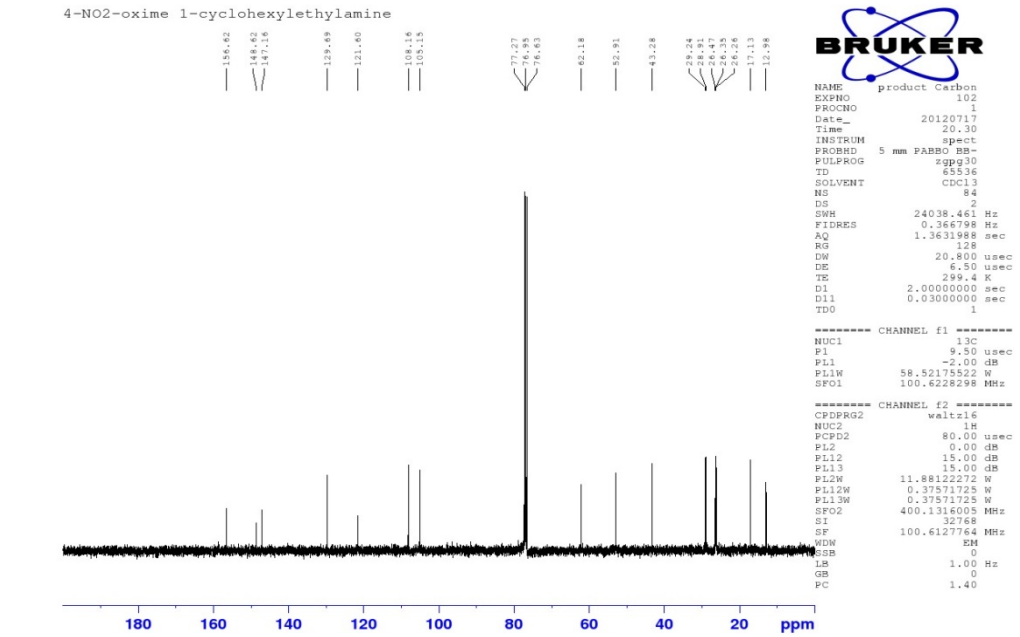

Figure A174. ^{1}H NMR of **10uk**

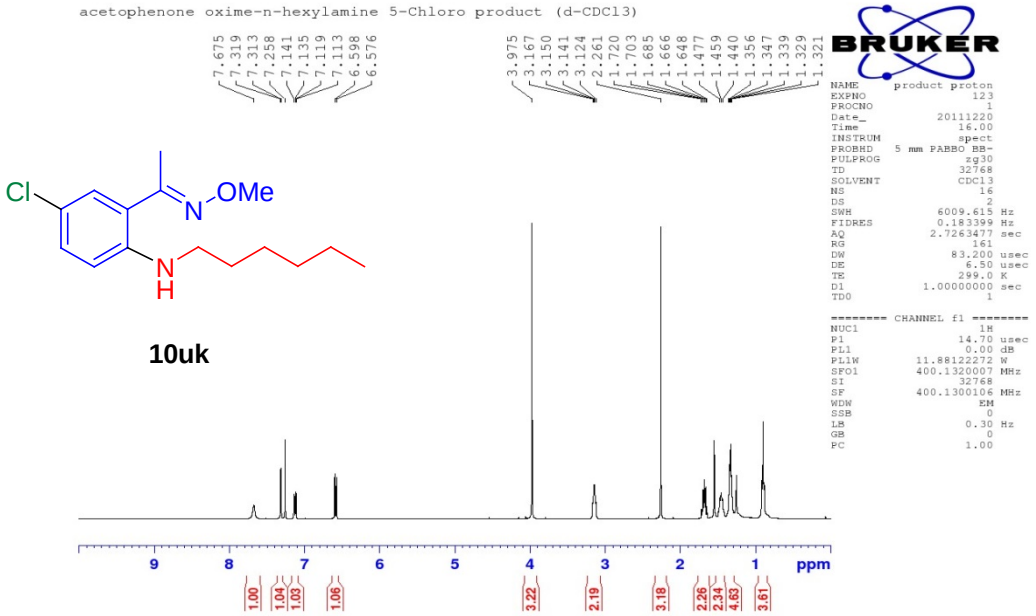

Figure A175. ^{13}C NMR of **10uk**

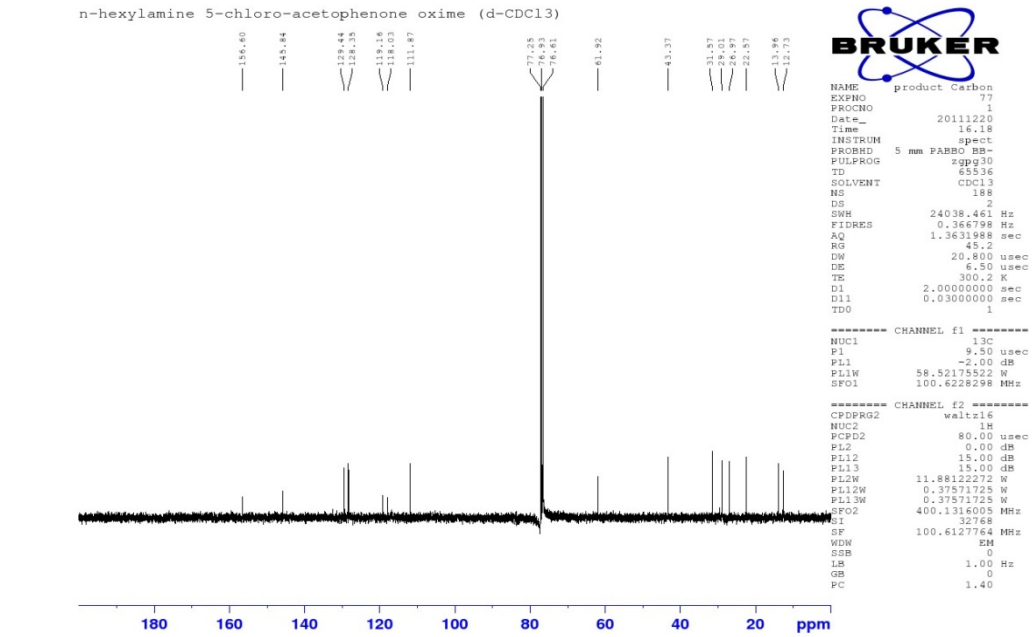

Figure A176. ^{1}H NMR of **10uk'**

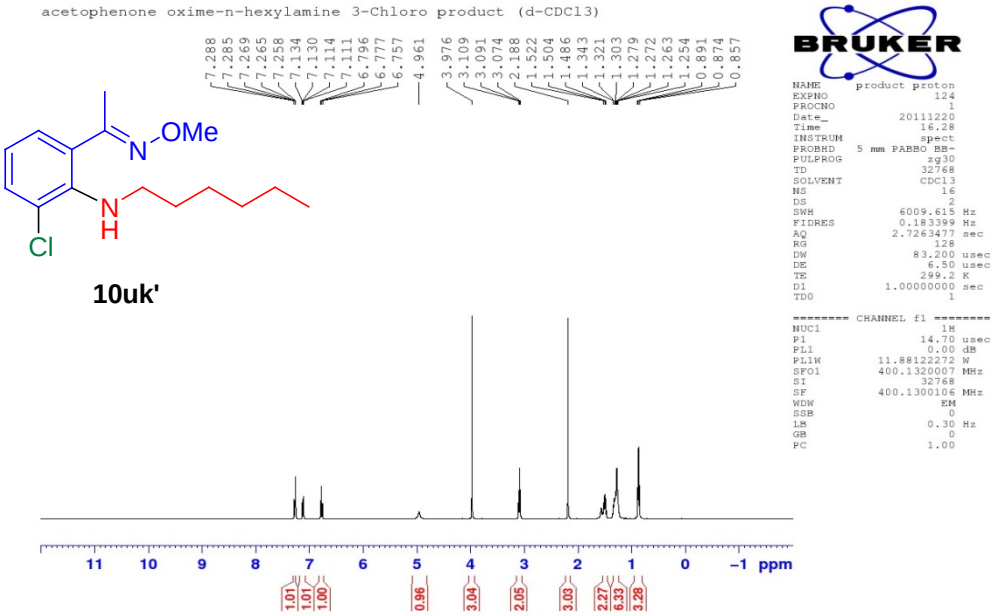

Figure A177. ^{13}C NMR of **10uk'**

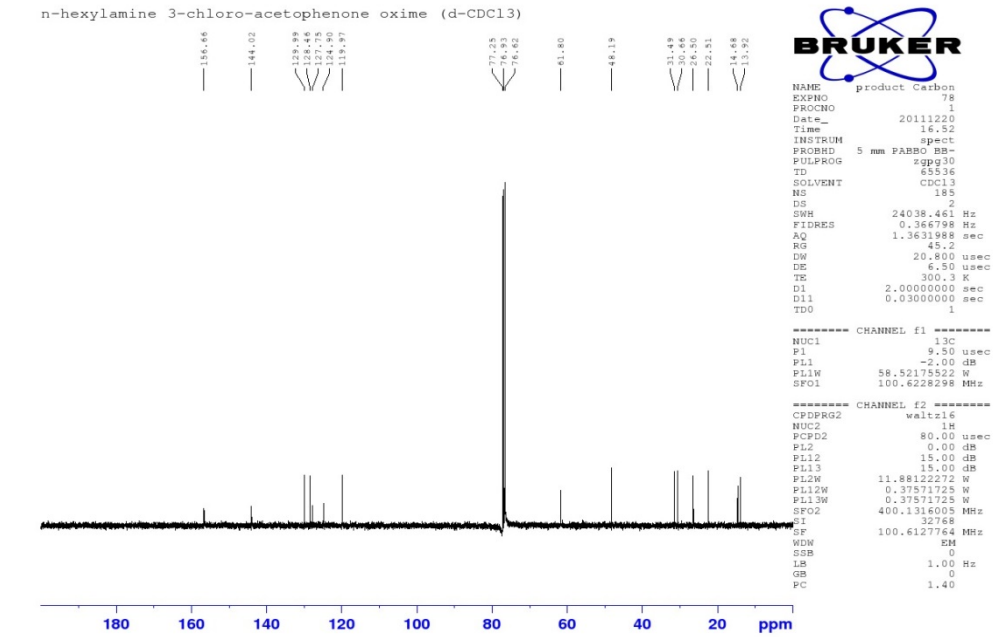

Figure A178. ^{1}H NMR of **10ak-DC**

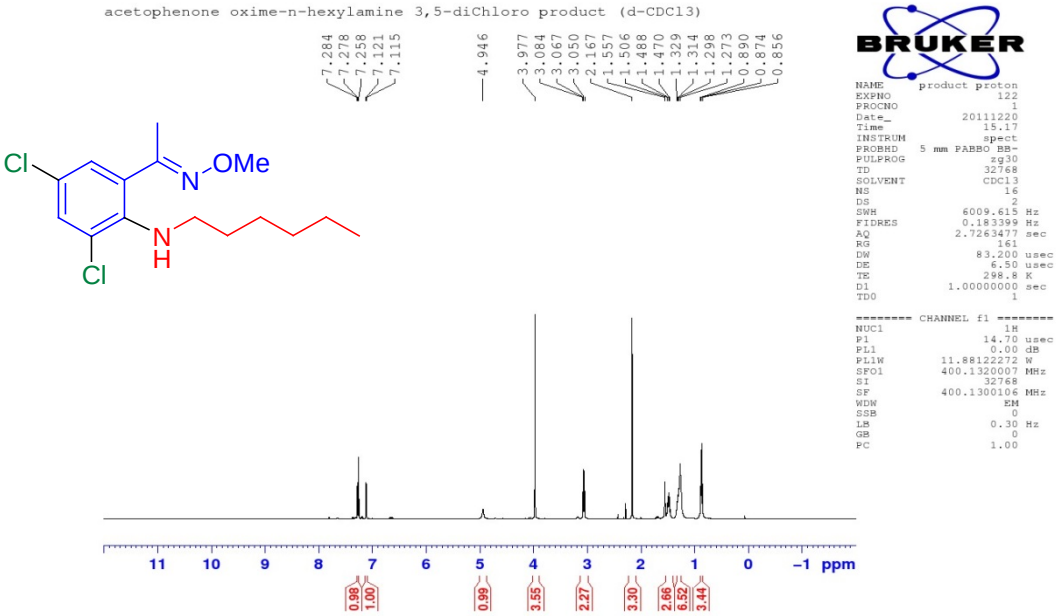

Figure A179. ^{13}C NMR of **10ak-DC**

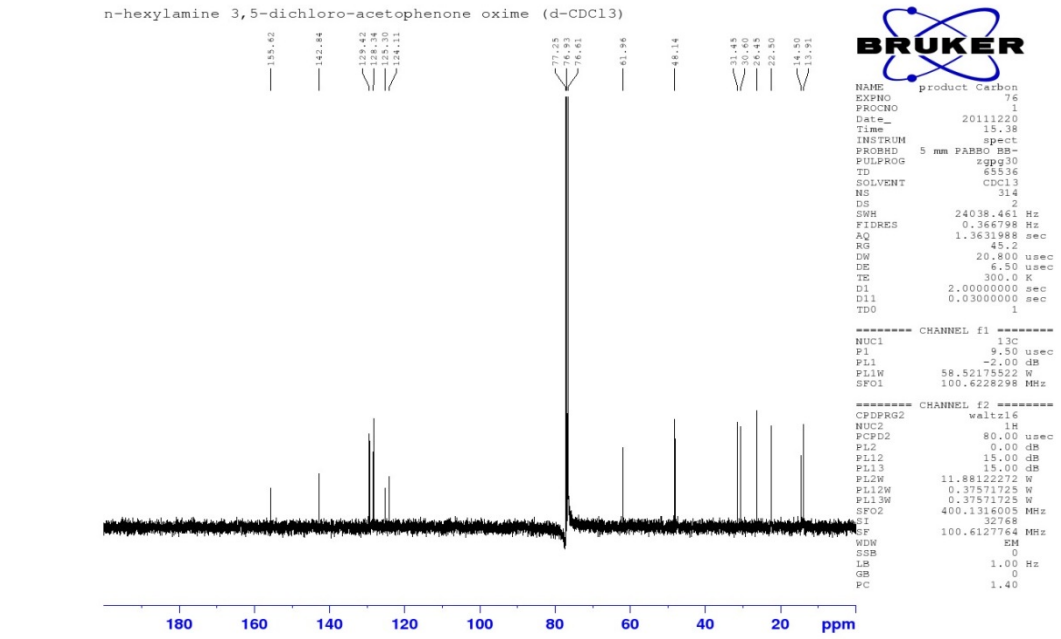

Figure A180. ^{1}H NMR of **8ab2**

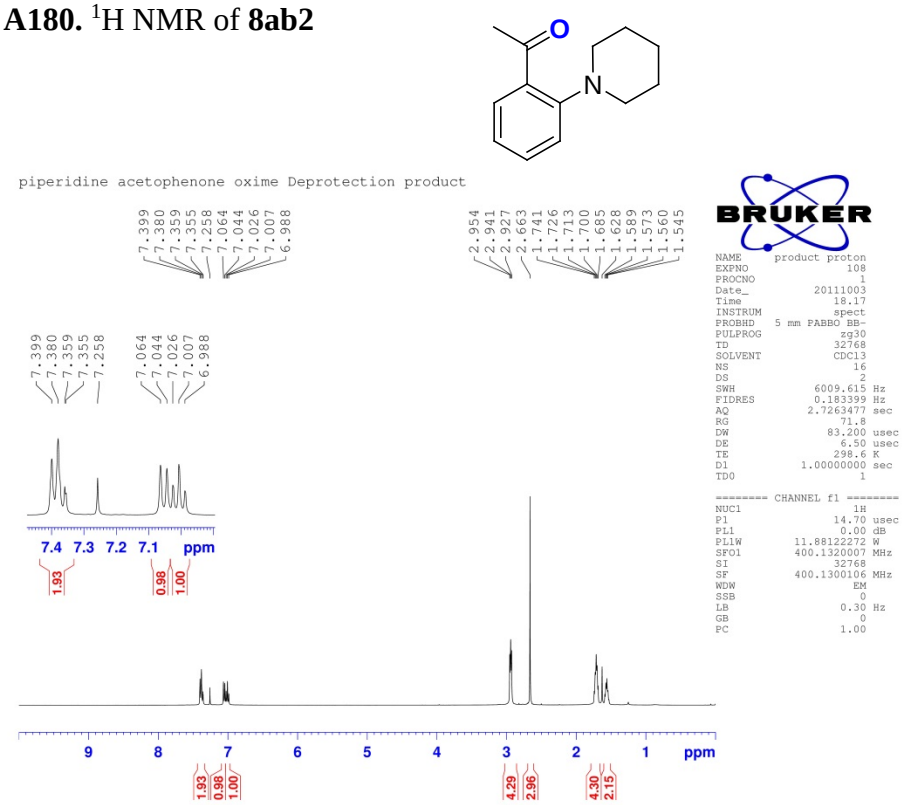

Figure A181. ^{13}C NMR of **8ab2**

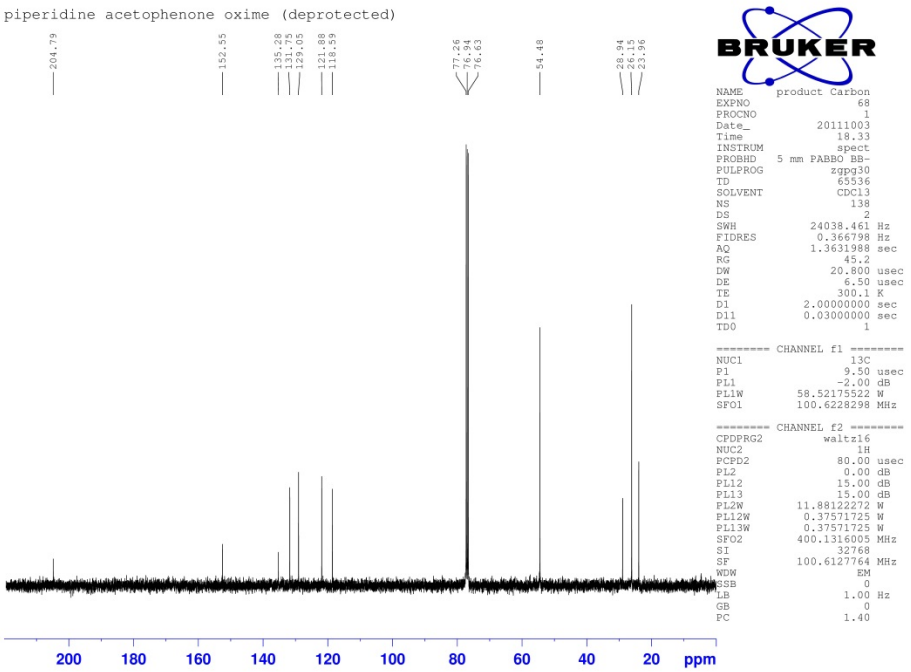

Figure A182. ^{1}H NMR of **10sf2**

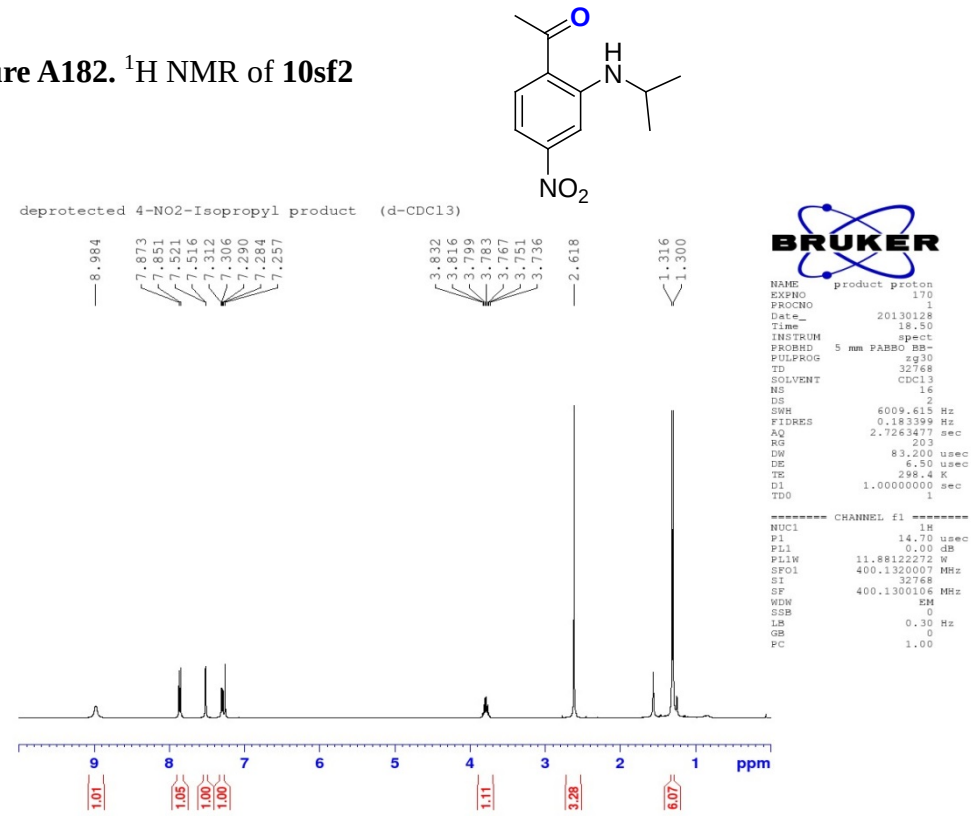

Figure A183. ^{13}C NMRof **10sf2**

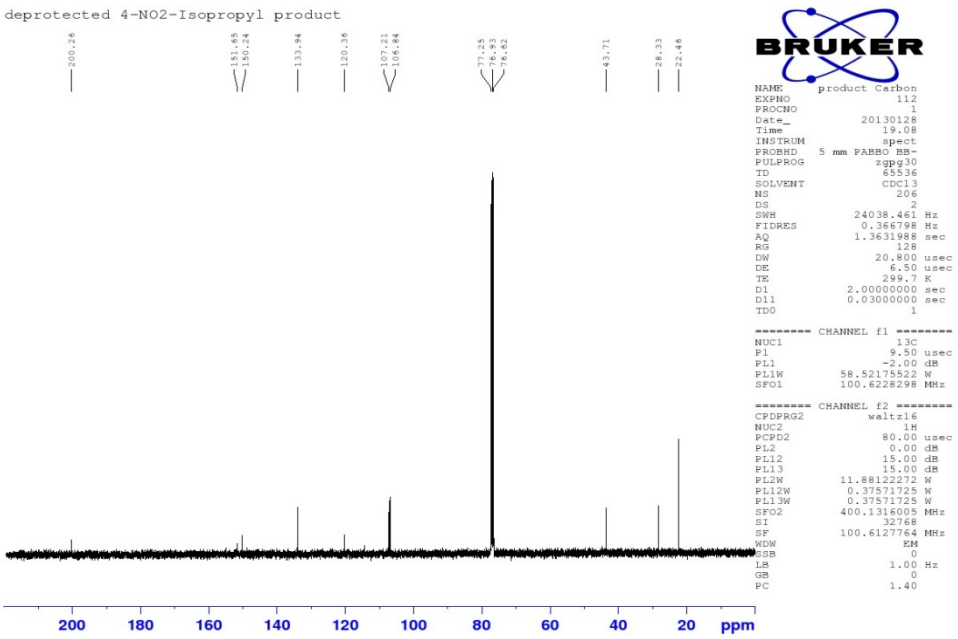

Figure A184. ^{1}H NMR of **10sa2**

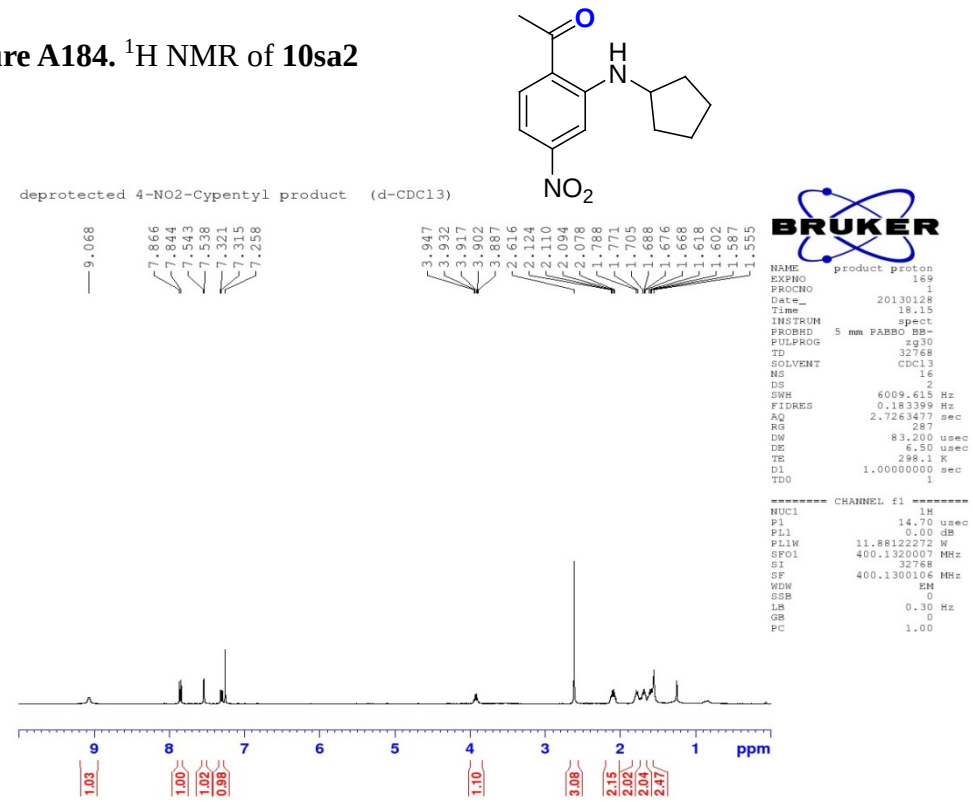

Figure A185. ^{13}C NMR of **10sa2**

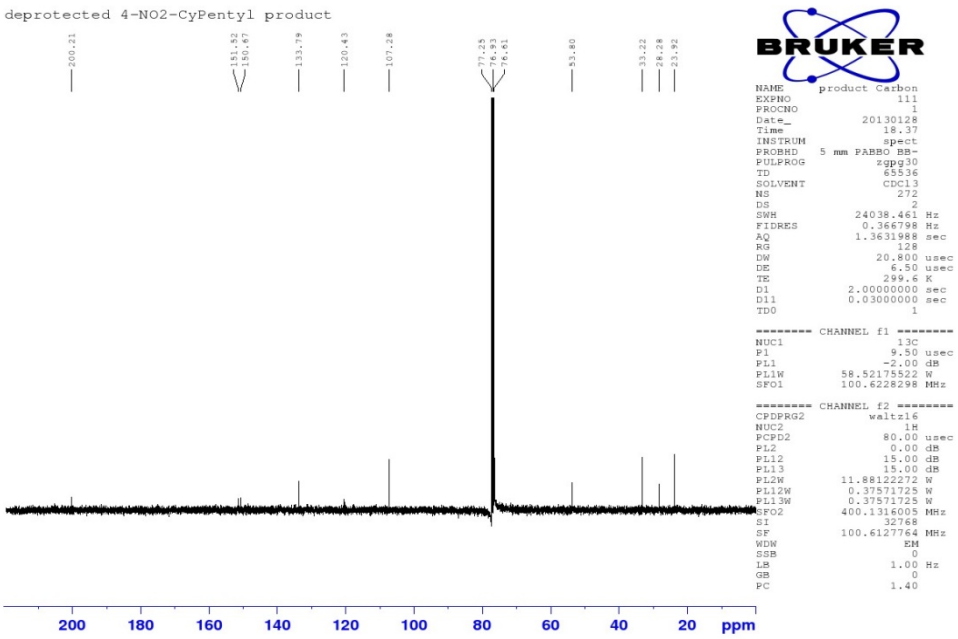

Figure A186. ^{1}H NMR of **10da2**

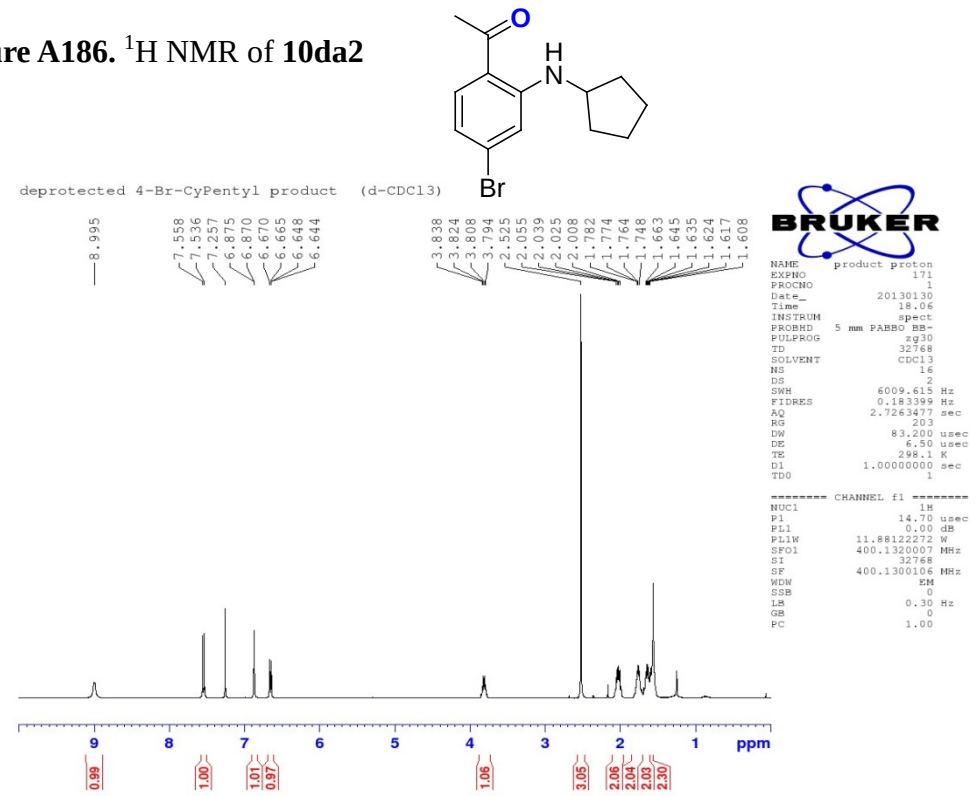

Figure A187. ^{13}C NMR of **10da2**

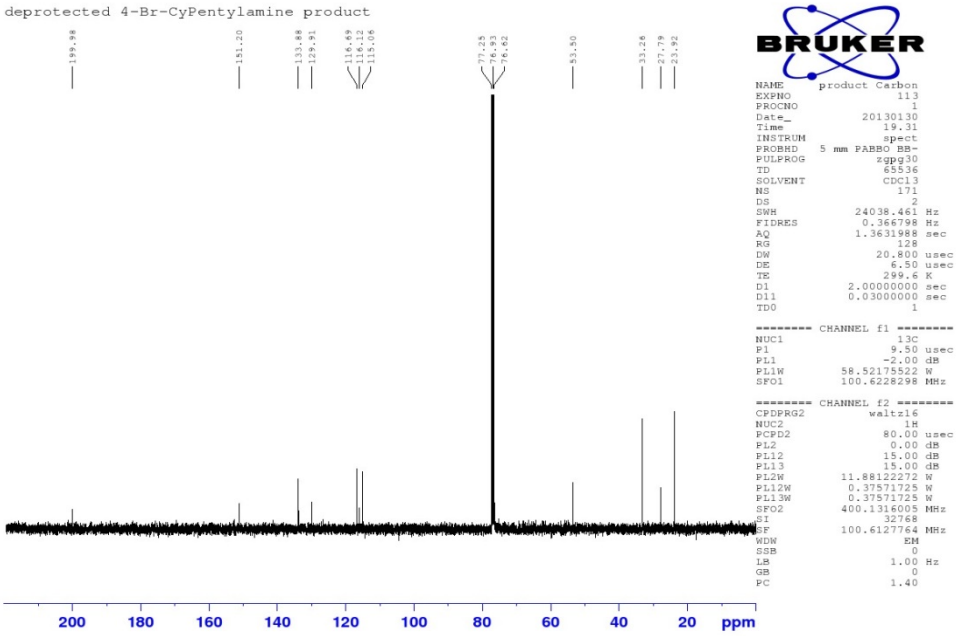

Figure A188. ^{1}H NMR of **10ea2**

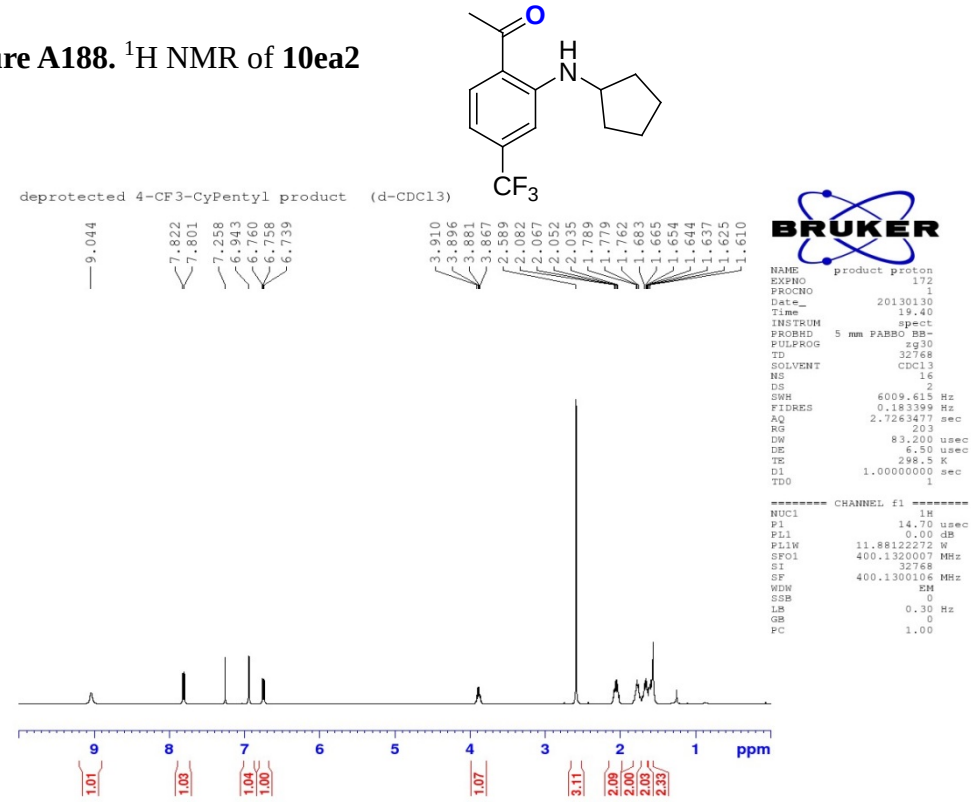

Figure A189. ^{13}C NMR of **10ea2**

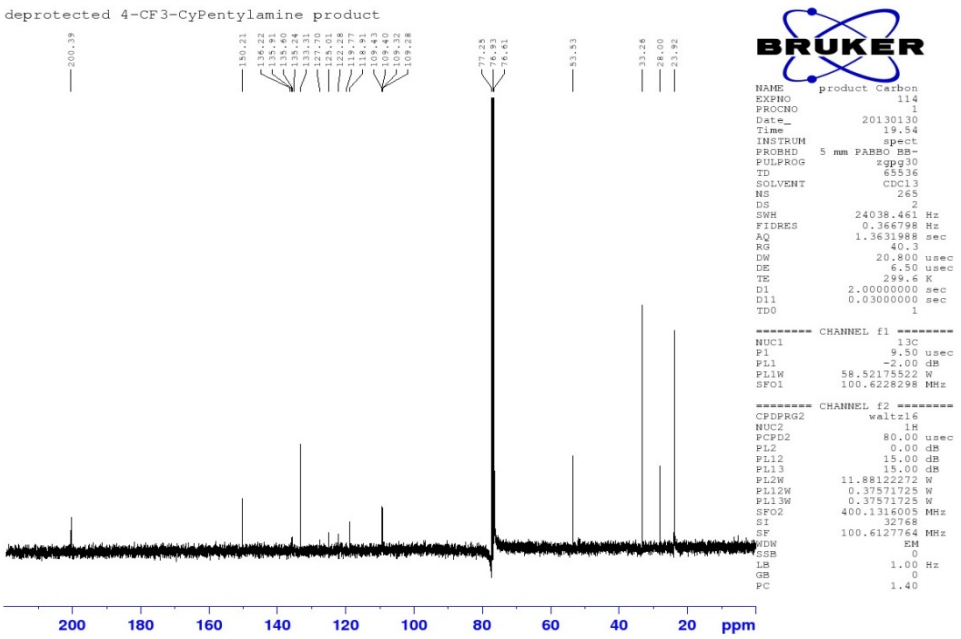

Figure A190. ^{1}H NMR of **12aa**

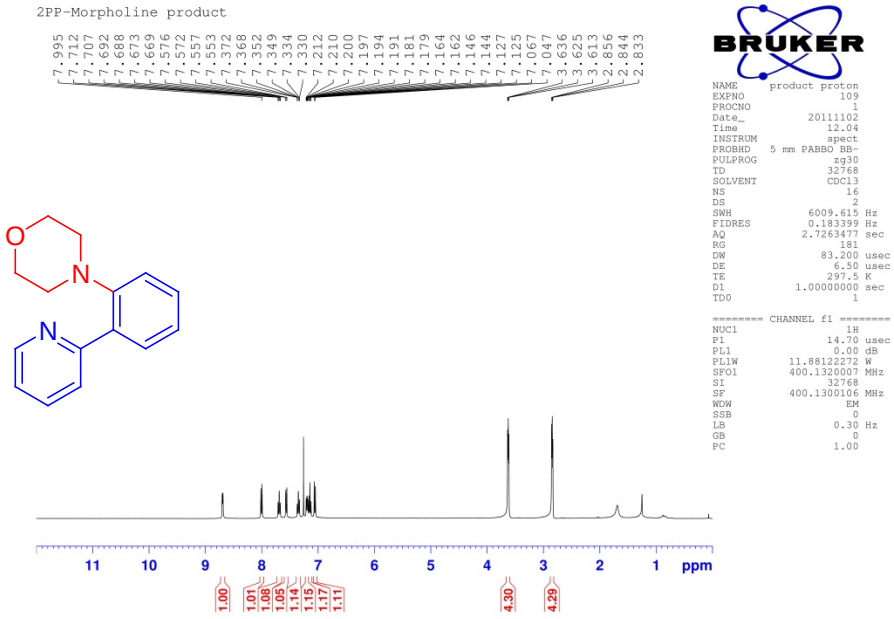

Figure A191. ^{13}C NMR of **12aa**

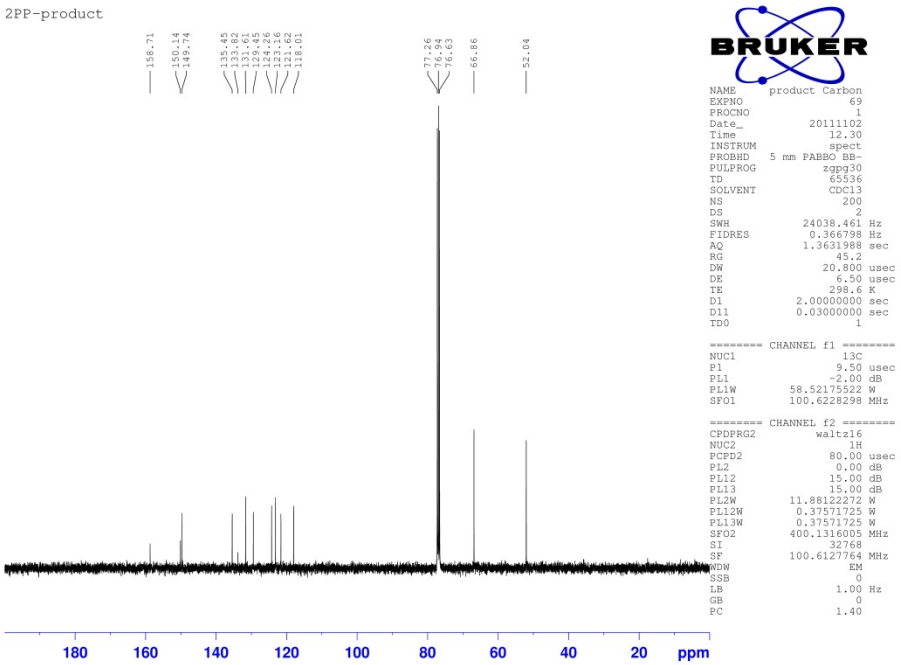

Figure A192. ^{1}H NMR of **13aa**

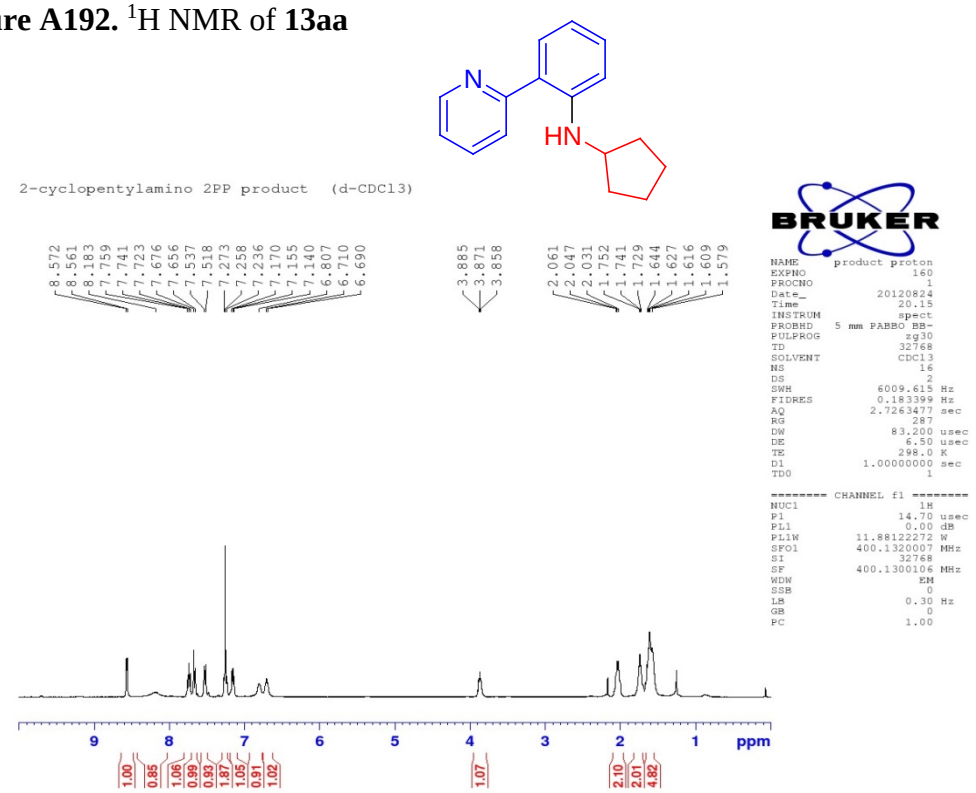

Figure A193. ^{13}C NMR of **13aa**

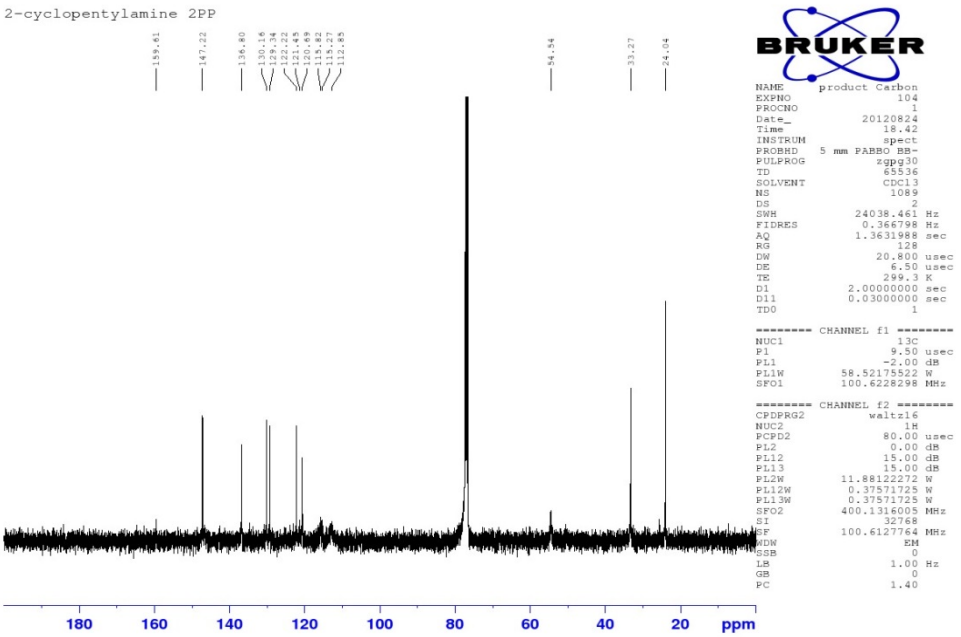

Figure A194. ^{1}H NMR of **13ac**

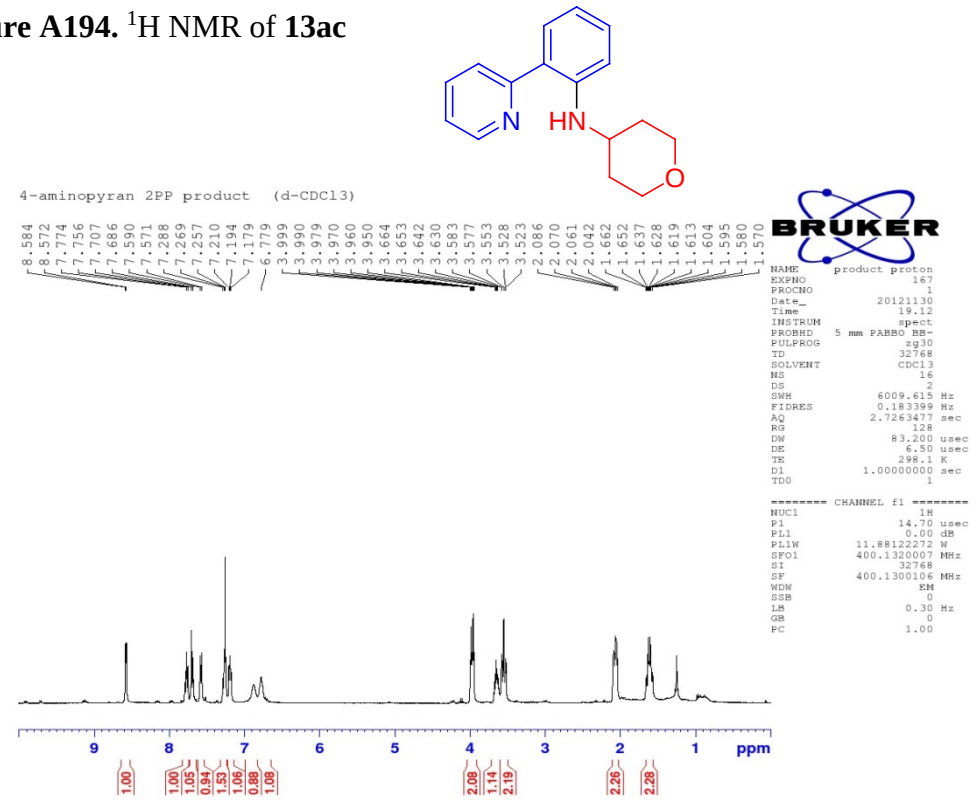

Figure A195. ^{13}C NMR of **13ac**

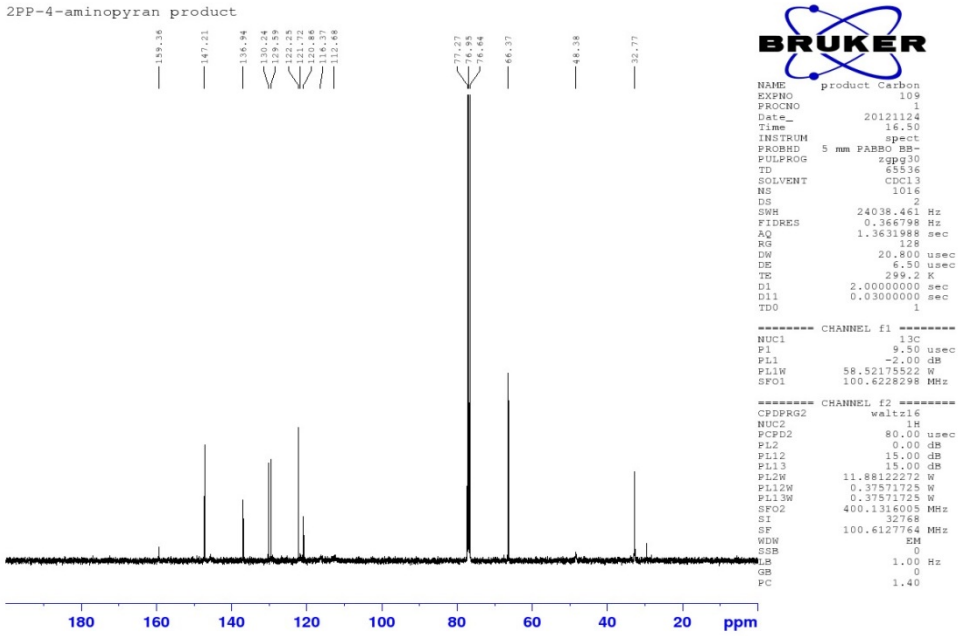

Figure A196. ^{1}H NMR of **13ah**

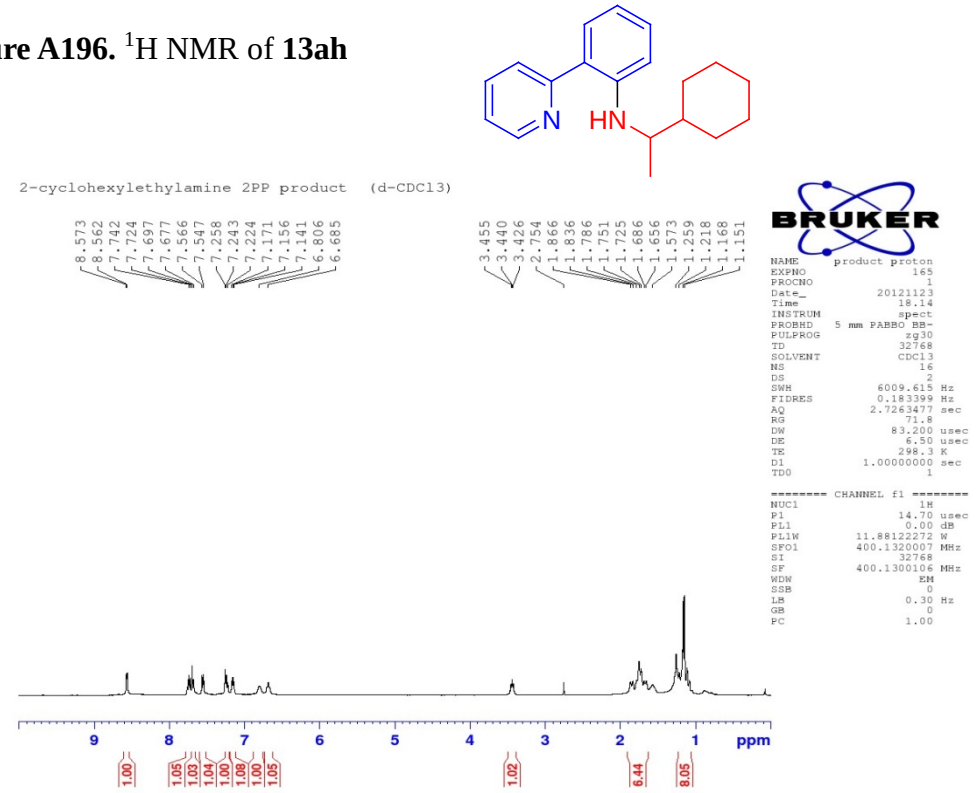

Figure A197. ^{13}C NMR of **13ah**

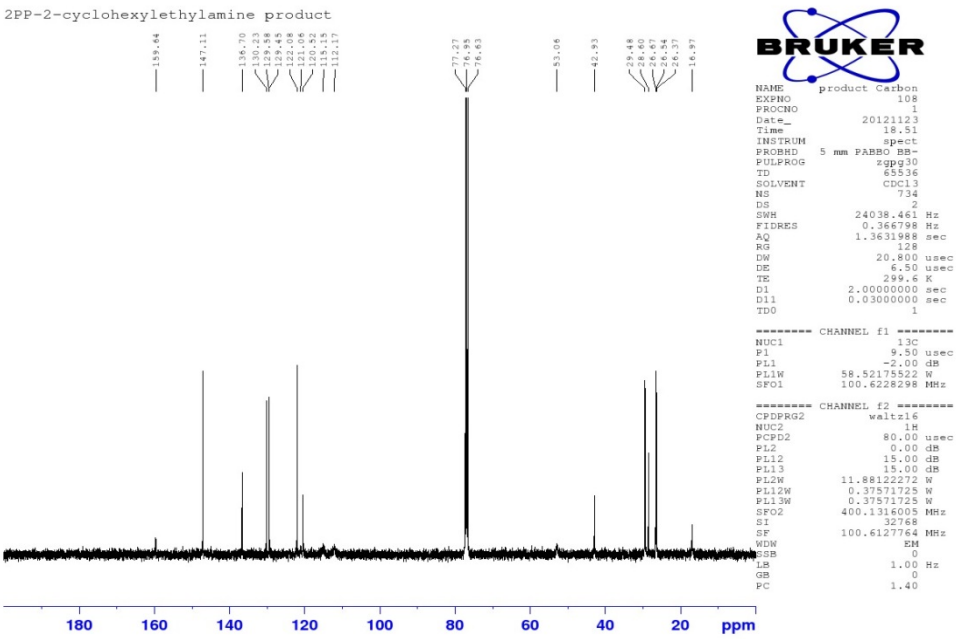

Figure A198. ^{1}H NMR of **13al**

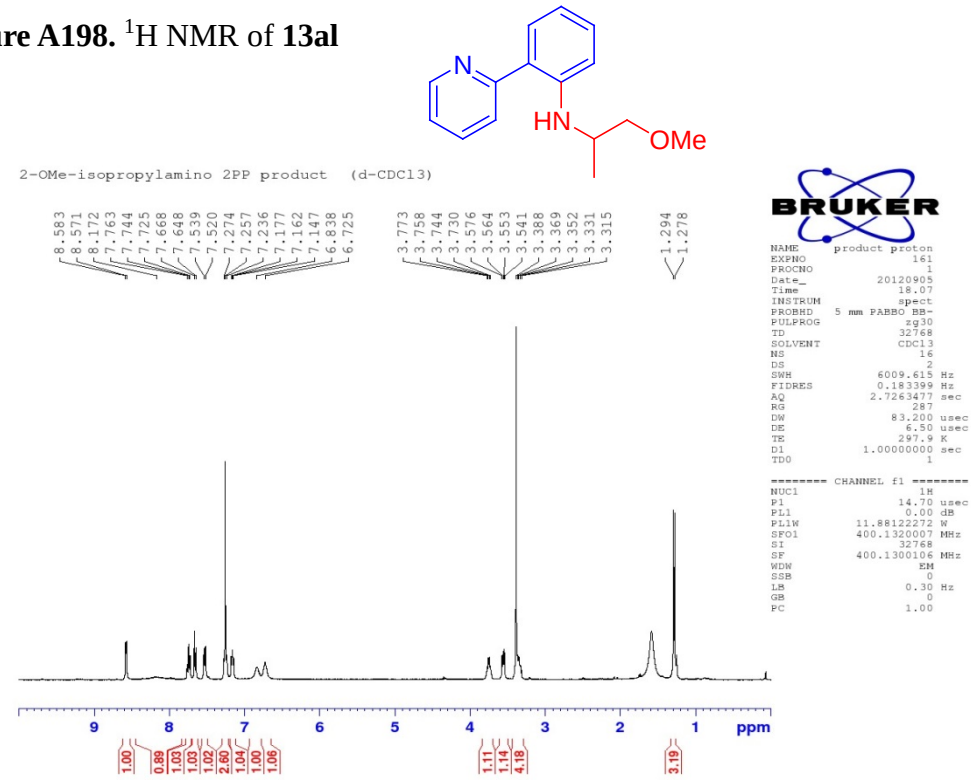

Figure A199. ^{13}C NMR of **13al**

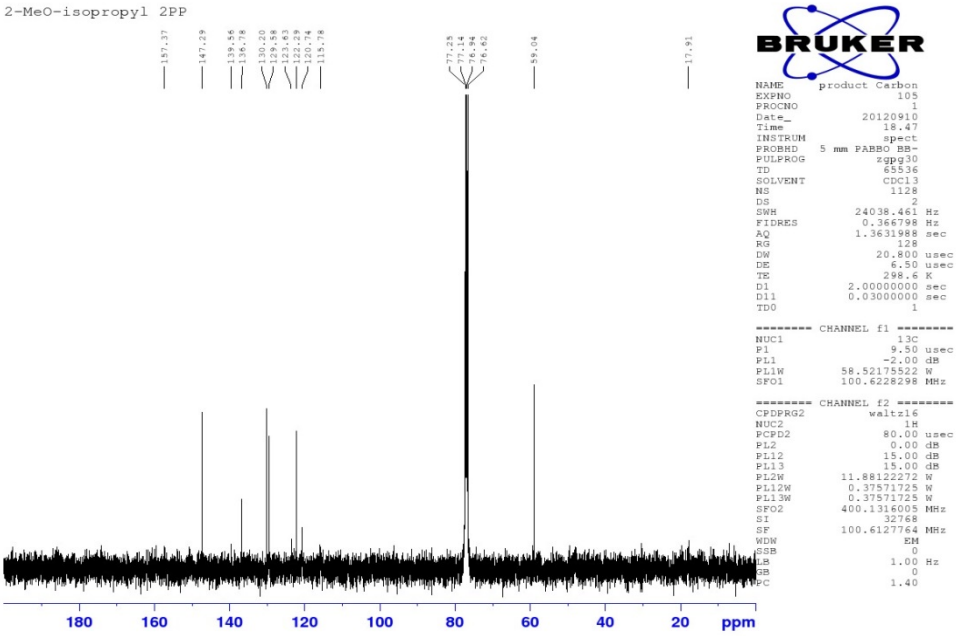

Figure A200. Molecular Structure of **8aa·HCl**

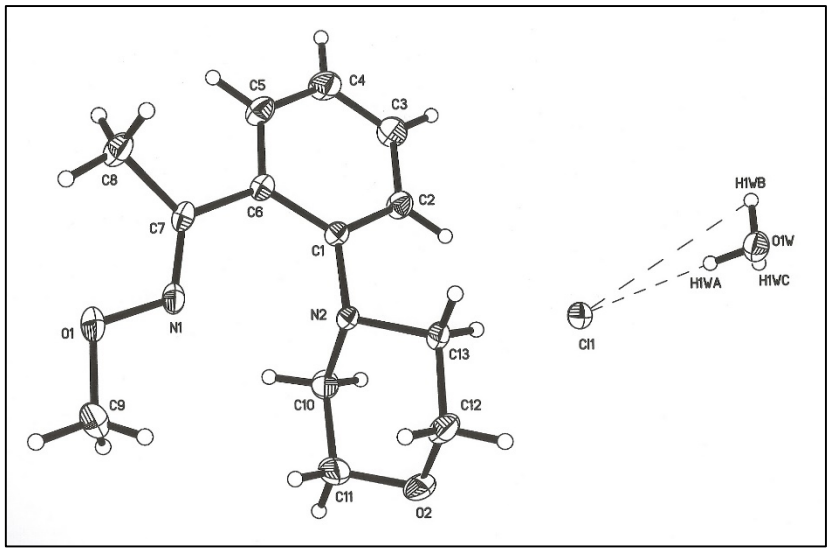

Table A1. Atomic coordinates (x 10^4) and equivalent isotropic displacement parameters ($Å^2$x 10^3) for **8aa·HCl**. U(eq) is defined as one third of the trace of the orthogonalized U^{ij} tensor.

	x	y	z	U(eq)
Cl(1)	2140(1)	3145(1)	9569(1)	51(1)
O(1)	8427(1)	1016(1)	14368(1)	61(1)
O(2)	7335(2)	1463(1)	9100(1)	71(1)
N(1)	7008(1)	1400(1)	14012(1)	47(1)
N(2)	5811(1)	2392(1)	11900(1)	35(1)
C(1)	4359(2)	2748(1)	13177(1)	37(1)
C(2)	2847(2)	3117(2)	12997(2)	48(1)
C(3)	1457(2)	3473(2)	14160(2)	60(1)
C(4)	1595(2)	3472(2)	15478(2)	65(1)
C(5)	3101(2)	3089(2)	15667(2)	56(1)
C(6)	4516(2)	2697(1)	14532(1)	40(1)
C(7)	6064(2)	2238(1)	14833(1)	42(1)
C(8)	6419(2)	2773(2)	16045(2)	61(1)
C(9)	9593(2)	323(2)	13226(2)	67(1)
C(10)	5669(2)	886(2)	11662(2)	55(1)
C(11)	7209(3)	584(2)	10379(2)	76(1)
C(12)	7556(2)	2877(2)	9283(2)	58(1)
C(13)	6046(2)	3329(1)	10505(1)	41(1)

O(1W)	1276(1)	5989(1)	8029(1)	57(1)

Table A2. Bond lengths [Å] and angles [°] for **8aa·HCl**.

O(1)-N(1)	1.4005(15)
O(1)-C(9)	1.436(2)
O(2)-C(11)	1.411(2)
O(2)-C(12)	1.411(2)
N(1)-C(7)	1.2756(18)
N(2)-C(1)	1.4791(14)
N(2)-C(10)	1.5030(17)
N(2)-C(13)	1.5099(16)
C(1)-C(2)	1.3846(18)
C(1)-C(6)	1.4059(18)
C(2)-C(3)	1.387(2)
C(2)-H(2A)	0.9300
C(3)-C(4)	1.367(3)
C(3)-H(3A)	0.9300
C(4)-C(5)	1.389(2)
C(4)-H(4A)	0.9300
C(5)-C(6)	1.3950(19)
C(5)-H(5A)	0.9300
C(6)-C(7)	1.4925(18)
C(7)-C(8)	1.500(2)
C(8)-H(8A)	0.9600
C(8)-H(8B)	0.9600
C(8)-H(8C)	0.9600
C(9)-H(9A)	0.9600
C(9)-H(9B)	0.9600
C(9)-H(9C)	0.9600
C(10)-C(11)	1.504(2)
C(10)-H(10A)	0.9700
C(10)-H(10B)	0.9700
C(11)-H(11A)	0.9700
C(11)-H(11B)	0.9700
C(12)-C(13)	1.5069(19)
C(12)-H(12A)	0.9700
C(12)-H(12B)	0.9700
C(13)-H(13A)	0.9700
C(13)-H(13B)	0.9700

O(1W)-H(1WA)	0.8208
O(1W)-H(1WB)	0.8845
O(1W)-H(1WC)	1.3410

N(1)-O(1)-C(9)	108.83(12)
C(11)-O(2)-C(12)	108.97(12)
C(7)-N(1)-O(1)	112.64(12)
C(1)-N(2)-C(10)	112.22(10)
C(1)-N(2)-C(13)	114.08(9)
C(10)-N(2)-C(13)	108.37(10)
C(2)-C(1)-C(6)	121.41(11)
C(2)-C(1)-N(2)	118.10(11)
C(6)-C(1)-N(2)	120.48(11)
C(1)-C(2)-C(3)	120.14(14)
C(1)-C(2)-H(2A)	119.9
C(3)-C(2)-H(2A)	119.9
C(4)-C(3)-C(2)	119.58(15)
C(4)-C(3)-H(3A)	120.2
C(2)-C(3)-H(3A)	120.2
C(3)-C(4)-C(5)	120.47(14)
C(3)-C(4)-H(4A)	119.8
C(5)-C(4)-H(4A)	119.8
C(4)-C(5)-C(6)	121.66(15)
C(4)-C(5)-H(5A)	119.2
C(6)-C(5)-H(5A)	119.2
C(5)-C(6)-C(1)	116.69(12)
C(5)-C(6)-C(7)	118.62(12)
C(1)-C(6)-C(7)	124.69(11)
N(1)-C(7)-C(6)	116.17(12)
N(1)-C(7)-C(8)	124.42(13)
C(6)-C(7)-C(8)	119.41(12)
C(7)-C(8)-H(8A)	109.5
C(7)-C(8)-H(8B)	109.5
H(8A)-C(8)-H(8B)	109.5
C(7)-C(8)-H(8C)	109.5
H(8A)-C(8)-H(8C)	109.5
H(8B)-C(8)-H(8C)	109.5
O(1)-C(9)-H(9A)	109.5

O(1)-C(9)-H(9B)	109.5
H(9A)-C(9)-H(9B)	109.5
O(1)-C(9)-H(9C)	109.5
H(9A)-C(9)-H(9C)	109.5
H(9B)-C(9)-H(9C)	109.5
N(2)-C(10)-C(11)	109.41(13)
N(2)-C(10)-H(10A)	109.8
C(11)-C(10)-H(10A)	109.8
N(2)-C(10)-H(10B)	109.8
C(11)-C(10)-H(10B)	109.8
H(10A)-C(10)-H(10B)	108.2
O(2)-C(11)-C(10)	111.70(14)
O(2)-C(11)-H(11A)	109.3
C(10)-C(11)-H(11A)	109.3
O(2)-C(11)-H(11B)	109.3
C(10)-C(11)-H(11B)	109.3
H(11A)-C(11)-H(11B)	107.9
O(2)-C(12)-C(13)	111.77(12)
O(2)-C(12)-H(12A)	109.3
C(13)-C(12)-H(12A)	109.3
O(2)-C(12)-H(12B)	109.3
C(13)-C(12)-H(12B)	109.3
H(12A)-C(12)-H(12B)	107.9
C(12)-C(13)-N(2)	109.58(11)
C(12)-C(13)-H(13A)	109.8
N(2)-C(13)-H(13A)	109.8
C(12)-C(13)-H(13B)	109.8
N(2)-C(13)-H(13B)	109.8
H(13A)-C(13)-H(13B)	108.2
H(1WA)-O(1W)-H(1WB)	97.2
H(1WA)-O(1W)-H(1WC)	76.8
H(1WB)-O(1W)-H(1WC)	74.9

Symmetry transformations used to generate equivalent atoms:

Table A3. Anisotropic displacement parameters ($Å^2 x\ 10^3$)for **8aa·HCl**. The anisotropicdisplacement factor exponent takes the form: $-2\pi^2 [h^2 a^{*2} U^{11} + ... + 2\ h\ k\ a^*\ b^*\ U^{12}]$

	U^{11}	U^{22}	U^{33}	U^{23}	U^{13}	U^{12}
Cl(1)	55(1)	52(1)	49(1)	-8(1)	-25(1)	9(1)
O(1)	62(1)	77(1)	58(1)	-6(1)	-39(1)	19(1)
O(2)	88(1)	92(1)	52(1)	-39(1)	-38(1)	31(1)
N(1)	52(1)	51(1)	45(1)	-1(1)	-29(1)	6(1)
N(2)	42(1)	37(1)	32(1)	-8(1)	-19(1)	5(1)
C(1)	37(1)	40(1)	34(1)	-6(1)	-14(1)	0(1)
C(2)	41(1)	63(1)	46(1)	-10(1)	-20(1)	3(1)
C(3)	38(1)	81(1)	61(1)	-11(1)	-16(1)	8(1)
C(4)	47(1)	87(1)	51(1)	-15(1)	-5(1)	9(1)
C(5)	54(1)	73(1)	35(1)	-8(1)	-11(1)	0(1)
C(6)	43(1)	43(1)	34(1)	-2(1)	-15(1)	-3(1)
C(7)	47(1)	47(1)	32(1)	4(1)	-18(1)	-6(1)
C(8)	63(1)	84(1)	46(1)	-15(1)	-29(1)	-1(1)
C(9)	68(1)	66(1)	77(1)	-9(1)	-39(1)	22(1)
C(10)	83(1)	37(1)	60(1)	-14(1)	-41(1)	6(1)
C(11)	108(1)	69(1)	77(1)	-42(1)	-54(1)	43(1)
C(12)	51(1)	88(1)	38(1)	-16(1)	-18(1)	6(1)
C(13)	45(1)	48(1)	35(1)	-3(1)	-20(1)	2(1)
O(1W)	57(1)	60(1)	49(1)	2(1)	-19(1)	2(1)

Table A4 Hydrogen coordinates (x 10^4) and isotropic displacement parameters (Å^{2}x 10^3) for **8aa·HCl**.

	x	y	z	U(eq)
H(2A)	2765	3126	12095	58
H(3A)	437	3710	14043	72
H(4A)	672	3729	16254	78
H(5A)	3169	3094	16572	67
H(8A)	7452	2386	16100	92
H(8B)	5476	2492	16945	92
H(8C)	6557	3782	15866	92
H(9A)	10571	55	13460	100
H(9B)	9965	953	12331	100
H(9C)	9023	-502	13124	100
H(10A)	4628	724	11485	67
H(10B)	5610	260	12521	67
H(11A)	8241	723	10576	91
H(11B)	7126	-393	10238	91
H(12A)	7702	3482	8389	70
H(12B)	8591	2986	9485	70
H(13A)	5015	3267	10289	50
H(13B)	6242	4301	10608	50
H(1WA)	1362	5219	8451	74
H(1WB)	328	6222	8710	86
H(1WC)	10	5191	7950	120

Table A5. Torsion angles [°] for **8aa·HCl**.

C(9)-O(1)-N(1)-C(7)	-168.19(12)
C(10)-N(2)-C(1)-C(2)	-83.24(14)
C(13)-N(2)-C(1)-C(2)	40.50(15)
C(10)-N(2)-C(1)-C(6)	96.13(14)
C(13)-N(2)-C(1)-C(6)	-140.13(12)
C(6)-C(1)-C(2)-C(3)	1.2(2)
N(2)-C(1)-C(2)-C(3)	-179.39(13)
C(1)-C(2)-C(3)-C(4)	0.7(3)
C(2)-C(3)-C(4)-C(5)	-1.4(3)
C(3)-C(4)-C(5)-C(6)	0.1(3)
C(4)-C(5)-C(6)-C(1)	1.8(2)
C(4)-C(5)-C(6)-C(7)	-177.33(14)
C(2)-C(1)-C(6)-C(5)	-2.42(19)
N(2)-C(1)-C(6)-C(5)	178.22(12)
C(2)-C(1)-C(6)-C(7)	176.61(12)
N(2)-C(1)-C(6)-C(7)	-2.75(19)
O(1)-N(1)-C(7)-C(6)	-179.78(10)
O(1)-N(1)-C(7)-C(8)	0.38(18)
C(5)-C(6)-C(7)-N(1)	153.48(13)
C(1)-C(6)-C(7)-N(1)	-25.53(18)
C(5)-C(6)-C(7)-C(8)	-26.67(18)
C(1)-C(6)-C(7)-C(8)	154.32(13)
C(1)-N(2)-C(10)-C(11)	-178.28(12)
C(13)-N(2)-C(10)-C(11)	54.85(15)
C(12)-O(2)-C(11)-C(10)	62.36(18)
N(2)-C(10)-C(11)-O(2)	-60.01(19)
C(11)-O(2)-C(12)-C(13)	-61.78(17)
O(2)-C(12)-C(13)-N(2)	58.89(15)
C(1)-N(2)-C(13)-C(12)	179.81(11)
C(10)-N(2)-C(13)-C(12)	-54.39(14)

Symmetry transformations used to generate equivalent atoms:

Table A6 Hydrogen bonds for **8aa·HCl** [Å and °].

D-H...A	d(D-H)	d(H...A)	d(D...A)	<(DHA)
O(1W)-H(1WA)...Cl(1)	0.82	2.37	3.1779(12)	169.4
O(1W)-H(1WA)...Cl(1)	0.82	2.37	3.1779(12)	169.4

Symmetry transformations used to generate equivalent atoms:

Figure A201. Molecular Structure of **10sb**

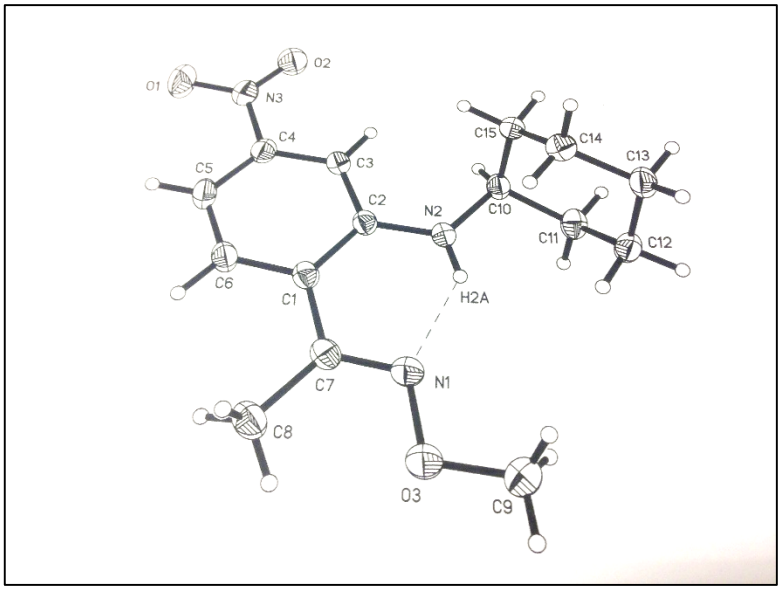

Table A7 Atomic coordinates (x 10^4) and equivalent isotropic displacement parameters ($Å^2$x 10^3) for **10sb.** U(eq) is defined as one third of the trace of the orthogonalized U^{ij} tensor.

	x	y	z	U(eq)
O(1)	2823(2)	945(1)	1678(1)	95(1)
O(2)	2353(1)	-115(1)	3132(1)	73(1)
O(3)	2027(1)	8251(1)	7625(1)	63(1)
N(1)	2116(1)	6772(1)	7009(1)	48(1)
N(2)	1905(1)	3846(1)	6728(1)	44(1)
N(3)	2592(1)	991(1)	2731(1)	53(1)
C(1)	2435(1)	5175(1)	5120(1)	38(1)
C(2)	2215(1)	3833(1)	5560(1)	36(1)
C(3)	2295(1)	2480(1)	4735(1)	39(1)
C(4)	2575(1)	2451(1)	3549(1)	42(1)
C(5)	2827(2)	3714(1)	3106(1)	51(1)
C(6)	2746(1)	5045(1)	3906(1)	47(1)
C(7)	2346(1)	6670(1)	5886(1)	40(1)
C(8)	2520(2)	8015(1)	5346(1)	55(1)
C(9)	1898(2)	8289(1)	8866(1)	78(1)
C(10)	1720(1)	2528(1)	7236(1)	40(1)
C(11)	739(1)	2906(1)	8417(1)	49(1)

C(12)	1961(2)	3861(1)	9429(1)	49(1)
C(13)	3776(2)	3154(1)	9595(1)	49(1)
C(14)	4795(1)	2861(1)	8436(1)	49(1)
C(15)	3592(1)	1885(1)	7429(1)	44(1)

Table A8 Bond lengths [Å] and angles [°] for **10sb**.

O(1)-N(3)	1.2117(12)
O(2)-N(3)	1.2144(12)
O(3)-N(1)	1.4059(10)
O(3)-C(9)	1.4167(15)
N(1)-C(7)	1.2835(12)
N(2)-C(2)	1.3583(11)
N(2)-C(10)	1.4594(12)
N(3)-C(4)	1.4722(12)
C(1)-C(6)	1.3934(13)
C(1)-C(2)	1.4391(13)
C(1)-C(7)	1.4774(12)
C(2)-C(3)	1.4040(12)
C(3)-C(4)	1.3712(13)
C(4)-C(5)	1.3762(15)
C(5)-C(6)	1.3749(14)
C(7)-C(8)	1.5038(14)
C(10)-C(15)	1.5266(14)
C(10)-C(11)	1.5300(13)
C(11)-C(12)	1.5215(14)
C(12)-C(13)	1.5121(15)
C(13)-C(14)	1.5200(14)
C(14)-C(15)	1.5194(13)

N(1)-O(3)-C(9)	109.02(8)
C(7)-N(1)-O(3)	112.01(8)
C(2)-N(2)-C(10)	124.77(7)
O(1)-N(3)-O(2)	122.65(9)
O(1)-N(3)-C(4)	118.40(9)
O(2)-N(3)-C(4)	118.94(8)
C(6)-C(1)-C(2)	117.75(8)
C(6)-C(1)-C(7)	118.77(8)
C(2)-C(1)-C(7)	123.48(8)
N(2)-C(2)-C(3)	119.96(8)
N(2)-C(2)-C(1)	122.10(7)
C(3)-C(2)-C(1)	117.93(8)
C(4)-C(3)-C(2)	120.53(9)

C(3)-C(4)-C(5)	122.95(9)
C(3)-C(4)-N(3)	117.48(9)
C(5)-C(4)-N(3)	119.57(8)
C(6)-C(5)-C(4)	116.92(9)
C(5)-C(6)-C(1)	123.90(9)
N(1)-C(7)-C(1)	118.01(8)
N(1)-C(7)-C(8)	121.86(8)
C(1)-C(7)-C(8)	120.14(8)
N(2)-C(10)-C(15)	112.00(8)
N(2)-C(10)-C(11)	109.45(8)
C(15)-C(10)-C(11)	110.65(8)
C(12)-C(11)-C(10)	112.80(8)
C(13)-C(12)-C(11)	111.12(8)
C(12)-C(13)-C(14)	110.95(8)
C(15)-C(14)-C(13)	110.61(9)
C(14)-C(15)-C(10)	112.63(7)

Symmetry transformations used to generate equivalent atoms:

Table A9. Anisotropic displacement parameters ($Å^2 x\ 10^3$)for **10sb**. The anisotropic displacement factor exponent takes the form: $-2\pi^2 [h^2 a^{*2} U^{11} + ... + 2\ h\ k\ a^*\ b^*\ U^{12}]$

	U^{11}	U^{22}	U^{33}	U^{23}	U^{13}	U^{12}
O(1)	169(1)	76(1)	39(1)	4(1)	25(1)	12(1)
O(2)	115(1)	50(1)	55(1)	6(1)	14(1)	7(1)
O(3)	102(1)	36(1)	49(1)	6(1)	6(1)	2(1)
N(1)	64(1)	35(1)	45(1)	8(1)	2(1)	4(1)
N(2)	66(1)	37(1)	33(1)	11(1)	7(1)	10(1)
N(3)	64(1)	57(1)	37(1)	6(1)	5(1)	9(1)
C(1)	34(1)	44(1)	38(1)	14(1)	1(1)	3(1)
C(2)	34(1)	43(1)	34(1)	13(1)	1(1)	5(1)
C(3)	43(1)	42(1)	36(1)	13(1)	2(1)	5(1)
C(4)	43(1)	49(1)	35(1)	8(1)	3(1)	6(1)
C(5)	60(1)	62(1)	34(1)	17(1)	9(1)	4(1)
C(6)	53(1)	51(1)	42(1)	20(1)	6(1)	2(1)
C(7)	36(1)	42(1)	45(1)	15(1)	-1(1)	0(1)
C(8)	67(1)	47(1)	57(1)	22(1)	5(1)	-2(1)
C(9)	131(1)	54(1)	45(1)	4(1)	5(1)	17(1)
C(10)	52(1)	38(1)	32(1)	10(1)	2(1)	-4(1)
C(11)	48(1)	61(1)	41(1)	16(1)	8(1)	-1(1)
C(12)	62(1)	51(1)	36(1)	8(1)	13(1)	4(1)
C(13)	65(1)	47(1)	35(1)	10(1)	-3(1)	-2(1)
C(14)	49(1)	51(1)	46(1)	10(1)	2(1)	6(1)
C(15)	62(1)	35(1)	37(1)	9(1)	7(1)	8(1)

Table A10. Hydrogen coordinates (x 10^4) and isotropic displacement parameters ($Å^2$x 10^3) for **10sb**.

	x	y	z	U(eq)
H(2A)	1842(15)	4697(12)	7181(10)	53(3)
H(3A)	2170(14)	1588(12)	4971(9)	49(3)
H(5A)	3034(16)	3700(13)	2327(11)	64(3)
H(6A)	2932(15)	5948(13)	3604(10)	59(3)
H(8C)	1860(20)	7856(17)	4561(14)	99(5)
H(8B)	1940(20)	8834(19)	5832(14)	110(5)
H(8A)	3710(20)	8222(19)	5242(15)	114(6)
H(9C)	1810(20)	9227(17)	9220(13)	92(5)
H(9B)	870(30)	7620(20)	8997(17)	140(7)
H(9A)	3010(30)	7880(20)	9174(18)	145(7)
H(10A)	938(13)	1765(10)	6683(8)	41(2)
H(11B)	364(16)	1955(13)	8639(10)	63(3)
H(11A)	-383(16)	3401(12)	8294(10)	58(3)
H(12B)	1328(16)	4034(12)	10184(10)	59(3)
H(12A)	2215(14)	4821(12)	9254(9)	49(3)
H(13B)	3502(15)	2219(13)	9833(10)	57(3)
H(13A)	4556(15)	3773(12)	10233(10)	55(3)
H(14B)	5085(14)	3834(12)	8214(9)	50(3)
H(14A)	5963(17)	2420(13)	8537(10)	64(3)
H(15B)	4284(14)	1701(11)	6687(9)	50(3)
H(15A)	3346(16)	904(13)	7601(10)	59(3)

Table A11. Torsion angles [°] for **10sb**.

C(9)-O(3)-N(1)-C(7)	-176.11(10)
C(10)-N(2)-C(2)-C(3)	2.94(14)
C(10)-N(2)-C(2)-C(1)	-178.27(8)
C(6)-C(1)-C(2)-N(2)	-179.91(9)
C(7)-C(1)-C(2)-N(2)	0.02(13)
C(6)-C(1)-C(2)-C(3)	-1.09(12)
C(7)-C(1)-C(2)-C(3)	178.83(8)
N(2)-C(2)-C(3)-C(4)	178.85(8)
C(1)-C(2)-C(3)-C(4)	0.00(13)
C(2)-C(3)-C(4)-C(5)	1.32(15)
C(2)-C(3)-C(4)-N(3)	-178.38(8)
O(1)-N(3)-C(4)-C(3)	179.43(10)
O(2)-N(3)-C(4)-C(3)	0.30(14)
O(1)-N(3)-C(4)-C(5)	-0.27(15)
O(2)-N(3)-C(4)-C(5)	-179.41(10)
C(3)-C(4)-C(5)-C(6)	-1.43(15)
N(3)-C(4)-C(5)-C(6)	178.26(9)
C(4)-C(5)-C(6)-C(1)	0.24(16)
C(2)-C(1)-C(6)-C(5)	0.99(15)
C(7)-C(1)-C(6)-C(5)	-178.93(9)
O(3)-N(1)-C(7)-C(1)	-179.06(8)
O(3)-N(1)-C(7)-C(8)	0.80(13)
C(6)-C(1)-C(7)-N(1)	-177.93(9)
C(2)-C(1)-C(7)-N(1)	2.15(13)
C(6)-C(1)-C(7)-C(8)	2.20(13)
C(2)-C(1)-C(7)-C(8)	-177.72(9)
C(2)-N(2)-C(10)-C(15)	76.36(11)
C(2)-N(2)-C(10)-C(11)	-160.55(9)
N(2)-C(10)-C(11)-C(12)	-72.25(11)
C(15)-C(10)-C(11)-C(12)	51.63(11)
C(10)-C(11)-C(12)-C(13)	-54.36(12)
C(11)-C(12)-C(13)-C(14)	56.70(11)
C(12)-C(13)-C(14)-C(15)	-57.34(11)
C(13)-C(14)-C(15)-C(10)	55.74(11)
N(2)-C(10)-C(15)-C(14)	69.94(10)
C(11)-C(10)-C(15)-C(14)	-52.47(11)

Symmetry transformations used to generate equivalent atoms:

Table A12. Hydrogen bonds for **10sb** [Å and °].

D-H...A	d(D-H)	d(H...A)	d(D...A)	<(DHA)
N(2)-H(2A)...N(1)	0.851(11)	1.973(11)	2.6554(11)	136.5(10)

Symmetry transformations used to generate equivalent atoms:

REFERENCES

Chapter 1

1 (a) Clayden, J.; Greeves, N.; Warren, S. *Organic Chemistry, 2nd Ed.*; Oxford University Press Inc.: New York, 2012. (b) Brown, J. M.; Carreira, E. M.; Fernandez, E.; Genet, J. –P.; Greck, C.; Hartwig, J. F.; Iikura, H.; Jørgensen, K. A.; Komatsu, M.; Kunz, H.; Lavergne, D.; Minakata, S.; Schultz-Kukula, M.; Tietgen, H.; Tomooka, C. S. *Modern Amination Methods*; Ricci, A., Ed.; WILEY-VCH: Weinheim, 2000. (c) Carey, F. A.; Sundberg, R. J. *Advanced Organic Chemistry Part B: Reactions and Synthesis*; Kluwer Academic / Plenum Publishers: New York, 2000; p 642-645.

2 D'Aprano, G.; Leclerc, M. *Chem. Mater.* **1995**, *7*, 33.

3 *Drug Top*. **2009**, *6*, 7. For information of the drugs see: www.yakup.com/download.html?mid=70407

4 (a) Surry, D. S.; Buchwald, S. L. *Angew. Chem. Int. Ed.* **2008**, *47*, 6338. (b) Hartwig, J. F. *Acc. Chem. Res.* **2008**, *41*, 1534. (c) Huang, X.; Anderson, k. W.; Zim, D.; Jiang, L.; Klapars, A.; Buchwald, S. L. *J. Am. Chem. Soc.* **2003**, *125*, 6653. (d) Yin, J.; Buchwald, S. L. *Org. Lett.* **2000**, *2*, 1101.

5 (a) Anslyn, E. V.; Dougherty, D. A. *Modern Physical Organic Chemistry*; Murdzek, J., Ed.; University Science Book: USA, 2006; p 91. (b) Blanksby, S. J.; Ellison, G. B. *Acc. Chem. Res.* **2003**, *36*, 255.

6 (a) Lyons, T. W.; Sanford, M. *Chem. Rev.* **2010**, *110*, 1147. (b) Dick, A. R.; Sanford, M. S. *Tetrahedron* **2006**, *62*, 2439.

7 (a) Ryabov, A. D. *Chem. Rev.* **1990**, *90*, 403. (b) Ryabov, A. D.; Sakodinskaya, I. K.; Yatsimirsky, A. K. *J. Chem. Soc., Dalton Trans.* **1985**, 2629.

8 (a) Bayler, A.; Canty, A. J.; Skelton, B. W.; White, A. H. *J. Organomet. Chem.* **2000**, *595*, 296. (b) Canty, A. J.; van Koten, G. *Acc. Chem. Res.* **1995**, *28*, 406. (c) Byers, P. K.; Canty, A. J.; Skelton, B. W.; White, A. H. *J. Chem. Soc., Chem. Commun.* **1986**, 1722.

9 (a) Davies, D. L.; Donald, S. M. A.; Al-Duaij, O.; Macgregor, S. A.; Pölleth, M. *J. Am. Chem. Soc.* **2006**, *128*, 4210. (b) Davies, D. L.; Donald, S. M. A.; Macgregor, S. A. *J. Am. Chem. Soc.* **2005**, *127*, 13754.

10 (a) Guimond, N.; Gorelsky, S. I.; Fagnou, K. *J. Am. Chem. Soc.* **2011**, *133*, 6449. (b) Guimond, N.; Gouliaras, C.; Fagnou, K. *J. Am. Chem. Soc.* **2010**, *132*, 6908. (c) Sun, H.-Y.; Gorelsky, S. I.; Stuart, D. R.; Campeau, L.-C.; Fagnou, K. *J. Org.*

Chem. **2010**, *75*, 8180. (d) Lafrance, M.; Fagnou, K. *J. Am. Chem. Soc.* **2006**, *128*, 16496

11 (a) Collect, F.; Dodd, R. H.; Dauban, P. *Chem. Commun.* **2009**, 5061. (b) Davies, H. M. L.; Manning, J. R. *nature* **2008**, *451*, 417. (c) Díaz-Requejo, M. M.; Pérez, P. J. *Chem. Rev.* **2008**, *108*, 3379. (d) Müller, P.; Fruit, C. *Chem. Rev.* **2003**, *103*, 2905. (e) Boche, G.; Lohrenz, J. C. W. *Chem. Rev.* **2001**, *101*, 697. (f) Horner, L.; Christmann, A. *Angew. Chem. Int. Ed.* **1963**, *2*, 599.

12 (a) Breslow, R.; Gellman, S. H. *J. Am. Chem. Soc.* **1983**, *105*, 6728. (b) Breslow, R.; Gellman, S. H. *J. Chem. Soc., Chem Commun.* **1982**, 1400.

13 (a) Liang, J.-L.; Huang, J.-S.; Yu, X.-Q.; Zhu, N.; Che, C.-M. *Chem. Eur. J.* **2002**, *8*, 1563. (b) Katsuki, T.; Kohmura, Y. *Tetrahedron Lett.* **2001**, *42*, 3339. (c) Yu, X.-Q.; Huang, J.-S.; Zhou, X.-G.; Che, C.-M. *Org. Lett.* **2000**, *2*, 2233. (d) Mahy, J. P.; Bedi, G.; Battioni, P.; Mansuy, D. *Tetrahedron Lett.* **1988**, *29*, 1927.

14 (a) Au, S.-M.; Huang, J.-S.; Che, C.-M.; Yu, W.-Y. *J. Org. Chem.* **2000**, *65*, 7858. (b) Au, S.-M.; Hunang, J.-S.; Yu, W.-Y.; Fung, W.-H.; Che, C.-M. *J. Am. Chem. Soc* **1999**, *121*, 9120. (c) Au, S.-M.; Zhang, S.-B.; Fung, W.-H.; Che, C.-M.; Cheung, K.-K.; *Chem. Commun.* **1998**, 2677 (d) Au, S.-M.; Fung, W.-H.; Cheng, M.-C.; Che, C-M.; Peng, S.-M. *Chem. Commun.* **1997**, 1655.

15 For examples other Ru-imido complexes that are inactive in nitrenoid transfer reactions, see: (a) Huang, J.-S.; Che, C.-M.; Poon, C.-K. *J. Chem. Soc., Chem. Commun.* **1992**, 161. (b) Danopoulos, A. A.; Wilkinson, G. *Polyhedron* **1992**, *11*, 2961.

16 (a) Albone, D. P.; Challenger, S.; Derrick, A. M.; Fillery, S. M.; Irwin, J. L.; Parsons, C. M.; Takada, H.; Taylor, P. C.; Wilson, D. J. *Org. Biomol. Chem.* **2005**, *3*, 107. (b) Albone, D. P.; Aujla, P. S.; Taylor, P. C. *J. Org. Chem.* **1998**, *63*, 9569.

17 (a) Fructos, M. R.; Trofimenko, S.; Díaz-Requejo, M.; Pérez, P. J. *J. Am. Chem. Soc.* **2006**, *128*, 11784. (b) Díaz-Requejo, M.; Belderrain, T. R.; Nicasio, M. C.; Trofimenko, S.; Pérez, P. J. *J. Am. Chem. Soc.* **2003**, *125*, 12078.

18 (a) Du Bois, J. *Org. Process Res. Dev.* **2011**, *15*, 758. (b) Kurokawa, T.; Kim, M.; Du Bois, J. *Angew. Chem. Int. Ed.* **2009**, *48*, 2777. (c) Kim, M.; Mulcahy, J. V.; Espino, C. G.; Du Bois, J. *Org. Lett.* **2006**, *8*, 1073. (d) Espino, C. G.; Fiori, K. W.; Kim, M.; Du Bois, J. *J. Am. Chem. Soc.* **2004**, *126*, 15378. (e) When, P. M.; Du Bois, J. *J. Am. Chem. Soc.* **2002**, *124*, 12950. (f) Espino, C. G.; Du Bois, J. *Angew. Chem. Int. Ed.* **2001**, *40*, 598.

19 Nakamura, E.; Yoshikai, N.; Yamanaka, M. *J. Am. Chem. Soc.* **2002**, *124*, 7181.

20 Dauban, P.; Dodd, R. H. *Synlett* **2003**, *11*, 1571.

21 (a) Lebel, H.; Huard, K. *Org. Lett.* **2007**, *9*, 639. (b) Lebel, H.; Huard, K.; Lectard, S. *J. Am. Chem. Soc.* **2005**, *127*, 14198.

22 (a) Shen, M.; Leslie, B. E.; Driver, T. G. *Angew. Chem. Int. Ed.* **2008**, *47*, 5056. (b) Stokes, B. J.; Dong, H.; Leslie, B. E.; Pumphrey, A. L.; Driver, T. G. *J. Am. Chem. Soc.* **2007**, *129*, 7500.

23 Alberico, D.; Scott, M. E.; Lautens, M. *Chem. Rev.* **2007**, *107*, 174.

24 (a) Fujiwara, Y.; Asano, R.; Moritani, I.; Teranishi, S. *J. Org. Chem.* **1976**, *41*, 1681. (b) Fujiwara, Y.; Moritani, I.; Danno, S.; Asano, R.; Teranishi, S. *J. Am. Chem. Soc.* **1969**, *91*, 7166. (c) Moritani, I.; Fujiwara, Y. *Tetrahydron Lett.* **1967**, *12*, 1119.

25 Kleiman, J. P.; Dubeck, M. *J. Am. Chem. Soc.* **1963**, *85*, 1544.

26 (a) Cope, A. C.; Friedrich, E. C. *J. Am. Chem. Soc.* **1968**, *90*, 909. (b) Cope, A. C.; Siekman, R. W. *J. Am. Chem. Soc.* **1965**, *87*, 3272.

27 (a) Constable, E. C.; Leese, T. A. *J. Organomet. Chem.* **1987**, *335*, 293. (b) Kasahara, A. *Bull. Chem. Soc. Jap.* **1968**, *41*, 1272.

28 (a) Li, L.; Brennessel, W. W.; Jones, W. D. *Organometallics* **2009**, *28*, 3492. (b) Li, L.; Brennessel, W. W.; Jones, W. D. *J. Am. Chem. Soc.* **2008**, *130*, 12414. (c) Davies, D. L.; Al-Duaij, O.; Fawcett, J.; Giardiello, M.; Hilton, S. T.; Russel, D. R. *Dalton Trans.* **2003**, 4132.

29 (a) Fahey, D. R. *J. Organomet. Chem.* **1971**, *27*, 283. (b) Fahey, D. R. *Chem. Commun.* **1970**, 417.

30 Arockiam, P. B.; Bruneau, C.; Dixneuf, P. H. *Chem. Rev.* **2012**, *112*, 5879.

31 (a) Kakiuchi, F.; Kochi, T.; Mizushima, E.; Murai, S. *J. Am. Chem. Soc.* **2010**, *132*, 17741 (b) Kakiuchi, F.; Matsuura, Y.; Kan, S.; Chatani, N. *J. Am. Chem. Soc.* **2005**, *127*, 5936. (c) Kakiuchi, F.; Kan, S.; Igi, K.; Chatani, N.; Murai, S. *J. Am. Chem. Soc.* **2003**, *125*, 1698. (d) Murai, S.; Kakiuchi, F.; Sekine, S.; Tanaka, Y.; Kamatani, A.; Sonoda, M.; Chantani, N. *nature*, **366**, 529.

32 (a) Oi, S.; Aizawa, E.; Ogino, Y.; Inoue, Y. *J. Org. Chem.* **2005**, *70*, 3113. (b) Oi, S.; Ogino, Y.; Fukita, S.; Inoue, Y. *Org. Lett.* **2002**, *4*, 1783. (c) Oi, S.; Fukita, S.; Hirata, N.; Watanuki, N.; Miyano, S.; Inoue, Y. *Org, Lett.* **2001**, *3*, 2579.

33 (a) Song, G.; Wang, F.; Li, W. *Chem. Soc. Rev.* **2012**, *41*, 3651. (b) Colby, D. A.; Bergman, R. G.; Ellman, J. A. *Chem. Rev.* **2010**, *110*, 624. (c) Satoh, T.; Miura, M. *Chem. Eur. J.* **2010**, *16*, 11212.

34 (a) Lim, Y.-G.; Kang, J.-B.; Kim, Y. H. *J. Chem. Soc., Perkin Trans.* **1996**, 2201. (b) Lim, Y.-G.; Kim, Y. H.; Kang, J.-B. *J. Chem. Soc., Chem. Commun.* **1994**, 2267.

35 (a) Lim, S.-G.; Ahn, J.-A.; Jun, C.-H. *Org. Lett.* **2004**, *6*, 4687. (b) Jun, C.-H.;

Chung, K.-Y.; Hong, J.-B. *Org. Lett.* **2001**, *3*, 785. (c) Jun, C.-H.; Hong, J.-B.; Kim, Y.-H.; Chung, K.-Y. *Angew. Chem. Int. Ed.* **2000**, *39*, 3440.

36 (a) Ueura, K.; Satoh, T.; Miura, M. *J. Org. Chem.* **2007**, *72*, 5362. (b) Ueura, K.; Satoh, T.; Miura, M. *Org. Lett.* **2007**, *9*, 1407.

37 (a) Tauchert, M. E.; Incarvito, C. D.; Rheingold, A. L; Bergman, R. G.; Ellman, J. A. *J. Am. Chem. Soc.* **2012**, *134*, 1482. (b) Tsai, A. S.; Tauchert, M. E.; Bergman, R. G.; Ellman, J. A. *J. Am. Chem. Soc.* **2011**, *133*, 1248. (c) Hesp, K. D.; Bergman, R. G.; Ellman, J. A. *J. Am. Chem. Soc.* **2011**, *133*, 11430.

38 Park, J.; Park, E.; Kim, A.; Lee, Y.; Chi, K.-W.; Kwak, J. H.; Jung, Y. H.; Kim, I. S. *Org. Lett.* **2011**, *13*, 4390.

39 Gómez, M.; Granell, J.; Martinez, M. *Organometallics* **1997**, *16*, 2539.

40 (a) Yeung, C. S.; Dong, V. M. *Chem. Rev.* **2011**, *111*, 1215. (b) Xu, L.-M.; Li, B.-J.; Yang, Z.; Shi, Z.-J. *Chem. Soc. Rev.* **2010**, *39*, 712. (c) Chen, X.; Engle, K. M.; Wang, D.-H.; Yu, J.-Q. *Angew. Chem. Int. Ed.* **2009**, *48*, 5094. (d) Beccalli, E. M.; Broggini, G.; Martinelli, M.; Sottocornola, S. *Chem. Rev.* **2007**, *107*, 5318. (e) Dupont, J.; Consorti, C. S.; Spence, J. *Chem. Rev.* **2005**, *105*, 2527.

41 Selected examples for Pd(II)-catalyzed C-H functionalizations of anilides: (a) Giri, R.; Lam, J. K.; Yu, J.-Q. *J. Am. Chem. Soc.* **2010**, *132*, 686. (b) Rauf, W.; Thompson, A. L.; Brown, J. M. *Chem. Commun.* **2009**, 3874. (c) Houlden, C. E.; Hutchby, M.; Bailey, C. D.; Ford, J. G.; Tyler, S. N. G.; Gagné, M. R.; Lloyd-Jones, G. C.; Booker-Milburn, K. I. *Angew. Chem. Int. Ed.* **2009**, *48*, 1830. (d) Yang, S.; Li, B.; Wan, X.; Shi, Z. *J. Am. Chem. Soc.* **2007**, *129*, 6066. (e) Wan, X.; Ma, Z.; Li, B.; Zhang, K.; Cao, S.; Zhang, S.; Shi, Z. *J. Am. Chem. Soc.* **2006**, *128*, 7416. (f) Daugulis, O.; Zaitsev, V. G. *Angew, Chem. Int. Ed.* **2005**, *44*, 4046. (g) Zaitsev, V. G.; Daugulis, O. *J. Am. Chem. Soc.* **2005**, *127*, 4156. (h) Boele, M. D. K.; van Strijdonck, G. P. F.; de Vries, A. H.; Kamer, P. C. J.; de Vries, J. G.; van Leeuwen, P. W. N. M. *J. Am. Chem. Soc.* **2002**, *124*, 1586. (i) Trernont, S. J.; Rahman, H. U. *J. Am. Chem. Soc.* **1984**, *106*, 5759. (j) Horino, H.; Inoue, N. *J. Org. Chem.* **1981**, *46*, 4416.

42 Cai, G.; Fu, Y.; Li, Y.; Wan, X.; Shi, Z. *J. Am. Chem. Soc.* **2007**, *129*, 7666.

43 (a) Chen, X.; Goodhue, C. E.; Yu, J.-Q. *J. Am. Chem. Soc.* **2006**, *128*, 12634.(b) Chen, X.; Li, J.-J.; Hao, X.-S.; Goodhue, C. E.; Yu, J.-Q. *J. Am. Chem. Soc.* **2006**, *128*, 78.

44 (a) Chiong, H. A.; Pham, Q.-N.; Daugulis, O. *J. Am. Chem. Soc.* **2007**, *129*, 9879. (b) Shabashov, D.; Daugulis, O. *Org. Lett.* **2005** *7*, 3657.

45 (a) Deprez, N. R.; Sanford, M. S. *J. Am. Chem. Soc.* **2009**, *131*, 11234. (b) Deprez,

N. R.; Sanford, M. S. *Inorg. Chem.* **2007**, *46*, 1924. (c) Kalyani, D.; Deprez, N.; Desai, L. V.; Sanford, M. S. *J. Am. Chem. Soc.* **2005**, *127*, 7330.

46 (a) Hull, K. L.; Sanford, M. S. *J. Am. Chem. Soc.* **2009**, *131*, 9651. (b) Brasche, G.; García-Fortanet, J.; Buchwald, S. L. *Org. Lett.* **2008**, *10*, 2207. (c) Li, B.-J.; Tian, S.-L.; Fang, Z.; Shi, Z.-J. *Angew. Chem. Int. Ed.* **2008**, *47*, 1115. (d) Hull, K. L.; Sanford, M. S. *J. Am. Chem. Soc.* **2007**, *129*, 11904.

47 (a) Houlden, C. E.; Hutchby, M.; Bailey, C. D.; Gair Ford, J.; Tyler, S. N. G.; Gagné, M. R.; Lloyd-Jones, G. C.; Booker-Milburn, K. I. *Angew. Chem. Int. Ed.* **2009**, *48*, 1830. (b) Giri, R.; Yu, J.-Q. *J. Am. Chem. Soc.* **2008**, *130*, 14082.

48 (a) Chan, C.-W.; Zhou, Z.; Yu, W.-Y. *Adv. Synth. Catal.* **2011**, *353*, 2999. (b) Chan, C.-W.; Zhou, Z.; Chan. A. S. C.; Yu, W.-Y. *Org. Lett.* **2010**, *12*, 3926. (c) Yu, W.-Y.; Sit, W. N.; Lai, K.-M.; Zhou, Z.; Chan, A. S. C. *J. Am. Chem. Soc.* **2008**, *130*, 3304.

49 (a) Tan, Y.; Hartwig, J. F. *J. Am. Chem. Soc.* **2010**, *132*, 3676. (b) Mei, T.-S.; Wang, X.; Yu, J.-Q. *J. Am. Chem. Soc.* **2009**, *131*, 10806. (c) Wasa, M.; Yu, J.-Q. *J. Am. Chem. Soc.* **2008**, *130*, 14058. (d) Li, J.-J.; Mei, T.-S.; Yu, J.-Q. *Angew. Chem. Int. Ed.* **2008**, *47*, 6452. (e) Jordan-Hore, J. A.; Johansson, C. C. C.; Gulias, M.; Beck, E. M.; Gaunt, M. J. *J. Am. Chem. Soc.* **2008**, *130*, 16184. (f) Tsang, W. C. P.; Zheng, N.; Buchwald, S. L. *J. Am. Chem. Soc.* **2005**, *127*, 14560.

50 (a) Xiao, B.; Gong, T.-J.; Xu, J.; Liu, Z.-J.; Liu, L. *J. Am. Chem. Soc.* **2011**, *133*, 1466. (b) Ke, Z.; Cundari, T. R. *Organometallics* **2010**, *29*, 821. (c) Dick, A. R.; Remy, M. S.; Kampf, J. W.; Sanford, M. S. *Organometallics* **2007**, *26*, 1365. (d) Thu, H.-Y.; Yu, W.-Y.; Che. C.-M. *J. Am. Chem. Soc.* **2006**, *128*, 9048,

51 (a) Kamaraj, K.; Bandyopadhyay, D. *Organometallics* **1999**, *18*, 438-446. (b) Kamaraj, K.; Bandyopadhyay, D. *J. Am. Chem. Soc.* **1997**, *119*, 8099-8100. (c) Valk, J.-M.; Boersma, J.; van Koten, G. *Organometallics* **1996**, *15*, 4366-4372. (d) Alsters, P. L.; Teunissen, H. T.; Boersma, J.; Spek, A.L.; van Koten, G. *Organometallics* **1993**, *12*, 4691-4696.

52 (a) Matsuda, N.; Hirano, K.; Satoh, T.; Miura, M. *Org. Lett.* **2011**, *13*, 2860. (b) Zhao, H.; Wang, M.; Su, W.; Hong, M. *Adv. Synth. Catal.* **2010**, *352*, 1301. (c) Kawano, T.; Hirano, K.; Satoh, T.; Miura, M. *J. Am. Chem. Soc.* **2010**, *132*, 6900. (d) Wang, Q.; Schreiber, S. L. *Org. Lett.* **2009**, *11*, 5178. (e) Monguchi, D.; Fujiwara, T.; Furukawa, H.; Mori, A. *Org. Lett.* **2009**, *11*, 1607.

Chapter 2

53 (a) Bhattacharya, S.; Chaudhuri, P. *Curr. Med. Chem.* **2008**, *15*, 1762. (b) Carta, A.;

Piras, S.; Loriga, G.; Paglietti, G. *Mini Rev. Med. Chem.* **2006**, *6*, 1179. (c) Kamal, A.; Reddy, K. L.; Devaiah, V.; Shankaraiah, N.; Rao, M. V. *Mini Rev. Med. Chem.* **2006**, *6*, 71. (d) Horton, D. A.; Bourne, G. T.; Smythe, M. L. *Chem. Rev.* **2003**, *103*, 893.

54 Xiao, B.; Fu, Y.; Gong, T.-J.; Dai, J.-J.; Yi, J.; Liu, L. *J. Am. Chem. Soc.* **2010**, *132*, 468.

55 (a) Palmer, B. D.; Woon, S.-T.; Sutherland, R.; Reddy, C.; Wang, L.-C. S.; Kieda, C.; Ching, L.-M. *J. Med. Chem.* **2007**, *50*, 3757. (b) Wiklund, P.; Bergman, J. *Curr. Org, Synth.* **2006**, *3*, 379.

56 Silva, J. F. M.; Garden, S. J.; Pinto, A. C. *J. Braz. Chem. Soc.* **2001**, *12*, 273.

57 Kunz, K.; Scholz, U.; Ganzer, D. *Synlett* **2003**, *15*, 2428.

58 (a) Shi, B.-F.; Zhang, T.-H.; Lam, J. K.; Wang, D.-H.; Yu, J.-Q. *J. Am. Chem. Soc.* **2010**, *132*, 460. (b) Zhang, Y.-H.; Yu, J.-Q. *J. Am. Chem. Soc.* **2009**, *131*, 14654. (c) Mei, T.-S.; Giri, R.; Maugel, N.; Yu, J.-Q. *Angew. Chem. Int. Ed.* **2008**, *47*, 5215. (d) Wang, D.-H.; Mei, T.-S.; Yu, J.-Q. *J. Am. Chem. Soc.* **2008**, *130*, 17676. (e) Giri, R.; Maugel, N.; Li, J.-J.; Wang, D.-H.; Breazzano, S. P.; Suaunders, L. B.; Yu, J.-Q. *J. Am. Chem. Soc.* **2007**, *129*, 3510.

59 (a) Donohoe, T. J.; Bataille, C. J. R.; Gattrell, W.; Kloesges, J.; Rossignol, E. *Org. Lett.* **2007**, *9*, 1725. (b) Herschhorn, A.; Lerman, L.; Weitman, M.; Gleenberg, I. O.; Nudelman, A.; Hizi, A. *J. Med. Chem.* **2007**, *50*, 2370. (c) Drent, E.; van Broekhoven, J. A. M.; Doyle, M. J. *J. Organomet. Chem.* **1991**, *417*, 235. (d) Bancroft, D. P.; Cotton, F. A.; Falvello, L. R.; Schwotzer, W. *Polyhedron* **1988**, *7*, 615.

Chapter 3

60 (a) Stowers, K. J.; Sanford, M. S. *Org. Lett*. **2009**, *11*, 4584. (b) Desai, L. V.; Stowers, K. J.; Sanford, M. S. *J. Am. Chem. Soc*. **2008**, *130*, 13285.

61 (a) Barani, M.; Fioravanti, S.; Loreto, M. A.; Pellacani, L.; Tardella, P. A. *Tetrahedron*, **1994**, *50*, 3829. (b) Lwowski, W.; Maricich, T. J. *J. Am. Chem. Soc.* **1965**, *87*, 3630. For a more recent example see: (v) Fioravanti, S.; Morreale, A.; Pellacani, L.; Tardella, P. A. *Eur. J. Org. Chem.* **2003**, 4549

62 (a) McMurray, L.; O'Hara, F.; Gaunt, M. J. *Chem. Soc. Rev.* **2011**, *40*, 1885. (b)Lersch, M.; Tilset, M. *Chem. Rev.* **2005**, *105*, 2471.

63 (a) Brown, H. C.; Stock, L. M. *J. Am. Chem. Soc.* **1957**, *79*, 5171. (b) De La Mare, P. B. D. *J. Chem. Soc.* **1954**, 4450.

64 (a) Chaudhuri, P. D.; Guo, R.; Malinakova, H. C. *J. Organomet. Chem.* **2008**, *693*, 567. (b) Guo, R.; Portscheller, J. L.; Day, V. W.; Malinakova, H. C. *Organometallics* **2007**, *26*, 3874.

65 Whitfield, S. R.; Sanford, M. S. *J. Am. Chem. Soc.* **2007**, *129*, 15142.

66 Kitamura, M.; Narasaka, K. *Chem. Rec.* **2002**, *2*, 268.

67 (a) Patureau, F. W.; Glorius, F. *Angew. Chem. Int. Ed.* **2011**, *50*, 1977. (b) Yu, S.; Wan, B.; Li, X. *Org. Lett.* **2013**, *15*, 3706. (c) Rakshit, S.; Grohmann, C.; Besset, T.; Glorius, F. *J. Am. Chem. Soc.* **2011**, *133*, 2350.

68 Xu, L.; Zhu, Q.; Huang, G.; Cheng, B.; Xia, Y. *J. Org. Chem.* **2012**, *77*, 3017.

Chapter 4

69 (a) Patureau, F. W.; Wencel-Delord, J.; Glorius, F. *Aldrichim. Acta* **2012**, *45*, 31. (b) Hyster, T. K.; Rovis, T. *J. Am. Chem. Soc.* **2010**, *132*, 10565. (c) Patureau, F. W.; Besset, T.; Glorius, F. *Angew. Chem. Int. Ed.* **2011**, *50*, 1064. (d) Stuart, D. R.; Alsabeh, P.; Kuhn, M.; Fagnou, K. *J. Am. Chem. Soc.* **2010**, *132*, 18326. (e) Staurt, D. R.; Bertrand-Laperie, M.; Burgess, K. M. N.; Fagnou, K. *J. Am. Chem. Soc.* **2008**, *130*, 16474.

70 (a) Erdick, E.; Ay, M. *Chem. Rev.* **1989**, *89*, 1947. (b) Stella, L. *Angew. Chem. Int. Ed.* **1983**, *22*, 337. (c) Kovacic, P.; Lowery, M. K.; Field, K. W. *Chem. Rev.* **1970**, *70*, 639.

71 (a) Hatakeyama, T.; Toshimoto, Y.; Ghorai, S. K.; Nakamura, M. *Org. Lett.* **2010**, *12*, 1516. (b) Barker, T, Jarvo, E. R. *J. Am. Chem. Soc.* **2009**, *131*, 15598. (c) He, C.; Chen, C.; Cheng, J.; Liu, C.; Liu, W.; Li, Q.; Lei, A. *Angew. Chem. Int. Ed.* **2008**, *47*, 6414. (d) Kabalka, G. W.; Wang, Z. *Organometalliics* **1989**, *8*, 1093. (e) Brown, H. C.; Kim, K.-W.; Srebnik, M.; Singaram, B. *Tetrahedron* **1987**, *43*, 4071. (f) Kabalka, G. W.; McCollum, G. W.; Kunda, S. A. *J. Org. Chem.* **1984**, *49*, 1656.

72 For more recent examples of Pd- and Rh-catalyzed intermolecular arene C-H aminations, see: (a) Grohmann, C.; Wang, H.; Glorius, F. *Org. Lett.* **2012**, *14*, 656. (b) Yoo, E. J.; Ma, S.; Mei, T.-S.; Chan, K. S. L.; Yu, J.-Q. *J. Am. Chem. Soc.* **2011**, *133*, 7652.

73 (a) Kamal, A.; Reddy, K. L.; Devaiah, V.; Shankaraiah, N.; Rao, M. V. *Mini Rev.*

Med. Chem. **2006**, *6*, 71. (b) Horton, D. A.; Bourne, G. T.; Smythe, M. L. *Chem. Rev.* **2003**, *103*, 893.

74 (a) Klemm, W. *Proc. Chem. Soc.* **1958**, 350. (b) Bachmann, W. E.; Cava, M. P.; Dreiding, A. S. *J. Am. Chem. Soc.* **1954**, *76*, 5554. (c) Fox, S. W.; Bullock, M. W. *J. Am. Chem. Soc.* **1951**, *73*, 2754. (d) Henry, R.; Dehn, W. M. *J. Am. Chem. Soc.* **1950**, *72*, 2280. (e) Soper, F. G. *J. Phy. Chem.* **1927**, *31*, 1192.

75 (a) Coleman, G. H.; Blomquist, R. F. *J. Am. Chem. Soc.* **1941**, *63*, 1692. (b) Coleman, G. H.; Forrester, R. A. *J. Am. Chem. Soc.* **1936**, *58*, 27. (c) Coleman, G. H. *J. Am. Chem. Soc.* **1933**, *55*, 3001.

76 (a) Beak, P.; Basha, A.; Kokko, B.; Loo, B. *J. Am. Chem. Soc.* **1986**, *108*, 6016. (b) Beak, P.; Basha, A.; Kokko, B. *J. Am. Chem. Soc.* **1984**, *106*, 1511.

77 (a) Erdik, E.; Ülhü, S. A. *J. Phys. Org. Chem.* **2007**, *20*, 671. (b) Erdik, E.; Eroğlu, F.; Kâhya, D. *J. Phys. Org. Chem.* **2005**, *18*, 950.

78 (a) Aggarwal, V. K.; Fang, G. Y.; Ginesta, X.; Howells, D. M.; Zaja, M. *Pure Appl. Chem.* **2006**, *78*, 215. (b) Bottoni, A; Lombardo, M.; Neri, A.; Trombini, C. *J. Org. Chem.* **2003**, *68*, 3397.

79 Donaruma, L. G. *J. Org. Chem.* **1957**, *22*, 1024.

80 Surry, D. S.; Buchwald, S. L. *Chem. Sci.* **2011**, *2*, 27.

81 Jo, Y. S.; van der Vlies, A. J.; Gantz, J.; Thacher, T. N.; Antonijevic, S.; Cavadini, S.; Demurtas, D.; Stergiopulos, N.; Hubbell, J. A. *J. Am. Chem. Soc.* **2009**, *131*, 14413.

82 Kang, J. W.; Moseley, K.; Maitlis, P. M. *J. Am. Chem. Soc.* **1969**, *91*, 5970.